



Polymerization of ethylene: from free radical homopolymerization to hybrid radical/catalytic copolymerization

Etienne Grau

► To cite this version:

Etienne Grau. Polymerization of ethylene: from free radical homopolymerization to hybrid radical/catalytic copolymerization. Polymers. Université Claude Bernard Lyon 1, 2010. English. NNT : . tel-02363216

HAL Id: tel-02363216

<https://hal.science/tel-02363216>

Submitted on 14 Nov 2019

HAL is a multi-disciplinary open access archive for the deposit and dissemination of scientific research documents, whether they are published or not. The documents may come from teaching and research institutions in France or abroad, or from public or private research centers.

L'archive ouverte pluridisciplinaire **HAL**, est destinée au dépôt et à la diffusion de documents scientifiques de niveau recherche, publiés ou non, émanant des établissements d'enseignement et de recherche français ou étrangers, des laboratoires publics ou privés.

THESE présentée

devant L'UNIVERSITE CLAUDE BERNARD - LYON 1

pour l'obtention du DIPLOME DE DOCTORAT

Spécialité CHIMIE
(arrêté du 7 août 2006)

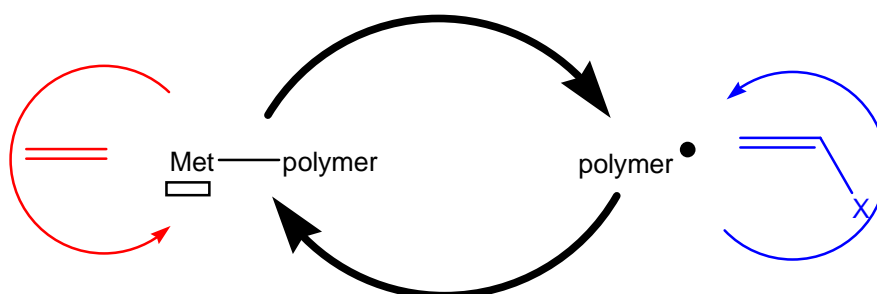
soutenue le 15 novembre 2010

par

M. GRAU Etienne

**Polymerization of ethylene:
from free radical homopolymerization to hybrid radical/catalytic copolymerization**

Directeur de thèse: M. BOISSON Christophe



JURY : M. L. BONNEVIOT
M. K. MATYJASZEWSKI,
M. S. MECKING,
M. C. BOISSON,
M. V. MONTEIL,
M. R. SPITZ,
M. S. MARQUE,
M. M. GLOTIN,

Examineur
Rapporteur
Rapporteur
Directeur de thèse
Co-encadrant
Co-encadrant
Examineur
Examineur

THESE

présentée

devant L'UNIVERSITE CLAUDE BERNARD - LYON 1

pour l'obtention

du DIPLOME DE DOCTORAT
Spécialité CHIMIE

(arrêté du 7 août 2006)

soutenue le 15 novembre 2010

par

M. GRAU Etienne

**Polymerization of ethylene:
from free radical homopolymerization to hybrid radical/catalytic copolymerization**

Directeur de thèse: M. BOISSON Christophe

JURY :	M. L. BONNEVIOT	Examineur
	M. K. MATYJASZEWSKI,	Rapporteur
	M. S. MECKING,	Rapporteur
	M. C. BOISSON,	Directeur de thèse
	M. V. MONTEIL,	Co-encadrant
	M. R. SPITZ,	Co-encadrant
	M. S. MARQUE,	Examineur
	M. M. GLOTIN,	Examineur

UNIVERSITE CLAUDE BERNARD - LYON 1

Président de l'Université

Vice-président du Conseil Scientifique

Vice-président du Conseil d'Administration

Vice-président du Conseil des Etudes et de la Vie Universitaire

Secrétaire Général

M. le Professeur L. Collet

M. le Professeur J-F. Mornex

M. le Professeur G. Annat

M. le Professeur D. Simon

M. G. Gay

COMPOSANTES SANTE

Faculté de Médecine Lyon Est – Claude Bernard

Faculté de Médecine Lyon Sud – Charles Mérieux

UFR d'Odontologie

Institut des Sciences Pharmaceutiques et Biologiques

Institut des Sciences et Techniques de Réadaptation

Département de Biologie Humaine

Directeur : M. le Professeur J. Etienne

Directeur : M. le Professeur F-N. Gilly

Directeur : M. le Professeur D. Bourgeois

Directeur : M. le Professeur F. Locher

Directeur : M. le Professeur Y. Matillon

Directeur : M. le Professeur P. Farge

COMPOSANTES ET DEPARTEMENTS DE SCIENCES ET TECHNOLOGIE

Faculté des Sciences et Technologies

Département Biologie

Département Chimie Biochimie

Département GEP

Département Informatique

Département Mathématiques

Département Mécanique

Département Physique

Département Sciences de la Terre

UFR Sciences et Techniques des Activités Physiques et Sportives

Observatoire de Lyon

Ecole Polytechnique Universitaire de Lyon 1

Institut Universitaire de Technologie de Lyon 1

Institut de Science Financière et d'Assurance

Institut Universitaire de Formation des Maîtres

Directeur : M. le Professeur F. Gieres

Directeur : M. le Professeur C. Gautier

Directeur : Mme le Professeur H. Parrot

Directeur : M. N. Siauve

Directeur : M. le Professeur S. Akkouche

Directeur : M. le Professeur A. Goldman

Directeur : M. le Professeur H. Ben Hadid

Directeur : Mme S. Fleck

Directeur : M. le Professeur P. Hantzpergue

Directeur : M. C. Collignon

Directeur : M. B. Guiderdoni

Directeur : M. le Professeur J. Lieto

Directeur : M. le Professeur C. Coulet

Directeur : M. le Professeur J-C. Augros

Directeur : M R. Bernard

A Mailys sans qui je ne suis rien.

Ce travail a été réalisé dans l'équipe Chimie et Procédés de Polymérisation au sein du laboratoire C2P2, UMR CNRS 5265, CPE, Université de Lyon sous la direction scientifique de Vincent MONTEIL, Roger SPITZ et Christophe BOISSON. Je tiens à les remercier particulièrement pour m'avoir accueilli dans leur équipe de recherche, leur disponibilité et pour m'avoir donné l'opportunité de réaliser ma thèse sur un sujet passionnant.

J'adresse mes sincères remerciements au Prof. Dr. Krzysztof MATYJASZEWSKI, Professeur à Carnegie Mellon University et au Prof. Dr. Stefan MECKING, Professeur à Konstanz University, pour avoir accepté d'être rapporteurs de ce manuscrit.

J'exprime toute ma reconnaissance au Dr. Michel GLOTIN, Directeur scientifique d'ARKEMA et au Prof. Dr. Sylvain MARQUE, Professeur à l'Université de Provence qui m'ont fait l'honneur de bien vouloir participer à mon jury de thèse.

Enfin je remercie Prof. Dr. Laurent BONNEVIOT, Professeur à l'ENS Lyon, d'avoir accepté de présider mon jury de thèse et surtout pour ses passionnantes et longues discussions (sur la morphologie et philosophie du Ni en particulier) devant la RPE.

Je remercie Roger SPITZ, l'ex-directeur du LCPP mais pour toujours l'âme du LCPP, pour m'avoir proposé l'asile politique au sein de son laboratoire. Grâce à vous en particulier j'appris et expérimentai qu'il y avait encore plein de choses à faire en chimie de polymérisation. (par effet ricochet je remercie donc Prof Dr Pierre AUDEBERT qui, en me déconseillant cette « science vieillissante » que sont les polymères, m'y a fait plonger à corps perdu). Roger, je vous remercie donc pour ses quatre années de discussions (chance réservée uniquement aux locataires des premiers bureaux puisque qu'à raison de 3-4h de discussion par bureau la visite se limite uniquement à trois chanceux par jour) en particulier sur des sujets scientifiques extrêmement variés ou sur des sujets très tendancieux, quel plaisir de pouvoir discuter avec quelqu'un ayant un esprit aussi ouvert. Et bien sûr toutes nos discussions sur Glee, BBT, House... Je me souviendrai aussi très longtemps de nos discussions sans fin sur la thermodynamique de l'éthylène qui m'ont permis de me pousser dans mes retranchements et qui m'ont fait passer plusieurs nuits blanches et week-ends à triturer les équations (désolé Maïlys). Enfin j'espère que vous continuerez longtemps à fournir une telle éducation aux jeunes thésards que nous sommes pour devenir de meilleurs scientifiques critiques et enthousiastes.

Je remercie aussi mon encadrant au jour le jour Vincent MONTEIL. Même si le début a été particulièrement difficile, au final tu m'as fait confiance et moi aussi. Tu m'as permis de prendre mes marques dans ce laboratoire et grâce à ton caractère assez semblable au mien j'ai trouvé au cours du temps un appui et un renfort. Enfin quel plaisir d'avoir pu titiller ton hypocondriasité quotidiennement. Alors j'espère que tes carrières scientifique et sentimentale vont se passer pour le mieux et à bientôt peut-être pour de futures interactions.

Je remercie enfin mon encadrant officiel Christophe BOISSON. Tu m'as fait confiance et permis de manager mon travail comme je l'entendais. Même si au final le contact est resté assez faible (peut-être dû à une trop grande différence de caractère), j'espère que l'on gardera contact.

Ce travail n'aurait pas pu être fait sans toutes les interactions avec des personnes d'origines diverses que j'ai eu la chance de côtoyer pendant ma thèse. Je tiens donc à remercier Jean-Pierre BROYER pour la chimie et la plomberies, Pierre-Yves DUGAS pour la TEM, Dr. Pierre-Antoine ALBOUI du LPS d'Orsay pour la RX sur les latex des PE et m'avoir accueilli pendant un court stage, Dr. Medhi ZEGHAL du LPS d'Orsay pour la RMN solide sur des Latex de PE, Dr. Christophe CHASSENIEUX du PCI du Mans pour m'avoir accueilli pendant 3 jours de SLS

intensive, David ALBERTINI de l'INL à Lyon pour l'AFM, Xavier JAURAND du CTM à Lyon pour la Tomo-TEM, Dr. Laurent BONNEVIOT et Dr. Belen ALBELA de l'ENS Lyon pour m'avoir formé à cette merveilleuse technique qu'est la RPE, Dr. Fernande BOISSON et Annick WATON pour l'analyse RMN des polymères, Dr. Vincent LEDENTU du LCTMM à Marseille pour les calculs DFT/MM, Dr. Robert BRULL and Chitta RAJESH du DKI à Darmstadt pour les analyses HT-LC-CC, Olivier BOYRON pour la HT-SEC, et pardon à tout ceux que j'ai oublié.

Un grand merci à Jean-Pierre BROYER, l'encyclopédie vivante du laboratoire en chimie pratique, Lyonnaiserie, et choses inutiles (avec spitzipedia et broyeurpedia wiki n'a qu'à bien se tenir). Tu m'as appris la plomberie ce qui m'est très utile aujourd'hui chez moi (comment faire un Y pour alimenter la machine à laver et un lavabo), et comme manier l'argon. Mais surtout en tant que cobureau tu m'as supporté au jour le jour surtout pendant les discussions avec Roger (tu me feras passer la note pour le Prozac et valium absolument nécessaires pour supporter ce rythme). Tu m'as fait découvrir certaines BD européennes avec succès, j'ai essayé de t'initier au 9^{ème} art US avec échec. Je te remercie pour m'avoir dégonflé le melon de temps en temps, etc. J'ai découvert des facettes inattendues de ta personnalité : oui, tu écoutes du Wagner, tu as un cœur et peu d'humour. Mais surtout je me rappellerai ta bonne humeur et ta gentillesse.

Je tiens particulièrement à remercier Pierre-Yves DUGAS qui en fin de thèse m'a fait découvrir l'émulsion. Une grande amitié est née entre nous bien avant (ça ne fait pas trop gay ?). Ensemble nous avons perverti le labo avec UBUNTU et des discussions sur l'informatique. Avec toi et Kessy on a partagé un grand nombre de bouffes à la bonne franquette et nos sorties du dernier jeudi du mois. Au fait je garde en otage quelque BD et DVD à toi en attendant de faire un échange avec les miens qui dorment chez toi. En espérant continuer à te voir pendant encore longtemps. Merci et à bientôt au tour d'un apéro.

Je tiens aussi à remercier les anciens du labo : les trois filles thésardes qui m'ont maltraité à mon arrivé au labo, Alexandra (merci de m'avoir formé), Magali, Gaëlle... et particulièrement Christian GRAILLAT qui avait toujours réponse à tout, son humour et son implication, bonne retraite. Je remercie aussi les stagiaires qui sont passés par le LCPP et qui ont travaillé avec moi : Alexandra, Christof (les allemands), Nérinel (bonne chance pour la suite), Clément, Alexandre et Cédric (ne détruis pas tout mes résultats stp). Et aussi les microprojets particulièrement Boa et Caca qui par erreur m'ont fait découvrir le radicalaire du PE (une longue histoire de 200 pages environ).

Finalement je remercie tout les personnes du labo qui reste : Franck, Muriel, Nathalie, Elodie, Bernadette, ainsi que tout les jeunes thésards et post-doc bonne chance pour la suite Florent, Elena (en espérant rester amis malgré mon humour douteux), Estevan, Ana (bonne chance pour ta future thèse), Miloud (à bientôt coloc), Pardal, Julien (l'ex nouveau post-doc)... et tout les autres.

Last but not least, je remercie ma famille, mes parents et mes frères. Un grand merci car ils m'ont toujours supporté et laissé libre de mes choix tout en me faisant pleinement confiance.

Enfin, Maillys je te remercie aussi pour m'avoir supporté pendant ces trois ans mais aussi au jour le jour depuis plus de 8 ans. Merci pour ton soutien, ta joie de vivre au quotidien, et tous ces merveilleux moments passés ensemble. Je t'aime.

Table of contents

Résumé

Glossary

Introduction 1

Chapter I: Homopolymerization of ethylene and copolymerization with polar vinyl monomers I-5

A. Generalities on polyethylene	I-9
1. Economical aspect	I-9
2. The different families of polyethylene	I-9
3. Physical properties of ethylene	I-13
B. Homopolymerization of ethylene	I-19
1. The different potential mechanisms of ethylene polymerization	I-19
2. Early works on synthesis of polyethylene	I-20
3. Free radical homopolymerization of ethylene	I-23
4. Kinetic studies of the free radical ethylene polymerization	I-28
5. Catalytic polymerization of ethylene	I-43
C. Homopolymerization of polar vinyl monomer	I-58
1. Radical polymerization	I-58
2. Polymerization of polar monomer with coordinated complexes	I-62
D. Copolymerization of ethylene with polar vinyl monomer	I-68
1. Radical copolymerization	I-68
2. Catalytic copolymerization	I-75
3. Conclusion and results obtained at the LCPP	I-84

Chapter II: Study of the free radical polymerization of ethylene in organic media under mild conditions

II-95

A. The free radical polymerization of ethylene in organic media	II-98
1. Polymerization in toluene	II-98
2. Polymerization without solvent	II-103
3. The activation by other solvents of the free radical polymerization of ethylene	II-105
4. Study of the initiator	II-113
5. Conclusion	II-117
B. Phase equilibrium in the Ethylene/solvent mixture	II-118
1. Solvent volume effect	II-118
2. Other experimental evidences of the phase equilibrium	II-121
3. Thermodynamic determination of the phase diagram	II-123
4. Conclusion	II-136
C. Solvent effect in the free radical polymerization	II-137
1. Polymerization of ethylene in various solvents	II-137
2. Rationalization of the solvent effect	II-142
3. Case of solvent mixtures	II-144
4. Arrhenius parameters of Toluene/DEC/THF	II-146
5. Solvent cohesive pressure interpretation	II-148
6. Interpretation of the solvent optimum	II-149
7. Case of other monomers	II-150
8. Conclusion	II-153
D. Lewis acid effect on the ethylene radical polymerization	II-154
1. Investigation of Lewis acids	II-154
2. Investigation of metal alkyl and alkoxides	II-156
E. Toward controlled radical polymerization	II-159
1. RAFT	II-159
2. Co mediated CRP	II-162
F. Conclusion	II-164

Chapter III: Free radical polymerization of ethylene in water	III-169
A. Ethylene free radical polymerization in emulsion	III-172
1. General mechanism of emulsion polymerization	III-172
2. Specific case of ethylene as monomer	III-174
B. Cationic stabilization of PE particles dispersion	III-175
1. Surfactant free emulsion	III-175
2. Emulsion stabilized by CTAB	III-187
3. Addition of an organic solvent	III-199
4. Rationalization of CTAB role	III-203
5. Conclusion	III-214
C. Case of anionic stabilization	III-216
1. Importance of the pH of the polymerization	III-216
2. Surfactant free emulsion	III-217
3. Polymerization with SDS as surfactant	III-219
4. SDS emulsion zone of stability	III-220
D. Toward more complex architectures	III-221
1. Hybrid organic-organic	III-221
2. Hybrid organic/inorganic	III-226
E. Conclusion	III-228

Chapter IV: Free radical copolymerization of ethylene with polar vinyl monomer

A. Parameters to consider for the ethylene copolymerization	IV-237
B. Ethylene-MMA copolymerization	IV-238
1. Influence of the ethylene pressure	IV-238
2. Influence of the solvent	IV-244
3. Influence of MMA initial concentration	IV-248
4. Conclusion	IV-255
C. Investigation of the copolymerization with various polar monomers	IV-256
1. Copolymerization with styrene	IV-256
2. Copolymerization with butyl acrylate	IV-262
3. Copolymerization with vinyl acetate	IV-269
4. Conclusion	IV-273
D. Copolymerization in emulsion	IV-274
1. Copolymerization with styrene	IV-274
2. Copolymerization with MMA	IV-277
3. Copolymerization with BuA	IV-279
4. Copolymerization with VAc	IV-280
5. Conclusion	IV-281
E. Conclusion	IV-282

Chapter V: Investigation on the hybrid radical/catalytic mechanism

A. Synergy effect between radical and catalytic polymerization	V-291
1. NiNO as a radical initiator of polymerization	V-291
2. Effect of additional AIBN on the radical polymerization initiated by NiNO	V-292
3. Effect of additional AIBN on the ethylene catalytic polymerization	V-295
B. Mechanistic investigation	V-299
1. Two different possible mechanisms	V-300
2. Evidence of the homolytic cleavage of the Ni carbon bond	V-303
3. Evidence of the radical addition on NiNO	V-306
4. Case of NiPO	V-307
C. Study of the phosphine effect during PMMA and PE syntheses	V-308
1. Influence of phosphorous ligand on the radical polymerization of MMA	V-308
2. Effect of the phosphorous ligand on the catalytic polymerization	V-316
D. Conclusion	V-323

Chapter VI: Application of the hybrid radical/catalytic mechanism to the copolymerization of ethylene with polar vinyl monomer	VI-327
A. Versatility in copolymerization available using hybrid copolymerization	VI-332
1. Copolymerization with NiNO alone	VI-332
2. Copolymerization from classical radical initiator: AIBN	VI-337
3. Copolymerization with the hybrid mechanism	VI-340
4. Conclusion	VI-346
B. Case of the ethylene MMA copolymerization	VI-347
1. Influence of the ethylene pressure	VI-347
2. Fine and original copolymer characterization by LC-CC at high-temperature	VI-348
3. Influence of the MMA concentration	VI-350
4. Effect of the catalyst and AIBN concentration	VI-351
5. Influence of the temperature	VI-354
6. ^{13}C NMR microstructure analysis of these copolymers	VI-355
7. Conclusion	VI-361
C. Case of styrene, BuA and VAc copolymerization with ethylene	VI-362
1. Ethylene copolymerization with styrene	VI-362
2. Ethylene copolymerization with BuA	VI-365
3. Copolymerization of vinyl acetate with ethylene	VI-366
4. Conclusion	VI-366
D. Hybrid copolymerization using an ATRP system	VI-368
1. Why ATRP system is a promising pathway?	VI-368
2. Introduction of radicals from ATRP equilibrium	VI-369
3. Case of reverse ATRP	VI-372
E. Conclusion	VI-374
Conclusion and perspectives	377

Table of contents

Experimental part	383
A. Synthesis of organometallic compounds	386
1. NiNO synthesis	386
2. NiPO synthesis	389
B. Method of polymerization	392
1. Polymerizations without ethylene	392
2. Ethylene homo- and copolymerization at low-pressure ($P < 25$ bar)	392
3. Ethylene homo- and copolymerization at high-pressure	393
C. Analytical methods	399
1. Polymer analyses	399
2. Colloidal analyses	400
3. Organometallics and organic compounds	402
Annex I: Influence of the PE microstructures on its melting point	I
A. Melting point of linear PE	I
B. Melting point of branched PE	II
C. Crystallinity of branched PE	V
Annex II: Calculation of comonomer molar insertion	VII
Annex III: Table of cohesive pressure, dielectric constant and dipole momentum of solvents	XI
Publications	

Résumé

Les polymères sont des macromolécules constituées d'unités de répétitions appelées monomères. Ils ont des propriétés physico-chimiques très intéressantes et surpassent dans beaucoup d'applications des matériaux classiques tels que le verre, le béton ou l'acier. Depuis le milieu des années 1970, les polymères sont partout (des avions au cœur artificiel) et certains disent que nous sommes rentrés dans « l'ère du plastique ».

Le polyéthylène (PE) est l'un des polymères les plus importants industriellement. En effet, on le retrouve dans la plupart des produits du quotidien tel que les films d'emballage, les jouets... Le polyéthylène a des propriétés physico-chimiques uniques et présente l'avantage de posséder une large gamme de propriétés différentes accessibles en variant sa microstructure (PEHD, PEBD, PEBDL) et donc sa cristallinité.

Actuellement, le polyéthylène est synthétisé industriellement par deux mécanismes différents : une polymérisation radicalaire qui nécessite des conditions expérimentales extrêmement dures (pression d'éthylène au delà de 2000 bar ou plus et température au dessus de 200°C), ou une polymérisation catalytique par coordination-insertion qui est généralement effectuée dans des conditions beaucoup plus douces (pression d'éthylène à 50 bar au plus et température le plus souvent en dessous de 100°C).

En général, ces deux méthodes ne donnent pas le même polymère. La polymérisation radicalaire produit un polyéthylène contenant des ramifications (PEBD – polyéthylène basse densité) et donc ayant un point de fusion et une cristallinité plus faible qu'un homopolyéthylène (PEHD – polyéthylène haute densité) qui peut être synthétisé par polymérisation catalytique.

Malgré l'importance considérable du polyéthylène, peu de groupes de recherche académique étudient le mécanisme et l'amélioration de sa synthèse. L'équipe Chimie et Procédés de Polymérisation du laboratoire C2P2 est une de celles-là. Depuis cinq ans, un nouveau projet de recherche y a été initié avec comme objectif la copolymérisation d'oléfines apolaires avec des comonomères polaires.

En effet, la copolymérisation est un outil extrêmement utile pour accéder à de nouvelles propriétés physico-chimiques. En effet, elle permet d'associer les propriétés différentes des homopolymères et en général d'ajouter des propriétés spécifiques à un matériau d'usage. La copolymérisation de l'éthylène avec d'autres oléfines non polaires a été

très étudiée avec des succès limités. Actuellement la microstructure du copolymère obtenu est bien contrôlée (teneur en comonomère, régio- and stéréo-sélectivité de l'insertion du comonomère...). Par contre la copolymérisation avec des monomères polaires par polymérisation radicalaire ou catalytique reste limitée voir inefficace. Il s'agit donc d'un verrou technologique important qu'il reste à briser.

Mon travail au cours de cette thèse suit la démarche originale initiées par Mlle Alexandra LEBLANC qui au cours de son doctorat a développé un nouveau concept de copolymérisation hybride pour effectuer la copolymérisation d'éthylène avec des monomères vinyliques polaires.

Ce travail repose sur deux idées principales :

- L'étude de la polymérisation radicalaire de l'éthylène dans des conditions beaucoup plus douces que les conditions industrielles. En effet, à des pressions d'éthylène en-dessous de 300 bar et des températures de polymérisations inférieures à 100°C, l'homopolymérisation de l'éthylène par voie radicalaire est souvent faussement considérée comme inefficace.
- Le développement de la copolymérisation hybride basée sur une croissance de chaîne alternant entre deux mécanismes de polymérisations différents, une croissance radicalaire pour les séquences riches en monomère vinylique polaire et une croissance par coordination/insertion pour les séquences polyéthylène. Le copolymère obtenu a alors une microstructure type multibloc.

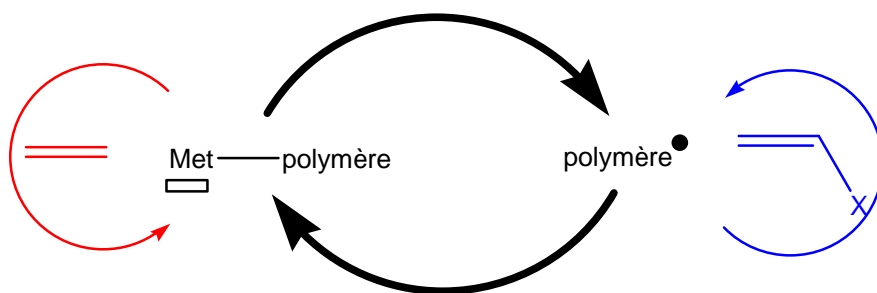


Figure 1. Copolymérisation de l'éthylène avec des monomères vinyliques polaires par un mécanisme hybride

Ce manuscrit de thèse est divisé en six chapitres qui décrivent la polymérisation de l'éthylène via polymérisation radicalaire classique jusqu'à la copolymérisation hybride par échange entre un système ATRP et une polymérisation catalytique.

Dans le premier chapitre, une étude bibliographique sur l'homopolymérisation de l'éthylène et la copolymérisation avec des monomères polaires a été effectuée.

Cette étude montre que l'homopolymérisation radicalaire de l'éthylène peut être effectuée dans des conditions expérimentales beaucoup plus diverses que celle généralement habituellement reportées (pression d'éthylène de 0.1 mbar jusqu'à 8000 bar et température de -80°C à plus de 400°C). Néanmoins, depuis plusieurs décennies très peu d'études ont été publiées sur cette polymérisation.

La copolymérisation, qu'elle soit catalytique ou radicalaire, ne permet pas la production de copolymères sur toute la gamme de compositions. De façon schématique, la polymérisation radicalaire sous des conditions douces permet l'insertion d'éthylène jusqu'à 20% pratiquement toujours isolé au sein du polymère. Et la polymérisation catalytique permet l'insertion de certains comonomères polaires jusqu'à 20% dans la chaîne (Figure 2).

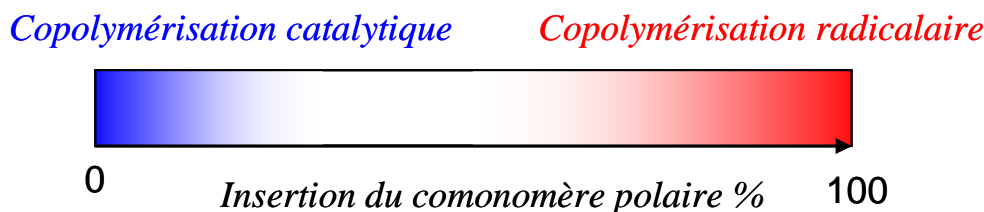


Figure 2. Copolymères accessibles par polymérisation radicalaire ou catalytique

Ces résultats démontrent bien l'importance de développer une nouvelle technique de polymérisation qui allierait les avantages des polymérisations catalytique et radicalaire afin d'obtenir des copolymères d'éthylène avec des monomères polaires.

La première partie de mon travail de thèse a concerné le développement de la polymérisation radicalaire de l'éthylène dans des conditions expérimentales qui sont généralement décrites comme étant inefficaces. De façon inattendu nous avons noté que la polymérisation radicalaire de l'éthylène peut être effectuée dans des conditions expérimentales aussi douces que des pressions de seulement 5 bar et à des températures de réaction de 10°C. Ainsi la synthèse de polyéthylène a été effectuée dans des conditions très

variables en température (10°C à 110°C) et pression (5 bar à 250 bar). Le polyéthylène obtenu possède moins de ramifications que le PEBD industriel. Sa masse molaire moyenne est faible en général (à cause de réaction de transfert au solvant) mais si la polymérisation est faite dans du diéthyle carbonate de hautes masses molaires sont atteintes (M_n de 20000 g/mol). Enfin, des températures de fusion allant de 85°C à 122°C sont obtenues.

La polymérisation radicalaire de l'éthylène peut être effectuée soit dans une phase unique supercritique (éthylène + solvant) soit dans un milieu biphasique. Dans ce cas, la polymérisation a lieu principalement dans la phase liquide où l'éthylène est dissous. La transition entre ses deux milieux a été étudiée à la fois théoriquement et expérimentalement avec un bon accord entre les deux.

Nous avons également noté que la polymérisation radicalaire de l'éthylène subit un fort effet activateur du solvant. En effet, la polymérisation sans solvant est presque inefficace contrairement à la polymérisation en présence de solvant. De plus la conversion dépend aussi du solvant utilisé. Ainsi la polymérisation dans le THF est six fois plus efficace que dans le toluène. Pour comprendre cet effet une large gamme de solvants a été étudiée. Seule l'étude par la théorie du complexe activé permet de rationaliser cet effet et il apparaît que l'interaction de Keesom induite par le solvant sur le radical en croissance contrôle la cinétique de polymérisation. En plus de cet effet activateur, les solvants peuvent être utilisés comme agents fonctionnalisants du polyéthylène par transfert au solvant. Par exemple des terminaisons par des fonctions chloro et THFyl ont été obtenues.

Enfin quelques résultats prometteurs ont été obtenus sur le contrôle de la polymérisation radicalaire de l'éthylène. En particulier les techniques RAFT (Reversible Addition Fragmentation Chain Transfer) et CMRP (Cobalt Mediated Radical Polymerization) semblent des méthodes qui permettront dans un avenir proche de contrôler la polymérisation radicalaire de l'éthylène et donc d'avoir accès à des architectures très intéressantes dans ces conditions douces.

Nous avons ensuite transposé ces résultats à la polymérisation radicalaire de l'éthylène en émulsion. Des latex stables à des taux de solides atteignant 40% en poids ont été synthétisés. Des diamètres de particules allant de 20 nm à 150 nm ont été obtenus. Deux morphologies de particules ont enfin été observées : des sphères lorsque la polymérisation est réalisée avec peu de tensioactif et des disques dans le cas contraire.

Après avoir étudié l'homopolymérisation de l'éthylène, nous avons abordé sa copolymérisation avec des monomères polaires dans des conditions expérimentales équivalentes en solution dans des solvants organiques ou bien en émulsion. Le caractère ambivalent du comonomère a été particulièrement souligné. En effet le comonomère est à la fois un solvant qui modifie la réactivité de l'éthylène et bien sûr un monomère qui peut s'insérer dans la chaîne. Ainsi les coefficients de réactivité peuvent être ajustés en modifiant le solvant organique de synthèse et la concentration initiale de comonomère utilisée. Les copolymères obtenus ont des taux d'insertion d'éthylène faibles et très peu de séquences d'unités éthylène sont présentes dans la chaîne. La copolymérisation de l'éthylène avec l'acétate de vinyle permet cependant d'atteindre des compositions extrêmement riches en éthylène.

Cette étude montre que malgré les conditions plus dures que celles décrites dans la littérature, la copolymérisation radicalaire de l'éthylène ne permet pas d'obtenir toutes les compositions possibles. En conséquence un nouveau type de copolymérisation doit être développé.

Dans la dernière partie de ce manuscrit nous avons étudié une copolymérisation hybride radicalaire/catalytique en vue d'obtenir une plus large gamme de compositions et de microstructures. Tout d'abord un complexe de nickel a été étudié qui est à la fois un catalyseur de polymérisation de l'éthylène et amorceur de la polymérisation radicalaire des monomères vinyliques polaires. En effet, la rupture homolytique de la liaison nickel carbone a été démontrée par spectroscopie RPE. De plus l'ajout d'une source supplémentaire de radicaux tel que l'AIBN permet d'activer cette rupture par un mécanisme de substitution radicalaire sur le nickel qui a été mise en évidence.

Le rôle de ligands supplémentaires comme des phosphines a aussi été étudié. En effet l'ajout de phosphine modifie l'amorçage par le complexe de nickel : à 70°C le temps de demi-vie varie de 60 min à 360 min en fonction du ligand ajouté et le facteur d'efficacité de 4% à 100%. De même l'activité du complexe en polymérisation de l'éthylène est aussi dépendant des ligands ajoutés, ainsi la polymérisation peut être totalement inhibée ou activée d'un facteur 4 par l'ajout de la phosphine adéquate. Ces résultats sont plutôt inattendus car en général un catalyseur est activé par l'ajout d'un acide de Lewis et pas d'une base qui peut se

complexer sur la lacune de coordination et donc entrer en compétition avec la coordination de l'éthylène.

Une fois ce catalyseur/amorceur étudié, la copolymérisation a été mise en place avec succès. En effet des copolymères ont été synthétisés avec de nombreux monomères vinyliques polaires. L'ajout d'une source additionnelle de radicaux augmente l'efficacité de la copolymérisation. Avec le MMA des copolymères allant de 1% à 99% ont été obtenus en utilisant le même système et en variant uniquement la pression d'éthylène et la quantité initiale de MMA. De même la nature multiblocs des copolymères a été démontrée grâce à plusieurs techniques analytiques. La microstructure obtenue est extrêmement intéressante car elle permet de conserver la cristallinité du copolymère même à des taux de comonomères polaire très élevé. Finalement l'amélioration de cette copolymérisation utilisant des techniques de polymérisation radicalaire contrôlées couplées à la catalyse a été abordée. L'ATRP (atom transfer radical polymerization) se révèle être un très bon candidat puisque qu'elle active l'homopolymérisation de l'éthylène tout en contrôlant la formation du bloc polaire.

En conclusion les objectifs initiaux de cette thèse ont été réalisés et de nouveaux domaines d'étude restent à approfondir tel que la polymérisation radicalaire contrôlée de l'éthylène, l'étude des propriétés des latex de PE ou la copolymérisation hybride contrôlée.

Glossary

Polymer:

ATRP: atom transfer radical polymerization
CMRP: cobalt mediated radical polymerization
CRP: controlled radical polymerization
FRP: free radical polymerization
HDPE: high-density polyethylene
LCB: long-chain branch
LDPE: low-density polyethylene
Mn: number average molecular weight
Mw: weight average molecular weight
MWD: molecular weight distribution
PDI: polydispersity index
PE: polyethylene
PP: polypropylene
RAFT: reversible addition-fragmentation chain transfer
SCB: short-chain branch

Molecules:

Initiators:

AIBN: azobisisobutyronitrile
AIBA: 2,2-azobis(2-amidinopropane)-dihydrochloride
APS: ammonium persulfate
KPS: potassium persulfate

Ligands:

Cy: cyclohexane
DPPB: 1,1-bis(diphenylphosphino)butane
DPPE: 1,1-bis(diphenylphosphino)ethane
DPPH: 1,1-bis(diphenylphosphino)hexane
DPPM: 1,1-bis(diphenylphosphino)methane
DPPP: 1,1-bis(diphenylphosphino)propane
DPPPe: 1,1-bis(diphenylphosphino)pentane
DPPPh: 1,1-bis(diphenylphosphino)benzene

Monomers:

AA: acrylic acid
AAm: acrylamide
AN: acrylonitrile
BuA: butyl acrylate
BuMA: butyl methacrylate
DCE: 1,1-dichloroethylene
MA: methyl acrylate
MAA: methacrylic acid
MAAm: methacrylamide
MAN: methacrylonitrile
MCr: methyl crotonate
MMA: methyl methacrylate
MSty: α -methylstyrene
PAC: isopropenyl acetate
Sty: styrene
tBuA: tert-butyl acrylate
tBuMA: tert-butyl methacrylate
VAc: vinyl acetate
VPiv: vinyl pivalate

Solvents:

DCM: dichloromethane
DEC: diethyl carbonate
DMF: dimethylformamide
DMSO: dimethylsulfoxide
THF: tetrahydrofuran

Surfactants:

CTAB: cetyltrimethylammonium bromide
SDBS: sodium dodecylbenzenesulfate
SDS: sodium dodecylsulfate

Techniques:

AFM: atomic force microscopy

DMA: dynamic mechanical analysis

DLS: dynamic light scattering

DSC: differential scanning calorimetry

EPR: electron paramagnetic resonance

GC-MS: gas chromatography-mass spectrometry

MALDI-TOF: matrix-assisted laser
desorption/ionisation – time-of-flight mass
spectrometry

NMR: nuclear magnetic resonance

SEC: size exclusion chromatography

TEM: transmission electron microscopy

TGA: thermogravimetric analysis

Miscellaneous:

cmc: critical micelle concentration

EoS: equation of state

P_c: critical pressure

T_b: boiling temperature

T_c: critical temperature

T_g: glass transition temperature

T_m: melting temperature

Introduction

Polymers are macromolecules constituted of repeated monomer units. They exhibit very interesting physico-chemical properties and they actually supplant classical materials such as glass, steel or concrete in many applications. Some authors even claim that mankind has entered in the “Polymer Era” since the mid 70s. Indeed polymers are everywhere, from cars to artificial hearts. Polymer science is a major domain of chemistry since about 50% of the world chemists work on polymer. Moreover research in polymer science undergoes exponential growth with major discoveries every year and is one of the most active communities.

Polyethylene is the top manufactured polymer. This polymer is present in the everyday life since the discovery of the first efficient polymerization of ethylene in the 40s. This polymer presents unique properties and can also cover a wide range of applications through different microstructures (HDPE, LDPE, LLDPE...).

The final properties are dependent on the molecular weight (and polydispersity index) of the polyethylene, and its crystallinities which are impacted by their branching content as well as the type of branches, and the possible comonomer content.

Polyethylene is synthesized by two efficient mechanisms: a free radical polymerization under severe experimental conditions (ethylene pressure over 2000 bar and temperature over 200°C), or a coordination-insertion catalytic polymerization which can be performed under milder experimental conditions.

Few academic research groups study the synthesis of polyethylene despite its industrial importance. The team “Chimie et Procédés de Polymérisation” in the C2P2 laboratory is one of them. Five years ago they began a project in order to copolymerize ethylene or other non polar olefins with polar vinyl monomers.

Indeed it is well known that copolymerization is a very efficient tool to access new physico-chemical properties by the variations of the polymer microstructure and their effect on the local and global properties. Copolymerization of ethylene with non polar olefins has been well investigated and the control of copolymer microstructure (comonomer content, regio- and stereoselectivity of the comonomer insertion...) is achieved from an academic point of view. For polar vinyl comonomer none of the two major mechanisms of polymerization (radical or catalytic) is able to give rise to an efficient copolymerization (in

activity, chemical composition and distribution, molecular weight, etc). Moreover none of them can produce the whole range of composition (see Figure 1) and comonomer distributions.

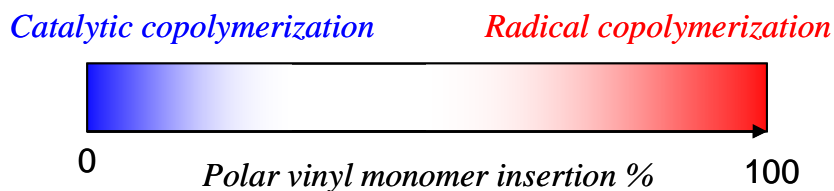


Figure 1. Range of polar insertion available up to now via radical or catalytic copolymerization

Therefore the copolymerization of ethylene with polar vinyl olefins remains one of the last challenges for polymer chemists. My work follows the initial study of Miss Alexandra LEBLANC who started to develop a new concept of hybrid copolymerization developed at the LCPP in order to solve this major issue.

The present work is based on two main ideas:

- A reinvestigation of the radical polymerization of ethylene under experimental conditions much milder than the industrial ones (see Figure 2). Indeed under ethylene pressure in the range of 0 to 300 bar and temperature of polymerization below 100°C this polymerization is often wrongly assumed to be inefficient.

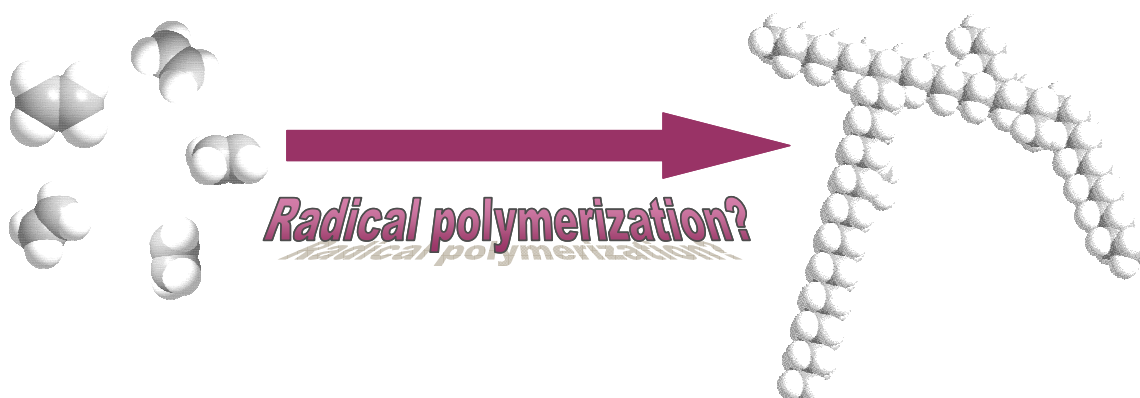


Figure 2. Free radical polymerization of ethylene

- The development of a new “hybrid” copolymerization based on the “shuttling” between two different polymerization mechanisms, a radical one for the polymerization of vinyl polar monomer and a catalytic one for the polymerization of ethylene (see Figure 3).

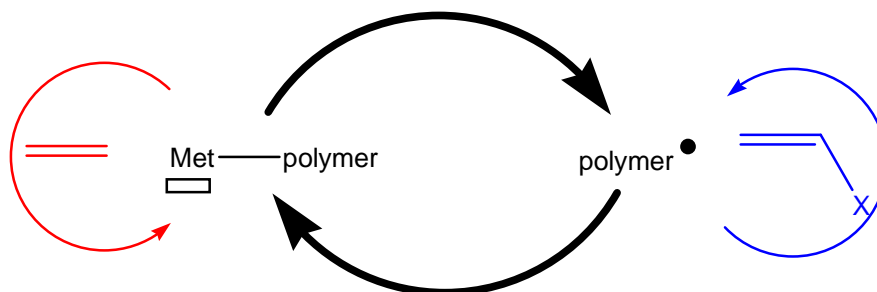


Figure 3. Hybrid radical/catalytic polymerization mechanism

The present manuscript is composed of six chapters each of them investigating a different aspect of the ethylene polymerization from a standard free radical polymerization to a controlled hybrid copolymerization with polar vinyl monomers.

In the first chapter, we will review the ethylene homopolymerization and copolymerization with polar vinyl monomer. This state-of-the-art will evidence that there is still a lack of knowledge in the free radical polymerization under medium ethylene pressure ($P < 250$ bar). Moreover the catalytic or radical copolymerization of ethylene with polar vinyl monomer does not provide the complete range of copolymer composition and microstructures. The conclusion of this study is that a new approach needs to be developed joining radical and catalytic polymerization in a hybrid mechanism.

In the second chapter, we will investigate the radical homopolymerization of ethylene. This polymerization exhibits some surprising behaviors. Ethylene free radical polymerization presents an unexpected high efficiency (due to an activation effect by the solvent) and this polymerization can even be performed under experimental conditions as mild as 10°C under 5 bar of ethylene pressure. The crucial role of solvent (activation of the polymerization and transfer agent leading to chain-end functionalization) and experimental conditions will be also rationalized. Finally, the possibility of performing controlled radical polymerization of ethylene will be briefly investigated.

In the third chapter, we will transpose this free radical polymerization in water in order to obtain high molecular weight polyethylenes and stable PE latexes. The influence of surfactant and initiator will be studied and the morphology of crystalline PE nanoparticles particularly highlighted. Finally, the formation of hybrid (organic/organic and organic/inorganic) nanoparticles is reported.

In the fourth chapter, the radical copolymerization of ethylene with various polar vinyl monomers is investigated. This copolymerization is performed in organic solvent or in aqueous dispersed medium. The particular roles of the comonomer as a solvent and as a monomer are highlighted.

In the last two chapters, we investigate in depth the possibility of performing a hybrid copolymerization.

In the fifth chapter, the synergy between radical and catalytic polymerization will be reported. Then we investigate the mechanism of “shuttling” between radical and catalytic polymerization. Finally the influence of additional ligands such as phosphine on radical and catalytic polymerization is rationalized.

In the last chapter, the copolymerization of ethylene with various polar vinyl monomers is presented. The high efficiency of this system is discussed. Then a fine investigation of the role of each compound in this copolymerization is performed. Finally the extrapolation to a shuttling between ATRP (atom transfer radical polymerization) and catalytic polymerization is investigated.

Chapter I : Homopolymerization of ethylene and copolymerization with polar vinyl monomers

A.	Generalities on polyethylene	I-9
1.	Economical aspect	I-9
2.	The different families of polyethylene	I-9
3.	Physical properties of ethylene	I-13
a)	Supercritical fluids	I-14
b)	Potential medium of polymerization	I-15
c)	Heat capacity	I-17
B.	Homopolymerization of ethylene	I-19
1.	The different potential mechanisms of ethylene polymerization	I-19
a)	Cationic polymerization	I-19
b)	Anionic polymerization	I-19
c)	Radical polymerization	I-20
d)	Catalytic polymerization	I-20
2.	Early works on synthesis of polyethylene	I-20
a)	Polyethylene synthesis without ethylene	I-20
b)	Paraffin synthesis via ethylene	I-21
(1)	Ethylene decomposition	I-21
(2)	Anionic polymerization of ethylene	I-22
(3)	Polymerization of ethylene assisted by Lewis acid	I-22
(4)	Radical polymerization of ethylene	I-22
(5)	Irradiation polymerization	I-22
(6)	Catalytic polymerization	I-22
3.	Free radical homopolymerization of ethylene	I-23
a)	Study of the high pressure and high temperature process	I-23
b)	Towards linear polyethylene at high pressure, low temperature	I-24
c)	Addition of diluents at high pressure and at high temperature	I-25
d)	Polymerization of ethylene in emulsion	I-25
e)	Process at low pressure and low temperature with diluent	I-25
(1)	In single supercritical phase	I-26
(2)	In diluents phase	I-26
f)	Activation of the ethylene radical polymerization by Lewis acid	I-27
g)	Polymerization in liquid ethylene	I-27
h)	Polymerization in gaseous ethylene	I-27

4.	Kinetic studies of the free radical ethylene polymerization	I-28
a)	Elementary steps of reaction	I-28
b)	Propagation and termination rate constants.....	I-28
(1)	Effect of ethylene pressure on the polymerization	I-29
(2)	Effect of the temperature on the polymerization.....	I-29
(3)	Determination of separate values of k_p and k_t	I-30
c)	Initiation of the polymerization.....	I-32
(1)	By Oxygen.....	I-32
(2)	Organic peroxides, azo initiators	I-35
(3)	Thermal initiation	I-35
(4)	Initiation by ionizing radiation.....	I-35
d)	Chain transfer and microstructures	I-36
(1)	Transfer to transfer agent.....	I-37
(2)	Short chain branching	I-39
(3)	Long chain branching	I-41
(4)	Unsaturation	I-42
5.	Catalytic polymerization of ethylene	I-43
a)	Generality about catalytic PE synthesis	I-43
b)	Different classes of catalyst	I-45
(1)	Group 4 transition metal complexes	I-46
(a)	With two monoanionic bidentate ligands.....	I-46
(b)	With one monoanionic tridentate ligand	I-47
(c)	With one dianionic tridentate or tetradentate ligand.....	I-47
(2)	Group 5 transition metal complexes	I-48
(3)	Group 6 transition metal complex.....	I-49
(4)	Group 7 transition metal complex.....	I-51
(5)	Group 8-9 transition metal complex	I-52
(6)	Group 10 transition metal complex.....	I-53
(a)	Brookhart type	I-54
(b)	Grubbs type	I-55
(7)	Group 11 transition metal complex.....	I-57
C.	Homopolymerization of polar vinyl monomer.....	I-58
1.	Radical polymerization	I-58
a)	Nitroxide Mediated Polymerization.....	I-59
b)	Reversible Addition Fragmentation Chain Transfer	I-59
c)	Iodide Degenerative Transfer Polymerization.....	I-60
d)	Atom Transfer Radical Polymerization.....	I-61
e)	Cobalt Mediated Radical Polymerization.....	I-61

2.	Polymerization of polar monomer with coordinated complexes.....	I-62
a)	Early transition metals and lanthanides catalysis	I-62
b)	Late transition metals	I-64
(1)	MAO ambiguous role during polymerization	I-64
(2)	Caution interpretation of radical trap test.....	I-65
(3)	Homolytic cleavage of a metal carbon bond.....	I-66
(4)	Results obtained at the LCPP.....	I-67
D.	Copolymerization of ethylene with polar vinyl monomer	I-68
1.	Radical copolymerization	I-68
a)	Copolymerization under “high pressure” polymerization conditions.....	I-69
(1)	Effect of pressure and temperature on reactivity ratios	I-70
(2)	Chemical structure and reactivity	I-71
b)	Copolymerization under “low pressure” polymerization conditions.....	I-72
c)	Copolymerization thanks to controlled radical polymerization.....	I-73
(1)	Nitroxide Mediated Polymerization.....	I-73
(2)	Reversible Addition Fragmentation Chain Transfer	I-73
(3)	Iodide Degenerative Transfer Polymerization	I-74
(4)	Atom Transfer Radical Polymerization.....	I-74
(5)	Cobalt Mediated Radical Polymerization	I-74
2.	Catalytic copolymerization	I-75
a)	Copolymerization of non-standard polar monomer	I-75
b)	Copolymerization with standard polar monomers	I-77
(1)	Acrylates.....	I-77
(a)	Cationic palladium α -diimine complex	I-78
(b)	Neutral palladium Phosphine-sulfonate catalyst	I-79
(c)	Nickel catalysts.....	I-79
(2)	Methacrylates	I-80
(3)	Acrylonitrile	I-81
(4)	Vinyl acetate.....	I-81
(5)	Vinyl halides.....	I-82
(6)	Vinyl ether.....	I-82
(7)	Other polar monomers	I-83
3.	Conclusion and results obtained at the LCPP	I-84

A. Generalities on polyethylene

1. Economical aspect

Polyolefins are the largest class of plastics [1, 2] and the market grows by 5-6% per year, because of their versatility with respect to physical and mechanical properties, their energy efficient and economically attractive production, their low cost and readily available primary materials. Among these, the commodity polymers linear low density polyethylene (LLDPE) and isotactic polypropylene (iPP) have shown the highest annual growth rates with more than 10% (see Table 1), followed by high density polyethylene (HDPE) and low density polyethylene (LDPE). In 2005, the world production of polyolefins amounted to more than 103 millions tons, nearly half of all plastics.

Table 1. World production of polyolefins in mTons [1, 2]

Year	LDPE	LLDPE	HDPE	PP	Total
1983	11.3	1.2	6.4	6.4	25.6
1990	14.0	4.0	11.4	12.6	42.7
1995	14.4	7.8	14.3	17.1	53.6
2001	15.8	15.2	20.9	27.7	79.6
2005	18.5	18.5	29.0	37.0	103.5
2010*	19.5	19.5	37.0	50.0	126.0

* : forecast

2. The different families of polyethylene

In this chapter, we will focus only on polyethylene. There are four principal classes of polyethylene (see Figure 1):

High-density polyethylene:

HDPE is chemically the closest in structure to pure polyethylene. It consists primarily of unbranched molecules with very few flaws to mar its linearity. With an extremely low level of defects to hinder organization, a high degree of crystallinity can be achieved, resulting in polymers that have a high density (relative to other types of polyethylene). Some polymers of this type produced using very small concentration of 1-alkenes comonomer in order to slightly reduce the crystallinity level and activate the ethylene polymerization. HDPE polymers typically have densities falling in the range of approximately 0.94-0.97 g/cm³.

Low-density polyethylene:

LDPE is so named because such polymer contains substantial concentrations of branches that hinder the crystallization process, resulting in relatively low density. The branches primarily consist of ethyl and butyl groups together with some long-chain branches. LDPE polymers typically have densities falling in the range of approximately 0.90-0.94 g/cm³.

Linear low-density polyethylene:

LLDPE polymers consist of macromolecules with linear polyethylene backbones to which are attached short alkyl groups at random intervals. These materials are produced by the copolymerization of ethylene with 1-alkenes. The branches most commonly encountered are ethyl, butyl, or hexyl groups. A typical average separation of branches along the main chain is 25-100 carbon atoms. Chemically these polymers can be seen as a compromise between linear polyethylene and low-density polyethylene. The short branches hinder crystallization to some extent, reducing density relative to HDPE. The result is a density range of approximately 0.90-0.94 g/cm³.

Very low-density polyethylene:

VLDPE is a specialized derivative of LLDPE. A typical separation of branches would fall in the range of 7-25 backbone carbon atoms. The high level of branching inhibits crystallization very effectively; consequently, the resulting materials are predominantly noncrystalline. The high levels of disorder are reflected in the very low densities, which fall in the range of 0.86-0.90 g/cm³.

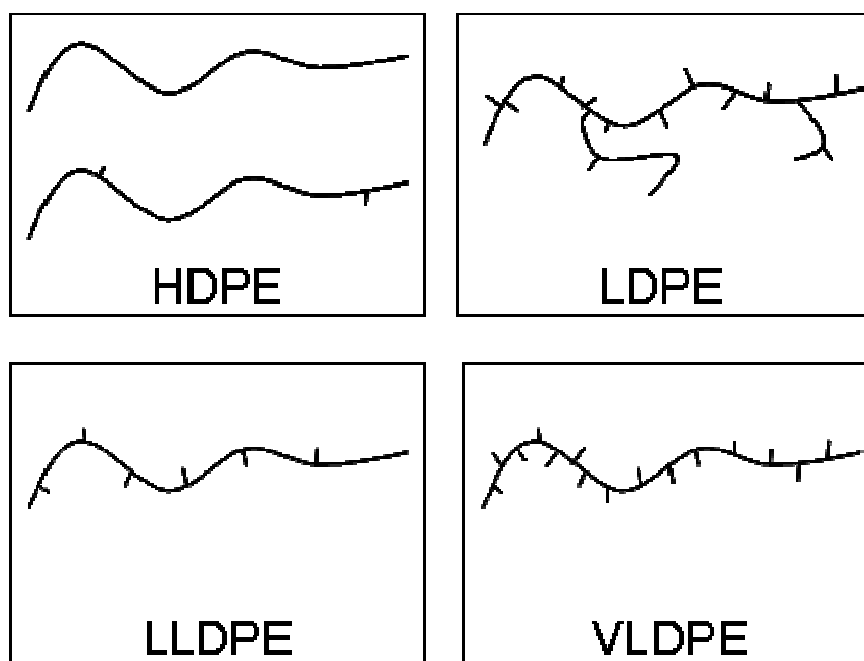


Figure 1. Schematic representations of the different classes of polyethylene

The various types of polyethylene (from high-density to very low-density) exhibit a wide range of properties, the specific attributes depending on the molecular and morphological characteristics of the polyethylene. Each variant of polyethylene possess its own characteristics, and within each type, there is a spectrum of properties. A numerical comparison of the different types of polyethylene [3], highlighting the typical ranges of some key solid-state properties, is presented in Table 2.

All these specificities explain the commercial importance of polyethylene in everyday life.

To produce these PE different processes have been developed. HDPE, LLDPE, and VLDPE are usually prepared by a catalytic polymerization such as Ziegler Natta or Phillips catalysis. LDPE is produced using free radical polymerization.

Table 2. Main properties of different types of polyethylene

Property	HDPE	LDPE	LLDPE	VLDPE
Density (g/cm ³)	0.94-0.97	0.91-0.94	0.90-0.94	0.86-0.90
Degree of crystallinity (% from calorimetry)	55-77	30-54	22-55	0-22
Melting temperature (°C)	125-132	98-115	100-125	60-100
Heat of fusion (J/g)	159-222	88-155	63-180	0-180
Flexural modulus (bar @ 23°C)	10000-16000	2500-3400	2800-11000	<2800
Tensile modulus (bar)	11000-14000	1700-3500	2700-9100	<2700
Tensile yield stress (bar)	180-310	90-200	80-200	<80
Tensile strength at break (bar)	220-310	80-310	130-450	170-350
Tensile elongation at break (%)	10-1500	100-650	100-950	100-600
Shore hardness Type D	66-73	44-50	55-70	25-55
Izod impact strength (ft-lb/in. of notch)	0.4-4.0	No break	0.35-No break	No break
Heat distortion temperature (°C @ 66 psi)	80-90	40-44	55-80	—
Thermal expansivity (10 ⁻⁶ in/in/°C)	60-110	100-220	70-150	150-270

3. Physical properties of ethylene

Before going in depth in the PE synthesis, we will focus on some different important specificities of the ethylene polymerizations.

Ethylene appears to have been discovered by Johann Joachim Becher in 1669, who obtained it by heating ethanol with sulfuric acid. Ethylene is industrially produced in the petrochemical industry by steam cracking. In this process, gaseous or light liquid hydrocarbons are heated to 750–950 °C, inducing numerous free radical reactions followed by immediate quenching to stop these reactions. This process converts large hydrocarbons into smaller ones and introduces unsaturations. Ethylene is separated from the resulting complex mixture by repeated compressions and distillations. The ethylene made is especially cheap thanks to this process (≈ 700 \$/tons compared with styrene ≈ 1100 \$/tons). This induces cheap polyethylene which also explains its wide commercial application: HDPE ≈ 900 -50000 \$/tons, LLPDE ≈ 900 -1200 \$/tons, LDPE ≈ 900 -1300 \$/tons.

As ethylene is also a vegetal hormone, which stimulates or regulates the ripening of fruit, the opening of flowers, and the abscission (or shedding) of leaves. Therefore, ethylene can be biosynthesized as well. Consequently, ethylene made by biosynthesis can be considered as a renewable and a bio-monomer, therefore poly(bio-ethylene) as a renewable resource. The current bio-ethylene is synthesized from bio-ethanol but a worldwide interest exists in the direct bacterial synthesis of ethylene.

At atmospheric pressure ethylene is a gas, which liquefies at -103.7°C and solidifies at -169.2°C . Critical point of ethylene is $T_c=9.2^{\circ}\text{C}$ and $P_c=50.4$ bar [4]. For comparison, styrene $T_b=145^{\circ}\text{C}$, $T_m=-31^{\circ}\text{C}$, $T_c=374^{\circ}\text{C}$, $P_c=39.9$ bar. Over this critical point in pressure and temperature, ethylene is a supercritical fluid (Figure 2).

In standard polymerization conditions, a gas or a supercritical fluid has to be manipulated, thus autoclaves techniques are mandatory.

As polymerization involves a non liquid monomer, most of the usual techniques to follow the reaction profile are unadapted. For example in a stainless reactor under 100 bar of ethylene pressure, withdrawal of a sample is not an easy task.

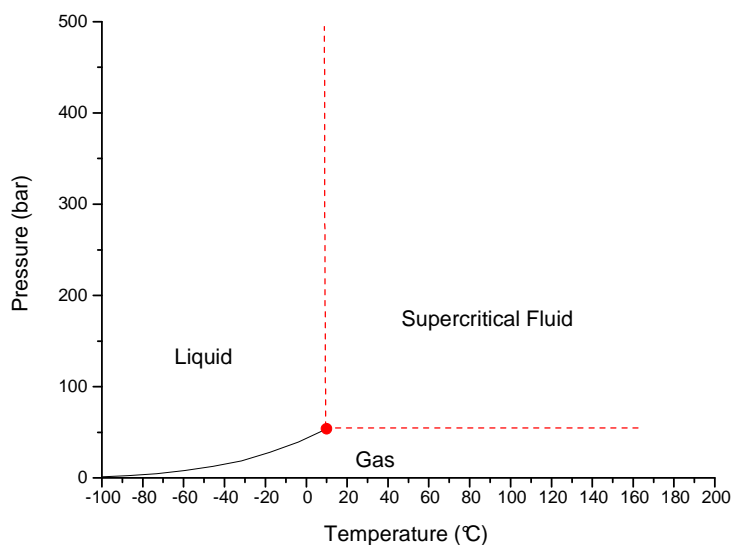


Figure 2. Phase diagram of ethylene

a) Supercritical fluids

Ethylene under standard polymerization conditions over 50 bar and 9°C is a supercritical fluid. This phase induces some specificities. Lot of pressurized gases are in fact supercritical fluids, such as CO₂ (T_c=31°C, P_c=73.8 bar), N₂ (T_c=-150°C, P_c=33.9 bar), O₂ (T_c=-118.5°C, P_c=50.4 bar), Ar (T_c=-122.3°C, P_c=48.7 bar), He (T_c=-269.1°C, P_c=1.1 bar) and also gaseous monomers such as propylene (T_c=91.7°C, P_c=46 bar) [4].

Supercritical fluids have properties between these of a gas and a liquid. In addition, there is no surface tension in a supercritical fluid, as there is no liquid/gas phase boundary. By changing the pressure and the temperature of the fluid, the properties can be “tuned” to be more liquid- or more gas-like. In first approximation, the liquid-gas phase transition can be extrapolated over the critical point. Below this curve, supercritical fluid is gas-like and over liquid-like.

One of the most important properties of a supercritical fluid is the solubility of material in the fluid. Indeed supercritical fluids have high solvation ability due to the prefer interaction with any other molecules than itself. Solubility in a supercritical fluid tends to increase with the density of the fluid (at constant temperature). Since density increases with pressure, solubility tends to increase with pressure. The relation with temperature is a little more complicated. At constant density, solubility will increase with temperature. The high solubility of compounds in a supercritical fluids and the easiness to remove the fluid explain the great interest about extraction via supercritical CO₂.

All supercritical fluids are completely miscible with each other. So for a mixture, a single phase can be guaranteed if the critical point of the mixture is exceeded. (It should be noted this principle originates the extraction of impurities by supercritical fluids). The critical point of a binary mixture can be estimated as the arithmetic mean of the critical temperatures and pressures of the two components, $Y_{c_{mix}} = x_a Y_{c_a} + x_b Y_{c_b}$, where x is the molar ratio and Y_c the critical temperature or pressure. For greater accuracy, the critical point can be calculated using equations of state (EoS), such as the Peng-Robinson equation, or group contribution methods. Other properties, such as density, can also be calculated using equations of state.

b) Potential medium of polymerization

For ethylene, this supercritical behavior means that the polymerization could take place in several media:

- Without diluent

1. Bulk polymerization in liquid phase:

If polymerization temperature is below 9°C and pressure over the gas-liquid phase transition.

2. Bulk polymerization in gaseous phase:

If polymerization pressure is below 50 bar and temperature over the gas-liquid phase transition.

3. Bulk polymerization in supercritical phase:

If polymerization pressure and temperature are over the critical point $T_c=9.2^\circ\text{C}$ and $P_c=50.4$ bar.

- With diluent

4. Slurry polymerization in diluent:

If polymerization pressure or temperature are below the critical point of the mixture ethylene-diluent then two phases exist. In this case, the polymerization will take place in the diluent, where some ethylene is dissolved. This is the polymerization medium of most of academics studies on the catalytic polymerization of ethylene. Ethylene phase can be gaseous or supercritical.

5. Homogeneous supercritical mixture polymerization

If polymerization pressure and temperature are over the critical point of the mixture ethylene-diluent. This is the case of some industrial process to synthesize LDPE.

6. Homogeneous gaseous or liquid mixture polymerization.

Homogeneous gaseous medium could exist with low boiling point and critical point mixture. Homogeneous liquid could also exist if the polymerization takes place below 9°C and at pressure over the gas-liquid transition.

One other important parameter is the solubility of the synthesized polyethylene. In slurry conditions PE always precipitates (due to the chain crystallization) during the polymerization except when highly branched PE is synthesized or with low molecular weight PE. For unique phase conditions, PE can precipitate during the polymerization or remain soluble in the liquid phase. We will call this system respectively heterogeneous and homogeneous system. PE has exactly the same effect as a normal diluent on the mixture. To estimate the critical parameters of PE, we could extrapolate T_c and P_c from heavy series of alkanes (see Figure 3).

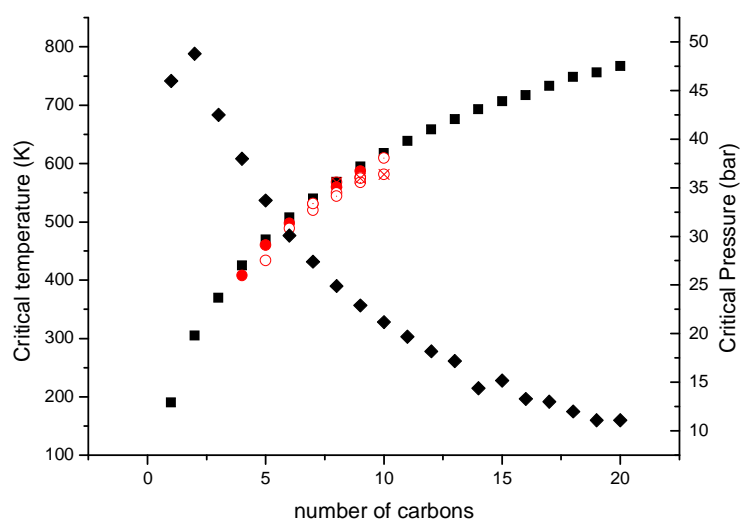


Figure 3. Critical parameters of alkanes $H(CH_2)_nH$; ■ linear alkanes critical temperature, ◆ linear alkane critical pressure, ●○○⊗ methyl alkanes critical temperature with respectively 1,2,3,4 methyl branches

From this data it has been extrapolated [5] that linear PE exhibits a virtual critical temperature of 1050 K. As shown in Figure 3, branches induce lower critical temperature thus homogeneity of the reaction medium will be easier with branched PE than linear one. Extrapolation of 2-methyl-n-alkane gives 950K [5] as result, 100K less than the linear one. These extremely high critical temperatures induce a high cloud point (over the cloud point, system is homogeneous (PE soluble in ethylene), below it is heterogeneous). Theoretical determination of cloud point is less easy because PE is a large entity and interacts with several ethylenes or diluents molecules. Consequently Van der Waals type of equation of states (EoS) cannot be used because they only consider interaction between 2 molecules. Much more complex EoS are used such as Span-Wagner or PC-SAFT (Perturbed-Chain Statistical Associating Fluid Theory) which include multiple points interaction [6-8].

In the standard ethylene free radical polymerization at high pressure and temperature PE is soluble in the supercritical phase, otherwise at lower pressure and/or temperature PE usually precipitates except with highly branched PE and/or low molecular weight PE.

c) Heat capacity

One of the most important parameters to control during the polymerization is the exothermicity of the reaction. In bulk polymerization, heat capacity of the monomer has to be significant compared to heat of polymerization. For ethylene, the heat of polymerization is very high 100 kJ/mol, for a comparison heat of styrene polymerization is only 70 kJ/mol [9]. Moreover heat capacity of ethylene (≈ 50 J/mol/°C at 100°C) is very low compared to styrene (≈ 200 J/mol/°C at 100°C, Figure 4, data from [10] and [4]).

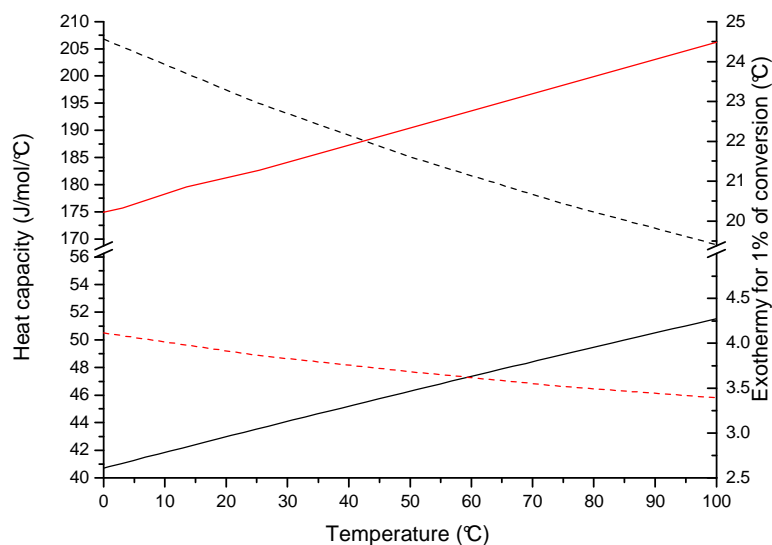


**Figure 4. Heat capacity vs. temperature; — ethylene vs. — styrene
Reactor temperature rises for each percent of conversion if none of the heat of polymerization is removed; -- ethylene, -- styrene**

Consequently if none of the heat of polymerization is removed, the increase of the reactor temperature during the polymerization will be much higher with ethylene than with styrene. For each percent of conversion the temperature of the reactor will rise of 23°C (only 3°C for styrene polymerization) if polymerization takes place at ambient temperature, 16°C at 200°C, and 13°C at 400°C. From another point of view, the adiabatic reactor temperature will rise from 20°C to 400°C with only 23% of ethylene conversion, only by heat of polymerization.

The heat of polymerization of ethylene is a drastic problem and has to be removed to control the polymerization. One of the solutions is to use diluents with high heat capacities such as heptane 2.23 kJ/kg/°C, toluene 1.71 kJ/kg/°C, tetrahydrofuran (THF) 1.72 kJ/kg/°C, diethyl carbonate (DEC) 1.81 kJ/kg/°C and water 4.17 kJ/kg/°C at 25°C [11].

Another important issue is to evacuate this heat. It is made through the reactor design which optimizes the heat transfer. This is a non trivial problem because reactors also have to resist to the ethylene pressure. Large reactor walls solve this pressure issue, but lead to adiabatic processes. This issue has been solved using loop reaction in tubular reactor filled with fluidized bed instead of batch reactor.

At the light of all these parameters, we understand the difficulty to provide a polymerization of ethylene at high pressure and temperature in safe conditions.

B. Homopolymerization of ethylene

In this section, we will focus on the polyethylene synthesis. Seminal papers on polyethylene synthesis will be first discussed; previous to the discovery of chemists at Imperial Chemical Industries (ICI) for the free radical polymerization and the discovery of Ziegler and Natta or Phillips for the catalytic polymerization. Then the research on the free radical polymerization of ethylene will be described, and finally the research on the catalytic polymerization.

1. The different potential mechanisms of ethylene polymerization

Theoretically, ethylene can be polymerized by four different chain polyaddition mechanisms: cationic, anionic, radical, and catalytic. The difficulty for all these mechanisms is that the active species (radical, cation, anion, metal carbon bond) are unstabilized and therefore highly reactive. Consequently, any inhibitor will have a dramatic effect on the ethylene polymerization.

a) Cationic polymerization

Many early works claim a cationic polymerization of ethylene thanks to strong Lewis acid (i.e. BF_3 , AlCl_3) [12-17], nevertheless no recent one describes this kind of polymerization and so these results may be catalytic polymerization misinterpreted, or a radical polymerization activated by Lewis acid. Moreover, primary carbocation undergoes multiple rearrangement reactions and elimination reactions. Consequently, cationic polymerization of ethylene appears highly improbable.

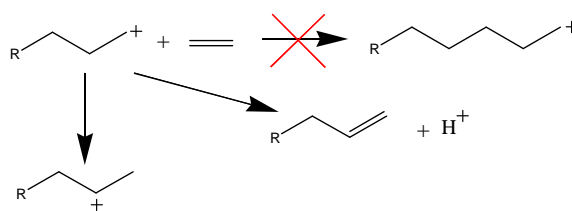


Figure 5. Cationic reaction with a 1-alkyl carbocation

b) Anionic polymerization

Anionic polymerization of ethylene is a mechanism proposed in the oligomerization of ethylene by “Aufbau reaction” [18, 19]. This reaction was discovered by Ziegler et al. and prefigured the discovery of the Ni effect.

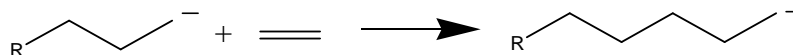


Figure 6. Propagation reaction in an anionic polymerization of ethylene

c) Radical polymerization

Radical polymerization is one of the two major mechanisms of polymerization of ethylene. Usually it provides branched PE. Industrial processes involve high temperatures ($T > 100^\circ\text{C}$) and high pressures ($P > 1000$ bar), which imply that it is difficult to conduct academics studies in such conditions. As for the cationic intermediate, 1-alkyl radical will surely undergo lot of different rearrangements.

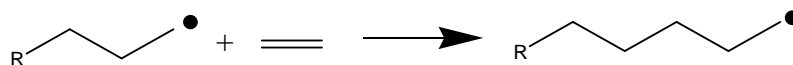


Figure 7. Propagation reaction in a radical polymerization of ethylene

d) Catalytic polymerization

Catalytic polymerization of ethylene provides vast ranges of PE from HDPE to VLDPE. Many research groups study this reaction academically and especially develop new catalysts or catalyst activators. Usually the reaction conditions are low temperature ($T < 100^\circ\text{C}$) and low pressure ($P < 50$ bar).

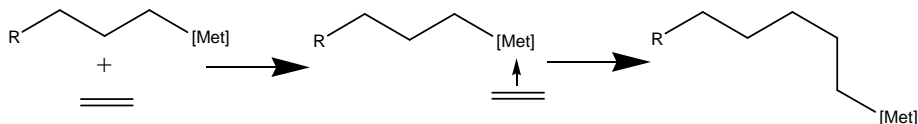


Figure 8. Coordination-insertion during a catalytic polymerization

2. Early works on synthesis of polyethylene

Previously to the initial discovery of chemists of ICI ethylene was usually described as a non-polymerizable monomer. Nevertheless, some groups tried to polymerize it using different pathways, in various experimental conditions, in order to obtain long chain alkanes which have many commercial applications. These tryouts did not yield polyethylenes of high molecular weight but only oligomers of ethylene.

a) Polyethylene synthesis without ethylene

Historically, the first synthesis of a high molecular weight hydrocarbon was probably polymethylene, produced from the decomposition of diazomethane accidentally in 1889 by von Pechmann [20] and understood in 1900 by Bamberger and Tschirner [21]. Later, polymethylenes of high molecular weight were prepared with high melting point ($M_w = 3 \cdot 10^6$ mol/g $T_m = 132^\circ\text{C}$) [22]. Some other polymers containing alkyl substituent were

also obtained by the same system [23]. This type of polymers is still used as model of polyolefins (equivalents of polypropylene, polyisobutene have been also synthesized).

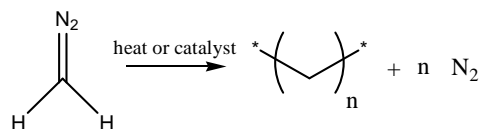


Figure 9. Polymethylene synthesis from diazomethane

The first LDPE must be the white solid obtained by Ling and Glockler [24] in 1929 by submitting ethane to a semi corona discharge. The waxy solid obtained was the first example of long alkane chains with various branches.

Fischer-Tropsch [25] reduction of carbon oxide by hydrogen discovered in the 1920s allows the production of hydrocarbon. By adjusting the process, the production of waxes up to 2000 g/mol was reported as early as 1935 [26]. Later, DuPont [27] reported the production of linear PE with average molecular weights as high as 9000 g/mol using a tungstite catalyst.

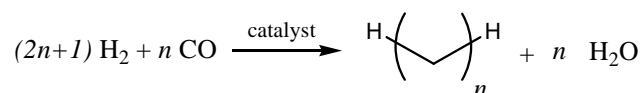


Figure 10. Fischer-Tropsch reaction yielding to hydrocarbons

Carothers [28] produced polymethylene by the condensation of decamethylene bromide with molecular weight up to 1000 g/mol. Finally, polyethylene can also be obtained by dehalogenation of polyvinyl chloride by lithium hydride [29]. (It should be noted that hydrogenated polybutadiene can also be considered as a polyethylene containing ethyl branches, and often use as model of branch PE, see Annex I).

b) Paraffin synthesis via ethylene

Oligomerization of ethylene was already well known before 1933. Some of these works were directed to produced gasoline or lubricants. But until 1933 no molecular weights over 6000 g/mol were reported.

(1) Ethylene decomposition

Oligoethylenes were produced as early as 1886 [30] by decomposition of ethylene under very high temperature (700°C) [31, 32] at low-pressure (10 bar). The products obtained were hydrocarbons of low molecular weights. The explosive decomposition and polymerization of ethylene to oils at 50 bar and 380°C was also reported [33]. This method only yields oligomers with maximum molecular weights of 500 g/mol.

(2) *Anionic polymerization of ethylene*

In 1930, Friedrich and Marvel reported the polymerization of ethylene to a “non-gaseous” product by the action of alkyl lithium [34]. In the same year, Carothers reported also the polymerization of ethylene by the action of sodium [35]. The maximum weight of the waxes obtained was approximately 1500 g/mol.

(3) *Polymerization of ethylene assisted by Lewis acid*

As early as 1927 ethylene and its analogues had been converted to oils by boron fluoride catalysts with cobalt as promoter [36], boron fluoride with hydrogen fluoride was also used [12]. Liquid mixtures of open-chain, cyclic, and aromatic hydrocarbons were formed by polymerizing ethylene at high pressures in the presence of phosphoric acid, anhydride, aluminum chloride, nickel or titanate acid at temperatures up to 800°C. [13-17]. The mechanism due to the method available at this time stays unknown but authors hypothesized a cationic one. However, we can also hypothesize a radical polymerization activated by strong Lewis acid or a catalytic polymerization. The cationic polymerization can also be a possibility but no cationic polymerizations were described up to now and must be improbable due to the extremely unstable carbocation involved.

(4) *Radical polymerization of ethylene*

Several papers were published on the polymerization of ethylene by free-radical initiation [37], particularly using biacetyl [38], ethylene oxide [39], methyl radicals [40, 41], and tetraethyl lead [42] under temperature over 300°C. All these methods produced only waxes ($M_n < 5000$ g/mol).

(5) *Irradiation polymerization*

McDonald and Norrish [43] discovered in 1936 that when ethylene was irradiated at pressures below 0.01 bar with light from a hydrogen discharge tube a solid polymer was deposited. This discovery initiated lot of works on photopolymerization of ethylene, in particular using acetone, mercury, cadmium, and zinc as photosensitizers [44-50].

(6) *Catalytic polymerization*

Catalytic polymerization at low pressures with cobalt and iron catalysts containing promoters was investigated at an early date [51-56], but the results were very poor and the products were of low molecular weight. Experiments at pressures up to 1800 bar gave no better result.

3. Free radical homopolymerization of ethylene

In the early 1930s the British company Imperial Chemical Industries established a research program with the goal of investigating the high pressure chemistry of selected organic compounds, including ethylene. On 29 March 1933, Eric Fawcett and Reginald Gibbon were investigating the high pressure reaction of ethylene with benzaldehyde. After an experiment that failed in its intended purpose (the benzaldehyde having been recovered unchanged) a sub gram quantity of a white waxy solid was found lining the vessel. The product was correctly identified as a polymer of ethylene. This reaction was not reproducible, and attempts to repeat it sometimes led to uncontrollable exothermic reactions with accompanying excessive pressure that damaged equipment. It was only in December 1935 that Michael Perrin established a set of conditions that could be used to polymerize ethylene consistently. The key to reproducibility laid in the contamination of the ethylene by traces of oxygen. Oxygen reacted with ethylene to produce peroxides that subsequently decomposed to create free radicals that initiated the polymerization of ethylene. The polyethylene made by Perrin et al. was a ductile material with a melting temperature of about 115°C. This material was what we know today as LDPE.

The seminal patent [57] broadly covered polymers consisting essentially of $-\text{CH}_2-$ groups, melting in the range 100-120°C, and having a molecular weights above 6000 g/mol. Solid polymers are obtained by mixing ethylene with approximately 0.01-0.05 % of oxygen, compressing the mixture to at least 500 bar, and heating in a well-stirred autoclave at 200°C or above. It is of the highest importance that the incoming ethylene steam was free from impurities, particularly acetylene. Usually the amount of oxygen is controlled by reducing the oxygen content of the incoming ethylene to 0.0001 % and adding the required amount of oxygen afterwards

a) Study of the high pressure and high temperature process

It was found out [58] that increasing the ethylene pressure lead to increase the molecular weight of the product and to accelerate the polymerization, and that increasing the temperature leads to accelerate the polymerization but gave a product of lower molecular weight and density (Figure 11). Increasing the oxygen quantity also reduced the molecular weight. The optimum conditions were difficult to define, but seemed to be 1500 bar, 0.03-0.1 % oxygen, and a temperature of 190-210°C. All of these results are summarized in the following figure.

One last point to highlight is the haze issue. Haze was found to decrease with pressure and increase with temperature. The processes have to minimize the haze in order to prevent the obstruction of the reactor.

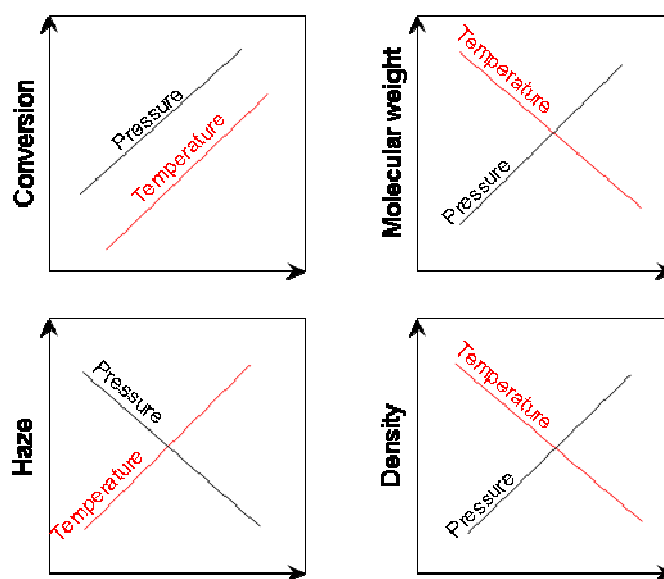


Figure 11. Schematic representation of process variable vs. product properties (variations are not necessarily linear)

b) Towards linear polyethylene at high pressure, low temperature

Density, thus inversely branching degree, decreases with temperature and increases with pressure. Consequently, some research groups attempted polymerization of ethylene under very high pressure and low temperature in order to synthesize linear PE.

As early as 1957 DuPont [59] discovered that ethylene radical polymerization under very high pressure (over 5000 bar) and low temperature (60°C) provides linear polyethylene. PE synthesized exhibit a melting point of 132°C with a density of 0.955, M_w over 100000 g/mol, and branching degree is below 1 branch per 1000C. At this early date, even catalytic polymerization recently discovered did not provide such linear polyethylenes.

Linear polymers, synthesized by free radical polymerization, were rediscovered in 2001 by Bini et al. [60] at ambient temperature under laser irradiation with similar results.

Under these extreme experimental conditions ethylene is close to a liquid phase behavior, consequently polymerization is extremely sensitive to exothermicity. Moreover, to provide this range of pressure, pistons need to be used. All these specifications explain why this procedure does not eclipse the catalytic polymerization, and has never been developed industrially.

c) Addition of diluents at high pressure and at high temperature

Since rapid heat transfer is a critical factor to obtain a controllable radical polymerization, diluents [61] have been used such as cracking still gases[58], aromatic solvents (benzene...) [62], alcohols [63], water, halogenobenzenes [64], ammonia [65], alkanes. All these diluents provide a better control of the reaction exothermicity and allow the functionalization by chain transfer to the diluents.

Machi et al also polymerized ethylene via γ rays radiation or thermal radical initiator in supercritical carbon dioxide [66, 67]. These experiments were initially designed in order to copolymerize ethylene with carbon dioxide, but only LDPE was obtained, no ethylene-CO₂ copolymerization was reported.

d) Polymerization of ethylene in emulsion

As early as 1944 [68-76] polymerizations in water were performed. Some of these works provided stable PE latexes. At this date only potassium persulfate (KPS) as water soluble initiator was known. Surprisingly the formation of PE latex was only obtained by controlling pH either over 11 [77, 78] or below 4 [79]. Control of pH at 2-4 with hydrogen chloride gave a shorter induction period, high intrinsic viscosity, and an improved yield compared to alkaline polymerization. Machi et al. [76] studied this emulsion by γ -rays initiation and also obtained latexes.

As dynamic light scattering (DLS) did not exist then the average diameters of particles could not be measured. Nevertheless, Kern et al. [68] referred to blueish latex therefore we can hypothesize that PE particles could have been quite small (20 nm).

Pressure conditions for polymerizations were usually over 1000 bar except for Machi's work in which pressure between 100 bar and 500 bar were used. Temperatures of polymerization were usually up to 200°C.

It should be noted that other works were performed in a supercritical homogeneous mixture of ethylene and water in order to produce high molecular weight alcohols.

e) Process at low pressure and low temperature with diluent

Since the initial disclosure of the ethylene radical polymerization, research groups all around the world have tried to bypass the initial patent [57], by trying to polymerize ethylene at pressure under 500 bar and temperature below 100°C.

(1) In single supercritical phase

In single supercritical phase, two major pathways were studied in order to induce an ethylene initiation under low temperature: initiation by a low temperature radical initiator (AIBN [80-82]), or initiation via radiation (γ -rays [83-90], or photo-polymerization [91]).

As it has been demonstrated [92] solubility of materials in supercritical fluids, is usually far greater than their vapor pressure exerted by the mixture even for solids. Therefore, the small amounts of initiator used can be expected to be soluble in ethylene supercritical phase. For polyethylene, calculations indicate that PE precipitated during the polymerization.

These kinds of polymerizations provided PE with lower yield than the industrial process which explains why these works were abandoned. One of the most surprising points developed in this supercritical monophasic heterogeneous condition is the hypothesis of a “living radical polymerization” as early as 1962 [82, 90, 93]. Evidence of a long-life alkyl radical has been proposed. Indeed, the crystallinity of the growing radical will drastically reduce the termination rate; therefore will increase its lifetime (see Figure 12). However, it is not yet a controlled radical polymerization due to the importance of transfer to the polymer.

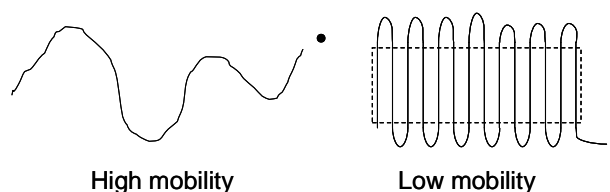


Figure 12. Schematic interpretation of long life time of a crystalline growing PE radical

(2) In diluents phase

Similar conditions of polymerization were applied with diluents [80, 82, 94-97].

In this case the polymerization media is a unique supercritical phase or a supercritical ethylene phase over the diluent liquid phase where some ethylene is dissolved (such as in the standard catalytic ethylene polymerization process). In the last case, initiator is nearly entirely dissolved in the liquid phase. To the best of our knowledge, ethylene-benzene [98] was the only system where the transition between the supercritical unique phase of the mixture ethylene/diluent and the biphasic medium was studied.

Khomiskovskii, Myshin and Machi observed that this polymerization is strongly dependent of the solvent. Khomiskovskii [99] was the first to report a solvent effect on the radical polymerization of ethylene. Myshkin [100] found a relation between solvent

permittivity and yield ($\ln k_p$ linearly decreases with $1/\epsilon_r$). Machi [97] hypothesized that solubility of polyethylene is a crucial factor (yield increases from good PE solvents to bad solvents).

f) Activation of the ethylene radical polymerization by Lewis acid

As radical polymerization of ethylene was inefficient under low pressure ($P < 100$ bar), some authors proposed to activate ethylene by strong Lewis acid (alkyl aluminum) [101, 102]. In these conditions, they managed the oligomerization of ethylene down to 50 bar of ethylene pressure.

The Lewis acid will activate the double bond of ethylene in order to drastically decrease the activation energy (see Figure 13).

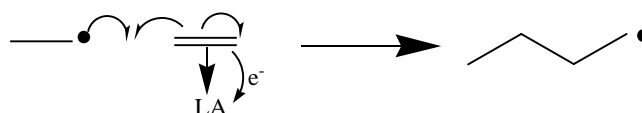


Figure 13. Activated radical polymerization of ethylene by Lewis acid

Recently, Russian and Michl [103, 104] succeeded in polymerizing ethylene respectively down to 10 bar and 1 bar, thanks to extremely strong Lewis acid (respectively TiBA with $Zr(Et)_4$ or $TiCl_3Me$ and for Michl a naked Li^+ ; $LiCB_{11}(CH_3)_{12}$). The maximum degree of polymerization by weight average (DPw) was 70. However, these strong Lewis acids induced low activities and are expensive which prohibits any further industrial use.

g) Polymerization in liquid ethylene

Some works [83, 105] in the 60s were performed in liquid ethylene at very low temperature. These studies were done especially to understand the mechanism and kinetic of ethylene free radical polymerization. As ethylene is liquid under these conditions, standard equipments for the polymerization of monomer can be used. At these low temperatures kinetics of polymerization are extremely slow and only polymers of low molar masses are obtained.

h) Polymerization in gaseous ethylene

Polymerization of gaseous ethylene was also studied, especially with irradiation initiation [43]. Nevertheless, polymerization is extremely inefficient and leads to very low molecular weights highly branched PE [106]. These polymerizations remain a laboratory curiosity.

4. Kinetic studies of the free radical ethylene polymerization

In this section, we will review some results on the kinetic of ethylene free radical polymerization and transfer reactions.

a) Elementary steps of reaction

The free radical polymerization of ethylene displays most of the typical characteristics of a vinyl monomer polymerization. Purposely omitting the initiation, which is probably identical to that in vinyl polymerization with typical peroxide and azo initiators, and poorly understood with oxygen, the main reaction steps are summarized in the following figure.

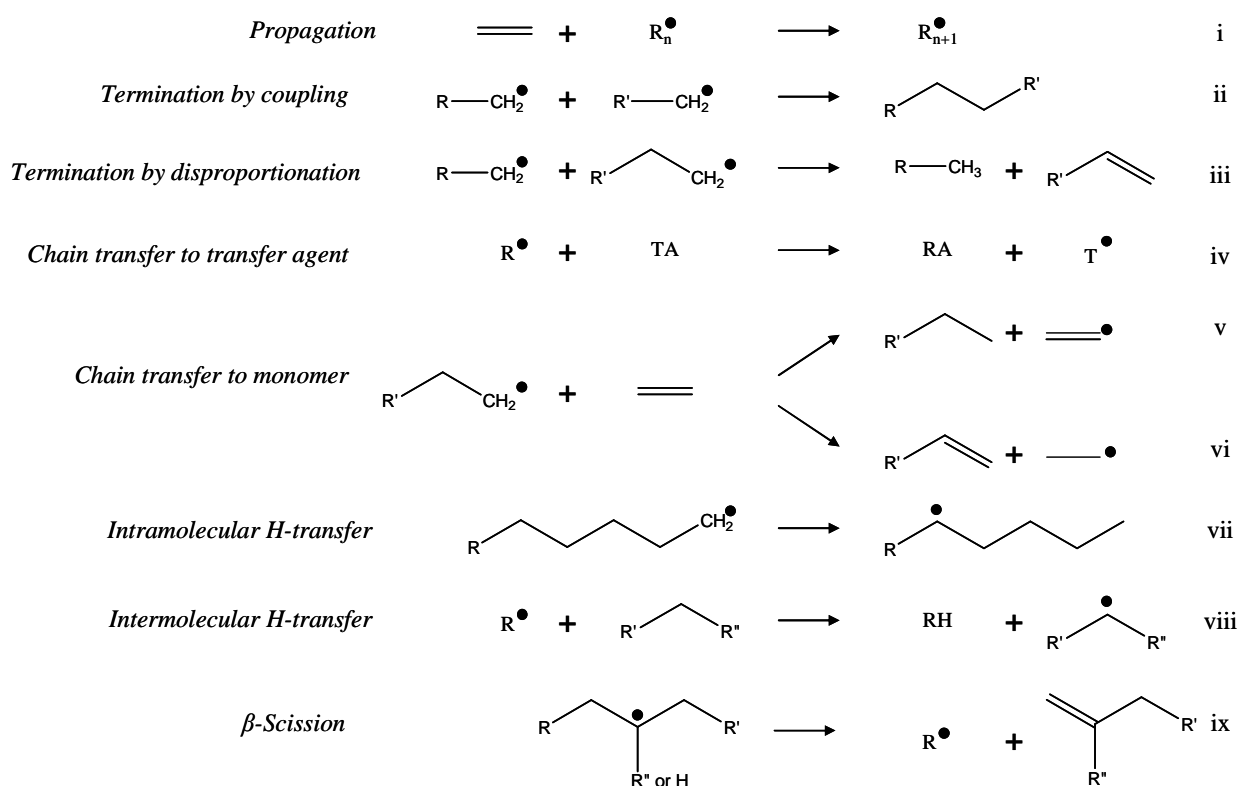


Figure 14. Elementary reaction steps of ethylene radical polymerization

Not all these reactions take place under a given set of experimental conditions. For example reactions iii, v and vi appear to be negligible, excepted at temperatures above 200°C. Reaction vii to ix explain the branched microstructure of the polyethylene: vii induces short chain branches (SCB, mostly butyl), viii long chain branches (LCB).

b) Propagation and termination rate constants

Determination of kinetic constants of ethylene free radical polymerization is a challenge due to the experimental conditions where ethylene polymerization takes place (supercritical fluids at high pressures and high temperatures). Most of the studies allow only

the determination of $k_p k_t^{-1/2}$ [107]. Only Luft [108] and more recently Buback [109] managed to use pulsed laser polymerization (PLP) to measure the propagation rate constant (k_p) and the termination rate constant (k_t) in the experimental conditions of the industrial process.

(1) *Effect of ethylene pressure on the polymerization*

$k_p k_t^{-1/2}$ increases with pressure (see Table 3) due to a negative value of the activation volume $\Delta V_{\ddagger}^{\circ}$. For example at 129°C in bulk, Ehrlich [110] calculated a value of -23 cm³/mol between 750 bar and 2500 bar. Some research groups calculated this factor in presence of benzene at 50-70°C between 3000 and 7600 bar and found very low values of -3 to -6 cm³/mol [111]. The interpretation of these results remain unclear however it is conceivable that polymerization in the liquid-like phase (supercritical fluid close to liquid behavior) in which polymer is virtually insoluble would indeed be associated with much smaller pressure coefficient and lower polymerization rates. Consequently in all cases rate of $k_p k_t^{-1/2}$ decreases when the pressure drops, so low-pressure polymerization will lead to oligomerization of ethylene.

Table 3. Values of $k_p k_t^{-1/2}$ at 129°C and at various pressures [110]

Pressure (bar)	$k_p k_t^{-1/2}$ (mol ^{-1/2} s ^{-1/2})
750	0.22
1000	0.30
1500	0.40
2000	0.54
2500	0.73

(2) *Effect of the temperature on the polymerization*

$k_p k_t^{-1/2}$ also drastically decreases with the temperature (see Table 4), consequently polymerization at low temperature usually leads to an oligomerization of ethylene. In order to confront different values, $k_p k_t^{-1/2}$ is extrapolated to 1 bar. Consequently, the activation volume effect is nullified and only the activation energy effect explains the variation of $k_p k_t^{-1/2}$.

Table 4. Values of $k_p k_t^{1/2}$ at different temperatures, extrapolated to 1 bar [107]

Temperature (°C)	$k_p k_t^{-1/2}$ (mol ^{-1/2} s ^{-1/2})
250	1.7
129	0.17
83	0.015
-20	0.009

Consequently if we do not consider the point in liquid ethylene, we can calculate the global Arrhenius parameters ($E_p - 1/2E_t = 43$ kJ/mol and $\ln(A_p A_t^{-1/2}) = 10.5$). This activation energy value is quite different from the one generally admitted in the standard ethylene free radical polymerization conditions of 30 kJ/mol [107]. It is partly due to the fact that the activation energy value is calculated at the pressure of polymerization without subtracting the activation volume effect.

(3) *Determination of separate values of k_p and k_t*

Luft [108] used pulsed laser polymerization (PLP) to measure k_p and k_t (see Table 5) but only at low pressure (up to 180 bar) and high temperature (132°C). As expected k_t drastically increases when the pressure decreases, and k_p increases with the pressure.

Table 5. Values of k_p and k_t at 132°C under various pressures [108]

Pressure (bar)	k_p (mol ⁻¹ .s ⁻¹)	k_t (10 ⁻⁶ mol ⁻¹ .s ⁻¹)
50	1200	1730
100	1800	580
150	2600	480
180	5400	400

Buback [109] also fully studied the propagation and termination rate by PLP between 190-230°C and 1950-2900 bar. He demonstrated that as for other radical polymerizations k_p and k_t are conversion dependent (see Figure 15).

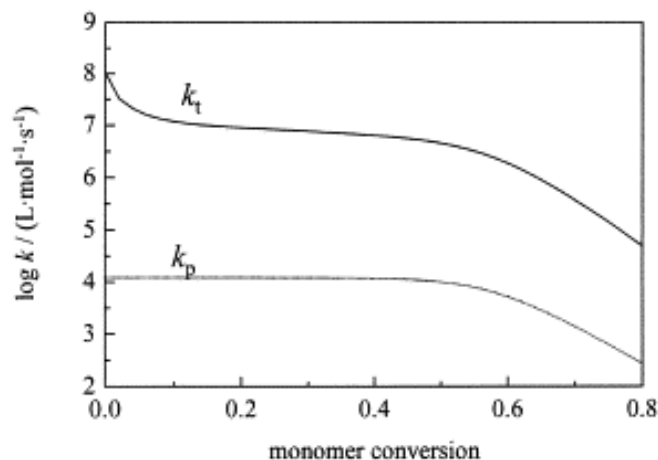


Figure 15. Variation of k_t and k_p with monomer conversion for ethylene polymerization at 230°C and 2500 bar from [109]

Buback summarized PLP experiments by the following equations valid between 190-230°C and 1950-2900 bar:

$$k_p = \frac{k_p^0}{1 + \frac{k_p^0}{1.13 \cdot 10^{10}} \eta_r}$$

$$k_p^0 = 1.88 \cdot 10^7 \exp\left(\frac{-4126 + 0.33P}{T}\right)$$

$$k_t = \left(0.832 \frac{1}{\eta_r} + 8.04 \cdot 10^{-6} (1-x) \frac{k_t^0}{1 + \frac{k_t^0}{1.13 \cdot 10^{10}} \eta_r} \right) k_t^0$$

$$k_t^0 = 8.11 \cdot 10^8 \exp\left(\frac{-553 - 0.190P}{T}\right)$$

Where k_p^0 and k_t^0 are respectively the initial propagation and termination rate, η_r the relative viscosity of the polymerization medium (also dependent of the monomer conversion), x is the monomer conversion and P the pressure in bar and T the temperature in K.

The activation energy for the propagation is 34.3 kJ/mol. The high value of E_a is due to the fact that ethylene double bond is not activated (for styrene 31.5 kJ/mol and MMA 22.4 kJ/mol).

Prior to these works, some research groups calculated by means of sector techniques the kinetics data at low temperature (see Table 6). For sector technique experiment, a liquid phase is mandatory so only slurry conditions of polymerization and liquid ethylene polymerization can be studied.

Table 6. Values of k_p and k_t measured by rotating sector techniques [107].

Temperature (°C)	k_p (mol.s)	k_t (10^{-6} mol.s)
132*	1200	1730
83	470	1050
-20	190	460

*: data obtained by PLP from Luft data [108]

Both kinetic constants decrease with the temperature as expected.

All these data show that the free radical polymerization of ethylene is only efficient to produce high molecular weights polymers under high pressure and high temperature. Under mild conditions, this will lead to an oligomerization of ethylene.

c) Initiation of the polymerization

(1) By Oxygen

Dioxygen is classically considered as an inhibitor of vinyl monomers polymerization carried out below 100-150°C. This explains why the action of oxygen as initiator of free radical polymerization had not been studied in detail prior to the extensive commercial use of high-pressure polyethylene processes. Some of the kinetic peculiarities associated with the initiating (as well as inhibiting) action of oxygen at temperature above 100°C were defined by Ehrlich and co-workers [112-114]. Several rather striking phenomena testified that, even when ethylene and oxygen were reacting isothermally in a well-stirred batch reactor, a steady-state free radical concentration could not be maintained. There was found to exist a sharply defined range of conditions depending, at given temperature, on pressure and oxygen concentration called “critical polymerization boundary” (see Figure 16). It separates a region of negligible polymerization rate from one in which polymerization is so rapid that, under some conditions, isothermal conditions could be barely maintained. This rapid polymerization

was preceded by a well-defined induction period which depended on pressure, the initial oxygen concentration and on temperature. Finally, it was found that the isothermal rate of oxygen consumption increased with the time, both above and below the critical polymerization boundary and that the major fraction, if not all, of initial oxygen had to be consumed prior to the onset of observable polymerization.

The induction period and its characteristics indicated the non-steady-state formation and destruction of a labile molecular intermediate, acting as polymerization initiator. The critical boundary was reminiscent of the explosion limits, often observed in the oxidation of hydrocarbons (In fact, this boundary is an extrapolation at lower temperature, pressure and oxygen content of the explosion limits of ethylene oxygen mixture). Both series of observation were consistent with viewing the oxygen-initiated polymerization as a “degenerated explosion” [107, 115].

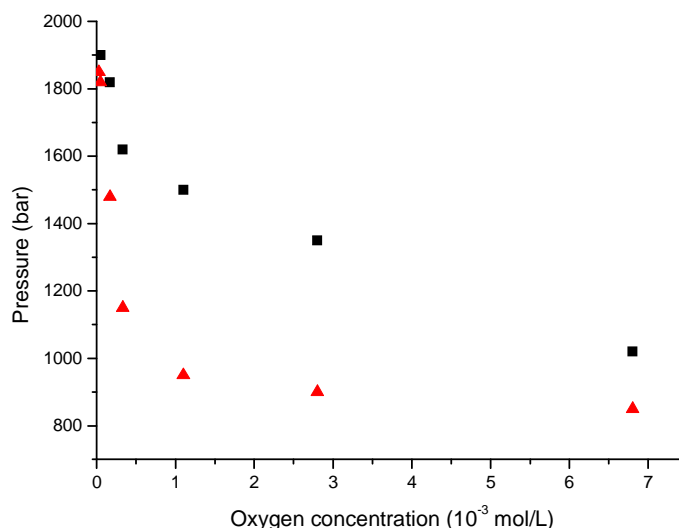


Figure 16. “Critical polymerization boundary” in the oxygen-initiated polymerization; ■ at 130°C, ▲ at 165°C [114]

Data on the duration of the induction period for polymerization, τ , variation on pressure, P , initial oxygen concentration $[O_2]_0$ and on temperature T , were presented by Ehrlich and Pittilo [114]. Their dependency is of the form $\tau = \text{const} \cdot P^{-1} [O_2]_0^{0.23} \exp(130000/RT)$ over pressures from about 700 to 1900 bar, initial oxygen molarities of 0.03 to 40 mol/kg and temperature from 100 to 180°C. The very slight increase of τ with $[O_2]_0$ indicates that an inhibiting effect of oxygen must coexist with its initiating action. The magnitude of the activation energy is consistent with the view that the rate-controlling step is the fission of a peroxide bond ($E_a=132.6\text{kJ/mol}$ for ethyl peroxide

homolytic cleavage). This induction period sets a lower limit on the temperature at which the oxygen-initiated polymerization can normally be initiated in continuous reactors.

The plot of oxygen concentration vs. time was originally reported to be S-shaped (see Figure 17) [114], with the end of induction period corresponding approximately to the inflection point. It appears that the latter part of the oxygen-depletion curve may be an artefact of the experimental procedure. Water and Mortimer [107] found the disappearance of oxygen to accelerate throughout the induction period, and rapid polymerization did not take place until the concentration of free oxygen was undetectable (below 1 ppm).

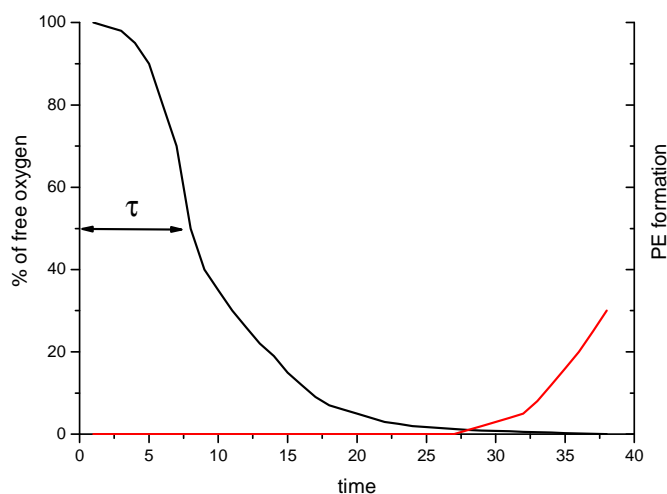


Figure 17. Schematic graphic on oxygen concentration versus PE formation.
—: free dioxygen concentration, —: PE yields

Numerous research groups have found that oxygen copolymerizes with vinyl monomers to give alternate peroxidic copolymers [116-119]. The key reaction steps are the following

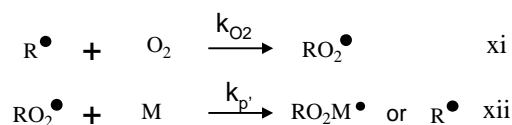


Figure 18. Peroxid formation

When O_2 is present, it competes with monomer for alkyl free radicals. Since k_{O_2} has been found to be in the range of 10^{10} to $10^{11} \text{ L}\cdot\text{mol}^{-1}\cdot\text{s}^{-1}$ where R^\bullet is ethyl radical, it explains why the free oxygen level must be extremely low for normal ethylene polymerization to occur in competition with reaction (xi). If $k_{\text{p}'} \ll k_{\text{p}}$ and the rate-determining step is the decomposition of peroxide linked in the alternating copolymer to generate new free radicals, the inhibiting effect of oxygen can be qualitatively understood [114].

(2) *Organic peroxides, azo initiators*

Organic peroxide and azo compounds are suitable for the initiation of ethylene polymerization. No specific behavior was observed in the initiation of ethylene with this type of initiator compared to another monomer such as styrene. AIBN was especially, in Machi et al studies, used as reference for ethylene polymerization. Initiators usually have low dissociation constants in order to perform the polymerization at high temperature: for example di-t-butyl peroxide $t_{1/2}=10$ h at 126°C.

Nevertheless initiation by peroxide and azo compounds remains an active domain of investigation for the ethylene radical polymerization [120-123]. Especially, very low half-time life initiator ($t_{1/2}<1$ s) and side reactions induced are analyzed intensively. The impacts of multi-initiators like diperoxide are also investigated.

Inorganic peroxides, such as KPS, are used to initiate ethylene polymerization in emulsion process. Surprisingly, results show that this initiation is efficient only in the acidic (below pH 2) [79] or basic range (over pH 10) [68]. Interpretation of this result remains open to discussion, as no initiation seems to take place at pH between 4 and 10.

(3) *Thermal initiation*

Data [107, 112-114] indicate that oxygen can initiate the polymerization of ethylene in trace amounts: even an oxygen concentration corresponding to 2 ppm will initiate polymerization at pressure above 1800 bar. In the course of the same studies, it was found that carefully deoxygenated ethylene did not polymerize under conditions as extreme as 200°C and 2000 bar. All “thermal” initiations at 200°C and at lower temperatures, occasionally reported in the literature, can therefore probably be safely attributed to oxygen. Beside no clear-cut proof of thermal initiation even at higher temperatures appears to have been established.

(4) *Initiation by ionizing radiation*

The γ -rays initiated polymerization of ethylene, under conditions in which high molecular weight polymer was formed, has been intensively studied by several groups of research throughout the world [83, 84, 86-88, 124-128]. The reaction has been carried out over a broad range of temperatures, pressures, and dose rates, sometimes in presence of solvents, and very often near or below room temperature where a separated, virtually pure phase of solid polymer was present. An increase in polymerization rate and in polymer

molecular weight with reaction time in batch systems is often observed under such conditions. Machi and al., among others, observed such effects suggesting that the termination reaction was virtually absent [90], inducing long living radicals. This behavior, which could be interpreted as a controlled radical polymerization, was in fact closer to the living radical polymerization as the radical lifetime is equal to the reaction time. Nevertheless, Munari and Russo [129] suggest that the auto-acceleration is caused by radiation-induced grafting on the precipitated polymer. This conclusion is in agreement with the observation that polyethylene made by radiation initiation at low temperatures often has a high degree of long-chain branching.

The kinetic study indicates that the nature and relative rates of the elementary reaction steps in the γ -rays initiated polymerization of ethylene, with the exception of initiation and occasional presence of radiation grafting, are quite similar to these occurring at similar pressures and temperatures in the course of free radical initiated polymerization.

The mechanism of polymerization using γ -rays initiation has been investigated. Meisels [130] suggested that hydrogen atoms are removed from ethylene by γ -ray energy and subsequently add to monomers to start polymer chains. By studying the initial stages of polymerization, Mitsui [131] found that one mole of acetylene was formed per mole of polymer (termination mode is mostly combination), which would indicate that the initiation reactions for pure ethylene can be written as below.

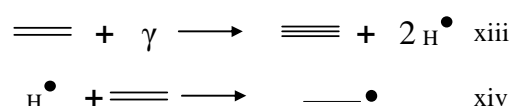


Figure 19. Initiation mechanism of ethylene polymerization under γ -rays

Numerous publications reported the addition of other components which accelerate the polymerization, presumably because they are fragmented by γ -rays energy more easily than ethylene. However, Machi interpreted this as a solvent activation effect of the polymerization [97]. Oxygen was found to inhibit the γ -rays initiated polymerization. Polymerization did take place after an induction period and the polymer was found to contain combined oxygen [131].

d) Chain transfer and microstructures

As it is well known, polyethylene prepared by catalysis such as Ziegler-Natta close to ambient temperature and pressure approaches more closely the ideal linear polymethylene

structure than free-radical polyethylene prepared at pressures over 1000 bar and at temperatures over 100°C. It has been known that most of the branches accounting for such non-linearity are short compared to the backbone chain (mostly ethyl and butyl groups) and that these short branches account for the lower crystallinity, density, melting point, and associated physical properties of commercial “high pressure” polyethylene.

Other structural “defects” known to exist in “high-pressure” polyethylene are vinyl and vinylidene type unsaturation. The former can result from the well-known disproportionation reaction (Figure 14 iii), whereas the latter, which is dominant, has been suggested to result from a chain transfer step associated with the depropagation of a tertiary radical (Figure 14 ix).

Consequently, the major defects in polyethylene appear to result from chain transfer reactions. It is important to understand the dependence of such defects according to polymerization temperature and pressure.

Table 7. Structural defects in various polyethylenes prepared by free radical method (last line corresponds to very high pressure linear radical polyethylene)

CH ₃ /1000C	Vinyl/1000C	Vinylidene/1000C
35	0.07	0.84
20.3	0.07	0.28
14	0.04	0.07
<0.8	<0.01	0.02

(1) *Transfer to transfer agent*

As illustrated (Figure 14 iv) a macroradical can react with a molecule to remove a fragment (A), generally a single atom, and leave the rest of the molecule with an unpaired electron. The kinetic chain is continued, that is no loss of radical occur, but the free radical site is transferred to another molecule. The new free radical can then add monomer, thus perpetuating the propagation reaction and creating a new polymer molecule. The chain transfer constant, C_s , is defined as the ratio of the transfer and propagation reaction rate constants, k_s/k_p . Chain-transfer constant are determinate under carefully controlled conditions in a homogeneous polymerization for a number of compounds [107] (see Table 8).

Table 8. Chain-transfer constant determined at 1360 bar and 130°C during the polymerization of ethylene [107].

Chain-transfer agent	C _s and standard deviation
Methane	0.0000±0.0002
t-Butanol	0.0001±0.0002
Ethane	0.0006±0.0005
Benzene	0.0009±0.0002
DMSO	0.0011±0.0003
Propane	0.00303±0.00007
Ethyl Acetate	0.0045±0.0003
Isobutane	0.0072±0.0003
Ethanol	0.0075±0.0003
n-heptane	0.0080±0.002
Cyclohexane	0.0095±0.0003
Acetonitrile	0.011±0.001
Toluene	0.0154±0.0005
DMF	0.026±0.002
THF	0.0288±0.0006
Dioxane	0.032±0.002
Butanone	0.060±0.005
Chloroform	0.27±0.03

From a study of the chain-transfer values, it is possible to see that the radical reactivity patterns, which are common for alkyl radicals in the gas phase and for radicals in solution, are also found for polyethylene in bulk polymerization. All other things being equal, tertiary hydrogens are abstracted more readily than secondary which in turn are abstracted more readily than primary. Hydrogens atoms activated by halogens, carbonyl, or other activating groups such as vinyl and phenyl are more reactive than hydrogen atoms on paraffins.

The chain-transfer constant is also dependent on pressure and temperature [107]. Most of the C_S seem to be mostly independent on pressure. For temperature dependence, compounds having low chain-transfer constants exhibit high activation energy, and vice-versa.

Chain transfer to monomer, a familiar reaction with other monomers is strikingly small with ethylene (for styrene 10^{-4} and MMA 0.2) [107]. A value of less than $3 \cdot 10^{-5}$ at 130°C has been calculated, assuming all vinyl end groups to be the result of chain transfer. Even at 250°C , the C_S value for ethylene is only $7 \cdot 10^{-5} \pm 2 \cdot 10^{-5}$, if the same assumption is made. Since termination by disproportion and β -scission are also giving rise to vinyl groups, the actual extent of chain transfers to ethylene is even less.

(2) *Short chain branching*

Roedel [132] first proposed an intramolecular chain-transfer or “back-biting” reaction to explain short-chain branches found in polyethylene. The absence of methyl, propyl and pentyl branches indicates great specificity in branch formation. These short chain branches (SCB) consist entirely (within limits of detection) of 2- and 4-carbon unit in length. The radical transfer mechanism for short-chain branching has been questioned by Wickham [133] and Van der Molen [134].

Free radical reactions can be very specific. It is well known that the free radicals are highly reactive intermediates and show limited discrimination between the various types of carbon-hydrogen bonds. This has led to the general feeling that free-radical reactions must be largely random and non-specific in character. This behavior is not in agreement with the regiochemistry observed for the short-chain branches formation. In studies of intramolecular hydrogen abstraction by alkoxy radicals, Walling and Padwa [135] have shown that the free radical abstracts almost exclusively the hydrogen bound to the fifth atom away from the radical site. Therefore, the transition state of the intramolecular hydrogen abstraction is a 6-

membered ring containing 5 chain atoms plus the hydrogen which has to be transferred. It was further shown that 1,5-transfer of unactivated hydrogens took place almost exclusively even when 1,4- or 1,6-hydrogen transfer was chemically favored by the presence of an activating group such as phenyl [136].

The “back-biting” or 1,5-hydrogen transfer mechanism not only accounts for the observed short-chain branching in polyethylene but also suggest an additional structural facet. Short-chain branches probably occur not as isolated branches, randomly spaced along the main chain, but as clusters separate by long linear sequences. If one molecule of ethylene adds after the first “back-bite”, and then a second “back-bite” occurs, two ethyl branches may be formed if it abstracts H of the branch. If the second “back-bite” abstracts H of the main chain, a 2-ethylhexyl branch would be formed (see Figure 20). Willborn [137] identified ethyl and butyl branches by infrared and concluded from a probability treatment that the occurrence of a second “back-bite” soon after the first was indeed likely. Experimental evidence has been presented for multiple “back-bites” and suggested that short-chain branches may be clustered or branched themselves [138-141].

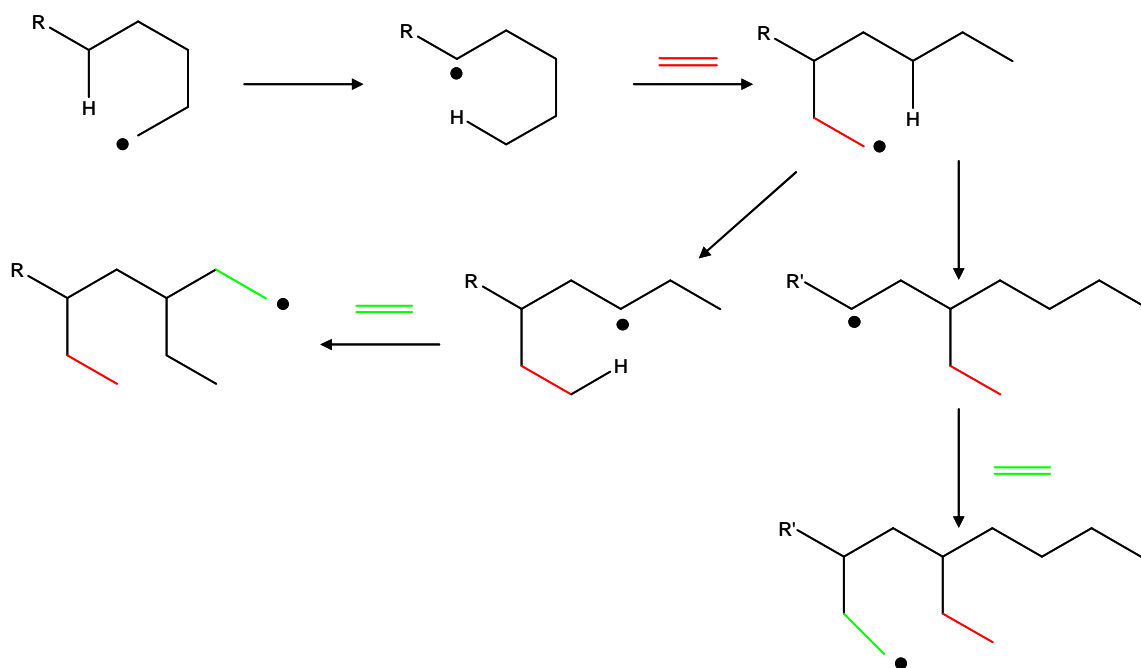


Figure 20. Extended Roedel mechanism

Assuming an intramolecular hydrogen-transfer mechanism for short-chain branching, it would be predicted that the extent of branching should vary as the pressure and temperature are varied, but should be independent of the nature and amount of chain transfer agents, conversion, as well as initiator type and amount. Indeed, all of these predictions have been

verified by monitoring the methyl/methylene ratio (specified $\text{CH}_3/1000\text{C}$) as the above variables have been changed [142-145]. There is general agreement that the $\text{CH}_3/1000\text{C}$ ratio increases with the temperature and drops with the pressure [143, 144, 146]. This observation was relevant with the almost linear polymer [59] formed at very high pressure 5000-7000 bar and low temperature and the very high branches level obtained by Jaacks and Mayo [106] in the gas phase near 1 bar.

(3) *Long chain branching*

Commercial polyethylene made by free radical polymerization always exhibits a broad molecular weight distribution (MWD) (polydispersity index $\text{PDI}=\text{Mn}/\text{Mw}$ over 5). The broad MWD has been attributed to the presence of long branches in the polymer backbone in addition to short ones. Convincing evidence for such long branches was presented by Roedel [132] and by Billmeyer [147].

Long-chain branches (LCB) arise probably from the abstraction by a growing radical of any hydrogen atoms at sites other than these allowing formation of a 6-membered ring. Except in a very dilute solution, a given radical will find a vast majority of such sites on other molecules. Long-chain branching will then be primarily the consequence of an intermolecular hydrogen abstraction (Figure 14 viii), in contrast to short-chain branching which is intramolecular.

Since both long and short branches are formed by abstracting a hydrogen atom from a polymer chain, it is expected and found [148, 149] that there is a high degree of correlation between the amounts of the two types of branching. The rate of formation of both types of branches should be affected similarly by changes in temperature and pressure. Consequently, LCB content decreases with pressure and increases with temperature. However, formation of a 6-membered ring must be highly favored, and this must account for the high concentration of short branches compared to long ones (typically 1 LCB for 20 SCB).

Beasley [150] was the first to attempt a quantitative calculation of the number and weight distribution of long-chain branches. He was able to show that the intermolecular abstraction mechanism could result in a great broadening of the MWD. This effect was shown to increase with the branching index. The mathematical models developed [151] allow to predict the MWD from the long chain branches index.

Some studies [132, 150] show that polymers made at high conversion contained more long chain branches with similar short-chain branches content. Mortimer [107] found an additional method to decrease the long-chain branches by synthesizing polyethylene in heterogeneous conditions (polyethylene precipitates). In this condition, the probability of intermolecular hydrogen abstraction drastically decreases due to the heterogeneity of the system.

(4) *Unsaturation*

Oakes and Richard [152] showed that the thermal degradation of polyethylene near 300°C did not yield monomers, and was associated with an increased vinyl and vinylidene content in the polymer. They suggested that this type of unsaturation resulted from the scission of secondary and tertiary radicals at a carbon-carbon bond located at the β -position (Figure 14 ix).

Since experimental evidence shows a substantial preponderance of vinylidene over vinyl groups [137, 146], the scission of tertiary radicals presumably plays a major role.

The “multiple backbiting” mechanisms, as outlined in the previous section, can lead to a tertiary radical which undergoes β -scission to vinylidene. Low-density polyethylene usually contains 0.1 to 1 vinylidene groups per molecule, and so β -scission of a tertiary radical might be expected to be the dominant mechanism for molecular transfer under some experimental conditions. The low ratio of vinylidene/methyl is consistent with the view that formation of a vinylidene group requires the prior formation of a succession of short-chain branches.

The vinyl contents of free radical polyethylene is usually substantially less than the vinylidene content. This testifies to the relative unimportance of molecular transfer by β -scission of a secondary radical and by chain transfer to monomer. At higher temperatures, however, such processes cannot be ruled out.

5. Catalytic polymerization of ethylene

The first efficient mechanism for ethylene polymerization was the radical pathway ($P > 1000$ bar and $T > 100^\circ\text{C}$). However free radical polymerization of ethylene, as just seen, leads to lot of flaws in the backbone except at very high pressure ($P > 5000$ bar) and low temperature ($T < 100^\circ\text{C}$). This linear polyethylene possesses very interesting properties but the experimental conditions are too severe to be developed as an industrial process. Consequently in order to access linear PE catalytic polymerizations of ethylene have been developed under low pressure ($P < 100$ bar) and low temperature ($T < 100^\circ\text{C}$).

Catalytic polymerization discovered in the early fifties is extensively used in the production of polyolefins; HDPE and LLDPE are produced using Ziegler-Natta [153, 154], Phillips [155] and metallocene catalysts [156]. These catalysts allow a good control of the polymer microstructure, but they are based on early transition metals, (Ti, Zr, Cr and V), which are highly oxophilic, hence interact with any polar function such as polar comonomer. Late transition metals (Ru, Co, Fe, Ni, Pd) are much less oxophilic and therefore they may be used in presence of polar function (solvent or polar monomer). Excellent reviews have been published on the catalytic polymerization of ethylene [157-159]. Only the latest main developments of catalysts for the ethylene polymerization will be reviewed here, focusing on late as these compounds represent the best candidates in order to copolymerize ethylene with polar vinyl monomer.

a) Generality about catalytic PE synthesis

Catalysis for ethylene polymerization provides PE via a coordination-insertion mechanism (see Figure 23). To enable this mechanism the metal complex needs a vacancy which coordinates ethylene and a metal carbon (or metal hydrogen) bond in *cis* position with the vacancy in which ethylene will be inserted.

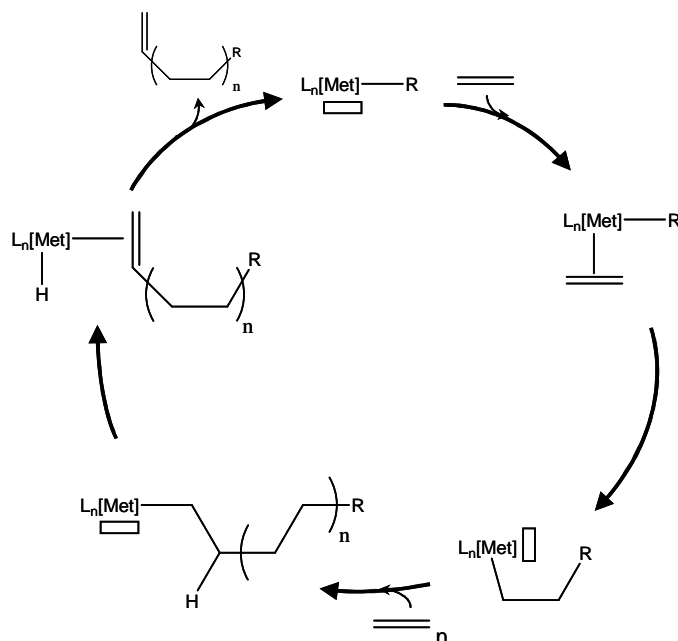


Figure 21. Schematic mechanism of catalytic polymerization of ethylene

Two major kinds of catalysts can be described: monocomponent catalyst and multicomponent catalyst. Multicomponent catalysts need the addition of cocatalyst to manage the polymerization of ethylene (see Figure 22). For example most of industrial catalysts such as Ziegler-Natta ones need an alkylating agent (TEA—triethylaluminum, MAO—methylaluminoxane) to create the first metal carbon bond in which ethylene will further insert, and/or create the vacancy on the metal center.

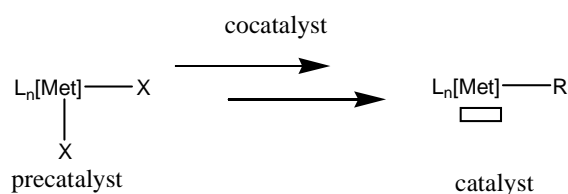


Figure 22. Schematic activation of a multicomponent catalyst with R a carbon or H

Cocatalysts in multicomponent systems usually do not act as spectator during the catalytic polymerization. Alkylating agents have another important role beside the activation of precatalyst, they are also scavenger. In some cases, alkylating agents are also directly involved in the active species via bimetallic complexes.

For monocomponent catalyst, the metal carbon bond preexists and usually an equilibrium exists to release the vacancy (see Figure 23). To favor the equilibrium toward the active species a ligand scavenger can be added to the system. For example a phosphine scavenger such as $\text{Ni}(\text{COD})_2$.

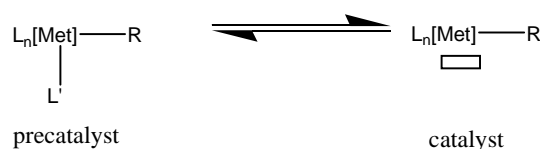


Figure 23. Schematic activation of a monocomponent catalyst, with R a carbon or H

In the following, we will call catalyst even compounds which need to be activated by a cocatalyst.

Most of the commercial processes for polyethylene synthesis are based on multicomponent catalysts and are usually used in heterogeneous phase with a solid catalyst. Important differences between homogeneous and heterogeneous catalyst are the PE particles formation and the homogeneity of both microstructures and molecular weights of PE synthesized. Homogeneous catalysts are often mono-site catalysts then all PE possess about the same molecular weight and chain microstructure. Heterogeneous catalysts are generally multi-site. Several different active species exist at the surface leading to several families of PE (in molecular weights and microstructures).

After a long time of development, the research in ethylene catalytic polymerization is now focusing on various aspects and the copolymerization with polar vinyl monomers is one of the most challenging (we will focus on this point in the subsection D.2).

b) Different classes of catalyst

This discussion focuses on the homogeneous catalyst families for ethylene polymerization. Since the initial discovery of activator of metallocene catalyst (see Figure 24 a) by Kaminsky, progress of catalysis using molecular early transition metal complexes during these three decades enabled control of molecular weights of polyethylenes and poly(α -olefin)s, control of stereochemistry of poly(α -olefin)s, synthesis of block copolymers... For example, bridged metallocene catalyst and half-metallocene, including constrained geometry catalyst (b, CGC), exhibit unique properties (such as efficient high α -olefin insertion).

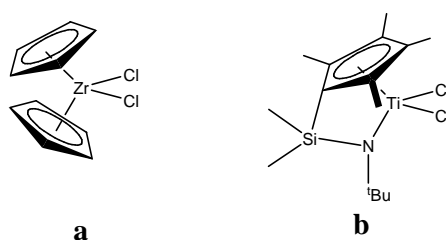


Figure 24. Example of metallocene and CGC catalysts

In this section, because of the huge amount of literature and reviews, only the last decade improvements and new classes of catalysts will be discussed, focusing on post-metallocene catalysts and excluding all bimetallic catalysts for ethylene polymerization (on this subject see the excellent review of Takeushi [160]). Lanthanocenes catalysts are also excluded due to the huge varieties of catalysts [161, 162] and a too high oxophilicity. Late transition metals will be specially highlighted since these compounds represent the best candidates in order to copolymerize ethylene with polar vinyl monomer.

(1) *Group 4 transition metal complexes*

(a) *With two monoanionic bidentate ligands*

The most outstanding catalysts for ethylene polymerization among these reported quite recently are bis(phenoxyimine) of group 4 transition metals (FI catalyst), which were discovered by Mitsui Chemical Co. [163] and Coates [164] independently. Varieties of related complexes having two bidentate monoanionic ligands have been explored (see Figure 25). These included Ti(IV) and Zr(IV) complexes with phenoxyimine ligands (**a**), pyrrolide-imine ligands (**b**), O,O- and N,O-chelating ligands (**c**, **d**) [165]. Ti(IV) complexes with enolateimine ligands (**e**) [166] and Zr(IV) complexes with phenoxyphosphine ligands (**f**) [167] and amionopyridine ligands (**g**) [168] are also active in ethylene polymerization.

FI catalysts show extremely high activities. For example, Ti FI catalysts with activities of $90 \cdot 10^3 \text{ kg mol}^{-1} \text{ h}^{-1} \text{ bar}^{-1}$ were reported [169]. For some FI catalysts, a living polymerization of ethylene was observed up to 75°C and block copolymers of ethylene and propylene were synthesized [166].

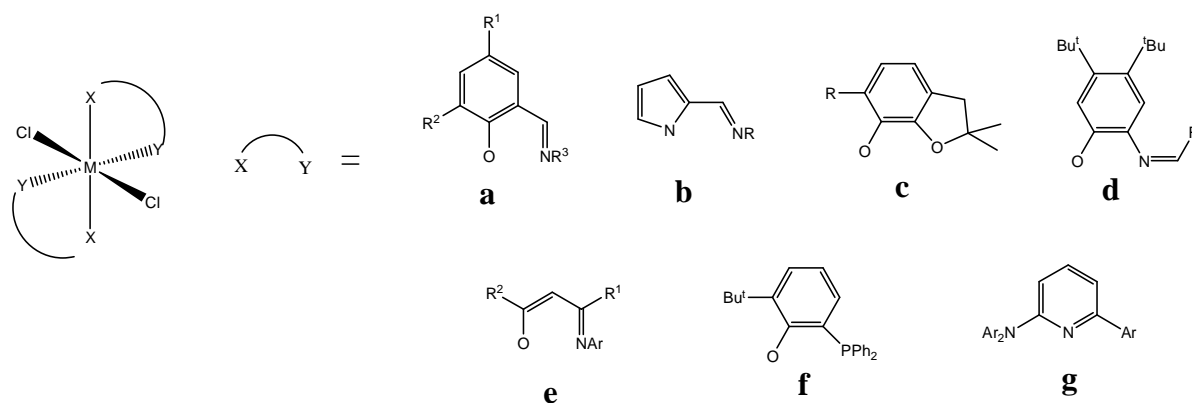


Figure 25. Group 4 transition metals with two bidentate monoanionic ligands

(b) With one monoanionic tridentate ligand

Group 4 metal complexes with one monoanionic tridentate ligand such as hydridotris(pyrazoyl)borate (Tp) catalyze ethylene polymerization [170, 171]. For example Tp ligand having bulky mesityl substituents (see Figure 26 **a**) show very high activities ($1.2 \cdot 10^6 \text{ kg mol}^{-1} \text{ h}^{-1} \text{ bar}^{-1}$). Jordan [172] found that Tp catalyst based on Hafnium is free from chain transfer, and the high PDI=1.6-3.0 are only due to a slow initiation of the polymerization.

Tang [173] reported Ti complexes that contain phenoxyimine or phenoxyamine ligand with P, S, or Se coordinating pendants in the meridional coordination (see Figure 26 **b**).

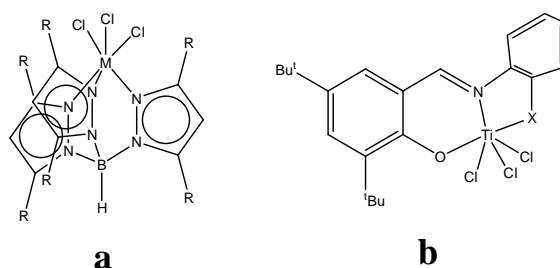


Figure 26. Group 4 transition metal with one tridentate monoanionic ligand

(c) With one dianionic tridentate or tetradentate ligand

Group 4 complexes with tridentate or tetradentate dianionic ligands active for ethylene polymerization (see Figure 27) include these with bisphenoxypyridine (**a**) [174], bisphenoxyphosphine (**b**) [175], bisphenoxydiphosphine (**c**) [176], salen (**d**) [177], and calixarene-based ligands (**e**) [178]. Highest activities were reported with bisphenoxypyridine Zr catalyst (up to $37 \cdot 10^3 \text{ kg mol}^{-1} \text{ h}^{-1} \text{ bar}^{-1}$). These catalysts usually afford ultra-high molecular weight polyethylene (for example Mn up to $4.2 \cdot 10^6 \text{ g/mol}$ for Ti calixarene-based catalyst).

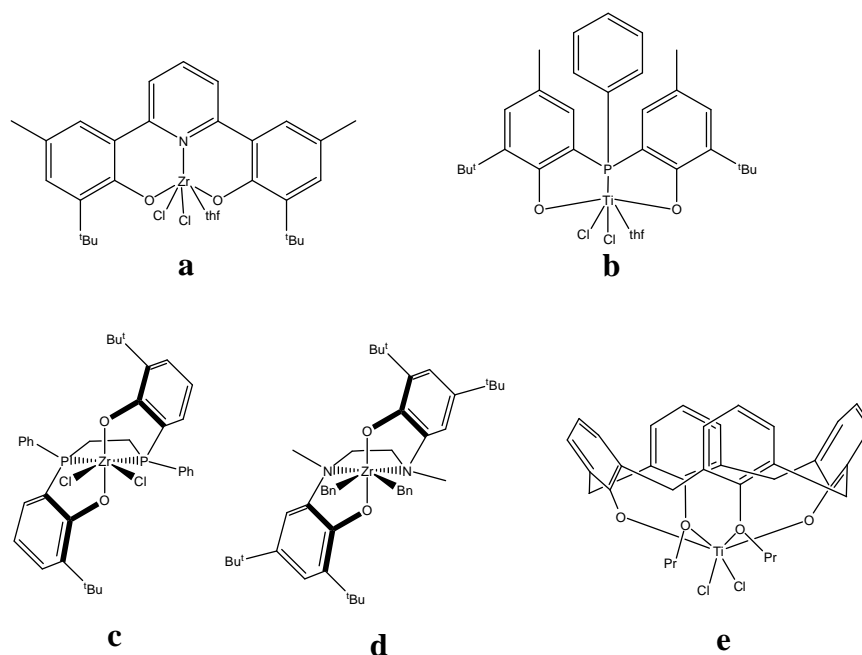


Figure 27. Group 4 transition metal with one tri- and tetradentate dianionic ligand

(2) *Group 5 transition metal complexes*

Studies of group 5 metal complexes with high catalytic activity for ethylene polymerization are limited [179], partly due to the thermal instability of the complexes and their tendency to be reduced to low valent species. However, appropriate design of the supporting ligand enabled catalysis with activity exceeding $10^4 \text{ kg mol}^{-1} \text{ h}^{-1}$.

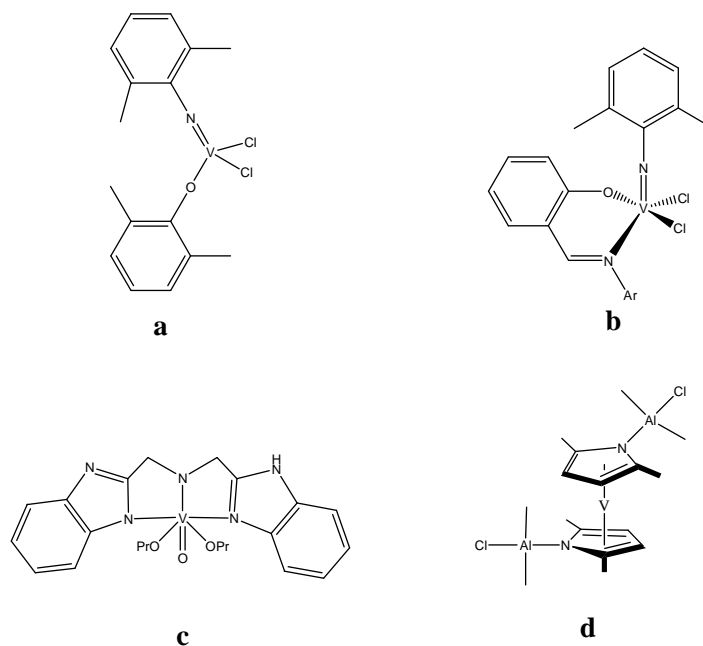


Figure 28. Different classes of vanadium catalysts

V(V) catalysts having phenoxy-based ligands (see Figure 28 **a, b**) have been found to be thermally stable and highly active for ethylene polymerization in the presence of an organoaluminum chloride co-catalyst (up to $640 \cdot 10^3 \text{ kg mol}^{-1} \text{ h}^{-1}$) [180].

V(V) and V(III) complexes with benzimidazoleamine ligand (see Figure 28 **c**) are also highly active for ethylene polymerization ($42 \cdot 10^3 \text{ kg mol}^{-1} \text{ h}^{-1}$), and the reaction requires a small excess amount of the aluminum cocatalyst [181].

Finally V complexes with pyrrolyl ligands (see Figure 28 **d**), without any carbon-vanadium bond, catalyzes ethylene polymerization without addition of a co-catalyst via an alkyl shift from aluminum to vanadium (see Figure 29) [182].

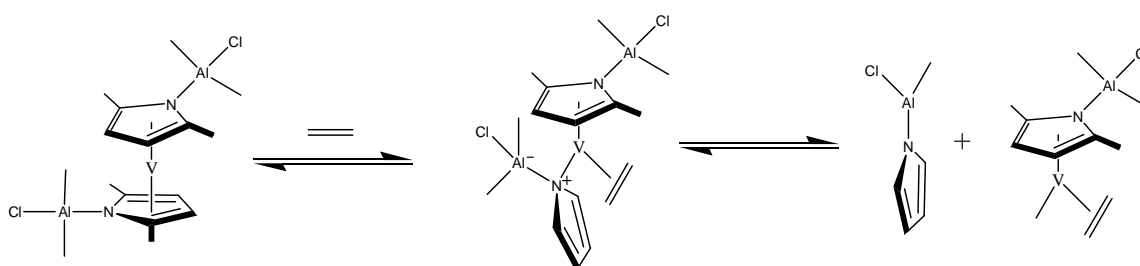


Figure 29. Proposed initiation mechanism for pyrrolyl vanadium complex

Nb and Ta complexes active for ethylene polymerization are limited [183], however these supported by calixarene ligands promote ethylene polymerization to produce linear polyethylene.

(3) Group 6 transition metal complex

Heterogeneous Cr catalysts are well known in the industrial production of polyethylene. Many homogeneous Cr catalysts with cyclopentadiene-based ligands (Cp) have been reported. Recently some Cp-based Cr complexes have been reported [184] to polymerize ethylene even in the presence of small amount of cocatalyst (for example using $[\text{Al}]/[\text{Cr}]=25$, activity of $4 \cdot 10^6 \text{ kg mol}^{-1} \text{ h}^{-1}$ was reported - see Figure 30 **a**).

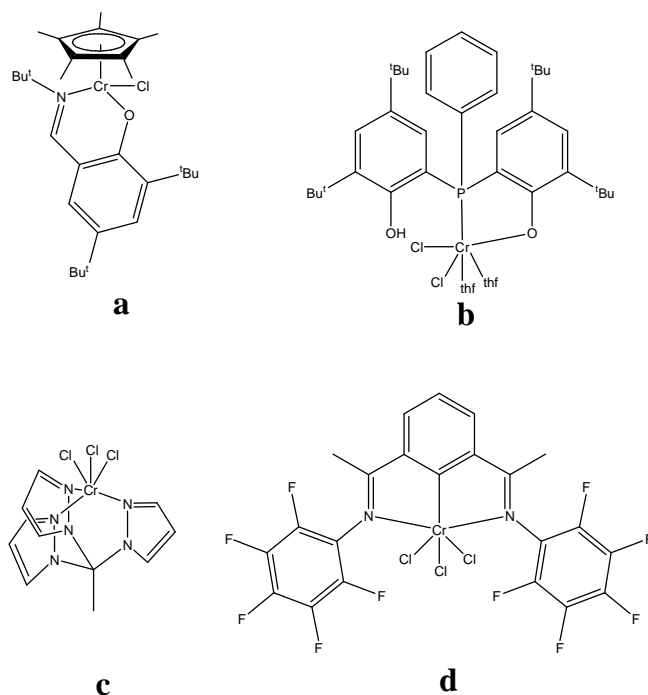


Figure 30. Different classes of chromium catalysts

Non-Cp Cr complexes (see Figure 30) with monoanionic ligands such as phosphinophenoxy ligand (**b**) [185] and neutral ligands such as tris(pyrazolyl)ethane ligand (**c**) [186] and with bis(imino)pyridine ligand (**d**) [187] are also highly active for ethylene polymerization with activity up to $113 \cdot 10^3 \text{ kg mol}^{-1} \text{ h}^{-1}$.

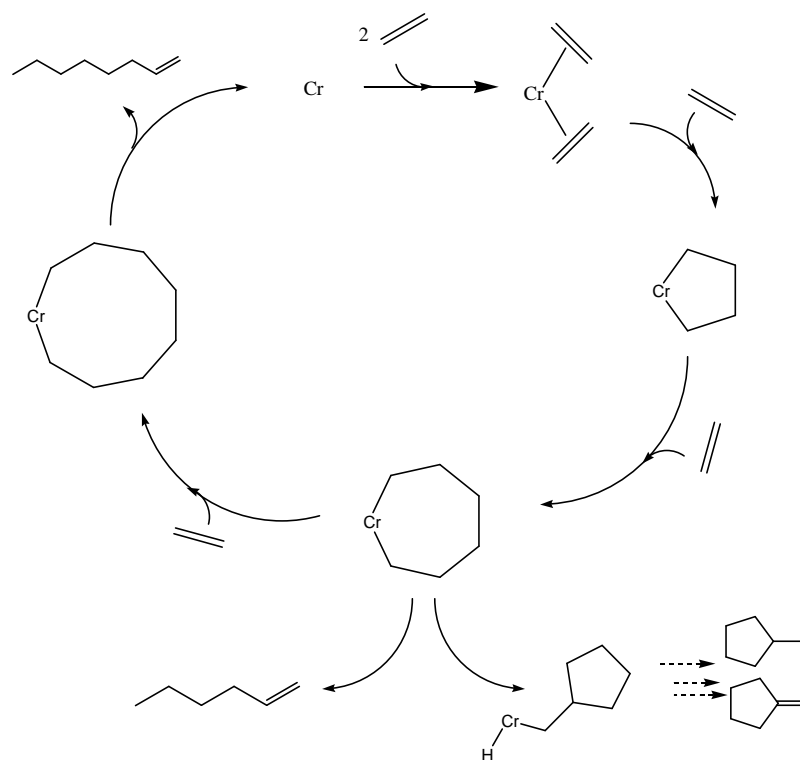


Figure 31. Mechanism of tri- and tetramerization of ethylene by chromium catalyst

Catalyst prepared from $\text{CrCl}_3(\text{thf})_3$ and diphenylphosphineamine (PNP) or dithioethylamine (SNS) ligands in conjunction with MAO, promote trimerization and tetramerization of ethylene, and have attracted increasing attention owing to their high productivity and selectivity (see Figure 31) [188]. Gambarotta and Duchateau [189] reported that a Cr complex with $^t\text{BuNPN}^t\text{Bu}$ ligand catalyzes ethylene polymerization (see Figure 32) to yield highly linear polyethylene (with activity up to $33 \cdot 10^3 \text{ kg mol}^{-1} \text{ h}^{-1} \text{ bar}^{-1}$) or its oligomerization, giving α -olefins, depending on the type and amount of organoaluminum co-catalyst. Polymerization of ethylene takes place without any cocatalyst addition to the polymerization solution.

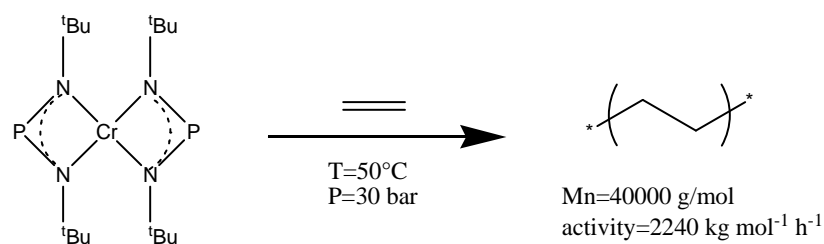


Figure 32. Monocomponent chromium catalyst for ethylene polymerization

(4) *Group 7 transition metal complex*

Mn complexes that are active for ethylene polymerization are rare (see Figure 33). Recently Fujisawa [190] reported a hydridatris(pyrazolyl)borate Mn (**a**) catalyst for ethylene polymerization (activity up to $7 \cdot 10^3 \text{ kg mol}^{-1} \text{ h}^{-1} \text{ bar}^{-1}$). A Mn catalyst with bispyridyldiamine ligands (**b**) [191] shows also low activity for ethylene polymerization ($<100 \text{ kg mol}^{-1} \text{ h}^{-1} \text{ bar}^{-1}$).

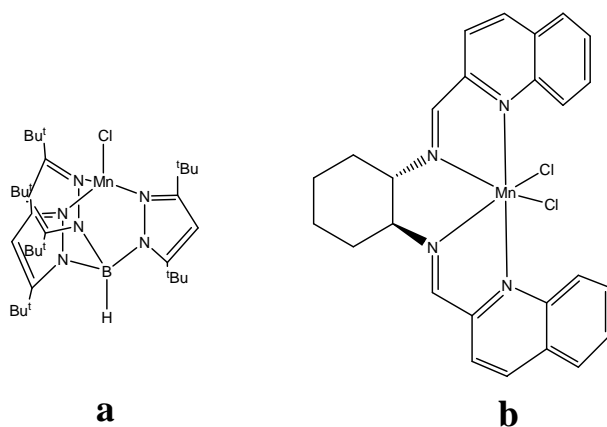


Figure 33. Examples of Mn catalysts

(5) Group 8-9 transition metal complex

Since initial reports of high performance of the Fe and Co complexes with bis(imino)pyridine ligands for ethylene polymerization by Gibson [192] and Brookhart [193], many research groups have studied olefin polymerization using modified bis(imino)pyridine ligands (see Figure 34 a). The Fe and Co catalysts exhibit unique advantages such as very high catalytic activity ($> 10^5 \text{ kg mol}^{-1} \text{ h}^{-1} \text{ bar}^{-1}$), formation of linear polyethylenes, production of high molecular mass polymer or oligomerization of ethylene, depending on the bulkiness of the arylimino groups of the ligand [194], and end-functionalization of polyethylene caused by addition of ZnR_2 as a chain transfer agent [195]. However, these complexes exhibit a major drawback since no efficient copolymerization with α -olefins has been reported yet. The alkyl Fe (b) complex catalyzes ethylene polymerization without the use of co-catalyst [196]; this is up to now the only example of monocomponent Fe catalyst for ethylene polymerization.

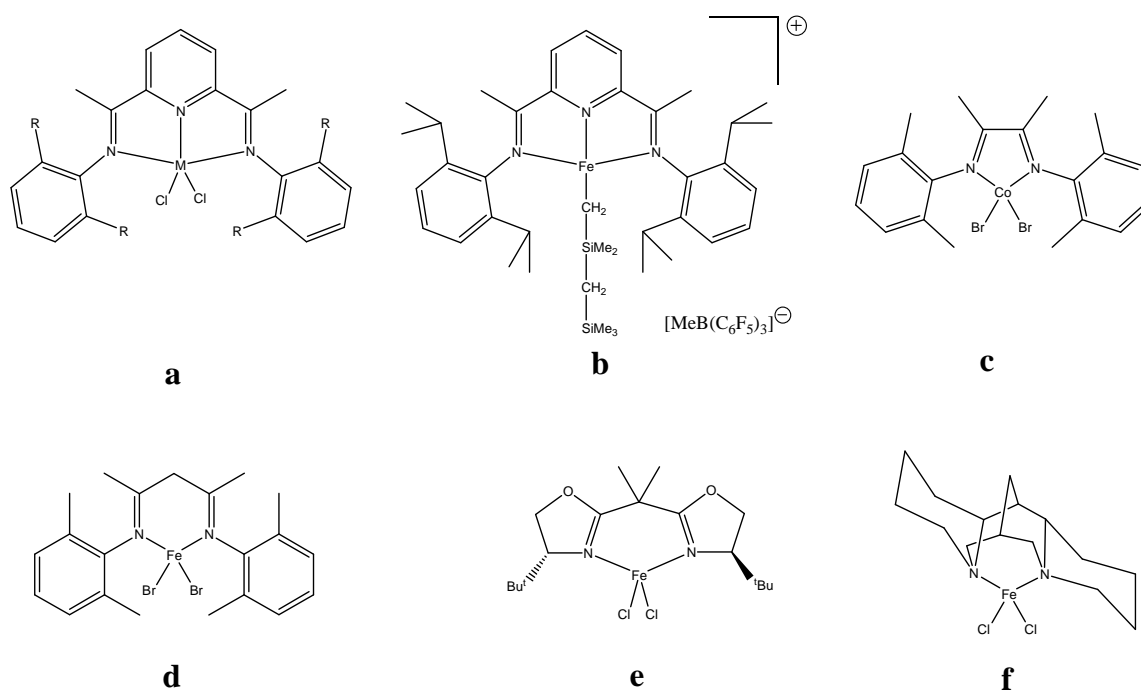


Figure 34. Different catalysts of group 8-9 for ethylene polymerization

Fe and Co complexes with other tridentate as well as bidentate N-ligands such as α - and β -diimine (c, d), bisoxazoline (e), and sparteine (f) have been shown to promote ethylene polymerization [197, 198], although their activities are not as high as the catalyst supported by bis(imino)pyridine ligands.

(6) Group 10 transition metal complex

The Ni and Pd catalysts for ethylene polymerization reported so far are categorized in two main groups (see Figure 35): complexes with diimines or bidentate neutral ligands (Brookhart type) [199] and complexes with phenoxyimine or monoanionic bidentate ligands (Grubbs type) [200]. The Grubbs type catalysts derive from the SHOP (Shell Higher Olefins Process) catalyst for ethylene oligomerization and are monocomponent catalysts.

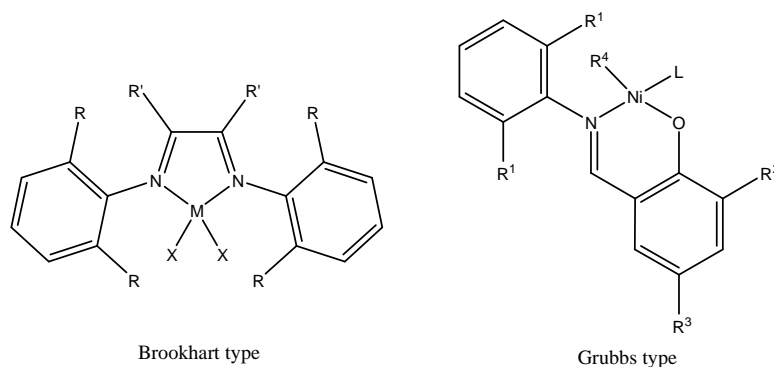


Figure 35. Two major classes of Ni and Pd catalysts

These catalysts tend to produce polyethylene with branched structure as a result of frequent β -hydrogen elimination followed by the re-insertion of the vinyl group terminated polyethylene (chain walking, see Figure 36). Diimine Ni complexes show higher catalytic activity than the corresponding Pd complexes. The Pd catalysts produce polyethylene with higher branches level than Ni equivalent complexes and their branching degree can be varied depending on ethylene pressure [201].

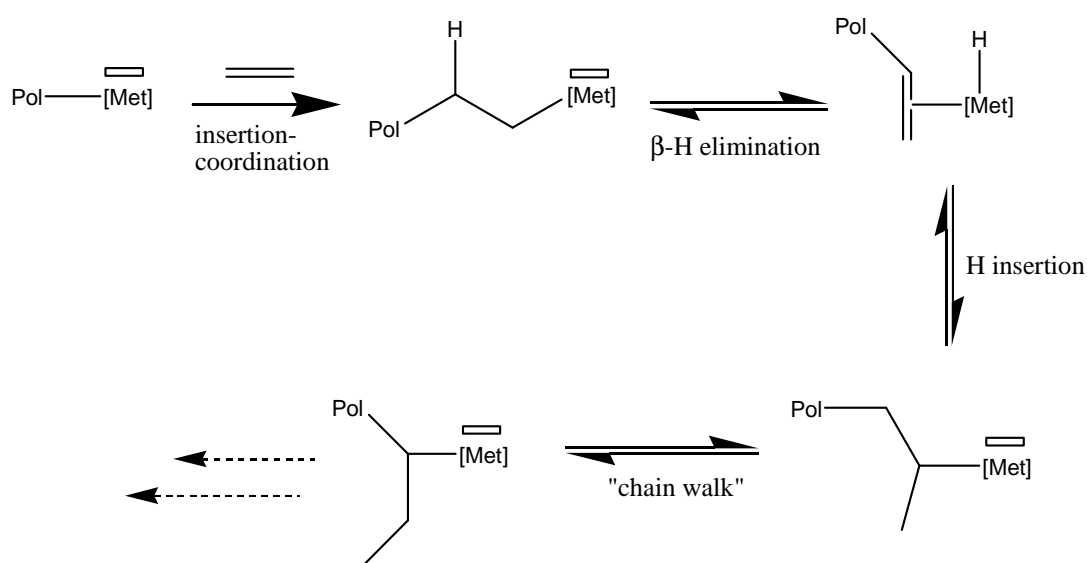


Figure 36. Chain walking mechanism

(a) Brookhart type

Owing to high tolerance of the Pd complex toward polar functional groups, the catalysis is successfully applied for ethylene copolymerization with varieties of polar comonomers. Brookhart Pd catalysts are also effective for living polymerization of ethylene. Pd complexes with functionalized alkyl ligands initiate the polymerization to produce branched polyethylenes (via a living ethylene polymerization) with specific end groups (see Figure 37) [202, 203].

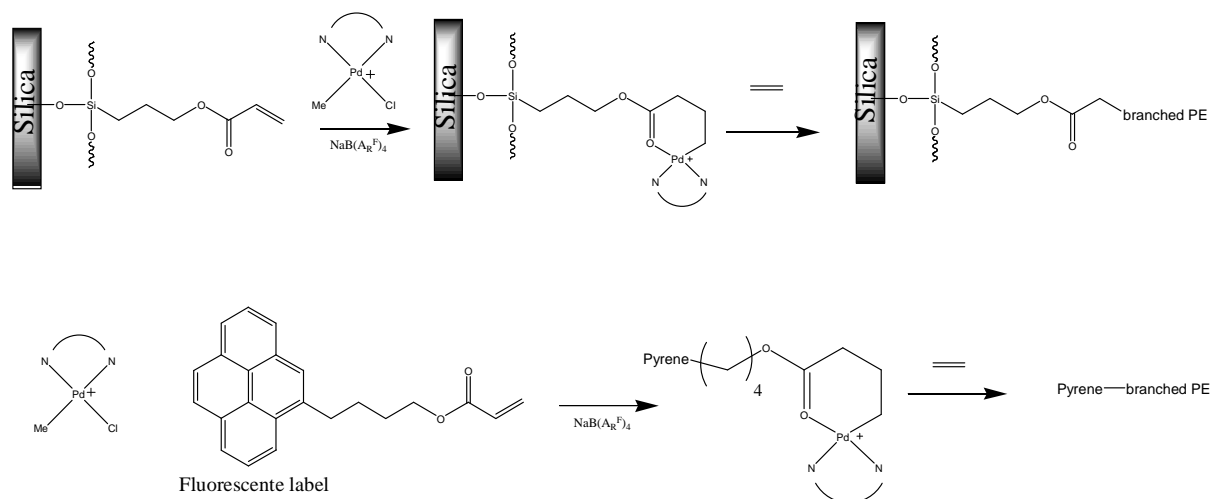


Figure 37. Example of functional PE synthesized thanks to functional alkyl ligands

Catalytic activity of Pd- and Ni-diimines complexes is affected by N-aryl groups of the ligand. Guan [204] investigated the electronic effect of the aryl group of diimine ligands on the ethylene polymerization systematically. Electron donation to aryl group stabilizes the cationic metal center, and increases the turnover number (TON) and molecular weight of the polyethylene.

Other bidentate neutral ligands have been developed for the ethylene polymerization. Jordan [205] reported that Pd complexes with bispyridyl methane ligand promote dimerization, oligomerization or polymerization of ethylene, depending on the bulkiness of substituents of the ligands (see Figure 38 a).

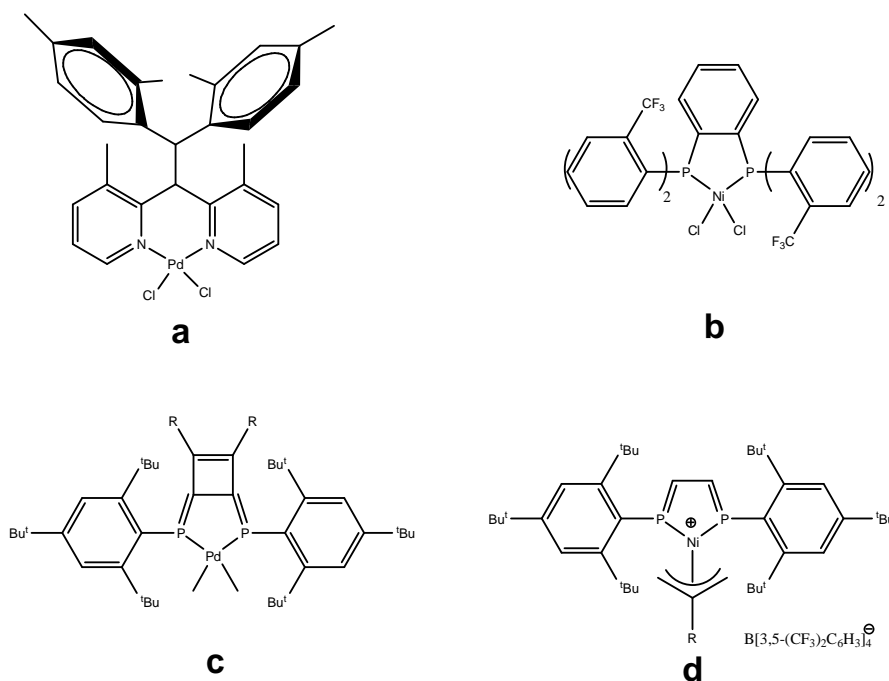


Figure 38. Other examples of Brookhart type catalysts

Ni complexes with diphosphine ligands (**b**) tend to afford ethylene oligomerization due to frequent chain transfer. The introduction of bulky substituents on the ligand enhances chain growth to enable formation of high molecular weight linear polymers (M_n up to 70000 g/mol with an activity of $10 \text{ kg mol}^{-1} \text{ h}^{-1}$) [206]. Ozawa and Ionkin prepared Pd (**c**) [207] and Ni (**d**) [208] complexes with bidentate phosphinidene ligands. These complexes catalyze ethylene polymerization to form polymer with a linear structure.

(b) *Grubbs type*

The Ni complexes with phenoxyimine ligands promote ethylene polymerization with or without activators such as $\text{Ni}(\text{cod})_2$ or $\text{B}(\text{C}_6\text{F}_5)_3$. The N-aryl *m*-substitution affects the degree of branching and molecular weight of the produced polyethylene, despite remote position from Ni center. The substituents on the phenoxy affect especially the activity of the catalyst [209].

The high tolerance of Ni complex toward polar functional groups even enables the polymerization of ethylene in water [210] and in supercritical CO_2 [211]. Therefore, the polymerization in aqueous media provides polyethylene nanoparticles [212].

Other bidentate monoanionic ligands have been developed to undergo catalytic polymerization of ethylene. Ni with anilinetropone (see Figure 39 **a**) or annilinoperinaphthenone (**b**) ligands [213, 214] promotes also polymerization of ethylene producing moderated-branched polyethylenes (35-55 branches/ 1000C).

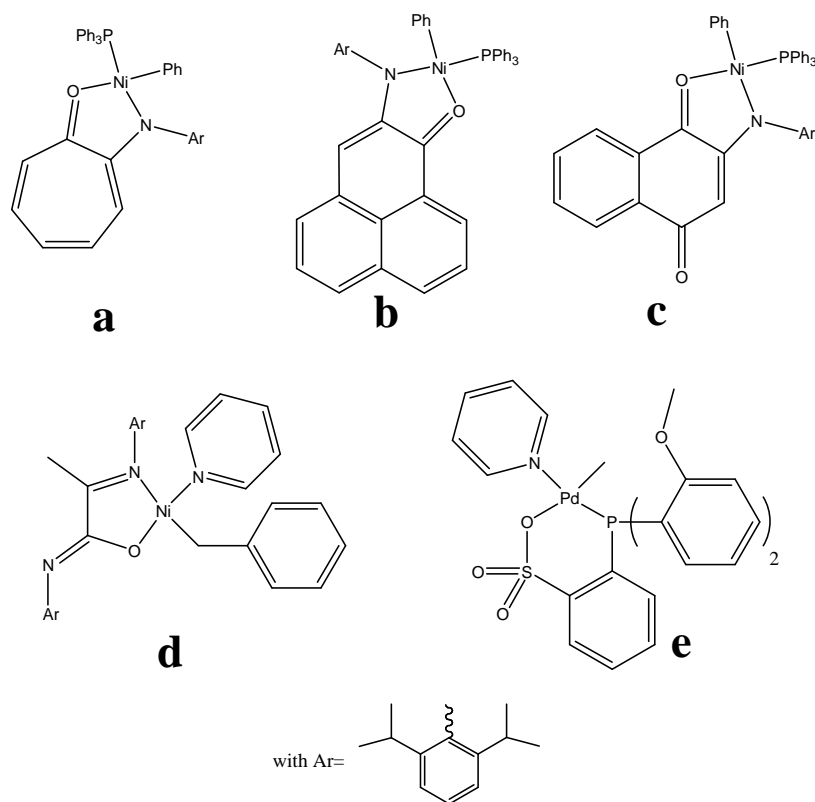


Figure 39. Other examples of Grubbs type catalysts

Shiono [215] reported that Ni complexes with an aminonaphthoquinone ligand (**c**) in conjunction with $B(C_6F_5)_3$ promotes polymerization of ethylene where the degree of branching depends on B to Ni ratio (low branches content without $B(C_6F_5)_3$ to highly branched with $B(C_6F_5)_3$).

Bazan [216] reported α -iminocarboxamide Ni complexes (**d**) with coordinating pyridine ligands which promote ethylene polymerization without any co-catalyst to give low-branched polyethylene with only Me branches.

Finally, Pd and Ni catalysts using phosphine-sulfonate ligands (**e**) have attracted recent attention for insertion-coordination catalysis. The catalysis was originally reported by Drent [217] who performed the copolymerization of ethylene with acrylate, to produce the copolymer containing acrylate repeating unit in the main chain (see section D-2 of this chapter). These catalysts provide linear PE with relative low molecular weights.

(7) *Group 11 transition metal complex*

Copper complexes with diimine and phenoxyimine ligands were claimed to catalyze homopolymerization of ethylene. However, more recent investigations of the reaction revealed that the aluminum complex, formed by the ligand exchange between catalyst and co-catalyst, is likely to be the active species in all these polymerizations (see Figure 40) [218].

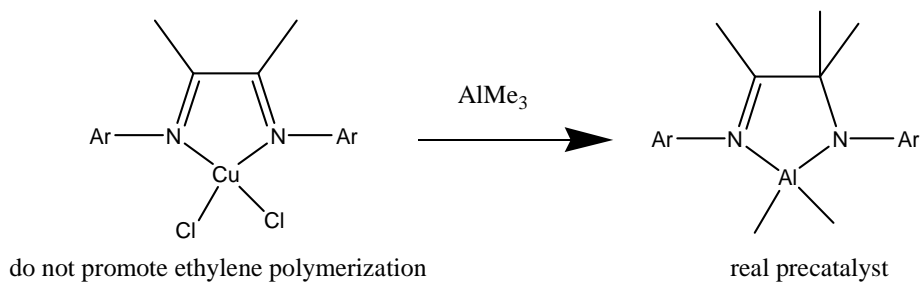


Figure 40. Metal exchange between Al and Cu

Gibson [219, 220] reported also Al compounds which promote the ethylene polymerization. The mechanism of the polymerization by a coordination-insertion is still unclear, theoretical calculations predict the involvement of polynuclear active species [221].

C. Homopolymerization of polar vinyl monomer

In order to copolymerize ethylene with polar vinyl olefins, the mechanism of polymerization needs to be chosen wisely. As already mentioned, ethylene can be polymerized via a radical pathway or a coordination-insertion mechanism using metal complexes. Polar vinyl monomers can be polymerized by a radical, cationic, anionic, or coordination-insertion mechanisms.

Consequently, only radical or coordination-insertion polymerization can be involved in a copolymerization of these monomers. In this section, we will shortly review radical and coordination polymerization of polar vinyl monomer. In particular, different methods of controlled radical polymerization will be presented in order to understand the results obtained for the copolymerization in the next section.

1. Radical polymerization

Polar vinyl monomer can be polymerized by a radical pathway as ethylene [222]. These polymerizations were intensively studied and radical polymerization represents one of the most versatile polymerization methods: wide range of solvents, temperatures and monomers can be used. Free radical polymerization of polar vinyl monomer follows the same mechanism as ethylene radical polymerization described in the previous section.

In this section, we will describe the major techniques for controlled radical polymerization (CRP). Indeed radical polymerization is one of the oldest techniques of polymerization; however, it induces major defects, mostly due to the radical itself (uncontrolled transfer and termination). Therefore, a challenge of free radical polymerization is to limit the effect of the irreversible terminations and transfer reactions. Controlled polymerizations induce linear molecular weight increase with conversion and the molecular weight distribution remains extremely narrow. Several different mechanisms of control have been developed in the last 20 years. All of them are based on the reduction of the radical concentration to drastically decrease the probability of irreversible termination. This extremely low concentration of growing radicals is controlled thanks to reversible reaction of transfer (leading to a non-propagating radical – see Figure 41) or termination (leading to compounds with no carbon radical – see Figure 41).

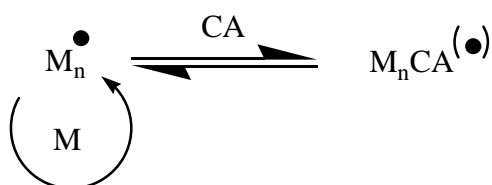


Figure 41. Schematic view of controlled radical polymerization mechanism

a) Nitroxide Mediated Polymerization

Nitroxide Mediated Polymerization (NMP) is a radical polymerization controlled by a reversible termination. Historically, NMP is the first controlled radical polymerization ever described. Georges [223] reported in 1993 the controlled polymerization of styrene in the presence of benzoyl peroxide and the stable radical TEMPO. Excellent reviews on NMP are available [224, 225].

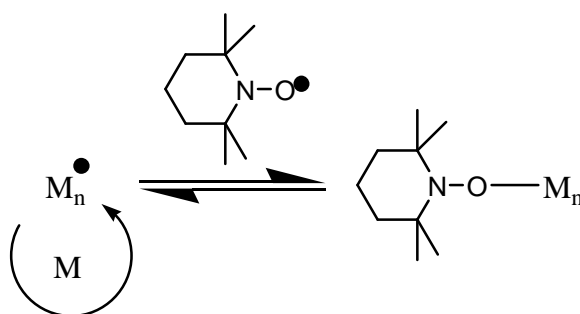


Figure 42. Schematic view of NMP using TEMPO as stable radical

Control in NMP is achieved with dynamic equilibrium between dormant alkoxyamines and propagating radicals (see Figure 42). Stable Free Radical Polymerization (SFRP) is a generalization of NMP where the stable radical is not a nitroxide. Several other organic or inorganic mediators have been developed. Wide ranges of monomers have been controlled by NMP but this method does not control easily monomers such as MMA. Two other disadvantages of NMP are that the mediated stable radical is usually expensive and that NMP needs high temperature (over 100°C).

b) Reversible Addition Fragmentation Chain Transfer

Reversible Addition Fragmentation Chain Transfer (RAFT) is a radical polymerization controlled by a reversible transfer. First RAFT was reported in 1998 [226]. It is efficient with a wide range of monomers and initiators to control radical polymerization. Excellent reviews have been published on RAFT [227, 228].

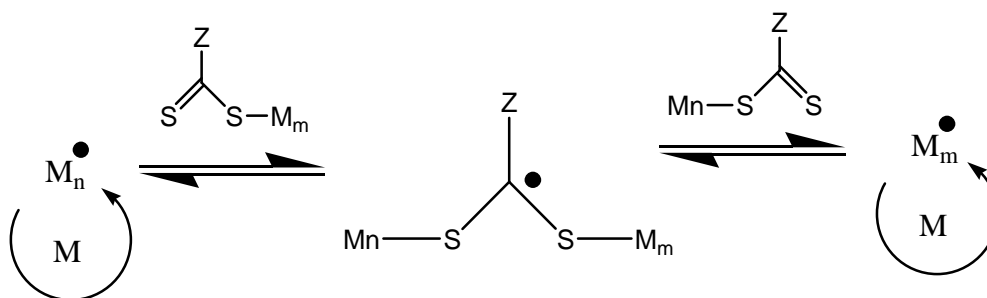


Figure 43. Schematic view of RAFT

RAFT controlled reaction is a chain transfer on the RAFT agent (see Figure 43). Several RAFT agents have been designed in order to control most of monomers in a broad range of experimental conditions. RAFT is one of the most successful CRP processes due to its applicability to a wide variety of monomers but the RAFT agent must be chosen wisely for each monomer.

c) Iodide Degenerative Transfer Polymerization

Iodide Degenerative Transfer Polymerization (IDTP) is a radical polymerization controlled by a reversible transfer. IDTP is certainly the oldest CRP process as it has been developed in the eighties by Tatemoto [229] especially for vinylidene fluoride polymerization. In this early period even block copolymers were synthesized. Nevertheless it is the work of Matyjaszewski [230, 231] in 1995 which reactivated the interest on IDTP.

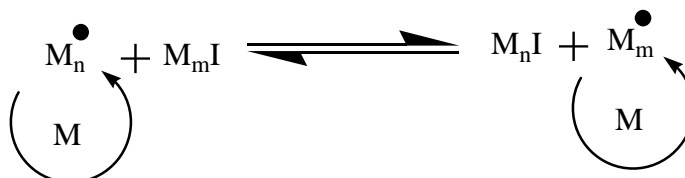


Figure 44. Schematic view of IDTP

IDTP controlled reaction is an iodine transfer between a dormant chain and an active chain (see Figure 44). IDTP is with RAFT one of the most universal techniques as lots of monomers can be polymerized by a controlled radical pathway (even vinyl acetate and vinyl chloride). However IDTP has one major drawback that iodinated transfer agents are not very stable upon storage.

d) Atom Transfer Radical Polymerization

The Atom Transfer Radical Polymerization (ATRP) is a radical polymerization controlled by reversible termination. First ATRP system was reported by Matyjaszewski [232, 233] in 1995 based on chloride copper complexed by a bipyridine ligand. This system shows good control of MA and MMA polymerization. Excellent reviews have been published on the ATRP [227, 234-236].

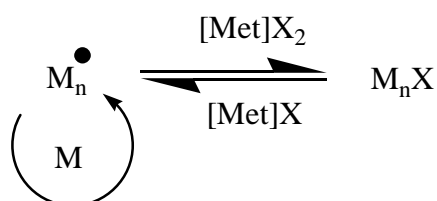


Figure 45. Schematic view of ATRP

ATRP controlled reaction is a reversible halogen atom transfer promoted by redox equilibrium between an alkyl halide and a metal complex (see Figure 45). Several metals have been used in ATRP (Ni, Fe, Pd, Ru, Te, Co), but the most used and studied one remains copper. Ligands have also an important influence on the behavior of the ATRP system; consequently several ligands have been investigated. ATRP can control most of the polar vinyl monomers (acrylates, methacrylates, styrenes). One disadvantage of ATRP is the important amount of metal needed. Two major approaches have been developed to solve this problem: the heterogenization of ATRP and the ARGET (Activators ReGenerated by Electron Transfer) ATRP technique and equivalents which allow to decrease drastically the metal concentration.

e) Cobalt Mediated Radical Polymerization

Cobalt Mediated Radical Polymerization (CMRP) was first reported by Wayland in 1994 [237]. The controlled reaction can be either a reversible termination or a reversible transfer (see Figure 46). An excellent review on CMRP has been published [238].

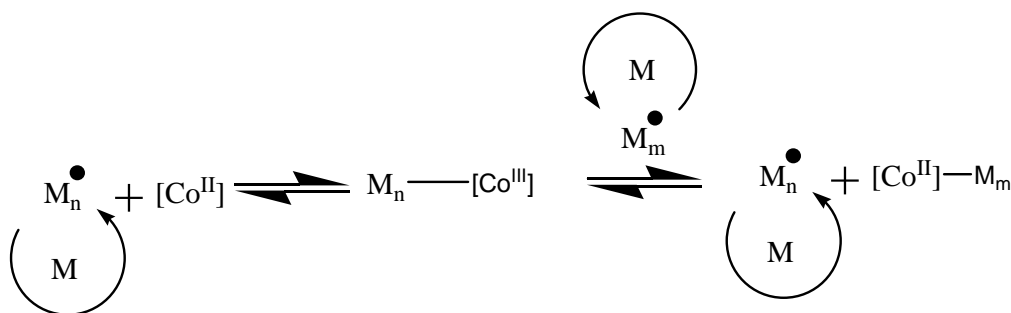


Figure 46. Schematic views of CMRP controlled by termination (left) or transfer (right)

Cobalt ligand and solvent have a great effect on the mechanism of CRP. Transfer or termination controls are solvent and ligand dependent. Several ligands were developed and even other metals were used. CMRP was the first efficient CRP technique reported to control VAc which induced a strong development of this method.

This technique is also the only one involving a metal-carbon bond (contrary to ATRP where metal-halogen bonds are involved). This dormant species induces interest since it present some similarity with an ethylene polymerization catalyst (possess a metal-carbon bond but without a vacancy in *cis* position).

2. Polymerization of polar monomer with coordinated complexes

Metal catalyzed homopolymerizations of polar vinyl monomers have been intensively studied. Conventional Ziegler-Natta type catalysts ($\text{TiCl}_4/\text{AlR}_3$) are employed for syndiospecific polymerization of MMA at low temperature since the sixties. Different mechanisms of polymerization have been proposed to explain this polymerization. For early transition metal complexes (as well as some late transition metal complexes) Group Transfer Polymerization (GTP) is usually the proposed mechanism. A coordination/insertion mechanism identical to the catalytic polymerization of ethylene is also proposed for complexes (usually late transition metal). The mechanism of polymerization can be sometimes unclear since in some cases, a radical initiation was also claimed due to the decomposition of the transition metal.

a) Early transition metals and lanthanides catalysis

In 1992 Yasuda (see Figure 47) [239] and Collins (see Figure 48) [240] reported the controlled polymerization of MMA using respectively samarocene and zirconocene complexes. Since this initial achievement, lots of research groups have studied this kind of polymerization: development of new catalysts, polymerization of broad range of polar monomers, improvement of the stereochemical control.

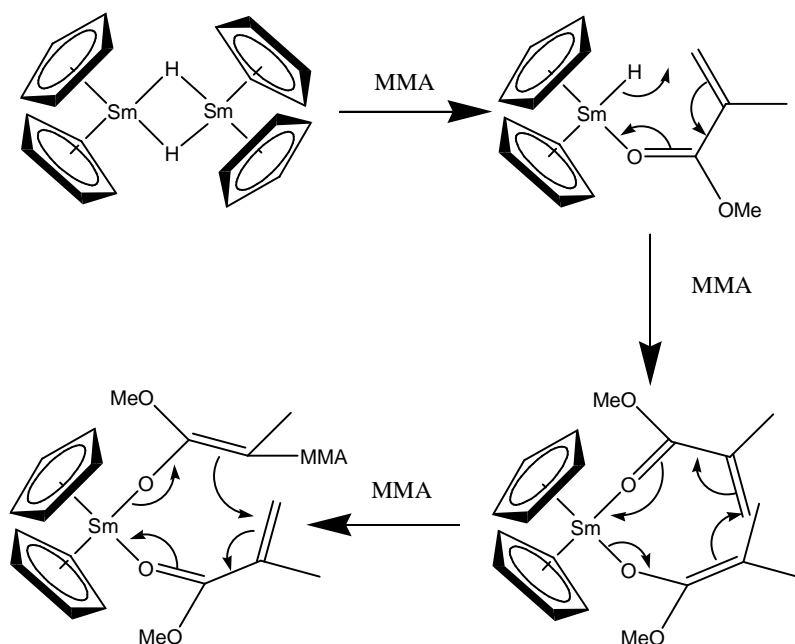


Figure 47. Chain initiation and propagation in MMA polymerization by samarocene catalyst

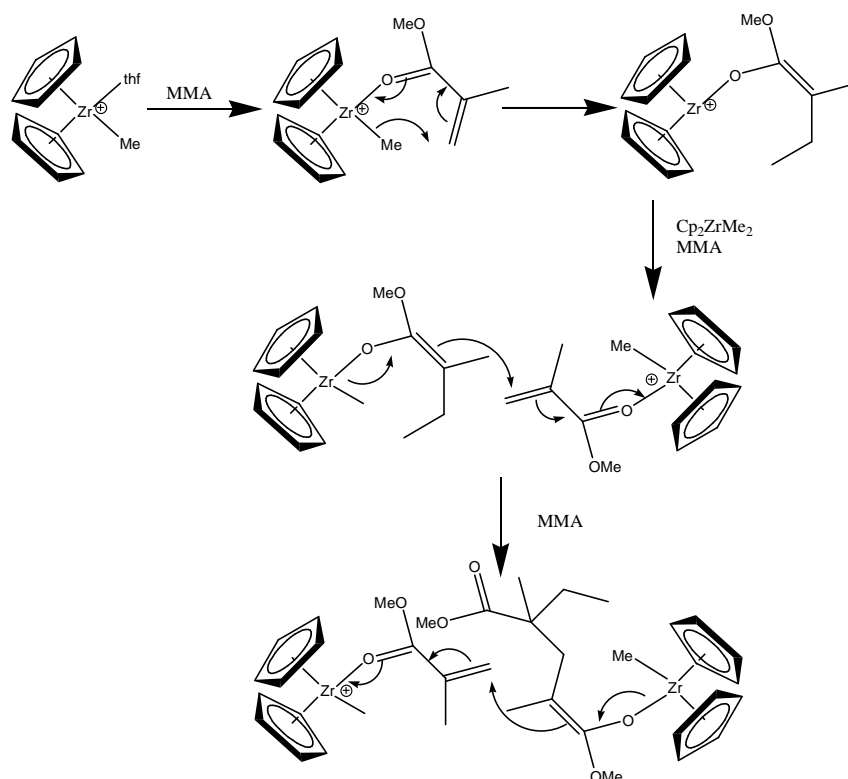


Figure 48. Chain initiation and propagation in MMA polymerization by zirconocene catalyst

Chen published recently an excellent review on the “coordination polymerization of polar vinyl monomer by single-site metal catalysts” [241]. Almost all polymerizations of polar monomers were done with lanthanides or early transition metals complexes.

It should be noted that up to now no coordination polymerization were reported for two of the most important classes of polar vinyl monomer: vinyl acetates and vinyl halides. It must be due to the same reason that we will develop in section D-2-b-(4) and (5) (OAc or halides elimination).

Some of these complexes can also polymerize ethylene by a living pathway. Consequently Yasuda [242] reported since 1992 the successive polymerization of ethylene with MMA to produce block copolymers.

b) Late transition metals

Some results have been reported with late transition metal like Fe [243, 244], Co [244], Ni [244-246], Pd [247, 248], and Cu [249]. Nevertheless, no clear-cut proofs of the mechanism have been reported up to now. Authors proposed either a radical, anionic or coordination/insertion mechanisms.

(1) *MAO ambiguous role during polymerization*

In all the polymerizations of MMA reported using a late transition metal complex, a large excess of MAO was used. Recently Po et al. [250] reported the polymerization of MMA or styrene in presence of MAO alone, with an unknown mechanism (radical, cationic, anionic, or coordination-insertion). The mechanism of polymerization seems to be mostly monomer dependent.

For MMA a radical polymerization is suspected. Microstructure of PMMA produced is the same as a radical PMMA initiated with AIBN [250]. Moreover Sivaram [251] demonstrated a radical initiation by the remaining AlMe_3 of MAO. However with specific ligands, aluminum complexes have been reported [252] to polymerize MMA via a group transfer polymerization.

For styrene, a cationic polymerization is suspected. Saegusa [253] reported as early as 1964 the cationic polymerization of styrene and isobutyl vinyl ether with TEA/water/acyl halides, which could form in situ aluminoxane.

Consequently, due to the similarity between the polymer produced by these metal/MAO systems and MAO alone, several other evidences must be produced to confirm a coordination/insertion mechanism on the transition metal complex.

(2) *Caution interpretation of radical trap test*

In many publications authors reported the addition of radical traps to the polymerization system in order to discriminate between a radical and non-radical polymerization. However as shown below this test is not adapted in presence of transition metal complexes and/or MAO (see Figure 49).

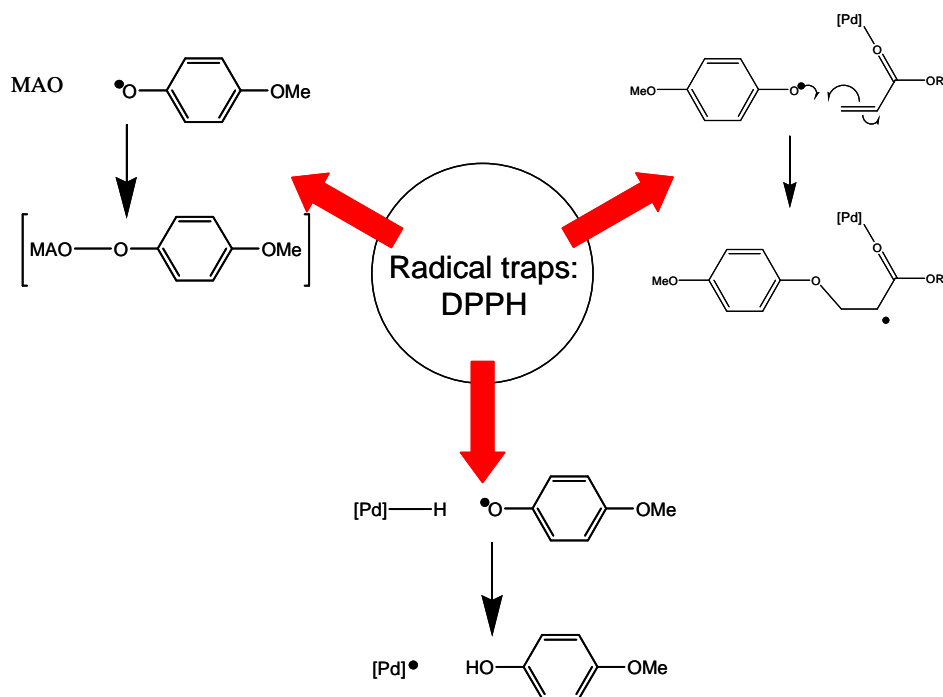


Figure 49. Summary of radical trap side reactions with late transition metal complexes and MAO

Sen [254] demonstrated that MAO interacts with typical radical traps employed to discriminate a radical process. He reported that for copper systems in presence of MAO, classical radical traps (TEMPO, DPPH, galvinoxyl) do not stop the polymerization despite the electron paramagnetic resonance (EPR) evidence of a radical polymerization. Consequently radical traps can give false-negative results.

Novak [248] reported an even more important fact. Radical traps in presence of Pd complexes can activate the polymerization of acrylate monomer. Novak proposed that the Pd complex activate the monomer via an O-binding and the radical trap acted as a radical initiator. Once again the radical trap can give a false-negative result.

Moreover, radical traps can also react with late transition metals as reported by Sen [255]. Then radical traps can also give a false-positive result.

Consequently, radical traps are inappropriate to discriminate radical polymerization with transition metal and their use should be banished. Other techniques such as EPR, analysis of the microstructure and determination of copolymerization reactivity ratios should be preferred to confirm a radical polymerization.

(3) Homolytic cleavage of a metal carbon bond

Sen [255] reported that a radical trap could induce a homolytic cleavage of a Pd-H bond. These results represent a great interest since if a metal carbon homolytic cleavage takes place, then the metal could be considered as a radical initiator since it release a organic radical which could initiate a polymerization.

Sen [256] reported also a homolytic cleavage of Pd-carbon bond of a Brookhart type Pd complex by adding phosphonium bromide (see Figure 50). This cleavage has been used to initiate radical polymerization of MA [257, 258]. Wu [259] proposed a similar mechanism with a Ni complex bearing N,O-ligands. The reversibility of the cleavage has been proposed but no clear-cut evidence has been provided up to now.

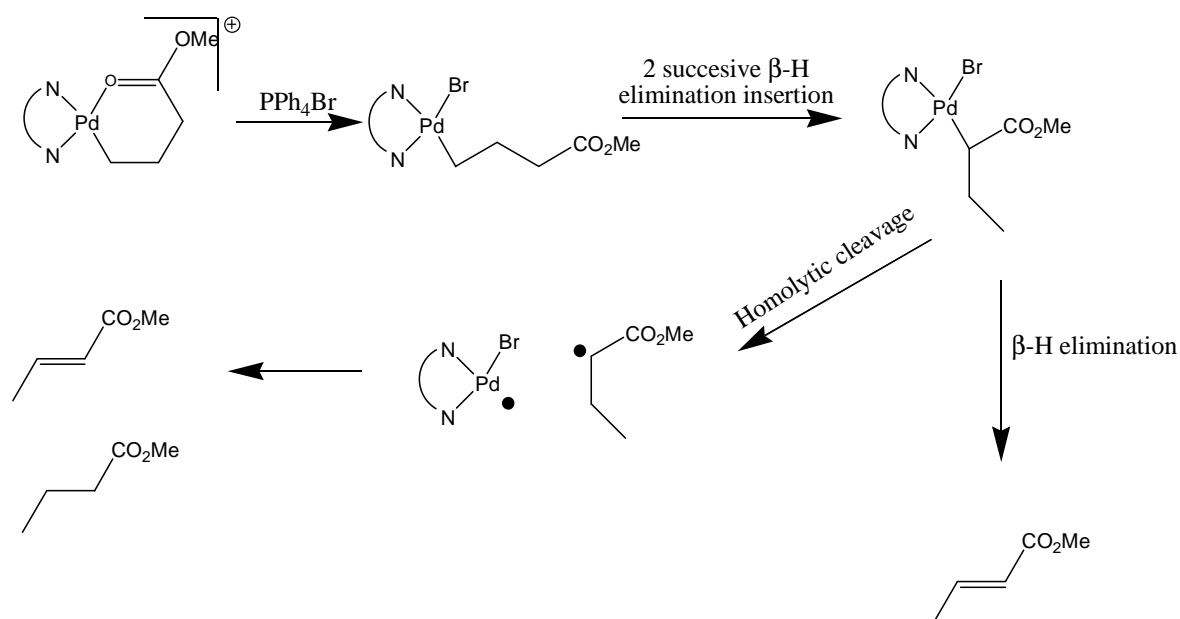


Figure 50. Proposed reaction pathway for the homolytic cleavage

(4) *Results obtained at the LCPP*

Alexandra Leblanc during her PhD [260, 261] at the LCPP demonstrated that some Grubbs catalysts (see Figure 51) can perform the homopolymerization of MMA, BuA and styrene. However, no homopolymerization of VAc takes place.

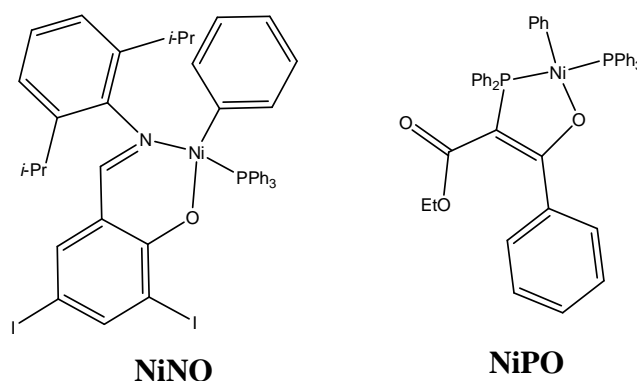


Figure 51. Ni complexes precursor for radical polymerization of polar vinyl monomer

Moreover a radical polymerization is clearly involved since the copolymerization reactivity ratios of Sty/BuA are identical to a polymerization initiated by AIBN. For Sty/MMA and MMA/BuA copolymerizations reactivity ratios are close to the ones obtained from a free radical copolymerization. In fact Sty and BuA seem to undergo radical polymerization initiated by the Grubbs catalyst. With MMA, copolymerization results indicated that an supplementary interaction should take place between the catalyst and MMA.

Temperature has a crucial importance on this polymerization since MMA polymerization yield to high conversion only at temperature over 70°C. Finally, the kinetics of the polymerization can be raised by the addition of supplemental phosphine to the reaction medium. The most intriguing point is that the addition of phosphine is mandatory to perform homopolymerization of BuA.

Homolytic cleavage of the nickel phenyl bond was proposed to explain the generation of radicals in the polymerization media. This is to the best of our knowledge the first example of radical polymerization initiated by an ethylene polymerization catalyst without any cocatalyst (such as MAO).

D. Copolymerization of ethylene with polar vinyl monomer

In order to directly copolymerize ethylene with polar vinyl monomers two different pathways have been proposed: a radical copolymerization or a catalytic polymerization.

In this section, only random copolymerization will be reviewed. All block copolymers will be excluded, as well as graft copolymer or other architectures. These copolymers were done in several steps. Excellent reviews are available on this kind of copolymerization [241, 262, 263].

1. Radical copolymerization

Copolymers of ethylene with polar monomers have a great industrial importance. Most of them contain a small amount of the polar comonomer and are so slightly different from the polyethylene itself that they are marketed as “improved polyethylene resins”. Usually for low comonomer content, polymerization conditions are close to the one of the standard industrial free radical ethylene polymerization process.

In most of the industrial applications less than 20 wt % comonomer content is used in order to keep some crystallinity. Acrylate, acetate, acrylic acids are the most common comonomers of ethylene used in industry.

Some of these copolymers are used as adhesives: EEA (ethylene/ethyl acrylate), EBAC (ethylene/butyl acrylate), EVA (ethylene/vinyl acetate), EAA (ethylene/acrylic acid), and EMAA (ethylene/methacrylic acid). EVA copolymers are primarily used in packaging films (meat packaging and stretch-wrap). EEA and EMA (ethylene/methyl acrylate) are useful in extrusion coating, coextrusions, and laminating applications; they are also used in soft blow molded articles, squeeze toys, disposable gloves. Acrylic or methacrylic acid copolymers properties are generally superior to these of EVA copolymers for these applications. These copolymers are used for coating on aluminum, in wire and cable applications. Ethylene carbon monoxide copolymers are used as “biodegradable” polyethylene: the ketone groups permit chain scission by enzymes or light.

a) Copolymerization under “high pressure” polymerization conditions

As we already discussed, ethylene can be polymerized by a free radical process under high pressure and high temperature. Consequently, several research groups [107, 264] use these conditions to undergo copolymerization of ethylene with various monomers. In the following table, main results are summarized.

Table 9. Reactivity ratios for copolymerization [107]

Comonomer	r_{ethylene}	$r_{\text{comonomer}}$	Pressure (bar)	Temperature (°C)
<i>VAc*</i>	<i>0.16</i>	<i>1.1</i>	<i>100</i>	<i>60</i>
VAc	0.82	0.99	1020-2040	120
MA	0.042	5.5	1360	130-152
BuA	0.052	3	1360	130-152
MMA	0.03	18	1360	130
BuMA	0.04	25	1430	130
AA	0.02	4	1160-2040	140-226
MAA	0.008	4	2040	160-200
Sty	0.04	2	1500-2500	100-280
1-butene	3.4	0.86	1020-1700	130-220

*: in this case, the copolymerization was performed in emulsion leading to VAE (an ethylene/vinyl acetate copolymer with low ethylene content)

In this case, copolymerization can be in first approximation rationalized thanks to the reactivity ratios of both monomers. The composition of the copolymer is determined by these four reactions.

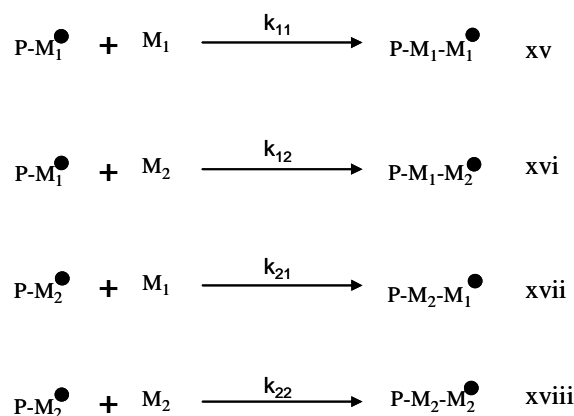


Figure 52. Reactions controlling the copolymer composition

Reactivity ratios r_1 and r_2 are defined by the ratios k_{11}/k_{12} and k_{22}/k_{21} respectively. Consequently, the copolymer composition is controlled by reactivity ratios and monomer feed compositions.

More recently, Buback et al. studied copolymerization of ethylene with various monomers: MA [265], BuA [266], BuMA [267], MAA, AA [268, 269]. Experimental conditions are generally 150-300°C and under 2000 bar of ethylene pressure. Results are quite similar to the previous ones but with improved precision.

(1) Effect of pressure and temperature on reactivity ratios

Generally, as the pressure is increased, the reactivity ratios tend toward unity and the $r_1 r_2$ product also tends toward unity. The same conclusion was obtained regarding the effect of pressure on copolymerization in general [270]. In addition, it can be seen that temperature has the same effect on r_{ethylene} values as pressure. It is noteworthy, however, that these trends are so slight that, at elevated pressures and temperatures where the reaction system is known to be homogeneous, little or no difference in r_{ethylene} values measured at pressures of 1000 to 2500 bar, and 130 to 220°C are reported [271].

Table 10. Effect of the temperature on reactivity ratios for Ethylene/BuA copolymerization at 2000 bar [266]

r_{ethylene}	r_{BuA}	Temperature (°C)
0.033±0.004	10±8	130
0.035±0.003	9±6	150
0.044±0.004	9.6±2.1	180
0.045±0.005	4.4±1.4	200
0.052±0.005	3.4±1.1	220

Nevertheless reaction system transition from homogeneous to heterogeneous (such as emulsion), due to temperature or pressure change leads to major variation of reactivity ratios (see for example line 1 and 2 of Table 9).

(2) *Chemical structure and reactivity*

Several trends on reactivity according to the different chemical functions can be highlighted. Olefins, vinyl ethers, allyl compounds, vinylene compounds and fluorinated olefins containing either one or two fluorines are, as general rule, less reactive than ethylene toward ethylene radical and their r_{ethylene} is in the range of 1 to 10. Vinyl esters and vinyl amines have about the same reactivity as ethylene: r_{ethylene} values are close to unity. All other monomers, based on a heteroatom in α of the double bond, other than nitrogen or oxygen (such as silicon, phosphorus, sulfur ...) and most halo-olefins are somewhat more reactive than ethylene: their r_{ethylene} values will be in the range of 0.1 to 1. Acrylic, maleic, and fumaric derivatives (nitriles, esters, or acids) are much more reactive than ethylene: r_{ethylene} values are substantially less than 0.1.

The considerations in the previous paragraph have only to do with the relative rates of incorporation of monomers into a copolymer. Something also should be said regarding the overall reaction rate at which a copolymerization might take place. In general, these compounds, which do not give resonance-stabilized radicals (acrylic esters, vinyl compounds,

olefins, etc), have little or no effect on polymerization rate. The rate is roughly the one observed for ethylene homopolymerization.

When the radical derived from comonomer is resonance stabilized, the rate of monomer addition will be decreased. For instance, when such a monomer is present to a low extent in the polymerization feed and r_{ethylene} is low, the comonomer will be a strong delaying agent. Examples of such monomer are butadiene, isoprene, styrene, and acrylonitrile.

Finally the copolymerizations of carbon monoxide, carbon dioxide, and sulfur dioxide do not obey to the normal copolymer model (k_{11} , k_{12} , k_{21} , k_{22}) and hence cannot be described by kinetic parameters which take into account only these reactions (r_1 , r_2). For example, Furrow [272] has shown that carbon dioxide will react with growing polyethylene chains in a free-radical reaction, but that it terminates the chains giving carboxylic acids. It does not copolymerize in the usual sense (which would give polyesters). Carbon monoxide and sulfur dioxide appear not to obey to the normal copolymer curve of feed composition versus polymer composition [273]. It has been reported that these compounds form a complex with ethylene which is more reactive than free CO or SO₂. Copolymerization has been carried out with ethylene and these monomers, and polyketones and polysulfones are the resultant products.

b) Copolymerization under “low pressure” polymerization conditions

Recently, some academics papers described the copolymerization of non-polar olefins with polar vinyl monomers under mild conditions. AIBN for example was used to initiate the copolymerization of MA with α -olefins and ethylene [274]. Insertion of ethylene is up to 40% but yield remains very low (0.2 g maximum produced in 18 hours).

This copolymerization was activated by adding a Lewis acid, such as Al₂O₃ [274], Sc(OTf)₃ [275]. These acids improve both yield and olefin insertion (insertion up to 50% and up 0.3 g of copolymer produced using the same conditions). This activation effect by Lewis acid has been predicted by Clark [276, 277], which calculated for the addition in gas phase of methyl radical on ethylene that the activation energy decrease from 60.3 kJ/mol to 25.1 kJ/mol for respectively free ethylene and ethylene complexed with Li⁺. Beside these effects, additions of Lewis acid induce a decrease of molecular weight of the polymer.

Sen et al. [278, 279] investigated the effect of a wide range of Lewis acids on the copolymerization of 1-hexene with MA. This study indicates a strong correlation between the strength of the interaction of the acid with a carbonyl of an acrylate group and the acids

ability to promote acrylate/1-hexene copolymerization (Figure 53). Moreover, they demonstrated that the activation effect of the acid is proportional to the acid concentration.

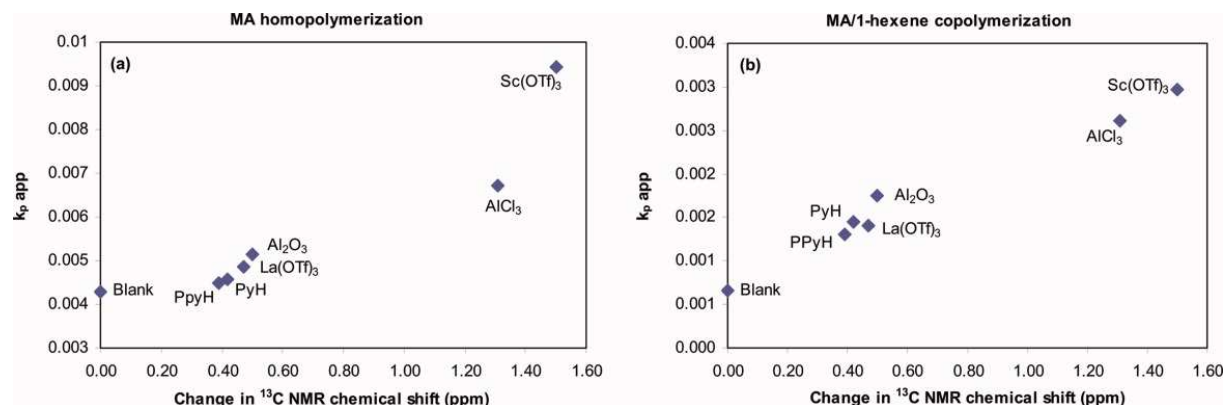


Figure 53. Copolymerization rate versus change in ^{13}C NMR chemical shift of the monomer carbonyl carbon [278]

With ethylene, copolymers produced have an alternating character and contain only isolated units of ethylene. In order to improve the copolymerization control in molecular weight and monomer insertion, controlled radical polymerizations have been developed.

c) Copolymerization thanks to controlled radical polymerization

Corresponding CRP techniques have been presented in the previous section.

(1) Nitroxide Mediated Polymerization

Sen [280] reported the copolymerization of MA with olefins from ethylene to 1-octene. Insertion of non-polar monomer remained below 15%, and only isolated units were observed. Evolution of molecular weight and polydispersity index evidenced a controlled radical copolymerization, however molecular weight remained low ($M_n < 10^4$ g/mol and $\text{PDI} < 1.1$). Yield was also extremely low: maximum of 0.5 g in 30 hours of reaction time.

(2) Reversible Addition Fragmentation Chain Transfer

Klumperman [281] copolymerized BuA or MMA with 1-octene by RAFT polymerization. Insertion up to 20% of octene was obtained, but molecular weight remains extremely low ($M_n < 1000$ g/mol).

Sen [282] also reported the copolymerization of MA with olefins from ethylene to 1-decene. Insertion of the non-polar unit is under 20%, and only isolated units were obtained.

(3) *Iodide Degenerative Transfer Polymerization*

Sen [283] reported the synthesis of an alternating copolymer of 1-octene or ethylene with MA, in presence of CH₃I or ethyl iodoacetate, with or without AlCl₃ to activate the non polar olefins insertion.

Sen [284] also reported the copolymerization of non-polar olefins with vinyl acetate. This polymerization occurs in pure vinyl acetate at 70°C with AIBN as initiator. Up to 40% of non-polar olefin can be inserted, but Mn remained below 10⁴ g/mol.

In both publications, the controlled behavior of the polymerization was not fully determined. Only the low PDI and the evolution of molecular weight with ethyl iodoacetate or CH₃I concentration indicated a controlled radical copolymerization.

Surprisingly, IDTP allows the insertion of ethylene units randomly distributed in the polymer chain. Ethylene long sequences have been identified by ¹³C NMR (peak at 30 ppm).

(4) *Atom Transfer Radical Polymerization*

Sen in 2001 [285] was the first to report the copolymerization of olefins with MA using a Cu based ATRP system. Ethylene was inserted up to 15%, and only isolated ethylene units were obtained. Once again molecular weight distributions were narrow and Mn was very low (Mn<10⁴ g/mol).

Klumperman [286-288] using an equivalent system synthesized copolymers of 1-octene with MA or MMA, with similar results (insertion up to 20%).

More recently, Matyjaszewski [289] reported the copolymerization of 1-octene with MMA or BuA using ATRP or ARGET ATRP systems. Using BuA, the incorporation of the 1-octene was about 20 % and using MMA 10 %. One important point is that the copolymerization with MMA stopped at low conversion and control over molecular weight distribution was poor, while ATRP of BuA and 1-octene proceeded to relatively high monomer conversion with lower polydispersity.

No adjacent ethylene units have been reported in all these publications.

(5) *Cobalt Mediated Radical Polymerization*

Jérôme et al [290] used CMRP to copolymerize ethylene or 1-octene with vinyl acetate. Polymerizations kinetics are extremely slow, with an important induction time, but copolymers were synthesized with insertion up to 20%. For ethylene, high molecular weights

were reached $M_n \approx 35000$ g/mol, $PDI \approx 2.4$. For 1-octene, molecular weights were lower but distributions were narrower ($PDI \approx 1.1-1.4$). The controlled behavior of the polymerization was not fully demonstrated.

CMRP as well as IDTP produced long sequences of ethylene in the copolymer chain under low pressure and low temperature. These results are quite unexpected due to the reactivity ratios of ethylene in a standard radical polymerization ($r_{\text{ethylene}} < 0.01$). Consequently these results suggest a non-standard behavior of the IDTP and CMRP during the copolymerization of ethylene with polar monomer (the reactivity ratio of ethylene must be drastically increased to produce ethylene long sequence).

2. Catalytic copolymerization

As ethylene can be polymerized by a radical or catalytic pathway, copolymerizations were also investigated using Ziegler-Natta catalysts. Very good and recent reviews [291-293] have been published; consequently, we will focus only on the major results.

a) Copolymerization of non-standard polar monomer

Until recently, most studies on the metal catalyzed coordination-insertion polymerization did not employed conventional polar vinyl monomers such as MA, MMA, VAC, etc. Instead of it, the monomers employed have a spacer between vinyl and polar function.

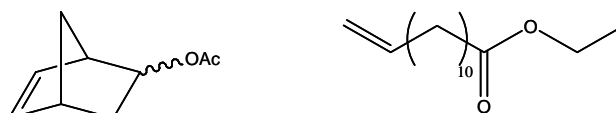


Figure 54. Examples of monomer containing “inaccessible” polar functions

These monomers allow the use of a wide range of catalysts as the polar function interact less with the metal centre. For example using vanadium-based Ziegler-Natta catalyst, Amiard copolymerized methyl-5-norbornen-2-yl ester with ethylene with 1-3% of incorporation [292].

Another method to introduce polar functions in PE is to protect the polar function. For example, monoboration of dienes with 9-BBN produces monomers which can be polymerized or copolymerized with ethylene [294]. Complexation with aluminum alkyl can also be used to hide the polar function to the metal catalyst.

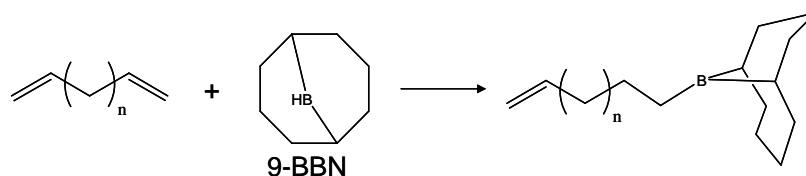


Figure 55. Example of protected polar monomer synthesis

One last very interesting method consist to the copolymerization of ethylene with 1,6-heptadiene bearing functional groups at 4-position (ester, acetal, imide and amide groups) using a Pd catalyst. A cyclization mechanism takes place giving trans-1,2-disubstitued cyclopentane group (see Figure 56). Once both double bonds are inserted the cyclopentane formed unit is too rigid to allow an efficient coordination of the polar function. Consequently, the poisoning by a polar function is highly reduced using this original method. Branched copolymers with incorporation of polar group up to 42% have been produced [295].

All these techniques show good results and copolymerization of ethylene with these monomers products up to 60% of polar function in the copolymer. Nevertheless these methods are specific and comonomers are expensive compared to standard monomers such as MA and MMA.

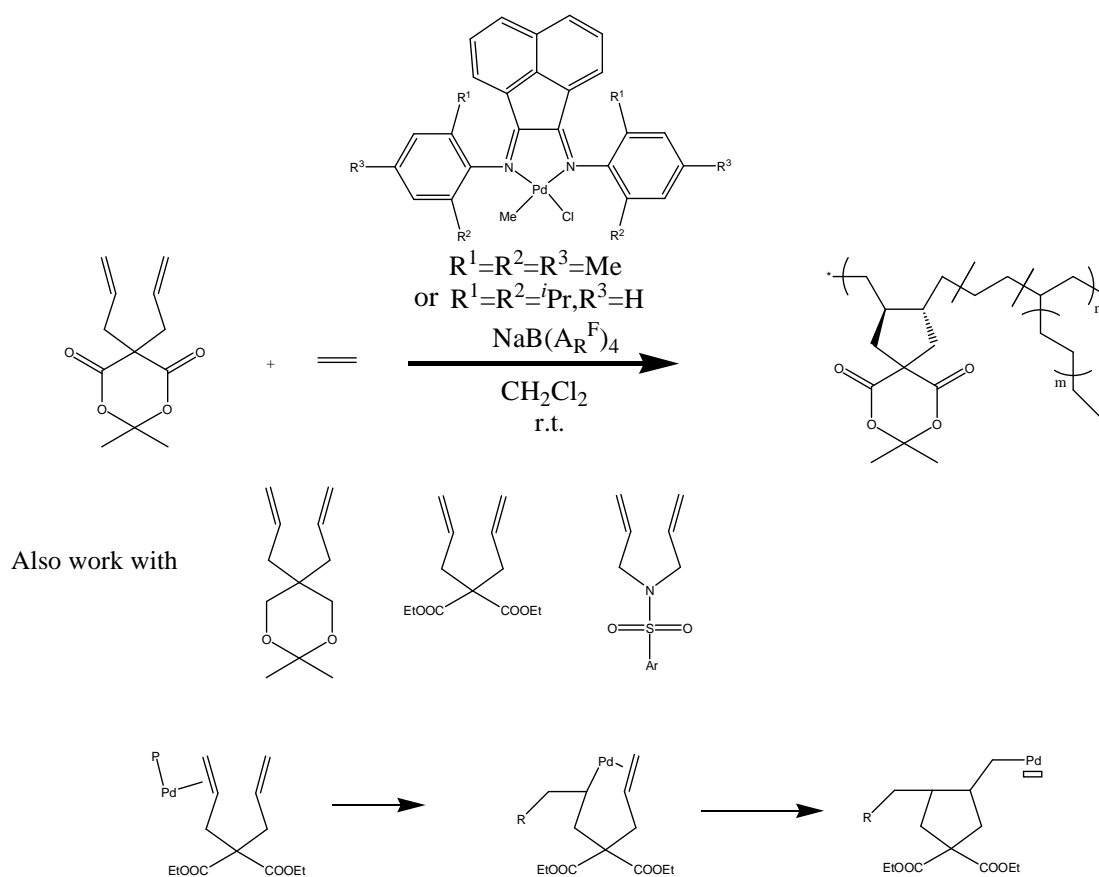


Figure 56. Copolymerization of ethylene using functional non conjugated dienes

b) Copolymerization with standard polar monomers

Several research groups have worked on the coordination-insertion copolymerization of ethylene with polar vinyl monomers for almost 40 years. No efficient systems with early transition metal have been reported up to now.

In 1996, a major breakthrough was achieved by Brookhart et al. [296], who reported copolymerization by cationic Ni(II) and Pd(II) α -diimine complexes. These catalysts were active for the copolymerization of ethylene with polar vinyl monomer such as acrylates. Nevertheless, these compounds yield highly branched polymers with polar units at the extremity of branches.

In 2002, a second breakthrough was performed by Drent et al. [217]. They obtained the copolymerization with a neutral Pd(II) complex which produced a linear copolymer of ethylene with MA.

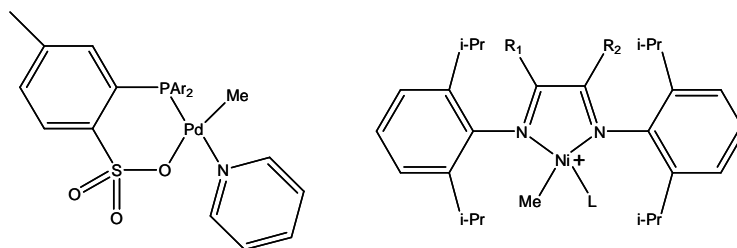


Figure 57. Examples of catalysts for the copolymerization of ethylene with polar vinyl monomer

The two major classes of ligands used for the copolymerization of ethylene with polar vinyl monomer are α -diimine and phosphine-sulfonate ligand (see Figure 57). In this section, different fundamental polar vinyl monomer copolymerizations with ethylene will be reviewed. Only single component systems will be discussed in this section. Systems with cocatalyst as MAO are excluded due to an unclear mechanism (see subchapter C).

(I) Acrylates

As we described in the previous section MA-ethylene copolymer can be synthesized thanks to controlled radical polymerization. In this case, ethylene insertions are up to 50% and molecular weights remain below 10^4 g/mol. However low M_n are due to chain transfer when polymerization is made by catalysis, contrary to CRP systems in which low M_n are due to the low conversion. Coordination-insertion polymerization process has been developed to obtain copolymers with less than 50% MA.

Due to the high oxophilicity of early transition metal all efficient catalysts described are based on late transition metals.

(a) *Cationic palladium α -diimine complex*

Brookhart [296] was the first who copolymerized efficiently MA with ethylene using a Pd α -diimine complex. Copolymers obtained were amorphous and highly branched (100 branches /1000C). The MA units were predominantly located at the end of the branches and were evenly distributed over all molecular weights. The productivity of the copolymerization of ethylene with MA was greatly reduced relatively to that of the homopolymerization of ethylene (by a factor 4). MA incorporations remain low (up to 12%) and Mn up to 10^5 g/mol were reached. Double or multiple insertions of MA have not been detected in the ethylene/MA copolymers. Control experiments [297] confirmed that the copolymerization proceeds through a coordination-insertion mechanism rather a radical or anionic polymerization.

Various other acrylic monomers (BuA, EA) were successfully used in copolymerization with ethylene.

Variation of the diimine backbone did not significantly affect the percentage of acrylates incorporation in the copolymer, although it influenced the productivities and molecular weights. However recently, Guan et al. [298] reported a Pd complex bearing cyclophane α -diimine (see Figure 58) which incorporated up to 20% of MA with a great efficiency.

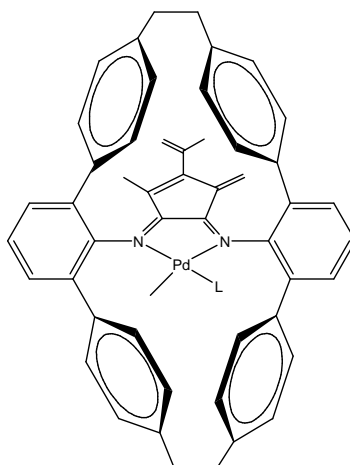


Figure 58. Guan catalyst for the ethylene MA copolymerization

The mechanism of the copolymerization of ethylene and MA catalyzed by Pd α -diimine complexes was confirmed by low temperature NMR experiments [299] as well as

theoretical calculations [300-302]. The MA insertion was mostly 2,1-insertion (>95%) to form a four-membered chelate. For more bulky acrylates such as tert-butyl acrylate 1,2-insertion also occurs. A theoretical study shows that ethylene can be further incorporated after an MA insertion, only after rearrangement to a six-membered chelate (see Figure 59).

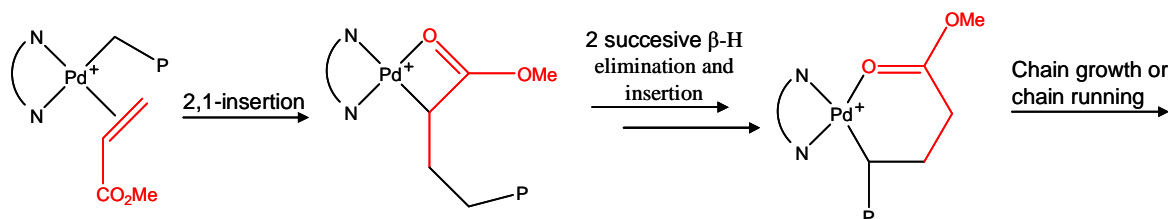


Figure 59. Methyl acrylates insertion and rearrangements catalyzed by Pd α -diimine complexes

(b) *Neutral palladium Phosphine-sulfonate catalyst*

In 2002 Drent et al. [217] obtained a linear copolymer of ethylene and MA (less than 1 branch /1000C) with MA incorporation up to 10%. No consecutive acrylate insertions were observed. Once again, with this phosphine sulfonate ligand, catalytic copolymerizations were performed with various acrylic monomers such as n-butyl, tert-butyl, and benzyl acrylates.

Mecking [303] using DMSO as ligand (occupying the vacancy for ethylene coordination) synthesized copolymer of ethylene with an MA content up to 52%.

With this catalyst, no rearrangements occur after MA insertion. Consequently, the MA units are located in the main linear chain.

(c) *Nickel catalysts*

Nickel catalysts exhibit low activities and low incorporation of MA compared to their Pd counterparts. Ziegler et al. [302] investigated the fundamental differences between Pd and Ni catalyst for the copolymerization of ethylene with MA. The most important difference between Pd and Ni is an initial poisoning of the catalyst by the O-binding of MA due to the higher oxophilicity of Ni.

Johnson [304, 305] reported a copolymerization using Ni α -diimine complex at high temperature (120°C) and pressure (340 bar). Less than 1% of acrylates was inserted in a moderately branched copolymer (50 branches /1000C).

Marks [306] also reported the ethylene MA copolymerization with Ni bimetallics complexes under mild conditions: 7 bar of ethylene pressure at 25°C. Up to 10% of MA was inserted in a moderately branched copolymer (30 branches/1000C). The mechanism proposed

to explain this high activity is O-binding on the other Ni to release the vacancy, thus allowing the further ethylene coordination-insertion.

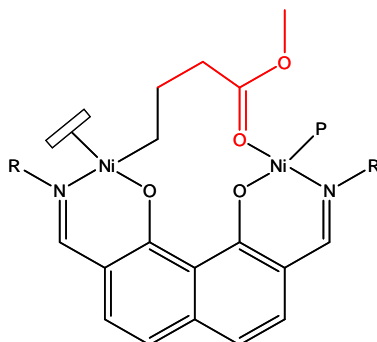


Figure 60. Proposed resting state after acrylate insertion for bimetallic complex

(2) *Methacrylates*

Methacrylates coordination-insertion copolymerization with ethylene is more challenging than acrylates. The coordination ability of 1,1-disubstituted olefins to metal center is indeed significantly decreased as compared to that of monosubstituted olefins. Indeed α -diimine and phosphine-sulfonate aforementioned catalysts which are active in copolymerization of ethylene with MA, have been reported inefficient for the copolymerization with MMA. One explanation is the impossibility of β -H elimination after a 1,2-insertion (the favorable insertion). Consequently, stable five-membered cyclic chelates are formed and cannot undergo further insertion of monomer. For example, Sen [307] was able to fully characterize this phenomenon.

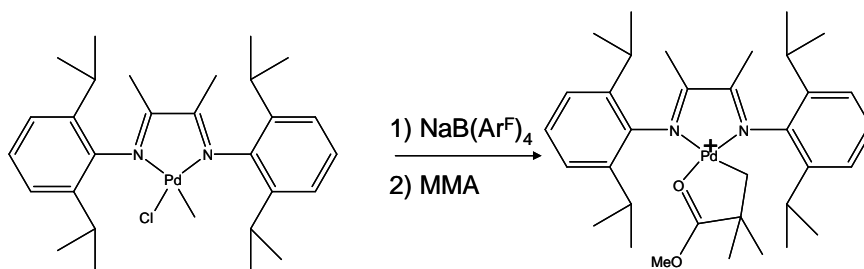


Figure 61. Reaction of MMA with Pd catalyst

In 2001, Gibson [308] produced ethylene/MMA copolymers using nickel catalysts with [P-O] ligand. Copolymers have low molecular weight and exhibit only chain-end MMA unit. This experimental result suggested that the chain-end MMA unit was formed via a mechanism involving 2,1-insertion of MMA into the growing chain following by β -H elimination. Marks [306] also managed to copolymerize ethylene with MMA, with incorporation up to 10% thanks to bimetallic catalysts.

Numerous other studies report the copolymerization of ethylene with MMA but in most cases, a MAO cocatalyst was added [293]. This result should be interpreted carefully because careful polymer separations often show that in fact two homopolymers were synthesized.

(3) Acrylonitrile

As for methacrylates, the major issue with acrylonitrile is the initial poisoning by N-binding to the metal. Consequently addition of AN prevents from not only the copolymerization but also the homopolymerization of ethylene. Various Pd catalysts were tested for this copolymerization but none was efficient [293].

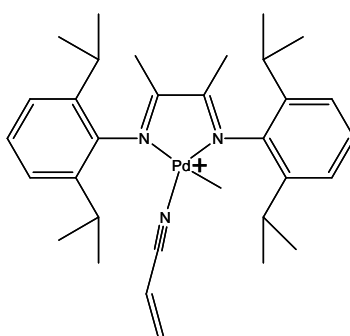


Figure 62. Acrylonitrile poisoning of Pd complexes

In 2007 Nozaki et al. [309] used a Pd phosphine-sulfonate complex which catalyzed the copolymerization of ethylene with AN. Incorporation of AN was up to 10% in linear copolymers.

(4) Vinyl acetate

For VAc, an other phenomenon contributed to the difficulty of the copolymerization with ethylene via a insertion-coordination mechanism. Brookhart et al [310] showed that for Pd and Ni α -diimine complexes the β -OAc elimination after 2,1-insertion of VAc (the favored insertion) is the major issue (see Figure 63). Moreover, for VAc, no initial O-binding seems to exist. Mecking [311] found similar results for [N-O]Ni complexes.

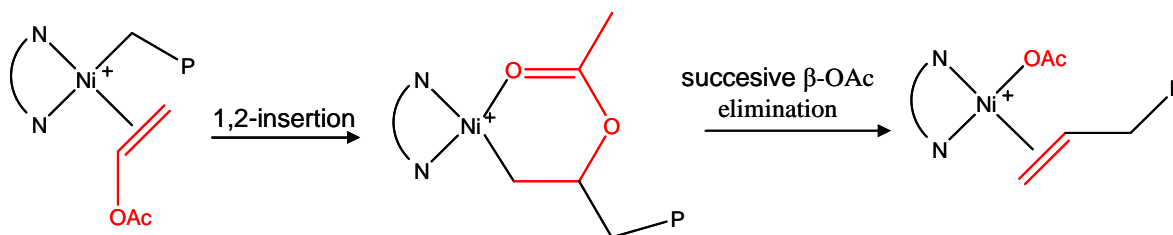


Figure 63. Insertion-elimination of vinyl acetate unit

Nozaki et al. [312] found a Pd complex which provides the copolymerization of ethylene with VAc. Insertion remains below 2% and molecular weights do not exceed 10^4 g/mol. This low molecular weight was due to a β -OAc elimination which terminates the growing polymer chain.

(5) Vinyl halides

The coordination-insertion copolymerization of ethylene with vinyl halides is limited due to the predominant β -halogen elimination (see Figure 64).

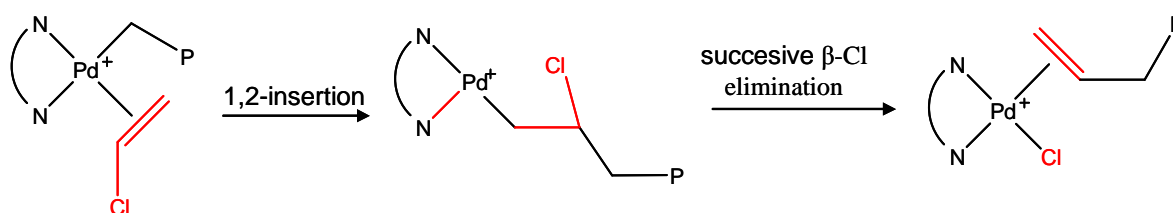


Figure 64. Insertion-elimination of vinyl chloride unit

Recently Jordan et al. [313] reported the copolymerization of ethylene with vinyl fluoride by using phosphine-sulfonate palladium complexes. This copolymerization is only efficient with fluoride vinyl. The vinyl fluoride content is below 1%. The actual direction of the vinyl halides insertion (1,2 or 2,1) remains unclear.

(6) Vinyl ether

Vinyl ether is theoretically one of the most challenging monomers to copolymerize by coordination-insertion mechanism. Indeed, these monomers are likely to undergo cationic polymerization in the presence of electrophilic metal compounds. Moreover, after insertion β -OR elimination is a favored reaction (see Figure 65).

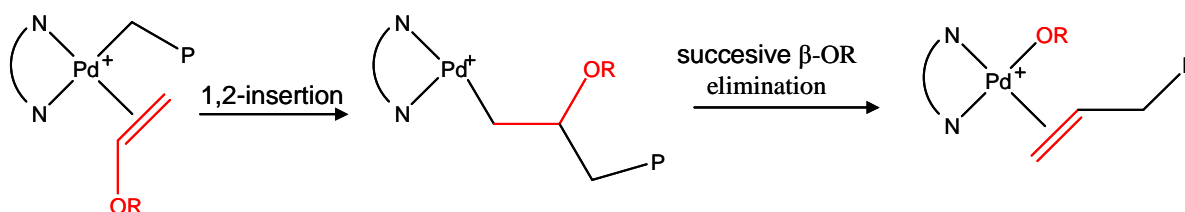


Figure 65. Insertion-elimination of vinyl ether unit

Triphenyl silyl vinyl ether was the first monomer which has been reported to undergo coordination-insertion copolymerization using a Pd α -diimine catalyst [314]. Indeed β -OSiPh₃ elimination is kinetically slow and this monomer does not undergo cationic polymerization.

Up to 20% of comonomer insertion was reported. Similar results were obtained with other silyl vinyl ethers.

Jordan [315] using phosphine-sulfonate palladium catalysts performed the copolymerization of ethylene with alkyl or aryl vinyl ether. Linear copolymers with low molecular weight were obtained ($M_n < 5000$ g/mol). Monomer insertion remained below 7%.

(7) *Other polar monomers*

Other polar monomers were investigated in the copolymerization with ethylene. In this section we will comment only the monomers possessing a polar function directly linked to the vinyl function [291-293].

Copolymerization of NIPAM (N-isopropylacrylamide) with ethylene was performed using Pd phosphine-sulfonate catalyst [316]. Insertion up to 4% has been obtained for a linear copolymer. The same system also copolymerizes NVP (N-vinyl pyrrolidinone) with ethylene [316].

Vinyl ketones were copolymerized using Pd α -diimine complexes with an insertion of 1.3% [296]. Pd phosphine-sulfonate catalyst was also used by Sen et al. [317] leading to a insertion of vinyl ketones up to 8%.

Recently Mecking et al [318] used a phosphine-sulfonate catalyst to copolymerize ethylene with methyl or phenyl vinyl sulfone comonomers. Insertions up to 14% in a linear copolymer were obtained.

3. Conclusion and results obtained at the LCPP

Copolymerization of polar vinyl monomer with ethylene remains one of the most challenging reactions. Both approaches catalytic and radical do not provide all the range of possible copolymers (in composition and comonomer available — see Figure 66).

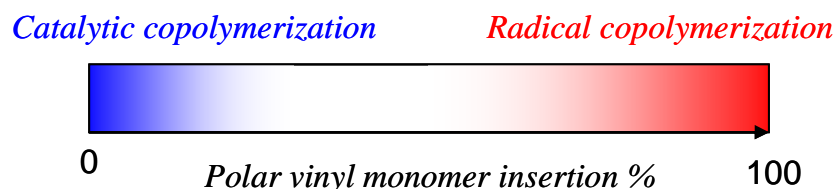


Figure 66. Range of polar insertion available up to now via radical or catalytic copolymerization

Indeed, under experimental conditions available in the laboratory ($P < 100$ bar), free or controlled radical copolymerization of ethylene with polar vinyl olefins provide only ethylene insertion up to 20% (40% using IDTP). Usually ethylene units are isolated in the polymer chain. At very high pressure, copolymers can be produced by free radical polymerization however, its structure is poorly controlled and lots of defect are present leading to not ultimate polymer properties.

Catalytic copolymerizations provide interesting results only with MA. Up to 50% of insertion is reached and successive MA units in the chain are reported. However, copolymerizations with other polar olefins such as MMA provide poor results and activities remain low.

Consequently, we were convinced at LCPP that a new approach of the copolymerization needs to be developed.

The fact that metal-carbon bond can suffer a homolytic cleavage and thus release a radical brought to us a huge interest especially if it takes place with an ethylene polymerization catalyst. Thanks to this result, a one-pot synthesis of multiblock copolymer of ethylene with polar vinyl monomer could be imagined. Indeed the ethylene polymerization catalyst initiates the formation of an ethylene block, then suffers a homolytic cleavage in order to initiate the formation of the polar vinyl monomer second block by radical mechanism. It remained to find a catalyst that releases its metal carbon bond during the ethylene polymerization to initiate a radical polymerization of the comonomer. Moreover, in order to access multiblock structure this cleavage has to be reversible (see Figure 67).

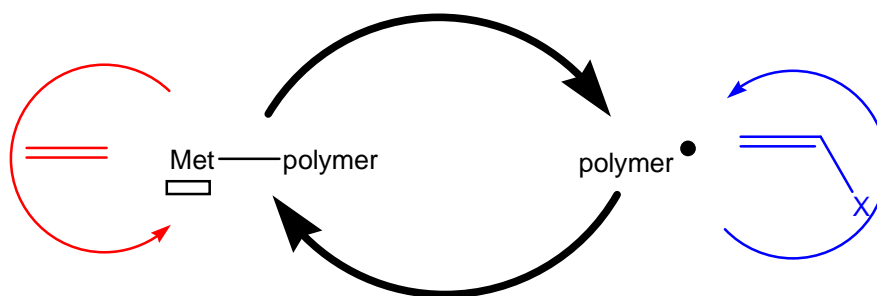


Figure 67. Hybrid radical/catalytic polymerization mechanism

Prior to this work, Alexandra Leblanc [260, 261, 319, 320] already investigated at the LCPP this hybrid system in order to synthesize copolymer of ethylene with MMA. Indeed she demonstrated that some ethylene polymerization catalyst can initiate the radical polymerization of polar vinyl monomers. Therefore using NiNO catalyst (see Figure 51), she was able to produce copolymers with ethylene molar content from 0% to 100%. She observed that the MMA insertion increases with the temperature of polymerization and decreases with the ethylene pressure (25-150 bar). The yield and copolymer composition was also impacted by the addition of phosphine such as triphenyl phosphine or tricyclohexyl phosphine. Usually the addition of phosphine increases the polar monomer insertion and decreases the yield of the copolymerization. Copolymer synthesized exhibit melting point even at MMA content of 25%. This may indicate that copolymers synthesized are not statistical but must contain ethylene blocks.

However the exact nature of copolymers produced remains unclear as well as the mechanism. ^{13}C NMR indicates that the copolymer synthesized must be diblock or composed of few blocks as the end block NMR signal was not identified in the spectrum. However, careful extraction by various solvent evidences that copolymers are produced. Moreover NiNO did not copolymerize efficiently other polar vinyl monomers such as BuA. She obtained similar results with NiPO as catalyst/initiator of the copolymerization

From these pioneer uncompleted investigations, the present manuscript will develop, understand and improve the original hybrid method of polymerization: a radical/catalytic “chain shuttling” polymerization (see Figure 67).

The initial idea of this work was to add an additional source of radical in order to improve this system by increasing the frequency of “shuttling” between the two mechanisms. The shuttling mechanism will be studied with and without the additional radical source. Then the copolymerization using this system with several polar vinyl monomer and ethylene will be investigated.

Before investigating the hybrid mechanism, we will focus first on the basic concept of ethylene radical polymerization and copolymerization under medium ethylene pressure conditions (up to 250 bar). Indeed there is a lack of study of this polymerization in our range of experimental conditions ($P < 250$ bar and $T < 100^{\circ}\text{C}$).

References:

- [1] P. Arjunan, "Global trends in polyolefins products/processes/catalysts," in *ACS Workshop Conference "Advances in Polyolefins VII"*, 2009.
- [2] W. Kaminsky *Macromol. Chem. Phys.*, vol. 209, p. 459, 2008.
- [3] A. J. Peacock, *Handbook of Polyethylene: Structures, Properties, and Applications*. Marcel Dekker, 2000.
- [4] R. C. Reaid, J. M. Prausnitz, and B. E. Poling, *The Properties of Gases and Liquids*. 1988.
- [5] J. Chickos, T. Wang, and E. Sharma *J. Chem. Eng. Data*, vol. 53, p. 481, 2008.
- [6] T. Tork, G. Sadowski, W. Arlt, A. D. Haan, and G. Krooshof *Fluid Phase Eq.*, vol. 163, p. 61, 1999.
- [7] H. Dörr, M. Kinzl, and G. Luft *Fluid Phase Eq.*, vol. 178, p. 191, 2001.
- [8] J. Gross and G. Sadowski *Ind. Eng. Chem. Res.*, vol. 40, p. 1244, 2001.
- [9] J. Brandrup, E. H. Immergut, and E. A. Grulke, *Polymere handbook*. WILEY-INTERSCIENCE, 1999.
- [10] K. S. Pitzer, L. Guttman, and E. F. Westrum *J. Am. Chem. Soc.*, vol. 68, p. 2209, 1946.
- [11] D. R. Lide, *CRC Handbook of Chemistry and Physics*. CRC Press, 2005.
- [12] F. Hofmann *Chem. Ztg.*, vol. 57, p. 5, 1933.
- [13] V. N. Ipatieff and H. Pines *Ind. Eng. Chem.*, vol. 27, p. 1364, 1935.
- [14] E. Desparmet *Bull. Soc. Chim.*, vol. 3, p. 2047, 1936.
- [15] A. D. Dunstan *Trans. Faraday Soc.*, vol. 32, p. 227, 1936.
- [16] V. N. Ipatieff and B. B. Corson *Ind. Eng. Chem.*, vol. 28, p. 860, 1936.
- [17] B. W. Malisher *Petroleum Z.*, vol. 32, p. 1, 1936.
- [18] K. Ziegler and H. Gellert *Angew. Chem.*, vol. 64, p. 323, 1952.
- [19] K. Ziegler, H. Gellert, E. Holzkamp, and G. Wilke *Angew. Chem.*, vol. 67, p. 425, 1955.
- [20] H. V. Pechmann. *Ber.*, vol. 31, p. 2643, 1898.
- [21] F. Bamberger and F. Tschirner *Ber.*, vol. 33, p. 959, 1900.
- [22] S. W. Kantor and R. C. Osthoff *J. Am. Chem. Soc.*, vol. 75, p. 931, 1953.
- [23] R. Raff and E. Lyle, *Crystalline olefin polymers*. John Wiley & sons Inc., 1965.
- [24] S. C. Lind and G. Glockler *J. Am. Chem. Soc.*, vol. 51, p. 2811, 1929.
- [25] F. Fischer and H. Tropsch *US 1746464*, 1926.
- [26] H. Koch and G. Ibing *Brennstoff-Chem.*, vol. 16, p. 141, 1935.
- [27] H. R. Arnold and E. C. Herrick *US 2726231*, 1953.
- [28] W. H. Carothers, J. W. Hill, J. E. Kirby, and R. A. Jacobson *J. Am. Chem. Soc.*, vol. 52, p. 5279, 1930.
- [29] W. Hahn *Makromol. Chem.*, vol. 64, p. 155, 1955.
- [30] R. Day *Am. Chem. J.*, vol. 8, p. 153, 1886.
- [31] V. Ipatiev *Zhu. Russ. Fiz.-Khi. Obs.*, vol. 43, p. 1420, 1912.
- [32] F. E. Frey and D. F. Smith *Ind. Eng. Chem.*, vol. 20, p. 948, 1928.
- [33] G. Egloff and R. E. Schaad *J. Inst. Petroleum Technol.*, vol. 19, p. 800, 1933.
- [34] M. E. P. Friedrich and C. S. Marvel *J. Am. Chem. Soc.*, vol. 52, p. 376, 1930.
- [35] W. H. Carothers, J. W. Hill, J. E. Kirby, and R. A. Jacobson *J. Am. Chem. Soc.*, vol. 52, p. 5279, 1930.
- [36] M. Otto *Brennstoff-Chem.*, vol. 8, p. 27, 1927.
- [37] O. Beeck and F. F. Rust *J. Chem. Phys.*, vol. 9, p. 480, 1941.
- [38] F. O. Rice and W. D. Walters *J. Am. Chem. Soc.*, vol. 63, p. 1701, 1941.
- [39] C. J. M. Fletcher and G. K. Rollefson *J. Am. Chem. Soc.*, vol. 58, p. 2135, 1936.
- [40] O. K. Rice and D. V. Sickman *J. Am. Chem. Soc.*, vol. 57, p. 1384, 1935.
- [41] D. V. Sickman and O. K. Rice *J. Chem. Phys.*, vol. 4, p. 608, 1936.
- [42] P. L. Cramer *J. Am. Chem. Soc.*, vol. 56, p. 12, 1934.
- [43] R. D. McDonald and R. G. W. Norrish *Proc. Roy. Soc.*, vol. 157, p. 480, 1936.
- [44] H. S. Taylor and J. C. Jungers *Trans. Faraday Soc.*, vol. 33, p. 1353, 1937.
- [45] G. G. Joris and J. C. Jungers *Bull. Soc. Chim. Belges*, vol. 47, p. 135, 1938.
- [46] D. J. L. Roy and E. W. R. Steacie *J. Chem. Phys.*, vol. 9, p. 829, 1941.
- [47] D. J. L. Roy and E. W. R. Steacie *J. Chem. Phys.*, vol. 10, p. 676, 1942.
- [48] H. Habeeb, D. J. L. Roy, and E. W. R. Steacie *J. Chem. Phys.*, vol. 10, p. 261, 1942.
- [49] E. W. R. Steacie and D. J. L. Roy *J. Chem. Phys.*, vol. 11, p. 164, 1943.
- [50] D. J. L. Roy *Can. Chem. Process Inds.*, vol. 28, p. 430, 1944.
- [51] Y. Konaka *J. Soc. Chem. Ind. Japan*, vol. 39, p. 447, 1936.
- [52] Y. Konaka *J. Soc. Chem. Ind. Japan*, vol. 40, p. 236, 1937.
- [53] Y. Konaka *J. Soc. Chem. Ind. Japan*, vol. 41, p. 22, 1938.
- [54] Y. Konaka *J. Soc. Chem. Ind. Japan*, vol. 43, p. 330, 1940.
- [55] Y. Konaka *J. Soc. Chem. Ind. Japan*, vol. 43, p. 363, 1940.

-
- [56] M. Koidzumi *J. Chem. Soc. Japan*, vol. 64, p. 257, 1943.
- [57] E. W. Fawcett, R. O. Gibson, and M. W. Perrin *US 2153553*, 1937.
- [58] M. W. Perrin, J. G. Paton, and E. G. Williams *US 2188465*, 1940.
- [59] R. A. Hines, W. M. D. Bryant, A. W. Larchar, and D. C. Pease *Ind. Eng. Chem.*, vol. 49, p. 1071, 1957.
- [60] D. Chezzazzi, M. Ceppatelli, M. Santoro, R. Bini, and V. Schettino *Nat. Mat.*, vol. 3, p. 470, 2001.
- [61] S. L. Aggarwal and O. J. Sweeting *Chem. Rev.*, vol. 57, p. 665, 1957.
- [62] E. Field and M. Feller *US 26912647*, 1955.
- [63] W. J. Cervený, D. E. Burney, and G. H. Weisemann *US 2685577*, 1955.
- [64] L. Squires *US 2395381*, 1946.
- [65] G. M. Whitman and S. L. Scott *US 2467245*, 1949.
- [66] M. Hagiwara, H. Mitsui, S. Machi, and T. Kagiya *J. Polym. Sci., Part A: General Papers*, vol. 6, p. 609, 1968.
- [67] M. Hagiwara, H. Mitsui, S. Machi, and T. Kagiya *J. Polym. Sci., Part A-1: Polym. Chem.*, vol. 6, p. 721, 1968.
- [68] H. Hopff and R. Kern *Modern Plastics*, p. 153, 1946.
- [69] A. F. Helin, H. K. Stryker, and G. J. Mantell *J. App. Polym. Sci.*, vol. 9, p. 1797, 1965.
- [70] H. K. Stryker, A. F. Helin, and G. J. Mantell *J. App. Polym. Sci.*, vol. 9, p. 1807, 1965.
- [71] H. K. Stryker, A. F. Helin, and G. J. Mantell *J. App. Polym. Sci.*, vol. 10, p. 81, 1966.
- [72] G. J. Mantell, H. K. Stryker, A. F. Helin, D. R. Jamieson, and C. H. Wright *J. App. Polym. Sci.*, vol. 10, p. 1845, 1966.
- [73] H. K. Stryker, G. L. Mantell, and A. F. Helin *J. App. Polym. Sci.*, vol. 11, p. 1, 1967.
- [74] H. K. Stryker, G. J. Mantell, and A. F. Helin *J. Polym. Sci., Polym. Symp.*, vol. 27, p. 35, 1969.
- [75] H. K. Stryker, G. J. Mantell, and A. F. Helin *Vinyl Polym.*, vol. 1, p. 175, 1969.
- [76] T. Suwa, H. Nakajima, M. Takehisa, and S. Machi *J. Polym. Sci., Polym. Let. Ed.*, vol. 13, p. 396, 1975.
- [77] R. E. Brooks, M. D. Peterson, and A. G. Weber *US 2388225*, 1946.
- [78] M. D. Peterson *US 2388178*, 1946.
- [79] W. E. Hanford *US 2405950*, 1946.
- [80] S. G. Lyubetskii, B. A. Dolgoplosk, and B. L. Erusalimskii *Vysokomolekulyarnye Soedineniya*, vol. 3, p. 734, 1961.
- [81] S. G. Lyubetskii, B. A. Dolgoplosk, and B. L. Erusalimskii *Vysokomolekulyarnye Soedineniya*, vol. 3, p. 1000, 1961.
- [82] S. G. Lyubetskii, B. A. Dolgoplosk, and B. L. Erusalimskii *Vysokomolekulyarnye Soedineniya*, vol. 4, p. 533, 1962.
- [83] R. H. Wiley, N. T. Lipscomb, F. J. Johnston, and J. E. Guillet *J. Polym. Sci.*, vol. 57, p. 867, 1962.
- [84] S. Machi and M. Hagiwara, M. Gotoda, and T. Kagiya *J. Polym. Sci.*, vol. 2, p. 765, 1964.
- [85] T. Kagiya, S. Machi, M. Gotoda, and K. Fukui *Kobunshi Kagaku*, vol. 22, p. 752, 1965.
- [86] S. Machi, T. Sakai, T. Tamura, M. Gotoda, and T. Kagiya *J. Polym. Sci., Part B: Polym. Let.*, vol. 3, p. 709, 1965.
- [87] S. Machi, T. Tamura, S. Fujioka, M. Hagiwara, M. Gotoda, and T. Kagiya *J. App. Polym. Sci.*, vol. 9, p. 2537, 1965.
- [88] S. Machi, M. Hagiwara, M. Gotoda, and T. Kagiya *J. Pol. Sci., Part A-1: Polym. Chem.*, vol. 4, p. 1517, 1966.
- [89] S. Machi, M. Hagiwara, M. Gotoda, and T. Kagiya *Bull. Chem. Soc. Jap.*, vol. 29, p. 675, 1966.
- [90] S. Machi, M. Hagiwara, M. Gotoda, and T. Kagiya *J. Polym. Sci., Part A: General Papers*, vol. 3, p. 2931, 1965.
- [91] S. Machi, M. Hagiwara, and T. Kagiya *J. Polym. Sci., Polym. Let. Ed.*, vol. 4, p. 1019, 1966.
- [92] J. S. Rowlinson and M. J. Richardson *Adv. Chem. Phys.*, vol. 2, p. 85, 1959.
- [93] S. Machi, S. Kise, M. Hagiwara, and T. Kagiya *J. Polym. Sci., Part B: Polym. Let.*, vol. 4, p. 585, 1966.
- [94] S. Machi, S. Kise, and T. Kagiya *Kogyo Kagaku Zasshi*, vol. 69, p. 1892, 1966.
- [95] H. Mitsui, F. Suganuma, S. Machi, M. Hagiwara, and T. Kagiya *J. Polym. Sci., Polym. Let. Ed.*, vol. 5, p. 997, 1967.
- [96] F. Suganuma, H. Mitsui, S. Machi, M. Hagiwara, and T. Kagiya *J. Polym. Sci., Part A-1: Polym. Chem.*, vol. 6, p. 3127, 1968.
- [97] F. Suganuma, S. Machi, H. Mitsui, M. Hagiwara, and T. Kagiya *J. Polym. Sci., Part A-1: Polym. Chem.*, vol. 6, p. 2069, 1968.
- [98] S. G. Lyubetskii *Zhurnal Prikladnoi Khimii*, vol. 35, p. 141, 1962.
- [99] V. F. Gromov and P. M. Khomiskovskii *Russ. Chem. Rev.*, vol. 48, p. 1943, 1979.
- [100] A. Shostenko and V. Myshkin *Doklady Akad. Nauk SSSR*, vol. 246, p. 1429, 1979.
- [101] K. Saito and T. Saegusa *Makromol. Chem.*, vol. 117, p. 86, 1968.
- [102] T. Yatsu, T. Ohno, H. Maki, and H. Fujii *Macromolecules*, vol. 10, p. 243, 1977.
-

- [103] P. Matkovskii and L. Russiyan *Doklady Chem.*, vol. 395, p. 54, 2001.
- [104] K. Vyakaranam, J. B. Barbour, and J. Michl *J. Am. Chem. Soc.*, vol. 128, p. 5610, 2006.
- [105] W. Rabel and K. Uebereitter *Ber. Bunsenges. Phys. Chem.*, vol. 514, p. 710, 1963.
- [106] V. Jaacks and F. R. Mayo *J. Am. Chem. Soc.*, vol. 87, p. 3371, 1965.
- [107] P. Ehrlich and G. A. Mortimer *Adv. Polymer Sci.*, vol. 7, p. 386, 1970.
- [108] P. C. Lim and G. Luft *Makromol. Chem.*, vol. 184, p. 207, 1983.
- [109] S. Beuermann and M. Buback *Prog. Polym. Sci.*, vol. 27, p. 191, 2002.
- [110] R. O. Symcox and P. Ehrlich *J. Am. Chem. Soc.*, vol. 84, p. 531, 1962.
- [111] A. L. Shiers, B. F. Dodge, and R. H. Bretton *Chem. Eng. Symp. Ser.*, vol. 2, p. 10, 1965.
- [112] P. Ehrlich, J. D. Cotman, and W. F. Yates *J. Polym. Sci.*, vol. 24, p. 283, 1957.
- [113] P. Ehrlich, R. N. Pittilo, and J. D. Cotman *J. Polym. Sci.*, vol. 32, p. 509, 1958.
- [114] R. N. Pittilo *J. Polym. Sci.*, vol. 43, p. 389, 1960.
- [115] N. Smenoff *Chem. Rev.*, vol. 6, p. 347, 1929.
- [116] F. R. Mayo and A. A. Miller *J. Am. Chem. Soc.*, vol. 80, p. 2493, 1958.
- [117] F. R. Mayo, A. A. Miller, and G. A. Russell *J. Am. Chem. Soc.*, vol. 80, p. 2500, 1958.
- [118] F. R. Mayo *J. Am. Chem. Soc.*, vol. 80, p. 2497, 1958.
- [119] F. R. Mayo *J. Am. Chem. Soc.*, vol. 80, p. 2465, 1958.
- [120] B. G. Kwag and K. Y. Choi *Ind. Eng. Chem. Res.*, vol. 33, p. 211, 1994.
- [121] R. Dhib and N. Al-Nidawy *Chem. Eng. Sci.*, vol. 57, p. 2735, 2002.
- [122] P. Becker, M. Buback, and J. Sandmann *Macromol. Chem. Phys.*, vol. 203, p. 2113, 2002.
- [123] M. Buback, B. Fischer, S. Hinrichs, S. Jauer, J. Meijer, and J. Sandmann *Macromol. Chem. Phys.*, vol. 208, p. 772, 2007.
- [124] R. K. Laird, A. G. Morrell, and L. Seed *Discussions Faraday Soc.*, vol. 22, p. 126, 1956.
- [125] R. H. Wiley, N. T. Lipscomb, C. F. Parrish, and J. E. Guillet *J. Polymer Sci.*, vol. 2, p. 2503, 1964.
- [126] L. E. Kukacka, P. Colombo, and M. Steinberg *J. Polymer Sci.*, vol. 16, p. 579, 1967.
- [127] S. S. Medvedev, A. D. Abkin, P. M. Khomikovskii, G. N. Gerasimov, V. F. Gromov, Y. A. Chikin, V. A. Tsingister, A. L. Auer, M. K. Yakovleva, L. P. Mezhirova, A. V. Matveeva, and Z. G. Bezzubik *Vysokomolekulyarnye Soedineniya*, vol. 2, p. 1960, 1960.
- [128] S. S. Medvedev, A. D. Abkin, P. M. Khomikovskii, G. N. Gerasimov, V. F. Gromov, Y. A. Chikin, V. A. Tsingister, A. L. Auer, M. K. Yakovleva, L. P. Mezhirova, A. V. Matveeva, and Z. G. Bezzubik *Polym. Sci. USSR*, vol. 2, p. 457, 1966.
- [129] S. Munari and S. Russo *J. Polym. Sci.*, vol. 4, p. 773, 1966.
- [130] G. G. Meisels *J. Am. Chem. Soc.*, vol. 87, p. 950, 1965.
- [131] H. Mitsui, S. Machi, M. Hagiwara, and T. Kagiya *J. Polym. Sci.*, vol. 4, p. 881, 1966.
- [132] M. J. Roedel *J. Am. Chem. Soc.*, vol. 75, p. 6110, 1953.
- [133] W. T. Wickham *J. Polym. Sci.*, vol. 60, p. 68, 1962.
- [134] T. J. V. der Molen in *IUPAC-conference*, p. 777, 1969.
- [135] C. Walling and A. Padwa *J. Am. Chem. Soc.*, vol. 83, p. 2207, 1961.
- [136] C. Walling and A. Padwa *J. Am. Chem. Soc.*, vol. 85, p. 1597, 1963.
- [137] A. H. Willbourn *J. Polym. Sci.*, vol. 34, p. 569, 1959.
- [138] D. A. Boyle, W. Simpson, and J. D. Waldron *Polymer*, vol. 2, p. 335, 1961.
- [139] K. Casey, C. T. Elston, and M. K. Phibbs *J. Polym. Sci.*, vol. 2, p. 1053, 1964.
- [140] K. Shirayama, T. Okada, and S. Kita *J. Polym. Sci.*, vol. 3, p. 907, 1965.
- [141] G. A. Tirpak *J. Polym. Sci.*, vol. 4, p. 111, 1966.
- [142] S. Kodama, Y. Matsushima, A. Ueashi, T. Shimidzu, T. Kagiya, S. Yuasa, and K. Fukui *J. Polym. Sci.*, vol. 41, p. 83, 1959.
- [143] G. A. Mortimer and W. F. Hammer *J. Polym. Sci.*, vol. 2, p. 1301, 1964.
- [144] S. Machi, T. Tamura, M. Hagiwara, M. Gotoda, and T. Kagiya *J. Polymer Sci.*, vol. 4, p. 283, 1966.
- [145] S. Machi, T. Tamura, M. Hagiwara, M. Gotoda, T. Kagiya, W. Kawakami, K. Yamaguchi, Y. Hosaki, M. Hagiwara, and T. Suga *J. Appl. Polymer Sci.*, vol. 12, p. 1639, 1968.
- [146] J. C. Woodbrey and P. Ehrlich *J. Am. Chem. Soc.*, vol. 85, p. 1580, 1963.
- [147] F. W. Billmeyer *J. Am. Chem. Soc.*, vol. 75, p. 6118, 1953.
- [148] L. D. Moore *J. Polym. Sci.*, vol. 36, p. 155, 1959.
- [149] W. L. Peticolas *J. Polym. Sci.*, vol. 58, p. 1405, 1962.
- [150] J. K. Beasley *J. Am. Chem. Soc.*, vol. 75, p. 6123, 1953.
- [151] L. Nicolas *J. Chem. Phys.*, p. 185, 1958.
- [152] W. G. Oakes and R. B. Richards *J. Chem. Soc.*, p. 2929, 1949.
- [153] G. Natta, P. Pino, P. Corradini, F. Danusso, E. Mantica, G. Mazzanti, and G. Moraglio *J. Am. Chem. Soc.*, vol. 77, p. 1708, 1955.
- [154] K. Ziegler, E. Holzkamp, H. Breil, and H. Martin *Angew. Chem. Int. Ed. Engl.*, vol. 67, p. 541, 1955.

-
- [155] J. P. Hogan and R. L. Banks *US 2825721*, 1958.
- [156] W. Kaminsky *J. Polym. Sci., Part A: Polym. Chem.*, vol. 42, p. 3911, 2004.
- [157] E. Y.-X. Chen and T. J. Marks *Chem. Rev.*, vol. 100, p. 1361, 2000.
- [158] R. Mulhaupt *Macromol. Chem. Phys.*, vol. 204, p. 289, 2003.
- [159] V. C. Gibson and S. K. Spitzmesser *Chem. Rev.*, vol. 103, p. 283, 2003.
- [160] D. Takeuchi *Dalton Trans.*, vol. 39, p. 311, 2010.
- [161] Z. Hou and Y. Wakatsuki *Coord. Chem. Rev.*, vol. 231, p. 1, 2002.
- [162] J. Gromada, J.-F. Carpentier, and A. Mortreux *Coord. Chem. Rev.*, vol. 248, p. 397, 2004.
- [163] H. Makio, N. Kashiwa, and T. Fujita *Adv. Synth. Catal.*, vol. 344, p. 477, 2002.
- [164] J. Tian and G. W. Coates *Angew. Chem. Int. Ed.*, vol. 39, p. 3626, 2000.
- [165] Y. Suzuki, Y. Inoue, H. Tanaka, and T. Fujita *Macromol. Rapid Comm.*, vol. 25, p. 493, 2004.
- [166] S.-M. Yu and S. Mecking *J. Am. Chem. Soc.*, vol. 130, p. 13204, 2008.
- [167] R. J. Long, V. C. Gibson, A. J. P. White, and D. J. Williams *Inorg. Chem.*, vol. 45, p. 511, 2006.
- [168] W. P. Kretschmer, B. Hessen, A. Noor, N. M. Scott, and R. Kempe *J. Organomet. Chem.*, vol. 692, p. 4569, 2007.
- [169] D. A. Pennington, S. J. Coles, M. B. Hursthouse, M. Bochmann, and S. J. Lancaster *Chem. Comm.*, p. 3150, 2005.
- [170] L. G. Furlan, M. P. Gil, and O. L. Casagrande *Macromol. Rapid Comm.*, vol. 21, p. 1054, 2000.
- [171] K. Michiue and R. F. Jordan *Organometallics*, vol. 23, p. 460, 2004.
- [172] H. Lee, K. Nienkemper, and R. F. Jordan *Organometallics*, vol. 27, p. 5075, 2008.
- [173] W.-Q. Hu, X.-L. Sun, C. Wang, Y. Gao, Y. Tang, L.-P. Shi, W. Xia, J. Sun, H.-L. Dai, X.-Q. Li, X.-L. Yao, and X.-R. Wang *Organometallics*, vol. 23, p. 1684, 2004.
- [174] M. C. W. Chan, K.-H. Tam, Y.-L. Pui, and N. Zhu *Dalton Trans.*, p. 3085, 2002.
- [175] H. Hanaoka, Y. Imamoto, T. Hino, and Y. Oda *J. Organomet. Chem.*, vol. 691, p. 4968, 2006.
- [176] R. J. Long, D. J. Jones, V. C. Gibson, and A. J. P. White *Organometallics*, vol. 27, p. 5960, 2008.
- [177] E. Y. Tshuva, I. Goldberg, and M. Kol *J. Am. Chem. Soc.*, vol. 122, p. 10706, 2000.
- [178] M. Frediani, D. Sémeril, A. Comucci, L. Bettucci, P. Frediani, L. Rosi, D. Matt, L. Toupet, and W. Kaminsky *Macromol. Chem. Phys.*, vol. 208, p. 938, 2007.
- [179] H. Hagen, J. Boersma, and G. V. Koten *Chem. Soc. Rev.*, vol. 31, p. 357, 2002.
- [180] Y. Onishi, S. Katao, M. Fujiki, and K. Nomura *Organometallics*, vol. 27, p. 2590, 2008.
- [181] A. K. Tomov, V. C. Gibson, D. Zaher, M. R. J. Elsegood, and S. H. Dale *Chem. Comm.*, p. 1956, 2004.
- [182] A. Jabri, I. Korobkov, S. Gambarotta, and R. Duchateau *Angew. Chem. Int. Ed.*, vol. 46, p. 6119, 2007.
- [183] C. Redshaw, M. Rowan, D. M. Homden, M. R. J. Elsegood, T. Yamato, and C. Pérez-Casas *Chem. Eur. J.*, vol. 13, p. 10129, 2007.
- [184] T. Xu, Y. Mu, W. Gao, J. Ni, L. Ye, and Y. Tao *J. Am. Chem. Soc.*, vol. 129, p. 2236, 2007.
- [185] H. Hanaoka, Y. Imamoto, T. Hino, T. Kohno, K. Yanagi, and Y. Oda *J. Polym. Sci., Part A: Polym. Chem.*, vol. 45, p. 3668, 2007.
- [186] T. Rüther, N. Braussaud, and K. J. Cavell *Organometallics*, vol. 20, p. 1247, 2001.
- [187] B. L. Small, M. J. Carney, D. M. Holman, C. E. O'Rourke, and J. A. Halfen *Macromolecules*, vol. 37, p. 4375, 2004.
- [188] D. F. Wass *Dalton Trans.*, p. 816, 2007.
- [189] K. Albahily, E. Koc, D. Al-Baldawi, D. Savard, S. Gambarotta, T. J. Burchell, and R. Duchateau *Angew. Chem. Int. Ed.*, vol. 47, p. 5816, 2008.
- [190] M. Nabika, Y. Seki, T. Miyatake, K.-i. O. Y. Ishikawa, and K. Fujisawa *Organometallics*, vol. 23, p. 4335, 2004.
- [191] K. Yliheikkilä, K. Axenov, M. T. Räisänen, M. Klinga, M. P. Lankinen, M. Kettunen, M. Leskelä, and T. Repo *Organometallics*, vol. 26, p. 980, 2007.
- [192] G. J. P. Britovsek, V. C. Gibson, S. J. McTavish, G. A. Solan, A. J. P. White, D. J. Williams, B. S. Kimberley, and P. J. Maddox *Chem. Comm.*, p. 849, 1998.
- [193] B. L. Small, M. Brookhart, and A. M. A. Bennett *J. Am. Chem. Soc.*, vol. 120, p. 4049, 1998.
- [194] F. A. R. Kaul, G. T. Puchta, G. D. Frey, E. Herdtweck, and W. A. Herrmann *Organometallics*, vol. 26, p. 988, 2007.
- [195] D. J. Arriola, E. M. Carnahan, P. D. Hustad, R. L. Kuhlman, and T. T. Wenzel *Science*, vol. 312, p. 714, 2006.
- [196] M. W. Bouwkamp, E. Lobkovsky, and P. J. Chirik *J. Am. Chem. Soc.*, vol. 127, p. 9660, 2005.
- [197] S. C. Bart, E. J. Hawrelak, A. K. Schmisser, E. Lobkovsky, and P. J. Chirik *Organometallics*, vol. 23, p. 237, 2004.
- [198] M. Tanabiki, Y. Sunada, and H. Nagashima *Organometallics*, vol. 26, p. 6055, 2007.
- [199] L. K. Johnson, C. M. Killian, and M. Brookhart *J. Am. Chem. Soc.*, vol. 117, p. 6414, 1995.
-

- [200] T. R. Younkin, E. F. Connor, J. I. Henderson, S. K. Friedrich, and R. H. Grubbs *Science*, vol. 287, p. 2320, 2000.
- [201] Z. Guan, P. M. Cotts, E. F. McCord, and S. J. McLain *Science*, vol. 283, p. 2059, 1999.
- [202] Y. Zhang and Z. Ye *Macromolecules*, vol. 41, p. 6331, 2008.
- [203] G. Chen, P. L. Felgner, and Z. Guan *Biomacromolecules*, vol. 9, p. 1745, 2008.
- [204] C. Propeney and Z. Guan *Organometallics*, vol. 24, p. 1145, 2005.
- [205] C. T. Burns and R. F. Jordan *Organometallics*, vol. 26, p. 6737, 2007.
- [206] J. N. L. Dennett, A. L. Gillon, K. Heslop, D. J. Hyett, J. S. Fleming, C. E. Lloyd-Jones, A. G. Orpen, P. G. Pringle, D. F. Wass, J. N. Scutt, and R. H. Weatherhead *Organometallics*, vol. 23, p. 6077, 2004.
- [207] S. Ikeda, F. Ohhata, M. Miyoshi, R. Tanaka, T. Minami, F. Ozawa, and M. Yoshifuji *Angew. Chem. Int. Ed.*, vol. 39, p. 4512, 2000.
- [208] A. Ionkin and W. Marshall *Chem. Comm.*, p. 710, 2003.
- [209] I. Göttker-Schnetmann, P. Wehrmann, C. Röhr, and S. Mecking *Organometallics*, vol. 26, p. 2346, 2007.
- [210] I. Gotter-Schnetmann, B. Korthals, and S. Mecking *J. Am. Chem. Soc.*, vol. 128, p. 7708, 2006.
- [211] A. Bastero, G. Franciò, W. Leitner, and S. Mecking *Chem. Eur. J.*, vol. 12, p. 6110, 2006.
- [212] C. H. M. Weber, A. Chiche, G. Krausch, S. Rosenfeldt, M. Ballauff, L. Harnau, I. Göttker-Schnetmann, Q. Tong, and S. Mecking *Nano Letters*, vol. 7, p. 2024, 2007.
- [213] F. A. Hicks and M. Brookhart *Organometallics*, vol. 20, p. 3217, 2001.
- [214] J. C. Jenkins and M. Brookhart *J. Am. Chem. Soc.*, vol. 126, p. 5827, 2004.
- [215] M. Okada, Y. Nakayama, T. Ikeda, and T. Shiono *Macromol. Rapid Comm.*, vol. 27, p. 1418, 2006.
- [216] R. S. Rojas, G. B. Galland, G. Wu, and G. C. Bazan *Organometallics*, vol. 26, p. 5339, 2007.
- [217] E. Drent, R. V. Dijk, R. V. Ginkel, B. V. Oort, and R. I. Pugh *Chem. Comm.*, p. 744, 2002.
- [218] J. A. Olson, R. Boyd, J. W. Quail, and S. R. Foley *Organometallics*, vol. 27, p. 5333, 2008.
- [219] M. P. Shaver, L. E. N. Allan, and V. C. Gibson *Organometallics*, vol. 26, p. 2252, 2007.
- [220] P. A. Cameron, V. C. Gibson, C. Redshaw, J. A. Segal, M. D. Bruce, A. J. P. White, and D. J. Williams *Chem. Comm.*, p. 1883, 1999.
- [221] G. Talarico and V. Busico *Organometallics*, vol. 20, p. 4721, 2001.
- [222] G. Moad and D. H. Solomon, *The chemistry of the free radical polymerization*. Pergamon, 1995.
- [223] M. K. Georges, R. P. N. Veregin, P. M. Kazmaier, and G. K. Hamer *Macromolecules*, vol. 26, p. 2987, 1993.
- [224] C. J. Hawker, A. W. Bosman, and E. Harth *Chem. Rev.*, vol. 101, p. 3661, 2001.
- [225] V. Sciannamea, R. Jérôme, and C. Detrembleur *Chem. Rev.*, vol. 108, p. 1104, 2009.
- [226] J. Chiefari, Y. K. Chong, F. Ercole, J. Krstina, J. Jeffery, T. P. T. Le, R. T. A. Mayadunne, G. F. Meijs, C. L. Moad, G. Moad, E. Rizzardo, and S. H. Thang *Macromolecules*, vol. 31, p. 5559, 1998.
- [227] W. A. Braunecker and K. Matyjaszewski *Prog. Polym. Sci.*, vol. 32, p. 93, 2007.
- [228] C. Barner-Kowollik, *Handbook of RAFT Polymerization*. WILEY-INTERSCIENCE, 2008.
- [229] Y. Yutani and M. Tatamoto *Eu. 489370*, 1992.
- [230] K. Matyjaszewski, S. Gaynor, and J.-S. Wang *Macromolecules*, vol. 28, p. 2093, 1995.
- [231] S. G. Gaynor, J.-S. Wang, and K. Matyjaszewski *Macromolecules*, vol. 28, p. 8051, 1995.
- [232] J.-S. Wang and K. Matyjaszewski *Macromolecules*, vol. 28, p. 7901, 1995.
- [233] J.-S. Wang and K. Matyjaszewski *J. Am. Chem. Soc.*, vol. 117, p. 5614, 1995.
- [234] M. Kamigaito, T. Ando, and M. Sawamoto *Chem. Rev.*, vol. 101, p. 3689, 2001.
- [235] K. Matyjaszewski and J. Xia *Chem. Rev.*, vol. 101, p. 2921, 2001.
- [236] N. V. Tsarevsky and K. Matyjaszewski *Chem. Rev.*, vol. 107, p. 2270, 2007.
- [237] B. B. Wayland, G. Poszmik, S. L. Mukerjee, and M. Fryd *J. Am. Chem. Soc.*, vol. 116, p. 7943, 1994.
- [238] A. Debuigne, R. Poli, C. Jérôme, R. Jérôme, and C. Detrembleur *Prog. Polym. Sci.*, vol. 34, p. 211, 2009.
- [239] H. Yasuda, H. Yamamoto, K. Yokota, S. Miyake, and A. Nakamura *J. Am. Chem. Soc.*, vol. 114, p. 4908, 1992.
- [240] S. Collins and S. G. Ward *J. Am. Chem. Soc.*, vol. 114, p. 5460, 1992.
- [241] E. Y.-X. Chen *Chem. Rev.*, vol. 109, p. 5157, 2009.
- [242] H. Yasuda, M. furo, H. Yamamoto, A. Nakamura, S. Miyake, and N. Kibino *Macromolecules*, vol. 25, p. 5115, 1992.
- [243] M. J. Fullana, M. J. Miri, S. S. Vadhavkar, N. Kolhatkar, and A. C. Delis *J. Polym. Sci., Part A: Polym. Chem.*, vol. 46, p. 5542, 2008.
- [244] I. Kim, J.-M. Hwang, J. K. Lee, C. S. Ha, and S. I. Woo *Macromol. Rapid Comm.*, vol. 24, p. 508, 2003.
- [245] E. Ihara, T. Fujimara, H. Yasuda, T. Maruo, N. Kanehisa, and Y. Kai *J. Polym. Sci., Part A: Polym. Chem.*, vol. 38, p. 4764, 2000.

-
- [246] X.-F. Li, Y.-G. Li, Y.-S. Li, Y.-X. Chen, and N.-H. Hu *Organometallics*, vol. 24, p. 2502, 2005.
- [247] E. Ihara, Y. Maeno, and H. Yasuda *Macromol. Chem. Phys.*, vol. 202, p. 1518, 2001.
- [248] G. Tian, H. W. Boone, and B. M. Novak *Macromolecules*, vol. 34, p. 7656, 2001.
- [249] R. T. Stibrany, D. N. Schulz, S. Kacker, A. O. Patil, L. S. Baugh, S. P. Rucker, S. Zushma, E. Berluche, and J. A. Sissano *Macromolecules*, vol. 36, p. 8584, 2003.
- [250] R. Po, L. Fiocaa, N. Cardi, F. Simone, M. A. Cardaci, S. Spera, and M. Salvalaggio *Polym. Bull.*, vol. 56, p. 101, 2006.
- [251] S. S. Reddy and S. Sivaram *J. Polym. Sci., Part A: Polym. Chem.*, vol. 34, p. 3427, 1996.
- [252] L. S. Baugh and J. A. Sissano *J. Polym. Sci., Part A: Polym. Chem.*, vol. 40, p. 1633, 2002.
- [253] T. Saegusa, H. Imai, and J. Furukawa *Makromol. Chem.*, vol. 79, p. 207, 1964.
- [254] M. Nagel, W. F. Paxton, A. Sen, L. Zakharov, and A. L. Rheingold *Macromolecules*, vol. 37, p. 9305, 2004.
- [255] A. C. Albeniz, P. Espinet, R. López-Fernandez, and A. Sen *J. Am. Chem. Soc.*, vol. 124, p. 11278, 2002.
- [256] M. Nagel and A. Sen *Organometallics*, vol. 25, p. 4722, 2006.
- [257] C. Elia, S. Elyashiv-Barad, A. Sen, R. Lopez-Fernandez, A. C. Albeniz, and P. Espine *Organometallics*, vol. 21, p. 4249, 2002.
- [258] A. C. Albeniz, P. Espinet, and R. Lopez-Fernandez *Organometallics*, vol. 22, p. 4206, 2003.
- [259] X. He and Q. Wu *Appl. Organometal. Chem.*, vol. 20, p. 264, 2006.
- [260] A. Leblanc, *Copolymerization d'oléfines et de monomères polaires: à la frontière des chimies de coordination et radicalaire*. PhD thesis, Université Claude Bernard-Lyon 1, 2008.
- [261] A. Leblanc, J.-P. Broyer, C. Boisson, R. Spitz, and V. Monteil *Macromolecules*, 2010, submitted.
- [262] M. Yanjarappa and S. Sivaram *Progr. Polym. Sci.*, vol. 27, p. 1347, 2002.
- [263] R. G. Lopez, F. D'Agosto, and C. Boisson *Prog. Polym. Sci.*, vol. 32, p. 419, 2007.
- [264] R. A. Terteryan, E. E. Braudo, and A. I. Dintses *Usp. Khim.*, vol. 34, p. 666, 1965.
- [265] M. Buback and T. Dröge *Macromol. Chem. Phys.*, vol. 198, p. 3627, 1997.
- [266] M. Buback, M. Busch, K. Lovis, and F.-O. Mähling *Macromol. Chem. Phys.*, vol. 197, p. 303, 1996.
- [267] M. Buback and T. Dröge *Macromol. Chem. Phys.*, vol. 200, p. 256, 1999.
- [268] M. Buback, L. Wittkowski, S. A. Lehmann, and F.-O. Mähling *Macromol. Chem. Phys.*, vol. 200, p. 1935, 1999.
- [269] M. Buback and L. Wittkowski *Macromol. Chem. Phys.*, vol. 201, p. 419, 2000.
- [270] R. D. Burkhart and N. L. Zutty *J. Polym. Sci.*, vol. 57, p. 793, 1962.
- [271] L. Boghetich, G. A. Mortimer, and G. W. Daues *J. Polym. Sci.*, vol. 61, p. 3, 1962.
- [272] C. L. Furrow *US 3168456*, 1965.
- [273] D. E. Hudgin *US 3968082*, 1976.
- [274] R. Luo and A. Sen *Macromolecules*, vol. 39, p. 7798, 2006.
- [275] M. Nagel, D. Poli, and A. Sen *Macromolecules*, vol. 38, p. 7262, 2005.
- [276] A. H. C. Horn and T. J. Clark *J. Chem. Soc., Chem. Commun.*, p. 1774, 1986.
- [277] A. H. C. Horn and T. J. Clark *J. Am. Chem. Soc.*, vol. 125, p. 2809, 2003.
- [278] R. Luo, Y. Chen, and A. Sen *J. Polym. Sci., Part A: Polym. Chem.*, vol. 46, p. 5499, 2008.
- [279] Y. Chen and A. Sen *Macromolecules*, vol. 42, p. 3951, 2009.
- [280] B. Gu, S. Liu, J. D. Leber, and A. Sen *Macromolecules*, vol. 37, p. 5142, 2004.
- [281] R. Venkatesh, B. B. P. Staal, and B. Klumperman *Chem. Comm.*, p. 1554, 2004.
- [282] S. Liu and A. Sen *J. Polym. Sci., Part A: Polym. Chem.*, vol. 42, p. 6175, 2004.
- [283] S. Liu, B. Gu, H. A. Rowlands, and A. Sen *Macromolecules*, vol. 37, p. 7924, 2004.
- [284] S. Borkar and A. Sen *J. Polym. Sci., Part A: Polym. Chem.*, vol. 43, p. 3728, 2005.
- [285] S. Liu, S. Elyashiv, and A. Sen *J. Am. Chem. Soc.*, vol. 123, p. 12738, 2001.
- [286] R. Venkatesh and B. Klumperman *Macromolecules*, vol. 37, p. 1226, 2004.
- [287] R. Venkatesh, S. Harrisson, D. M. Haddleton, and B. Klumperman *Macromolecules*, vol. 37, p. 4406, 2004.
- [288] R. Venkatesh, F. Vergouwen, and B. Klumperman *Macromol. Chem. Phys.*, vol. 206, p. 547, 2005.
- [289] K. Tanaka and K. Matyjaszewski *Macromol. Symp.*, vol. 261, p. 1, 2008.
- [290] R. Bryaskova, N. Willet, P. Degée, P. Dubois, R. Jérôme, and C. Detrembleur *J. Polym. Sci., Part A: Polym. Chem.*, vol. 45, p. 2532, 2007.
- [291] S. D. Ittel, L. K. Johnson, and M. Brookhart *Chem. Rev.*, vol. 100, p. 1169, 2000.
- [292] L. S. Boffa and B. M. Novak *Chem. Rev.*, vol. 100, p. 1479, 2000.
- [293] A. Nakamura, S. Ito, and K. Nozaki *Chem. Rev.*, vol. 109, p. 5215, 2009.
- [294] T. C. Chung *Prog. Polym. Sci.*, vol. 27, p. 39, 2002.
- [295] S. Park, D. Takeuchi, and K. Osakada *J. Am. Chem. Soc.*, vol. 128, p. 3510, 2006.
- [296] L. K. Johnson, S. Mecking, and M. Brookhart *J. Am. Chem. Soc.*, vol. 118, p. 267, 1996.
-

-
- [297] J. Heinemann, R. Mülhaupt, P. Brinkmann, and G. Luinstra *Macromol. Chem. Phys.*, vol. 200, p. 384, 1999.
- [298] C. S. Popeney, D. H. Camacho, and Z. Guan *J. Am. Chem. Soc.*, vol. 129, p. 10062, 2007.
- [299] S. Mecking, L. K. Johnson, L. Wang, and M. Brookhart *J. Am. Chem. Soc.*, vol. 120, p. 888, 1998.
- [300] A. Michalak and T. Ziegler *J. Am. Chem. Soc.*, vol. 123, p. 12266, 2001.
- [301] D. M. Philipp, R. P. Muller, W. A. Goddard, J. Storer, M. McAdon, and M. Mullins *J. Am. Chem. Soc.*, vol. 124, p. 10198, 2002.
- [302] A. Michalak and T. Ziegler *Organometallics*, vol. 22, p. 2660, 2003.
- [303] D. Guironnet, P. Roesle, T. Runzi, I. Gottker-Schnetmann, and S. Mecking *J. Am. Chem. Soc.*, vol. 131, p. 422, 2009.
- [304] S. J. McLain, K. J. Sweetman, L. K. Johnson, and E. McCord *Polym. Mater. Sci. Eng.*, vol. 86, p. 320, 2002.
- [305] L. Johnson, A. Bennett, K. Dobbs, E. Hauptman, A. Ionkin, S. Ittel, E. McCord, S. McLain, C. Radzewich, Z. Yin, L. Wang, Y. Wang, and M. Brookhart *Polym. Mater. Sci. Eng.*, vol. 86, p. 319, 2002.
- [306] B. A. Rodriguez, M. Delferro, and T. J. Marks *J. Am. Chem. Soc.*, vol. 131, p. 5902, 2009.
- [307] S. Borkar, H. Yennawar, and A. Sen *Organometallics*, vol. 26, p. 4711, 2007.
- [308] V. C. Gibson and A. Tomov *Chem. Comm.*, p. 1964, 2001.
- [309] T. Kochi, S. Noda, K. Yoshimura, and K. Nozaki *J. Am. Chem. Soc.*, vol. 129, p. 8948, 2007.
- [310] B. S. Williams, M. D. Leatherman, P. S. White, and M. Brookhart *J. Am. Chem. Soc.*, vol. 127, p. 5132, 2005.
- [311] A. Berkefeld, M. Drexler, and H. M. M. and S. Mecking *J. Am. Chem. Soc.*, vol. 131, p. 12613, 2009.
- [312] S. Ito, K. Munakata, A. Nakamura, and K. Nozaki *J. Am. Chem. Soc.*, vol. 131, p. 14606, 2009.
- [313] W. Weng, Z. Shen, and R. F. Jordan *J. Am. Chem. Soc.*, vol. 129, p. 15450, 2007.
- [314] S. Luo and R. F. Jordan *J. Am. Chem. Soc.*, vol. 128, p. 12072, 2006.
- [315] S. Luo, J. Vela, G. R. Lief, and R. F. Jordan *J. Am. Chem. Soc.*, vol. 129, p. 8946, 2007.
- [316] K. M. Skupov, L. Piche, and J. P. Claverie *Macromolecules*, vol. 41, p. 2309, 2008.
- [317] S. Borkar, D. K. Newsham, and A. Sen *Organometallics*, vol. 27, p. 3331, 2008.
- [318] C. Bouilhac, T. Runzi, and S. Mecking *Macromolecules*, vol. 43, p. 3589, 2010.
- [319] C. Navarro, A. Leblanc, V. Monteil, R. Spitz, C. Boisson, and J.-P. Broyer *FR 2937643*, 2010.
- [320] C. Navarro, A. Leblanc, V. Monteil, R. Spitz, C. Boisson, and J.-P. Broyer *WO 2010049633*, 2010.
-

Chapter II : Study of the free radical polymerization of ethylene in organic media under mild conditions

A.	The free radical polymerization of ethylene in organic media.....	II-98
1.	Polymerization in toluene	II-98
a)	Effect of the ethylene pressure.....	II-98
b)	Kinetic investigations of the ethylene polymerization	II-101
(1)	Kinetics of polymerization.....	II-101
(2)	Effect of the initiator concentration	II-102
2.	Polymerization without solvent.....	II-103
3.	The activation by other solvents of the free radical polymerization of ethylene.....	II-105
a)	Polymerization of ethylene in THF or DEC.....	II-105
(1)	Pressure effect	II-105
(2)	Toward free radical polymerization of ethylene under low pressure.....	II-108
(3)	Kinetics of polymerization.....	II-109
b)	Comparison of the Arrhenius parameters of three solvents.....	II-110
4.	Study of the initiator	II-113
a)	Initiation efficiency of different initiator.....	II-113
b)	Toward polymerization of ethylene at low temperature.....	II-116
5.	Conclusion	II-117
B.	Phase equilibrium in the Ethylene/solvent mixture.....	II-118
1.	Solvent volume effect	II-118
2.	Other experimental evidences of the phase equilibrium	II-121
a)	Practical determination of the phase state	II-121
b)	Isodensity pressure and temperature behaviors.....	II-122
3.	Thermodynamic determination of the phase diagram.....	II-123
a)	Experimental measurement of the ethylene solubility in various solvents.....	II-123
(1)	Pressure effect	II-124
(2)	Temperature effect.....	II-124
b)	Phase diagram of Ethylene/solvent mixture	II-125
(1)	Theoretical consideration.....	II-125
(2)	Example for Ethylene/THF medium.....	II-127
(3)	Other equations of state	II-127
(4)	Effect of the solubility	II-132
(5)	Correlation to the experimental evidences.....	II-133
(6)	Effect of the solvent on the phase transition	II-134
4.	Conclusion	II-136

C.	Solvent effect in the free radical polymerization	II-137
1.	Polymerization of ethylene in various solvents.....	II-137
a)	Free ethylene radical polymerization in a wide range of solvents.....	II-138
b)	Molecular weight controlled by solvent.....	II-139
c)	No simple relation between conversion and the solvent properties.....	II-141
2.	Rationalization of the solvent effect	II-142
a)	Theoretical consideration.....	II-142
b)	Validation of the law.....	II-143
3.	Case of solvent mixtures	II-144
4.	Arrhenius parameters of Toluene/DEC/THF	II-146
a)	Relation with the solvent parameters	II-146
b)	Optimum calculation.....	II-147
5.	Solvent cohesive pressure interpretation.....	II-148
6.	Interpretation of the solvent optimum.....	II-149
7.	Case of other monomers	II-150
a)	Solvent activation effect with other monomers.....	II-150
b)	Possible interpretation of the solvent activation effect.....	II-152
8.	Conclusion	II-153
D.	Lewis acid effect on the ethylene radical polymerization.....	II-154
1.	Investigation of Lewis acids	II-154
2.	Investigation of metal alkyl and alkoxides.....	II-156
E.	Toward controlled radical polymerization	II-159
1.	RAFT	II-159
2.	Co mediated CRP.....	II-162
F.	Conclusion.....	II-164

In order to fully understand the hybrid polymerization (concept described in Chapter I) developed in the last chapter of this thesis (see Figure 1), we have to investigate the efficiency of the free radical polymerization of ethylene under our experimental conditions (ethylene pressure up to 250 bar and temperature below 100°C). Indeed the composition of the block synthesized by radical polymerization could either be purely composed of the polar monomer or contain some amounts of ethylene. Before investigating the radical copolymerization of ethylene with polar vinyl monomer, the free radical polymerization of ethylene will be discussed.

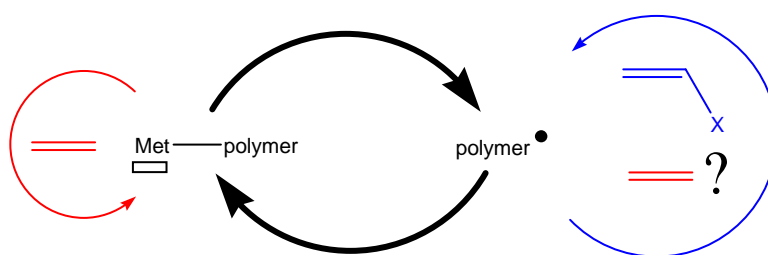


Figure 1. Hybrid radical/catalytic polymerization mechanism

Free radical polymerization of ethylene is a well-known industrial process used to synthesize LDPE. Industrially it requires severe experimental conditions: a high temperature ($T > 200^\circ\text{C}$) and a high pressure ($P > 2000$ bar). Nowadays, the free radical polymerization of ethylene under milder conditions is assumed to be inefficient. Nevertheless, as mentioned in the first chapter, this polymerization can be performed in conditions very different from the industrial process. With strong Lewis acids, polymerization can take place even under 1 bar of ethylene pressure. Based on these results, free radical polymerization of ethylene has not to be underestimated and need to be fully investigated.

Recently in our laboratory, a new 160 mL reactor has been developed in order to reach safely ethylene pressures up to 250 bar. In this range of experimental conditions ($P < 250$ bar, and $T < 100^\circ\text{C}$) ethylene free radical polymerization has been studied and some unexpected phenomena (solvent activation effect, phase transition) take place. These investigations are reported in this chapter.

A. The free radical polymerization of ethylene in organic media

The work developed in this section was partly published in *Macromolecules* [1].

1. Polymerization in toluene

First, we confirm that free radical polymerization is possible at low temperature (70°C) and low pressure ($P < 250$ bar) in toluene. Toluene is first chosen as solvent because it is also the solvent of our catalytic polymerization, which will be presented in the chapter VI. AIBN is defined as our reference radical initiator. All polymerizations are performed using inert atmosphere (argon) and Schlenk techniques with purified compounds in order to eliminate all impurities (especially O_2 and peroxides that interact with radicals).

a) Effect of the ethylene pressure

We perform the ethylene polymerization at 70°C in 50 mL toluene during 4 hours. We use AIBN (50 mg, 305 μmol) as radical initiator. As shown in Table 1 polyethylene can be synthesized under these conditions but the yield remains low.

Table 1. Ethylene pressure influence on the free radical polymerization of ethylene^a

Ethylene pressure (bar)	Yield (g)	Melting point (°C) ^b [crystallinity (%)] ^b	Mn (g/mol) ^c [PDI ^c]
25	0	- [-]	- [-]
50	0.25	105.9 [49]	950 [1.7]
100	0.65	115.9 [63]	2340 [1.9]
150	0.8	118.3 [56]	2900 [1.9]
200	1	118.4 [58]	2990 [1.9]
250	1.3	118.7 [66]	4320 [1.8]

^a: Polymerizations are performed during 4 hours with 50 mg of AIBN at 70°C in 50 mL of toluene. ^b: determined by DSC. ^c: determined by HTSEC

Polymerization occurs only over 50 bar of ethylene pressure, since the quantity of PE synthesized at 25 bar is negligible. Over 50 bar yield raises almost linearly with the ethylene pressure (up to 1.3 g at 250 bar). This increase is mostly due to the increase of initial concentration of ethylene. Indeed, the range of pressure is too narrow to observe other pressure effects such as volume activation effect. In fact conversion is almost constant (around 2-3%) with ethylene pressure. However at this point of the discussion it is not possible to calculate the total initial concentration of ethylene in our system because the composition of the polymerization medium is unknown (this will be discussed in the following section B).

The polyethylene produced exhibits low molecular weights ($M_n < 5000$ g/mol) which increase with the ethylene pressure from 950 g/mol at 50 bar to 4300 g/mol at 250 bar. These low molecular weights are due to the transfer of the macroradical to toluene during the polymerization and to the low value of $k_p/k_t^{1/2}$. As molecular weight of PE synthesized at 50 bar is extremely low, we could expect that the hypothetical molecular weight of a PE synthesized at 25 bar for example would be so low that only oligomers would be synthesized which cannot be isolated by our method of yield determination (evaporation of the solvent, then drying of polymer under vacuum).

Transfer to toluene has been shown by ^{13}C NMR (see Figure 3). If the decomposition rate of AIBN is independent of the ethylene pressure, the variation of the number of PE chains synthesized (yield/ M_n) represents the variation of transfer probability to the solvent. The number of chains transferring to solvent slightly increases with the pressure. This effect cannot be due to the predicted activation volume from the activated state theory because pressure variation is too small. This increase may evidence a raise of the local concentration of toluene in the neighbourhoods of the PE macroradical.

Melting points of PE are surprisingly high ($T_m > 115^\circ\text{C}$) excepted for polyethylene synthesis at 50 bar ($T_m = 105.9^\circ\text{C}$). In this case it must be due to the low molecular weight of this PE ($M_n = 950$ g/mol, for a linear alkane of 970 g/mol the melting point is 105°C , see annex I). This melting point indicates low branching level (10 branches per 1000 C) of PE compared to the high pressure LDPE. In order to quantify this branching level ^{13}C NMR are performed (see Figure 3).

We used Galland et al. [2] notations for branches (see Figure 2). Only butyl and longer branches seem to be present in the synthesized PE. This branch type is very different

from the one obtained for PE synthesized by catalysis in which methyl, ethyl, and propyl branches are produced. More surprisingly is that contrary to the classical LDPE no ethyl branches seem to be present. It indicates that the branches content is very low and no cumulating back-biting takes place (see extended Roedel mechanism in the first chapter). Integration of the ^{13}C NMR spectrum leads to a total of 7 branches per 1000 C. This branching level is in agreement with the melting point values.

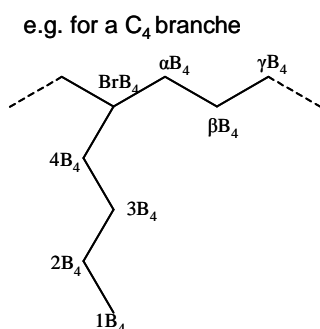


Figure 2. Example of Galland notation for PE branches

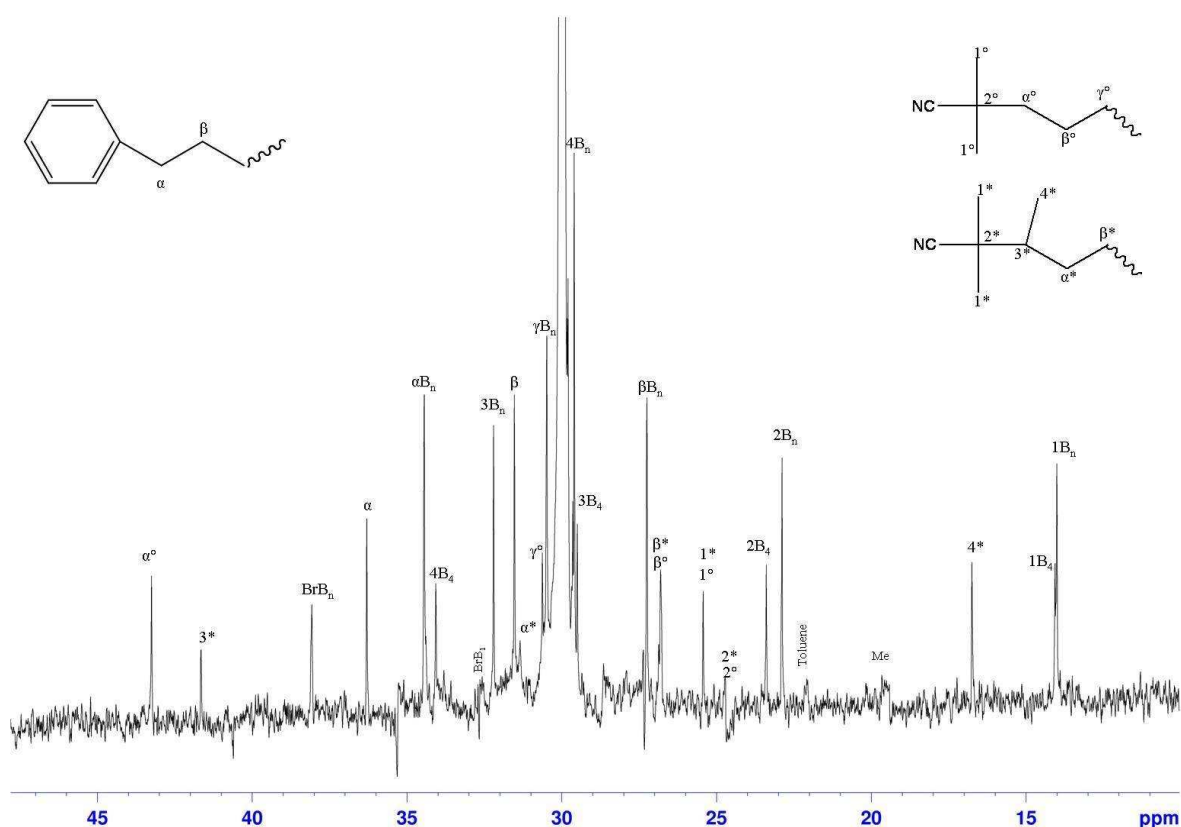


Figure 3. Example of ^{13}C NMR spectrum for PE synthesized in toluene (notation from Galland [2])

As the molecular weight is low, chain-ends can also be characterized. Consequently, AIBN fragment (from initiation) and tolyl fragment (from transfer to solvent as already mentioned) have been identified (see Figure 3). This transfer to organic compounds could be an efficient way to functionalize polyethylene oligomers or very low molecular weight polymers.

b) Kinetic investigations of the ethylene polymerization

We demonstrated that polyethylene can be synthesized by a radical polymerization initiated by AIBN radical initiator. Nevertheless, free radical polymerization kinetics and dependence on initiator concentration have to be studied in order to confirm that the polymerization follows conventional free radical kinetic law:

$$\frac{1}{1-x} \frac{\partial x}{\partial t} = k_p \sqrt{\frac{2fk_d[I]}{k_t}} = k_{tot} \quad (1)$$

Where x is the ethylene conversion, $[I]$ the initiator concentration, f the efficiency factor of the initiator, k_p , k_d and k_t respectively the propagation, decomposition and termination rate.

(1) Kinetics of polymerization

Under 100 bar of ethylene pressure at 70°C, a kinetic study of ethylene free radical polymerizations (see Figure 4) is performed. It should be noted that, under such high pressure and with a small reactor size, samples collection cannot be easily and accurately achieved. Therefore, for each point a polymerization needs to be carried out. Each of these polymerizations must be done in the identical conditions, same temperature (the reactor is not cooled down between the different points), same ethylene fill up (initial conditions (T, P) of the intermediate tank are identical), same AIBN concentration (a master solution was prepared and stored in the fridge). Consequently, establishing a reaction profile in our experimental conditions is not an easy task.

To confirm the kinetics of a free radical polymerization, the initial concentration of ethylene needs to be known. This determination is not trivial, and will be fully discussed in the following (see subchapter B). In our conditions, we calculated that initially 24.9 g of ethylene are contained in the reactor (at 70°C, 50 mL of toluene under 100 bar of ethylene pressure).

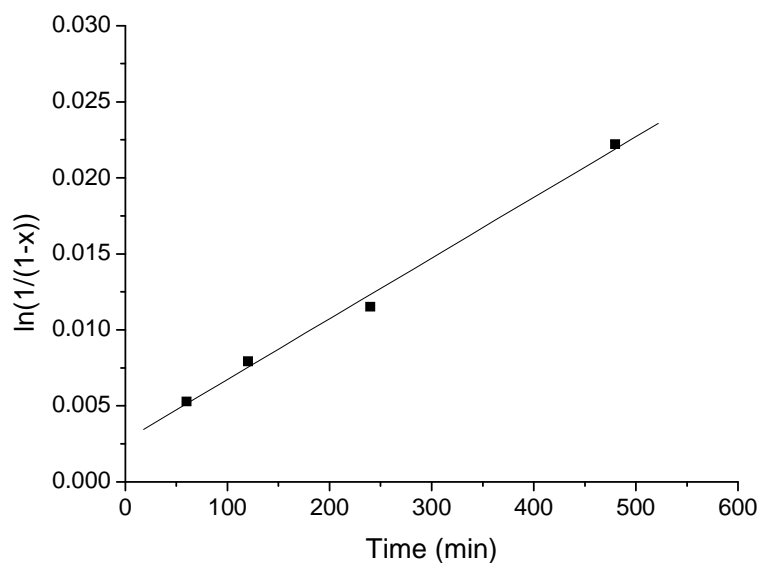


Figure 4. Reaction profile of ethylene polymerization initiated by AIBN: ■ 50 mg of AIBN under 100 bar of ethylene pressure at 70°C in 50 mL of toluene

Our system seems to follow the classical 1st order kinetics of a free radical polymerization of ethylene since $\ln \frac{1}{1-x}$ is proportional to time. After 8 hours of polymerization 1.3 g of PE are synthesized. This kinetics profile excludes a possible Trommsdorff effect. Indeed, the viscosity variations during the polymerization do not induce any variation of the kinetic rate. This is an expected result as PE is not soluble (whatever the ethylene conversion) in toluene, therefore polymerization medium remains almost identical during the polymerization.

(2) *Effect of the initiator concentration*

AIBN concentration influence has been also confirmed to be in agreement to the standard free radical kinetic law. Polymerizations are performed at 70°C under 100 bar of ethylene during 4 hours with various initial concentrations of AIBN. The following figure shows that $\ln \frac{1}{1-x}$ is proportional with $[AIBN]^{1/2}$ as expected.

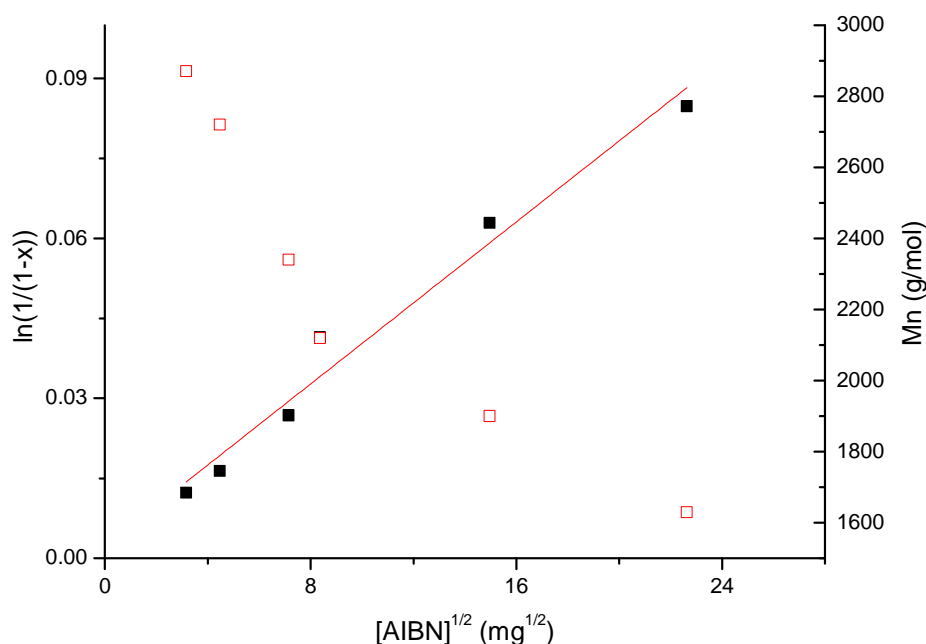


Figure 5. Influence of initiator concentration on ethylene radical polymerization: ■ yield and □ molecular weight* vs AIBN concentration under 100 bar of ethylene pressure during 4 h in 50 mL of toluene at 70°C. * determined by HTSEC

A maximum yield of 2 g was obtained with 512 mg of AIBN. The molecular weights only slightly decrease (from 3000 g/mol to 1500 g/mol) with the AIBN content which is in agreement with the molecular weight being primarily controlled by transfer to solvent rather than termination. From 10 mg to 512 mg of AIBN, the number of PE chains only increases by a factor 10 (50 is expected if no transfer and no variation of termination mode takes place).

All these sets of experiments confirm that a free radical polymerization of ethylene in solution can be done under mild conditions.

2. Polymerization without solvent

Polymerization of ethylene by a free radical pathway is a well known mechanism, but traditionally occurs under harsh conditions (industrially, $P > 1000$ bar and $T > 100^\circ\text{C}$) and usually in bulk. We demonstrated that ethylene free radical polymerization under mild condition with toluene can be performed. Without solvent, in the same conditions, polymerization is surprisingly ineffective:

Table 2. Free radical polymerization of ethylene without solvent^a

Ethylene pressure (bar)	Yield (g)	Melting point (°C) ^b [crystallinity (%) ^b]	Mn (g/mol) ^c [PDI ^c]
100	0.1	105.3 [46]	3010 [1.3]
200	0.2	106.7 [53]	5830 [1.5]

^a: Polymerizations are performed at 70°C during 4 hours with 50 mg of AIBN. ^b: determined by DSC. ^c: determined by HTSEC

Polymerization in supercritical ethylene only produce 0.2 g of PE under 200 bar of ethylene pressure while in the presence of toluene 1 g of PE is produced.

It should be noted that without any organic solvent, AIBN is dissolved in ethylene itself. Consequently, experiments need some modifications compared to the standard modus operandi. AIBN was directly put into the hot open reactor under argon, then reactor was quickly closed and ethylene injected (duration of the whole operation is less than 2 min).

Even in these conditions where no transfer agent is present in the reactor (only PE itself acts as a transfer agent and AIBN), molecular weight remains extremely low ($M_n < 6000$ g/mol). As we already mentioned in the first chapter ethylene is not an efficient transfer agent. If we assume that the AIBN dissociation as well as k_t are identical in toluene and in ethylene, toluene transfer capacity can be calculated. In toluene, about 8 additional chains are synthesized for each chain synthesized in ethylene alone (therefore $v_{tr} \approx 8v_t$).

Moreover, melting points are lower than for PE synthesized in toluene (105°C which is standard for a LDPE vs. 115°C). Consequently, PE synthesized exhibit a higher branching level (about 20 branches per 1000C). These effects could be due to the slow termination rate and the high probability of intramolecular transfer.

Since the growing PE chain is not soluble in supercritical ethylene far below the melting point, PE precipitates, and consequently dramatically decreases the termination probability. The local concentration of transferable hydrogen from the PE itself dramatically increases therefore transfer to PE increases as well as branching content of the synthesized

PE. In toluene the macroradical will precipitate too but some toluene will swell it leading to lower branching content.

Polymerization in toluene is about 6 times more efficient than without solvent in the exactly same experimental conditions. This indicates that the solvent has a crucial role in the free radical polymerization of ethylene. This effect can be due to an increase of the local concentration of ethylene in the polymerization medium or to the solvent itself.

3. The activation by other solvents of the free radical polymerization of ethylene

As the toluene solvent activated the polymerization of ethylene, other solvents have to be investigated, in order to discriminate between an effect on ethylene solubility or of the solvent itself. Two other solvents are studied tetrahydrofuran (THF) and diethyl carbonate (DEC). THF is a highly polar solvent compared to toluene and DEC is a low transferring solvent.

a) Polymerization of ethylene in THF or DEC

(1) Pressure effect

Ethylene free radical polymerizations are performed at 70°C during 4 hours with 50 mg of AIBN as radical initiator in two other solvents: THF and DEC (see Figure 6).

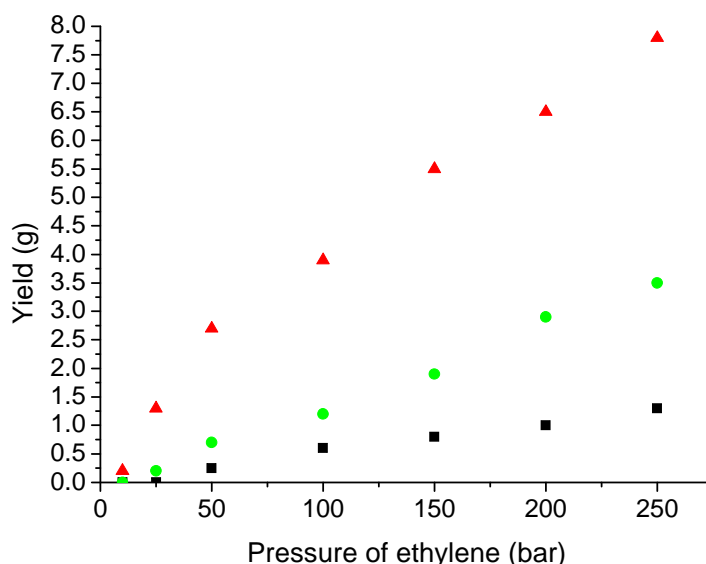


Figure 6. Pressure of ethylene influence on radical polymerization of ethylene in different solvents: 50 mg of AIBN during 4 hours at 70°C in 50 mL ■ of toluene, ▲ of THF, ● of DEC

Surprisingly, yield of the free radical polymerization is highly solvent dependent. Polymerization in THF is 6 times more efficient than polymerization in toluene, and about 40 times more than the solvent-free polymerization. Polymerization in DEC is less efficient than in THF but about 2 times more than in toluene. In all cases the yield increases almost linearly with the ethylene pressure. In THF almost 8 g of PE are synthesized in 4 hours under 250 bar of ethylene pressure (corresponding to 16% of conversion, and only 5% in DEC).

This solvent activation effect could be due to a difference in the initial ethylene concentration. Nevertheless solubility measurements show that ethylene content is about the same in various solvents (see subchapter B). Therefore this activation effect can only be due to the solvent properties (see subchapter C).

The melting point of the PE is mostly independent of the solvent. Indeed in the same experimental conditions, 100 bar, $T_m=115.2^\circ\text{C}$ for PE synthesized in THF, 117.8°C in DEC and 115.9°C in toluene. It indicates that the branching level is almost independent of the solvent. Crystallinity of PE is in the range of 50-70%. The thermal properties of polyethylene are intermediate between the standard properties of LDPE ($T_m=98-115^\circ\text{C}$, crystallinity=30-54%) and HDPE ($T_m=125-135^\circ\text{C}$, crystallinity=55-80%).

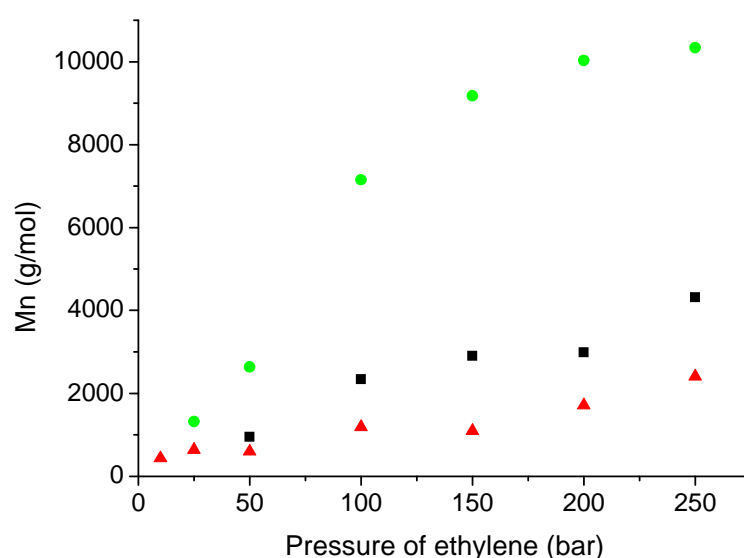


Figure 7. Pressure of ethylene influence on PE molecular weight* synthesized by free radical polymerization in different solvent: 50 mg of AIBN during 4 hours at 70°C in 50 mL ■ of toluene, ▲ of THF, ● of DEC. *: determined by HTSEC

Molecular weights strongly depend on the solvent (see Figure 7, PDI remain constant 1.5~2). Under 100 bar of pressure, Mn are respectively 2340 g/mol with toluene, 1190 g/mol

with THF and 7150 g/mol with DEC. Molecular weight increases with the pressure from oligomer at low ethylene pressure to $M_n > 1000$ g/mol. PE synthesized in DEC provides the highest molecular weight (M_n up to 10000 g/mol, $DP_n > 400$), as expected from its low transferring ability. Polymerization in THF leads to the lowest M_n , while it is the most efficient solvent for activity. THF is therefore the most transferring solvent. This transfer has been confirmed by ^{13}C NMR (see Figure 8).

If we assume that AIBN dissociation is equivalent in each solvent, we can estimate the transfer to solvent capacity by calculating the number of chains formed. It confirms that DEC is the less transferring solvent, in the case of ethylene polymerization about 2 times less than toluene. THF was about 20 times more transferring than DEC.

THF-ended polyethylenes are fully identified by ^{13}C NMR (see Figure 8). About 80% of the PE chains possess a THF-end. These end-functional PE can be considered as macromonomers. For example the copolymerization of 1- and 2-polyethylenyl-THF with THF via cationic ring opening polymerization could lead to a poly(THF) with PE branches.

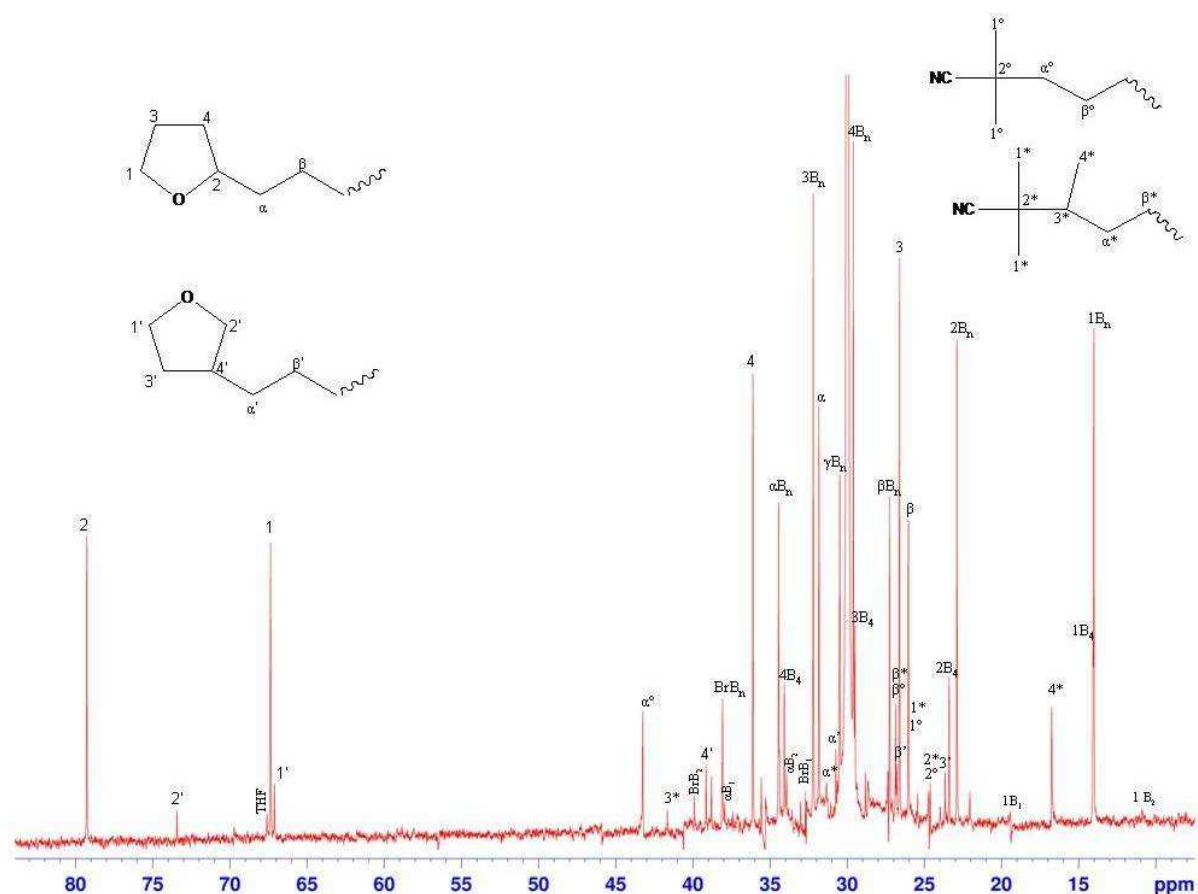


Figure 8. Example of ^{13}C NMR spectrum for PE synthesized in THF (notation from Galland et al [2])

^{13}C NMR allows to measure the branching level. PE synthesized in THF is the most branched with 9 branches per 1000 carbons (in toluene 7 branches and DEC 6 branches).

Contrary to toluene, where the polymerization leads to significant quantities of PE over 50 bar only, free radical polymerization in DEC allows PE to be synthesized at only 25 bar of ethylene, but the molecular weight at this pressure is very low: $M_n=1320$ g/mol, $PDI=2.2$. With THF, free radical polymerization of ethylene can even be performed under lower ethylene pressure. At 10 bar 0.2 g of PE is synthesized, but it is only oligomers ($M_n=440$ g/mol, $PDI=1.3$).

(2) *Toward free radical polymerization of ethylene under low pressure*

One development of interest is to perform polymerization of ethylene in the mildest experimental conditions without using complex methods such as strong Lewis acid used for example by Michl [3] to synthesize PE by a radical polymerization at 1 bar.

In THF, as it allows the synthesis of PE in the lowest pressure range, polymerizations are performed to study this low-pressure area at 70°C with 500 mg of AIBN in 250 mL of THF during 12 hours (a conventional 500 mL steel reactor was used for these experiments).

Table 3. Polymerization of ethylene under very low pressure^a

Ethylene pressure (bar)	Yield (g)
1	0
5	0.2
10	1.9
20	8.1

^a: Polymerizations are performed at 70°C during 12 hours with 500 mg of AIBN in 250 mL of THF

Free radical polymerization of ethylene in THF allows synthesis of PE at ethylene pressure down to 5 bar. Nevertheless, only oligomerization takes place. PE synthesized

exhibit a melting point below 50°C. These kinds of polyethylene do not have the interesting properties of PE itself but may be used further as macromonomers.

(3) Kinetics of polymerization

At 70°C under 100 bar of ethylene pressure, the kinetics of the polymerization and the yield vs. AIBN concentration dependencies were investigated. A good agreement with a free radical polymerization kinetic law (equation 1) is obtained (see Figure 9 and Figure 10).

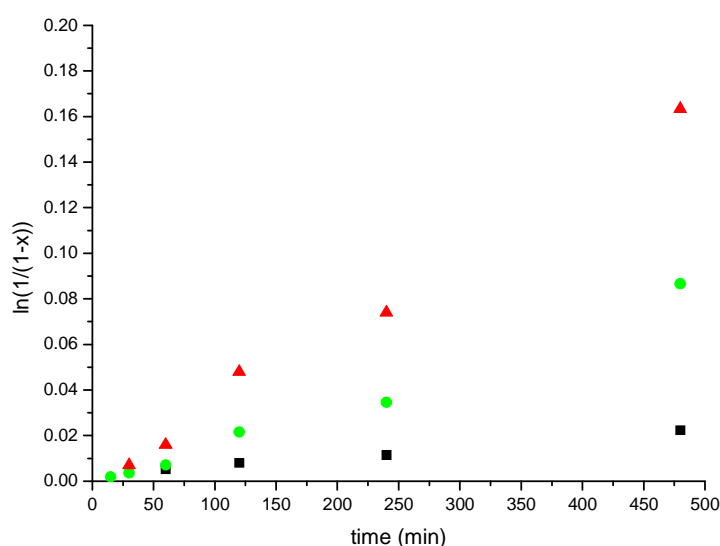


Figure 9. Reaction profile of ethylene polymerization initiated by AIBN: 50 mg of AIBN under 100 bar of ethylene pressure at 70°C in 50 mL ■ of toluene, ▲ of THF, ● of DEC

Polymerizations in all solvents follow the standard free radical polymerization kinetic behavior (see Figure 9). These kinetics profiles show that no auto-acceleration takes place. As PE is not soluble in any of these solvents, PE precipitates in situ, consequently solvent viscosity is not modified by PE synthesized. This set of experiment infirm the likelihood that activation effect of solvent is due to the Trommsdorff effect.

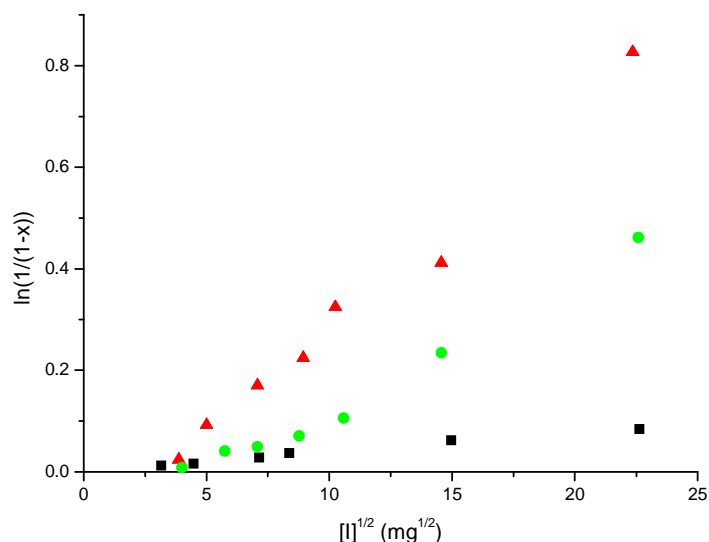


Figure 10. Influence of initiator concentration on the free ethylene polymerization in different solvents: at 70°C under 100 bar of ethylene pressure during 4 hours in 50 mL
 ■ of toluene, ▲ of THF, ● of DEC

Yield dependence on AIBN initiator concentration is also in agreement with the standard kinetic law (see Figure 10). At high AIBN concentration, up to 14 g of PE (60% of conversion) has been obtained in only 4 hours at 100 bar of ethylene pressure in THF. Surprisingly a minimal amount of AIBN is required to polymerize ethylene in our conditions. Below 5 mg of AIBN ($6 \cdot 10^{-4}$ mol/L) no polymerization takes place, and all AIBN is consumed by a secondary reaction. As this required quantity seems mostly independent of the solvent, the secondary reaction must be due to impurities in the ethylene itself (or some oxygen adsorbed at the surface of the reactor).

Molecular weights decreases as expected with increasing AIBN concentration but this decrease remains slight. As with toluene, M_n decrease from 14620 g/mol to 4010 g/mol for DEC and for THF from 2000 g/mol to 1250 g/mol. In the last case M_n is mostly controlled by transfer to solvent.

b) Comparison of the Arrhenius parameters of three solvents

For each of these three solvent, polymerizations at 50°C, 70°C and 90°C and pressures of 50 bar, 100 bar, 150 bar, 200 bar, 250 bar during 4 hours are performed in order to determine the global Arrhenius parameters (see equation 2).

$$k_{tot} = k_p \sqrt{\frac{2fk_d[I]}{k_t}} = A_{tot} \cdot \exp\left(\frac{-E_{tot}}{RT}\right) \begin{cases} E_{tot} = E_p - \frac{1}{2}E_t + \frac{1}{2}E_d & (2a) \\ A_{tot} = A_p \sqrt{\frac{2fA_d[I]}{A_t}} & (2b) \end{cases}$$

With T the temperature in Kelvin, R the ideal gas constant, E the activation energy of propagation (E_p), termination (E_t) and initiator decomposition (E_d), and A the pre-exponential fact of propagation (A_p), termination (A_t) and initiator decomposition (A_d).

Figure 11 shows the yield obtained in THF at various ethylene pressures. Yield drastically increases with the temperature, for example at 100 bar of ethylene pressure, 0.6 g of PE is synthesized at 50°C, 3.9 g at 70°C and 9 g at 90°C.

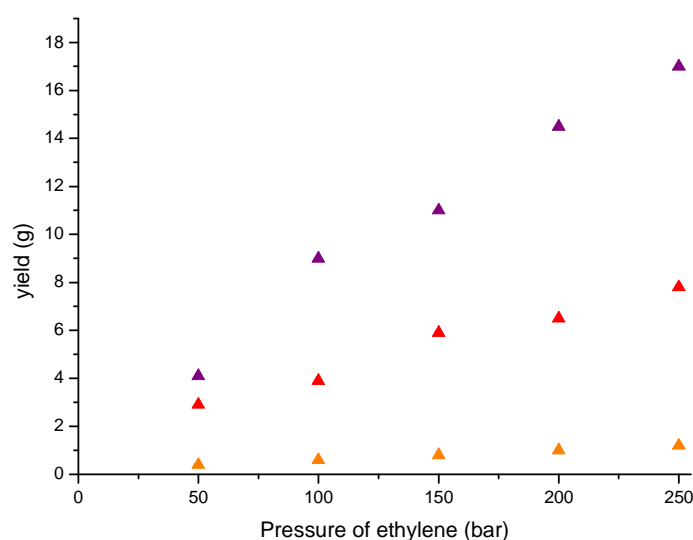


Figure 11. Influence of the temperature of the ethylene free radical polymerization: 50 mg of AIBN during 4 hours in 50 mL of THF ▲ at 50 °C, ▲ at 70°C, ▲ at 90°C

For all solvents, melting points and crystallinity decrease with pressure. For example in THF, the PE synthesized under 100 bar of ethylene pressure at 50°C melts at 117.1 °C, 115.2°C at 70°C and only 108.2°C at 90°C. Crystallinity decreases from 69% to 49%. This decrease is expected because at higher temperature PE macroradicals possess a higher mobility, therefore transfer reactions to polymer are more frequent.

For the same reason, PE molecular weights decrease with increasing temperature. For toluene, PE synthesized at 50°C under 200 bar of ethylene pressure possesses a M_n of 3630 g/mol, 2990 g/mol at 70°C and only 2370 g/mol at 90°C. As the crucial parameters to

control molecular weight distribution is transfer to solvent, these results indicate that this transfer is more frequent with temperature. The higher mobility of PE macroradical may explain this result.

From these findings the global Arrhenius parameters for each solvent can be calculated (see Table 4).

Table 4. Activation energy and pre-exponential factor for each of the solvent.

Solvent	E_{tot} - Global activation energy (kJ/mol)	$\ln(A_{\text{tot}})$ – Global pre-exponential factor
Toluene	27.7	7.6
THF	32.8	10.3
DEC	40.0	12.2

Ideally, the determination of the Arrhenius parameters should be performed for each polymerization step, but this kind of study is currently incompatible with our conditions of pressure (since stopped flow or pulsed laser polymerizations techniques cannot be used).

Global activation energy and pre-exponential factor values cannot explain simply the activity dependence of solvents. Indeed global activation energy factor alone predicts the following reactivity order toluene>THF>DEC while pre-exponential factor alone predicts another order of reactivity DEC>THF>toluene. It is the combination of both that explains the actual order of reactivity. For low energy barriers, the reaction is controlled by the efficiency of the reaction, while at high-energy barriers; it is the activation energy.

If these Arrhenius parameters are suitable for a wide range of temperature (from 100 K to 700 K) Figure 12 shows the relative activity in each solvent. Toluene is the best solvent below 258 K (-15°C). DEC is the most efficient solvent over 456K (183°C). Between these two temperatures, THF is the optimum solvent. Finally DEC is a better solvent than toluene over 321 K (48°C). This last result has been confirmed by doing polymerization at low temperature (30°C) using another low temperature radical initiator (V70 – see Figure 15). At 200 bar of ethylene pressure, 0.4 g of PE were synthesized in toluene and 0.2 g in DEC (1.3 g in THF).

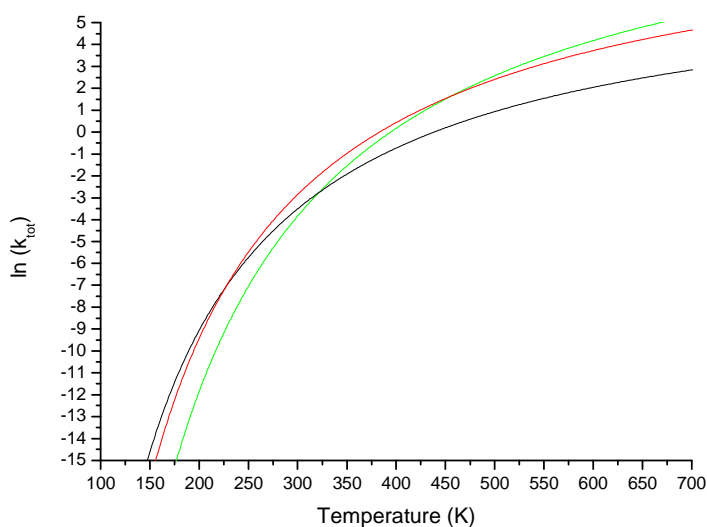


Figure 12. Influence of temperature on the global kinetic constant: — for toluene, — for THF, — for DEC

4. Study of the initiator

Up to now, all polymerizations have been performed using AIBN as radical initiator. In the following, we will study the influence of various initiators on ethylene free radical polymerization in THF.

a) Initiation efficiency of different initiator

Several radical initiators (see Table 5) are used in the same molar amount in order to estimate their relative efficiency factor. All polymerizations are performed at 70°C in THF during 4 hours (see Figure 13).

PE synthesized with all these initiators possess similar melting temperatures and molecular weight distributions (Mn and PDI). Consequently initiators seem to play a role only on the initiation mechanism of the free radical polymerization.

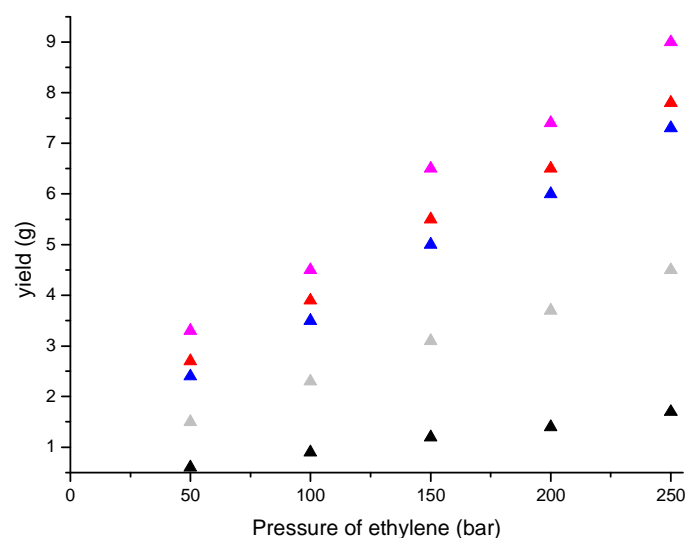


Figure 13. Polymerization of ethylene with different radical initiators: 50 mL of THF during 4 hours at 70°C with 160 μmol \blacktriangle of V40, \triangle of DBP, \triangle of V601, \triangle of AIBN, \triangle of V65

All radical initiators possess different k_d therefore lead to different polymerization yields. To obtain the relative efficiency factors (f/f_{AIBN}), the efficiency of the ethylene polymerization compared to the efficiency of the polymerization with AIBN ($\ln\left(\frac{1}{1-x}\right) / \ln\left(\frac{1}{1-x}\right)_{\text{AIBN}}$) was plotted versus the relative initiator reactivity (see Figure 14).

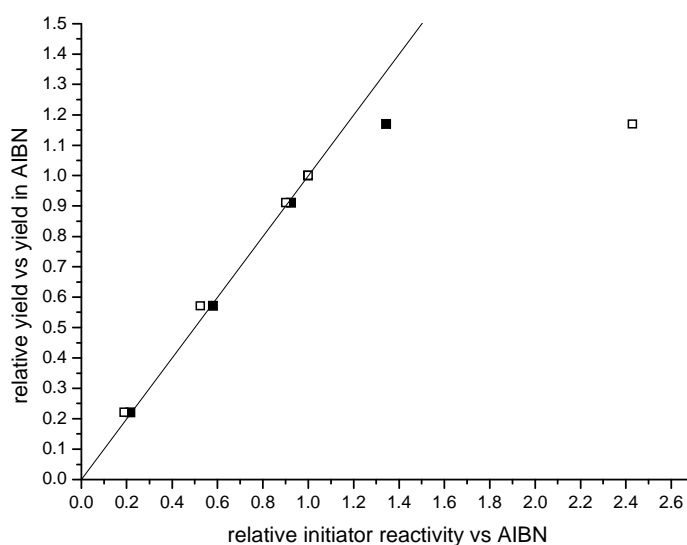
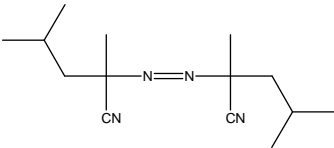
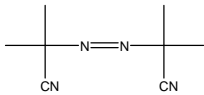
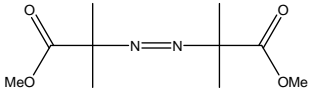
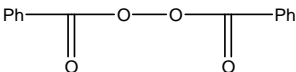
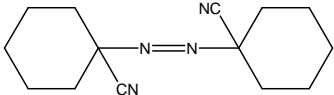


Figure 14. Correlation of the efficiency of the polymerization vs. the initiator reactivity: \square first approximation, \blacksquare second order correction, — 1:1 line

Relative initiator reactivity is in first approximation $\left(k_d/k_{d,AIBN}\right)^{1/2}$ nevertheless in order to include the time of reaction a second order relative initiator reactivity is calculated as $\left(k_d/k_{d,AIBN}\right)^{1/2} \frac{1 - \exp\left(-k_{d,AIBN}t/2\right)}{1 - \exp\left(-k_d t/2\right)}$ (see Figure 14). A good correlation is obtained especially with the second order relative initiator reactivity. Consequently, relative efficiency factors of initiators can be determined (see Table 5).

Table 5. Efficiency factor of different initiator for the ethylene free radical initiation

Initiator	Formula	$t_{1/2}$ (min) ^a	f/f_{AIBN}
V65		50	0.76
AIBN		290	1
V601		350	0.97
DBP		1050	0.97
V40		8100	1.04

^a: half-life time of the initiator at 70°C

Except for V65, efficiency factors of initiators are almost identical. Peroxide initiator (DBP) exhibits the same initiation efficiency as azo initiators such as AIBN. For V65, efficiency is especially low. This can be due to the too high dissociation constant at 70°C ($t_{1/2}=50$ min).

b) Toward polymerization of ethylene at low temperature

As free radical polymerization is mostly independent of the initiator, experiments are performed using V70 (see Figure 15), a low temperature radical initiator, at 30°C ($t_{1/2}=10\text{h}$ at 30°C) during 4 hours in 50 mL of THF (see Figure 16).

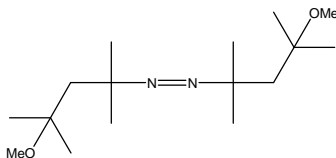


Figure 15. V70 molecule

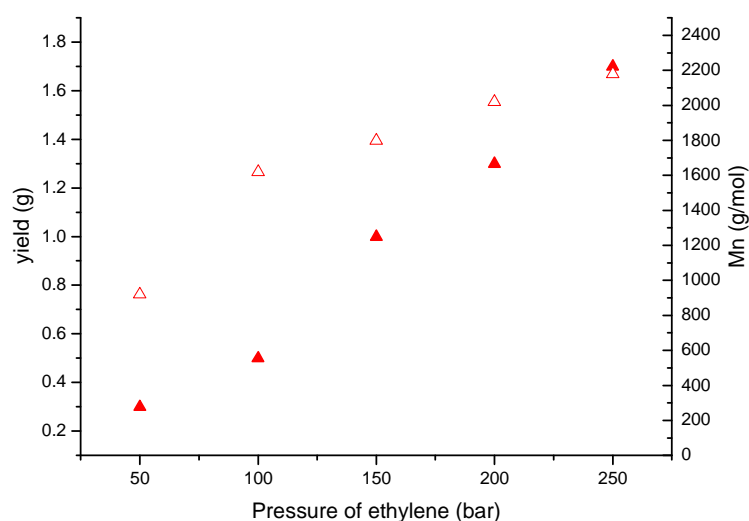


Figure 16. Free radical polymerization of ethylene at low temperature: ▲ yield and ▲ molecular weight* vs. ethylene pressure 160 μmol of V70 during 4 hours at 30°C in 50 mL of THF. *: determined by HTSEC

At this low temperature, PE still can be synthesized by free radical polymerization. Molecular weights are slightly increased in comparison to standard polymerization in THF at 70°C (at 200 bar of pressure $M_n=2000\text{ g/mol}$ at 30°C compared to 1700 g/mol at 70°C).

As already mentioned, melting temperature of PE increases for low temperature of synthesis. Melting points up to 122°C have been observed (for a standard LDPE 100-115°C). This corresponds to a moderate branching level (5 branches per 1000 carbon).

It should be noted that to obtain linear PE, free radical polymerization of ethylene could be theoretically performed at very low temperature (ideally below the T_g of PE) using for example photoinitiators. In this case the mobility of the macroradical would drastically decrease the probability of chain branching.

As THF induced a high efficiency of the free radical polymerization of ethylene, polymerizations are performed at 20 bar, 10°C overnight with 500 mg of V70 in 250 mL of THF.

In this condition 1.5 g of polyethylene is synthesized with melting point around 60°C. Consequently, even at low temperature ($T=10^{\circ}\text{C}$) and low pressure ($P=20$ bar), free radical oligomerization of ethylene can be performed.

This method of efficient radical polymerization of ethylene under easy-to-access experimental conditions allows transfer all classic tools of the radical polymerization (controlled polymerization, emulsion, macromonomer synthesis ...) to the ethylene free radical polymerization.

5. Conclusion

Free radical polymerization can be performed under milder experimental conditions than the industrial well-known process. Under these conditions solvents used have a dramatic influence. The presence of solvent increases the activity and PE melting point in comparison to bulk polymerization.

Surprisingly, activity of the polymerization is also solvent dependent. At 70°C, free radical polymerization in THF is almost 6 times more efficient than in toluene and 2 times more than in DEC. In THF, PE polymerization can be performed at pressure as low as 5 bar.

Moreover, the average molecular weights depend on the solvent. DEC is the less transferring solvent and PE with M_n up to 10000 g/mol are synthesized. Toluene and THF produce lower polyethylene molecular weight with respectively toluene- and THF-ended chain. These polymers could be used further for example as macromonomer.

Finally, various initiators can be used to perform this polymerization, even low temperature radical initiator such as V70 which permit the PE synthesis at ambient temperature.

B. Phase equilibrium in the Ethylene/solvent mixture

An activating solvent effect seems to be identified for the free radical polymerization of ethylene. This effect can be due to the solvent itself, or can also be explained by physical variation of the polymerization medium according to polymerization experimental conditions.

In our experimental conditions, two polymerization media can exist: a monophasic supercritical medium, in which ethylene and solvent form a unique phase, or a biphasic medium, in which some ethylene is dissolved in the solvent where the radical polymerization takes place. Consequently, as the initial system is not the same (different initial concentrations of ethylene, initiator...), this could explain the polymerization efficiency difference between solvents.

The work developed in this section was partly published in *Physical Chemistry Chemical Physics* [4].

1. Solvent volume effect

The transition between the two systems depends mostly on four parameters: temperature, ethylene pressure, solvent critical properties (T_c and P_c) and solvent volume. To characterize this transition, polymerizations are performed at different volumes of solvent for toluene, THF and DEC using same experimental conditions ($P=100$ bar, $T=70^\circ\text{C}$, during 4 hours using 50 mg of AIBN as initiator, see Figure 17) in order to explore from single supercritical phase to biphasic.

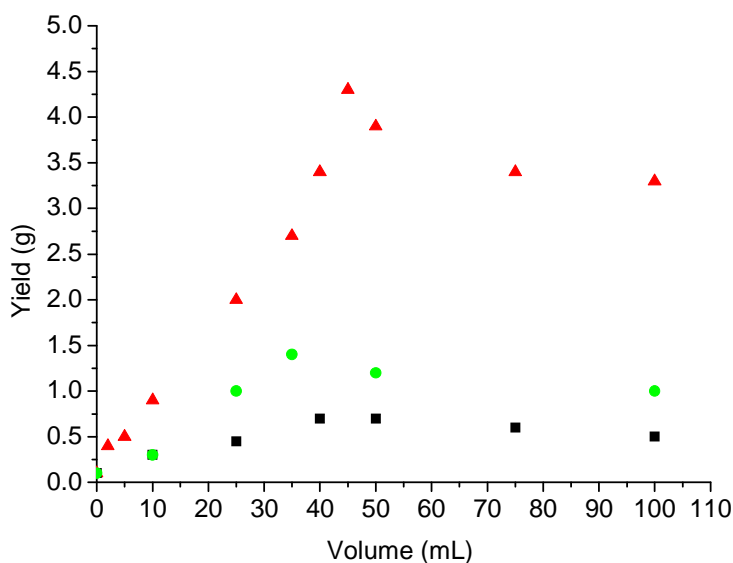


Figure 17. Influence of solvent volume on free radical polymerization of ethylene: 50mg of AIBN during 4 hours at 70°C under 100 bar of ethylene pressure ■ in toluene, ▲ in THF, ● in DEC

Λ-shaped curves are observed for each solvent. At low solvent volume, yield increases with the volume; and at high solvent volume yield decreases. Maxima seem to be solvent dependent. Different curves were obtained for each solvent (in yield and maximum), therefore a solvent activation effect exists.

At high solvent volume, yield decreases with the solvent volume. In this case, a biphasic medium is expected. Therefore, as ethylene concentration remains constant (same solubility) while initiator concentration decreases, conversion and consequently yield decreases.

At low solvent volume, yield increases with the solvent volume. In a monophasic medium, initiator concentration remains constant with the quantity of solvent and ethylene concentration slightly decreases. The only factor which can explain this gain of yield is the increase of solvent concentration.

Consequently, the free radical polymerization of ethylene is activated by the presence of solvent.

As expected polyethylene molecular weights decreases with increasing solvent volumes due to transfer of the propagating radical to solvent (see Figure 18). In addition molecular weights drop after the maximum due to the sudden increase of solvent concentration in the liquid phase after the assumed phase transition. Over this transition as the local concentration of solvent remains almost constant, molecular weights reach a plateau.

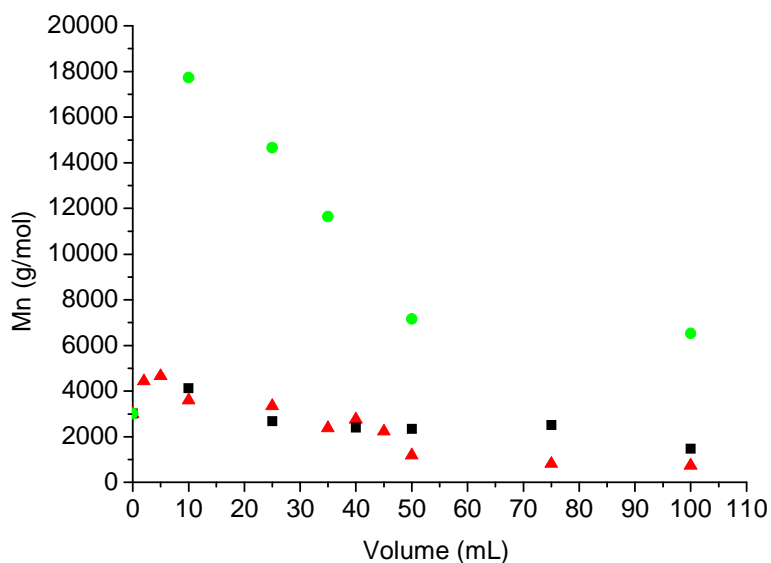


Figure 18. Influence of solvent volume on Mn of polyethylene synthesized: 50 mg of AIBN during 4 hours at 70°C under 100 bar of ethylene pressure ■ in toluene, ▲ in THF, ● in DEC

The maximum yield in THF and toluene is almost obtained for the same solvent volume (45 mL). In DEC maximum is reached at lower volume (35 mL). This can be explained by the solvent physical properties. Indeed, as we already mentioned in the first chapter, critical pressure and temperature are crucial parameters to describe the transition. DEC is a much more stringent solvent (the most relevant factor to determine this is $\frac{d}{M}T_c$ - see Table 6) than THF or toluene. Therefore the transition between monophasic and biphasic system will occur at lower volume.

Table 6. Important parameters to determine ethylene/solvent phase transition [5]

Compounds	Pc (Bar)	Tc (°C)	M (g/mol)	d (g/cm ³) at 25°C	$\frac{d}{M}T_c$ (mol. K/cm ³) at 25°C
Ethylene	50.4	9.2	28.05	-	-
Toluene	41.1	319	92.14	0.87	5.59
THF	51.9	267	72.11	0.89	6.67
DEC	33.9	303	118.13	0.97	4.73

In addition, if no phase transition takes place, the set of experiments varying AIBN concentration or solvent volume should be identical. As shown in the following figure for THF at low AIBN concentration (thus high solvent volume) yield per unit of volume is identical (for AIBN concentration and solvent volume variations). The two set of experiments then diverge from the ratio AIBN/THF of 1.11 g/L corresponding to 45 mL of THF (with 50 mg AIBN).

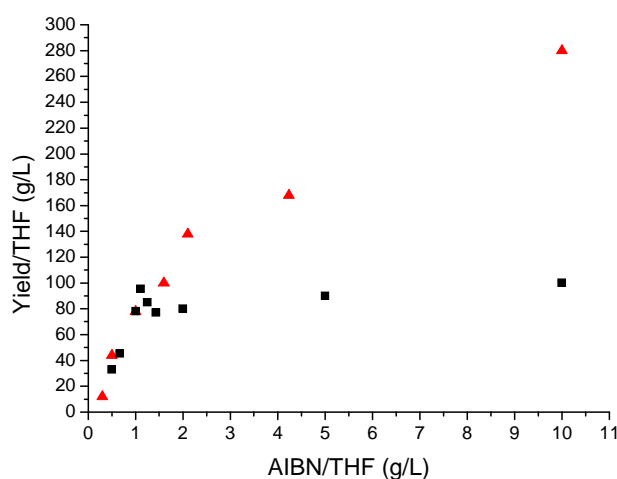


Figure 19. Influence of AIBN/THF ratio on free radical polymerization of ethylene
■: 50 mg AIBN, 4h at 70°C under 100 bar of ethylene pressure, various volume of THF
▲ : 50 mL of THF, 4h at 70°C under 100 bar of ethylene pressure, various amounts of AIBN

All these results indicate that a transition takes place between a biphasic medium at high solvent volume and a monophasic one at low solvent volume.

2. Other experimental evidences of the phase equilibrium

Some other investigations can be performed in order to characterize this transition.

a) Practical determination of the phase state

This phase transition can be identified in several other ways. A practical one is that when a polymerization is performed in a unique supercritical fluid, PE synthesized lines all the reactor walls which is not the case for a biphasic medium.

This observation is in agreement with the previous set of experiments: at low solvent volume, PE lines the entire reactor and at high solvent volume, PE is present only in suspension in the liquid solvent phase. Experimentally we observed that PE lines all the reactor when polymerization are performed over 150 bar of ethylene pressure at 70°C with 50 mL of solvent (THF, toluene and DEC).

It should be noted that these observations confirm that no polymerization takes place in the supercritical phase in the biphasic medium as no PE lines the headspace of the reactor.

b) Isodensity pressure and temperature behaviors

A thermodynamical study can also be performed in order to identify these transitions. Reactor is filled at ambient temperature by a given pressure of ethylene and a given volume of solvent. At this initial time, we are in presence of a biphasic medium. Then the reactor is slowly heated until a pressure of 300 bar is reached and cooled down afterwards, in order to cross the boundary between biphasic and monophasic medium. Temperature and pressure of the reactor are then analyzed in order to identify change of Clapeyron slope ($\ln P \propto 1/T$), which testifies the transition (see Figure 20).

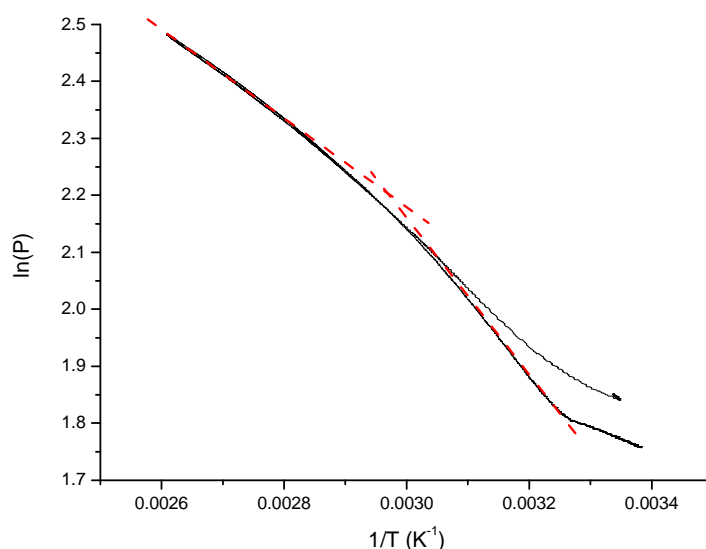


Figure 20. Example of Clapeyron curve of Ethylene/Toluene (50 mL) mixture

A slight change of the slope is observed and corresponds to the transition between the monophasic and biphasic medium. However this method needs much time as for each point the thermodynamic equilibrium needs to be reached. This is impossible for the heating part but manageable to reach a repeatable result for the cooling part by cooling the reactor very slowly (less than 1°C per hour). Consequently the experiment needs almost one week for just one point and therefore is highly sensitive to even very small ethylene leaks.

The phase transition (P and T) can be calculated as the value at the connection of the Clapeyron slopes of the biphasic medium and monophasic one. Similar results than the previous method are then obtained.

Nevertheless due to all the drawbacks of this technique we will not use it to experimentally determine the coordinates of the transition. We will prefer the maximum of yield versus solvent volume for the radical polymerization.

3. Thermodynamic determination of the phase diagram

In order to get the transition conditions between monophasic and biphasic medium, the solubility of ethylene in solvent has to be measured in a wide range of experimental conditions.

Solubility of ethylene has been well investigated in the literature in various organic solvents but as far as we know solubility is available in the literature only up to 50 bar of ethylene pressure [6-8].

a) Experimental measurement of the ethylene solubility in various solvents

As solubilization is kinetically extremely slow without stirring, we develop a simple *modus operandi* to measure this solubility directly in our reactor. First the reactor containing solvent is charged at a given ethylene pressure and temperature (without stirring) then we record over stirring the pressure drop until the equilibrium.

A Peng-Robinson equation of state is chosen after examination of numerous available equations of state as an excellent compromise between simplicity and efficiency. According to it, the density of ethylene (d) is known in the supercritical phase for each P , T (equations 3-4). The difference in density between the initial step (i) (before stirring) and the equilibrium (f) is due to the solubilization of ethylene in the solvent (s_E). To perform the calculation the total inner volume of the reactor is determined ($V_R = 230$ mL is calculated by studying the pressure fall of the intermediate tank when we charge the empty reactor. A mass balance gives us: $d_i(V_T) = d_f(V_T + V_R)$ with V_T the tank volume). The volume of the solvent being known (V_S), solubility was calculated by mass balance through the equation 5. The dilatation of solvent (V_E) due to the solubilization of ethylene was determined by varying the volume of solvent at a constant P_f .

$$d_i = EOS(P_i, T_i) \quad (3)$$

$$d_f = EOS(P_f, T_f) \quad (4)$$

$$d_i(V_R - V_S) - d_f(V_R - V_S - V_E) = s_E V_S \quad (5)$$

(1) Pressure effect

We perform these experiments with our three reference solvents at 70°C. We are able to measure the solubility of ethylene up to 140 bar of ethylene pressure (see Figure 21).

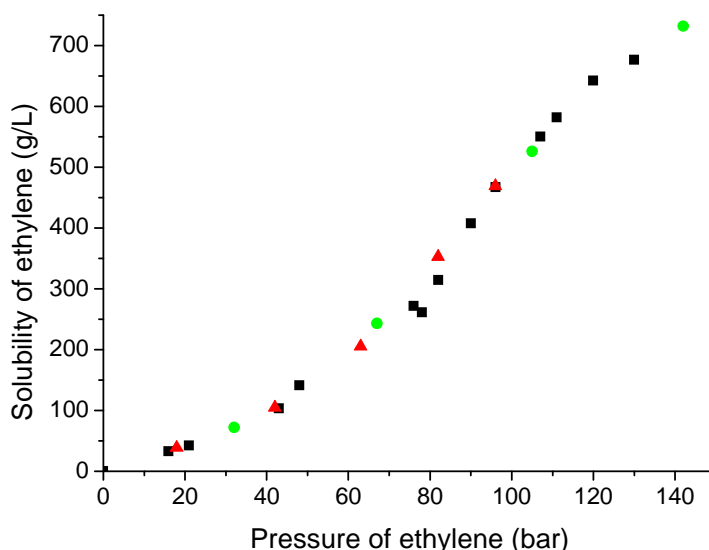


Figure 21. Solubility of Ethylene at 70°C (in grams of ethylene per initial volume of solvent) ■: in toluene, ▲: in THF, ●: in DEC

As the figure shows solubility seems to be mostly independent on the solvent itself and only dependent on the ethylene pressure. Under 50 bar, solubility vs. pressure is almost linear with a slope of about $2 \text{ g.L}^{-1}.\text{bar}^{-1}$. This observation has been already reported in the literature but no recent study calculated the solubility of ethylene over 50 bar. Over 60 bar, an increase of slope occurs up to $9 \text{ g.L}^{-1}.\text{bar}^{-1}$.

(2) Temperature effect

Same procedures are performed at 50°C and 90°C with toluene. Solubility decreases with the temperature at equivalent ethylene pressure. In order to rationalize these results, we plot the ethylene solubility in function of the ethylene density (see Figure 22).

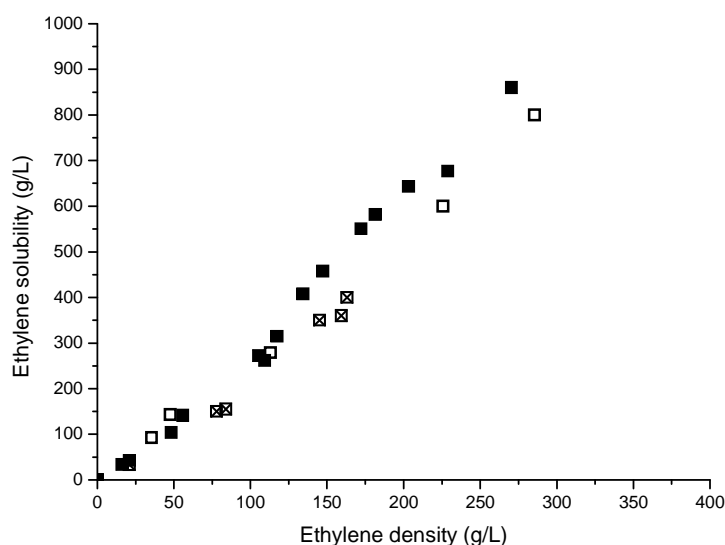


Figure 22. Correlation between ethylene density and solubility in toluene □: at 50°C; ■: at 70°C; ☒: at 90°C

Solubility seems to be almost linear with ethylene density and follows the same straight line for each temperature. Consequently, we assume in the following that ethylene solubility will be equal to three times the ethylene density ($s_E = 3d_E$).

b) Phase diagram of Ethylene/solvent mixture

Thanks to the solubility measurement, we are able to describe fully the initial system for the biphasic medium. The monophasic medium can also be described entirely. However, at this point of the discussion, the frontier between the two systems remains unknown.

(1) Theoretical consideration

Ethylene solubility has been determined up to 130 bar, but the phase transition between a biphasic medium at low pressure and a monophasic medium at higher pressure still has to be determined. This is done using the Peng-Robinson equation of state (equations 6-10) [5] and the standard mixing rules for a and b coefficients (equations 11-12) [5] for a bicomponent system (ethylene and solvent).

Peng-Robinson equation of state:

$$P = \frac{RT}{V-b} - \frac{a}{V^2 + 2bV - b^2} \quad (6)$$

$$a = \frac{0.45724R^2T_c^2}{P_c} \left[1 + f\omega(1 - T_r^{1/2}) \right]^2 \quad (7)$$

$$\text{where } f\omega = 0.37464 + 1.54226\omega - 0.26992\omega^2 \quad (8)$$

$$\text{and } T_r = \frac{T}{T_c} \quad (9)$$

$$b = \frac{0.07780RT_c}{P_c} \quad (10)$$

Mixing rules:

$$a = \sum_{i=1}^N \sum_{j=1}^N x_i x_j a_{ij} \text{ where } a_{ij} = \sqrt{a_i a_j} \quad (11)$$

$$b = \sum_{i=1}^N \sum_{j=1}^N x_i x_j b_{ij} \text{ where } b_{ij} = \frac{b_i + b_j}{2} \quad (12)$$

where P is the pressure in Pascal, T the absolute temperature in Kelvin, V the molar volume, R the ideal gas constant, P_c the pressure at the critical point, T_c the absolute temperature at the critical point, ω the acentric factor, x_i the molar fraction of compound i (solvent or ethylene).

To calculate the transition we have to determine at each temperature (because a varies with T), the critical pressure and temperature of the ethylene-solvent mixture using equations 7-12 for all compositions.

Mixture composition depends on three parameters only: temperature, pressure of ethylene (which determines the amount of ethylene), and volume of solvent (which determines the amount of solvent). For each composition and temperature a and b are then calculated using equations 11 and 12. Then critical parameters of the mixture are determined (equations 7 and 10). These critical parameters also depend on ethylene pressure, temperature and solvent volume.

At a given temperature if $T_{c,mixture} < T$ and $P_{c,mixture} < P$, the medium is supercritical and monophasic. If $T_{c,mixture} > T$ a biphasic system is expected with a liquid phase of solvent containing dissolved ethylene. $P_{c,mixture} > P$ and $T_{c,mixture} < T$ never occurs due to the intrinsic properties of the mixture.

(2) Example for Ethylene/THF medium

From these calculations, a phase transition surface can be obtained depending on temperature, ethylene pressure, and amount of solvent as shown in the Figure 23 and the composition of the medium can be estimated for each coordinate.

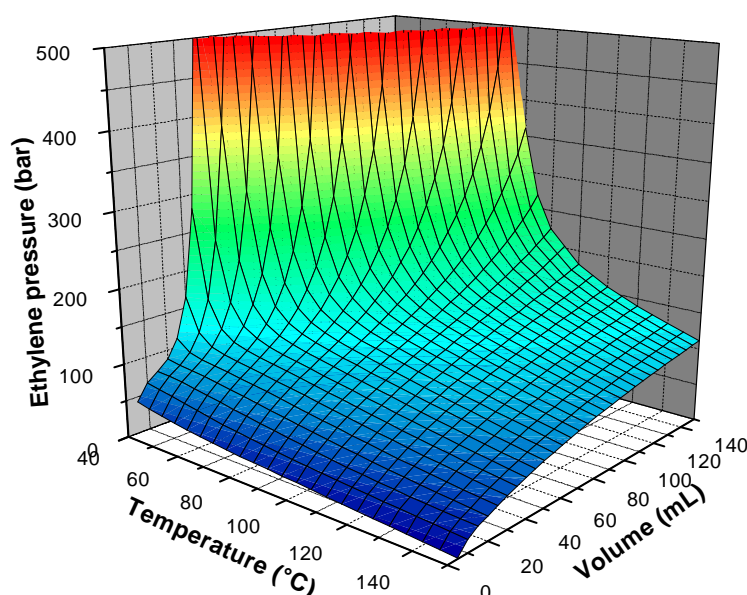


Figure 23. Phase diagram for Ethylene/THF mixture

The transition pressure increases with solvent volume and decreases with temperature. Above the phase transition surface the system will be a supercritical monophasic medium (THF and ethylene in a unique supercritical phase) and below the surface it will be biphasic (2 phases with ethylene in both).

It is noteworthy to mention that the transition surface possesses a certain thickness (second order transition) which cannot be precisely determined using our calculation method.

(3) Other equations of state

We also performed these calculations with various other equations. Two main families are used: 1) equation of state such as Peng-Robinson previously described with a

standard mixing rule of the a and b parameters, or 2) mixing rules on the critical parameters themselves.

- Equations of states
 - Cubic equations of state

Cubic equations of state takes into account only interactions between two particles, contrary to ideal gas equation in which molecules do not interact. Consequently this kind of equation is able to good prediction if the multi-center interactions (3, 4 centers) can be neglected.

$$P = \frac{RT}{V-b} - \frac{a}{V^2 + ubV + wb^2} \quad (13)$$

In this equation b represents the covolume of the particles and a the interaction between molecules. P is the pressure in Pascal, T the absolute temperature in Kelvin, V the molar volume, R the ideal gas constant.

- Van der Waals EoS (VdW) [5]

$$u = 0, w = 0, b = \frac{RT_c}{8P_c} \text{ and } a = \frac{27R^2T_c^2}{64P_c}$$

With P_c the pressure at the critical point, T_c the absolute temperature at the critical point.

- Redlich-Kwong EoS (RK)

$$u = 1, w = 0, b = \frac{0.08664RT_c}{P_c} \text{ and } a = \frac{0.42748R^2T_c^{5/2}}{P_c T^{1/2}}$$

This equation takes into account that the interactions between particles are temperature dependent.

▪ Redlich-Kwong-Soave EoS (RKS) [5]

$$u = 1, \quad w = 0, \quad b = \frac{0.08664RT_c}{P_c} \quad \text{and} \quad a = \frac{0.42748R^2T_c^2}{P_c} \left[1 + f\omega(1 - T_r^{1/2}) \right]^2 \quad \text{where}$$

$$f\omega = 0.48 + 1.574\omega - 0.176\omega^2$$

In this EoS, $f\omega$ takes into account the anisotropy of interactions between particles. With ω the acentric factor, and $T_r = T/T_c$.

▪ Peng-Robinson EoS (PR) [5]

$$u = 2, \quad w = -1, \quad b = \frac{0.07780RT_c}{P_c} \quad \text{and} \quad a = \frac{0.42714R^2T_c^2}{P_c} \left[1 + f\omega(1 - T_r^{1/2}) \right]^2 \quad \text{where}$$

$$f\omega = 0.37464 + 1.5226\omega - 0.26992\omega^2$$

Peng-Robinson equation uses a mathematical trick to take into account a part of the interaction between 3 particles via the factor $-b^2$. This equation usually has a better estimation in high density areas due to this consideration.

○ Non-cubic equations of state

▪ Sako-Wu-Prausnitz EoS (SWP) [9-11]

This equation was developed in order to take into account multiple interactions via an additional parameter c which represents a number of external freedoms (number of particles with which a molecule can interact at the same time).

$$P = \frac{RT(V - b - bc)}{V(V - b)} - \frac{a}{V(V + b)} \quad (14)$$

$$\text{Where } a = a_c \alpha(T), \quad b = \frac{D_0 RT_c}{P_c} \quad \text{and} \quad D_0^3 + (6c - 3)D_0^2 + 3D_0 - 1 = 0$$

$$\alpha(T) = \frac{\alpha_0(1 - T_r)^2 + 2T_r^2}{1 + T_r^2}, \quad a_c = f(D_0) \frac{RT_c^2}{P_c}$$

$$\alpha_0 = 1.1920 + 0.11060 \ln(V_w) + 0.30734 \cdot 10^{-3} V_w$$

$$f(D_0) = \frac{(1 - 2D_0 + 2cD_0 + D_0^2 - cD_0^2)(1 + D_0^2)}{3(1 - D_0)^2(2 + D_0)}$$

D_0 and V_w are calculated from the Lennard-Jones potential and are representing respectively the first ionisation potential and the Van der Waals volume.

- Mixing rule on the critical parameters

Critical temperature and pressure can also be estimated using mixing rules directly on the critical parameters of the compounds.

- Molar average of critical coordinates (CrAv) [5]

$$T_{c,mixture} = \sum_i x_i T_{c,i} \text{ and } P_{c,mixture} = \sum_i x_i P_{c,i}$$

With x_i the molar fraction of compound i (solvent or ethylene).

- Kay mixing rules (KPG) [5]

$$T_{c,mixture} = \sum_i x_i T_{c,i} \text{ and } P_{c,mixture} = \frac{R \left(\sum_i x_i Z_{c,i} \right) T_{c,mixture}}{\sum_i x_i V_{c,i}}$$

With V_c the critical molar volume and $Z_c = \frac{P_c V_c}{T_c}$.

- Barner and Quinian mixing rules (BQPG) [5]

$$T_{c,mixture} = \sum_i \sum_j x_i x_j T_{c,ij} \text{ with } T_{c,ii} = T_{c,i} \text{ and } T_{c,ij} = k_{ij}^* \frac{T_{c,i} + T_{c,j}}{2}$$

$$P_{c,mixture} = \frac{R \left(\sum_i x_i Z_{c,i} \right) T_{c,mixture}}{\sum_i x_i V_{c,i}}$$

With k_{ij}^* the Barner and Quinian interaction factor between i and j compounds. The exact value of k_{ij}^* is only known for ethylene/heptane mixture ($k_{ij}^* = 1.13$), otherwise we choose $k_{ij}^* = 1$ and assume that the interaction is neglected.

○ Lee-Kesler mixing rules (LK) [5]

$$T_{c,mixture} = \frac{1}{V_{c,mixture}^{1/4}} \sum_i \sum_j x_i x_j V_{c,ij}^{1/4} T_{c,ij}, \quad V_{c,mixture} = \sum_i \sum_j x_i x_j V_{c,ij} \quad \text{and} \quad \omega_{mixture} = \sum_i x_i \omega_i$$

$$P_{c,mixture} = (0.2905 - 0.085\omega_{mixture}) \frac{RT_{c,mixture}}{V_{c,mixture}}$$

$$\text{With } T_{c,ij} = (T_{c,i} T_{c,j})^{1/2} k'_{ij} \quad \text{and} \quad V_{c,ij} = \frac{1}{8} (V_{c,i}^{1/3} + V_{c,j}^{1/3})^3$$

With k'_{ij} the Lee and Hesler interaction factor between i and j compounds. The exact volume of k'_{ij} is only known for ethylene/heptane mixture ($k'_{ij} = 1.16$), otherwise we choose $k'_{ij} = 1$ and assume that the interaction is neglected.

Calculations have been done for each of these methods and results have been summarized in the following figure. The transition between the monophasic and biphasic medium is plotted at constant volume of toluene (50 mL).

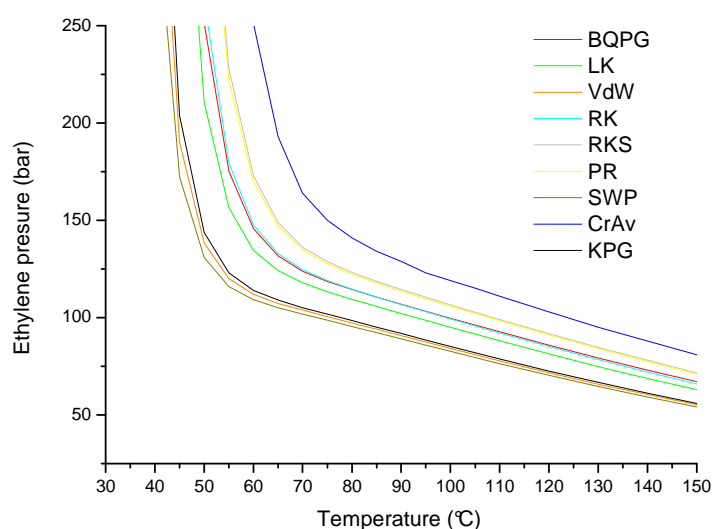


Figure 24. Phase transition for 50 mL of toluene with various EoS

The shapes are similar in all cases but the transition coordinates are strongly dependent of the equation used to calculate it. For example at 70°C the Sako–Wu–Prausnitz (SWP) predicts a transition at 101 bar and the molar average of critical coordinates (CrAv) at 165 bar.

Peng-Robinson (PR) equation is preferred: it provides the best fit with the experimental transition point and the Peng-Robinson equation describes accurately ethylene itself.

(4) *Effect of the solubility*

Solubility of ethylene in the solvent phase has also a huge importance in the determination of the transition. Molar content of ethylene at a given pressure in the case of a biphasic medium is drastically impacted by the solubility of ethylene ($m_{E,tot} = m_{E,sol} + m_{E,gas}$).

In the following figure we predict the transition with or without taking into account the solubility of ethylene in 50 mL of toluene.

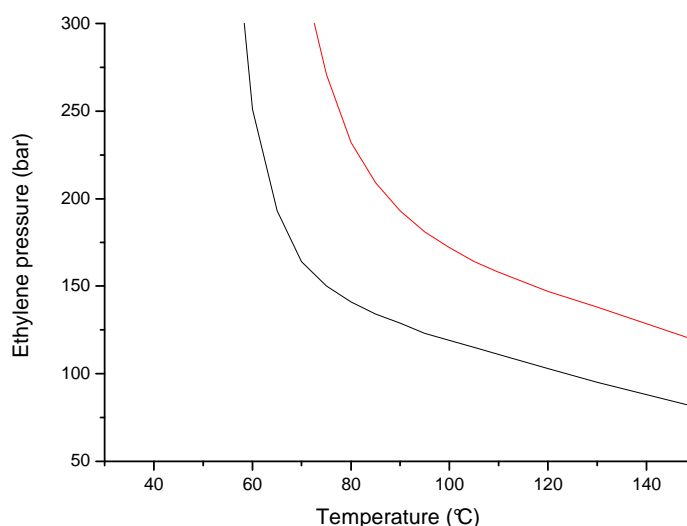


Figure 25. Phase transition for 50 mL of toluene with (—) or without (—) taking into account ethylene solubility in liquid toluene using the average of critical parameters technique (CrAv)

As the figure shows the solubility drastically decreases the transition to milder conditions. For example at 70°C without taking into account ethylene solubility the transition takes place at 330 bar and only at 165 bar by taking into account ethylene solubility. Similar results are obtained with the other EoS.

Consequently solubility is a crucial parameter and the more ethylene is soluble in the liquid, the lower in temperature and ethylene pressure the transition between the biphasic and monophasic medium takes place.

(5) *Correlation to the experimental evidences*

In order to confirm our theoretical calculations using the Peng-Robinson equation of state, we have to confront the prediction to the experimental data assuming that the maximum of activity corresponds to the phase transition (see Figure 17).

(a) *Phase transition at different pressures*

In this purpose we perform at several ethylene pressures, some sets of experiment in order to determine the optimum THF volume at 70°C. As shown in Figure 26 a quite good correlation is observed between theoretical and experimental data which confirm that the maximum of yield is got around the transition.

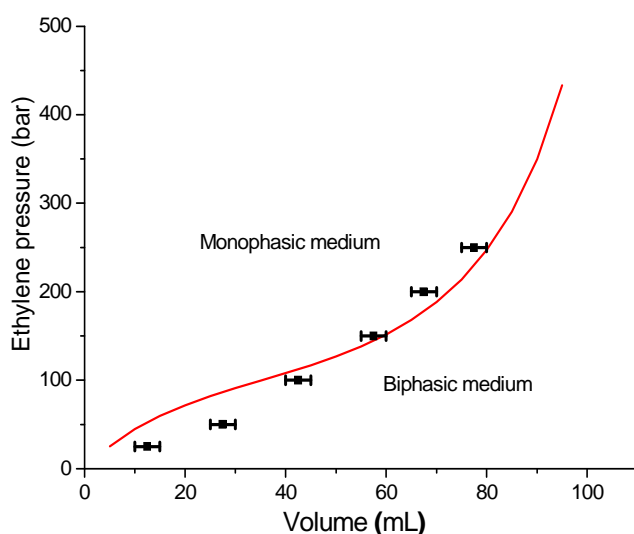


Figure 26. Phase diagram for Ethylene/THF mixture at 70°C —: computed values, ■: experimental measurement based on polymerization studies

The slight divergence between the experiment and the theory could be only due to the non-ideality of the mixture ethylene-THF ($a_{ij} = \sqrt{a_i a_j} (1 - k_{ij})$ $k_{E/THF} \neq 0$).

(b) *Phase transition at different temperatures*

We also determined the optimal volume for THF at two other temperatures: 50°C and 90°C. Again results are in agreement with the theoretical data with a slight difference due to the non-ideality of THF-ethylene mixture (see Figure 27).

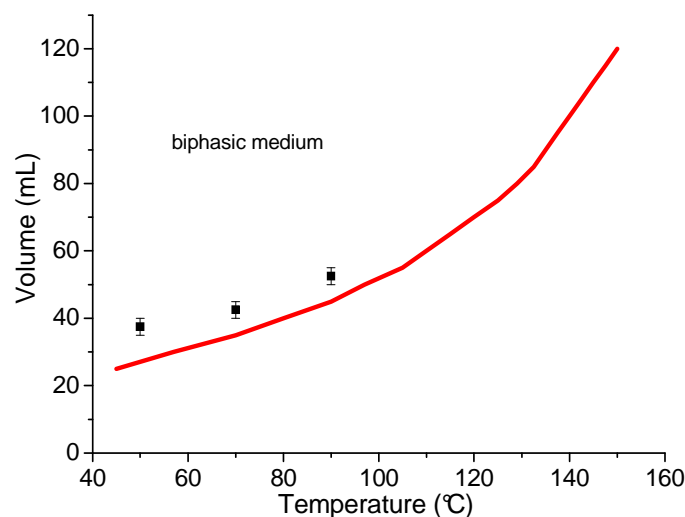


Figure 27. Phase diagram for Ethylene/THF mixture at 100 bar —: computed values, ■: experimental measurement based on polymerization studies

This difference between experimental and theoretical data may slightly decrease with the temperature which would indicate that the interaction parameters between ethylene and THF depend on the temperature ($k_{E/THF} = k_{E/THF}^0 + k_{E/THF}^1 T$). This could be confirmed with more experimental data.

(6) *Effect of the solvent on the phase transition*

Similar calculations are applied to toluene and DEC respectively. As shown in Figure 28 and Figure 29, from Peng-Robinson EoS, THF is the “lighter” solvent and DEC the “heavier”. However, these solvents exhibit similar behavior.

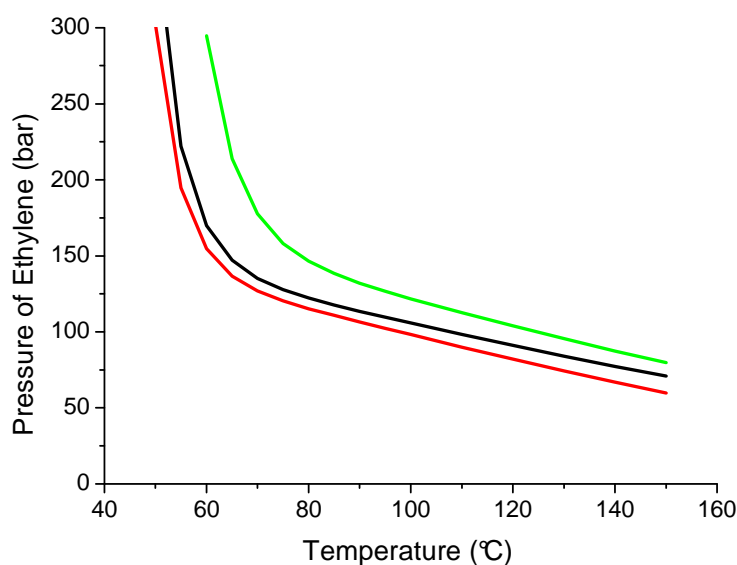


Figure 28. Phase diagram of Ethylene/Solvent system —: with 50 mL toluene, —: with 50 mL THF, —: with 50 mL DEC

Theoretical calculations predict a transition with THF at 70°C and 100 bar at 37 mL compared to 40-45 mL obtained experimentally (see Figure 29); for toluene 33 mL compared to 35-40 mL and for DEC 27 mL vs. 25-30mL. Our experimental approach is in really good agreement with our calculations. As we already mentioned, prediction can be more accurate by considering a non-ideal mixture and therefore determine the interaction parameters (k_{ij}).

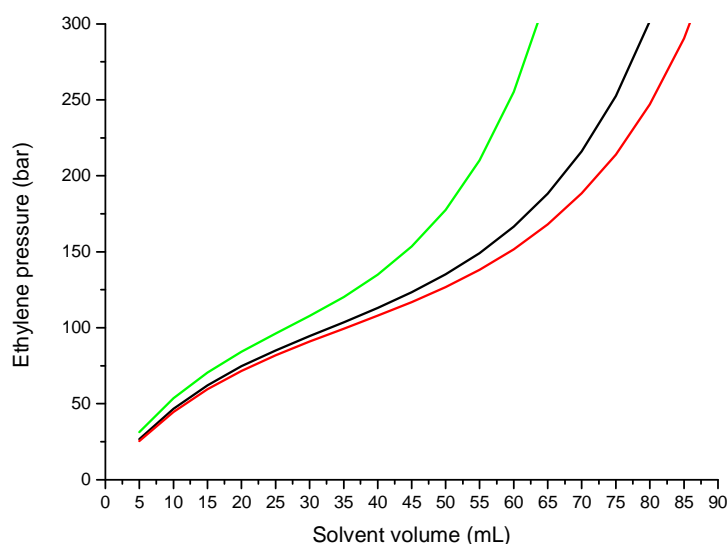


Figure 29. Phase diagram of Ethylene/Solvent system —: at 70°C in toluene, —: at 70°C in THF, —: at 70°C in DEC

In the standard experimental conditions 70°C, 100 bar and 50 mL of solvent, in all cases polymerization take place in a biphasic medium. Consequently, the differences in kinetics observed (see Figure 9) are not due to differences of the medium phase composition. It has to be a solvent effect.

4. Conclusion

In the experimental conditions used to polymerize ethylene, a phase transition takes place between a biphasic (at low pressure and/or low temperature and/or high solvent volume) and monophasic medium (at high pressure and/or high temperature and/or low solvent volume). In the biphasic medium, the ethylene free radical polymerization occurs only in the liquid phase.

This transition has been theoretically and experimentally determined with relative good accuracy.

No dramatic difference of behavior (in ethylene solubility and phase transition) has been obtained between the three solvents investigated (toluene, DEC and THF). Moreover, the study of the monophasic zone of polymerization confirms that the solvent itself activates the free radical polymerization of ethylene.

C. Solvent effect in the free radical polymerization

All these results show that the polymerization medium (monophasic or biphasic) does not explain the differences of yield between our three solvents. Then it has to be an effect of the solvent itself.

The influence of the solvent on free radical polymerization of vinyl compounds was previously reported by Kamachi [12]. For almost all monomers, it is a tiny effect except for vinyl acetate [13] and ethylene [14, 15]. For these two monomers, the kinetics of radical polymerization could vary by a factor up to 10 depending on the solvent.

The early studies for ethylene remain partial due to the experimental conditions available at this time (before 1980s). Machi [16] suggested that the solubility of growing polyethylene chain could induce the solvent activation effect through a Trommsdorff-Norish effect, but his interpretation is still controversial [17]. Myshkin [14] assumed it was a fully different mechanism based on the dielectric constant ϵ of the solvent.

For other monomers, several explanations for this influence have been proposed but none of them is consistent with all sets of data. The influences of solvent on the free radical polymerization are due to variations of kinetic rate constants. Variation of the termination rate [12, 13] was partially related to the viscosity of the solvent due to diffusion mechanisms. For variation in the propagation rate [12, 13, 18, 19], different origins have been proposed as polarity, interactions between polymer and solvent, interactions between monomer and solvent, and complexation between the propagating macroradical and the solvent. Others authors [20-22] suggested that local monomer concentration could also play a major role in the solvent activating effect of the free radical polymerization.

1. Polymerization of ethylene in various solvents

In order to rationalize this solvent effect we performed the polymerization in a wide range of solvents using same experimental conditions (100 bar of ethylene pressure, at 70°C during 4 hours using 50 mg of AIBN).

a) Free ethylene radical polymerization in a wide range of solvents

The results of this set of experiments have been summarized in the Table 7.

Table 7. Solvent effect on free radical polymerization of ethylene^a

Run	Solvent	Yield (g)	Melting point (°C) ^b	Crystallinity (%) ^b	Mn (g/mol) ^c	PDI ^c
1	None	0.1	105.3	46	3010	1.3
2	Cyclohexane	0.6	115.5	58	4800	2.2
3	Heptane	0.65	116.7	55	4700	2.1
4	Toluene	0.7	115.9	63	2340	1.9
5	DMSO	1	112.7	43	1910	3.5
6	Acetonitrile	1.1	115.5	59	1370	2.2
7	DEC	1.2	117.8	62	7150	2.5
8	DMF	1.3	108.5	47	530	2.9
9	Dibutylether	1.3	109.0	52	1370	1.4
10	Ethanol	1.4	117.6	63	2130	2.4
11	Acetone	1.5	115.2	62	1710	2.0
12	Dimethylcarbonate	1.6	117.9	57	11720	2.5
13	Butanone	1.8	61	nd	370	1.2
14	Butyrolactone	1.8	nd	nd	570	1.4
15	Butan-2-ol	1.9	116.4	68	2070	2.8
16	Cyclohexanone	2.1	nd	nd	1760	1.5

Run	Solvent	Yield (g)	Melting point (°C) ^b	Crystallinity (%) ^b	Mn (g/mol) ^c	PDI ^c
17	Butan-1-ol	2.2	117.8	58	4130	2.4
18	Ethyl acetate	2.3	115.2	54	3760	3.3
19	Dichloromethane	2.7	105.1	46	1050	1.6
20	1,4-dioxane	3.2	118.9	65	1300	2.2
21	THF	3.9	115.2	58	1190	1.9

^a: Polymerizations are performed during 4 hours with 50 mg of AIBN at 70°C in 50 mL of solvent under 100 bar of ethylene pressure. ^b: determined by DSC. ^c: determined by HTSEC

As illustrated by the Table 7, yield is highly dependent on the solvent of the polymerization (from 0.1 g to 4 g). If we consider that solubility of ethylene is almost the same for all solvents (470 g/L under 100 bar at 70°C, the same solubility is measured in toluene, heptane, THF, DEC, styrene, MMA, BuA and VAc consequently we hypothesize that the ethylene solubility in an organic solvent is almost independent of the solvent itself) then conversion without solvent is less than 0.3% whereas in presence of solvent it is from 3% to 17%.

b) Molecular weight controlled by solvent

The molecular weight is strongly related to the solvent due to transfer reactions to solvent. The highest molecular weight is reached in dimethylcarbonate (Mn=11700 g/mol – run 12), and the lowest in butanone (Mn=370 g/mol – run 13). The transfer capacity of the solvent can be related to the calculated number of chains per initiator if we assume that the initiator decomposition is almost identical in all solvents. Cyclohexane (Mn=4800 g/mol – run 2) is the less transferring solvent, while butanone is the highest. Toluene (run 4) is the non polar solvent with the highest transfer capacity, 2.4 times more than cyclohexane. Dimethylcarbonate is the less transferring polar solvent (only 1.1 more than cyclohexane).

Solvents with high solvent transfer capacity can be used to obtain functionalized polyethylenes. One of the most transferring solvent is THF, 26 times higher than cyclohexane.

This transfer has been already shown with toluene and THF by ^{13}C NMR (see Figure 3 and Figure 8). Transfers to solvent are also identified with ^{13}C NMR for other solvents such as dioxane (run20, Figure 30), DCM (run 19, Figure 31).

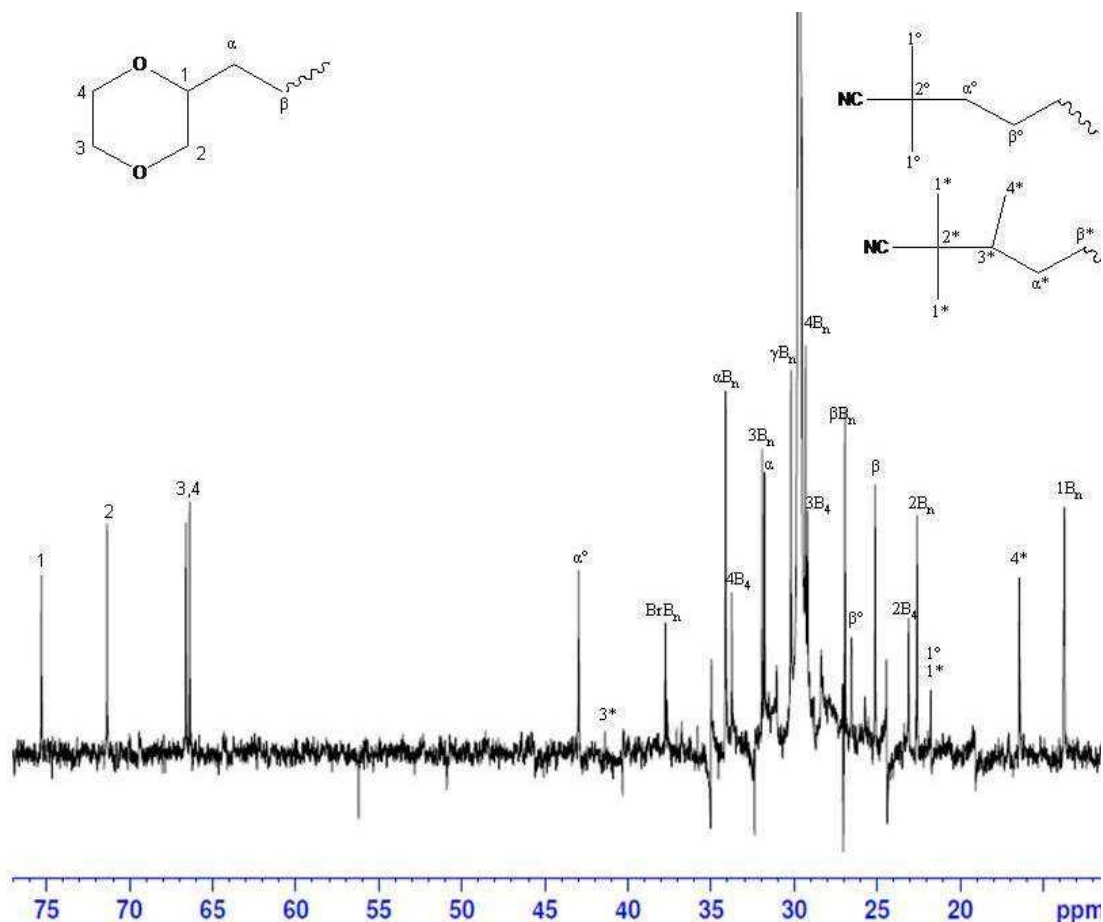


Figure 30. Typical ^{13}C NMR of polyethylene prepared in dioxane (notation from Galland et al [2])

One interesting solvent for further use of the chain-end functionalized PE is the butyrolactone (run 14). It could be used to copolymerize via ring-opening polymerization with a lactone in order to obtain polyester with PE branches.

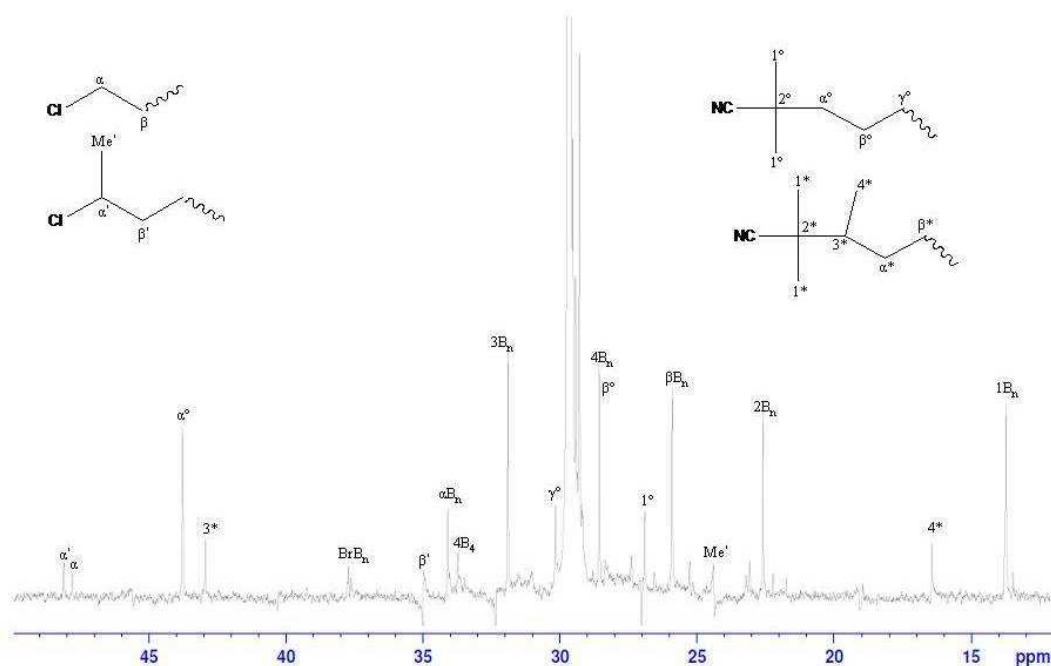


Figure 31. Typical ^{13}C NMR of polyethylene prepared in dichloromethane (notation from Galland et al [2])

The chloro functionalization obtained if polymerization takes place in dichloromethane could also be used further in order to access specific functionalities of PE.

On the contrary, solvents with low transfer ability and high activity provide no functional polyethylene. Usually, high activating solvents are highly transferring, except for ethyl acetate (run 18) which is a particularly poor transferring solvent (but still 4.9 times more transferring than cyclohexane), for butan-1-ol (run 17), and for carbonates (run 7 and 12). These solvents could be used to provide PE with relatively high molecular weight (over 10000 g/mol).

In summary, free radical polymerization of ethylene in solvent can provide either, non-functional/high-molecular weights polyethylenes or functional/low-molecular weights polyethylenes.

c) No simple relation between conversion and the solvent properties

Free radical polymerization of ethylene is strongly dependent on the solvent. This high solvent activation effect could not be related directly to any solvent parameters such as solvent viscosity, dipole momentum, dielectric constant or solubility parameters (see Annex III). THF activates the polymerization 2.8 times more than ethanol (run 12) despite similar dipole momenta. Toluene is 4.6 times less efficient than 1,4-dioxane while they exhibit the same dielectric constants.

2. Rationalization of the solvent effect

a) Theoretical consideration

To quantify the solvent effect we use the theory of the activated complex (equation 15) [23] which links a kinetic constant in a solvent to a kinetic constant without solvent. In this theory, the solvent effect is due to the preferential interactions between the solvent and the activated complex or the reactants.

In the case of the free radical polymerization of ethylene, this stabilization is mostly due to Van der Waals interactions, that is, Keesom (dipole-dipole), Debye (dipole-induced dipole) and London (instantaneous dipole-induced dipole) interactions (equation 16-18). Keesom interactions are the main interactions which stabilize the macroradical ($E_{Keesom} > E_{Debye}$ and E_{London}), since the 1-alkyl radical possesses a dipole momentum.

Consequently, each kinetic constant of the polymerization (k_d , k_p and k_t) exhibits a relation (equation 19) with different solvent properties (ϵ , μ). Therefore, according to the free radical kinetic law (equation 1), yield can be related to $\left(\frac{\mu}{\epsilon}\right)^2$ (equation 20).

$$\ln k = \ln k_0 - \frac{1}{RT} \left(\Delta G_{R,solv} + \Delta G_{M,solv} - \Delta G_{(RM)^*,solv} \right) \quad (15)$$

$$E_{Keesom} = -\frac{1}{3r^6} \left[\frac{\mu_{solvent}^2 \cdot \mu_{radical}^2}{(4\pi \cdot \epsilon_0 \cdot \epsilon_{solvent})^2 k_B T} \right] \quad (16)$$

$$E_{Debye} = -\frac{1}{r^6} \left[\frac{\mu_{solvent}^2 \cdot \alpha_{radical} + \mu_{radical}^2 \cdot \alpha_{solvent}}{(4\pi \cdot \epsilon_0 \cdot \epsilon_{solvent})^2} \right] \quad (17)$$

$$E_{London} = -\frac{1}{r^6} \left[\frac{3}{4} \cdot \frac{h \cdot \nu \cdot \alpha_{solvent} \cdot \alpha_{radical}}{(4\pi \cdot \epsilon_0)^2} \right] \quad (18)$$

$$\ln k \propto \left(\frac{\mu}{\epsilon} \right)^2 \quad (19)$$

$$\ln \ln \frac{1}{1-x} \propto \left(\frac{\mu}{\epsilon} \right)^2 \quad (20)$$

Where k is any kinetic constant in the solvent, k_0 the constant without solvent, R the ideal gas constant, T the absolute temperature, ΔG the solvation Gibbs energy of the

initial and activated state, r the distance between the molecules, μ the dipole momentum, α the polarizability, ε_0 the permittivity of the vacuum, ε the dielectric constant, h the Planck constant, ν the absorbing electromagnetic radiation frequency, x the conversion of the polymerization assuming a free radical kinetic law.

b) Validation of the law

We plot the conversion versus $\left(\frac{\mu}{\varepsilon}\right)^2$ (Figure 32), in order to confirm our relation.

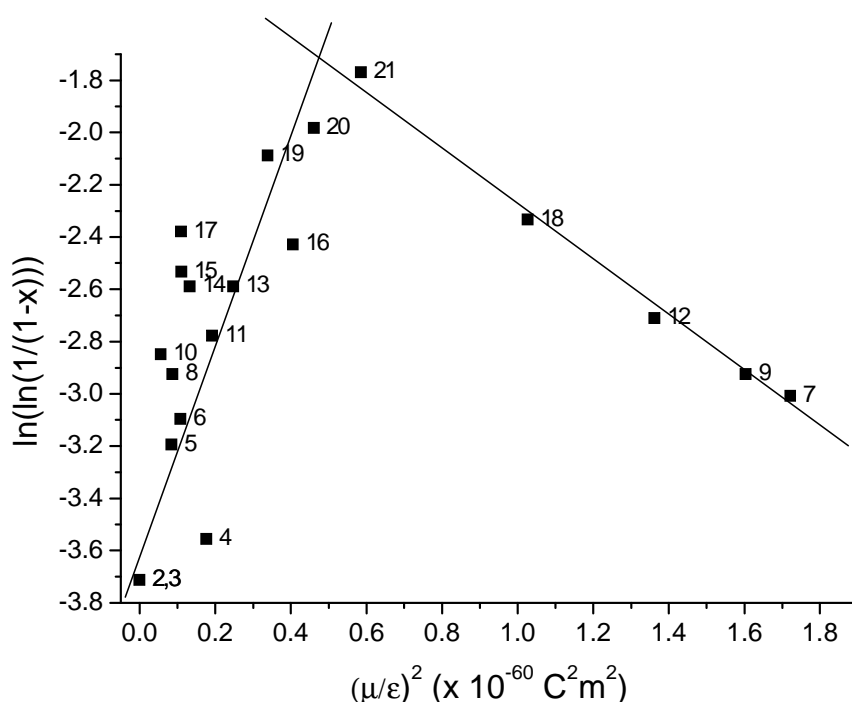


Figure 32. Solvent effect due to Keesom interactions on free radical polymerization of ethylene (labels correspond to run numbers in Table 7) ■ : 50 mg AIBN, 50 mL of solvent 4 h at 70°C under 100 bar of ethylene pressure

The curve obtained is unexpectedly Λ -shaped. A change of behavior is observed for Keesom interactions higher than the ones for THF ($\left(\frac{\mu}{\varepsilon}\right)_{\text{optimum}}^2 \approx 0.58 \cdot 10^{-60} \text{ C}^2\text{m}^2$). At lower value of $\left(\frac{\mu}{\varepsilon}\right)^2$, yield increases with this parameter, over it decreases. Most of the solvents showed a good correlation between polymerization yield and $\left(\frac{\mu}{\varepsilon}\right)^2$.

For alcohols (run 10,15,17) such as ethanol an “over” yield is observed. This can be due to the H-bond interaction which has been neglected in the theory. Indeed in these solvents

stabilization takes place not only by Van der Waals interactions but also by H-bond interactions.

3. Case of solvent mixtures

In order to validate this interpretation of solvent activating effect we perform the polymerization in the same experimental conditions with different mixtures of toluene, THF, and diethylcarbonate (DEC) as solvent (Figure 33). By this way, we artificially change the $\left(\frac{\mu}{\epsilon}\right)^2$ of the solvent by mixing three solvents.

Standard mixing rules [5] used are respectively for relative permittivity $\epsilon_{Mixture} = \sum_{i=1}^N x_i \epsilon_i$, with x_i the volume fraction of solvent i and ϵ_i the relative permittivity of solvent i , and for dipole momentum $\mu_{Mixture} = \sum_{i=1}^N \sum_{j=1}^N x_i x_j \sqrt{\mu_i \mu_j}$, with μ_i the dipole momentum of the solvent i .

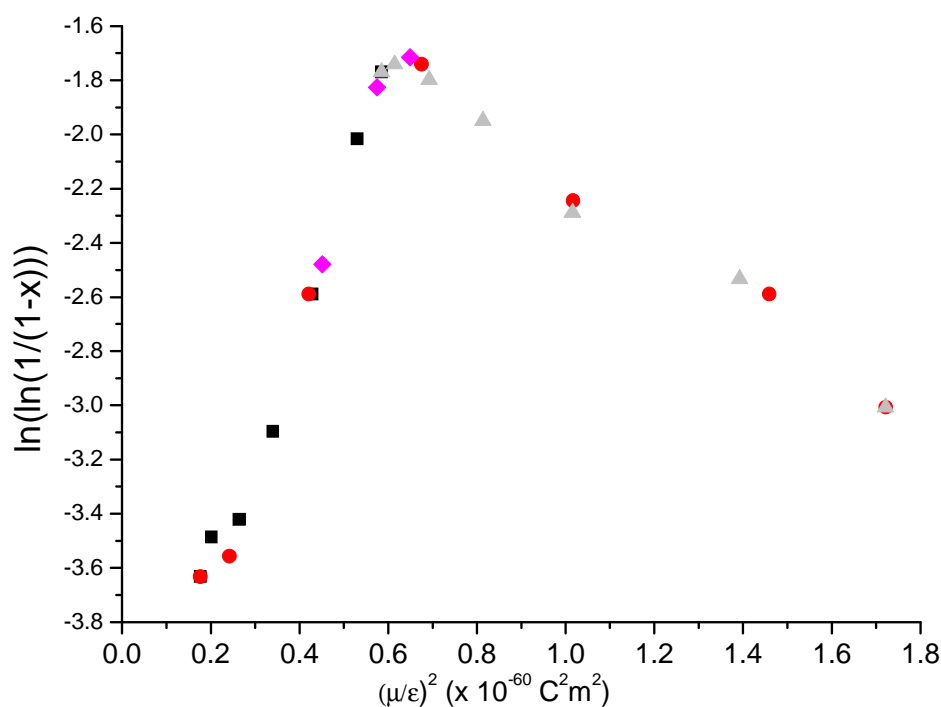


Figure 33. Mixture composition effect due to Keesom interactions on free radical polymerization of ethylene: 50 mg of AIBN during 4 hours under 100 bar of ethylene pressure with 50 mL ■ of THF-toluene, ▲ of THF-DEC mixture, ● of toluene-DEC mixture, ◆ of THF-toluene-DEC mixture

In all cases, whatever the mixture composition, the same Λ -shaped curve is observed between conversion and $\left(\frac{\mu}{\epsilon}\right)^2$ (see Figure 33). The maximum of activity (yield 4.1 g) is reached for $\left(\frac{\mu}{\epsilon}\right)^2_{\text{optimum}} \approx 0.65 \cdot 10^{-60} \text{ C}^2 \text{ m}^2$. Polymerization in Toluene-DEC mixture follows the same curve than toluene-THF and THF-DEC mixtures.

So by tuning the proportion of toluene-DEC mixture we are able to provide the same activity as the ethylene polymerization in THF. This evidences that the solvent interaction with the alkyl radical is an exact average of the solvent composition and is not due to the solvent itself (only dependent on the average $\left(\frac{\mu}{\epsilon}\right)^2$). In other words the solvation shell presents the same composition than the overall solvent composition; there is no favorable interaction of one of the solvents.

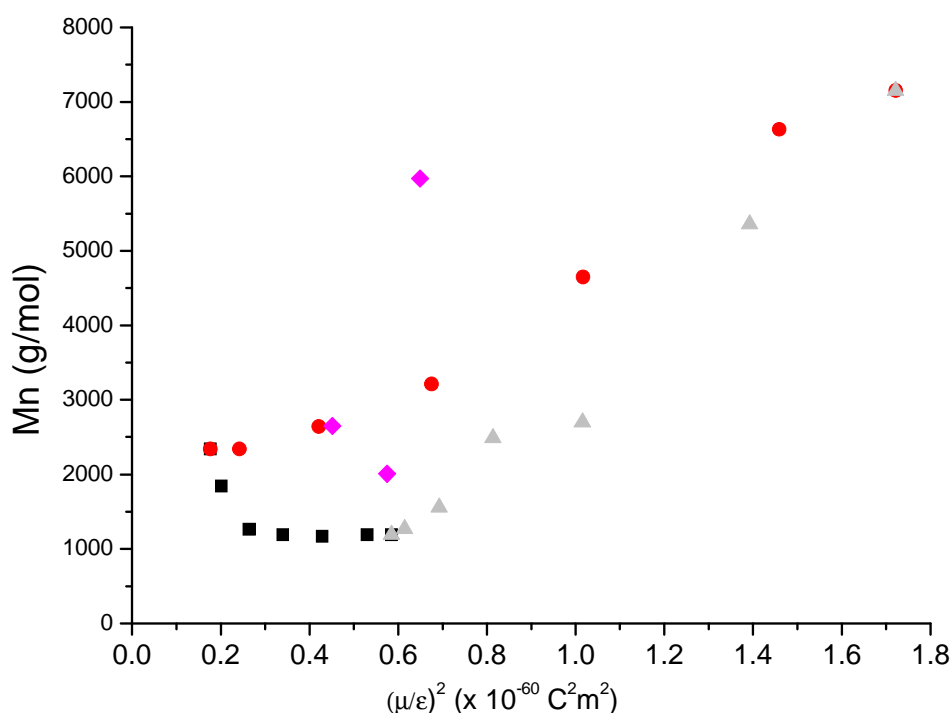


Figure 34. Mixture composition influences by Keesom interactions molecular weight of PE synthesized: 50 mg of AIBN during 4 hours under 100 bar of ethylene pressure with 50 mL ■ of THF-toluene, ▲ of THF-DEC mixture, ● of toluene-DEC mixture, ◆ of THF-toluene-DEC mixture

Using solvent mixtures, a better solvent than THF is provided. Moreover solvent mixtures are able to lead to the same activity than any third solvent but the molecular weights of the synthesized polyethylenes will be different (see Figure 34).

For example, a toluene/DEC 50/50 v/v mixture provides about the same polymerization activity as THF but does not lead to the same molecular weight: respectively 3200 g/mol and 1200 g/mol.

Therefore as the solvent activation effect is a global solvent effect only related to μ and ε , and molecular weight mostly controlled by the composition of the solvent used, yield and average molecular weight can be tuned easily by choosing a suitable mixture of solvents.

4. Arrhenius parameters of Toluene/DEC/THF

To investigate further the Arrhenius parameters of the free radical polymerization of ethylene in toluene, DEC and THF are compared to $\left(\frac{\mu}{\varepsilon}\right)^2$ values of these solvents (see Table 8).

Table 8. Arrhenius parameters of ethylene polymerization (assuming the validity of Arrhenius law)

Solvent	$\left(\frac{\mu}{\varepsilon}\right)^2$ ($10^{-60} \text{ C}^2.\text{m}^2$)	E_{tot} - Global activation energy (kJ/mol)	$\ln(A_{\text{tot}})$ – Global pre- exponential factor
Toluene	0.18	27.7	7.6
THF	0.58	32.8	10.3
DEC	1.72	40.0	12.2

a) Relation with the solvent parameters

Both global activation energy and pre-exponential factor increase with $\left(\frac{\mu}{\varepsilon}\right)^2$. Lower global activation energy is usually linked to a more favorable reaction. In all solvents the polymerization mechanism is considered to be the same, so the change in the global activation energy is only due to the relative stabilization of reactant and activated states, which differs from one solvent to the other [23]. Solubilization by toluene provides a lower energy barrier than in THF and DEC.

The global pre-exponential factor is proportional to the frequency of efficient collisions. With a higher pre-exponential factor the probability of the mechanism involved to occur is supposed to increase. Differences in geometry of activated states in toluene, in THF and in DEC could explain the difference of pre-exponential factors. Toluene is less electron donor than THF; therefore, more toluene molecules will be necessary to stabilize the radical. Consequently, the radical should have a harder solvation shell in toluene than in THF. This could explain why the pre-exponential factor is higher in THF than in Toluene. The same interpretation could be applied for DEC.

For these three solvents, a linear relationship seems to exist between E_{tot} and $\left(\frac{\mu}{\epsilon}\right)^2$, in the same way $\ln(A_{tot})$ vs $\left(\frac{\epsilon}{\mu}\right)^2$ is linear.

b) Optimum calculation

These two relations allow to estimate the Arrhenius parameters for every $\left(\frac{\mu}{\epsilon}\right)^2$ and to predict the optimum of solvent activation.

Free radical polymerization kinetics law links monomer conversion to the global kinetic constant. Since we know the Arrhenius parameters dependence to the solvent properties $\left(\frac{\mu}{\epsilon}\right)^2$, the conversion dependence to $\left(\frac{\mu}{\epsilon}\right)^2$ can be calculated.

$$\ln \frac{1}{1-x} \propto k_{tot} \text{ and } \ln k_{tot} = \ln A_{tot} - \frac{E_{tot}}{RT}$$

$$\text{With } X = \left(\frac{\mu}{\epsilon}\right)^2 > 0$$

$$\text{Then } \ln A_{tot} = a \frac{1}{X} + b \text{ and } E_{tot} = cX + d$$

Then we can calculate the optimum dependence with the temperature.

$$\frac{\partial \ln k_{tot}}{\partial X} = 0 \text{ and } \frac{\partial \ln k_{tot}}{\partial X} = \frac{\partial \ln A_{tot}}{\partial X} - \frac{1}{RT} \frac{\partial E_{tot}}{\partial X}$$

$$\text{Then } 0 = -a \frac{1}{X_{optimum}^2} - \frac{c}{RT}, \text{ consequently } X_{optimum} = \sqrt{-\frac{aRT}{c}}$$

The optimum depends of the temperature (in Kelvin the relation is $\left(\frac{\mu}{\varepsilon}\right)_{optimum}^2 \approx 0.03\sqrt{T} \cdot 10^{-60} C^2 m^2$). Using Arrhenius parameters, at 70°C the predicted optimum is $\left(\frac{\mu}{\varepsilon}\right)_{optimum}^2 \approx 0.56 \cdot 10^{-60} C^2 m^2$.

5. Solvent cohesive pressure interpretation

Solvent Van der Waals interactions are also well described by the cohesive pressure parameters. These parameters correspond to the energy to put a solvent molecule at an infinite distance to other solvent particles. Consequently, it testifies for the strength of the solvent/solvent interactions therefore the rigidity of the solvation cage.

Therefore, we plot yield versus solvent cohesive pressure (see Figure 35).

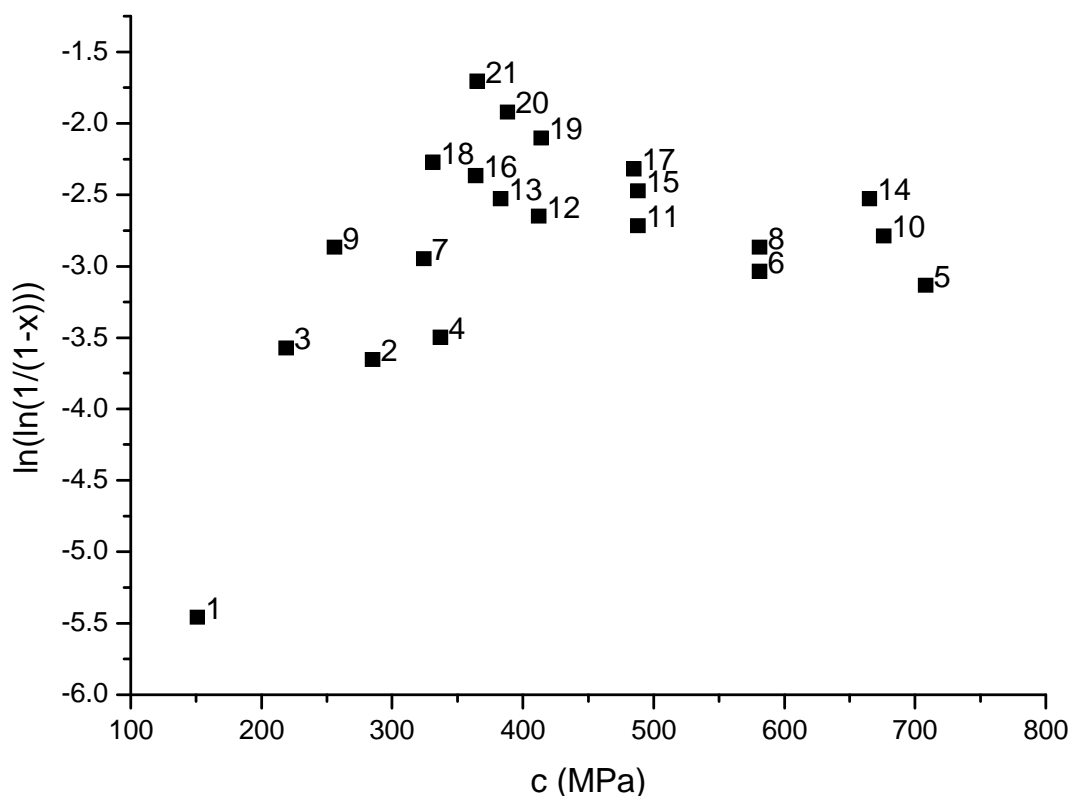


Figure 35. Solvent influence by cohesive pressure parameters on radical polymerization of ethylene (labels correspond to run numbers in Table 7) ■ : 50 mg AIBN, 50 mL of solvent 4 h at 70°C under 100 bar of ethylene pressure

The curve obtained is Λ -shaped with lower correlation than $\left(\frac{\mu}{\varepsilon}\right)^2$ alone. This kind of curve testifies for a change of behavior with the cohesive pressure parameters. A two-stage

process of the addition of ethylene on the macroradical could explain the experimental results (Figure 36).

At low solvent cohesive pressure, the macroradical and the ethylene solvation cages are too labile to confine efficiently ethylene with the macroradical, and consequently induce a low efficient addition. By increasing this cohesive pressure, half-life time of this intermediate species will increase therefore k_p increases. At high cohesive pressure, the limiting process is the interpenetration of the two initial solvation cages. The more cohesive the solvent is, the less ethylene penetrates the solvent cage of the macroradical, therefore k_p decreases.

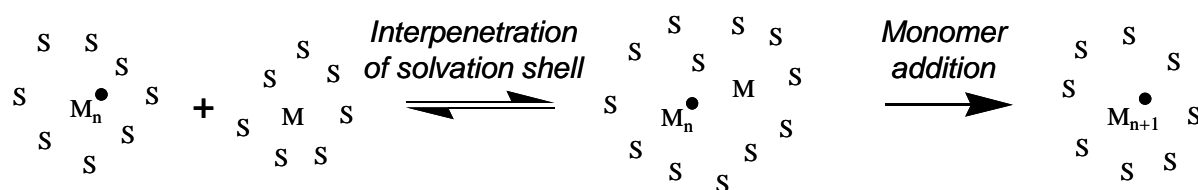


Figure 36. Schematic interpenetration of the solvent effect thanks to two step mechanism. With M a monomer, S a solvent, M_n^\bullet a macroradical.

It should be noted that the solvent repartition is totally different when Keesom interactions or cohesive pressure are used.

This method leads to a less accurate correlation than $\left(\frac{\mu}{\epsilon}\right)^2$. This may reflect that only the solvent/solvent interaction is taken into account. The nature of the reactant and product, which lead to different interactions with the solvent (and consequently weaken or strengthen the solvation cage) is not considered in this theory.

6. Interpretation of the solvent optimum

The optimum of solvent properties is calculated by three different techniques $\left(\frac{\mu}{\epsilon}\right)_{optimum}^2 \approx 0.56 - 0.65 \cdot 10^{-60} C^2 m^2$ at $70^\circ C$ (using different solvents, the mixtures of solvents and Arrhenius parameters) with little discrepancy.

This optimum is close to the $\left(\frac{\mu}{\epsilon}\right)_{optimum}^2 \approx 0.62 \cdot 10^{-60} C^2 m^2$ of an alkyl radical ($\mu \approx 1.5 \cdot 10^{-30} Cm$ and $\epsilon \approx 1.9$). The optimum solvent properties could be then correlated to the macroradical properties. Dipole momentum μ is the punctual dipole momentum of the radical 1-hexyl. It is determined by MOPAC calculation of partial charge and geometry of the

radical $\mu_{\text{radical}} = \sum_i q_i \vec{r}_i$ with q_i the partial charge of the i atom, and \vec{r}_i a vector from some reference to the atom i . The relative permittivity ϵ corresponds to the permittivity of the growing end chain, it could be approximated to a molecule similar to the saturated end chain (for macroradical of the free radical polymerization of ethylene we choose heptane).

Consequently optimum solvent is reached when its $\left(\frac{\mu}{\epsilon}\right)^2$ is the closest to the $\left(\frac{\mu}{\epsilon}\right)^2$ of the propagating radical.

7. Case of other monomers

In order to confirm this correlation between the solvent optimum activation of polymerization and the radical properties, the radical polymerization of 1-hexene, vinyl acetate (VAc) and 1,1-dichloroethylene (DCE) are performed.

a) Solvent activation effect with other monomers

These three monomers are known to exhibit a high solvent effect in free radical polymerization [12, 13]. Moreover polymerization of these monomers could be used within a certain limits as models of the radical polymerization of ethylene. 1-hexene, a liquid non stabilized olefin like ethylene, and VAc free radical polymerization is based on non stabilized alkyl radical as ethylene. Finally PDCE is a semi-crystalline polymer as PE.

Again Λ -shaped curves are obtained for two of the three monomers for conversion vs $\left(\frac{\mu}{\epsilon}\right)^2$ (Figure 37).

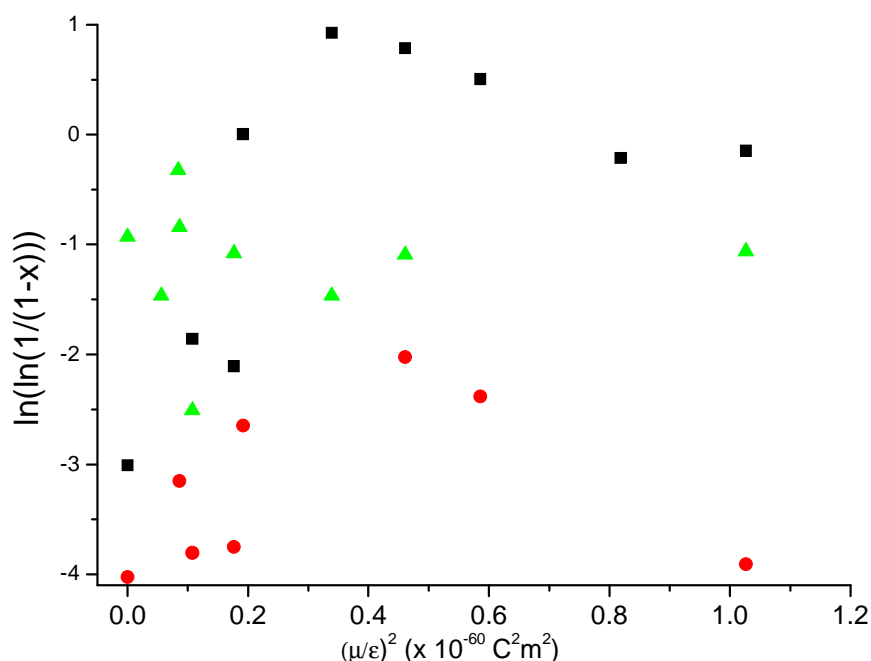


Figure 37. Solvent influence by Keesom interaction on free radical polymerization

■ : 100 mg AIBN, 90 ml of solvent and 10 mL of VAc 4 hours at 70°C

● : 100 mg AIBN, 90 ml of solvent and 10 mL of 1-hexene 4 hours at 70°C

▲ : 100 mg AIBN, 80 ml of solvent and 20 mL of DCE 4 hours at 70°C

For VAc, a change of slope is observed for Keesom interactions higher than those in dichloromethane ($(\mu/\epsilon)^2 \approx 0.35 \cdot 10^{-60} \text{ C}^2\text{m}^2$). At lower value of $(\mu/\epsilon)^2$ yield increases with this parameter, over yield decreases. The optimal $(\mu/\epsilon)^2$ seems to occur at about $0.3 \cdot 10^{-60} \text{ C}^2\text{m}^2$. This optimum is well correlated with the $(\mu/\epsilon)^2 \approx 0.25 \cdot 10^{-60} \text{ C}^2\text{m}^2$ of the corresponding radical ($\mu \approx 3 \cdot 10^{-30} \text{ Cm}$ and $\epsilon \approx 6$) calculated with the same approximation as for ethylene (μ of radical 1-ethyl acetate and ϵ of ethyl acetate).

For 1-hexene, the same kind of curve is observed with a maximum around $0.4 \cdot 10^{-60} \text{ C}^2\text{m}^2$. Once again this maximum could be correlated to the corresponding radical, $(\mu/\epsilon)^2 \approx 0.4 \cdot 10^{-60} \text{ C}^2\text{m}^2$ of the alkyl radical ($\mu \approx 1.2 \cdot 10^{-30} \text{ Cm}$ of radical 2-hexyl and $\epsilon \approx 1.9$ of heptane).

For DCE, a non Λ -shaped curve is obtained. It can be explained because $\left(\frac{\mu}{\varepsilon}\right)^2 \approx 0.1 \cdot 10^{-60} C^2 m^2$ ($\mu \approx 3.3 \cdot 10^{-30} Cm$ radical 1-(1,1-dichloro)ethyl and $\varepsilon \approx 10.4$ of 1,1-dichloroethane) of DCE radical is too low, then the first part of the curve cannot be observed.

b) Possible interpretation of the solvent activation effect

The solvent activation effect on the free radical polymerization is correlated to the Keesom interactions between the radical and the solvent. This interaction is not punctual but due to the average composition of the solvation shell of the macroradical. The decrease of the Keesom interaction lowers the global activation energy (due to a decrease of the stabilization), as the global pre-exponential factor (due to a thickening of the macroradical solvation shell). The intensity of the solvent effect remains an open question. A different optimum was observed for each monomer. This optimum $\left(\frac{\mu}{\varepsilon}\right)^2$ is close to the corresponding same parameters of the radical $\left(\frac{\mu}{\varepsilon}\right)^2$.

However, the optimum corresponds to the monomer radical, not to the radical AIBN fragment. So the initiation (first addition of the monomer) is not determining in the solvent activation effect. Indeed if it was the case the optimum $\left(\frac{\mu}{\varepsilon}\right)^2$ would be the same for each monomer and would correspond to the $\left(\frac{\mu}{\varepsilon}\right)^2 \approx 0.02 \cdot 10^{-60} C^2 m^2$ of the radical AIBN ($\mu \approx 1.1 \cdot 10^{-30} Cm$ and $\varepsilon \approx 25$). Consequently it must be the propagation and/or termination steps which are influenced by the solvent.

For standard monomers (MMA, Sty, BuA), the solvent effect remains tiny [12, 13]. These monomers possess higher propagation rate and lower termination rate than the monomers which exhibit a solvent activation effect. As the activity is proportional to $\frac{k_p}{\sqrt{k_t}}$ the absolute variation of these kinetics rates must be higher to exhibit a solvent effect. So only monomers, which possess low propagation rate or high termination rate, seem to express a high solvent effect.

8. Conclusion

Free radical polymerization of ethylene can be performed under mild conditions ($P < 250$ bar and $T < 100^\circ\text{C}$) in a wide range of solvents. These polymerizations exhibit some unexpected behaviors such as a high solvent activation effect and a phase transition of the polymerization medium between a monophasic one and a biphasic one.

At this point of the discussion we investigated two major effects on the free radical polymerization of ethylene: the phase transition behavior and solvent effect. No correlation exists between these factors. Phase transition depends mostly of the critical parameters of the solvent (T_c and P_c) while the solvent activation effect depends of $\left(\frac{\mu}{\epsilon}\right)^2$.

In order to reach higher activity we demonstrate that polymerization must be done near the frontier (between monophasic and biphasic medium) and with an optimal $\left(\frac{\mu}{\epsilon}\right)^2$.

Solvent transfer capacities have also crucial importance on the synthesized PE. Since the alkyl radical possesses a high reactivity, the transfer constants to solvents are high and for most of the solvents it is the transfer which controls the molecular weight of the PE synthesized. This transfer to solvent can be used to functionalize PE by chlorine (with DCM) or lactone (with γ -butyrolactone) for example. Then the functional PE can be used as a macromonomer in order to access novel architecture, or as reactant. Finally, carbonates are the less transferring solvents and M_n values up to 15000 g/mol are reached. This molecular weight over the entanglement mass should lead to some interesting properties.

In the next sections we will investigate the role of additional compounds such as Lewis acid or controlled agents on the radical polymerization of ethylene.

D. Lewis acid effect on the ethylene radical polymerization

Free radical polymerization of ethylene is solvent dependent. Therefore, in order to activate the polymerization the solvent must be chosen wisely.

Another method to increase activity of the polymerization was demonstrated by Clark [24, 25] using activation of the ethylene double bond by Lewis acid. Consequently, in this section we will investigate the influence of Lewis acid on the radical polymerization of ethylene.

1. Investigation of Lewis acids

In classical experimental conditions (100 bar of ethylene pressure, 70°C 4 hours in 50 mL of solvent with 50 mg of AIBN), we add 50 mg of Lewis acid. Bipyridine is also added to the mixture in order to dissolve the Lewis acid (polymerization with bipyridine alone does not affect the polymerization compared to the reference). Results are summarized in the following table.

Table 9. Lewis acid influence on the free radical polymerization of ethylene^a

Solvent	Lewis acid	Yield (g)	Mn (g/mol) ^b	PDI ^b
Toluene	–	0.65	2340	1.9
Toluene	CuCl	1.0	2170	1.9
Toluene	CuCl ₂	0.7	2310	1.8
Toluene	FeCl ₂	0.8	2940	1.8
Toluene	FeCl ₃	1	3100	1.8
Toluene	AlCl ₃	0.5	1780	2.1
Toluene	ScTf ₃	0.6	2850	1.8
THF	–	3.9	1190	1.9

Solvent	Lewis acid	Yield (g)	Mn (g/mol) ^b	PDI ^b
THF	CuCl	1.8	1910	1.8
THF	CuCl ₂	2.2	1380	1.9
THF	FeCl ₂	2.3	1660	2.0
THF	FeCl ₃	1.6	1830	1.7
THF	AlCl ₃	1.6	1860	1.6
THF	ScTf ₃	3.0	1590	1.7
DEC	—	1.2	7150	2.5
DEC	CuCl	1.5	6880	2.6
DEC	CuCl ₂	1.2	6730	2.5
DEC	FeCl ₂	1.3	6540	2.5
DEC	FeCl ₃	1.8	6540	2.4
DEC	AlCl ₃	1.3	5360	3.4
DEC	ScTf ₃	2.0	7450	2.8

^a: Polymerizations are performed during 4 hours with 50 mg of AIBN at 70°C in 50 mL of solvent under 100 bar of ethylene pressure with 50 mg of Lewis acid and 150 mg bipyridine.

^b: determined by HTSEC

In toluene almost all Lewis acids lead to a better activity (especially for CuCl and FeCl₃). As we mentioned previously toluene interaction with radical and ethylene is negligible (almost no solvent activation effect), then the addition of a Lewis acid could increase slightly the efficiency of the free radical polymerization of ethylene via an activation of the ethylene double bond as predicted by Clark.

In THF, all Lewis acids investigated decrease the efficiency of the polymerization. THF exhibits a high solvent activation effect therefore these Lewis acids seems to disturb the activation by THF.

In DEC all Lewis acid increase yield. ScTf₃ and FeCl₃ lead to the highest activity. Surprisingly the strong Lewis acid ScTf₃ is an activator only in DEC.

The rationalizations of these effects are not an easy task as Lewis acid and solvent play major roles in the free radical polymerization of ethylene. Clark calculations predict a drastic increase of the yield of polymerization. This is not the case here and it is mostly due to Clark hypothesis of a gaseous polymerization in which no interaction occurs between ethylene and solvent.

2. Investigation of metal alkyl and alkoxides

Metal alkyl effect on the free radical polymerization is also studied. We perform the polymerization in the same experimental condition (100 bar of ethylene pressure, 70°C during 4 hours in toluene and using 50 mg of AIBN). In each case, we perform the polymerization at the same organometallic concentration 0.02 mol/L, therefore corresponding to an excess of 3 times of the AIBN contained. In this study, only toluene is used as solvent. Results are summarized in the following table.

Table 10. Metal alkyls influence on the free radical polymerization of ethylene^a

Metal alkyl	Yield (g)	Mn (g/mol) ^b	PDI ^b
-	0.65	2340	1.9
ZnMe ₂	1.1	2950	1.6
ZnEt ₂	0.6	840	1.1
BuMgOct	0.2	410	1.6
BEt ₃	0.8	4070	1.6
MAO [*]	0.4	3580	2.0
AlEt ₃	1.3	970	1.1
Al(iBu) ₃	0.5	2510	1.9
Al(nOct) ₃	0.2	1140	1.1
Al(OiPr) ₃	0.7	2370	2.1

^a: Polymerization are performed during 4 hours with 50 mg of AIBN at 70°C in 50 mL of toluene under 100 bar of ethylene pressure with 0.02 mol/L of metal alkyl. ^b: determined by HTSEC. ^{*}: AlMe₃ free

ZnMe₂ and AlEt₃ are the only activating agent of the polymerization. If longer alkyl chains are used the activity drastically decreases: for example from 1.3 g to 0.2 g for the aluminum series.

MAO and BuMgOct deactivate the free radical polymerization of ethylene. Al(OiPr)₃ seems to have no effect on the polymerization yield and the MWD of the polyethylene produced. BEt₃ leads to a slight activation of the polymerization together with an increase of molecular weight.

For ZnEt₂ and AlEt₃ molecular weight also decreases and MWD became extremely narrow. This narrowing with important decrease of Mn could be due to a control of molecular

weight by metal alkyl. With ZnEt_2 , 2.6 times more chains are synthesized, 4.8 for AlEt_3 , compared to the polymerization without alkyl metal. This means that 1.7 times more chains are synthesized with AlEt_3 vs. ZnMe_2 , almost equal to the ratio of Al-C bond/Zn-C bond 1.5. Moreover, total number of chains is 1.3 chains per Al-C bond and 0.7 Zn-C bond.

This effect is not due to an “Aufbau” reaction since the polymerization with the metal alkyl alone is inefficient with all metal alkyl studied.

Consequently, these compounds (ZnEt_2 and AlEt_3) could play the role of a controlling agent via a mechanism of degenerative transfer similar to RAFT (see Figure 38). These results are promising toward the possibility of controlling the ethylene radical polymerization and will require to be investigated further.

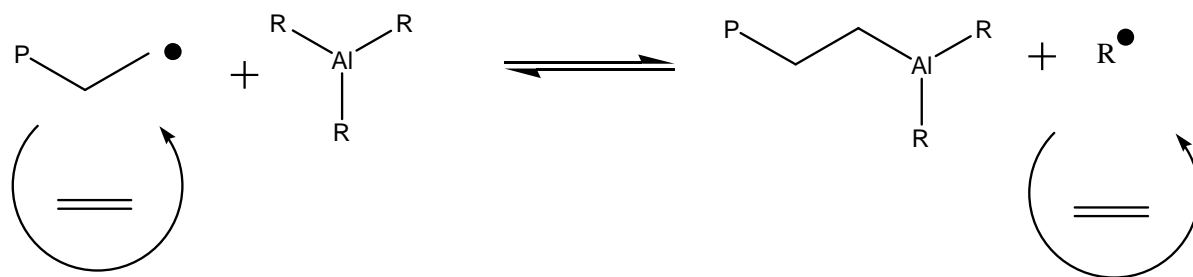


Figure 38. Proposed mechanism of controlled of ethylene radical polymerization by AlEt_3 (similar mechanism should be involved for ZnEt_2)

E. Toward controlled radical polymerization

Free radical polymerization of ethylene can be performed with significant yield. One point of interest is to develop controlled polymerization of ethylene. Two systems are chosen for some tryouts of CRP: RAFT and Co mediated CRP. These methods are promising for the ethylene CRP as they are already reported to control efficiently VAc which polymerizes via a non stabilized radical as ethylene does.

We also perform tryouts in NMP, under 250 bar of ethylene at 110°C using TEMPO or SG1 but no polyethylene has been synthesized. Under this temperature, no homolytic fragmentation of the carbon-nitroxide bond takes place and therefore the ethylene polymerizations are totally inhibited.

1. RAFT

In order to assess the controlled behavior of the polymerization we studied the kinetics profile of the reaction. We perform set of experiments at 100°C in THF under 250 bar of ethylene pressure with in all cases a RAFT agent (O-ethyl-S-(1-ethyl acetate)dithiocarbonate (xanthate of vinyl acetate, Figure 39) with a ratio RAFT/AIBN 10/1 (see Figure 40).

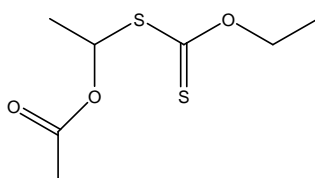


Figure 39. RAFT agent used

The RAFT agent itself has a crucial role. For example the polymerization has been also performed in the same conditions with O-ethyl-S-(1-phenylethyl)dithiocarbonate (xanthate of styrene) and O-ethyl-S-ethyldithiocarbonate (xanthate of ethylene), but no polymer has been synthesized.

Moreover solvents are also important as no polymer is synthesized in DEC or toluene in the same experimental conditions using 50 mg of AIBN. Finally under lower pressure (100 bar) and temperature (70°C) no PE is synthesized as well. Consequently the harsh conditions used are mandatory in order to obtain some polymer.

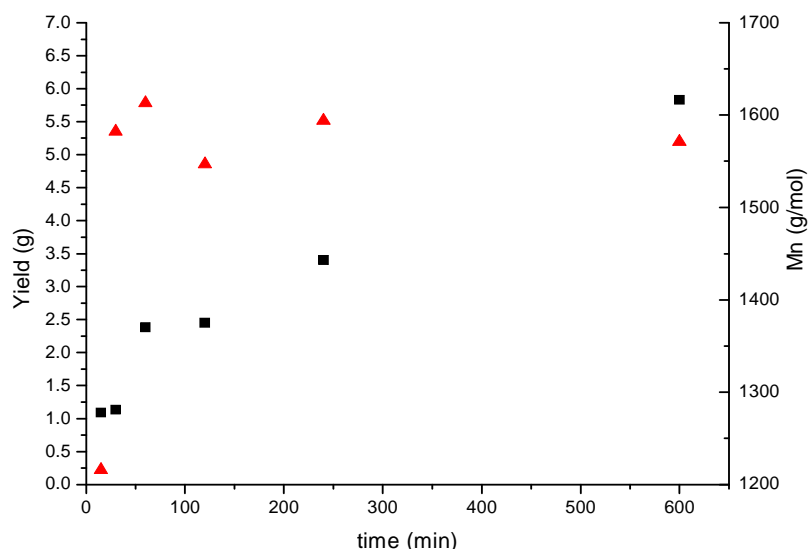


Figure 40. Reaction profile of the radical polymerization of ethylene with a RAFT agent and 10 mg of AIBN at 100°C under 250 bar of ethylene pressure in 50 mL of THF: ■ yield versus time, ▲ molecular weight* versus time. *: determined by HT-SEC

With low AIBN concentration (10 mg) molecular weights remain almost constant with the conversion. Polymerization without RAFT agent provides 8 g of PE in 4 hours with molecular weight of 1520 g/mol compared to 3.4 g of PE with Mn equal to 1590 g/mol in the presence of the RAFT agent. Consequently activity is lower with the RAFT agent which indicates a interaction between the radical and the xanthate. However Mn is almost identical to the polymerization without the RAFT agent therefore the transfer to THF seems to control the MWD. Consequently we do not control the radical polymerization of ethylene.

Two methods can be developed in order to reach a better control of the polymerization, to increase the control agent concentration or to choose a less transferring solvent. As we already mentioned polymerization is inefficient in toluene or DEC. Consequently we perform a second set of experiment using 50 mg of AIBN (see Figure 41).

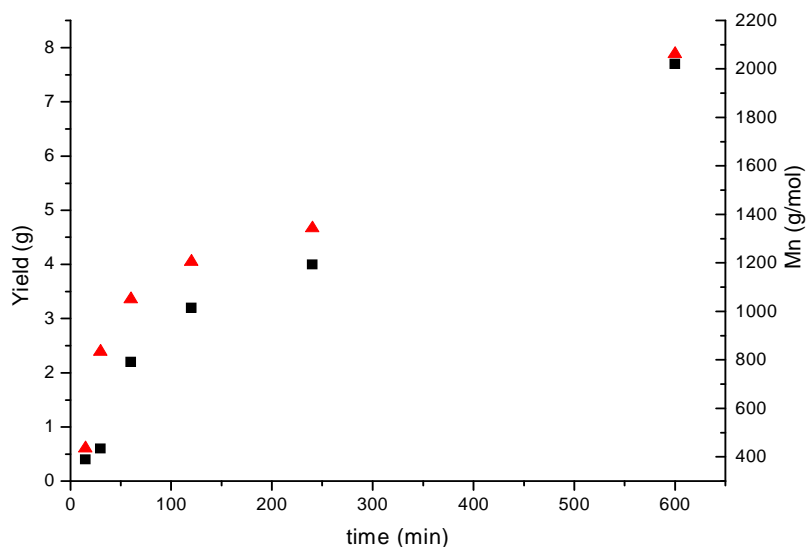


Figure 41. Reaction profile of the radical polymerization of ethylene with a RAFT agent and 50 mg of AIBN at 100°C under 250 bar of ethylene pressure in 50 mL of THF: ■ yield versus time, ▲ molecular weight* versus time. *: determined by HTSEC

In this case with 5 times more RAFT agent than the previous set of experiment, a good correlation between Mn and ethylene conversion seems to be observed (see Figure 41 and Figure 42). PDI remains about 1.5. Polymerization without xanthate provides in 4 hours 23 g of polyethylene with $M_n \approx 1500$ g/mol in the same experimental condition (compared to 4 g of polyethylene with $M_n \approx 1340$ g/mol). However control is not perfect as the number of polyethylene chains increase with the conversion which indicates that some dead chains are produced (see Figure 42).

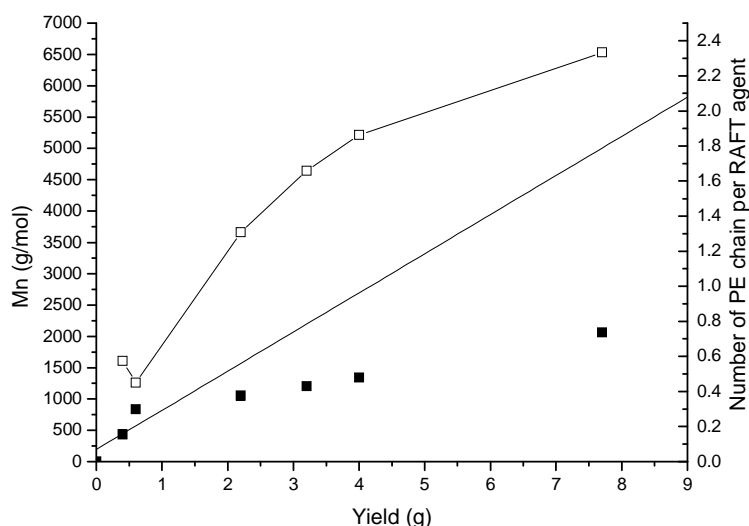


Figure 42. Evolution of the molecular weight* and chain number with yield: — theoretical curve for molecular weight, ■ molecular weight, —□— number of chain per RAFT agent. *: determined by HTSEC

These results are very interesting and lot of complementary study needs to be done in order to progree in the direction of the controlled radical polymerization behavior of ethylene.

2. Co mediated CRP

Another promising controlled radical polymerization of ethylene is the cobalt mediated one. We perform the polymerization at 90°C under 250 bar of ethylene pressure in THF with 50 mg of AIBN using 10 equivalents of $\text{Co}(\text{Acac})_2$ (see Figure 43).

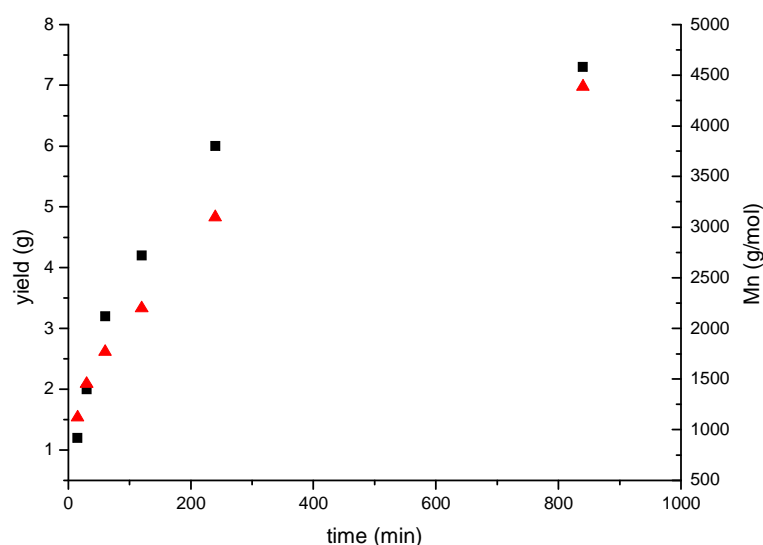


Figure 43. Reaction profile of the radical polymerization of ethylene with $\text{Co}(\text{Acac})_2$ and 50 mg of AIBN at 90°C under 250 bar of ethylene pressure in 50 mL of THF: ■ yield versus time, ▲ molecular weight* versus time. *: determined by HTSEC

In this case, molecular weights increase with time and yield. As shown in Figure 44, variation of the molecular weight versus the yield is close to the theoretical one. PDI is almost constant with the yield and remains about 1.5. Moreover number of chains per Co is nearly constant during the polymerization and remains at approximately 1 (see Figure 44).

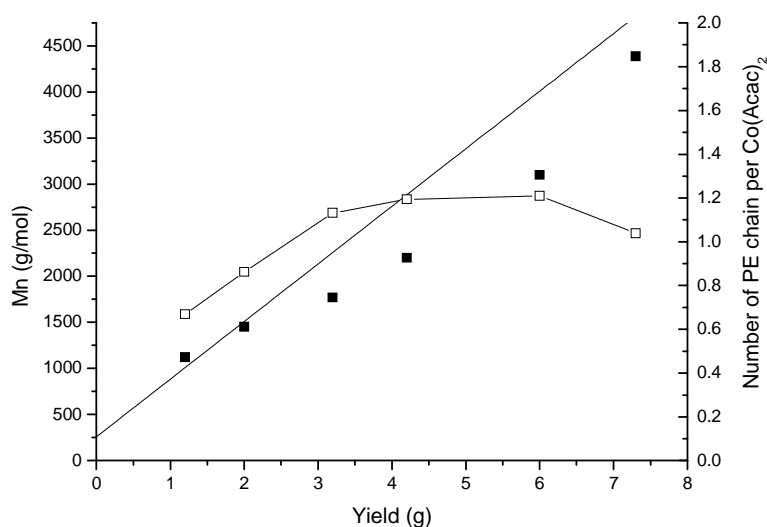


Figure 44. Evolution of the molecular weight* and chain number with yield:
— theoretical curve for molecular weight, ■ molecular weight, —□— number of chain
per Co(Acac)₂. *: determined by HTSEC

Cobalt mediated radical polymerization at the light of these tryouts seems to be a very promising method in order to reach the control of the radical polymerization of ethylene. However other experiments need to be performed in order to confirm the controlled behavior of this polymerization (such as block copolymerization).

It should be noticed that a branched PE is produced in all cases, consequently intramolecular transfer takes place even in these “controlled” conditions. Up to now we reached a control of the molecular weight but not of the branching level.

F. Conclusion

From an industrial process which requires extremely high energy consuming experimental conditions ($P > 1000$ bar and $T > 100^{\circ}\text{C}$) we develop the polymerization under milder conditions, previously assumed to be inefficient. Solvent activation effect and transition between mono and biphasic medium have been investigated.

Solvents have a crucial importance for the yield of the polymerization with conversions from 0.3% to 16% in the same experimental conditions. This solvent activation effect has been rationalized using Keesom parameters. Moreover molecular weights also are solvent dependent from 400 g/mol to 12000 g/mol. This dependence is due to transfer to solvent which can be used to functionalize PE. Indeed THF-ended or chloro-ended polyethylene are obtained. This can be used to produce macro-monomer for example.

Using specific solvents allows the free radical polymerization of ethylene under very low pressure (5 bar) and temperature (10°C). PE produced under low temperature exhibits particularly high melting point 122°C for polyethylene produced by a free radical polymerization.

The transition between the monophasic and biphasic medium has also a crucial importance on the polymerization. Indeed the monophasic medium could induce some safety issue (if PE synthesized block degassing tube or safety valves for example). Yield and molecular weight of PE are also dependent to the phase as the solvent concentration is different in the two possible media.

Finally, we investigate the possibility to activate the polymerization by Lewis acid. This study does not give thorough results in their purpose but shows promising results in the control of ethylene radical polymerization by metal alkyl. Then we tried to control this polymerization by a system reported for the VAc CRP. CoAcac systems show very promising results which need further investigations.

This polymerization has two major drawbacks: it requires organic solvent and leads to low molecular weight compared to industrial LDPE. In order to overcome these issues we will develop in the next chapter the radical polymerization of ethylene in water.

Regarding to the final objective of hybrid polymerization mechanism, we saw in this chapter that the likelihood of the radical polymerization of ethylene during the synthesis of the radical block can not be neglected anymore. Consequently the investigation of the radical copolymerization of ethylene with various polar vinyl monomers needs to be investigated (see chapter IV).

References:

- [1] E. Grau, J.-P. Broyer, C. Boisson, R. Spitz, and V. Monteil *Macromolecules*, vol. 42, p. 7279, 2009.
- [2] G. B. Galland, R. F. de Souza, R. S. Mauler, and F. F. Nunes *Macromolecules*, vol. 32, p. 1620, 1999.
- [3] K. Vyakaranam, J. B. Barbour, and J. Michl *Journal of the American Chemical Society*, vol. 128, p. 5610, 2006.
- [4] E. Grau, J.-P. Broyer, C. Boisson, R. Spitz, and V. Monteil *Phys. Chem. Chem. Phys.*, vol. 12, p. 11665, 2010.
- [5] R. C. Reid, J. M. Praunsiitz, and B. E. Poling, *The properties of gases and liquids*. McGraw-Hill Book Compagny, 1988.
- [6] M. Atiqullah, H. Hammawa, and H. Hamid *Eur. Polym. J.*, vol. 34, p. 15511, 1998.
- [7] L. S. Lee, H. J. Ou, and H. L. Hsu *Fluid Phase Equilib.*, vol. 231, p. 221, 2005.
- [8] L. S. Lee, R. F. Shih, H. L. Ou, and L. S. Lee *Ind. Chem. Res.*, vol. 42, p. 6977, 2003.
- [9] J. García, M. M. Piñeiro, L. Lugo, and J. Fernández *Fluid Phase Equilib.*, vol. 210, p. 77, 2003.
- [10] T. Tork, G. Sadowski, W. Arlt, A. D. Haan, and G. Krooshof *Fluid Phase Equilib.*, vol. 163, p. 61, 1999.
- [11] T. Tork, G. Sadowski, W. Arlt, A. D. Haan, and G. Krooshof *Fluid Phase Equilib.*, vol. 163, p. 79, 1999.
- [12] M. Kamachi *Adv. Polym. Sci.*, vol. 38, p. 55, 1981.
- [13] S. Beuermann and M. Buback *Prog. Polym. Sci.*, vol. 27, p. 191, 2002.
- [14] A. G. Shostenko and V. E. Myshkin *Doklady Akademii Nauk SSSR*, vol. 246, p. 1429, 1979.
- [15] V. F. Gromov and P. M. Khomikovskii *Russ. Chem. Rev.*, vol. 48, p. 1943, 1979.
- [16] F. Suganuma, S. Machi, H. Mitsui, M. Hagiwara, and T. Kagiya *J. Polym. Sci., Part A-1: Polym. Chem.*, vol. 6, p. 2069, 1968.
- [17] S. Munari and S. Russo *J. Polym. Sci.*, vol. 4, p. 773, 1966.
- [18] S. Beuermann and N. García *Macromolecules*, vol. 37, p. 3018, 2004.
- [19] O. F. Olaj and E. Scnoll-Bitai *Mon. Chem.*, vol. 130, p. 731, 1999.
- [20] G. Henrichi-Olivé and S. Olivé *Z. Phys. Chem. NF*, vol. 47, p. 286, 1965.
- [21] G. Henrichi-Olivé and S. Olivé *Z. Phys. Chem. NF*, vol. 48, p. 35, 1966.
- [22] L. A. Smirnova, N. A. Kopylova, and V. V. Izvolenskii *Eur. Polym. J.*, vol. 32, p. 1213, 1996.
- [23] C. Reichardt, *Solvents and solvent effects in organic chemistry*. VCH:Weinheim, 1988.
- [24] A. H. C. Horn and T. J. Clark *J. Am. Chem. Soc.*, vol. 125, p. 2809, 2003.
- [25] A. H. C. Horn and T. J. Clark *J. Chem. Soc., Chem. Commun.*, p. 1774, 1986.

Chapter III : Free radical polymerization of ethylene in water

A.	Ethylene free radical polymerization in emulsion.....	III-172
1.	General mechanism of emulsion polymerization.....	III-172
a)	Interval I.....	III-172
(1)	Heterogeneous nucleation.....	III-173
(2)	Homogeneous nucleation.....	III-173
(3)	Coagulative nucleation	III-173
b)	Interval II	III-174
c)	Interval III.....	III-174
2.	Specific case of ethylene as monomer	III-174
B.	Cationic stabilization of PE particles dispersion.....	III-175
1.	Surfactant free emulsion	III-175
a)	Effect of the ethylene pressure.....	III-175
b)	Kinetics of polymerization.....	III-178
c)	Effect of the AIBA concentration	III-179
d)	Influence of water volume	III-179
e)	Effect of the temperature.....	III-181
f)	PE nanoparticles morphology	III-182
(1)	Microscopy analysis	III-182
(2)	X-rays scattering.....	III-186
g)	Conclusion	III-186
2.	Emulsion stabilized by CTAB	III-187
a)	Effect of the ethylene pressure.....	III-187
b)	Kinetics of polymerization.....	III-189
c)	Effect of the AIBA concentration	III-190
d)	Influence of water volume	III-192
e)	Effect of the temperature.....	III-193
f)	PE nanoparticles morphology	III-194
(1)	Microscopy analysis	III-194
(2)	X-ray scattering	III-199
g)	Conclusion	III-199
3.	Addition of an organic solvent.....	III-199
a)	Effect of organic solvents on emulsion polymerization	III-199
b)	Role of the initiator	III-202

4.	Rationalization of CTAB role	III-203
a)	Effect of the CTAB concentration	III-203
b)	Correlation between CTAB concentration and particles morphology.....	III-205
c)	Possible mechanism for disappearance of large particles.....	III-207
(1)	Evidence of the disappearance.....	III-208
(2)	Effect of stirring	III-210
(3)	Evidence of the ejection of cylinder particles	III-212
(4)	Density of the PE particles.....	III-214
5.	Conclusion	III-214
C.	Case of anionic stabilization	III-216
1.	Importance of the pH of the polymerization	III-216
2.	Surfactant free emulsion	III-217
3.	Polymerization with SDS as surfactant.....	III-219
4.	SDS emulsion zone of stability	III-220
D.	Toward more complex architectures	III-221
1.	Hybrid organic-organic	III-221
a)	PMMA/PE particles	III-221
(1)	PMMA core.....	III-221
(2)	PE core	III-222
b)	PS/PE particles using a PS core	III-223
2.	Hybrid organic/inorganic	III-225
a)	Silica hybrid particles	III-225
b)	Clay hybrid particles	III-226
E.	Conclusion.....	III-227

In the previous chapter we reported the free radical polymerization of ethylene in organic solvents. This polymerization takes place under mild experimental conditions ($T < 100^{\circ}\text{C}$ and $P < 250$ bar) with an unexpected high activity. Nevertheless two major drawbacks have been identified. PE synthesized exhibit low molecular weights even with low transfer capacity solvents such as DEC ($M_n < 15000$ g/mol). And the polymerization takes place at high pressure in a single supercritical phase. Consequently, PE lines reactor walls therefore generating safety issue. In order to solve these problems, we will develop the polymerization in water in this chapter.

Indeed, transposition to an emulsion polymerization in aqueous dispersed medium (benefiting from the compartmentalization of radicals and from the low transfer ability of water) should be useful to increase both molecular weight and yield and at the same time to solve the “lining” issue.

As already mentioned in the first chapter, PE latexes were obtained by free radical polymerization as early as 1940 [1-9]. Research groups reported the polymerization in water under γ -rays or initiated by KPS (only if $\text{pH} < 2$ or > 10). But due to the lack of characterization available at that time (no DLS, HT-SEC, NMR, etc), interpretation of results is quite difficult.

More recently PE latexes have also been obtained by catalytic polymerization of ethylene [10-12]. In most of publications, research groups used the miniemulsion process, using an oil soluble catalyst. Some recent works propose to use a water soluble catalyst and then performed a standard emulsion polymerization, by catalytic mechanism. Almost linear to high branched degree PE can be synthesized by these methods. However solid content of the synthesized latexes remains limited as most of publication reported only PE content below 20%.

In this chapter, we will study the free radical polymerization of ethylene in water using a water soluble initiator. First, we will simply transpose the free radical polymerization in water using a water-soluble equivalent of AIBN, 2,2-azobis(2-amidinopropane)-dihydrochloride (AIBA – see Figure 1).

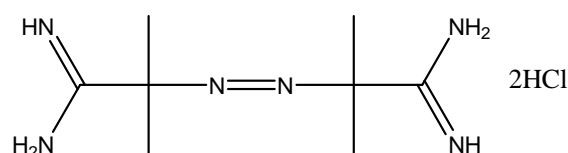


Figure 1. AIBA initiator

The so obtained stable latexes will be fully studied and the influence of surfactant addition will be investigated. Then the polymerization with the anionic initiator ammonium persulfate (APS) will be reported. And finally we will review some tryouts to produce more complex nanostructures such as hybrid PE latexes.

A. Ethylene free radical polymerization in emulsion

1. General mechanism of emulsion polymerization

In this thesis, emulsion polymerization refers to a process allowing to produce sub-micronic polymer particles dispersed in water via a free radical mechanism. Emulsion polymerization is used to produce latexes at high polymerization rates, high molecular weight, and with some controlled properties. One main advantage of emulsion is the low viscosity of the resulting product. In addition this process presents an excellent heat removal capacity.

The original qualitative description of the mechanism of polymerization was given by Harkins [13-15] who separates the polymerization in three distinct intervals. Smith and Eward [16] completed the description in 1948.

A typical emulsion polymerization formulation is composed of monomer of low water solubility, a surfactant, water as continuous phase and a water-soluble initiator. The surfactant is an amphiphilic molecule which presents the ability to stabilize hydrophobic compounds in water phase. In this process, the monomer is originally dispersed in aqueous media in the form of droplets (1-10 μm) stabilized by surfactant, in micelles (5-20 nm – if surfactant concentration is over the critical micelle concentration) and a limited amount is dissolved in the aqueous phase.

a) Interval I

Particles formation occurs during Interval I also called nucleation step. At the beginning of the polymerization, the initiator, dissolved in water, decomposes to form free radicals which initiate the polymerization by reacting with monomer present in the water phase in order to form oligoradicals. Then these non-water soluble oligoradicals will form particles where the polymerization will continue.

In this interval, the polymerization rate raises due to the increase in the number of particles. The diffusion of monomer through the water phase is usually the rate determining step. Three different particle nucleation mechanisms can usually compete.

(1) *Heterogeneous nucleation*

Also called micellar nucleation, this nucleation is characterized by the entry of a radical or an oligoradical in the monomer-swollen micelles giving rise to the formation of primary particles. This requires a surfactant concentration higher than the critical micelle concentration (cmc, for example SDS – sodium dodecylsulfate cmc is about 2 g/L and for CTAB – cetyltrimethylammonium bromide 0.3 g/L) and enough monomer present in the aqueous phase to produce oligoradicals.

It should be noted that the number of particles formed by heterogeneous nucleation is lower than the initial number of micelles.

(2) *Homogeneous nucleation*

This nucleation begins also in the water phase, however the growing oligoradicals become hydrophobic and insoluble so they precipitate and form new polymer particles, stabilized by surfactant or by charges present at the initiator fragment, before they enter into micelle or an existing particle.

This is generally a significant mean of particles generation when no micelle is present in the water phase, or if the monomer is relatively highly soluble in water.

(3) *Coagulative nucleation*

This nucleation is an extension of homogeneous nucleation. Oligoradicals form unstable precursor polymer particles so that they coagulate to form larger particles with enough surface charge density to be stable.

There is a competition between these different mechanisms of nucleation. Their relative importance depends on different parameters such as the solubility of monomer in water (favoring homogeneous nucleation) and/or the concentration of surfactant (favoring heterogeneous nucleation).

b) Interval II

The second interval begins when enough particles are nucleated to efficiently capture the radicals formed in water. It consists of the growth of particles and is called stationary step. During this interval, the number of particles remains unchanged. The particles growth occurs thanks to monomer diffusion from droplets which act as reservoir to particles. The rate of polymerization stays constant because the concentration of radical and the monomer concentration within the particles remains constant. Particles growth depends on the number of particles and the time between two radical captures.

c) Interval III

At the end of stationary step, there are no monomer droplets anymore. The disappearance of the monomer droplets constitutes the onset of the interval III. The monomer, present only in the particles and water phase, continues to polymerize. The number of particles remains unchanged while polymerization rate and monomer concentration decrease.

2. Specific case of ethylene as monomer

The emulsion process for ethylene polymerization can not be a classical one. Ethylene is a supercritical fluid and consequently no ethylene droplets should exist during the polymerization. The reservoir able to feed particles is then the ethylene headspace. Moreover, as the pressure of ethylene remains constant during the polymerization, interval III does not take place in our polymerization.

Ethylene has a low water solubility of $50 \text{ mg bar}^{-1} \text{ L}^{-1}$ at 70°C [17] (comparable to styrene 0.7 g/L at 70°C). Consequently a homogeneous or coagulative nucleation is favored without surfactant and a micellar one with surfactant over the critical micelle concentration.

It is noteworthy to mention that no liquid unreacted monomer can remain in the latex after polymerization whatever the conversion since the latexes is analyzed after degassing of the reactor ethylene pressure. Consequently latexes synthesized are totally VOC-free.

In addition PE is a crystalline material contrary to most conventional polymers produced by free radical polymerization in emulsion.

B. Cationic stabilization of PE particles dispersion

This work was partly published in *Angewandte Chemie International Edition* [18].

With AIBA initiator inducing a cationic stabilization of PE particles, two different systems are discussed in this part: a surfactant free emulsion, and an emulsion in the presence of 1 g/L of cetyltrimethylammonium bromide (CTAB – see Figure 2), a standard cationic surfactant.

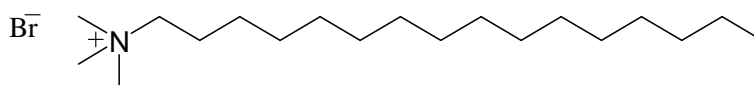


Figure 2. CTAB surfactant

1. Surfactant free emulsion

This system is the analogue of the polymerization of ethylene in solution. Indeed organic solvent is replaced by water and AIBN by an equivalent water-soluble initiator AIBA. Moreover same amount of solvent, initiator are used at the same temperature.

a) Effect of the ethylene pressure

The polymerization is performed in 50 mL of water during 4 hours at 70°C using 80 mg of AIBA (305 μ mol) as water soluble radical initiator. Results are summarized in the following table.

Table 1. Ethylene pressure influences on the free radical polymerization of ethylene in water^a

Ethylene Pressure (bar)	Yield (g)	Melting point (°C) ^b	Crystallinity (%) ^b	Mn (g/mol) ^c	PDI ^c	Dp (nm) ^d	PI ^d
50	0.3	70.3	12	10800	3.4	32 (±2)	0.07 (±0.01)
100	1.3	96.5	35	21600	6.0	89 (±1)	0.04 (±0.01)
150	1.8	100.9	30	31100	7.3	104 (±1)	0.06 (±0.03)
200	2.2	106.0	40	20800	6.1	109 (±1)	0.03 (±0.01)
250	2.5	104.6	37	21000	7.9	113 (±1)	0.03 (±0.02)

^a: Polymerizations are performed during 4 hours with 80 mg of AIBA at 70°C in 50 mL of water. ^b: determined by DSC. ^c: determined by HTSEC. ^d: determined by DLS.

In the surfactant-free system, yield is lower than the one obtained using the same molar amount of initiator in THF but higher than in toluene, for example at 100 bar of ethylene pressure, yields are respectively 1.3 g in water, 3.9 g in THF and 0.7 g in toluene. Polymerization yield increases with the ethylene pressure as expected.

Surprisingly, stable PE latexes are obtained even after degassing 250 bar of ethylene pressure. No flocculation is observed for any of these polymerizations. The stabilization of PE particles is assumed to result from the cationic fragments of the initiator attached at the chain ends which induces electrostatic repulsion. Solid contents of these latexes are up to 5%.

Average particle diameters (D_p) measured by DLS (dynamic light scattering) increases with the ethylene pressure (and consequently with the yield) from 30 nm to 110 nm. Polydispersity indexes remain very low ($PI \sim 0.05$) indicating the monodisperse character of particle size distribution.

In addition, the $yield/D_p^3$ ratio, standing for the number of particles, remains constant whatever the ethylene pressure. This indicates that the formation of PE particles is mostly independent of the ethylene pressure. Difference in yield can be due to a difference in ethylene diffusion to the growing particle or to a faster nucleation of the particles (since solubility of ethylene in water increase linearly with pressure $50 \text{ mg bar}^{-1} \text{ L}^{-1}$).

PE latexes synthesized are stable under standard storage conditions (in a transparent glass bottle at ambient temperature). No flocculation is observed over one year. For the sample synthesized at 100 bar, DLS measurements are done regularly over two months (see Figure 3) and no significant change is observed in average particles diameters and polydispersity.

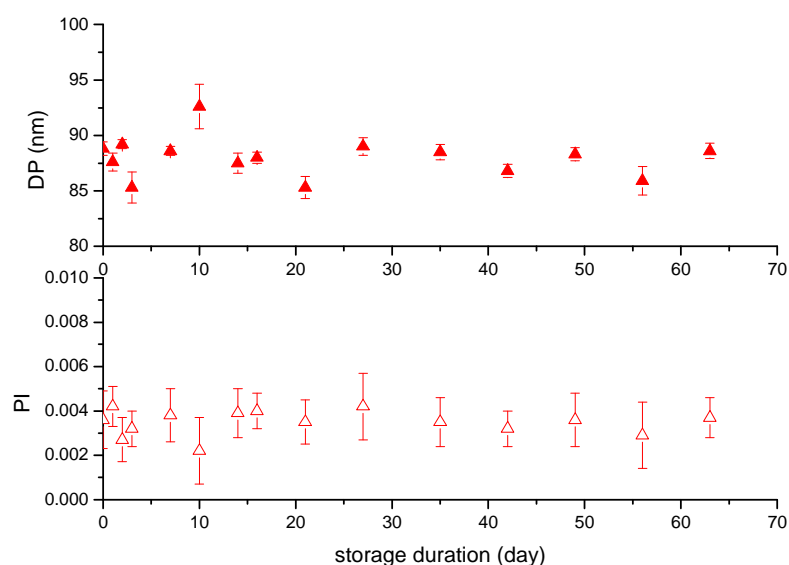


Figure 3. Evolution of particles diameters and distribution with storage duration.
▲ average particles diameters^a and ▲ polydispersity index^a vs. storage duration.
^a: determined by DLS

Molecular weights are higher in emulsion than in solution (for example $M_n=31000 \text{ g/mol}$ at 100 bar of ethylene pressure – see Table 1). These molecular weights are the highest reported up to now by a free radical polymerization in this range of experimental conditions. Moreover, MWD is quite broad, $PDI \approx 6-7$ due to the emulsion process. Indeed molecular weight of the polymer is partly controlled by the time between two radical captures

which depends of the surface of particles therefore varying during the polymerization. Due to this broad MWD, Mw values fall in the range of 10^6 g/mol. This “high” molecular weight polyethylene could possess some interesting physical properties since their molecular weight are far above the entanglement mass of PE (10^4 g/mol).

After coagulation and washing by water, the PE produced exhibits a low melting point ($T_m \sim 100^\circ\text{C}$) and low crystallinity (30-40%). This is lower than the one determined with PE produced in solution ($T_m \sim 115^\circ\text{C}$) under similar experimental conditions. This is due to a higher branches content of 30 branches per 1000 C (determined by ^{13}C NMR).

This higher branching level in water than in an organic solvent (in THF: 9 branches/1000C or in toluene: 7 branches/1000C) can be explained by the compartmentalization of the PE growing chains which increases transfer reactions to the polymer. The proportion of short chain branches (ratio short chain branches over total chain branches) is lower in emulsion (25% vs. 35% in organic solvent) due to favored intermolecular over intramolecular transfer reactions in a confined environment.

b) Kinetics of polymerization

In order to understand the particles formation, a kinetic study is performed at 100 bar of ethylene pressure and 70°C (see Figure 4). As for a standard emulsion polymerization, particle diameters increase with time as well as yield does.

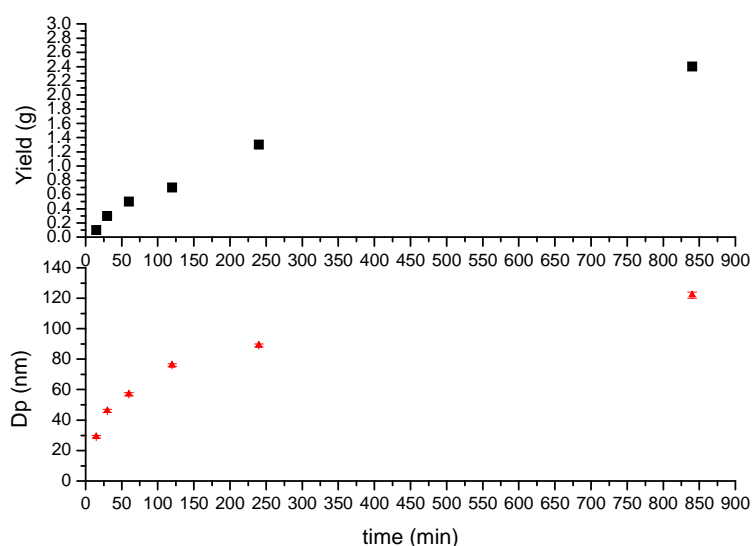


Figure 4. Reaction profile of free radical polymerization of ethylene in aqueous dispersed medium. ■ yield and ▲ average particles diameters^a vs. time under 100 bar of ethylene pressure at 70°C with 80 mg of AIBA in 50 mL of water. ^a: determined by DLS

For the surfactant-free system, particles diameters increases with yield and the yield/D_p^3 ratio remains constant, therefore no renucleations and/or aggregation take place during the polymerization. This behavior is classic for an emulsion during the Smith-Ewart phase II.

c) Effect of the AIBA concentration

We also investigate the AIBA concentration effect on the PE latex synthesis. In this purpose, polymerizations are performed at 100 bar of ethylene pressure during 4 hours in 50 mL of water at 70°C with various amounts of AIBA (see Figure 5).

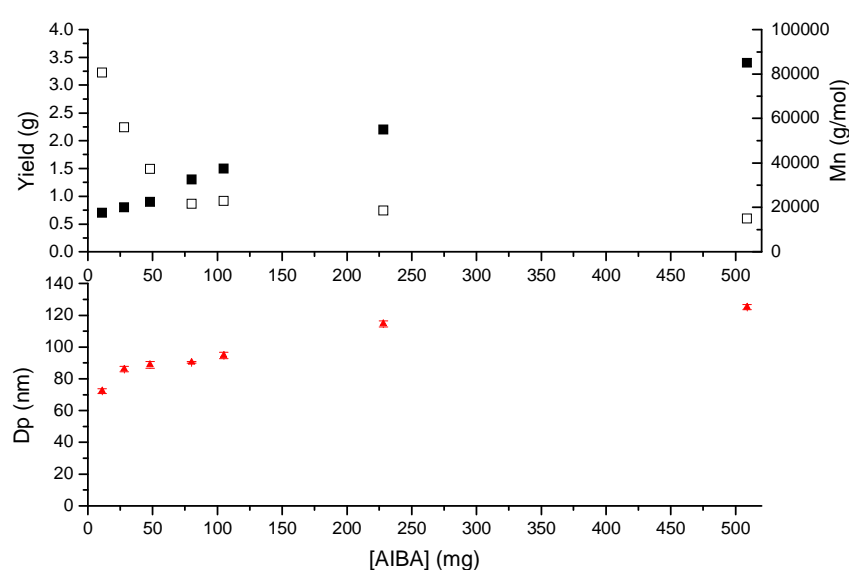


Figure 5. Influence of AIBA concentration on yield and particles diameters of PE latexes. ■ yield, □ molecular weight^a and ▲ average particles diameters^b vs. AIBA concentration under 100 bar of ethylene pressure at 70°C during 4 hours in 50 mL of water. ^a: determined by HT-SEC, ^b: determined by DLS

Yield and particles diameters increase with AIBA concentration. Moreover the yield/D_p^3 ratio remains almost constant. Consequently whatever the AIBA concentration, the number of PE particles synthesized remains even ($N_p \propto [AIBA]^{0.01}$).

Molecular weights of PE decrease with AIBA concentration. Indeed Mn decrease only from 81000 g/mol to 15000 g/mol (loss by a factor of 5.4) for AIBA content respectively of 11 mg and 509 mg (increase by a factor of 46).

d) Influence of water volume

The influence of water volume has been also investigated. Indeed as for the ethylene polymerization in solution, a phase transition could take place between a biphasic medium

where the polymerization occurs in water in order to form latex and a monophasic medium (ethylene and water in a unique supercritical phase) where no latex can be obtained. With water the transition between a biphasic and a monophasic medium is expected to be much higher in pressure and temperature than in any other organic solvents. This represents an additional advantage of water as solvent for ethylene polymerization.

This high transition point can be explained because ethylene is almost not soluble in water (almost $50 \text{ mg L}^{-1} \text{ bar}^{-1}$ at 70°C below 200 bar compared to $2\text{--}9 \text{ g L}^{-1} \text{ bar}^{-1}$ in the same conditions for organic solvents). Moreover critical conditions indicate that water is one of the “heaviest” solvents ($T_c=373.9^\circ\text{C}$, $P_c=220 \text{ bar}$, $M=18 \text{ g/mol}$, $d=1$, therefore $\frac{d}{M}T_c=20.7 \text{ mol K/cm}^3$ compared to 6.7 mol K/cm^3 for THF). Consequently calculations using Peng-Robinson equation of state predict that the transition does not take place in our experimental conditions: i.e. for 50 mL of water at 150°C the transition takes place under 345 bar of ethylene pressure.

In consequence whatever the water volume used, polymerizations are performed in a biphasic medium and stable latexes will be obtained.

A set of experiments is performed at 70°C under 100 bar of ethylene pressure with 80 mg of AIBA as radical initiator at various water volumes (see Figure 6).

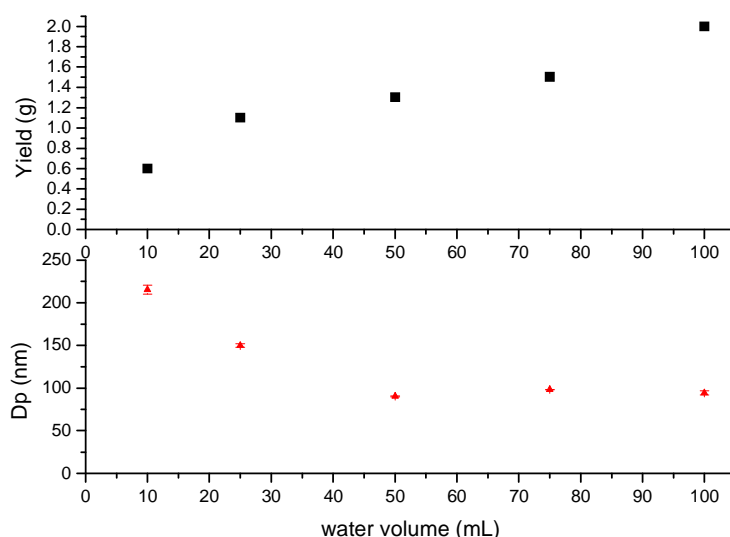


Figure 6. Influence of water volume on yield and particles diameters of PE latexes.
■ yield and ▲ average particles diameters^a vs. water volume under 100 bar of ethylene pressure with 80 mg of AIBA at 70°C . ^a: determined by DLS

All experiments lead to stable PE latexes. Yield increases with water volume but solid content of PE latexes decreases from 5.7 % in 10 mL to 2% in 100 mL of water. As expected, average particles diameters decrease and the concentration of PE particles (Np/V) remains almost constant.

Moreover, this set of experiments is in agreement with the set in which AIBA concentration varies. Indeed, water volume influence is only due to an AIBA concentration variation. Therefore if solid content is plotted vs. AIBA concentration the same curve is obtained for the two sets of experiments.

e) Effect of the temperature

Finally, polymerizations are also performed at 50°C, 70°C and 90°C under 100 bar of ethylene pressure during 4 hours with 80 mg of AIBA in order to characterize an effect of the temperature. In all cases, stable PE latex is obtained (see Table 2).

Table 2. Effect of the temperature on the ethylene polymerization in water^a

Temperature (°C)	Yield (g)	Melting point (°C) ^b	Crystallinity (%) ^b	Mn (g/mol) ^c	PDI ^c	Dp (nm) ^d	PI ^d
50	0.3	105.6	40	24600	7.8	77 (±2)	0.15 (±0.03)
70	1.3	96.5	35	21600	6.0	89 (±1)	0.04 (±0.01)
90	0.8	85.6	10	48500	7.1	45 (±1)	0.04 (±0.01)

^a: Polymerizations are performed during 4 hours with 80 mg of AIBA under 100 bar of ethylene pressure in 50 mL of water. ^b: determined by DSC. ^c: determined by HTSEC. ^d: determined by DLS

Yield and particles diameters are maximal at 70°C but the number of particles increases with the temperature. Consequently, the nucleation of PE particles is more efficient at higher temperature.

As expected melting point and crystallinity of PE decrease with the temperature of polymerization, from 105.6°C at 50°C to 85.6°C at 90°C. This must be due to the same phenomenon than in solution. At higher temperature, the mobility of the macroradical is higher and so transfer to the polymer is more favored. Therefore, PE synthesized contained more branches so the melting point and crystallinity decrease with the temperature of synthesis.

Molecular weight seems to slightly increase with temperature from 20000 g/mol to 48500 g/mol. Polydispersity index remain between 6 and 8.

It should be noted that the PE synthesized in our experimental conditions contain a non-negligible amount of long chain-branches. This type of branches can affect significantly the HT-SEC calibration since molecular weights are determined by coupling RI, and viscosity measurements. Therefore, LCB reduce the polymer intrinsic viscosity and consequently the measured molecular weight value must be lower than the real one.

f) PE nanoparticles morphology

All these sets of experiments show that ethylene polymerization in water exhibits a standard behavior of emulsion: the number of particles remains constant during the polymerization. In this section the morphology of PE nanoparticles synthesized will be studied.

(1) *Microscopy analysis*

PE particles obtained are observed by TEM. An example is shown below (see Figure 7). It should be noted that all pictures present in this section are performed on the same native PE latex. This latex is synthesized without surfactant under 150 bar of ethylene pressure during 2 hours with 80 mg of AIBA radical initiator.

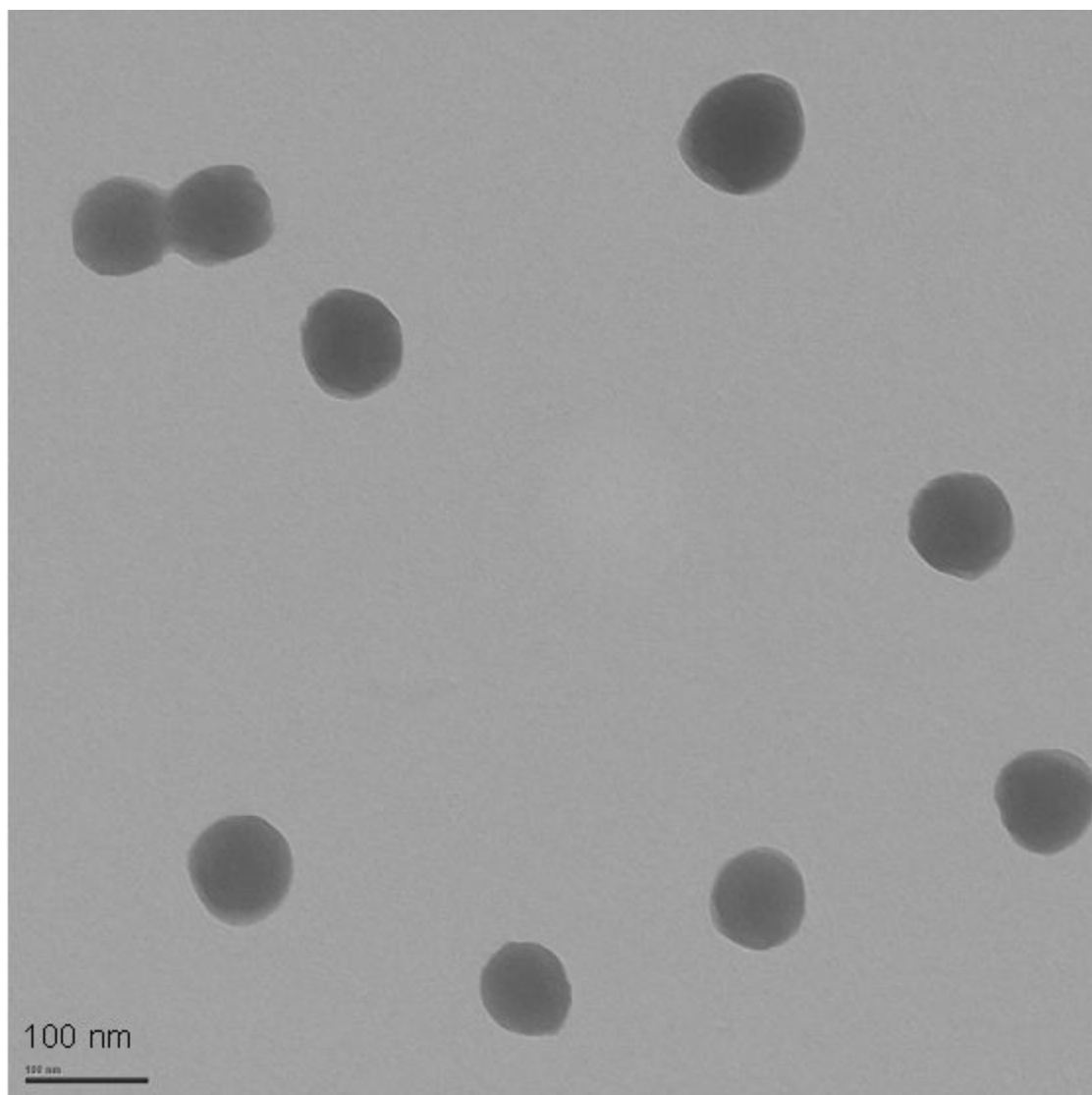


Figure 7. Typical TEM picture obtained for free-surfactant polymerization

The most interesting fact is that the particles obtained are not perfect spheres (contrary to polystyrene for example). This is due to the crystallinity of PE. Indeed crystalline PE lamellas prohibit the formation of perfect sphere. Therefore at the surface of PE particles, some facets can be observed and could be attributed to PE lamella.

It should be noted that if no crystalline region exists in the native particles, no distinct particles would be observed by TEM due to the low $T_g \approx -100^\circ\text{C}$ of amorphous PE. Consequently native PE particles possess some crystallinity.

This morphology has been confirmed by TEM tomography. In this purpose a TEM picture of a single PE particle is taken every 2° tilt, and then 3D PE particle image can be constructed. The following figure shows the projection of this 3D surface.

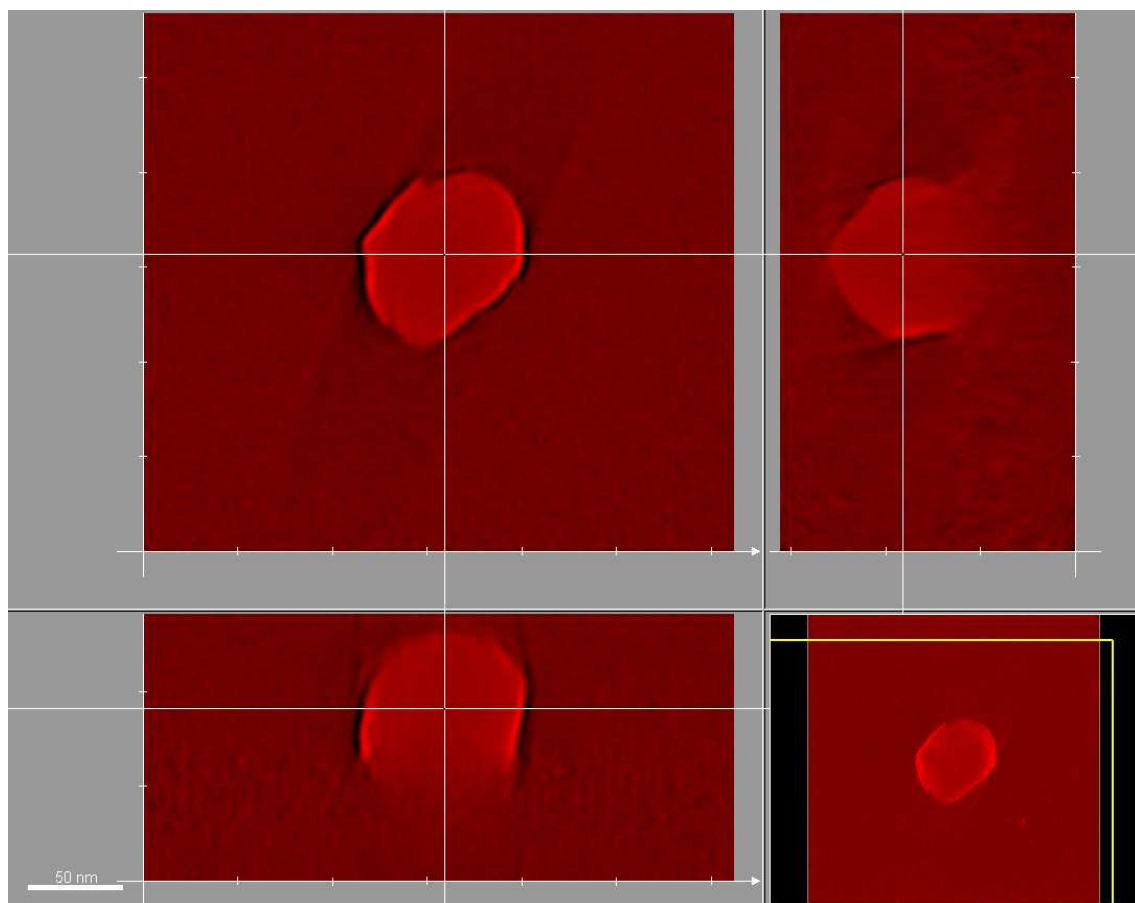


Figure 8. TEM tomography result on a PE particle synthesized without surfactant

Once again facets can be well identified at the surface of the PE particles. This facet dimension is about 20 nm.

Height of the particles is almost identical to the particle diameter which confirms the sphere-like morphology. It should be noted that due to the amorphous part of PE the particles flatten a little when there are deposited on a surface.

In order to confirm this morphology, AFM are also performed on these particles (see Figure 9).

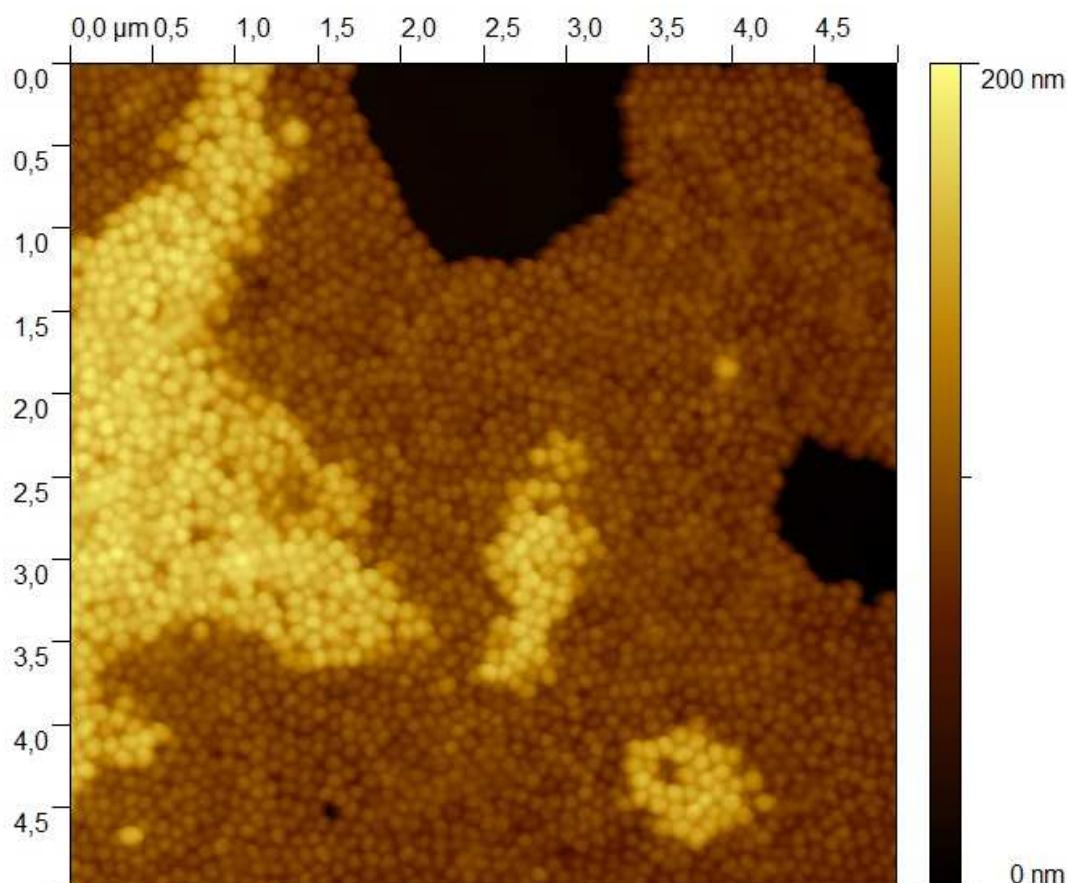


Figure 9. AFM obtained for PE particles synthesized without surfactant

Using AFM, the height of the different layers can be determined and compared to the particles diameters. First, well organized layers (close to face-centered cubic organization) are observed which testify a good monodispersity of PE particle size distribution.

On this sample, average particles diameter is 82.3 ± 1.6 nm (determined by DLS). The first layer has an average thickness of 76.5 ± 1.6 nm and the second layer 66.8 ± 9.1 nm. This confirms a sphere-like morphology.

It should be noted that PE particles height is about 5 nm smaller than particles diameters. Indeed particles flatten a little on surface due to the large amount of amorphous PE part ($\sim 70\%$ of amorphous PE, $T_g \sim -100^\circ\text{C}$).

(2) *X-rays scattering*

Finally, as PE is a semicrystalline polymer, X-rays scattering on the native latex could also be performed. Two important data are accessible by this technique: the average crystallite dimension and the crystallinity of the polymer inside the native PE particles.

Two latexes were studied: one synthesized under 150 bar of ethylene pressure using 80 mg of AIBA and the other synthesized at 100 bar using 500 mg of AIBA. Initial particles diameters are respectively 104 nm and 125 nm (determined by DLS).

The native crystallite diameters are measured respectively at 23 nm and 18 nm. It should be noted that the thickness of the crystallites can not be measured by our technique. This small crystallite dimension, compared to the particles dimension, indicates that several crystallites are present inside the PE particles. Moreover the dimension of the crystallites could correspond to the dimension of some facet observed at the surface of particles.

PE native crystallinities are also determined: respectively at 38% and 25%. These crystallinities are in agreement to the one obtained by DSC respectively at 30% and 23%. Consequently, the difference in crystallization mechanism seems to be small between the one inside nanoparticles and the bulk PE. However, a slight over-crystallinity is observed in the PE latexes and can be due to a Laplace pressure effect (higher pressure inside the particles which could induce a higher crystallization than bulk PE).

g) **Conclusion**

In this section we confirmed that we can transpose the polymerization from an organic medium to ethylene free radical polymerization in water. Moreover, PE synthesized form a stable aqueous dispersion of semi-crystalline nanoparticles.

Solid content of the latexes obtained are up to 6% with particles diameters up to 120 nm. These PE particles are sphere-like and possess some facets at their surface.

PE synthesized exhibit high molecular weights over 10^4 g/mol with a broad MWD ($PDI \approx 6$). Melting points fall in the range of 95°C to 105 °C indicating a high branches content (≈ 30 -40 branches per 1000 carbons).

2. Emulsion stabilized by CTAB

PE synthesized in water provides stable latexes with high molecular weight but yield remains lower than in THF. In order to improve the yield of ethylene emulsion we perform the same study in presence of CTAB (1 g/L, over its cmc) as cationic surfactant.

a) Effect of the ethylene pressure

We perform the polymerization in 50 mL of water at 1 g/L of CTAB during 4 hours at 70°C, and 80 mg of AIBA (305 μ mol) as water soluble initiator. Results are summarized in the Table 3.

Table 3. Ethylene pressure influence on the free radical polymerization of ethylene in an aqueous solution of 1g/L of CTAB^a

Ethylene Pressure (bar)	Yield (g)	Melting point (°C) ^b	Crystallinity (%) ^b	Mn (g/mol) ^c	PDI ^c	Dp (nm) ^d	PI ^d
50	0.7	69.5	10	38800	2.8	97 (± 3)	0.71 (± 0.03)
100	4.6	92.8	31	50500	8.7	24 (± 1)	0.52 (± 0.08)
150	7.9	97.3	31	60500	7.3	51 (± 1)	0.17 (± 0.02)
200	12.3	99.4	29	73800	8.1	52 (± 1)	0.22 (± 0.02)
250	19.9	97.0	31	119000	6.3	46 (± 2)	0.33 (± 0.09)

^a: Polymerizations are performed during 4 hours with 80 mg of AIBA at 70°C in 50 mL of water. ^b: determined by DSC. ^c: determined by HTSEC. ^d: determined by DLS.

When polymerizations are performed in the presence of a standard cationic surfactant (CTAB) at 1 g/L (above the critical micelle concentration: 0.3 g/L at 25°C), much higher activities are observed. For example, under 100 bar of ethylene pressure, 4.6 g of PE are synthesized compared to 1.3 g without CTAB. This emulsion system is even more efficient than the polymerization in THF (3.9 g at 100 bar) which is the most efficient system described in the previous chapter.

As expected, yield dramatically increases with the ethylene pressure. Indeed in these non-optimized conditions, up to 40% of solid content is obtained. This represents to the best of our knowledges the highest solid content even reported for a PE latex.

In all cases stable latexes are obtained and no flocculation is observed. Average particle diameters seem to reach a plateau at 50 nm when increasing ethylene pressure. This indicates that the number of particles increases with the yield. Compared to the previous set of experiment (surfactant-free) number of particles are higher except for polymerization performed under 50 bar of ethylene pressure.

Moreover, polydispersity indexes measured by DLS remain surprisingly higher (PI ~ 0.5) than for the surfactant-free process. This indicates that the particles formed are not homogeneous in size.

As already mentioned the number of particles increases dramatically with the ethylene pressure ($Np \propto [P]^{3.48}$). This high influence of the ethylene pressure on the number of particles is unexpected. Indeed without CTAB this number remains constant with the ethylene pressure. Consequently this could be due to a better efficiency of the particles nucleation with higher ethylene pressure. Therefore the nucleation mechanism in the presence of CTAB should be different than in the surfactant free process.

As for PE latexes synthesized without surfactant, these latexes are stable under standard storage conditions (in a glass bottle at ambient temperature). No flocculation is observed over one year. For the sample synthesized at 100 bar, DLS measurements are done over two months (see Figure 10) and no significant change is observed.

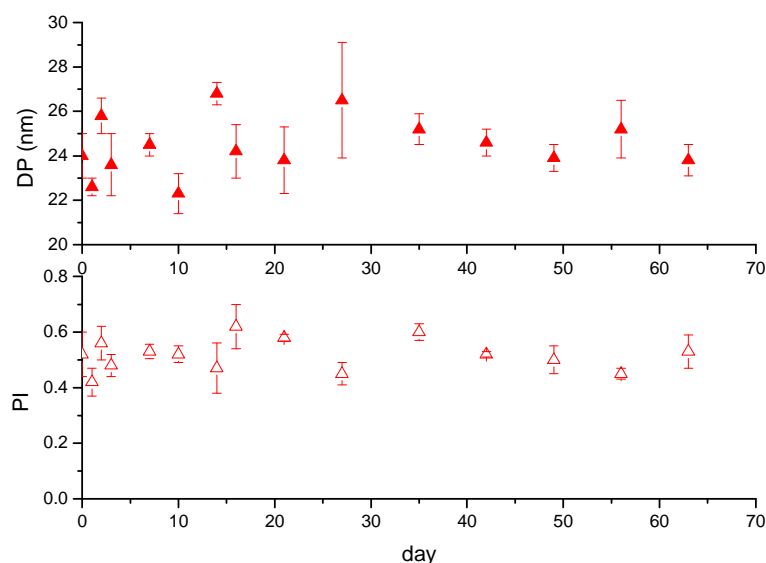


Figure 10. Evolution of particles diameters and distribution with storage duration.
▲ average particles diameters^a and ▲ polydispersity index^a vs. storage duration.
^a: determined by DLS

Coagulated and isolated PE are analyzed further by HT-SEC and DSC (see Table 3). As expected, molecular weights increase with ethylene pressure. Mn values are interestingly high from 40000 g/mol to 120000 g/mol at 250 bar. The PE synthesized under similar experimental conditions exhibit higher molecular weights than those prepared without CTAB.

Melting points of PE synthesized as well as crystallinity are lower with surfactant than without. Moreover, both increase with the ethylene pressure. Consequently branches content should be higher for PE synthesized in presence of CTAB. Using ^{13}C NMR the branches content is determined: 37 branches per 1000C compared to 30 branches without CTAB.

b) Kinetics of polymerization

In order to understand the particles formation, we perform a kinetic study under 100 bar of ethylene pressure, at 70°C using 80 mg of AIBA (see Figure 11). Contrary to the surfactant free emulsion in which particles diameters increase with yield, in the presence of CTAB yield increases with time but particles diameters seem to decrease until reaching a plateau at 20 nm.

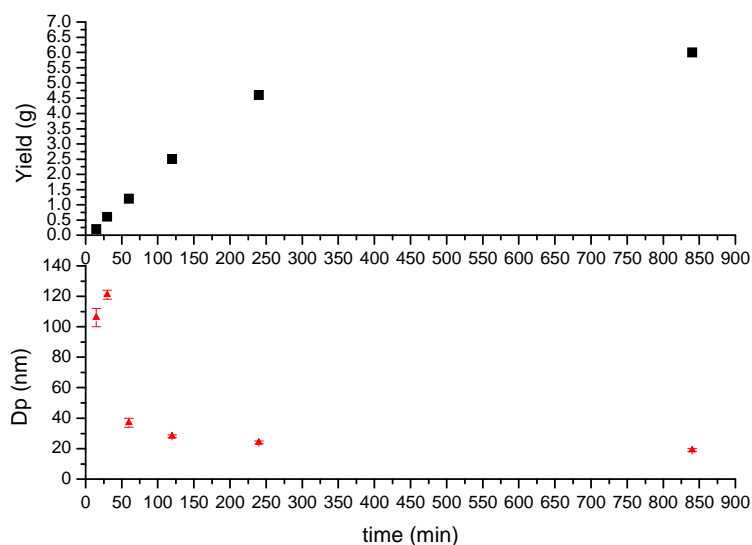


Figure 11. Reaction profile of free radical polymerization of ethylene in aqueous dispersed medium. ■ yield and ▲ average particles diameters^a vs. time under 100 bar of ethylene pressure with 80 mg of AIBA at 70°C in 50 mL of a CTAB aqueous solution at 1 g/L. ^a: determined by DLS

This unexpected behavior testifies that the number of PE particles increases with time of polymerization. Moreover, the final particles produced have always the same dimension which seems to be independent of the ethylene conversion. Finally, the particles produced first seem to have a greater size. These particles disappear after 1 hour of reaction.

The number of particles increases with time following this law $Np \propto t^{3.03}$. This is about the same exponent as the dependence in ethylene pressure.

This mechanism of polymerization is totally different from the surfactant free-system. Indeed the system behavior appears to be still in the nucleation step during all the polymerization. Moreover no growing of the particles takes place.

c) Effect of the AIBA concentration

The influence of AIBA concentration has been also investigated in order to have a better understanding of this system. Polymerizations are performed at 70°C during 4 hours, in 50 mL of an aqueous solution of 1 g/L of CTAB with various amounts of AIBA (see Figure 12).

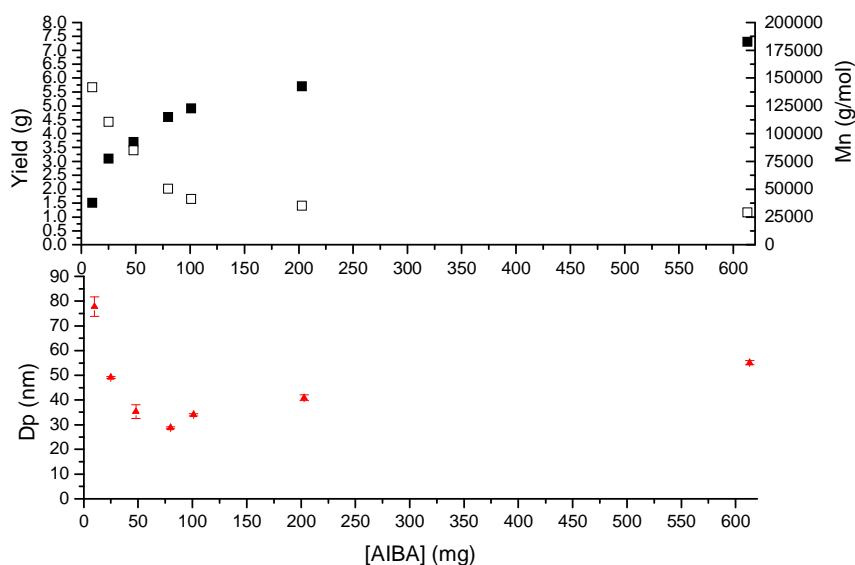


Figure 12. Influence of AIBA concentration on yield and particles diameters of PE latexes. ■ yield, □ molecular weight^a and ▲ average particles diameters^b vs. AIBA concentration at 70°C under 100 bar of ethylene pressure during 4 hours in 50 mL of an aqueous CTAB solution at 1 g/L. ^a: determined by HT-SEC, ^b: determined by DLS

Two zones are observed. One below 80 mg of AIBA in which yield increases and average particles diameters decrease with the AIBA concentration. And the other one, over 80 mg of AIBA in which yield and particles diameters increase with the AIBA concentration.

This induces that the number of particles first increase ($Np \propto [AIBA]^{1.98}$) then decrease ($Np \propto [AIBA]^{-0.68}$) with the AIBA concentration.

This phenomenon can be explained if we take into account two different mechanisms of the PE particle formation. At low AIBA concentration almost each oligoradical creates a particle as the CTAB present in the solution can stabilize all particles (via a micellar or homogeneous nucleation). At higher AIBA concentration, therefore higher yield, there are too many particles to be stabilized thanks to CTAB only, consequently several oligoradicals are involved in a unique particle (it could be a coagulative nucleation).

After measuring the area of absorption of a CTAB molecule on these PE particles (77 \AA^2 per molecule of CTAB for PE particles synthesized in presence of CTAB which is about the same for PE particles synthesized without CTAB 84 \AA^2) we calculate the ratio of stabilization by CTAB (equal to the ratio between the surface covered per CTAB molecules present in the latex and the total surface of PE particles: 100 % if the PE particles are fully

covered by CTAB). Therefore, we plot this ratio and the number of PE particles vs. AIBA concentration (see Figure 13).

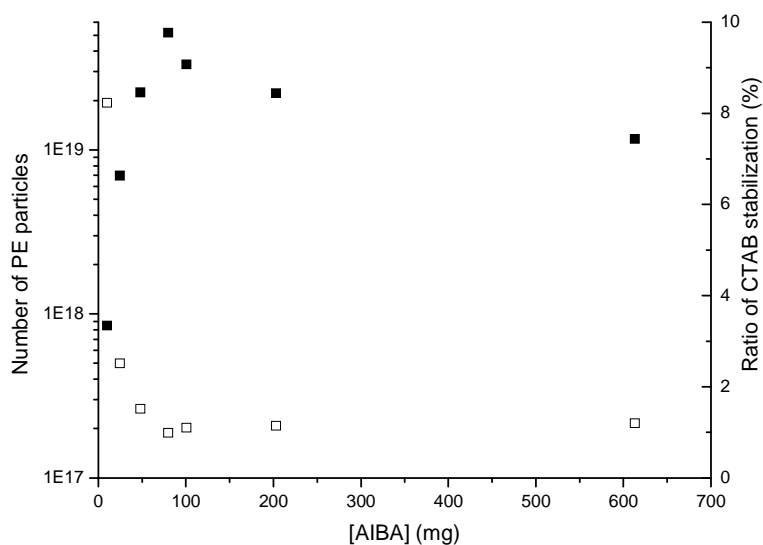


Figure 13. Evolution of ■ number of PE particles and □ absolute ratio of CTAB stabilization vs. the AIBA concentration

This curve confirms our hypothesis that CTAB coverage decreases with AIBA concentration until reaching a plateau at 1% of CTAB stabilization which seems to be the minimum amount of CTAB mandatory to stabilize PE particles. Therefore, the mechanism of nucleation seems to be controlled by CTAB concentration.

Finally as for the surfactant free system, molecular weights decrease with the AIBA concentration (see Figure 12), from 142000 g/mol to 29000 g/mol for respectively 10 mg and 613 mg of AIBA.

d) Influence of water volume

Once again, we perform a set of experiments using various volumes of water (see Figure 14). In this case no correlation with the previous set of experiment is observed. This is partially due to the evolution of the ratio CTAB/AIBA, which is different in these two sets of experiments.

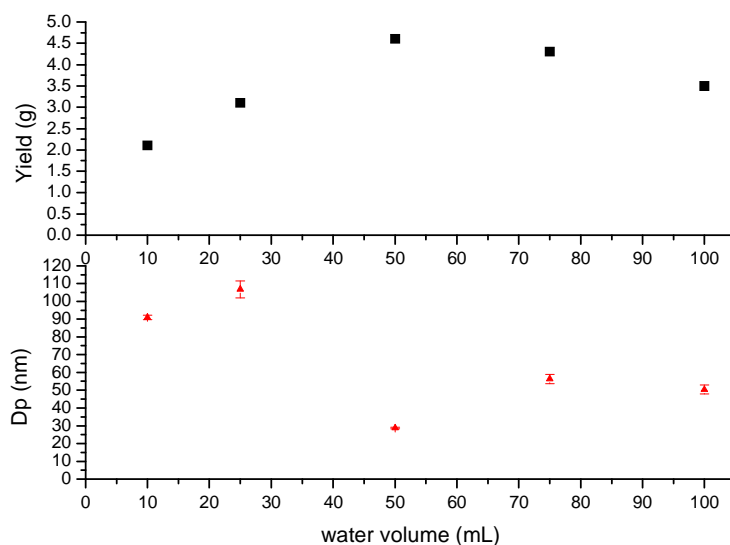


Figure 14. Influence of water volume on yield and particles diameters of PE latexes.
 ■ yield and ▲ average particles diameters^a vs. water volume under 100 bar of ethylene pressure at 70°C with 80 mg of AIBA in an aqueous CTAB solution at 1 g/l during 4 hours. ^a: determined by DLS

We first observe that yield increases with water volume until 50 mL then decreases. The solid content decreases as well with water volume from 16.7% with 10 mL to 3.4% with 100 mL. The particles diameters roughly decrease from 100 nm at low water volume to 50 nm.

This behavior could be explained by the same hypothesis than the previous set of experiments. At low water volume, too few CTAB molecules are present and cannot stabilize fully PE particles. This leads to high diameters particles and low particles number. At high water volume, CTAB can stabilize all PE particles therefore smaller particles are formed.

Consequently these experiments are in agreement with our previous hypothesis that CTAB amount plays a crucial role during the polymerization.

e) Effect of the temperature

Finally, polymerizations are also performed at 50°C, 70°C and 90°C under 100 bar of ethylene pressure during 4 hours with 80 mg of AIBA and 1 g/L of CTAB in order to identify a temperature effect (see Table 4). Stable PE latexes are obtained excepted at 90°C.

Table 4. Effect of the temperature on the ethylene polymerization in an aqueous solution of 1g/L of CTAB^a

Temperature (°C)	Yield (g)	Melting point (°C) ^b	Crystallinity (%) ^b	Mn (g/mol) ^c	PDI ^c	Dp (nm) ^d	PI ^d
50	2.9	106.0	42	34700	5.5	17 (±1)	0.28 (±0.02)
70	4.6	92.8	31	50500	8.7	24 (±1)	0.52 (±0.08)
90	1.3	82.5	9	69500	6.2	420 (±12)	0.68 (±0.11)

^a: Polymerizations are performed during 4 hours with 80 mg of AIBA under 100 bar of ethylene pressure in 50 mL of water. ^b: determined by DSC. ^c: determined by HTSEC. ^d: determined by DLS

Yield is maximal at 70°C and particles diameters increase with temperature. Finally contrary to surfactant free system, the number of particles decreases with the temperature. At 90°C the latex is not stable anymore and some flocculations occur during the polymerization.

As expected melting point and crystallinity decrease with the temperature for the same reason as previously (see section B-1-e of this chapter). Molecular weights increase with the temperature: Mn from 34700 to 69500 g/mol.

f) PE nanoparticles morphology

(1) Microscopy analysis

All these sets of experiments show that ethylene polymerization in water with CTAB as surfactant does not follow the same behavior that the surfactant free system. One of the most intriguing point is that PI remains high whatever the experimental conditions (contrary to surfactant free polymerization). This indicates that the size of the PE particles is broadly distributed.

In order to understand this point we perform the TEM analysis of these particles (see Figure 15). All pictures present in this section are performed on the same PE latex synthesized under 250 bar of ethylene pressure during 4 hours with 80 mg of AIBA.

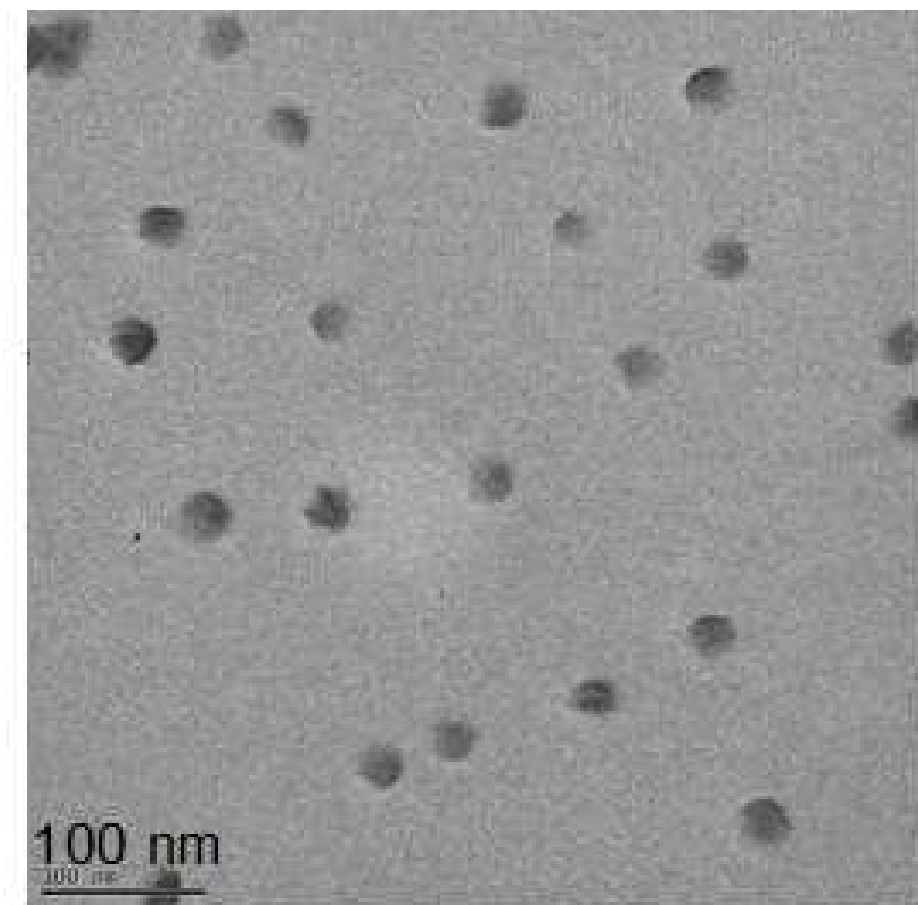


Figure 15. Standard TEM picture obtained for PE particles synthesized with 1 g/L of CTAB

In a first approach, the overall apparent shape of the particles seems almost identical to the particles synthesized without CTAB. Diameters of particles appear to be quite homogeneous and cannot explain the high PI (>0.5) observed by DLS. In addition, the particles appear to be lowly contrasted compared to particles obtained in the surfactant free system.

As already mentioned, CTAB adsorption surface is identical ($\sim 80 \text{ \AA}^2$) for the two kinds of particles (synthesized with or without CTAB), consequently particles surfaces are identical (both are composed of PE containing fragments of AIBA from the initiation). Therefore the contrast should be the same between these two kinds of particles except if the thickness of PE particles synthesized with CTAB is much smaller than their diameters.

By tilting at 60° the same sample we do not observe round shapes anymore but ellipses (see Figure 16) which implies that the 3D shape of these particles is not sphere-like but more cylinder-like.

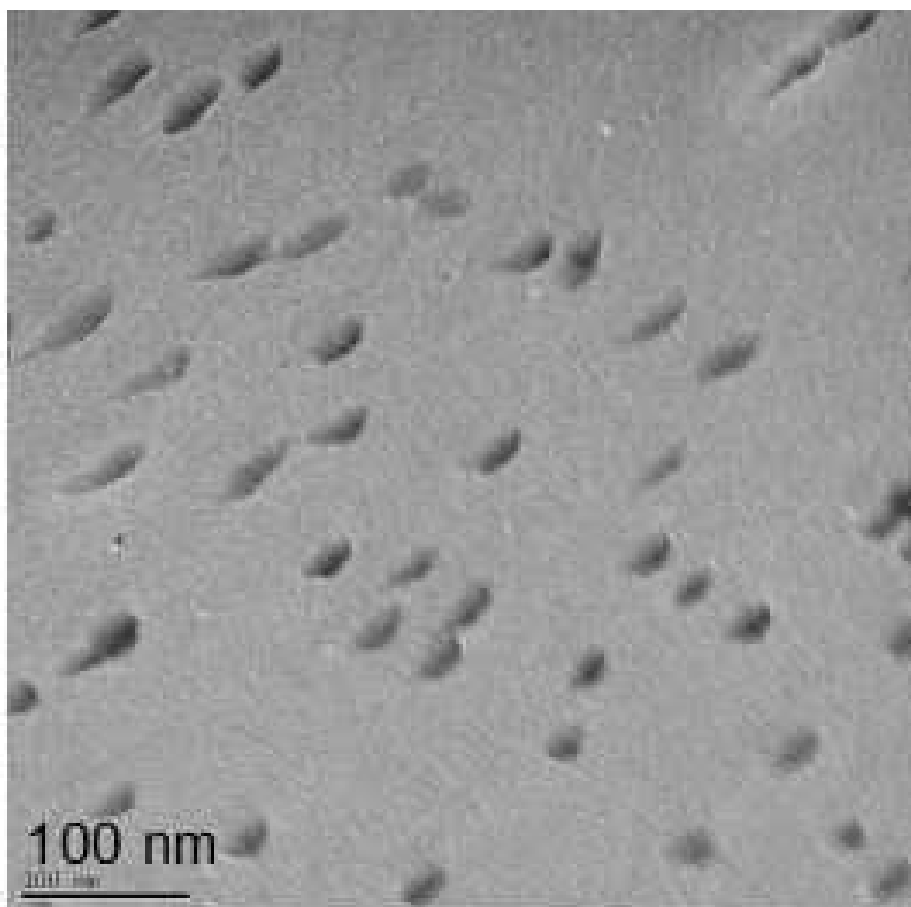


Figure 16. Standard TEM picture tilted at 60° obtained for PE particles synthesized with 1 g/L of CTAB

It is noteworthy that high diameters particles (which are present in the first instants of the polymerization) are never observed in TEM image of latexes polymerized during 4 hours. As no flocculation is observed these particles should desegregate in order to form smaller PE particles.

In order to confirm this cylinder-like morphology, TEM tomography is performed. The analysis is more complex than for sphere-like particles since the studied particles possess smaller diameter and thickness. In the following pictures we observe a PE particle on a formvar/carbon film.

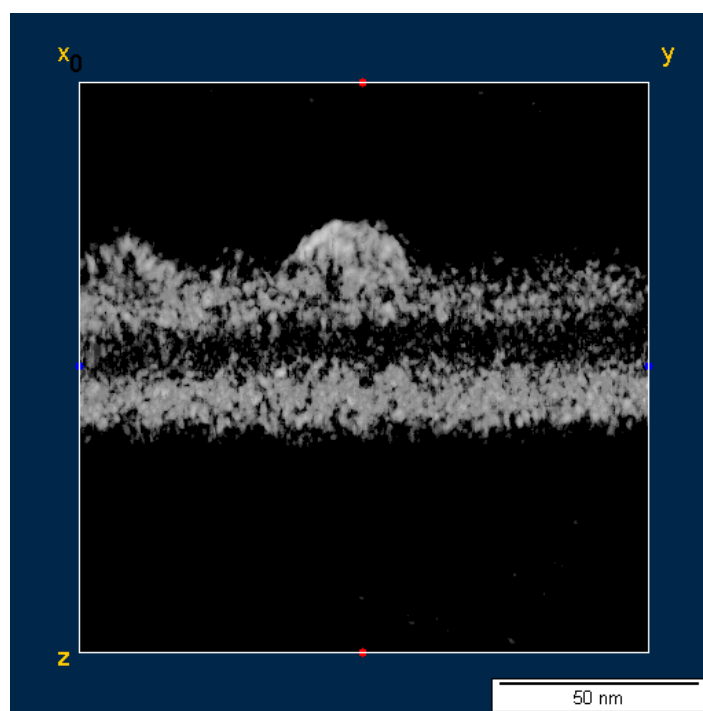


Figure 17. TEM tomography of a PE particle synthesized with 1 g/L of CTAB

Thickness is about 10 nm for a particle diameter of 40 nm. Consequently PE particles synthesized in presence of CTAB are not sphere-like but cylinder-like.

The high PI ($PI \approx 0.5$) of the PE particles can be due to the morphology of the particles and/or due to the broad distribution of the thickness of the PE particles.

In order to obtain a thickness distribution AFM analyses are performed on the same PE latex (see Figure 18).

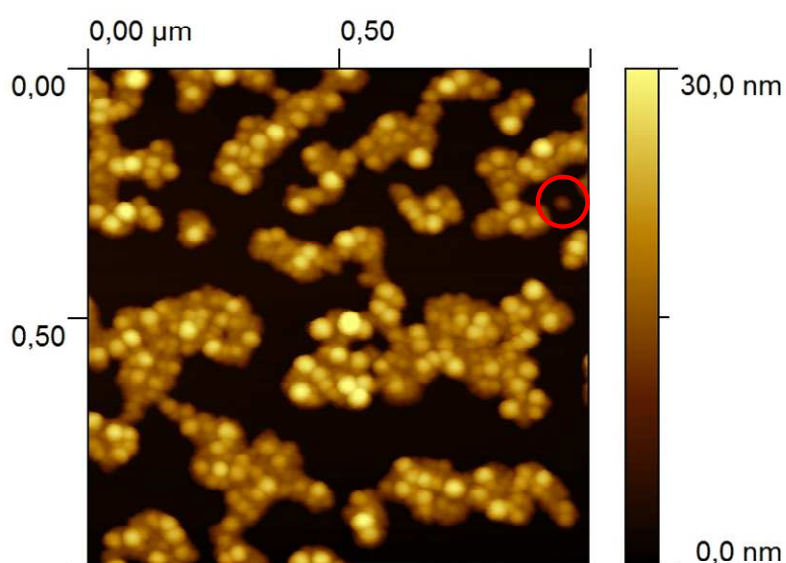


Figure 18. AFM obtained for PE particles synthesized with 1 g/L of surfactant

With cylinder-like particles, it is not easy to determine the thickness because the particles are tilted, each particle partly covering adjacent particles (see Figure 19). This arrangement can be pictured as plates in a dish-washer. Consequently the apparent height is not the thickness of PE particles. It should be noted that this organization confirms that PE particles are not sphere-like.

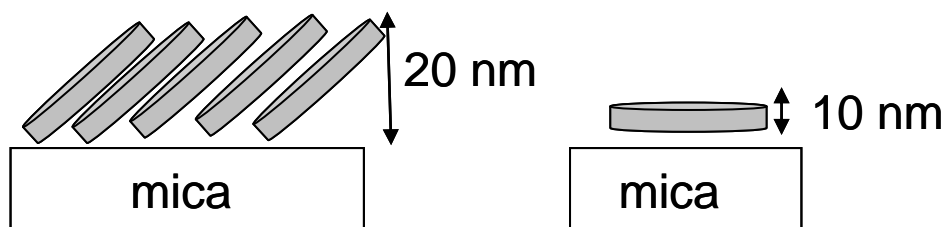


Figure 19. Schematic representation of group of PE particles and isolated particles at the mica surface

Nevertheless we are able to obtain the thickness of some isolated particles (such as the one at the high right corner of the Figure 18). The average of measure performed on ten isolated particles gives a thickness of 9.6 ± 1.3 nm. Consequently, no broad distribution is observed in thickness nor in diameters.

Therefore the high PI is ascribed to the morphology of the particles only. Indeed DLS algorithm uses a sphere particles model with only one relaxation time to calculate the average particles diameters and PI. But cylinder-like particles have two characteristic dimensions (diameters and thickness) therefore two relaxation times which are interpreted by the DLS algorithm as two different populations and consequently the DLS algorithm will predict a broad particles distribution.

Consequently this high PI is an additional evidence that cylinder-like particles are present in the solution and that the observations are not due to spheres which flatten at the surface of the microscopy film (formvar/carbon or mica).

(2) *X-ray scattering*

Finally, two latexes are characterized by X-ray scattering: one synthesized under 150 bar of ethylene pressure with 80 mg of AIBA and 1 g/L of CTAB and another synthesized at 100 bar with 200 mg of AIBA and 1 g/L of CTAB. DLS measurements indicate that particles diameters are respectively 51 nm and 40 nm with PI about 0.4.

The corresponding native crystallite diameters are respectively measured by X-ray scattering at 35 nm and 33 nm, with native crystallinity of 24% and 21%. Surprisingly average crystallite dimension is higher with CTAB than without (~20nm) and exhibits lower crystallinity level (~30%). These crystallite diameters are well correlated to the particles diameters and consequently one particle could only contain a couple of crystallites.

g) **Conclusion**

In this section the free radical polymerization of ethylene was performed in water with surfactant in order to increase the efficiency of the system.

Stable PE latexes are synthesized with solid content up to 40%. This represents the highest solid content reported for PE up to now. Moreover this process is even more efficient in activity than the free radical polymerization of ethylene in THF, our previous best system. Particles diameters remain low between 20 nm and 100 nm. Surprisingly these PE particles are not sphere-like but cylinder-like.

Finally, PE synthesized exhibit high molecular weights over 10^4 g/mol with a broad MWD ($PDI \approx 6$). Melting points falls in the range of 95°C to 105 °C indicating that high branches content PE are synthesized. Moreover, this low crystalline PE with a high level of chain branches could exhibit some interesting physical properties.

3. **Addition of an organic solvent**

a) **Effect of organic solvents on emulsion polymerization**

In order to link solvent and emulsion processes, the influence of the addition of organic solvents to water (water miscible – THF – or non-miscible – toluene) has been investigated. Different experiments are performed using 20 % in volume of organic solvent with or without CTAB using AIBA as radical initiator. In all cases stable PE dispersions are obtained.

Table 5. Influence of additional organic solvent on free radical polymerization of ethylene in aqueous dispersed medium^a

Water (mL)/ Solvent (mL) [solvent]	CTAB (g/L)	Yield (g)	Melting point (°C) ^b	Crystallinity (%) ^b	Mn (g/mol) ^c	PDI ^c	Dp (nm) ^d	PI ^d
50/0	0	1.3	96.5	35	21600	6.0	89 (±1)	0.04 (±0.01)
50/0	1	4.6	92.8	31	50500	8.7	24 (±1)	0.52 (±0.08)
0/50 [THF]		3.9	115.2	58	1190	1.9	-	-
40/10 [THF]	0	1.3	105.0	44	1760	3.8	129 (±2)	0.03 (±0.02)
40/10 [THF]	1	3.2	103.1	40	2350	3.2	16 (±1)	0.39 (±0.07)
0/50 [toluene]		0.7	115.9	63	2340	1.9	-	-
40/10 [toluene]	0	0.4	104.5	27	17100	2.6	72 (±5)	0.14 (±0.02)
40/10 [toluene]	1	3.2	99.9	22	8300	3.2	121 (±32)	0.88 (±0.11)

^a: Polymerizations are performed during 4 hours with 80 mg of AIBA under 100 bar of ethylene pressure in 50 mL of solution at 70°C. ^b: determined by DSC. ^c: determined by HTSEC. ^d: determined by DLS

In all cases, no activation effects are observed. Indeed the addition of organic solvent does not increase yield of polymerization. Additions of these organic solvents are therefore used to understand the mechanism of the polymerization such as the type of particles nucleation.

PE molecular weights drop in the presence of organic solvents. M_n drops from 50500 g/mol in water to 8300 g/mol and 2350 g/mol for toluene/H₂O (1/4) and THF/H₂O mixtures respectively in the presence of CTAB. This decrease can be related to an increased frequency of transfer reactions to solvent (contrary to water, THF and toluene exhibit high transfer capacities) which has been confirmed by ¹³C NMR analysis. Indeed in both cases the toluene-chain end or THF-chain end are identified by NMR. Moreover the PDI reaches a value close to 2 in presence of organic solvent indicating that MWD is mostly controlled by transfer.

With THF, the transfer reaction should take place in the continuous aqueous phase or at the particle surface and not inside the particles, because THF is not an efficient swelling agent for amorphous PE (same D_p is observed before and after removal of THF by partial reduced pressure evaporation of the latex). For toluene, the D_p drops by about 10 nm by removing the organic solvent (toluene is a swelling solvent for PE) so transfer could additionally take place inside the particles.

Finally, since PE is strongly non-soluble in water, PE growing radical must form particles (or enter in existing particles) very soon (at molecular weight far below the one measured by HT-SEC). Consequently the drop in molecular weight evidences that the growing macroradical of PE must be at the surface of PE particles in order to undergo the transfer to organic solvent such as THF.

PE nanoparticles synthesized in these conditions are more crystalline than usual. Consequently, due to the high crystallinity of PE, particle surfaces are extremely irregular. This has been confirmed by TEM (see Figure 20).

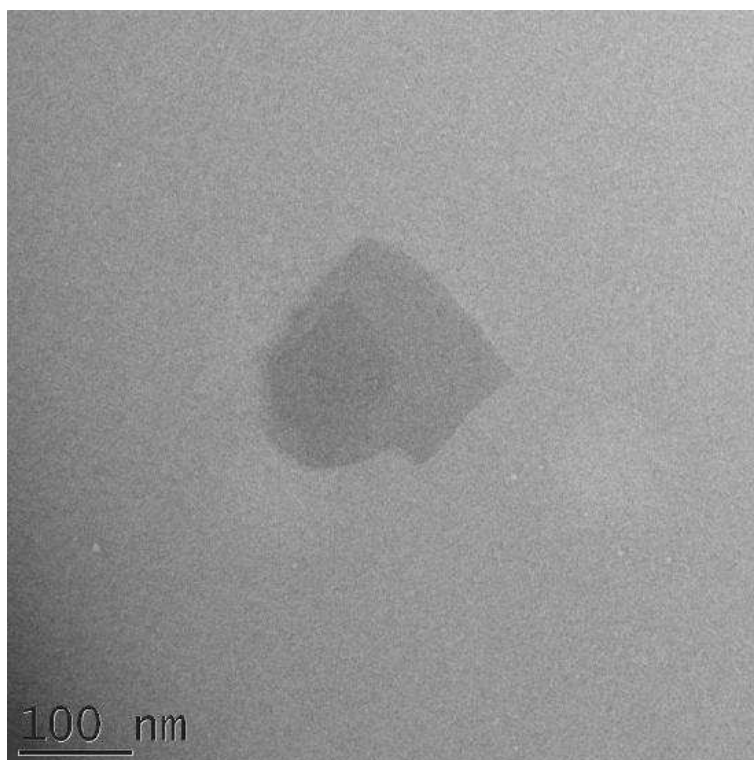


Figure 20. Example of TEM picture obtained for PE particles synthesized in THF/water mixture without CTAB

b) Role of the initiator

The difference in yield between polymerization in solution and in emulsion could be partly due to the difference in efficiency factor and dissociation constant between AIBA and AIBN.

In this purpose two experiments are performed in water/THF (1/1) mixture in which both AIBA and AIBN are soluble. With the same molar amount of radical initiator, the polymerizations provide in both cases exactly the same yield (1.8 g). However the dispersion is not stable. This identical yield shows that, as the decomposition is about the same for both of these initiators; the efficiency factor of AIBA is approximately equal to the efficiency factor of AIBN. Molecular weights are also identical for both polymers respectively $M_n=1910$ g/mol, $PDI=2.6$ for AIBA and $M_n=2020$ g/mol, $PDI=1.9$ for AIBN.

These experiments demonstrate that the effects on yield and molecular weight observed during the polymerization in emulsion are only due to the emulsion itself and not to the initiator.

4. Rationalization of CTAB role

PE particles shapes seem to be CTAB dependent. Without CTAB, sphere-like particles are synthesized and with 1 g/L of CTAB, cylinder-like particles are obtained. In this section, the boundary between sphere and cylinder particles is investigated and the particles formation discussed.

a) Effect of the CTAB concentration

Several series of experiment are performed in aqueous solution of CTAB with concentration from 0 g/L to 4 g/L. All polymerizations are done at 70°C during 4 hours at ethylene pressure from 100 bar to 250 bar, using 80 mg AIBA as radical initiator in 50 mL of aqueous solution.

Results are summarized in the following figures.

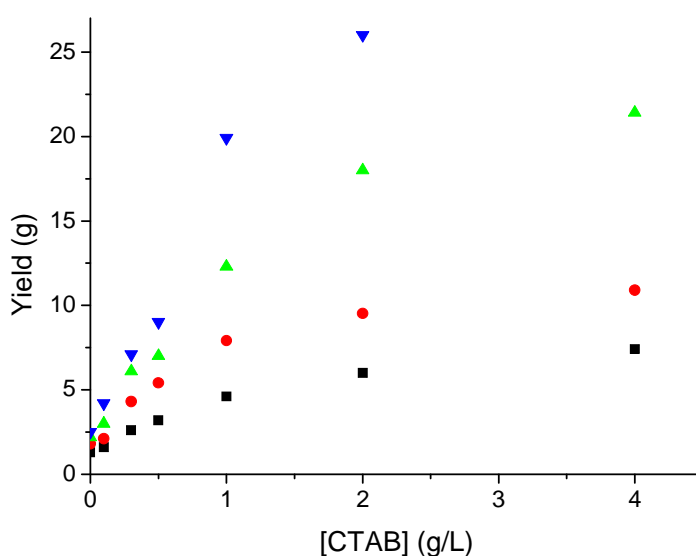


Figure 21. Influence of CTAB concentration on the polymerization yield. ■ at 100 bar of ethylene pressure, ● at 150 bar, ▲ at 200 bar, ▼ at 250 bar

As already mentioned, whatever the CTAB concentration, solid contents increase with ethylene pressure and with CTAB concentration. Polymerizations at 4 g/L of CTAB yield the highest solid content at constant ethylene pressure. At this CTAB concentration under 250 bar, the polymerization is so efficient that the latex flocculates (indeed the particles double layer must interact when a certain amount of solid content is reached and leads to particles aggregation) and almost 30 g of PE are synthesized.

Concerning average particles diameter, two different behaviors are observed (see Figure 22). The first one is below 0.5 g/L of CTAB, the average particles diameters decrease with the CTAB concentration until reaching the second one, a plateau over 0.5 g/L. Moreover below 0.3 g/L average particles diameters increase with pressure, which is not the case over 0.5 g/L of CTAB.

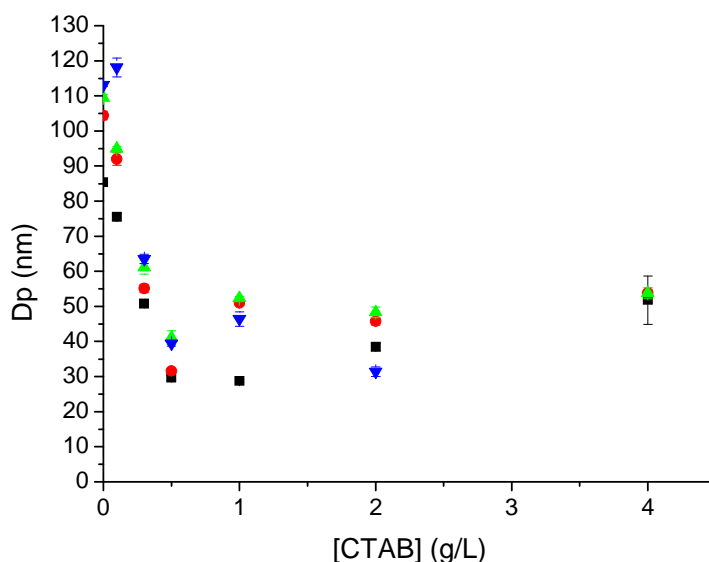


Figure 22. Influence of CTAB concentration on the average particles diameters.^a
 ■ at 100 bar of ethylene pressure, ● at 150 bar, ▲ at 200 bar, ▼ at 250 bar.
^a: determined by DLS

In regards to the variation of the number of particles with CTAB, it should be noted that below 0.5 g/L the number of particles is almost constant with the ethylene pressure ($Np \propto P^0$) and it increases with the CTAB concentration ($Np \propto [CTAB]^2$).

Over 0.5 g/L of CTAB, the number of particles increases with the ethylene pressure ($Np \propto [P]^3$). Finally at constant pressure of ethylene, the number of particles is almost independent of the CTAB concentration ($Np \propto [CTAB]^0$).

PI of the particles distribution determined by DLS (see Figure 23) remains extremely low below 0.5 g/L (PI \approx 0.05) and high over 0.5 g/L (PI $>$ 0.2).

All these results confirm that CTAB concentration exhibits a dramatic influence on the PE particles morphology. Over 0.5 g/L of CTAB cylinder-like particles are obtained and below 0.5 g/L sphere-like.

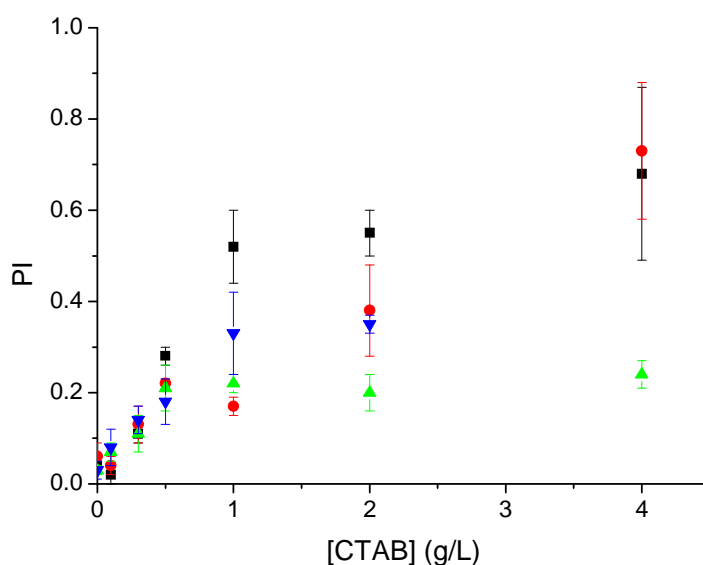


Figure 23. Influence of CTAB concentration on the polydispersity index.^a ■ at 100 bar of ethylene pressure, ● at 150 bar, ▲ at 200 bar, ▼ at 250 bar
^a: determined by DLS

Indeed all these data indicate a change of behavior around the critical micelle concentration of CTAB. As micelles have a crucial importance during phase I of the emulsion it could be partly due to a change of the prevailing nucleation mechanism.

b) Correlation between CTAB concentration and particles morphology

The crucial influence of CTAB on PE morphology has been confirmed by TEM analysis (see Figure 24). Indeed cylinder-like particles can be identified by their low contrast compared to sphere-like particles.

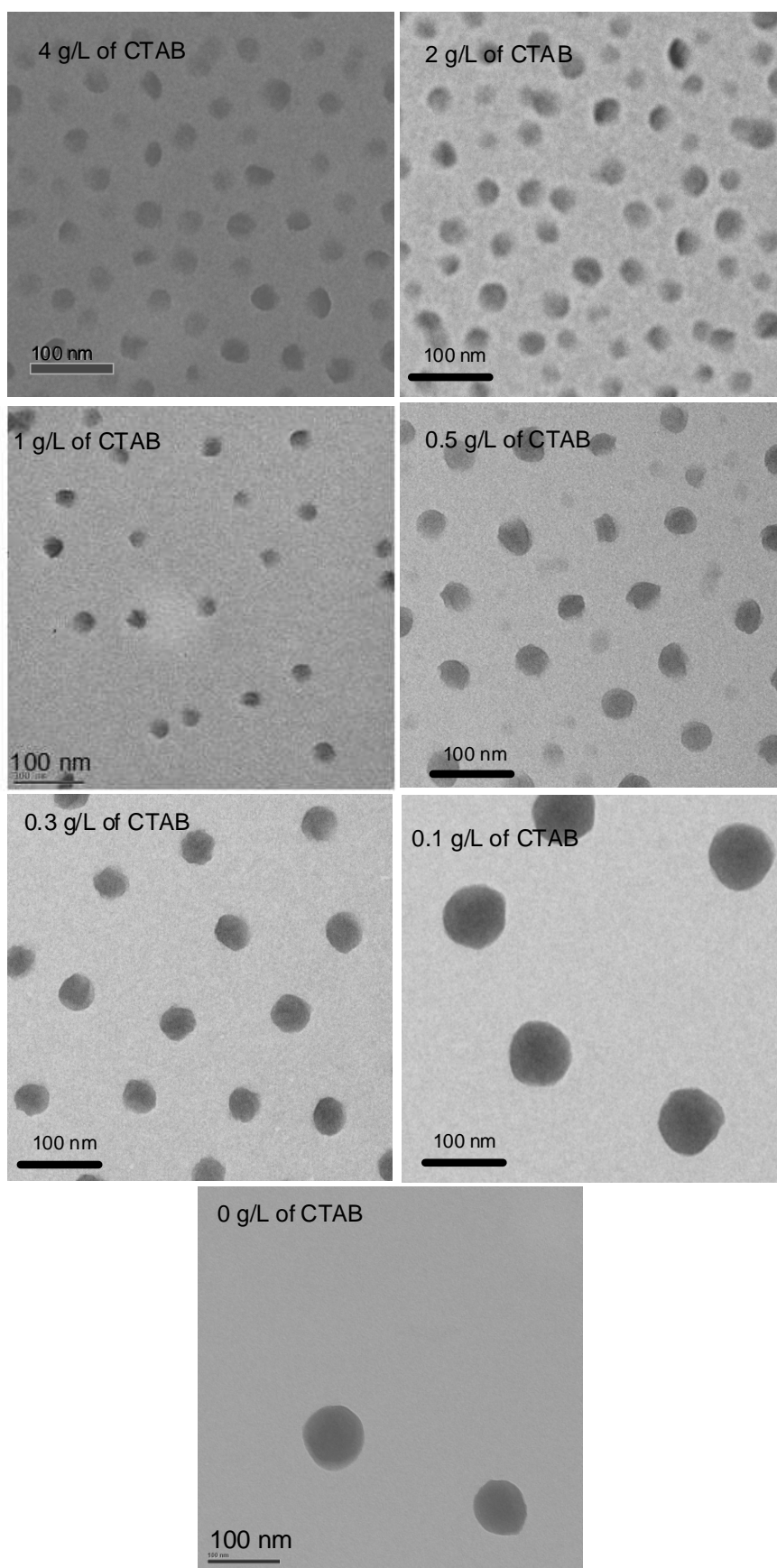


Figure 24. Standard TEM pictures for PE particles synthesized at various CTAB concentrations under 150 bar of ethylene pressure

For PE particles synthesized in aqueous solution at 4 g/L of CTAB, cylinder-like particles are observed as expected. Same kinds of particles are obtained at 2 g/L and 1 g/L of CTAB. These results are in agreement with DLS results (high PI therefore cylinder-like particles).

For cylinder-like particles, the contrast seems to increase when CTAB concentration decreases. This should indicate that the thickness of the cylinder decreases with increasing CTAB concentration. However, these results need to be confirmed by TEM tomography analysis or AFM.

At 0.5 g/L of CTAB, we observe both highly contrasted particles (sphere-like) and lowly contrasted particles (cylinder-like) with the same apparent diameters. This CTAB concentration appears to be the boundary between the two particles morphologies.

At lower CTAB concentration only highly contrasted particles are observed. No more cylinder-like particles are identified. However at 0.3 g/L of CTAB, particles appear to be less sphere-like (particles surface are more erratic) than that PE particles obtained without CTAB.

Finally at 0.1 g/L of CTAB no apparent difference exists between these particles and particles synthesized without CTAB.

Consequently these results show how important the influence of CTAB concentration is on the PE particles morphology. Above 0.5 g/L of CTAB cylinder-like particles are synthesized while under 0.5 g/L sphere like particles are formed.

This boundary between the two different morphologies is well correlated with the critical micelle concentration of CTAB. Consequently, we can assume that micelles of CTAB play an essential role in the formation of these PE particles.

c) Possible mechanism for disappearance of large particles

Now it remains to understand the particles formation and why at high CTAB concentration cylinder-like particles are synthesized.

(1) *Evidence of the disappearance*

Kinetics profiles have been determined at 100 bar, 70°C using 80 mg of AIBA with increasing CTAB concentration from 0 g/L to 4 g/L (see Figure 25, Figure 26) with the aim to determine the emulsion of behavior has. This behavior can be either “standard” in which yield and particles diameters increase with time and number of particles remains constant, or “non-standard” in which yield increases and particles diameters decrease with time, consequently the number of particles increases with time.

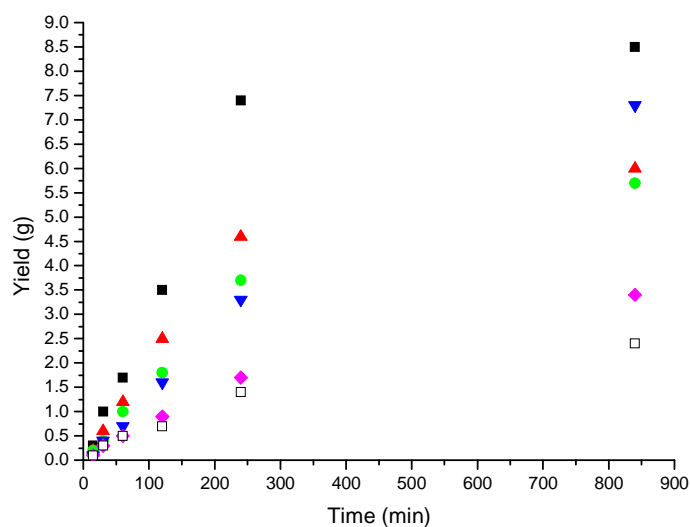


Figure 25. Influence of CTAB concentration on the reaction profiles: yield vs. time.
 ■ at 4 g/L of CTAB, ▲ at 1 g/L ● at 0.5 g/L, ▼ at 0.3 g/L, ◆ at 0.1 g/L and □ at 0 g/L

As expected, yield increases with time and with CTAB concentration. Concerning the evolution of particles diameters two different behaviors are observed (see Figure 26).

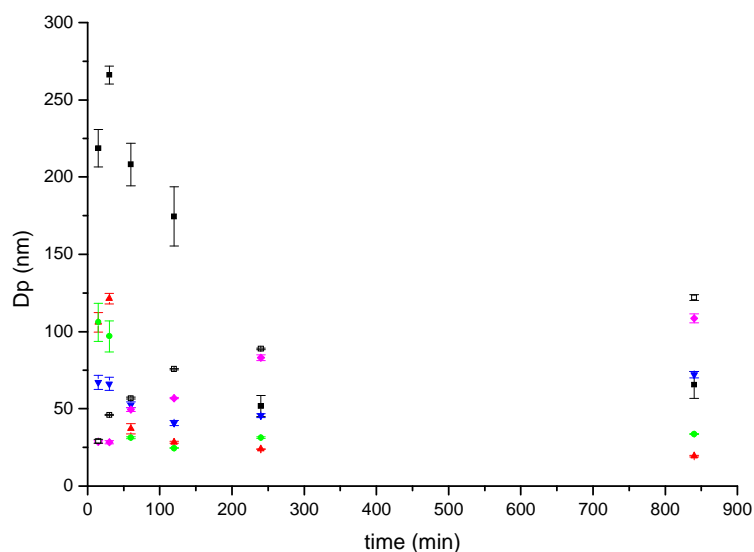


Figure 26. Influence of CTAB concentration on the reaction profiles: average particles diameters^a vs. time. ■ at 4 g/L of CTAB, ▲ at 1 g/L ● at 0.5 g/L, ▼ at 0.3 g/L, ◆ at 0.1 g/L and □ at 0 g/L. ^a: determined by DLS

For kinetics performed between 4 g/L and 0.5 g/L of CTAB particles diameter decreases and reaches a plateau after 2-4 hours of polymerization. For 0 g/L and 0.1 g/L of CTAB particles diameter increases with time and the number of particles remains even during the polymerization. Finally at 0.3 g/L of CTAB, particles diameter decreases in a first period and then after 1 hour of polymerization this diameter increases and the number of particles remains constant.

Consequently, over 0.3 g/L of CTAB, a “non-standard” behavior is observed. Cylinder-like particles are synthesized and the number of particle increases with the time of polymerization. Below 0.3 g/L of CTAB a “standard” behavior is obtained. Number of particles remains constant with time (and ethylene pressure) and sphere-like particles are synthesized. Therefore, the morphology seems to be interconnected with the kinetic behavior of the polymerization.

At the beginning of the reaction, large particles are synthesized over 0.5 g/L of CTAB. TEM pictures of the latex obtained after 30 min of reaction shows large particles surrounded by other smaller particles (see Figure 27). Those large particles seem to disappear during the polymerization; since no flocculation is observed they must disaggregate.

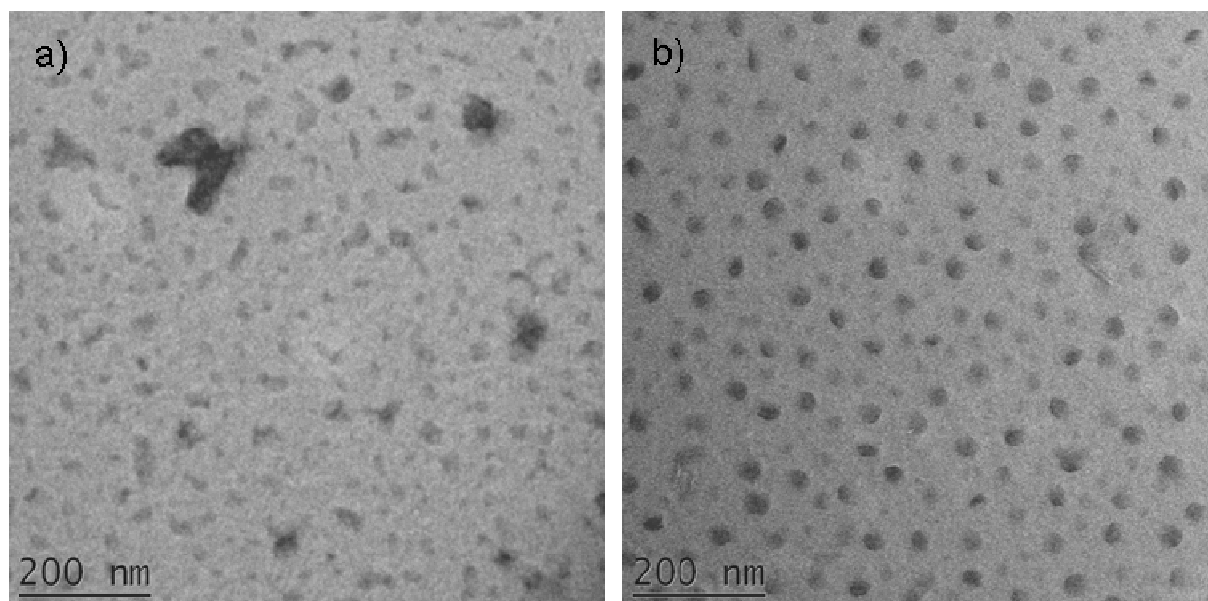


Figure 27. TEM pictures of PE latex after 30 min at 70°C (a) and 4h (b) with 1g/L of CTAB

These large particles synthesized in the first minutes of the polymerization have disappeared by an unknown mechanism. In order to obtain some clues we performed several additional sets of experiments.

(2) *Effect of stirring*

Polymerizations are performed at 70°C with 50 mL of an aqueous solution of 0.5 g/L of CTAB under 100 bar of ethylene pressure during 4 hours with 80 mg of AIBA (see Figure 28). In this set of experiments, the influence of stirring rate is investigated.

It should be noted that the stirring rate is constant for all of the previous experiments (at around 250 tr/min).

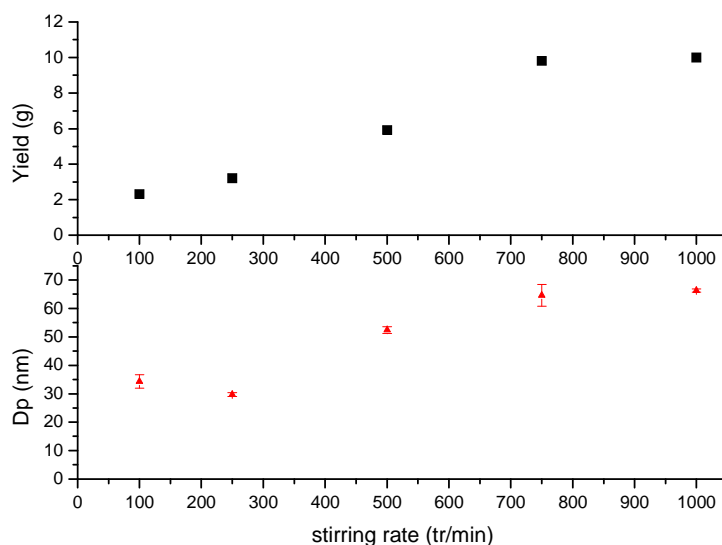


Figure 28. Influence of stirring rate on polymerization of ethylene in water. ■ yield and ▲ average particles diameters^a vs. stirring grade under 100 bar of ethylene pressure with 80 mg of AIBA in 50 mL of 0.5 g/L of CTAB aqueous solution during 4 hours.
^a: determined by DLS

A drastic effect of the stirring on the polymerization yield and the particles diameters is observed. Indeed, both increase with the stirring rate. It should be noted that there is no significant effect if polymerizations are performed in THF or without CTAB (same yield, particles diameters, and molecular weight).

Ethylene polymerization is more efficient at higher stirring rate (higher yield and particles diameters). As the number of particles slightly decreases with the stirring rate ($Np \propto S_R^{-0.22}$), the higher yield cannot be due to the number of particles (usually kinetic rate increases with the number of particles) but may be due to the fragmentation of native large particles.

Indeed the sooner these particles disaggregate to form cylinder-like PE particles the higher will be the yield. As stirring grade increases, the probability of collision between particles increases thus the desegregation of large particles.

Consequently it seems that the stirring facilitates the disappearance of the PE large particles. Now it remains to understand the role of CTAB.

(3) *Evidence of the ejection of cylinder particles*

In order to fully understand the influence of CTAB, we perform the polymerization of ethylene with 0.1 g/L of CTAB. Consequently, sphere-like particles are obtained with an average particles diameter of 92 nm and a PI of 0.03. Then after the polymerization end we add CTAB up to a concentration of 1 g/L and then this latex is stirred at 70°C during 4 hours. Using DLS, we observe that the average particles diameter decreases to about 10 nm and PI increases to 0.15. Moreover TEM pictures on the latex stirred with CTAB shows two different populations of particles: the native large particles, with a sphere-like morphology, and small particles with low contrasted cylinder-like morphology (see Figure 29).

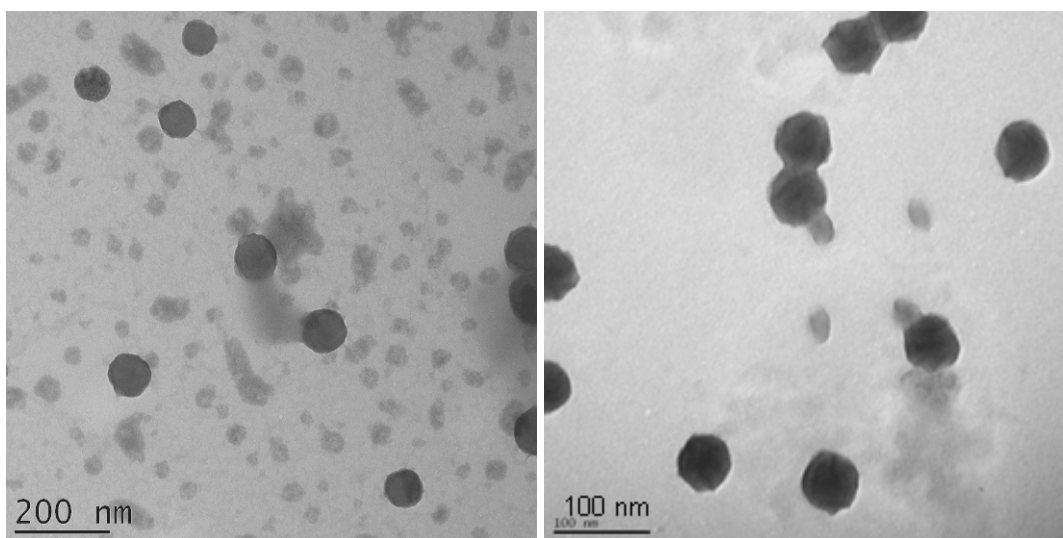


Figure 29. TEM pictures of the PE latex after stirring during 4 hours at 70°C with 1 g/L of additional CTAB

It should be noted that a blank experiment has been performed by stirring at 70°C during 4 hours the latex without addition of CTAB. No change in the morphology is observed by TEM or DLS (see Figure 30).

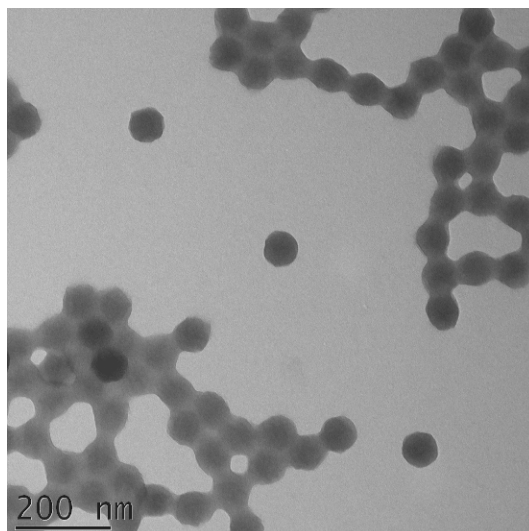


Figure 30. TEM picture of the PE latex after stirring during 4 hours at 70°C

Moreover no change in morphology by TEM or DLS is observed if the latex is not heated whatever the CTAB concentration added.

Consequently the decrease of average particles diameter observed by DLS is due to the apparition of a new population of smaller cylinder-like particles. These cylinders could be ejected from the native particles thanks to the CTAB itself and the temperature. Then these particles are stabilized by CTAB.

This mechanism appears also to be related to the temperature. Consequently the PE should be ductile enough to allow the ejection of some material (indeed PE is low crystalline, $T_m < 105^\circ\text{C}$, crystallinities $< 30\%$). Then high CTAB concentration is mandatory in order to stabilize the ejected PE particles.

(4) Density of the PE particles

It is worthy to mention that during these aforementioned experiments density of PE particles vary. To determine the density of PE particles, we simply measure the density of the native latex. Below 0.3 g/L of CTAB, PE nanoparticles synthesized have density of 0.7-0.8. This value is below the PE amorphous density (0.855). Consequently, some cavities should exist inside the particles. Over 0.5 g/L of CTAB, density of PE particles is around 0.9 which is in agreement with the PE crystallinity, therefore no hole must be present.

After stirring at 70°C with or without CTAB, we observe that the density increases from 0.75 to 0.87. Consequently, there is a reorganization of PE particles themselves. Therefore when CTAB is added during this reorganization some material can be ejected in order to form smaller cylinder-like PE particles. This mechanism explains why a certain temperature is mandatory (no PE particles ejected at ambient temperature) as PE has to be ductile in order to permit this reorganization. .

It should be noted that density increases when the PE particles are heated at 70°C, however the polymerization was also performed at 70°C. Consequently these holes could be due to unreacted ethylene present inside the particles at the end of the reaction.

5. Conclusion

In this section, we demonstrated that PE can be synthesized in aqueous media which leads to the formation of a stable PE dispersion. Moreover due to the compartmentalization effect, this system is more efficient than the ethylene free radical polymerization in THF (our previous best system). Indeed stable PE latexes with solid contents up to 40% are obtained. Particles average diameters available by these techniques are from 20 nm to 200 nm which leads from transparent to white latexes (see Figure 31).

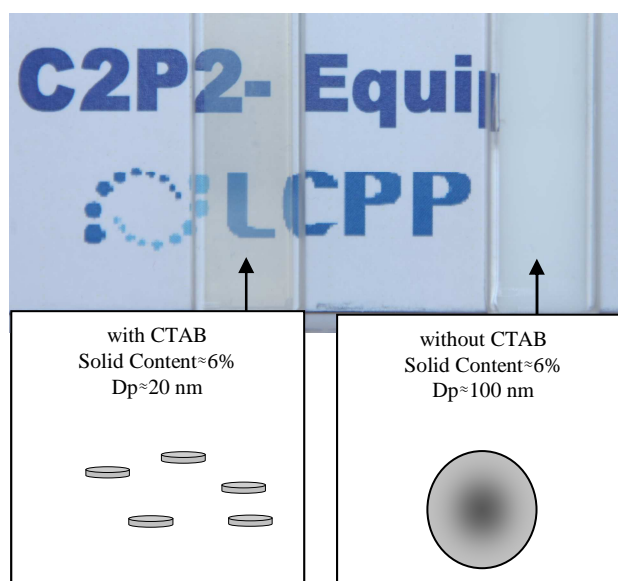


Figure 31. Two different native PE latexes obtained at 6% of solid content

Moreover MWD exhibits higher molecular weight over the entanglement weight with PDI between 5 and 8. Consequently this PE could possess some interesting physical properties. Melting points fall in the range of 95°C to 105°C corresponding to a PE of important branches content (between 30 and 40 branches per 1000 carbons).

Additionally since these PE possess low crystallinities, these latexes should exhibit some interesting coating properties which remain to be investigated.

Finally two different morphologies of PE particles are identified: sphere-like particles if the PE is synthesized with a CTAB concentration below 0.5 g/L, and cylinder-like particles if polymerization is performed with CTAB concentration over 0.5 g/L. Moreover these cylinder particles possess bigger crystallites than sphere-like particles. The crystallite dimension has a crucial role in the PE particles morphology since for sphere-like particles their dimension corresponds to the facets dimension and for cylinder-like to the diameters of the particle itself.

Some important clues in the formation mechanism of the cylinder-like particles have been found: temperature and high CTAB concentration seem to play a crucial role. Moreover stirring rate leads also to a dramatic effect on the polymerization indicating that some physical force such as collision should impact the cylinder-like particles formation.

C. Case of anionic stabilization

Up to now, all latexes are synthesized using a cationic stabilization since radical initiator (AIBA) and a cationic surfactant (CTAB) are used. The most used anionic stabilization and initiator have been also investigated (surfactant: sodium dodecylsulfate, SDS; initiator: ammonium persulfate, APS) in this section.

1. Importance of the pH of the polymerization

In the literature, authors reported that this polymerization is only efficient if the pH is acidic ($\text{pH} < 2$) [19] or basic ($\text{pH} > 10$) [20, 21]. In this section we will confirm these results in our range of pressure and temperature.

In this purpose, polymerizations are performed in 50 mL of aqueous solution containing 305 μmol of ammonium persulfate (APS) or potassium persulfate (KPS) with or without 4 g/L sodium dodecylsulfate (SDS). After 4 hours at 70°C whatever the ethylene pressure, no PE is synthesized.

In order to infirm an inhibition by SDS itself, we perform polymerizations with another anionic surfactant SDBS (sodium dodecylbenzenesulfate) at the same concentration (4 g/L). In this case also no PE is synthesized.

Finally, in order to infirm an effect of the anionic stabilization we perform polymerizations using a non-ionic surfactant (Disponil A 3065 based on PEG). Once again no PE is synthesized.

This confirms the literature results already mentioned, that free ethylene polymerization initiated by persulfate is only efficient at basic or acidic pH. Indeed polymerizations are performed under 200 bar of ethylene pressure at 70°C during 4 hours in 50 mL of an aqueous solution containing 305 μmol of APS, 0.005% in volume of NH_3 or 0.1 mol/L of HCl. In both cases, stable PE nanoparticles dispersions are obtained. Solid contents are by the acidic pathway about 4% and only 2.4% in basic solution with average particles diameters respectively of 95 nm and 127 nm.

As we use a steel reactor, we choose in the following to study only the emulsion initiated by APS in basic solution in order to prevent the corrosion of the reactor.

2. Surfactant free emulsion

Polymerizations of ethylene in basic aqueous solution are first studied without any surfactant. Reactions are performed at 70°C during 4 hours in 50 mL of an aqueous solution containing 70 mg of APS and 0.005% in volume of NH₃. Results are summarized in the following table.

Table 6. Ethylene pressure influence on the free radical polymerization of ethylene in water^a

Ethylene Pressure (bar)	Yield (g)	Melting point (°C) ^b	Crystallinity (%) ^b	Mn (g/mol) ^c	PDI ^c	Dp (nm) ^d	PI ^d
50	0.1	nd	nd	nd	nd	300 (±20)	0.66 (±0.12)
100	0.3	95.3	25	nd	nd	92 (±1)	0.09 (±0.02)
150	0.7	99.2	28	6500	4.5	94 (±1)	0.04 (±0.04)
200	1.2	105.3	41	14300	6.5	127 (±3)	0.03 (±0.01)
250	2	103.2	38	17200	5.2	105 (±1)	0.03 (±0.02)

^a: Polymerizations are performed during 4 hours with 70 mg of APS at 70°C in 50 mL of water at 0.005% in volume of NH₃. ^b: determined by DSC. ^c: determined by HTSEC. ^d: determined by DLS.

Yield of polymerization initiated by APS remains lower than with AIBA in similar experimental conditions. It is partly due to the lower decomposition rate of the APS in basic solution compared to the one of AIBA.

In all these experiments (except the polymerization performed under 50 bar of ethylene pressure) stable latexes are obtained.

As usual, yield increases with the ethylene pressure. Maximum solid content of PE latex synthesized is 4 %. Average particles diameter slightly increases with the ethylene pressure. Number of particles increases as well ($Np \propto P^{3.8}$). PI remains low indicating sphere like particles homogeneous in dimension. This has been confirmed using TEM pictures (Figure 32).

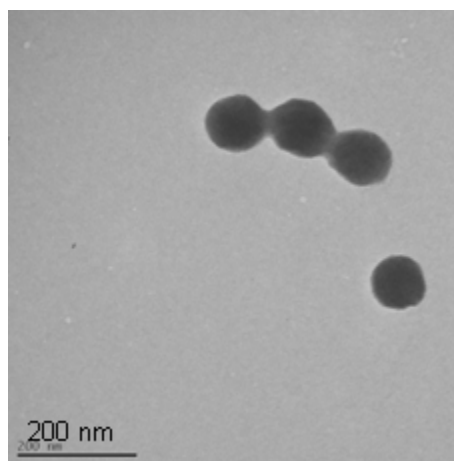


Figure 32. Standard TEM picture obtained for PE particles synthesized in alkaline solution without SDS

PE synthesized exhibit similar melting points as the PE synthesized with AIBA while molecular weights are lower: for example, respectively 105.3°C and 106°C for PE synthesized under 200 bar of ethylene pressure.

One important point is to understand the origin of the particles stabilization. Indeed we perform this polymerization in basic aqueous solution. It is known that in this case the initiated radical is mostly a hydroxyl radical. Consequently the chain-end is functionalized by an alcohol group which cannot explain the particles stabilization.

Moreover if the latex undergoes dialysis, PE particles flocculate (it should be noted that latexes synthesized using AIBA do not flocculate). Consequently the molecules which stabilize PE particles could possess a low molecular weight. We hypothesize that the sulphate radical can initiate some ethylene and undergo the oligomerization of PE, synthesizing in-situ surfactant for PE particles. This should be mostly an oligomerization otherwise dialyse will not destabilize the latex. Moreover surfactant in-situ synthesized seems to be in small amount since no measurable yield is obtained during the reaction of APS in water without NH_3 whatever the ethylene pressure.

3. Polymerization with SDS as surfactant

In order to improve this polymerization we performed the same set of experiments with 4 g/L of SDS (over the cmc – see Table 7).

Table 7. Ethylene pressure influence on the free radical polymerization of ethylene in an aqueous solution of 4 g/L of SDS^a

Ethylene Pressure (bar)	Yield (g)	Melting point (°C) ^b	Crystallinity (%) ^b	Mn (g/mol) ^c	PDI ^c	Dp (nm) ^d	PI ^d
50	0.3	nd	nd	4600	2.7	nd	nd
100	0.6	97.3	25	14900	1.9	nd	nd
150	1.4	102.5	35	17800	4.2	nd	nd
200	2	103.2	37	29500	5.6	nd	nd
250	2.3	105.5	41	53000	4.7	nd	nd

^a: Polymerizations are performed during 4 hours with 70 mg of APS at 70°C in 50 mL of an aqueous solution containing 4 g/L of SDS and 0.005% in volume of NH₃. ^b: determined by DSC. ^c: determined by HTSEC. ^d: determined by DLS.

In all cases no stable latex is obtained. This is an unexpected result as SDS is a surfactant which usually improves efficiently the stabilization of the particles.

Yield of polymerization is slightly higher with SDS than without and increases with the ethylene pressure.

Molecular weights also increase with the pressure (up to 53000 g/mol) and are higher than without SDS. Finally, PE melting point is also higher with SDS, than without.

These results are unexpected. Indeed we demonstrate that the stabilization of PE nanoparticles in the surfactant-free polymerization must be due to oligoethylene terminated by a sulphate. These molecules are close in chemical formula to SDS. Then it remains to understand why 4 g/L of SDS destabilize the dispersion.

4. SDS emulsion zone of stability

This destabilization of PE particles in presence of SDS is an unexpected result. Polymerizations with the same surfactant concentration using SDBS ($\text{cmc} \approx 0.5 \text{ g/L}$) are also performed and lead to similar result.

In order to understand this flocculation phenomenon, we perform polymerizations with several concentration of SDS from 0 g/L to 10 g/L. All experiments are done in the same conditions: 70°C, during 4 hours with 70 mg of APS in 50 mL of an aqueous solution containing 0.005% and ethylene pressure from 50 bar to 250 bar. Over 1 g/L whatever the ethylene pressure no stable latexes are obtained. But below, an area of stability is identified (see Figure 33).

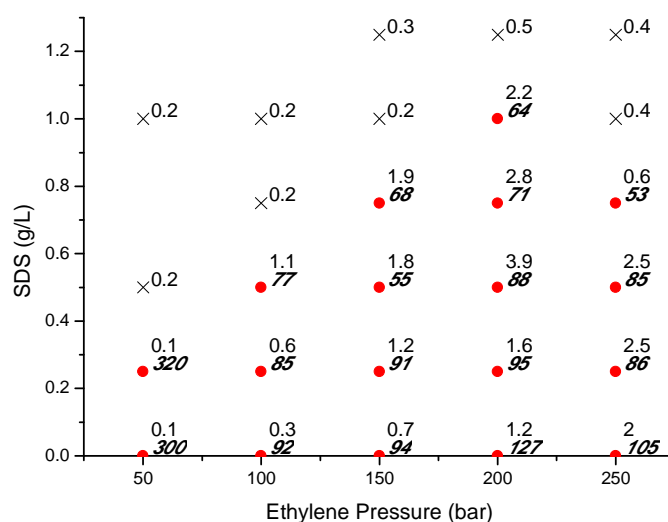


Figure 33. Area of latex stability. ● stable latex, x: flocculation. Labels are yield and average particles diameters^a. ^a: determined by DLS

At 0 g/L and 0.25 g/L of SDS yield increases with the ethylene pressure. The particles diameter, except at 50 bar, increases up to a maximum value at 200 bar then decreases. Over 0.25 g/L the optimum in yield is obtained at 200 bar. This pressure seems to be the optimum of polymerization since with 1 g/L of SDS polymerizations of ethylene at 150 and 250 bar provide unstable latex. At constant pressure, yield increases with the SDS concentration and average particles diameters decreases with the SDS concentration.

The explanation for the existence of this area of stability remains unclear and some complementary studies need to be performed in order to understand how SDS can destabilize PE particles. However it appears that the concentration of SDS has a crucial role on the destabilization mechanism.

D. Toward more complex architectures

In order to access more complex nanostructures, we performed some tryouts in order to obtain hybrid nanoparticles (organic/organic or organic/inorganic).

1. Hybrid organic-organic

In this section polymerizations are performed using a native latex (PMMA, PS, PE) in order to obtain organic-organic hybrid nanoparticles.

a) PMMA/PE particles

(1) PMMA core

First we perform a MMA polymerization in water with AIBA and CTAB in order to obtain a 20 % solid content PMMA latex with a narrow particles diameters distribution around 50 nm. The conversion of MMA is over 95%.

Then, we prepare a latex at 10 % of solid content with an additional CTAB concentration of 4 g/L, with 80 mg of AIBA, and perform the polymerization during 4 hours at 70°C under ethylene pressure up to 250 bar. Results are summarized in the following table.

Table 8. Tryouts of PMMA/PE hybrid particles^a

Ethylene Pressure (bar)	PE Yield (g)	Dp (nm) ^b	PI ^b
native	0	48 (±1)	0.03 (±0.01)
50	0.9	60 (±2)	0.13 (±0.05)
100	3.9	76 (±4)	0.14 (±0.06)
150	5.3	70 (±5)	0.11 (±0.03)
200	7.3	77 (±3)	0.15 (±0.06)
250	13.3	71 (±6)	0.16 (±0.04)

^a: Polymerizations are performed during 4 hours with 80 mg of AIBA at 70°C in 50 mL of a PMMA latex at 10% of solid content 4 g/L of CTAB. ^b: determined by DLS.

We observe that the solid content after polymerization is above the native solid content. Moreover the average particles diameters are also increased compared to the native PMMA latex. Consequently, some PE has been synthesized. However as the PI also increases (from 0.03 to 0.16) we cannot be sure that a core-shell architecture is obtained. It is possible that additional particles are synthesized. However, the number of particles is almost constant with ethylene pressure which is compatible with a core-shell morphology. Unfortunately TEM analyses are unable to confirm that PE shell surrounding PMMA core particles are synthesized (see Figure 34).

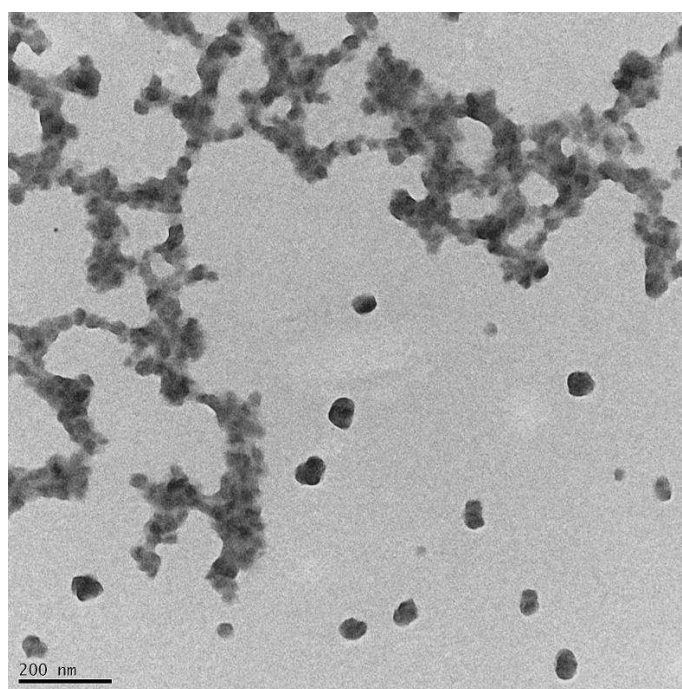


Figure 34. Standard TEM picture obtained for PE/PMMA latex synthesized under 150 bar of ethylene pressure

Indeed no core-shell architecture is identified. However the picture obtained does not correspond to the one usually obtained for PE particles or PMMA particles (For PMMA latexes, cryo-TEM is mandatory in order to observe nanoparticles). Consequently the particles observed could be PE/PMMA hybrids.

(2) *PE core*

The opposite synthesis based on PE cores has been also investigated. But in this case a second population appears then latex flocculates. Since PE is not swollen by MMA, the core-shell synthesis is ineffective (since no MMA is inside the native particles) and consequently novel PMMA particles are synthesized.

b) PS/PE particles using a PS core

For PS another strategy is tested. Large PS latex particles are chosen (narrow distribution around 100 nm synthesized without CTAB). Two experiments are performed at 150 bar of ethylene pressure with a native PS latex at 10 % of solid content. In the first one 80 mg of AIBA was added. Without any surfactant the nucleation of new particles will be disfavored.

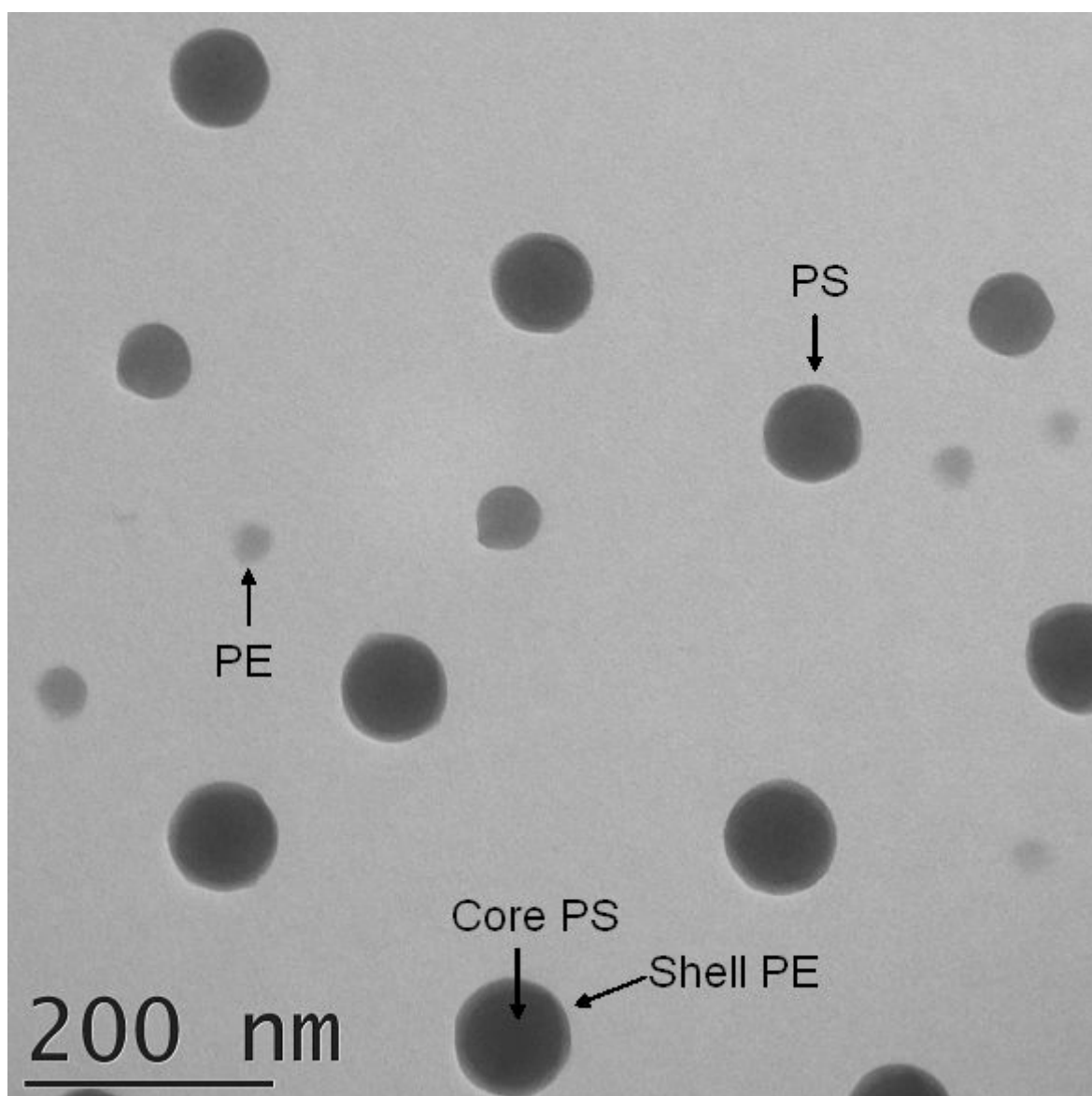


Figure 35. TEM picture of core-shell PS/PE using AIBA as initiator

Yield shows that 0.6 g of PE were synthesized and DLS shows an increase of average diameter to 108 nm (native PS latex 101 nm) with a polydispersity index of 0.07 (0.03 for the native PS).

By TEM analysis (see Figure 35) new smaller PE particles were observed. Moreover, some larger particles with a PS core and a thin shell of PE can be identified.

In order to reduce the formation of new particles a new route of synthesis has been chosen. We add to the native PS latex 2 mL of styrene in which 50 mg of AIBN is dissolved in order to swell the native PS particles. Then the polymerization is performed at 150 bar of ethylene pressure at 70°C during 4 hours.

Solid content indicates that 1.6 g of PE has been synthesized and particles diameters increase to 113 nm with a polydispersity index of 0.06. TEM show less PE particles and the PE shell appears thicker (see Figure 36).

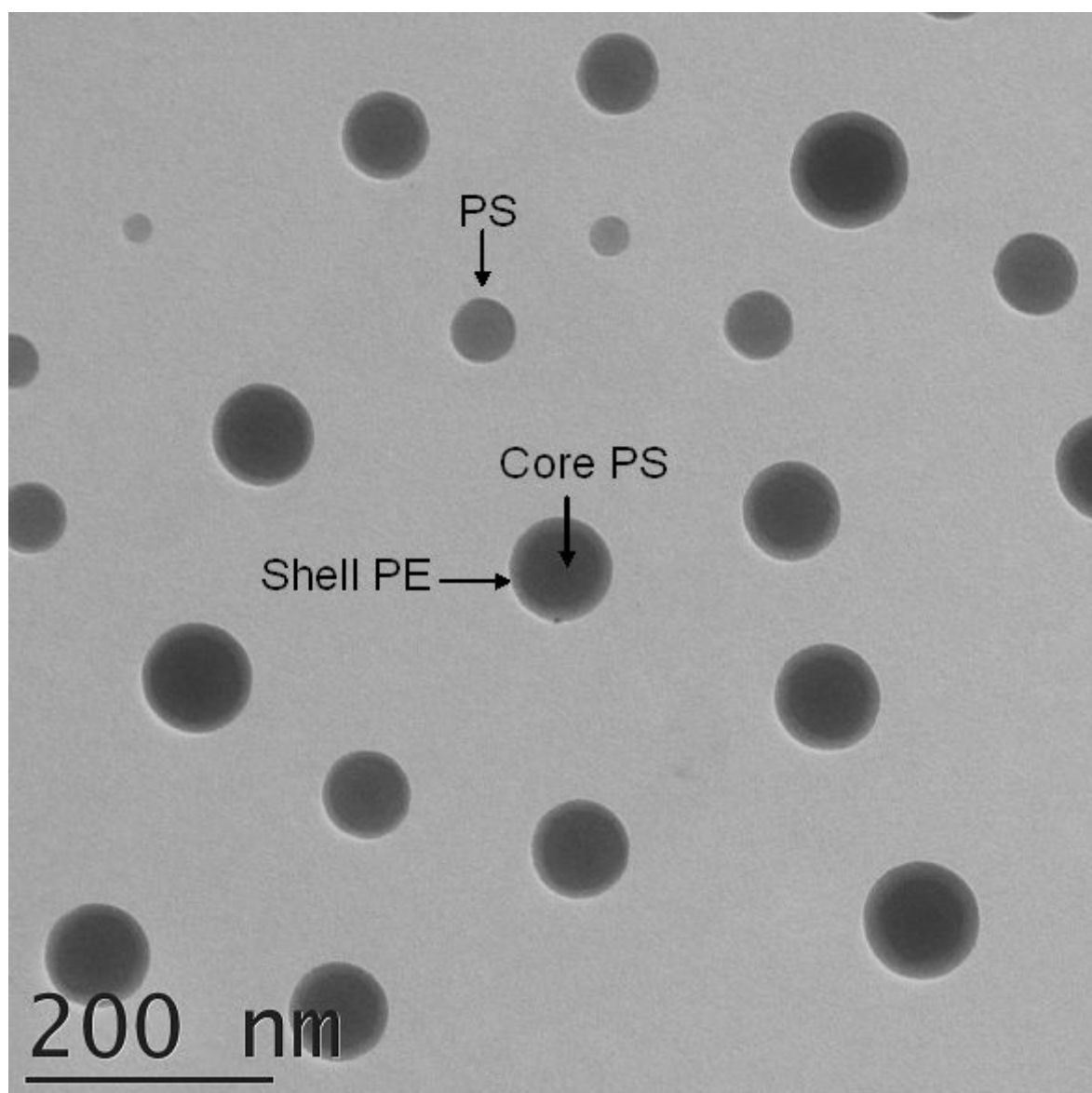


Figure 36. TEM picture of core-shell PS/PE using AIBN as initiator

These examples show some promising preliminary results but further studies needs to be done in order to obtain fully characterized core-shell nanoparticles with a PE core or shell.

2. Hybrid organic/inorganic

In this section we try to perform a radical ethylene polymerization with a stable dispersion of inorganic compounds in order to obtain stable hybrid latex. In all cases the polymerizations are performed under 150 bar of ethylene pressure at 70°C during 4 hours with 80 mg of AIBA.

a) Silica hybrid particles

We perform the polymerization with two kinds of silica, the Klebosol 50R50 ($D_p \approx 65$ nm, and narrow distribution in alkaline solution) and Klebosol 30R12 ($D_p \approx 25$ nm, and broad distribution in alkaline solution) at 0.5% of inorganic solid content.

We obtain with 50R50 a stable latex at 3.3% of solid content with particles diameters of 139 nm ($PI=0.01$). Theoretical inorganic content (18%) is in agreement with the experimental determination by ATG (17%). Moreover one population only is observed by TEM (see Figure 37).

All these results indicate that core-shell particles should be present with a silica core and a PE shell. However the silica core cannot be identified on TEM pictures.

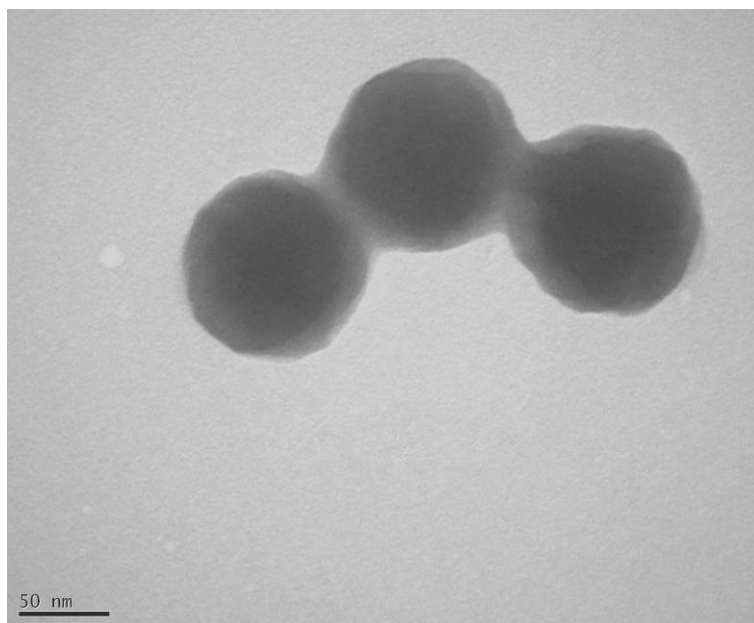


Figure 37. Standard particles observed by TEM after the polymerization of ethylene in presence of 50R50

For 30R12 a stable latex of 1.8% of solid content with particles diameters of 148 nm ($PI=0.03$) is obtained. Theoretical inorganic content (27%) is well correlated with the experimental determination by ATG (22%). As for 50R50 only one population is observed by TEM.

It should be noted that in both cases the inorganic content experimentally determined is lower than the theoretical one. Since the solid content is determined after filtration of the latex, it is possible that some silica aggregates during the polymerization.

These results are promising but no direct evidence of the silica core is obtained and consequently additional experiments have to be performed.

b) Clay hybrid particles

We perform the polymerization with a water dispersion of laponite, an artificial clay, at a solid content of 0.2%. We obtain a latex of 1.4% of solid content with particles diameters of 149 nm ($PI=0.05$). No free laponite particles were observed by TEM (see Figure 38). Inorganic content (12%) determined by ATG is in good agreement with the theoretical value (14%).

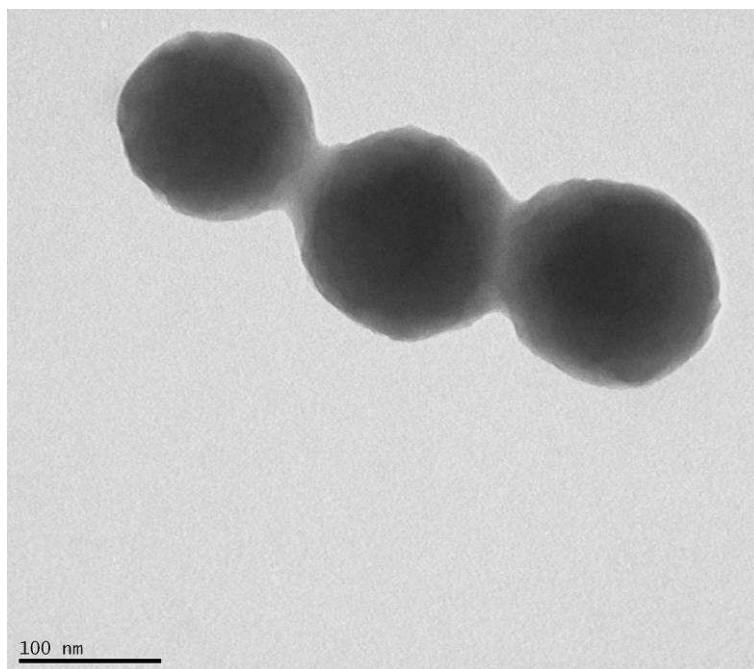


Figure 38. Standard particles observed by TEM after the polymerization of ethylene in presence of clay

Once again, ATG indicates that some clay is present in the latex or at the surface of particles but no clay is evidenced by TEM. In consequence clay must be present inside the particles and further investigations needs to be done in order to characterize these particles.

E. Conclusion

In this chapter, we reported that polyethylene can be easily synthesized by a free radical polymerization with a water soluble radical initiator which provides stable latexes. Latexes obtained with solid content up to 40 % and a good control of the particles diameters (20-200 nm) are formed.

Moreover the polymer exhibits higher molecular weights compared to the polymerization performed in organic media, with molecular weights far above the entanglement weight and PDI between 5 and 8. Consequently, these PE could possess some interesting physical properties. Moreover, melting points fall in the range of 95°C to 105°C corresponding to an important branches content PE.

Two different morphologies of PE particles are identified: sphere-like particles if the PE is synthesized with a CTAB concentration below 0.5 g/L, and cylinder-like particles if polymerization is performed with CTAB concentration over 0.5 g/L. Moreover these cylinder particles possess bigger crystallites than sphere-like particles. The crystallite dimension plays a crucial role in the PE particles morphology since for sphere-like particles their dimension corresponds to the facets dimension and for cylinder-like to the diameters of the particle itself.

Some important clues in the mechanism of the cylinder-like particles formation have been reported. Indeed temperature and high CTAB concentration seem to play an important role. Moreover, stirring rate leads also to a dramatic effect on the polymerization which indicated that some physical forces such as collision should impact the cylinder-like particles formation.

The properties of these latexes such as coating properties remain to be investigated but their low crystallinity should lead to an easy film formation.

Polymerization in aqueous solution using standard emulsion radical initiator (persulfate) and standard surfactant (SDS) are also performed. In this case the polymerization takes place only if the aqueous solution is basic or acid. In basic solution, an aqueous dispersion of PE particles is obtained. However, these experimental conditions are less efficient than the polymerization initiated by AIBA with CTAB as surfactant. Moreover, SDS appears to have an unexpected behavior since flocculation is observed when too high concentrations of SDS are used.

Finally, this emulsion process could be used to generate hybrid particles (organic/organic and organic/inorganic). However up to now no clear-cut proof of the nature of the particles formed is available.

As we will report in the following chapter, polymerization of ethylene in emulsion can be transposed to the copolymerization of ethylene with polar vinyl monomers in emulsion. This copolymerization will be compared to the direct copolymerization in solution.

References:

- [1] A. F. Helin, H. K. Stryker, and G. J. Mantell *J. App. Polym. Sci.*, vol. 9, pp. 1797–1805, 1965.
- [2] H. Hopff and R. Kern *Modern Plastics*, pp. 153–220, 1946.
- [3] G. J. Mantell, H. K. Stryker, A. F. Helin, D. R. Jamieson, and C. H. Wright *J. App. Polym. Sci.*, vol. 10, pp. 1845–1862, 1966.
- [4] H. K. Stryker, A. F. Helin, and G. J. Mantell *J. App. Polym. Sci.*, vol. 9, pp. 1807–1822, 1965.
- [5] H. K. Stryker, A. F. Helin, and G. J. Mantell *J. App. Polym. Sci.*, vol. 10, pp. 81–96, 1966.
- [6] H. K. Stryker, G. J. Mantell, and A. F. Helin *Vinyl Polym.*, vol. 1, pp. 175–186, 1969.
- [7] H. K. Stryker, G. J. Mantell, and A. F. Helin *J. Polym. Sci., Polym. Symp.*, vol. 27, pp. 35–48, 1969.
- [8] H. K. Stryker, G. L. Mantell, and A. F. Helin *J. App. Polym. Sci.*, vol. 11, pp. 1–22, 1967.
- [9] T. Suwa, H. Nakajima, M. Takehisa, and S. Machi *J. Polym. Sci., Polym. Let. Ed.*, vol. 13, pp. 396–375, 1975.
- [10] A. Held, F. Bauers, and S. Mecking *Chem. Comm.*, p. 301, 2000.
- [11] S. Mecking *Coll. Polym. Sci.*, vol. 285, p. 605, 2007.
- [12] R. Soula, C. Novat, A. Tomov, R. Spitz, J. Claverie, X. Drujon, J. Malinge, and T. Saudemont *Macromolecules*, vol. 34, p. 2022, 2001.
- [13] W. D. Harkins *J. Chem. Phys.*, vol. 13, p. 381, 1945.
- [14] W. D. Harkins *J. Chem. Phys.*, vol. 14, p. 47, 1946.
- [15] W. D. Harkins *J. Am. Chem. Soc.*, vol. 69, p. 1428, 1947.
- [16] W. V. Smith and R. H. Ewart *J. Chem. Phys.*, vol. 16, p. 592, 1948.
- [17] R. G. Anthony and J. J. McKetta *J. Chem. Eng. Data*, vol. 12, p. 17, 1967.
- [18] E. Grau, P.-Y. Dugas, J.-P. Broyer, C. Boisson, R. Spitz, and V. Monteil *Angew. Chem. Int. Ed.*, vol. 49, p. 6810, 2010.
- [19] W. E. Hanford *US 2405950*, 1946.
- [20] R. E. Brooks, M. D. Peterson, and A. G. Weber *US 2388225*, 1946.
- [21] M. D. Peterson *US 2388178*, 1946.

Chapter IV : Free radical copolymerization of ethylene with polar vinyl monomer

A. Parameters to consider for the ethylene copolymerization	IV-235
B. Ethylene-MMA copolymerization	IV-236
1. Influence of the ethylene pressure.....	IV-236
a) Preliminary remarks.....	IV-237
b) Study of the ethylene-MMA copolymerization in toluene.....	IV-238
c) Chemical composition distribution of copolymers.....	IV-240
2. Influence of the solvent.....	IV-242
3. Influence of MMA initial concentration	IV-246
a) Preliminary remarks.....	IV-247
b) Interpretation of the results	IV-248
c) Conclusion	IV-252
4. Conclusion	IV-253
C. Investigation of the copolymerization with various polar monomers.....	IV-254
1. Copolymerization with styrene	IV-254
a) Influence of the solvent.....	IV-254
b) Influence of styrene initial concentration.....	IV-258
2. Copolymerization with butyl acrylate	IV-260
a) Influence of the solvent.....	IV-260
b) Influence of BuA initial concentration.....	IV-265
3. Copolymerization with vinyl acetate	IV-267
a) Influence of the solvent.....	IV-267
b) Influence of VAc initial concentration.....	IV-269
4. Conclusion	IV-271
D. Copolymerization in emulsion	IV-272
1. Copolymerization with styrene	IV-272
2. Copolymerization with MMA.....	IV-275
3. Copolymerization with BuA	IV-277
4. Copolymerization with VAc	IV-278
5. Conclusion	IV-279
E. Conclusion.....	IV-280

In the previous chapters, the efficiency of the free radical polymerization of ethylene was demonstrated under mild experimental conditions ($T < 100^{\circ}\text{C}$ and $P < 250$ bar). Indeed polyethylene can be synthesized in a wide range of organic solvents at pressure as low as 5 bar and temperature as low as 10°C via a radical mechanism. PE can also be synthesized in water using a water-soluble radical initiator. In this case stable PE latexes are obtained with solid content up to 40%. In this last case PE synthesized possess high molecular weight ($M_n > 10^6 \text{ g mol}^{-1}$).

These results have a crucial importance in the understanding of the hybrid radical/catalytic mechanism (that will be developed in the final chapter). During the “shuttling” between the radical mechanism and the catalytic mechanism, the influence of ethylene on the radical polymerization cannot be neglected anymore (see Figure 1). Therefore, the polar block synthesized by free radical polymerization could insert a certain amount of ethylene. Consequently, the multiblock copolymer synthesized by this mechanism should be composed of a polyethylene block synthesized by catalytic polymerization and another block rich in polar vinyl monomer (polar block) synthesized by radical polymerization.

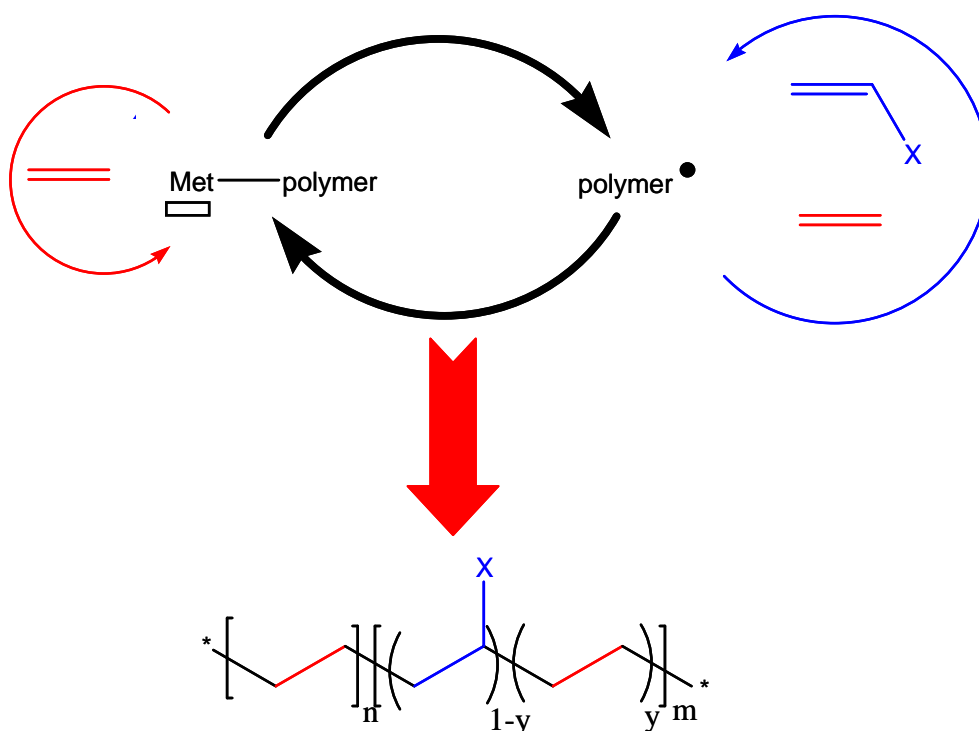


Figure 1. Hybrid mechanism of copolymerization

Therefore the fine study of the free radical copolymerization of ethylene needs to be done in order to estimate the composition of the polar block synthesized by hybrid copolymerization.

Free radical copolymerization of ethylene has been well investigated using experimental conditions close to the industrial conditions ones ($P > 2000$ bar and $T > 200^{\circ}\text{C}$) [1]. Indeed these kinds of copolymers are industrially produced in these conditions with polar vinyl monomer content below 20% in weight in order to keep some crystallinity in polymers. Low content of ethylene in poly(vinyl acetate) is also industrially produced (VAE) in emulsion under lower pressure and temperature. Recently some tryouts are reported for the ethylene polar vinyl monomer copolymerization at lower pressure and temperature ($P < 50$ bar and $T < 100^{\circ}\text{C}$) [2] even using CRP techniques [3-6]. Copolymers produced exhibit low olefin content and usually only isolated ethylene units are present in the polymer chain. However, to the best of our knowledge no study has been reported in experimental conditions close to ours.

In this chapter, we will investigate the radical copolymerization of ethylene with polar vinyl monomer under ethylene pressure up to 250 bar at 70°C . First the ethylene-methyl methacrylate (MMA) system will be studied in toluene, THF and DEC. The influence of solvent properties such as $\left(\frac{\mu}{\epsilon}\right)^2$ and comonomer concentration on the copolymerization (reactivity ratios) will be highlighted.

Then we will transpose this study to other monomers: styrene (Sty), butyl acrylate (BuA) and vinyl acetate (VAc). Copolymerization in emulsion will be also studied. Finally, the influence of additional Lewis acid will be investigated.

A. Parameters to consider for the ethylene copolymerization

In this chapter, the determination of the reactivity ratio is crucial in order to rationalize copolymerization of ethylene (E) with a polar monomer (Pol). For this purpose Kelen Tüdös linearization method [7-9] is used to determine $r_E = \frac{k_{EE}}{k_{EPol}}$ and $r_{Pol} = \frac{k_{PolPol}}{k_{PolE}}$. Note that, we will called in the following ethylene radical the final ethyl radical of the polymer growing chain (and also respectively MMA radical, BuA radical, etc).

During copolymerization of ethylene with polar vinyl olefins, several parameters need be taken into account.

1. Since ethylene homopolymerization is dependent of $\left(\frac{\mu}{\varepsilon}\right)^2$ of the polymerization media, k_{EE} must be also dependent on this parameter. Therefore k_{EPol} and k_{PolE} should also be impacted by the $\left(\frac{\mu}{\varepsilon}\right)^2$.
2. Moreover, since polar vinyl monomer possesses their own μ and ε , concentration of the comonomer will impact the initial μ and ε of the polymerization media thus kinetic rates of the copolymerization and reactivity ratios.
3. The polar monomer concentration will decrease since during the copolymerization this monomer is incorporated to the polymer chain. Therefore, $\left(\frac{\mu}{\varepsilon}\right)^2$ of the polymerization media will vary with the conversion of the polar vinyl monomer.
4. Finally, ratio itself of polar monomer over solvent will impact the copolymerization. Indeed, comonomer can originate from the solvation shell of the growing radical or from another one. The first process will be more probable at high initial concentration polar vinyl monomer.

All these parameters have to be taken into account in order to give an interpretation of the variation of the copolymerization reactivity ratios. From a thermodynamic point of view, $\left(\frac{\mu}{\epsilon}\right)^2$ effect corresponds to an enthalpy effect of the relative stabilization by Van der Waals interactions of the radicals and monomers with solvent and the influence of the comonomer initial concentration correspond to an entropic effect in which the frequency of efficient shocks vary with the solvation shell composition.

Consequently, for each copolymerization we will perform the copolymerization study at constant polar vinyl monomer over solvent ratio in different organic solvents in order to investigate the effect of the initial $\left(\frac{\mu}{\epsilon}\right)^2$ of the polymerization medium. Then series of experiments will be performed at different polar vinyl monomer over solvent ratio in toluene in order to investigate the influence of the comonomer concentration.

B. Ethylene-MMA copolymerization

In this section, the copolymerization of ethylene with MMA will be investigated and detailed before applying this study to other comonomers in the next part. As already demonstrated ethylene free radical polymerization is strongly dependent of the properties of the solvent (μ , ϵ). It will be the same for the copolymerization of ethylene; i.e. k_{MMAE} and k_{EMMA} should be dependent of the solvent. Moreover MMA/solvent ratio will also impact the reactivity ratios of the copolymerization.

Consequently, as MMA influences the initial μ and ϵ of the solvent polymerization medium, copolymerization will be studied at constant MMA/solvent ratio.

1. Influence of the ethylene pressure

The copolymerization of ethylene with MMA is performed at different ethylene pressures at 70°C during 4 hours initiated by 305 μmol of AIBN in toluene with 20% v/v of MMA. Results are summarized in the following table.

Table 1. Ethylene/MMA copolymerization in toluene^a

Ethylene pressure (bar)	Yield (g)	MMA content (mol %) ^b	Glass transition (°C) ^c	Mn (g/mol) ^d [PDI ^d]
0	5	100	105	nd
25	4.8	95	109.1	34100 [1.7]
50	3.3	90	102.1	26500 [1.8]
100	1.4	78	77.4	10300 [1.4]
150	1	74	75.4	10000 [1.5]
200	0.9	73	74.9	14700 [1.6]
250	1.5	68	67.7	12400 [1.7]

^a: Polymerizations are performed during 4 hours with 50 mg of AIBN at 70°C in 40 mL of toluene with 10 mL of MMA. ^b: determined by ¹H NMR. ^c: determined by DSC. ^d: determined by HT-SEC

a) Preliminary remarks

Before considering the copolymerization, we verify that the homopolymerization of MMA is not disturbed by pressure itself and solvent. In this purpose, homopolymerizations are performed under various argon pressures up to 200 bar. No effect of the argon pressure is identified. Contrary to the homopolymerization of ethylene, no solvent activation effect is highlighted with MMA (same yield in toluene, THF and DEC using the same initial concentration of MMA). Consequently, MMA homopolymerization is independent of the pressure and the solvent used.

Another point to take into consideration is the solubility of ethylene in MMA. As already mentioned in the second chapter, no difference in solubility has been identified between vinyl monomers such as MMA, styrene, BuA, VAc and organic solvents: DEC, toluene, THF.

Moreover the phase transition between a monophasic and a biphasic medium is also not drastically changed. With all these polar monomers, whatever their initial concentrations, below 100 bar the system is biphasic and over 150 bar of ethylene pressure monophasic at 70°C.

Consequently, the ethylene content is known for each polymerization conditions and therefore reactivity ratios can be calculated.

b) Study of the ethylene-MMA copolymerization in toluene

The copolymerization of ethylene with MMA is performed at different ethylene pressures from 25 bar to 250 bar (see Table 1). First, yield decreases with the pressure below 100 bar. Then yield reaches a plateau from 100 to 200 bar and increases over 200 bar. The decrease of activity below 100 bar can be related to the ethylene insertion, since ethylene is usually described as a poorly reactive monomer (compared to MMA). Moreover since the solubility of ethylene in the polymerization medium increases the MMA is diluted by ethylene and consequently the reaction slows down.

The average ethylene content of the copolymer is calculated thanks to ^1H NMR. The ethylene insertion increases as expected with the ethylene pressure up to 35%. Below 200 bar, decrease of yield vs. ethylene insertion is almost linear, therefore the decrease in yield is due to the insertion of ethylene which slows down the copolymerization. Finally, over 250 bar a slight increase of yield is observed while the ethylene insertion increases.

Average molecular weights of copolymers first decrease with pressure below 100 bar then increase over 150 bar. The initial decrease can be explained by a higher transfer capacity of ethylene radical compared to MMA radical. In all experiments, MWD is narrow which may indicate that only one family of copolymer is synthesized.

Since we are able to determine the number of phases of the medium of polymerization (biphasic up to 100 bar and monophasic over 150 bar) and their composition, the reactivity ratio of the copolymerization can be calculated by Kelen Tüdös method: $r_{\text{MMA}}=28.1$ and $r_{\text{E}}=0.07$ using a terminal model.

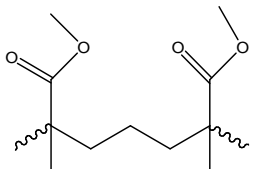
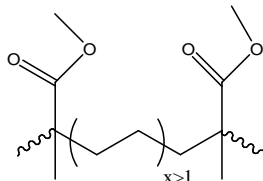
We can calculate the reactivity ratios because the ratio MMA/toluene is constant so the initial permittivity and dipole moment of the polymerization medium are almost unchanged in all these experiments. Therefore no variation of the kinetic rate via a solvent activating effect should take place.

However, the solvent properties change with MMA content and so with the conversion of MMA but the variation of $\left(\frac{\mu}{\varepsilon}\right)^2$ remains low, for instance below 5% with MMA conversion up to 15% (this will be developed in the following section, see Figure 5). For the experiments over 100 bar of ethylene pressure, the MMA conversion remains between 7% and 12% whatever the ethylene pressure corresponding to a variation of $\left(\frac{\mu}{\varepsilon}\right)^2$ below 5% during the polymerization compared to the initial value. Moreover, differences between all the final values of $\left(\frac{\mu}{\varepsilon}\right)^2$ remain below 2% between all experiments performed at different ethylene pressures over 100 bar. At 25 bar and 50 bar the MMA conversions are respectively 48% and 31% corresponding to higher variation of $\left(\frac{\mu}{\varepsilon}\right)^2$, 16% and 11% respectively.

Consequently, k_{EE} , k_{MMAE} , k_{EMMA} , k_{MMAMMA} are assumed constant in this series of experiments and during the copolymerization except for the two experiments at ethylene pressure below 50 bar.

The reactivity ratios of ethylene/MMA copolymerization ($r_{MMA}=28.1$ and $r_E=0.07$) induce a copolymer with a high probability of isolated ethylene units. Indeed, the average length of ethylene sequence $x_E = 1 + r_E \frac{[E]}{[MMA]}$ remains close to 1. This has been confirmed by ^{13}C NMR (see Table 2). Under 100 bar of ethylene pressure no consecutive ethylene units have been identified.

Table 2. Ethylene microstructures of the copolymer from ^{13}C NMR^a

Pressure (bar)	25	50	100	150	200	250
Ethylene content (% mol)	5%	10%	22%	26%	27%	32%
	100%	100%	82%	59%	59%	52%
	0%	0%	18%	41%	41%	48%
x_E	1	1	1.18	1.62	1.6	2.1

^a: determined by ^{13}C NMR for isolated ethylene by peak at 43.8 and 19 ppm and for longer sequence peak at 41, 24 and 32.4 ppm.

Finally, glass transition temperatures of the copolymers decrease with the ethylene insertion as expected from 105°C to 68°C. No melting point has been identified therefore no homopolyethylene has been synthesized during the copolymerization. Moreover, the glass transition remains quite narrow. Consequently, the distribution in composition of the chain should be narrow. These results indicate that no homopolymers (PE or PMMA) have been synthesized.

c) Chemical composition distribution of copolymers

In order to go further these samples are analyzed at the DKI (Deutsches Kunststoff-Institut, Darmstadt, Germany) using high temperature liquid chromatography in critical conditions of MMA (LC-CC PMMA exhibit same elution volume whatever their molecular weights). This technique uses an elution method designed to separate the polymers according to their chemical composition. Examples of chromatograms are shown in the following figure.

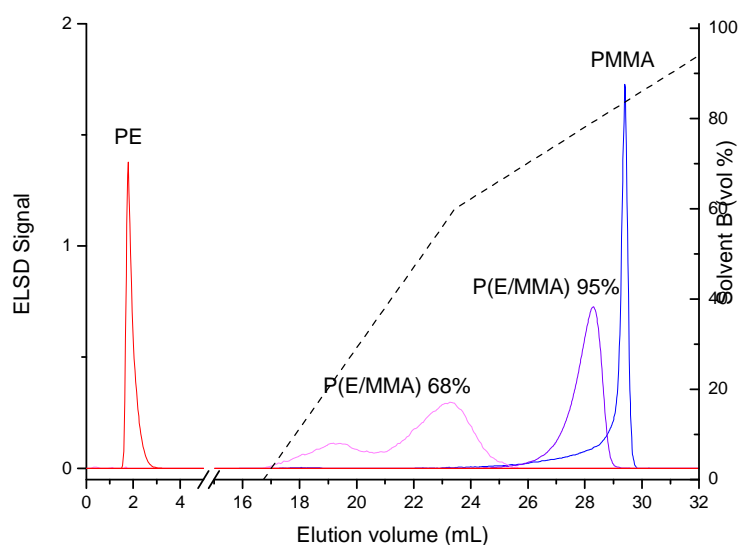


Figure 2. Overlay of chromatograms of P(E/MMA) samples. Stationary phase: Perfectsil 300. Mobile phase: TCB and gradient TCB → TCB/cyclohexanone (20/80 v/v). Temperature: 140°C. Gradient of solvent is indicated by a dotted line

Elution times increase with the MMA content of the copolymer from 2 mL for PE to 29.5 mL for PMMA. Except when synthesized at 250 bar of ethylene pressure, copolymers exhibit only one peak between the PE and PMMA peak. Moreover, no trace of homopolymers is identified in the copolymer analyzed.

Consequently, the elution time can be correlated to the MMA content determined by ^1H NMR (see Figure 3). Therefore, the two distributions of the copolymer synthesized under 250 bar of ethylene pressure can be related to two average compositions of respectively 54% and 72% of MMA content. Average composition of MMA for this copolymer determined by NMR is 68% consequently the highest ethylene content distribution represents 25% of the copolymer which is in good agreement with the chromatogram.

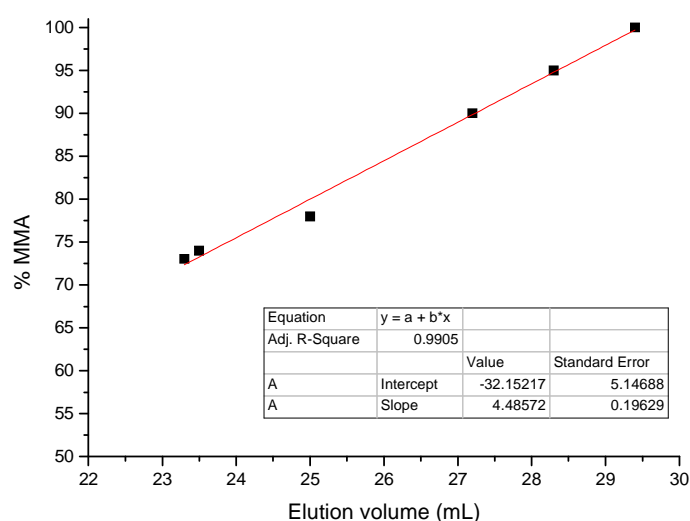


Figure 3. Correlation between elution time determined by LC-CC and MMA insertion determined by ^1H NMR.

It is noteworthy to mention that the bimodal distribution obtained for free radical copolymerization of ethylene with MMA under 250 bar of pressure is quite unexpected. It indicates that the polymerization is poorly controlled and probably two different media of polymerization exist.

Indeed, at 250 bar the toluene/MMA/ethylene mixture is supercritical monophasic. However, the synthesized copolymer should “precipitate” and form therefore a second medium of polymerization since this copolymer can be swollen by MMA and toluene and therefore produces a second family of copolymer. It should be noted that it is not the case during ethylene homopolymerization because PE is not swollen by solvent and therefore does not create a second medium of polymerization.

2. Influence of the solvent

The same set of experiments is performed in THF and DEC in order to characterize a solvent activation effect on the ethylene copolymerization with MMA. Indeed initial $\left(\frac{\mu}{\epsilon}\right)^2$ will be different in each solvent and consequently lead to different reactivity ratios. Results are summarized in the following figure.

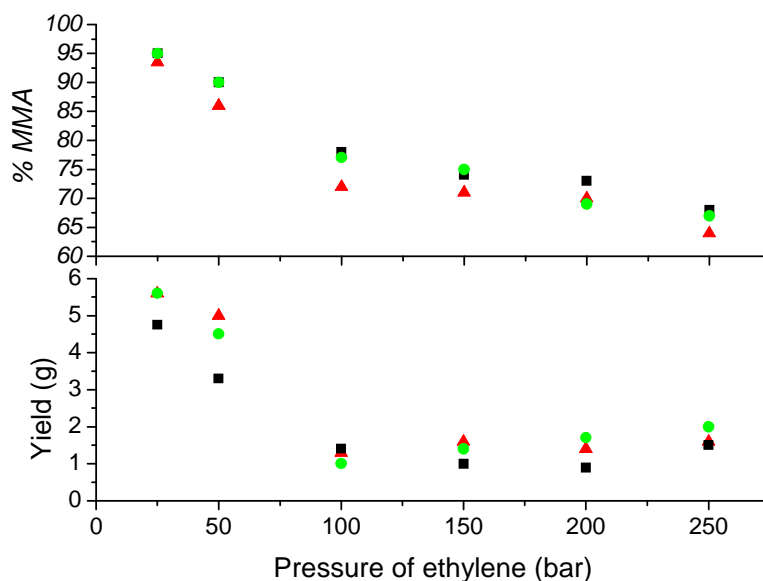


Figure 4. Influence of ethylene pressure on yield and MMA insertion^a during radical copolymerization of ethylene with MMA in different solvents: 50 mg of AIBN during 4 hours at 70°C with 10 mL of MMA in 40 mL of toluene, ▲ of THF, ● of DEC.
^a: determined by ¹H NMR

Yield and MMA insertion follow similar curves in all solvents. Yield decreases with ethylene pressure until reaching a plateau at 100 bar then slightly increases. MMA insertion decreases with ethylene pressure. Contrary to the homopolymerization of ethylene, no important differences in yield are observed between THF, toluene and DEC, indeed the copolymers are mostly composed of MMA which does not exhibit solvent activation effect.

In THF, homopolymerization of ethylene is more efficient than in the two other solvents and as expected, the insertion of ethylene is higher than in toluene.

Reactivity ratios in THF are calculated $r_{\text{MMA}}=20.6$ and $r_{\text{E}}=0.20$. Once again, the solvent properties change with the MMA conversion but the variation in this case is very low (only 1% with up to 20% of MMA conversion see Figure 5).

In DEC, homopolymerization of ethylene is slightly more efficient than in toluene, consequently the ethylene insertions are almost similar. Reactivity ratio in DEC are calculated $r_{\text{MMA}}=28.4$ and $r_{\text{E}}=0.14$. Once again, the solvent properties change with the MMA conversion but in this case $\left(\frac{\mu}{\epsilon}\right)^2$ increases significantly with MMA conversion (consequently, it will favor ethylene propagation – see Figure 5). For example, $\left(\frac{\mu}{\epsilon}\right)^2$ increases of 5% with 20% of MMA conversion (see Figure 5).

Compared to toluene r_{MMA} is smaller by a factor 1.4 in THF and almost identical in DEC. The homopolymerization of MMA follows the same kinetics in all these solvents so k_{MMAMMA} should be constant. Consequently, k_{MMAE} should be higher by a factor 1.4 in THF than in toluene and DEC (see Table 3).

This means that the addition of a radical MMA on ethylene monomer is more efficient in THF than in toluene. As MMA is not known to exhibit a solvent activation effect, we can assume that this effect is only due to the ethylene itself. Consequently, the interaction between solvent and ethylene favors the addition of radical MMA by a factor 1.4 in THF compared to toluene. This effect is due to the interaction of the solvent with the ethylene reactant and/or the alkyl radical resulting from ethylene addition.

The same methodology can be applied to r_{E} , which is higher in THF (2.8) and DEC (2.0) than in toluene. As shown in chapter II, homopolymerization of ethylene is solvent dependent. Previously we demonstrated that a relation exists between the kinetic of reaction and the solvent parameter $\left(\frac{\mu}{\epsilon}\right)^2$ (see subsection C of chapter II). We assume that this solvent activation effect is only due to the propagation rate of ethylene in the different solvent (or that the effect of solvent is similar for propagation and termination), consequently k_{EE} can be compared for each copolymerization. For example, in toluene $\left(\frac{\mu}{\epsilon}\right)^2 = 0.17 \cdot 10^{-60} \text{ C}^2.\text{m}^2$, $\mu = 1 \cdot 10^{-30} \text{ C.m}$ and $\epsilon = 2.4$) k_{EE} is about 6 time smaller than in THF $\left(\frac{\mu}{\epsilon}\right)^2 = 0.59 \cdot 10^{-60} \text{ C}^2.\text{m}^2$, $\mu = 5.8 \cdot 10^{-30} \text{ C.m}$ and $\epsilon = 7.6$).

This relation is also valid for solvents mixtures, therefore $\left(\frac{\mu}{\epsilon}\right)^2$ can be calculated for any MMA mixture with solvent: MMA/toluene 1/4 v/v $\left(\frac{\mu}{\epsilon}\right)^2 = 0.25 \cdot 10^{-60} \text{ C}^2.\text{m}^2$, MMA/THF 1/4 v/v $\left(\frac{\mu}{\epsilon}\right)^2 = 0.61 \cdot 10^{-60} \text{ C}^2.\text{m}^2$ and MMA/DEC 1/4 v/v $\left(\frac{\mu}{\epsilon}\right)^2 = 1.36 \cdot 10^{-60} \text{ C}^2.\text{m}^2$ using the standard mixing rule for relative permittivity $\epsilon_{\text{Mixture}} = \sum_{i=1}^N x_i \epsilon_i$, with x_i the volume fraction of solvent i and ϵ_i the solvent i relative

permittivity and for dipole $\mu_{Mixture} = \sum_{i=1}^N \sum_{j=1}^N x_i x_j \sqrt{\mu_i \mu_j}$, with μ_i the dipole moment of the solvent i , with for MMA $\mu = 5.6 \cdot 10^{-30}$ C.m and $\epsilon = 6.5$.

Thanks to the relation between $\left(\frac{\mu}{\epsilon}\right)^2$ and k_{EE} (see chapter II-C), we can estimate that k_{EE} in MMA/THF will be about 5 time higher than in MMA/toluene, and k_{EE} in MMA/DEC 2.4 times higher than in MMA/toluene (see Table 3).

It is noteworthy to mention that k_{EE} during the copolymerization can be different to the one of the equivalent homopolymerization with same $\left(\frac{\mu}{\epsilon}\right)^2$, however we assume that their relative value are similar.

Therefore based on the determination of r_E in each solvent, we can estimate that k_{EMMA} is respectively 1.8 times higher in THF and 1.2 smaller in DEC than in toluene (see Table 3).

Consequently, the addition of a non-substituted alkyl radical on MMA monomer is more efficient in THF than in toluene and DEC. Again we assume that this effect is only due to the alkyl radical itself since no solvent activation effect has been identified during the homopolymerization of MMA. For k_{EE} , contributions on both ethylene monomer and alkyl radical exist.

These sets of experiments show that even during the copolymerization solvent exhibit a crucial influence on the kinetic rate of propagation: k_{EE} , k_{MMAE} and k_{EMMA} are dependent of the $\left(\frac{\mu}{\epsilon}\right)^2$ of the polymerization medium. These results are summarized in the following table.

Table 3. Reactivity ratios and relative kinetic rates of the ethylene-MMA copolymerization

Solvent	$\left(\frac{\mu}{\varepsilon}\right)^2$ ($10^{-60} \text{ C}^2\text{m}^2$)	r_{MMA}	relative k_{MMAMMA}	relative k_{MMAE}	r_{E}	relative k_{EE}	relative k_{EMMA}
Toluene	0.25	28.1	1	1	0.07	1	1
THF	0.61	20.6	1	1.4	0.20	5	1.8
DEC	1.36	28.4	1	1	0.14	2.4	0.8

In THF, the three kinetics rates (k_{EE} , k_{EMMA} and k_{MMAE}) appear to be maximal. Other solvent need be investigated in order to determine if a Λ -shaped curve is obtained (see k_{tot} during the ethylene homopolymérisation in chapter II).

3. Influence of MMA initial concentration

The previous work evidences that ethylene monomer and ethylene radical are more reactive in THF than in toluene and DEC while MMA monomer and MMA radical exhibit the same reactivity in all three solvents.

Moreover, it is important to highlight the ambivalence of the comonomer in the ethylene copolymerization. Indeed, MMA is a monomer and also a solvent which modifies the $\left(\frac{\mu}{\varepsilon}\right)^2$ of the mixture. Consequently, the copolymerization of ethylene/MMA in toluene with different amounts of MMA would not lead to the same reactivity ratios (see Table 4). Moreover these experiments will also be impacted by the change of MMA/toluene ratio.

This behavior is shown by experiments performed for various MMA initial concentrations in toluene at ethylene pressures between 50 bar and 250 bar during 1 hour at 70°C with 50 mg of AIBN.

Table 4. Reactivity ratios of ethylene MMA copolymerization vs. initial MMA content^a

MMA volume (% vv)	10	20	40	60	80	100
r_{MMA}	5.52	8.85	17.0	21.6	37.0	51.6
r_{E}	0.06	0.08	0.12	0.41	0.54	1.07

^a: Polymerizations are performed between 50 bar and 250 bar of ethylene pressure during 1 hour at 70°C with 50 mg of AIBN in 50 mL of toluene/MMA mixture.

Both reactivity ratios increase with the concentration of MMA from 5.5 to 52 for r_{MMA} and from 0.06 to 1.07 for r_{E} . It should be noted that since polymerizations are performed at a given initial concentration of MMA in toluene in order to work at constant $\left(\frac{\mu}{\varepsilon}\right)^2$, the only way to change the ratio MMA/Ethylene in the feed is to play on the ethylene pressure.

a) Preliminary remarks

Surprisingly the reactivity ratio differs from the previous set of experiment at identical MMA concentration: $r_{\text{MMA}}=28.1$ and $r_{\text{E}}=0.07$ for an experiment performed during 4 hours at 20% v/v of MMA (see Table 3) and $r_{\text{MMA}}=8.85$ and $r_{\text{E}}=0.08$ for an experiment performed during 1 hour at 20% vv of MMA (see Table 4).

Only r_{MMA} decreases (28.1 vs. 8.85), r_{E} seems to be time independent (0.07 vs. 0.08). Is it an artefact? It cannot be explained by composition derivation of the monomer mixture (indeed a decrease of r_{MMA} is expected at high MMA conversion), but by the derivation of the solvent composition. Indeed, during the polymerization MMA is incorporated into the polymer chain. The overall solvent properties change consequently during the polymerization:

e.g. $\left(\frac{\mu}{\varepsilon}\right)^2$ decreases vs. the MMA insertion in toluene while it increases in DEC (see Figure

5). As a consequence, during the copolymerization, kinetic rates are dependent of $\left(\frac{\mu}{\varepsilon}\right)^2$, therefore they change leading to differences in reactivity ratios with the comonomer conversion. This impact will be more important with the increase of the MMA initial concentration (see Figure 5).

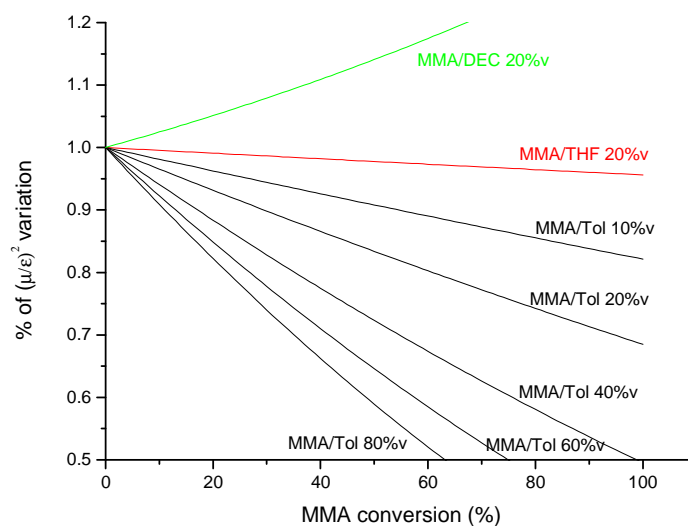


Figure 5. Variation of $\left(\frac{\mu}{\varepsilon}\right)^2$ with the MMA conversion

In order to apply copolymerization kinetic laws we have to neglect this variation. In this purpose we work in all series of experiments at extremely low MMA conversion.

b) Interpretation of the results

Both r_{MMA} and r_{E} increase with the MMA amount. For r_{MMA} this increase should only be due to a decrease of k_{MMAE} with the MMA amount as k_{MMAMMA} is expected to be constant (no solvent activation effect on MMA homopolymerization). A relation is observed between $\ln(1/r_{\text{MMA}})$ and $\left(\frac{\mu}{\varepsilon}\right)^2$ (see Figure 6a).

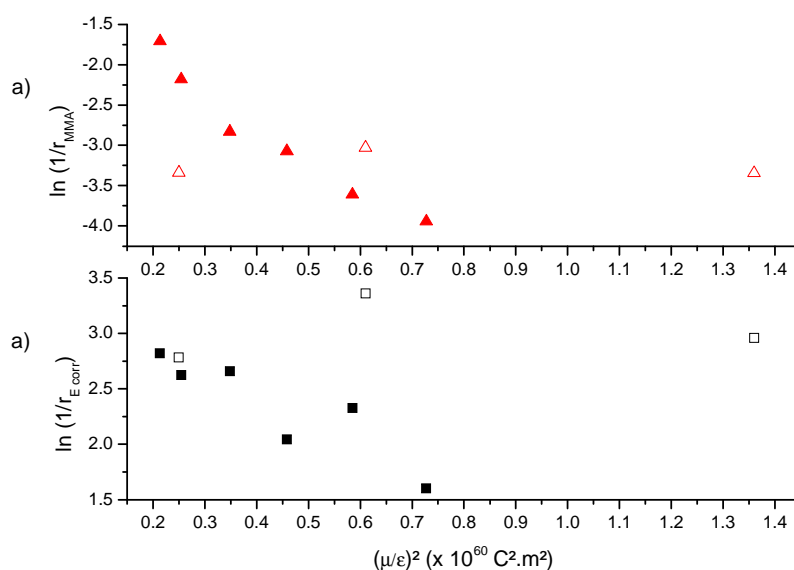


Figure 6. Influence of the initial $\left(\frac{\mu}{\varepsilon}\right)^2$ on the reactivity ratio: variation of ▲ r_{MMA} and ■ r_{E} with different contents of MMA (▲ and □ correspond to values measured with toluene, THF and DEC for 4 hours copolymerizations)

Indeed according to the activated states theory (equation 1, see section C-2 of chapter II), $\ln(k_{\text{MMAE}})$ is proportional to $\left(\frac{\mu}{\varepsilon}\right)^2$ which was observed (see Figure 6a).

$$\ln k \propto \left(\frac{\mu}{\varepsilon}\right)^2 \quad (1)$$

These results show that k_{MMAE} decreases with $\left(\frac{\mu}{\varepsilon}\right)^2$. Consequently, the stronger the interaction with the solvent is, the lower is k_{MMAE} . This is not in agreement with the previous study performed with different solvents in which the k_{MMAE} is almost constant with $\left(\frac{\mu}{\varepsilon}\right)^2$ (even if r_{MMA} value are different, dependence with $\left(\frac{\mu}{\varepsilon}\right)^2$ are expected to be similar). However, in this case the MMA over solvent ratio remains constant.

Indeed, MMA concentrations have a crucial importance since the solvation shell of the ethylene is partly made of MMA monomer which will more and more hide the ethylene to the growing radical (the radical will react with the MMA which solvates ethylene and not the ethylene itself- see Figure 7) when the MMA ratio over toluene increases. Consequently the frequency of efficient shocks should dramatically decrease with MMA concentration.

Contrary to $\left(\frac{\mu}{\epsilon}\right)^2$, it is not an enthalpic effect due to the relative interactions of radicals and monomers with the solvent but an entropic effect. In order to summarize we can consider that

$$k_{MMAE} = A \exp \frac{-E_a}{RT}, \quad A \text{ decrease with } [MMA] \text{ and } E_A \text{ depends of } \left(\frac{\mu}{\epsilon}\right)^2.$$

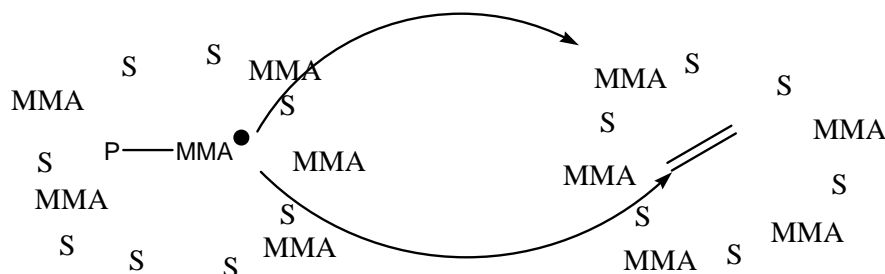


Figure 7. Effect of the MMA concentration on k_{MMAE} with S the solvent

Therefore k_{MMAE} decreases with MMA monomer initial content (see Figure 7).

Consequently, k_{MMAE} depends on the solvent $\left(\frac{\mu}{\epsilon}\right)^2$ and on the concentration of MMA.

Moreover this induces that k_{MMAMMA} will also depend of the MMA concentration. Indeed MMA macroradical is surrounded by a solvation shell more and more composed of MMA. Therefore, the addition of MMA is most probably coming from outside the solvation shell at low MMA concentration and from inside at high MMA concentration (see Figure 8). These mechanisms must have different kinetic rates ($k_{MMAMMA\text{inside}} > k_{MMAMMA\text{outside}}$). Consequently k_{MMAMMA} should increase with the MMA concentration.

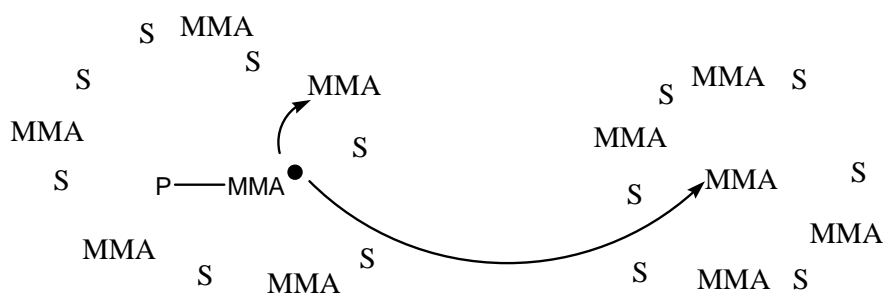


Figure 8. Effect of the MMA concentration on k_{MMAMMA} with S the solvent

For r_E , the same *modus operandi* can be applied except that a correction must be done to unlink k_{EE} variation (known for the homopolymerization experiments) and k_{EMMA} unknown variation. Again a linear relation seems to exist between $\ln(1/r_{E\text{ cor}})$ and $\left(\frac{\mu}{\epsilon}\right)^2$ (see Figure 6b).

Surprisingly k_{EMMA} seems to decrease with $\left(\frac{\mu}{\epsilon}\right)^2$. In the first series of experiments k_{EMMA} slightly increases with this solvent parameters in this range of $\left(\frac{\mu}{\epsilon}\right)^2$. Once again it may be a MMA concentration effect.

It can be explained by the same argumentation as for k_{MMAMMA} . Indeed as shown in Figure 9, k_{EMMA} is expected to increase with MMA concentration because at low MMA concentration the additional monomer comes from another solvation shell and at high concentration from the radical solvation shell.

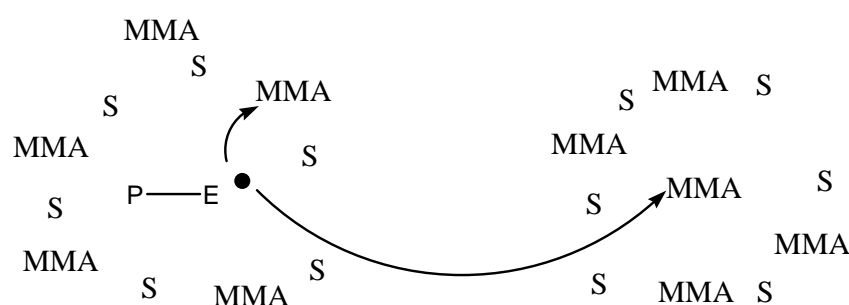


Figure 9. Effect of the MMA concentration on k_{EMMA} with S the solvent

Consequently, the observed decrease must be due to the fact that k_{EE} was wrongly estimated. Indeed we use for k_{EE} the variation of the homopolymerization of ethylene, while the concentration of MMA increases from one set of experiment to the other. In this case the comonomer is more and more present in the solvation shell, consequently the ethyl macroradical will more and more react with the MMA of the solvation shell. This leads to a decrease of k_{EE} . It is exactly the same argument that for k_{MMAE} .

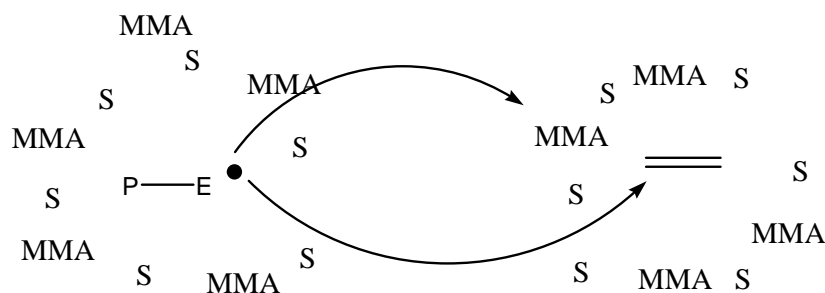


Figure 10. Effect of the MMA concentration on k_{EE} with S the solvent

In this section, we highlight that kinetic rate can also be impacted by entropic effect due to the variation of MMA initial concentration. Since an enthalpic effect due to stabilization by $\left(\frac{\mu}{\varepsilon}\right)^2$ is also impacted by the MMA monomer content, the decorrelation of both influences on the reactivity ratios need a more fine study.

c) Conclusion

These series of experiments show that the concentration of MMA itself in toluene leads to a variation of kinetic rate. However the $\left(\frac{\mu}{\varepsilon}\right)^2$ exhibits also an important role on the reactivity ratios. Consequently the apparent variation of reactivity ratios is due to two distinct mechanisms the MMA concentration in toluene and the $\left(\frac{\mu}{\varepsilon}\right)^2$ of the MMA toluene mixture (see Table 5).

Table 5. Different factors to take into consideration in order to understand reactivity ratios variation

	r_{MMA}		r_{E}	
	k_{MMAMMA}	k_{MMAE}	k_{EE}	k_{EMMA}
$\left(\frac{\mu}{\varepsilon}\right)^2$ value	-	X	X	X
variation of $\left(\frac{\mu}{\varepsilon}\right)^2$	-	X	X	X
MMA over solvent ratio	X	X	X	X

X means impacting and – not impacting.

4. Conclusion

In this section, we demonstrated that the ethylene-MMA copolymerization takes place in various experimental conditions. Ethylene insertions are up to 50%. However, the copolymer is mostly composed of isolated ethylene units.

Solvents and MMA concentration have a crucial role on the copolymerization reactivity ratio. Indeed solvent and MMA concentration impact the $\left(\frac{\mu}{\epsilon}\right)^2$ of the medium of polymerization, which is a crucial parameter to quantify the activation effect of the solvent. Moreover $\left(\frac{\mu}{\epsilon}\right)^2$ is not stable during the copolymerization since MMA concentration decrease with the conversion leading to variation of kinetics rates thus reactivity ratios during the copolymerization. Finally, MMA concentration itself inside the solvation shell of radicals and monomer impacts also the reactivity ratios. This last effect is an entropic contribution compared to the enthalpic contribution described by $\left(\frac{\mu}{\epsilon}\right)^2$.

In the following we will confirm these effects using other polar vinyl monomers in copolymerization with ethylene.

C. Investigation of the copolymerization with various polar monomers

Different polar vinyl monomers such as styrene, butyl acrylate and vinyl acetate have been copolymerized with ethylene using AIBN radical initiation. A similar study than the ethylene MMA copolymerization is performed for each of these comonomers.

1. Copolymerization with styrene

Styrene is studied despite its non-polarity because this monomer simplifies the investigation of the comonomer effect. Indeed comonomers are ambivalent in the copolymerization of ethylene: they are both monomers and solvents, thus modify the kinetic copolymerization rates and therefore the reactivity ratios.

For styrene, its low $\left(\frac{\mu}{\epsilon}\right)^2 = 0.03 \cdot 10^{-60} \text{ C}^2\cdot\text{m}^2$ ($\mu = 0.41 \cdot 10^{-30} \text{ C}\cdot\text{m}$, $\epsilon = 2.47$) close to the value of toluene ($\left(\frac{\mu}{\epsilon}\right)^2 = 0.17 \cdot 10^{-60} \text{ C}^2\cdot\text{m}^2$) induces that for series of experiments at different styrene concentrations in toluene only the concentration effect of styrene will lead to variation of kinetic rate. Consequently the copolymerization in styrene allows the separate study of the monomer concentration effect and $\left(\frac{\mu}{\epsilon}\right)^2$ effect.

a) Influence of the solvent

Polymerizations are performed at 70°C using 50 mg of AIBN with 20% in volume of styrene in toluene under ethylene pressure up to 250 bar during 4 hours. Results are summarized in the following table.

Table 6. Ethylene/Sty copolymerization in toluene^a

Ethylene pressure (bar)	Yield (g)	Sty content (mol %) ^b	Glass transition (°C) ^c
0	3	100	100
25	1.5	97.5	87.9
50	1	93	80.7
100	0.4	82	64.6
150	0.4	74	64.8
200	0.3	72	62.8
250	0.45	70	66.9

^a: Polymerizations are performed during 4 hours with 50 mg of AIBN at 70°C in 40 mL of toluene with 10 mL of styrene. ^b: determined by ¹H NMR. ^c: determined by DSC

As for MMA, copolymerization yield decreases with pressure up to 100 bar then reaches a plateau and slightly increases over 200 bar. Ethylene insertion increases with ethylene pressure up to 30%. Once again, the decrease in yield is mostly due to the insertion of slowly reacting ethylene monomer and also by the dilution of styrene by ethylene.

As exact composition of the system is known for each ethylene pressure (ethylene content and phases), reactivity ratios of this copolymerization can be calculated $r_{\text{Sty}}=66.3$ and $r_{\text{E}}=0.51$.

Due to the lower reactivity of styrene compared to MMA, yield in all these experiments are much lower. Moreover, compared to MMA, r_{Sty} is higher than r_{MMA} and r_{E} is higher with styrene than with MMA.

Finally, glass transition decreases with the ethylene pressure and content. This glass transition remains sharp and no melting point is observed which indicates that no homopolymer is synthesized and the composition distribution is narrow.

The same set of experiments is performed under identical conditions in THF and DEC (see Figure 11).

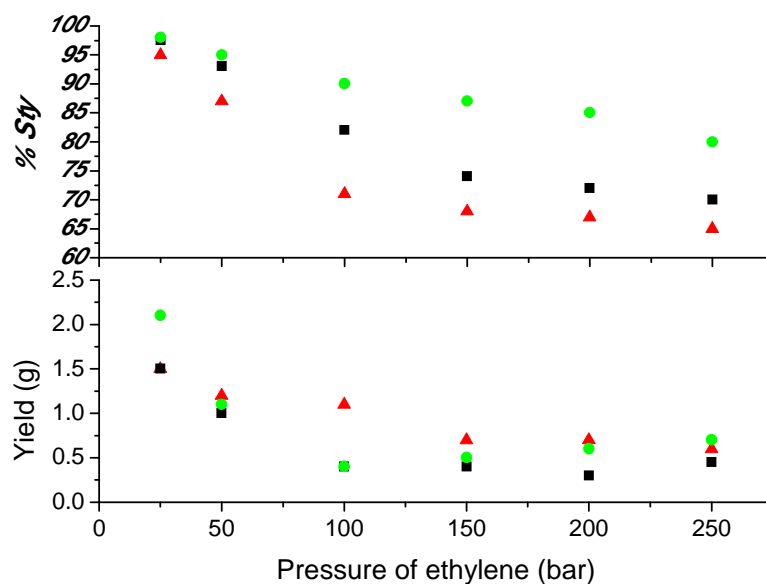


Figure 11. Influence of ethylene pressure on yield and styrene insertion^a during radical copolymerization of ethylene with styrene in different solvents: 50 mg of AIBN during 4 hours at 70°C with 10 mL of styrene in 40 mL ■ of toluene, ▲ of THF, ● of DEC.
^a: determined by ¹H NMR

Solvents exhibit a dramatic effect on the ethylene insertion. In DEC, ethylene insertion is lower than in toluene and THF. The higher content of ethylene is obtained in THF. For example at 250 bar of ethylene pressure 35% of ethylene is inserted in THF, 30% in toluene and only 20% in DEC.

Reactivity ratios are calculated in THF, $r_{\text{Sty}}=30.0$ and $r_{\text{E}}=0.51$ and in DEC $r_{\text{Sty}}=78.5$ and $r_{\text{E}}=0.39$ (see Table 7).

In the free radical homopolymerization of styrene, no solvent activation effect has been identified therefore k_{StySty} is independent of the solvent. Consequently, k_{StyE} is 2 times higher in THF than in toluene and in DEC k_{StyE} is 1.3 times higher than in toluene (see Table 7). Therefore, styryl radical addition on ethylene monomer is favored in THF compared to DEC and toluene.

This result is in agreement with the result obtained for MMA copolymerization with ethylene. This indicates that this effect should be mostly due to specific interactions between solvent and ethylene itself, since similar results are obtained with two distinct comonomers.

For k_{EE} , $\left(\frac{\mu}{\varepsilon}\right)^2$ needs to be calculated for each mixture in order to determine relative k_{EE} : Sty/toluene 1/4 v/v $\left(\frac{\mu}{\varepsilon}\right)^2 = 0.13 \cdot 10^{-60} \text{ C}^2.\text{m}^2$ and Sty/THF 1/4 v/v $\left(\frac{\mu}{\varepsilon}\right)^2 = 0.41 \cdot 10^{-60} \text{ C}^2.\text{m}^2$, Sty/DEC 1/4 v/v $\left(\frac{\mu}{\varepsilon}\right)^2 = 1.02 \cdot 10^{-60} \text{ C}^2.\text{m}^2$. Consequently, k_{EE} is respectively 3 times higher in THF and 4 times in DEC than in toluene (see Table 7).

Therefore k_{ESty} can be estimated: k_{ESty} in THF is almost equal to 3 times k_{ESty} in toluene and k_{ESty} in DEC is 6.5 higher than in toluene (see Table 7). Consequently, the addition of an ethyl radical on a styrene monomer is favored in DEC compared to THF and toluene.

Contrary to MMA copolymerization with ethylene, k_{ESty} increases with $\left(\frac{\mu}{\varepsilon}\right)^2$. However, the range of $\left(\frac{\mu}{\varepsilon}\right)^2$ is between 0.1 to $1 \cdot 10^{-60} \text{ C}^2.\text{m}^2$ during styrene copolymerization. For MMA copolymerization k_{EMMA} increases between 0.25 to $0.6 \cdot 10^{-60} \text{ C}^2.\text{m}^2$ and then decrease for $\left(\frac{\mu}{\varepsilon}\right)^2 = 1.4 \cdot 10^{-60} \text{ C}^2.\text{m}^2$. Consequently, a drop of k_{ESty} could take place over $1 \cdot 10^{-60} \text{ C}^2.\text{m}^2$ in order to obtain result similar to the ethylene MMA copolymerization.

Ethylene-styrene copolymerization results are summarized in the following table.

Table 7. Reactivity ratios and relative kinetic rates of the ethylene-styrene copolymerization

Solvent	$\left(\frac{\mu}{\varepsilon}\right)^2$ ($10^{-60} \text{ C}^2.\text{m}^2$)	r_{sty}	relative k_{StySty}	relative k_{StyE}	r_E	relative k_{EE}	relative k_{ESty}
Toluene	0.13	66.3	1	1	0.51	1	1
THF	0.41	30.0	1	2	0.51	3	3
DEC	1.02	78.5	1	0.8	0.39	4	6.5

Once again a crucial effect of the solvent on the reactivity ratios has been identified. This kinetic rate variation vs. $\left(\frac{\mu}{\varepsilon}\right)^2$ seems to be in agreement with the results obtained for the ethylene-MMA copolymerization.

b) Influence of styrene initial concentration

In order to understand the influence of the initial styrene concentration on the ethylene radical copolymerization, sets of experiments are performed in order to determine reactivity ratios (see Table 8). Copolymerizations conditions are during 1 hour between 50 bar and 250 bar of ethylene pressure in toluene initiated by 50 mg of AIBN.

Table 8. Reactivity ratios of ethylene styrene copolymerization vs. initial styrene content^a

Sty volume (% vv)	10	20	40	60	80	100
r_{Sty}	-	-	7.0	26.6	17.7	19.0
r_{E}	-	-	0.20	0.58	0.62	0.74

^a: Polymerizations are performed between 50 bar and 250 bar of ethylene pressure during 1 hour at 70°C with 50 mg of AIBN in 50 mL of toluene/styrene mixture.

Reactivity ratios as expected are dependent on the styrene content: r_{Sty} increases with the concentration of styrene as well as r_{E} . We are unable to calculate reactivity ratios at styrene concentration below 20 % because yields of polymerization are too low.

In toluene, variations of $\left(\frac{\mu}{\varepsilon}\right)^2$ between the different series of experiment remain extremely low (from 0.02 to 0.1 $10^{-60} \text{ C}^2.\text{m}^2$). Therefore the difference in stabilization by Van der Waals interactions should not induce important variation of kinetics rates. Consequently only the concentration of styrene must impact the reactivity ratios.

In the following figure we plot $\ln(1/r_{\text{Sty}})$ and $\ln(1/r_{\text{E corr}})$ versus $\left(\frac{\mu}{\varepsilon}\right)^2$.

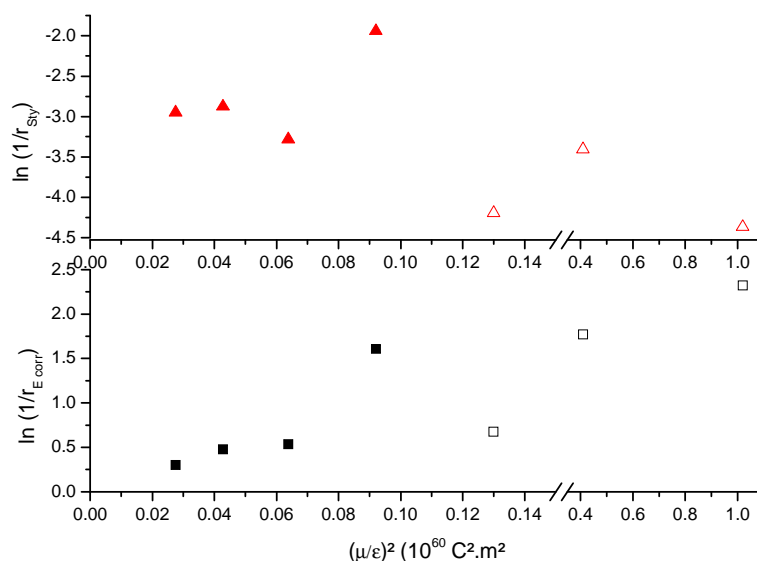


Figure 12. Influence of the initial $\left(\frac{\mu}{\epsilon}\right)^2$ on the reactivity ratio: variation of \blacktriangle r_{Sty} and \blacksquare r_{E} with different contents of styrene (\blacktriangle and \square correspond to values measured with toluene, THF and DEC for 4 hours copolymerizations)

We observe that k_{ESty} and k_{StyE} seem to decrease with initial styrene concentration (increase with $\left(\frac{\mu}{\epsilon}\right)^2$). At high concentration of styrene (over 60% in volume) the reactivity ratio appears to be almost constant.

Over this concentration, macroradicals are mostly surrounded by styrene monomer and therefore the styrene, which will react with the radical, has a higher probability to be from the solvation shell of the radical. Therefore as no solvent activation by $\left(\frac{\mu}{\epsilon}\right)^2$ takes place all kinetics rate must be constant over this styrene concentration.

Below this concentration, the styrene could come from outside the solvation shell therefore k_{ESty} and k_{StySty} would depend on the styrene concentration and increase with the styrene concentration. For k_{EE} and k_{StyE} a decrease is expected.

The increase of r_{Sty} with the styrene concentration is in agreement with the argumentation.

The increase of r_E at low styrene concentration indicates that k_{EE} is unexpected indeed k_{EE} and k_{ESty} theoretical variation should lead to a decrease. This result must indicate that a solvent activation effect exist event at this low $\left(\frac{\mu}{\epsilon}\right)^2$ variation.

Consequently, even with a monomer which do not exhibit a solvent activation effect, a concentration effect exist. This system is especially important since it allows to unlink the concentration effect by performing polymerization under various styrene concentrations and the solvent effect by performing the polymerization using different solvents.

Then to fully understand the copolymerization of ethylene with polar vinyl monomer three distinct parameters have to be taken into account: the solvent activation effect, the variation of this solvent effect with the monomer incorporation and the concentration of comonomer effect.

2. Copolymerization with butyl acrylate

Acrylates are another important class of monomers with solvent properties (μ and ϵ) close to MMA but exhibiting higher reactivity ($k_{BuABuA} > k_{MMAMMA}$). In this section butyl acrylate (BuA) copolymerization with ethylene is reported.

a) Influence of the solvent

Polymerizations are performed in a initial mixture of BuA/Toluene 1/4 v/v at 70°C using AIBN during 4 hours. Results are summarized in the following table.

Table 9. Ethylene/BuA copolymerization in toluene^a

Ethylene pressure (bar)	Yield (g)	BuA content (mol %)^b	Mn (g/mol)^c [PDI^c]
0	5	100	nd
25	7.5	78	26100 [2.9]
50	7	65	25300 [2.7]
100	4	55	28900 [1.9]
150	4	54	30000 [2.0]
200	4.5	51	18600 [2.2]
250	5.5	41	30100 [2.5]

^a: Polymerizations are performed during 4 hours using 50 mg of AIBN at 70°C in 40 mL of toluene with 10 mL of BuA. ^b: determined by ¹H NMR. ^c: determined by HTSEC

As for styrene and MMA copolymerization with ethylene, yield first decreases until reaching a plateau at 100 bar and then increases over 200 bar. As expected, yield is higher with BuA than styrene or MMA due to the higher reactivity of acrylate.

Ethylene insertion increases with pressure up to 60%. This high ethylene insertion is quite surprising and testifies that r_{BuA} must be smaller than r_{MMA} , while r_{E} during the copolymerization with BuA must be higher than with MMA.

In all of these copolymers, no melting point is identified by DSC, therefore no homopolyethylene is synthesized.

Once again, as solubility of ethylene and the frontier between the monophasic and biphasic media are known, reactivity ratios can be calculated: $r_{\text{BuA}}=5.6$ and $r_{\text{E}}=0.59$. Compared to other investigated comonomers (MMA and styrene); ethylene insertion is favored during the copolymerization.

However, insertions of ethylene are surprisingly high therefore we performed further analysis at the DKI. HT-HPLC techniques with an elution designed to separate the polymer in function of their chemical composition are used in order to determine the composition distribution of this copolymer. Examples of chromatograms are shown in the following figure

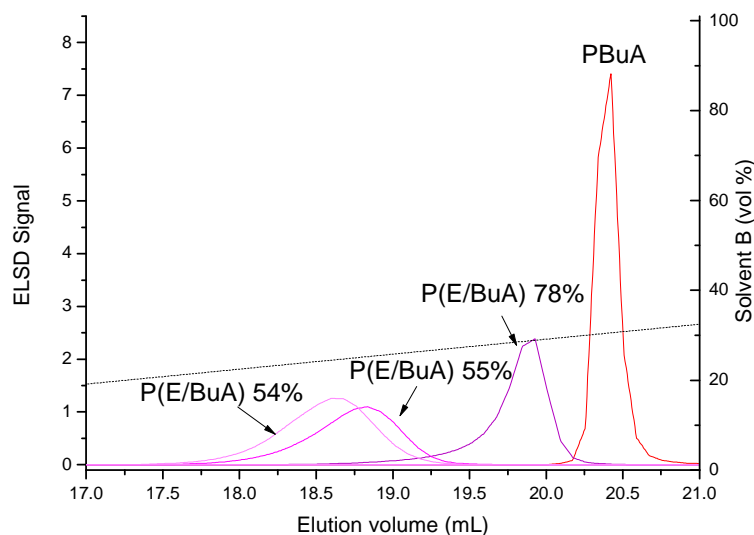


Figure 13. Overlay of chromatograms of P(E/BuA) samples. Stationary phase: Perfectsil 250. Mobile phase: TCB and gradient TCB → TCB/cyclohexanone (30/70 v/v). Temperature: 140°C. Gradient of solvent is indicated by a dotted line

In all cases, only monomodal distributions are observed and no homopolymers are detected. Therefore a linear relation can be found with quite good agreement between the elution time and the BuA average incorporation determined by NMR (see Figure 14).

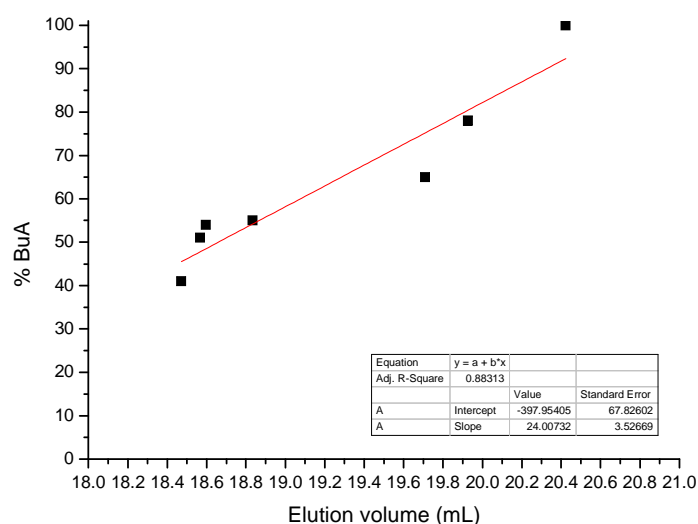


Figure 14. Correlation between elution time determined by LC-CC and BuA insertion determined by ^1H NMR.

These results confirmed that under our experimental conditions, copolymer with ethylene content up to 60% can be synthesized.

The same set of experiments is performed in DEC and THF, and similar results are obtained (see Figure 15). Reactivity ratios are also calculated in these two other solvents: in THF $r_{BuA}=2.7$ $r_E=0.13$ and in DEC $r_{BuA}=4.2$ $r_E=0.51$ (see Table 10).

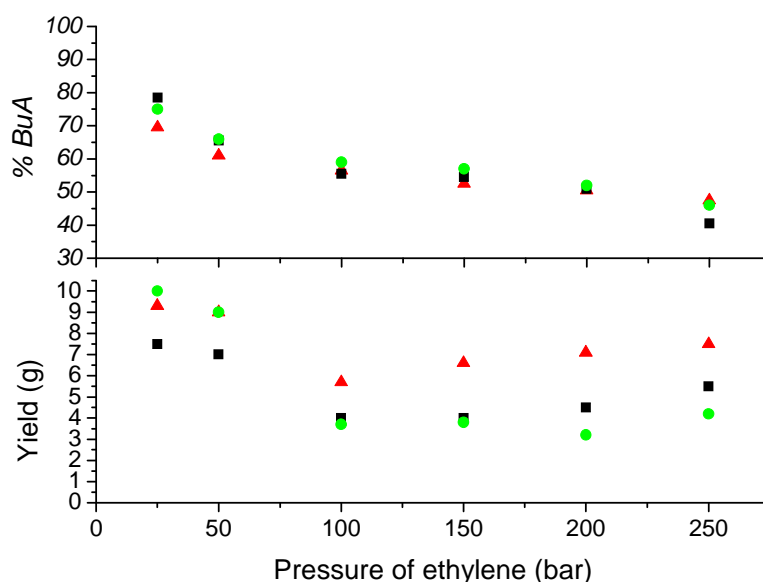


Figure 15. Influence of ethylene pressure on yield and BuA insertion^a during radical copolymerization of ethylene with BuA in different solvents: 50 mg of AIBN during 4 hours at 70°C with 10 mL of BuA in 40 mL ■ of toluene, ▲ of THF, ● of DEC.
^a: determined by ¹H NMR

As expected, yields are higher with THF as solvent than with other solvents due to the higher reactivity of ethylene in this solvent of ethylene. For each solvent the same type of curve is obtained. After a decrease of yield versus ethylene pressure a plateau is reached and followed by an increase over 200 bar. Moreover as expected ethylene insertion increases with ethylene pressure.

These variations of reactivity ratios should be partially due to the solvent effect. Indeed $\left(\frac{\mu}{\epsilon}\right)^2$ is different for each series of experiments: BuA/toluene 1/4 v/v

$\left(\frac{\mu}{\epsilon}\right)^2 = 0.34 \cdot 10^{-60} \text{ C}^2 \cdot \text{m}^2$ and BuA/THF 1/4 v/v $\left(\frac{\mu}{\epsilon}\right)^2 = 1.38 \cdot 10^{-60} \text{ C}^2 \cdot \text{m}^2$, BuA/DEC 1/4 v/v

$\left(\frac{\mu}{\epsilon}\right)^2 = 1.62 \cdot 10^{-60} \text{ C}^2 \cdot \text{m}^2$ with $\mu = 6.3 \cdot 10^{-30} \text{ C} \cdot \text{m}$, $\epsilon = 5.07$ for BuA.

All these experiments are performed at the same initial BuA concentration then k_{BuABuA} is constant and only variation of BuA concentration effect takes place. Consequently, k_{BuAE} is respectively 2.1 times higher in THF and 1.3 times higher in DEC than in toluene (see Table 10). Therefore the addition of ethylene on acrylate radical is favored in THF compared to DEC or toluene.

These results are similar to the previous ones obtained with styrene and MMA in copolymerization with ethylene. This indicates that the effect is mostly independent of the radical and only due to specific interactions between ethylene (monomer or radical) and the solvent.

Ethylene reactivity ratio (r_E) is also $\left(\frac{\mu}{\epsilon}\right)^2$ dependent. As already mentioned k_{EE} variation can be estimated: k_{EE} is 1.7 times higher in THF and 1.3 in DEC than toluene (see Table 10).

Consequently k_{EBuA} is respectively 7.6 higher in THF and 1.5 higher in DEC than in toluene (see Table 10). The effect of solvent is particularly high with THF as the reactivity of ethyl radical toward butyl acrylate is increased by almost a factor 8. These results are in agreement with the results obtained during the MMA copolymerization with ethylene. Therefore the mechanisms involved must be similar.

Ethylene-BuA copolymerization results are summarized in the following table.

Table 10. Reactivity ratios and relative kinetic rates of the ethylene-BuA copolymerization

Solvent	$\left(\frac{\mu}{\epsilon}\right)^2$ ($10^{-60} \text{ C}^2\text{m}^2$)	r_{BuA}	relative k_{BuABuA}	relative k_{BuAE}	r_E	relative k_{EE}	relative k_{EBuA}
Toluene	0.34	5.6	1	1	0.59	1	1
THF	1.38	2.7	1	2.1	0.13	1.7	7.6
DEC	1.62	4.2	1	1.3	0.51	1.3	1.5

Once again a crucial effect of the solvent on the reactivity ratios has been identified.

This kinetic rate variation vs. $\left(\frac{\mu}{\varepsilon}\right)^2$ seems to be in agreement with the results obtained for the ethylene-MMA copolymerization. Indeed kinetics rates (k_{BuAE} , k_{EE} , k_{EBuA}) are higher in THF than in the two other solvents studied.

b) Influence of BuA initial concentration

Copolymerizations with different initial amounts of BuA are also performed in order to calculate the reactivity ratios. Results are summarized in the following table. Copolymerizations are done during 1 hour between 50 bar and 250 bar of ethylene pressure in toluene initiated by AIBN.

Table 11. Reactivity ratios of ethylene BuA copolymerization vs. initial BuA content^a

BuA volume (% vv)	10	20	40	60	80	100
r_{BuA}	9.8	9.2	9.5	6.1	5.6	-
r_{E}	0.21	0.22	0.16	0.03	0.30	-

^a: Polymerizations are performed between 50 bar and 250 bar of ethylene pressure during 1 hour at 70°C with 50 mg of AIBN in 50 mL of toluene/BuA mixture.

Contrary to previous monomers, reactivity ratios first decrease with the increase of BuA concentration until 60-80% then increase. Copolymerization in pure BuA are not easy to perform since there is an important lack of control of the reaction (exothermy up to 50°C has been observed, the high pressure reactor being not to study very fast reactions).

Another specificity is that the reactivity ratios are in good agreement with the reactivity ratio calculated in the previous series of experiment. Consequently, neither the variation of $\left(\frac{\mu}{\varepsilon}\right)^2$ during the polymerization nor the decrease of BuA concentration will have a significant effect in this case.

The different reactivity ratios are plotted versus $\left(\frac{\mu}{\varepsilon}\right)^2$ using the aforementioned calculation.

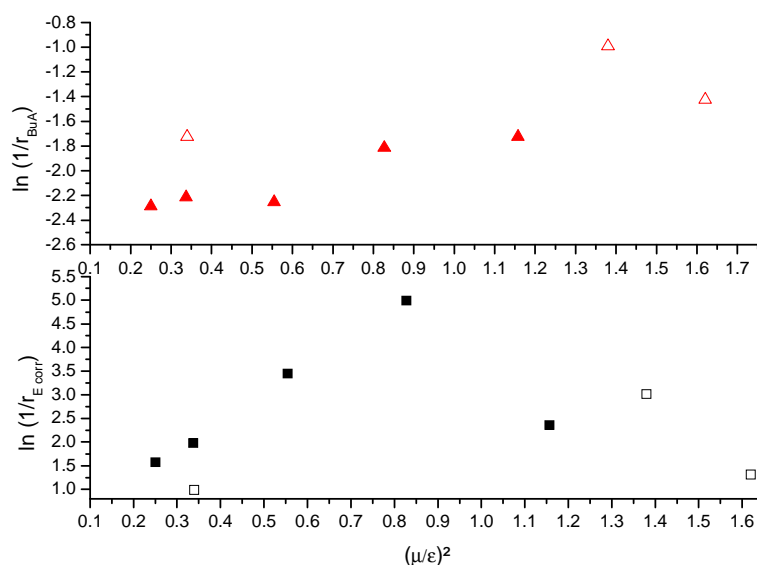


Figure 16. Influence of the initial $\left(\frac{\mu}{\varepsilon}\right)^2$ on the reactivity ratio: variation of \blacktriangle r_{BuA} and \blacksquare r_{E} with different contents of styrene (\triangle and \square correspond to values measured with toluene, THF and DEC for 4 hours copolymerizations)

r_{BuA} is almost constant with the BuA concentration leading to a constant k_{BuAE} , only a slight increase is observed. This means that the impact of BuA concentration on k_{BuABuA} and k_{BuAE} is equivalent.

For k_{EBuA} a Λ -shaped curve is observed as for ethylene homopolymerization. Optimum for the addition of ethyl radical on BuA monomer is for a BuA initial concentration of 60 % in volume over $\left(\frac{\mu}{\varepsilon}\right)^2 = 1 \cdot 10^{-60} \text{ C}^2.\text{m}^2$. These results are in agreement with the previous results obtained for copolymerization performing during 4 hours which may indicate that the BuA concentration effect is negligible for k_{EE} and k_{EBuA} .

Compared to the other monomers studied up to now, BuA copolymerization with ethylene exhibits a specific behavior. Indeed BuA concentration effect seems to be negligible.

However an important effect mostly due to $\left(\frac{\mu}{\varepsilon}\right)^2$ takes place for r_{E} with variation from 0.03 to 0.58 (almost a factor 20). Consequently ethylene successive additions are very improbable except if the copolymerization takes place in THF or in toluene at 60% in volume of BuA.

3. Copolymerization with vinyl acetate

Up to now three major monomers were studied: MMA, styrene, BuA. All of these monomers do not exhibit a solvent activation effect during their homopolymerization. In this section we will study the copolymerization with vinyl acetate (VAc) known for exhibiting a solvent activation effect in free radical polymerization such as ethylene.

a) Influence of the solvent

Ethylene vinyl acetate copolymerizations are performed in the same experimental conditions in three solvents: toluene, THF, DEC. Results are summarized in the following figure.

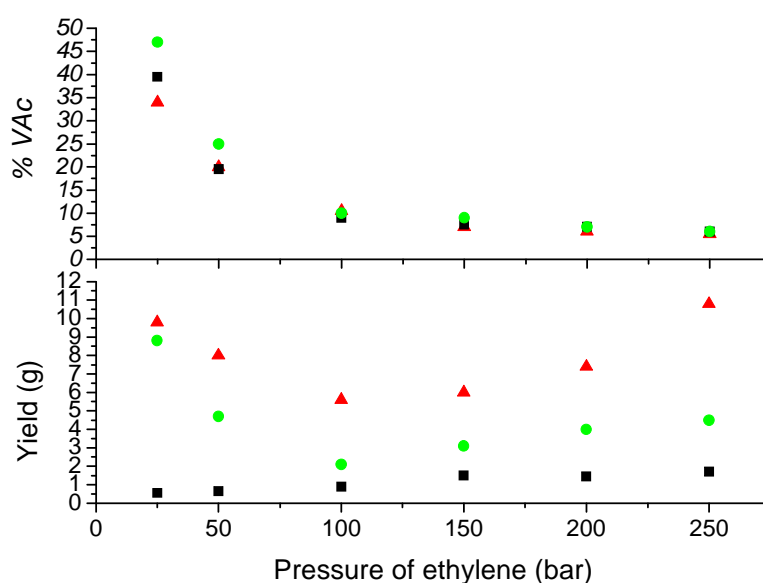


Figure 17. Influence of ethylene pressure on yield and VAc insertion^a during radical copolymerization of ethylene with VAc in different solvents: 50 mg of AIBN during 4 hours at 70°C with 10 mL of VAc in 40 mL ■ of toluene, ▲ of THF, ● of DEC.
^a: determined by ¹H NMR

Contrary to the other copolymerizations performed up to now, yield is strongly dependent on the solvent used. Indeed THF is an efficient solvent for ethylene and VAc homopolymerization, DEC only for VAc and toluene for none of them.

Consequently as expected at high VAc content polymerizations in DEC and THF are highly more efficient than in toluene. At low VAc content THF is the most efficient system and DEC is slightly more efficient than toluene.

Another particularity is that the ethylene insertion is very high up to 95%. Therefore reactivity ratios of these copolymerizations are calculated: $r_{VAc}=0.11$ $r_E=13.8$ in toluene, $r_{VAc}=0.19$ $r_E=16.8$ in THF and $r_{VAc}=0.98$ $r_E=10.1$ in DEC (see Table 12).

In this case the interpretations of the reactivity ratios are more complex due to the solvent dependence of all kinetic rates, k_{VAcVAc} , k_{EE} , k_{EVAc} and k_{VAcE} .

In the second chapter the study of the VAc homopolymerization in different solvents has been performed (see section C-7 of the chapter II). Consequently the relative rate of k_{VAcVAc} can be estimated if we assume that the solvent activation effect is only due to the variation of propagation kinetic rate and not influenced by ethylene pressure. In THF VAc homopolymerization is 7 times more efficient than in toluene (4 in DEC – see Table 12).

Therefore k_{VAcE} is respectively 3.9 times higher in THF and 2.3 lower in DEC than in toluene (see Table 12). Consequently the VAc radical addition on ethylene monomer is more efficient in THF than toluene and DEC.

Efficiency of the ethylene homopolymerization can also be estimated in each solvent as VAc/toluene $1/4 \text{ v/v} \left(\frac{\mu}{\epsilon} \right)^2 = 0.28 \cdot 10^{-60} \text{ C}^2 \cdot \text{m}^2$, VAc/THF $1/4 \text{ v/v} \left(\frac{\mu}{\epsilon} \right)^2 = 0.64 \cdot 10^{-60} \text{ C}^2 \cdot \text{m}^2$ and VAc/DEC $1/4 \text{ v/v} \left(\frac{\mu}{\epsilon} \right)^2 = 1.40 \cdot 10^{-60} \text{ C}^2 \cdot \text{m}^2$ with $\mu = 5.69 \cdot 10^{-30} \text{ C} \cdot \text{m}$ and $\epsilon = 6.1$ for vinyl acetate. Consequently, in THF k_{EE} will be 4.6 times higher (2.1 for DEC) than in toluene (see Table 12).

Moreover k_{EVAc} is 3.8 times higher in THF (2.9 for DEC) than in toluene (see Table 12). Consequently the ethylene radical addition on vinyl acetate monomer is more efficient in THF and DEC than in toluene.

These results are again similar to the previous variations observed during the different copolymerizations.

Ethylene-VAc copolymerization results are summarized in the following table.

Table 12. Reactivity ratios and relative kinetic rates of the ethylene-VAc copolymerization

Solvent	$\left(\frac{\mu}{\epsilon}\right)^2$ ($10^{-60} \text{ C}^2\text{m}^2$)	r_{VAc}	relative k_{VAcVAc}	relative k_{VAcE}	r_{E}	relative k_{EE}	relative k_{EVAc}
Toluene	0.28	0.11	1	1	13.8	1	1
THF	0.64	0.19	7	3.9	16.8	4.6	3.8
DEC	1.40	0.98	4	0.4	10.1	2.1	2.3

Once again a crucial effect of the solvent on the reactivity ratio has been identified. This kinetic rate variation vs. $\left(\frac{\mu}{\epsilon}\right)^2$ seems to be in agreement with the results obtained for the ethylene-MMA copolymerization. It should be noted that contrary to other copolymerization studied up to now $r_{\text{E}} > r_{\text{Pol}}$ and therefore high ethylene insertion is reached.

b) Influence of VAc initial concentration

Polymerizations are also performed in toluene with different VAc initial concentrations in order to determine the reactivity ratios and their dependence to the monomer concentration and solvent properties. Results are summarized in the following table.

Table 13. Reactivity ratios of ethylene VAc copolymerization vs. initial VAc content^a

VAc volume (% vv)	10	20	40	60	80	100
r_{AcV}	0.43	0.14	0.46	0.64	0.77	1.7
r_{E}	4.8	5.1	5.1	4.6	4.6	3.2

^a: Polymerizations are performed between 50 bar and 250 bar of ethylene pressure during 1 hour at 70°C with 50 mg of AIBN in 50 mL of toluene/VAc mixture.

As expected reactivity ratios are strongly dependent on the initial VAc concentration. r_{VAc} increases with the VAc concentration and r_{E} roughly decreases.

Once again we plot the different reactivity ratios in function of $\left(\frac{\mu}{\varepsilon}\right)^2$ using the aforementioned calculation.

Both series of experiments (copolymerization performed during 1 hour and 4 hours) provide similar results on the dependence of the reactivity ratio vs. $\left(\frac{\mu}{\varepsilon}\right)^2$ (see Figure 18). Values are almost identical for r_{VAc} but r_E is lower if the polymerizations are performed during 1 hour. This slight influence of polymerization duration is mostly due to the low conversion of VAc during the copolymerization since insertion of VAc in polymer chain remains low, therefore $\left(\frac{\mu}{\varepsilon}\right)^2$ variation remains low.

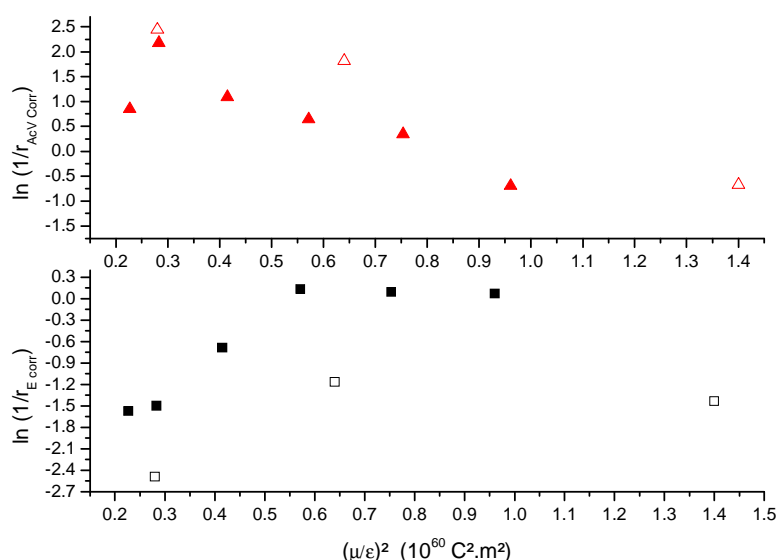


Figure 18. Influence of the initial $\left(\frac{\mu}{\varepsilon}\right)^2$ on the reactivity ratio: variation of ▲ r_{VAc} and ■ r_E with different content of styrene (▲ and □ correspond to values measured with toluene, THF and DEC for 4 hours copolymerizations)

Calculations indicate that k_{EVAc} increases with the VAc concentration until reaching a plateau over 60% in volume of VAc. For k_{VAcE} a decrease is observed. Once again this variation is due to a global solvent effect $\left(\frac{\mu}{\varepsilon}\right)^2$ and to the VAc concentration. Indeed, if the solvent is mostly composed of VAc the monomer which will react with the macroradical is from the inner of the solvation shell. Therefore, k_{EVAc} should increase and k_{VAcE} decreases with the VAc concentration using the same argumentation aforementioned.

For both k_{EVAc} and k_{VAcE} the slight difference in behaviors indicates that some entropic effect could take place but the effect should be very low compared to the enthalpic effect.

4. Conclusion

Copolymerization of ethylene with polar vinyl monomers has been performed. Insertion of ethylene up to 60% is obtained. In the specific case of VAc even higher ethylene insertions can be reached.

All these copolymerizations exhibit a solvent dependence of the reactivity ratios. Indeed the solvent modifies the kinetic rate of copolymerization and therefore favor or disfavor the ethylene insertion. Similar effects on k_{PoIE} and k_{EPoI} are observed since in almost all cases their values are maximal for THF (Table 14).

Table 14. Relative k_{PoIE} and k_{EPoI} for different copolymerization studied

	MMA		Styrene		BuA		VAc	
Solvent	k_{MMAE}	k_{EMMA}	k_{StyE}	k_{ESty}	k_{BuAE}	k_{EBuA}	k_{VAcE}	k_{EVAc}
Toluene	1	1	1	1	1	1	1	1
THF	1.4	1.8	2	3	2.1	7.6	3.9	3.8
DEC	1	0.8	0.8	6.5	1.3	1.5	0.4	2.3

Another effect identified is the monomer concentration effect itself. The comonomer, which will react, can come from the inside or outside of the solvation shell of the macroradical. The high concentrations of comonomer are in favor of the inner shell mechanism.

D. Copolymerization in emulsion

Ethylene copolymerization in solution exhibits specific behaviors: some are usual in copolymerization (comonomer concentration effect) and some specific of ethylene (solvent activation effect). During these copolymerizations the ambivalence of comonomer as a monomer and a solvent is highlighted.

In this section we report the copolymerization in water dispersed medium. Latexes synthesized could represent some interesting film properties due to their non negligible amount of ethylene in the polymer chain.

Copolymerizations are performed without surfactant at 10% v/v of comonomer and initiated by water soluble AIBA. Stable latexes of ethylene copolymers with polar vinyl monomers are so obtained.

Ethylene behavior in these emulsions will be completely different than during the homopolymerization in water since ethylene is soluble in the comonomer. Indeed, in this case ethylene is present in the comonomer droplets and therefore the diffusion in water will be faster (due to the higher surface of diffusion).

1. Copolymerization with styrene

Before investigating the copolymerization, the homopolymerization of the styrene in emulsion without surfactant under argon pressure was studied (see Figure 19).

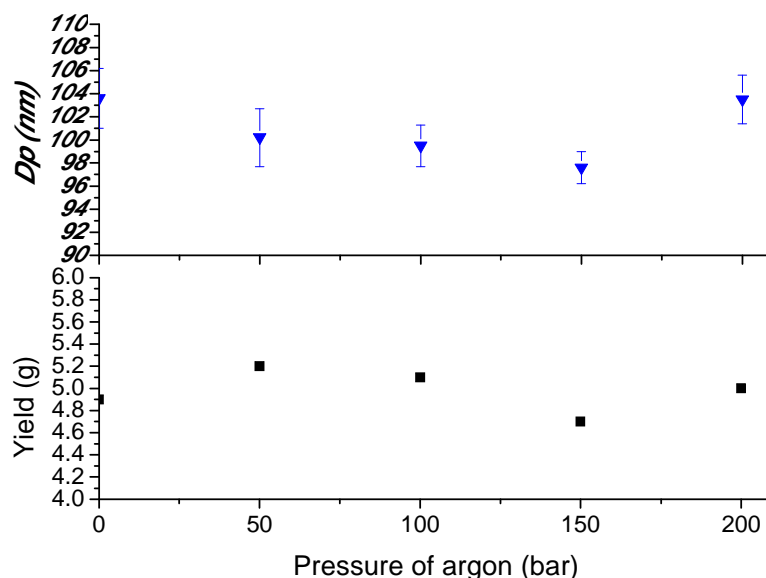


Figure 19. Styrene emulsion polymerization under various argon pressures. ■ yield and ▼ average particles diameters^a vs. argon pressure at 70°C with 80 mg of AIBA in 45 mL of water with 5 mL of styrene during 2 hours. ^a: determined by DLS

No important variation in yield or final particles diameters is identified after polymerizing during 2 hours at 70°C under various argon pressures (up to 200 bar) at 10% in volume of styrene with 80 mg of AIBA as radical initiator. Consequently, we assume that nucleation, diffusion of styrene and propagation are mostly independent of the pressure itself.

Copolymerization of styrene in similar experimental conditions are performed under a given ethylene pressure using 305 μmol of AIBA as water soluble radical initiator dissolved in a mixture of water and styrene 9/1 v/v at 70°C during 2 hours. Results are summarized in the following figure.

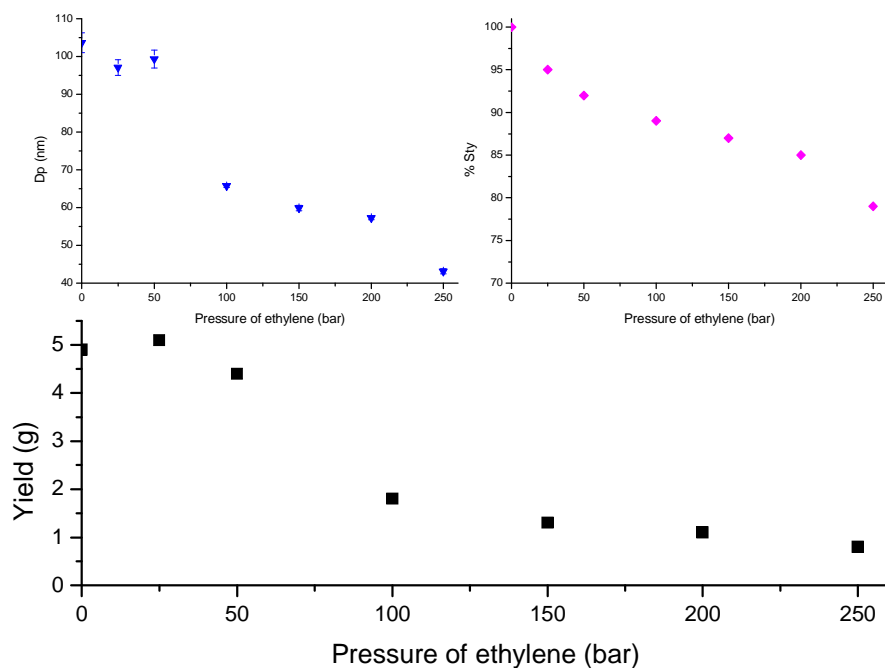


Figure 20. Ethylene styrene copolymerization in emulsion under various ethylene pressures. ■ yield, ▼ average particles diameters^a and ♦ styrene insertion^b vs. ethylene pressure at 70°C with 80 mg of AIBA in 45 mL of water with 5 mL of styrene during 2 hours. ^a: determined by DLS. ^b: determined by ¹H NMR

After the polymerization, ethylene is slowly degassed. In all experiments, stable latex without flocculation is isolated. It is important to note that no surfactant are present, consequently the stabilization is due to AIBA fragment at the end-chain of polymer.

Yield decreases with ethylene pressure from 5 g to 1 g. As ethylene insertion increases with polymerization pressure, this decrease is due to the insertion of lowly reactive ethylene in the polymer chain.

Average particles diameters decreases from 100 nm to 50 nm with the ethylene pressure. PI remains close to 0.15 in all experiments which could indicate that the particles diameters are broadly distributed. Finally, the number of particles remains almost constant in all these experiments; therefore the nucleation mechanism should be almost independent of the ethylene pressure.

No melting points are observed by DSC consequently homopolyethylene was synthesized. TEM has been performed on these latexes (see Figure 21).

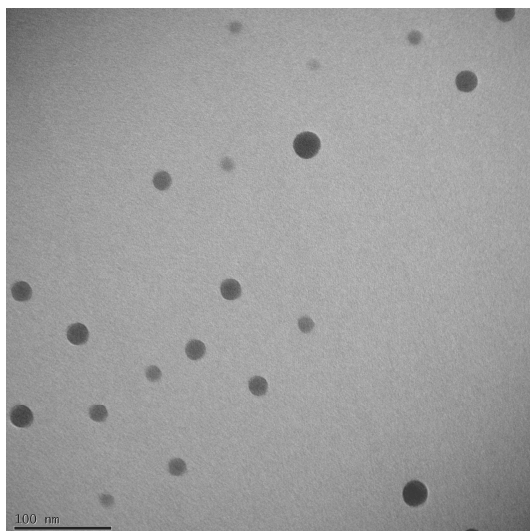


Figure 21. Standard TEM picture obtained for an ethylene/styrene copolymer synthesized at 200 bar of ethylene pressure

Particles show a high distribution in diameters as expected from DLS measurement which should be due to a low control of the nucleation step. Particles are spherical and no facet is observed contrary to PE particles. No difference with standard polystyrene particles is observed.

Finally, reactivity ratio can be calculated: $r_{\text{Sty}} \approx 16$ and $r_{\text{E}} \approx 0.01$. These reactivity ratios are close to the ones obtained in solution. This indicates that the relative reactivity of the monomer remains unchanged in emulsion compared to solution process.

2. Copolymerization with MMA

The same series of experiments is performed with MMA instead of styrene in free-surfactant emulsion. Results are summarized in the Figure 22.

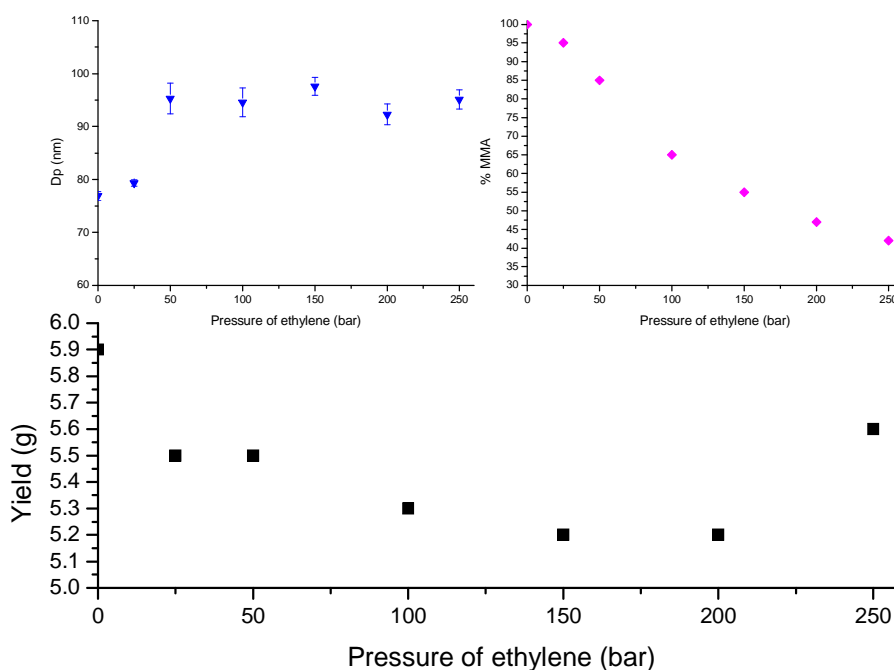


Figure 22. Ethylene MMA copolymerization in emulsion under various ethylene pressures. ■ yield, ▼ average particles diameters^a and ♦ MMA insertion^b vs. ethylene pressure at 70°C with 80 mg of AIBA in 45 mL of water with 5 mL of MMA during 2 hours. ^a: determined by DLS. ^b: determined by ¹H NMR

In all experiments stable latexes are obtained after copolymerization.

Contrary to styrene copolymerization, yield is almost constant with the ethylene pressure (from 5.2 g to 5.9 g). A slight expected decrease of yield at low pressure and increase at high pressure is observed.

Moreover, ethylene insertions drastically increase with pressure. This behavior is very different from the solution polymerization in which the insertion of ethylene dramatically slows down the polymerization. Indeed since the yield is almost independent from the ethylene insertion, the ethylene reactivity should be similar to the MMA reactivity during the copolymerization in emulsion.

Average particles diameter remains constant around 90 nm over 50 bar of ethylene pressure. However at 25 bar and for the homopolymerization of MMA smaller particles of 80 nm are obtained. Therefore the number of particles slightly increases with the ethylene pressure.

No particles can be observed by TEM due to the film formation of the particles and DSC analysis did not allow to show any melting point. Consequently, no homopolyethylene is produced.

Finally, reactivity ratios are calculated $r_{\text{MMA}} \approx 15$ and $r_{\text{E}} \approx 0.3$. These values are close to the solution copolymerization. Therefore, the relative reactivities of ethylene and MMA are similar in emulsion and in solution.

3. Copolymerization with BuA

Copolymerizations are also performed with butyl acrylates in the same experimental conditions: 80 mg of AIBA during 2 hours at 70°C with 45 mL of water and 5 mL of BuA under different ethylene pressures.

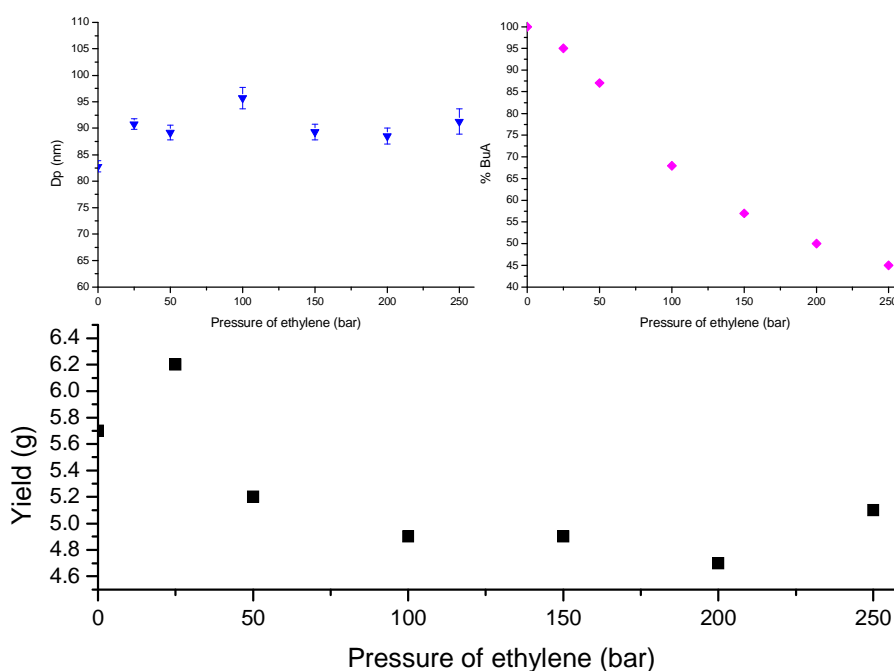


Figure 23. Ethylene BuA copolymerization in emulsion under various ethylene pressures. ■ yield, ▼ average particles diameters^a and ♦ BuA insertion^b vs. ethylene pressure at 70°C with 80 mg of AIBA in 45 mL of water with 5 mL of BuA during 2 hours. ^a: determined by DLS. ^b: determined by ¹H NMR

Once again stable latexes are obtained.

Yield follows a similar curve than in solution. Indeed at low pressure, yield decreases with the ethylene pressure until reaching a plateau and then increases over 200 bar of ethylene pressure. Insertion of ethylene also increases with the ethylene pressure up to 55 % at 250 bar.

Average particles diameters remain almost constant around 90 nm whatever the ethylene pressure. Therefore, the number of particles slightly increases with the ethylene pressure.

Reactivity ratios are calculated using Kelen Tüdös method, $r_{\text{BuA}} \approx 80$ and $r_{\text{E}} \approx 0.3$. r_{E} is close to the value obtained in solution copolymerization, however contrary to the precedent set r_{BuA} is surprisingly higher.

4. Copolymerization with VAc

Finally vinyl acetate copolymerization was also investigated.

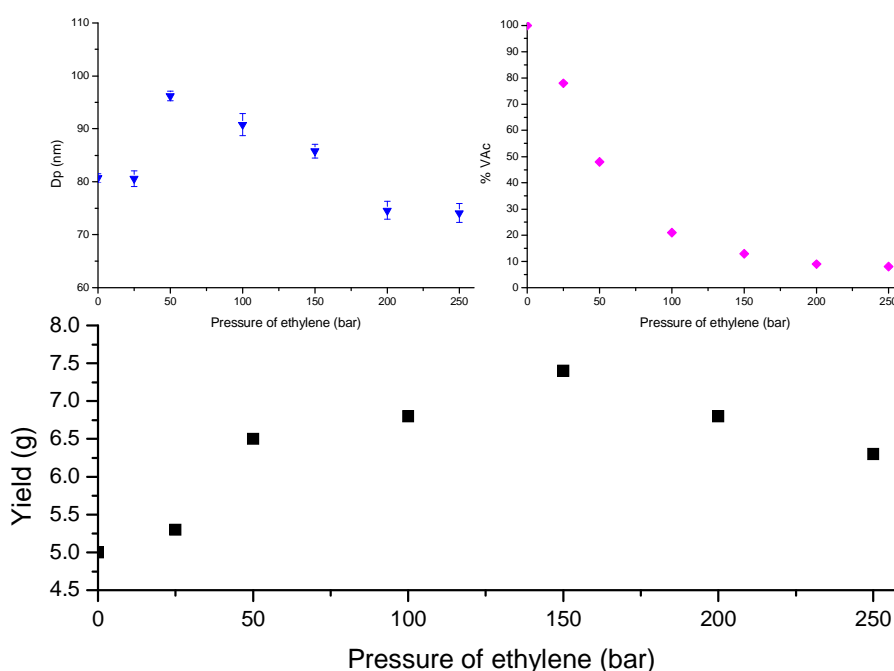


Figure 24. Ethylene VAc copolymerization in emulsion under various ethylene pressures. ■ yield, ▼ average particles diameters^a and ♦ VAc insertion^b vs. ethylene pressure at 70°C with 80 mg of AIBA in 45 mL of water with 5 mL of VAc during 2 hours. ^a: determined by DLS. ^b: determined by ¹H NMR

Stable latexes are obtained whatever the ethylene pressure used.

VAc copolymerization in emulsion exhibits a very different behavior than the other copolymerizations studied up to now. Indeed, yield increases with ethylene pressure up to 150 bar then decreases. This is the exact opposite of the copolymerization in solution of THF or DEC and closer to the behavior with toluene. Ethylene insertion increases up to 90% at 250 bar.

Moreover, particles diameters decrease with ethylene pressure from 100 nm to 70 nm. Therefore the number of particles increases with the ethylene pressure.

Reactivity ratios are calculated $r_{VAc}=1.7$ and $r_E=17.7$. r_E is close to the value obtained in solution (see Table 12) however r_{VAc} is surprisingly higher. This means that the relative reactivity of VAc compared to ethylene is increased in emulsion compared to solution. It could be due to the high water solubility of VAc (25 g/L at 20°C).

5. Conclusion

In this section, stable latexes of ethylene copolymers are obtained with similar ethylene insertion than the solution process. Consequently, these copolymers can be produced without organic solvent. Moreover, contrary to the solution process, in most of the case ethylene pressure impacts only the ethylene insertion. Indeed yield and average particles diameters remain almost constant whatever the ethylene pressure.

The mechanisms of these copolymerizations remain to investigate, especially the droplet existence at high ethylene pressure. Indeed in this case polar monomer can be entirely present in headspace supercritical phase of the reactor with ethylene.

E. Conclusion

In this chapter we report the free radical copolymerization of ethylene with four major polar vinyl monomers: MMA, BuA, styrene and VAc. Yield and ethylene insertion are as expected solvent dependent.

Solvent and comonomer concentration have a crucial role on the copolymerization reactivity ratios. Indeed, at constant initial comonomer concentration, solvents induce an important variation of reactivity ratio via a solvent activation effect. Moreover, experiments performed at different comonomer concentrations show also variation of reactivity ratios. This is due to both effects: a solvent activation effect and a comonomer concentration effect.

These effects correspond from the thermodynamic point of view in an enthalpic one in which the stabilization of monomers and radicals influence the kinetics of the copolymerization and an entropic one in which the frequency of efficient shocks is impacted.

Copolymerizations in three different organic solvents are performed. High molar amounts of ethylene have been inserted in the polymer chain for each comonomer studied.

Therefore the radical polymerization is able to insert important amounts of ethylene inside the polar chain. These inserted ethylene units are mostly isolated and no crystallinity is obtained except with VAc.

In addition copolymerizations in aqueous dispersed medium are performed. In this case also similar copolymers are synthesized with reactivity ratios usually close to the one obtained in emulsion. These processes represent an important interest as the final copolymer synthesized could easily form films.

However, for MMA, styrene and BuA copolymerization with ethylene, no long sequences of ethylene have been obtained since no melting point is observed whatever the experimental conditions used. Therefore, in order to obtain long sequences of ethylene and a semi-crystalline polymer another type of polymerization should be investigated.

The insertion-coordination polymerization of ethylene on metal complexes is one of the most efficient systems to produce sequences of ethylene. However no efficient and versatile catalyst has been reported up to now for the copolymerization with polar vinyl monomer.

Consequently the hybrid mechanism (catalytic/radical polymerization) need be developed to obtain a wide range of new ethylene copolymers. To obtain an efficient system the “shuttling” between the two mechanisms has to be of several orders faster than termination and transfer rate in order to produce polymer chains with several catalytic-made and radical-made blocks. In the next chapter we will investigate the efficiency of the shuttling.

References:

- [1] P. Ehrlich and G. A. Mortimer *Adv. Polymer Sci.*, vol. 7, p. 386, 1970.
- [2] R. Luo, Y. Chen, and A. Sen *J. Polym. Sci., Part A: Polym. Chem.*, vol. 46, p. 5499, 2008.
- [3] R. Bryaskova, N. Willet, P. Degée, P. Dubois, R. Jérôme, and C. Detrembleur *J. Polym. Sci., Part A: Polym. Chem.*, vol. 45, p. 2532, 2007.
- [4] R. Venkatesh, B. B. P. Staal, and B. Klumperman *Chem. Comm.*, p. 1554, 2004.
- [5] S. Borkar and A. Sen *J. Polym. Sci., Part A: Polym. Chem.*, vol. 43, p. 3728, 2005.
- [6] K. Tanaka and K. Matyjaszewski *Macromol. Symp.*, vol. 261, p. 1, 2008.
- [7] T. Kelen and F. Tudos *React. Kinet. Catal. Lett.*, vol. 1, p. 487, 1974.
- [8] T. Kelen and F. Tudos *J. Macromol. Sci.-Chem.*, vol. A9, p. 1, 1975.
- [9] T. Kelen and F. Tudos *Makromol. Chem.*, vol. 191, p. 1863, 1990.

Chapter V : Investigation on the hybrid radical/catalytic mechanism

A.	Synergy effect between radical and catalytic polymerization.....	V-289
1.	NiNO as a radical initiator of polymerization	V-289
2.	Effect of additional AIBN on the radical polymerization initiated by NiNO	V-290
a)	Case of MMA polymerization	V-290
b)	Case of styrene polymerization	V-292
3.	Effect of additional AIBN on the ethylene catalytic polymerization	V-293
B.	Mechanistic investigation.....	V-297
1.	Two different possible mechanisms	V-298
a)	With no additional source of radical	V-298
b)	With an additional source of radicals	V-299
(1)	Exchange type S_{R1}	V-300
(2)	Exchange type S_{R2}	V-300
2.	Evidence of the homolytic cleavage of the Ni carbon bond.....	V-301
3.	Evidence of the radical addition on NiNO	V-304
4.	Case of NiPO	V-305
C.	Study of the phosphine effect during PMMA and PE syntheses	V-306
1.	Influence of phosphorous ligand on the radical polymerization of MMA	V-306
a)	Effect of triphenyl phosphine.....	V-307
b)	Effect of other phosphines	V-308
c)	Effect of phosphites	V-309
d)	Rationalisation of the phosphorous ligand effect	V-310
e)	Case of multidentate phosphine ligands	V-313
2.	Effect of the phosphorous ligand on the catalytic polymerization	V-314
a)	Effect of phosphines	V-315
b)	Effect of phosphites	V-316
c)	Rationalization of the activity in presence of phosphorous ligands	V-317
d)	Effect of diphosphines	V-318
e)	Other ligands.....	V-320
D.	Conclusion.....	V-321

In the previous chapters we demonstrated the efficiency of the free radical polymerization of ethylene in organic solvent or in water. Then we investigated the free radical copolymerization of ethylene with other polar vinyl monomers. The ambivalent role of the comonomer as monomer and solvent has been highlighted in order to understand copolymerization mechanisms. Indeed reactivity ratios obtained depend of the solvent used and the comonomer concentration.

However, these copolymerizations, excepted for vinyl acetate do not provide the full range of copolymer composition under our experimental conditions. Indeed ethylene insertions over 50 % are difficult to access using the pure radical pathway.

By a catalytic polymerization, accessible copolymers have limited polar content and polar function (see chapter I). Insertion of methyl acrylate, the most studied comonomer, is reported up to 50% in the main chain [1], however activity and molecular weight are very low. Moreover for other polar monomers, insertion is rarely over 10% [2] and these polar units are mostly isolated in the polymer chain.

Since all systems used for copolymerization of ethylene with polar vinyl monomer present important limitations, the investigation of a new hybrid way, developed at the LCPP, seems mandatory in order to access the full range of copolymer composition (see Figure 1).

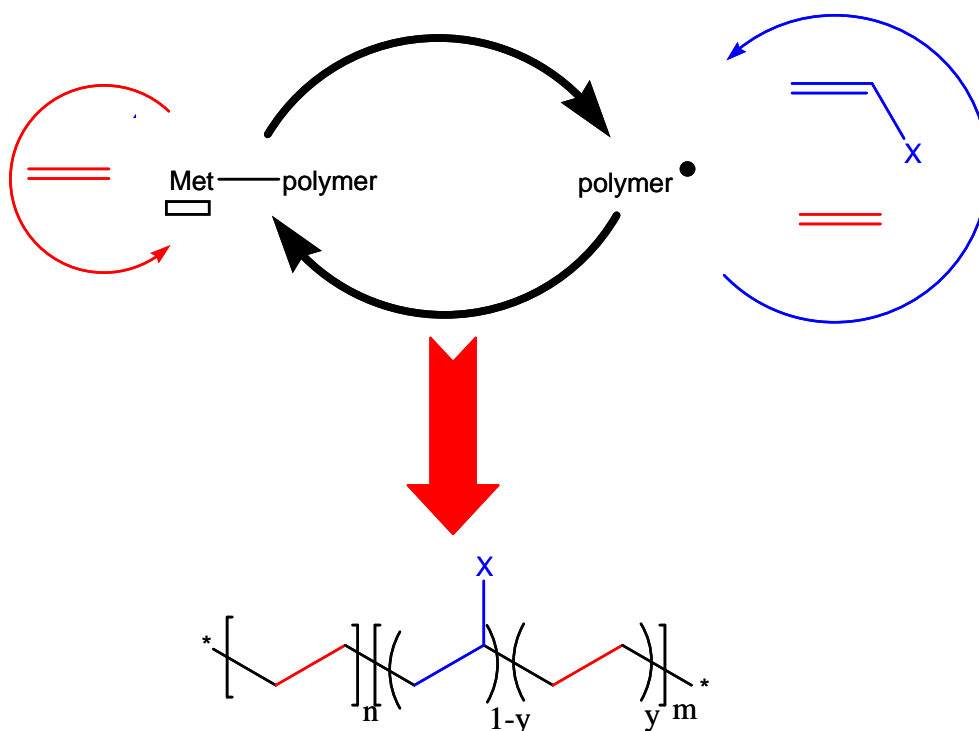


Figure 1. Hybrid mechanism of polymerization

This copolymerization concept is based on the homolytic cleavage of a metal carbon bond in an ethylene polymerization catalyst, followed by the initiation of a radical polymerization of polar monomers by the radical released. Consequently multiblock copolymers of ethylene and a polar vinyl monomer can be synthesized if the metal carbon bond can be formed again by radical readdition. The ethylene block will be synthesized by catalytic polymerization and the polar by radical one. This multiblock architecture presents the additional advantage to allow the conservation of the polymer crystallinity even at high polar content.

Alexandra Leblanc [3-6] demonstrated that the catalyst NiNO (see Figure 2) can initiate a radical polymerization in bulk of MMA and styrene. BuA can also be polymerized if triphenylphosphine is added to the system. This compound is to our knowledge the first example of an ethylene catalyst which initiates a radical polymerization with some efficiency. Indeed the reactivity ratios obtained during copolymerizations of MMA/BuA, MMA/styrene and BuA/styrene are close to the ones of a free radical copolymerization which confirms a radical mechanism. Consequently she used this compound to perform ethylene/MMA hybrid copolymerization with some promising results.

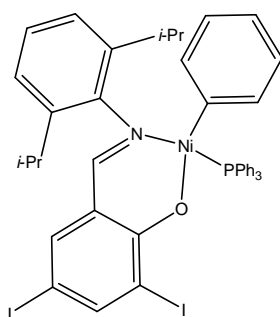


Figure 2. NiNO catalyst study

In this chapter we will investigate further the nickel carbon bond cleavage and the interaction of NiNO with organic radicals. Indeed in order to control this type of copolymerization the homolytic cleavage of the metal carbon bond and the reformation of this bond need to be fully studied. Firstly polymerization in solution of polar vinyl monomer and ethylene initiated by NiNO will be studied and the influence of addition of AIBN investigated. In this chapter the mechanism of this cleavage will be studied and optimized. Finally, the addition of a variety of additional phosphorous ligands on this catalyst will be reported during polar vinyl monomer polymerization and ethylene polymerization.

A. Synergy effect between radical and catalytic polymerization

In this section the effect of a radical source on the radical polymerization of polar vinyl monomer initiated by NiNO and the catalytic polymerization of ethylene initiated by NiNO is investigated.

1. NiNO as a radical initiator of polymerization

In order to confirm that NiNO can polymerize polar vinyl monomers in solution such as MMA, we perform polymerization at 70°C with 54 μmol of NiNO in 50 mL of a mixture toluene/monomer 4/1 v/v. Then kinetic profiles are determined via samples collections. Results are summarized in the following figure for MMA, BuA, styrene and VAc polymerizations.

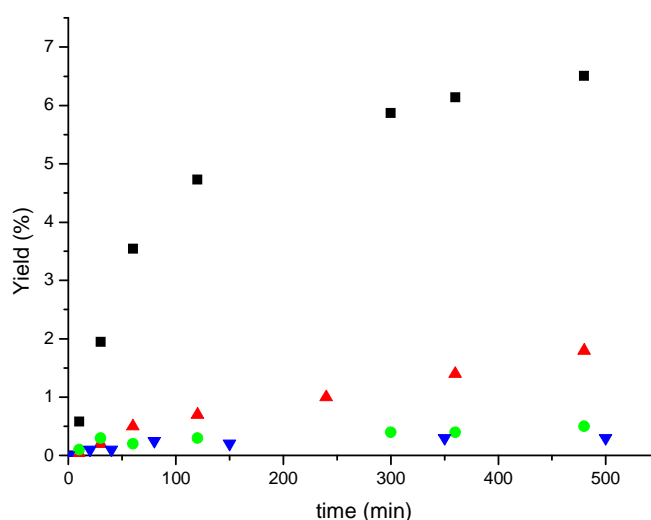


Figure 3. Reaction profiles of the polar vinyl monomer polymerizations initiated by NiNO. 50 mg of NiNO at 70°C in 40 mL of toluene and 10 mL of ■ MMA, ▲ Sty, ● BuA and ▼ VAc.

The results obtained are similar to these obtained during the same polymerizations initiated by NiNO in bulk [3, 6]. Indeed NiNO is able to polymerize MMA and styrene even in solution. However, conversions remain low (<7% for MMA and 2% for styrene after 8 hours of polymerization).

Polymerizations of BuA and VAc surprisingly do not occur. Indeed BuA is one of the most reactive monomer for radical polymerization (compared to MMA and styrene).

Consequently the initiation mechanism seems to be inhibited by the presence of BuA. This may indicate that the monomer does not act as a spectator during the initiation.

The reaction profiles follow the classical 1st order kinetics of a free radical polymerization since $\ln \frac{1}{1-x}$ is proportional to time. Consequently, the half-life time of the species which initiates the polymerization can be calculated using the standard treatment of the kinetics profile [7].

For MMA, at 70°C a half-life time ($t_{1/2}$) of 200 min is measured. With styrene 260 min is obtained. This difference in $t_{1/2}$ between MMA and styrene, and the fact that the polymerization is not efficient with BuA, indicates that the initiator species interacts with the monomer. Consequently the initiator species is monomer dependent. For example the nickel carbon bond cleavage could take place after the monomer coordination to the NiNO or after a first monomer insertion (see Figure 4).

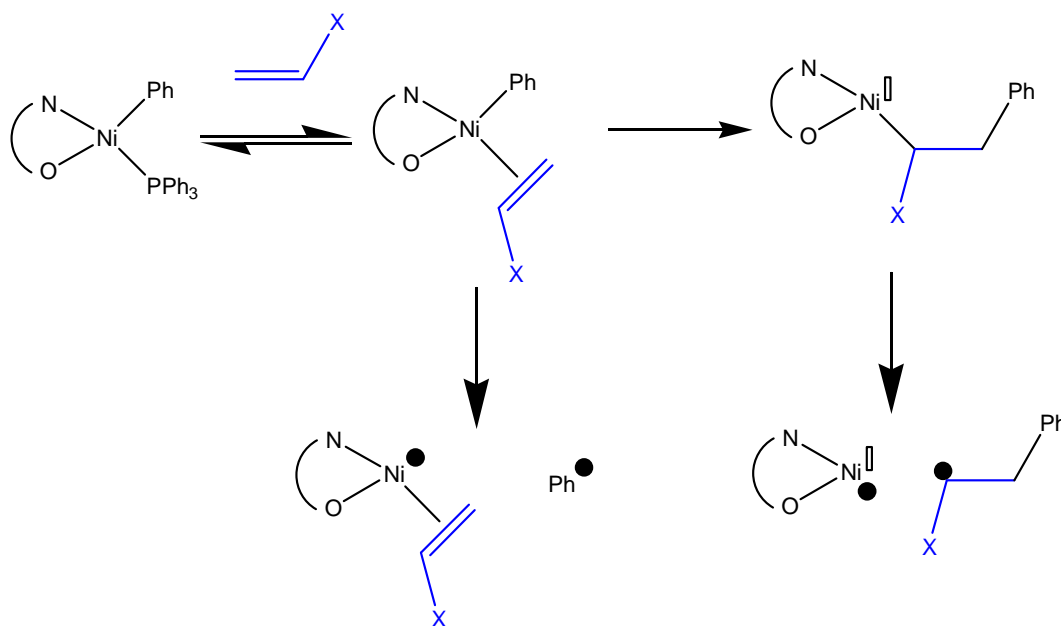


Figure 4. Schematically possible radical initiation by NiNO with $\text{CH}_2=\text{CHX}$ a polar vinyl monomer (2,1 and 1,2 insertion could take place)

2. Effect of additional AIBN on the radical polymerization initiated by NiNO

a) Case of MMA polymerization

NiNO is able to initiate the polymerization of some polar vinyl monomers but the conversion remains low (<10%). In order to increase the efficiency of the free radical

polymerization of MMA we add to the solution $\frac{1}{2}$ molar equivalent of AIBN per NiNO (see Figure 5).

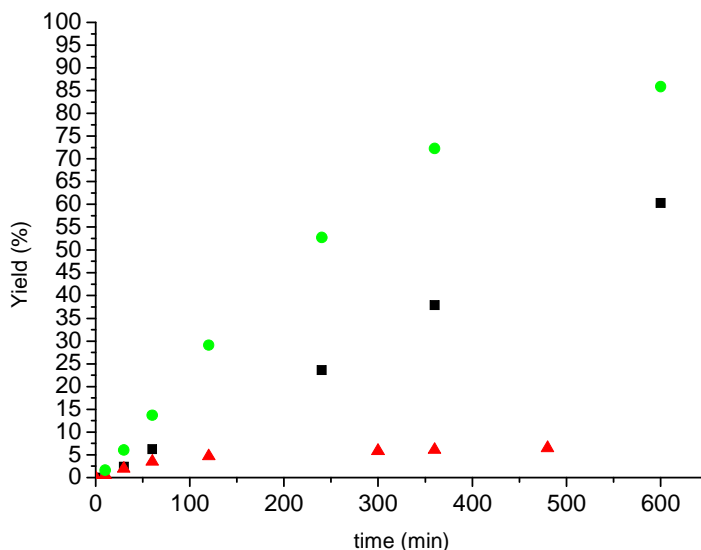


Figure 5. Reaction profiles of the free radical polymerization of MMA. Polymerizations are performed at 70°C in 40 mL of toluene with 10 mL of MMA with ■ 27μmol of AIBN, ▲ 54μmol of NiNO, ● 27μmol of AIBN and 54μmol of NiNO

In all cases 1st order kinetics of free radical kinetic profiles are obtained since $\ln \frac{1}{1-x}$ is proportional to time. AIBN is more efficient than NiNO alone to polymerize MMA. The best system is the addition of both initiators in which conversion reaches almost 85% in 10 hours.

If we assume that the propagation rate (k_p) and termination rate (k_t) remain constant in each experiment (therefore NiNO acts only as a initiator of a radical polymerization), the efficiency factor for NiNO can be estimated.

$$\ln \frac{1}{1-x} = k_p \sqrt{\frac{2fk_d[I]_0}{k_t}} \left(1 - \exp \frac{-k_d t}{2} \right)$$

Therefore, for NiNO initiation alone $f[I]_{NiNO} = 0.15[NiNO]$, consequently either all NiNO are poorly efficient initiators or only 15% of NiNO form an efficient initiator. The later possibility is in agreement with the initiation mechanism dependent on the monomer proposed in the Figure 4.

With both initiators a synergy is observed as the rate of polymerization with NiNO and AIBN is over the sum of polymerization rate with each compound

($R_{P_{NiNO+AIBN}} > R_{P_{NiNO}} + R_{P_{AIBN}}$). However, if we assume that $f[I]_{NiNO} = [NiNO]$ (therefore a NiNO efficiency factor gets close to 100%) then equality is obtained. Consequently the addition of AIBN to the system increases dramatically the efficiency of NiNO initiation.

This effect can be due to the interaction of the AIBN nitrile function and/or the organic radical with NiNO. However, this increase of the NiNO efficiency factor is not due to the nitrile function of AIBN since radical polymerization of MMA with NiNO and one molar equivalent of isobutyronitrile (IBN) per Ni does not disturb significantly the reaction profile. Consequently it is the interaction of the organic radical with the NiNO complex which increases the efficiency of the initiation.

b) Case of styrene polymerization

A similar set of experiments is performed with styrene instead of MMA leading to comparable findings (see Figure 6).

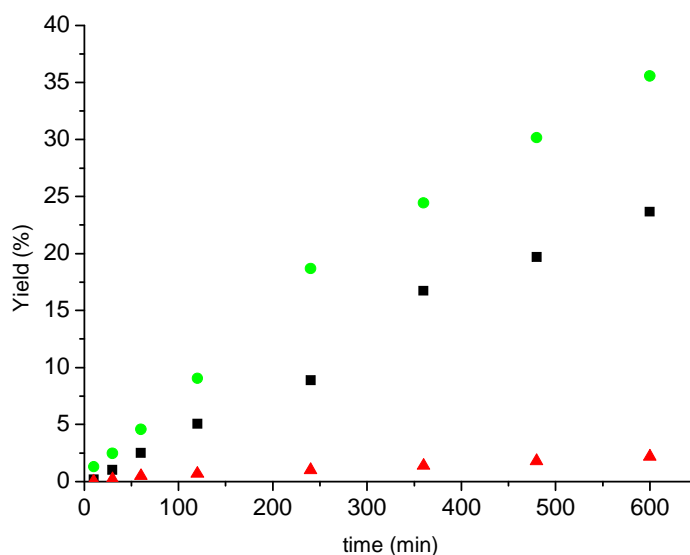


Figure 6. Reaction profiles of the free radical polymerization of styrene. Polymerizations are performed at 70°C in 40 mL of toluene with 10 mL of styrene with ■ 27μmol of AIBN, ▲ 54μmol of NiNO, ● 27μmol of AIBN and 54μmol of NiNO

Once again having NiNO and AIBN together is the most efficient system and conversion reaches 35 % in 10 hours.

NiNO initiation parameters can be estimated if we assume that the propagation rate and termination rate of styrene are independent of the initiator. Then calculation predicts that

$f[I]_{NiNO} = 0.25[NiNO]$. Once again, two possibilities exist: either only a low fraction of NiNO act as initiator or NiNO is a poorly efficient radical initiator.

In the presence of the two initiators, a synergy effect is also observed and the effective efficiency factor of NiNO appears to reach 100%.

Since NiNO initiation does not give similar efficiencies and half-life times in styrene and MMA polymerization, we assume that the real initiator is not NiNO itself but another species such as a complex between Ni and the monomer, which explains the differences in behaviors (see Figure 7). Indeed since the actual initiators are different their parameters (efficiency factor and half-life time) will differ as well. Consequently, NiNO is not a poor radical initiator but only a small fraction of the initial NiNO quantity acts as an initiator.

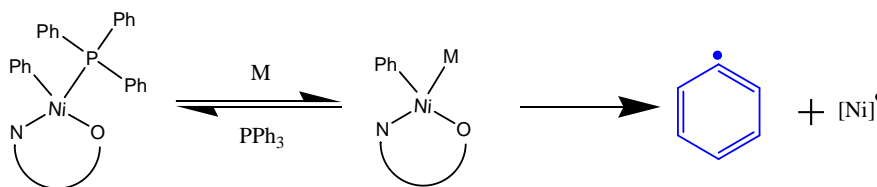


Figure 7. Proposed NiNO decomposition mechanism, with M a monomer

If the real initiator is a complex between nickel and the monomer, other additional ligands could be added in the system in order to modify half-life time and efficiency factor of the initiator (see section C.1). Alexandra Leblanc already observed this ligand effect since she reported that BuA polymerization initiated by NiNO is only efficient in presence of additional triphenyl phosphine [3].

Finally, it should be underlined that the real initiation mechanism remains unknown and it could also be a cleavage of the nickel carbon bond after a first insertion of the polar vinyl monomer.

3. Effect of additional AIBN on the ethylene catalytic polymerization

NiNO is also a well known ethylene polymerization catalyst [8]. In this section we investigate the effect of AIBN on the catalytic polymerization of ethylene initiated by NiNO. In this purpose, we perform the polymerization in toluene under several ethylene pressures at 70°C using 20 mg of NiNO with or without ½ molar equivalent of AIBN in 50 mL of toluene.

It should be noted that under these experimental conditions AIBN alone does not produce polyethylene by a free radical mechanism. Indeed only 2 mg of AIBN are present in the solution. At this low concentration, AIBN can produce some polyethylene in THF under

high ethylene pressure (0.2 g under 250 bar at 70°C during 4 hours), however in THF no polymerization occurs using NiNO alone (THF probably poisons the catalyst).

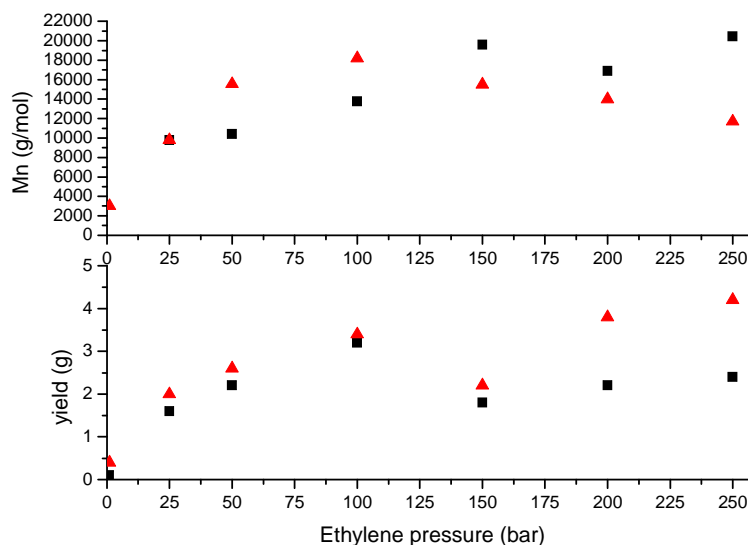


Figure 8. Influence of ethylene pressure on yield and PE molecular weight.*
Polymerizations are performed at 70°C in 50 mL of toluene during 4 hours with 20 mg of NiNO and without AIBN (■) or with ½ molar equivalent AIBN (▲).
 *: determined by HT-SEC

Yield increases with ethylene concentration. The drop observed between 100 bar and 150 bar of ethylene pressure correspond to the transition between monophasic and biphasic polymerization medium (see chapter II).

Surprisingly the AIBN does not deactivate the polymerization of ethylene. Indeed higher activities are observed in the presence of AIBN. These activation effects remain tiny below 100 bar of ethylene pressure (below 20%). Over it, activation up to 70% (at 250 bar of ethylene pressure) is obtained.

Using NiNO alone, Mn increases with ethylene pressure until reaching a plateau at 150 bar. In the presence of AIBN, Mn increases then decreases over 100 bar of ethylene pressure.

PEs synthesized in the presence of AIBN exhibit higher Mn below 100 bar of ethylene pressure and lower over 150 bar. The number of PE chain synthesized per Ni is similar below 100 bar but dramatically increases with the presence of AIBN over 150 bar of ethylene pressure.

Moreover PE melting point decreases of about 5°C in the presence of AIBN. Since these PE exhibit high molecular weights, this decrease must be due to an increase of the branching content.

These results may indicate that the nitrile function of AIBN interacts with NiNO. However polymerizations are performed with varying amount of isobutyronitrile (IBN) as AIBN analogue and no trend on the yield, molecular weight and melting point is observed (see Table 1).

Table 1. Influence of isobutyronitrile on the catalytic polymerization of ethylene^a

IBN/NiNO (mol/mol)	Activity (g/mmol/h)	Molecular weight (g/mol) ^b [PDI] ^b	Melting point (°C) ^c
0	95	9800 [2.3]	115.8
0.1	98	10500 [2.5]	115.2
0.5	93	10200 [1.9]	116
1	103	9500 [2.1]	114.7
2	96	12000 [2.2]	115.3
5	100	10000 [2.0]	111.2
10	90	8900 [2.5]	112.3
100	85	11500 [2.7]	110.3

^a: Polymerizations are performed during 1 hour using 50 mg of NiNO at 70°C in 250 mL of toluene. ^b: determined by HTSEC. ^c: determined by DSC.

Consequently the increase in activity and of the number of PE chain per Ni is due to an interaction between the AIBN radical and the catalyst itself during the polymerization (see Figure 9).

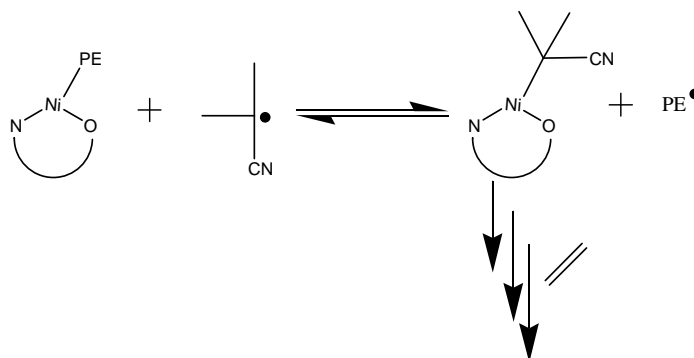


Figure 9. Possible interaction between catalyst and radical

Indeed this figure shows that AIBN radical can act as a chain transfer agent and therefore increases the number of PE chain per Ni.

The increase of activity can be due to the reactivation of “dead” catalyst by AIBN radical. Indeed we demonstrate that NiNO may suffer at 70°C a homolytic cleavage of the nickel carbon bond. Therefore if this cleavage also takes place during the ethylene polymerization, this could be a deactivation pathway of the NiNO ethylene polymerization catalyst. Then AIBN radical can recreate the metal-carbon bond and therefore regenerates in-situ an ethylene catalyst. Consequently this reactivation mechanism increases the activity of the ethylene polymerization catalyst (see Figure 10).

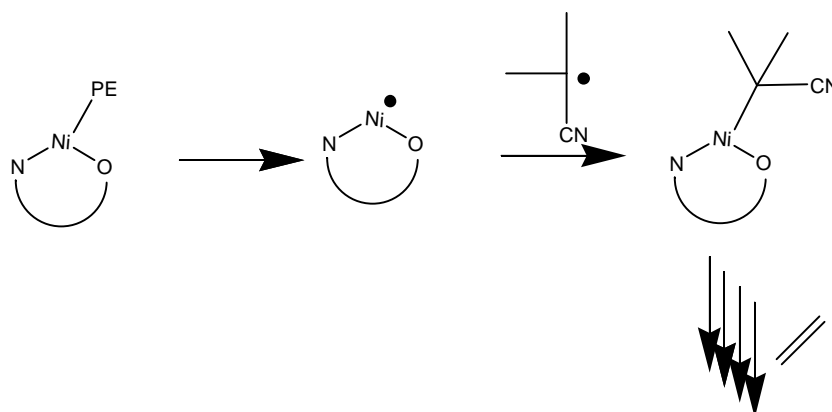


Figure 10. Proposed reactivation mechanism of NiNO by AIBN

B. Mechanistic investigation

NiNO is a catalyst which reveals some specific behaviors in presence of radicals. Indeed we demonstrated that NiNO can initiate the free radical polymerization of MMA and styrene in solution. The efficiency of this initiation step remains low and monomer dependent. However in presence of AIBN, the initiation by NiNO becomes almost 100% efficient.

Moreover the addition of AIBN during the polymerization leads to higher activity and a larger number of chains per nickel. Then it seems that AIBN radical can interact with NiNO catalyst via a transfer reaction during the ethylene catalytic polymerization.

Consequently we demonstrated that this NiNO complex is not only an ethylene polymerization catalyst but also an initiator of radical polymerization (see Figure 11). The mechanisms of initiation of radical polymerization as well as the synergy with AIBN need to be investigated.

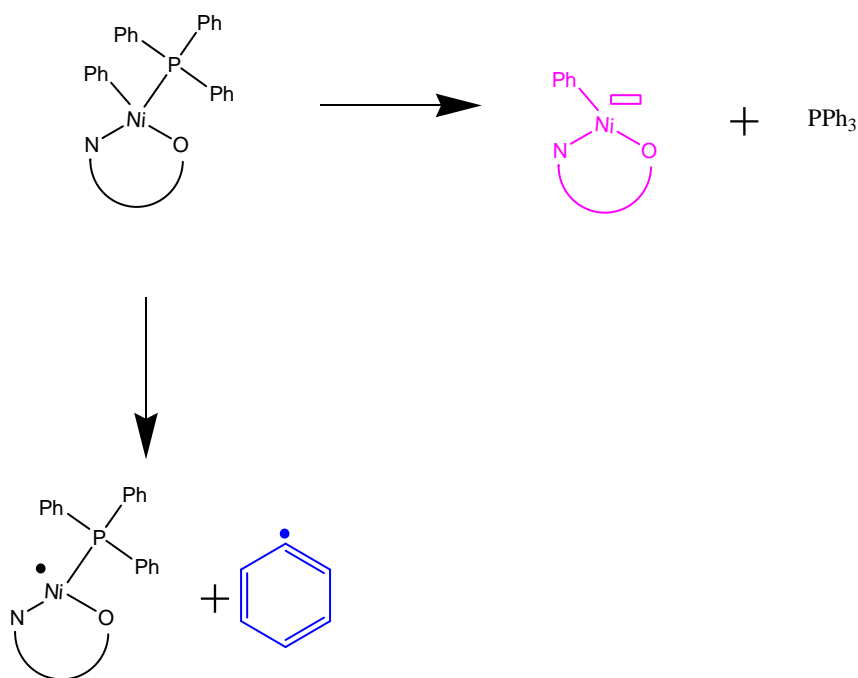


Figure 11. Ambivalence of the NiNO complexes

1. Two different possible mechanisms

We demonstrate that NiNO can suffer a homolytic cleavage of the nickel-carbon bond. This cleavage controls the average length of blocks during the hybrid radical/catalytic copolymerization.

a) With no additional source of radical

With no additional source of radicals the mechanism of hybrid radical/catalytic polymerization can be summarized as follow.

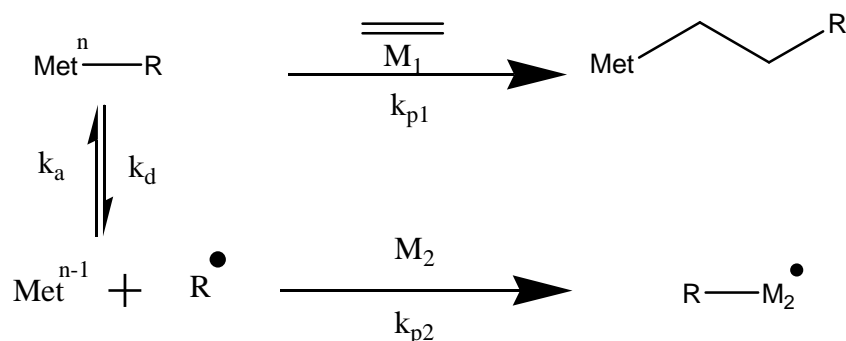


Figure 12. Schematic kinetic steps of the polymerization with no additional radical source

If we assume that k_d and k_a are independent of the R fragment as well as k_{p1} and k_{p2} then the average block length can be estimated by simple kinetic calculations.

$$L_1 = \frac{k_{p1}[M_1]}{k_d} \quad (1)$$

$$L_2 = \frac{k_{p2}[M_2]}{\sqrt{k_d k_a [\text{Met-R}]}} \quad (2)$$

Usually as the component (Met-R) is quite stable ($t_{1/2}$ about 200 min at 70°C) propagation rate is orders of magnitude over k_d and k_a . Therefore average block lengths can be extremely long and only diblock copolymers could be synthesized.

In order to decrease this average block length an additional radical source need to be added to the system. Indeed to obtain shorter block with monocomponent systems k_a and k_d should be in the same order of magnitude than k_{p1} and k_{p2} . However no organometallic ethylene polymerization catalyst with this kind of specification is known yet (Cobalt complexes involved in the CMRP can be considered as potential candidates but they do not homopolymerize ethylene.)

b) With an additional source of radicals

Consequently an additional source of radicals is used in order to artificially increase the exchange rate between radical and catalytic polymerization and therefore decrease the average block length (see Figure 13).

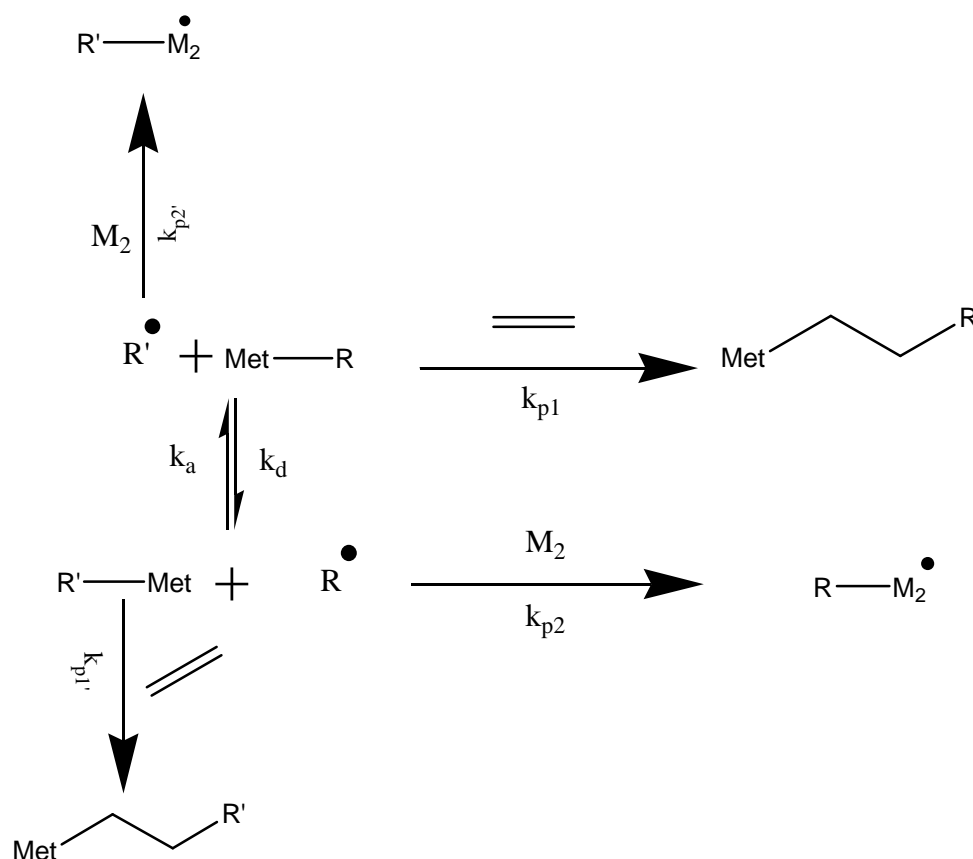


Figure 13. Schematic kinetic steps of the polymerization with an additional radical source

This figure summarizes the ideal bi-component hybrid polymerization. Indeed ethylene does not interfere during the radical polymerization and the polar vinyl monomer does not interfere during the catalytic one.

We assume that $k_{p1'}$ is equal to k_{p1} as well as $k_{p2'}$ to k_{p2} . The exchange mechanism can be performed by S_{R1} and/or S_{R2} therefore $k_a = k_d = k$ (because $v_a = v_d$).

Therefore average block length can be calculated.

$$L_1 = \frac{k_{p1}[M_1]}{k[R^\bullet]}$$

$$L_2 = \frac{k_{p2}[M_2]}{k[Met-R]}$$

This exchange may be more efficient than the previous one. Then average block length would be shorter.

Two different exchange mechanisms can be assumed: radical substitution of type 1 (S_R1) or type 2 (S_R2) equivalents to S_N1 and S_N2 .

(1) *Exchange type S_R1*

S_R1 can be characterized by the presence of Met^{n-1} , which is for NiNO Ni^I species (see Figure 14).

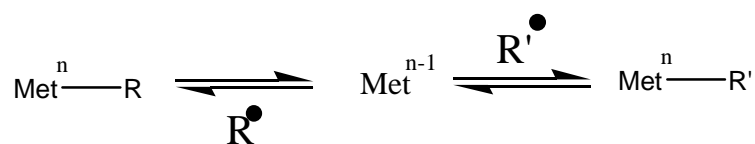


Figure 14. S_R1 mechanism

(2) *Exchange type S_R2*

S_R2 can be characterized by the presence of Met^{n+1} , which is for NiNO Ni^{III} species (see Figure 15).

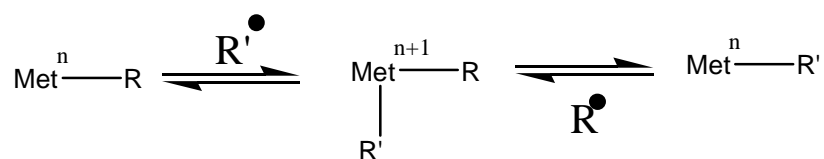


Figure 15. S_R2 mechanism

Consequently the mechanism of exchange can be identified by isolating Ni^I or Ni^{III} using spectroscopic techniques. As both of these compounds are paramagnetic, EPR (Electron Paramagnetic Resonance) technique is used.

2. Evidence of the homolytic cleavage of the Ni carbon bond

Firstly, direct evidence of the cleavage of the metal carbon bond need to be found. In this purpose a concentrated solution of NiNO (5 mL of toluene with 250 mg of NiNO) is heated at 70°C during 24 hours, the coupling product of phenyl radical, biphenyl, is then identified by GC-MS (see Figure 16 and Figure 17).

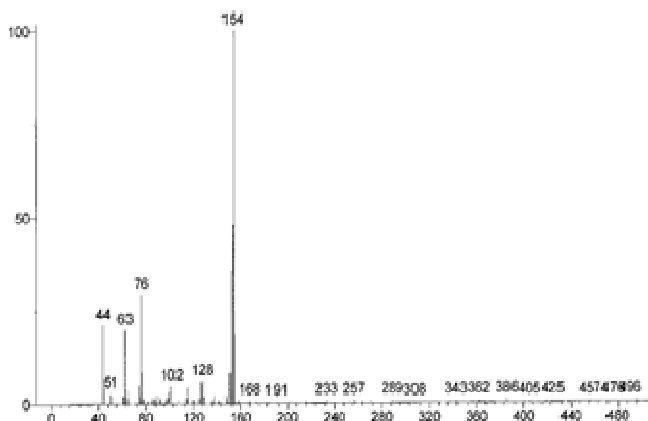


Figure 16. Experimental mass spectrum obtained

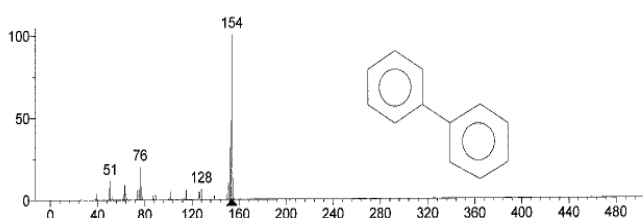


Figure 17. Theoretical mass spectrum of biphenyl

Experimental (Figure 16) and theoretical (Figure 17) mass spectra are correlated. Since no coupling product is obtained with unheated NiNO, this molecule is not produced during the analysis. Consequently, biphenyl is synthesized when NiNO is heated. This result is in agreement with a homolytic cleavage of the nickel phenyl bond and could explain the deactivation of the catalyst at high temperature.

To go further EPR spectroscopy is performed at 110 K (see Figure 18) on a solution of NiNO in toluene. Three signals characteristic of a Ni^{I} anisotropic complex are observed ($g_1=2.019$, $g_2=2.208$, $g_3=2.340$). It should be noted that the last signal (at high field) is observed without EPR probe and corresponds to a contamination of the EPR cavity.

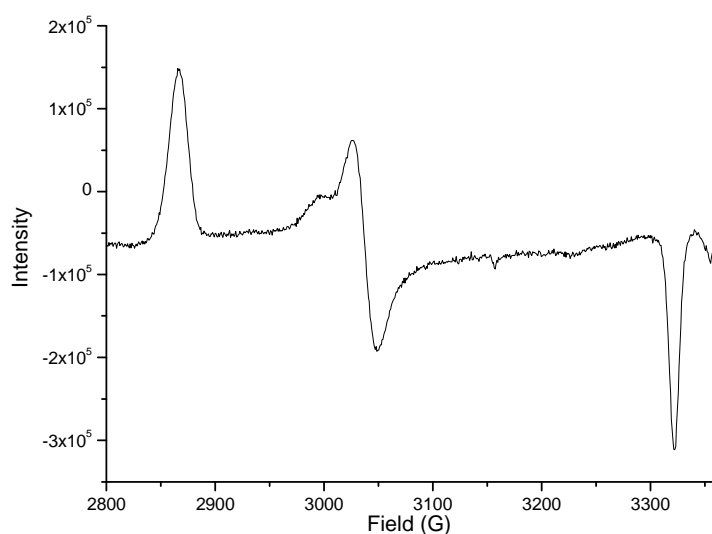


Figure 18. EPR spectrum of Ni^I (Acquisition from 2800 G to 3400 G in 5min, 10 G of modulation at 9 dB at 110 K)

This spectrum indicates that the Ni^I complex is strongly anisotropic. Only one species is present and in low concentration (indeed acquisition parameters are tuned to obtain this signal while in the most usual cases the signal of a paramagnetic species is so intense that the cavity signal can not be seen which is not the case for NiNO).

Moreover no hyperfine coupling with phosphorous atoms is observed, consequently either no initial triphenyl phosphine is present on the Ni^I or the orbital which possesses the single electron does not expand on triphenyl phosphine ligand (for example d_{xy}^1 with phosphine along z axis).

However we assume that phosphine plays a predominant role in the homolytic cleavage since Alexandra Leblanc demonstrated that the radical polymerization of BuA is only efficient with additional triphenyl phosphine [3]. Consequently triphenyl phosphine should interact with the initiator system and be present in the resulting Ni^I species.

At 70°C we observe a unique signal $g_{iso}=2.192$. This corresponds to the average of g_1 , g_2 , and g_3 ($\frac{g_1 + g_2 + g_3}{3}=2.189$) therefore the same complex is observed at high temperature as expected.

Finally an organic radical signal can be also identified by EPR (see Figure 19) but the resolution is too low to determine the hydrogen hyperfine coupling and therefore the

chemical structure of this radical. This spectrum must be accumulated at lower temperature in liquid helium in order to confirm the expected phenyl radical structure.

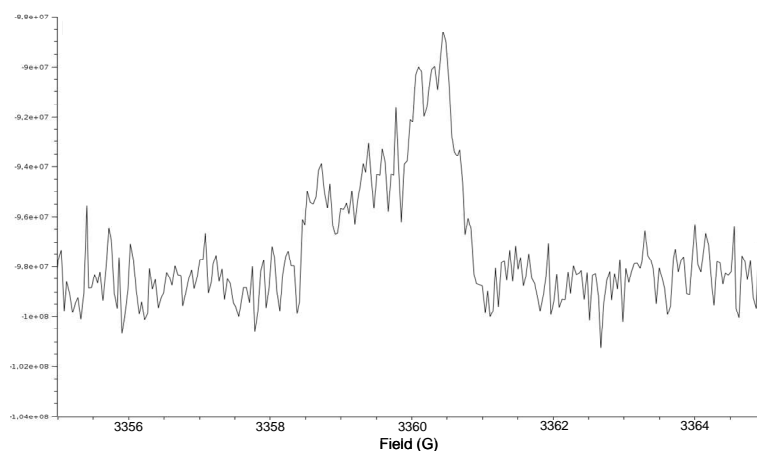


Figure 19. EPR signal of a organic radical (Accumulation of 2000 scans from 3315 G to 3395 G in 2 sec, 0.1G of modulation at 33 dB at 110 K)

In addition this organic radical resonance is in agreement with a carbon radical (not O, N, or I radical). This EPR signal is extremely weak and 2000 scans need to be accumulated to observe this radical signal. This indicates that concentration of radical is low due to their efficient coupling in order to product diphenyl.

The same behaviour is observed for Ni^{I} as the signal disappears if the sample is heated for too long (after 30 min no signal remains). Therefore two Ni^{I} species may dimerize to produce a diamagnetic bimetallic complex.

3. Evidence of the radical addition on NiNO

If we perform the EPR spectrum of NiNO in toluene in presence of $\frac{1}{2}$ molar equivalent of AIBN at 70°C we observe three signals (see Figure 20). The same g_{iso} of the Ni^I previously observed, g_{iso} corresponding to organic radical (at high field) and an intermediate g_{iso} at 2.07. This last species could be a Ni^{III} species.

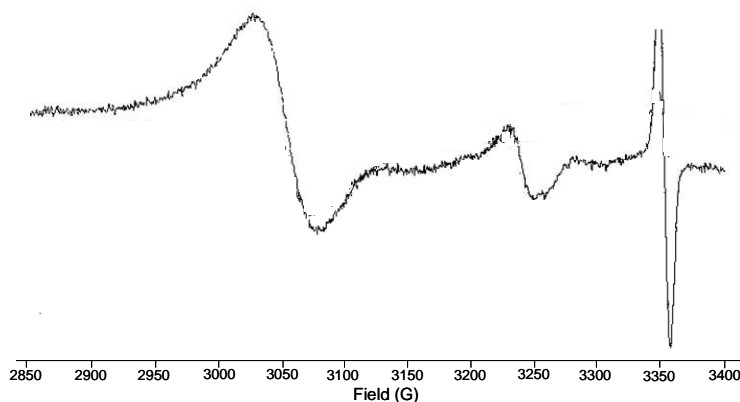


Figure 20. EPR spectrum at 70°C of NiNO in presence of AIBN (Acquisition from 2800 G to 3400 G in 5min, 10G of modulation at 9dB)

We are unable to clearly identify a peak at 110 K in order to determine the exact nature of the paramagnetic specie. However the g_{iso} obtained at 70°C is close to 2 indicating a more intern single electron therefore a higher oxidation degree. As only nickel is present in the EPR tube we assume that this signal corresponds to a Ni^{III} species.

Consequently, EPR proves that Ni^I and Ni^{III} species are generated in similar experimental conditions therefore S_R1 and S_R2 mechanism can take place at the same time. The same Ni^I species seems to be present during the S_R1 mechanism and the homolytic cleavage of NiNO without AIBN, consequently the spontaneous nickel carbon fragmentation mechanism may be very close to the one during S_R1 .

For both observed paramagnetic species, the presence of triphenyl phosphine on nickel atom can not be determined since no phosphorous hyperfine coupling is observed.

4. Case of NiPO

Alexandra Leblanc also used NiPO (see Figure 21) as a radical initiator [3-5]. This catalyst for ethylene polymerization can polymerize MMA and Sty in similar experimental conditions than NiNO.

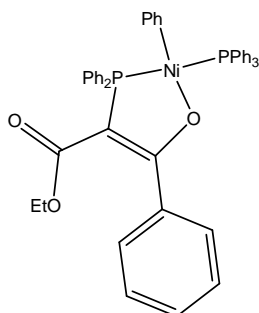


Figure 21. NiPO catalyst

We perform a similar study than with NiNO. For MMA polymerization, NiPO system seems more efficient since half life time of 300 min and efficiency factor of 70% are measured. However, no synergy effect with AIBN is identified: the same efficiency factor and half-life time is obtained with or without AIBN.

Moreover the ethylene polymerization initiated by NiPO is almost totally deactivated by the addition of ½ equivalent of AIBN to the system. Indeed activity without AIBN is equal to $7.5 \cdot 10^3 \text{ g mmol}^{-1} \text{ h}^{-1}$ at 70°C under 20 bar of ethylene pressure during 30 min using 20 mg of NiPO in 250 mL of toluene compared to $1.3 \cdot 10^3 \text{ g mmol}^{-1} \text{ h}^{-1}$ in the presence of AIBN.

This catalyst is also promising, however no synergy takes place between radical and catalytic polymerization (AIBN inhibits the catalytic polymerization and acts as spectator of the MMA polymerization initiated by NiNO). Moreover EPR and GC-MS do not indicate any direct evidence of the homolytic cleavage on the nickel carbon bond (no biphenyl, Ni^{I} and Ni^{III} species have been observed).

Moreover, the polyethylenes synthesized possess low molecular weight ($M_n < 1000 \text{ g/mol}$). Consequently we did not further study this compound for hybrid catalytic/radical polymerization.

C. Study of the phosphine effect during PMMA and PE syntheses

Mechanistic study is unable to confirm the role of phosphine in the cleavage process of the nickel carbon bond while it is experimentally observed that the addition of phosphine favors the homolytic cleavage. Indeed Alexandra Leblanc [3] demonstrated that BuA polymerization is initiated by NiNO only in presence of additional PPh₃. Moreover, MMA and styrene polymerizations are also activated by the addition of phosphine. These results indicate that an interaction must exist between phosphine and NiNO.

In this section we investigate the interaction between phosphines and NiNO. For this purpose we perform MMA polymerizations and ethylene polymerizations both initiated by NiNO in the presence of additional phosphorous ligand.

1. Influence of phosphorous ligand on the radical polymerization of MMA

These series of experiments are performed at 70°C in 40 mL of toluene with 10 mL of MMA, using 50 mg of NiNO and 3 molar equivalents of phosphorous atoms per Ni. In all this section, we will assume that propagation and termination rates remain unchanged whatever the additional phosphorous ligand used and we will discuss only on an initiation step variation (half-life time and efficiency factor) caused by phosphine ligand addition.

a) Effect of triphenyl phosphine

Firstly we compare the polymerization of MMA with and without additional triphenyl phosphine (see Figure 22).

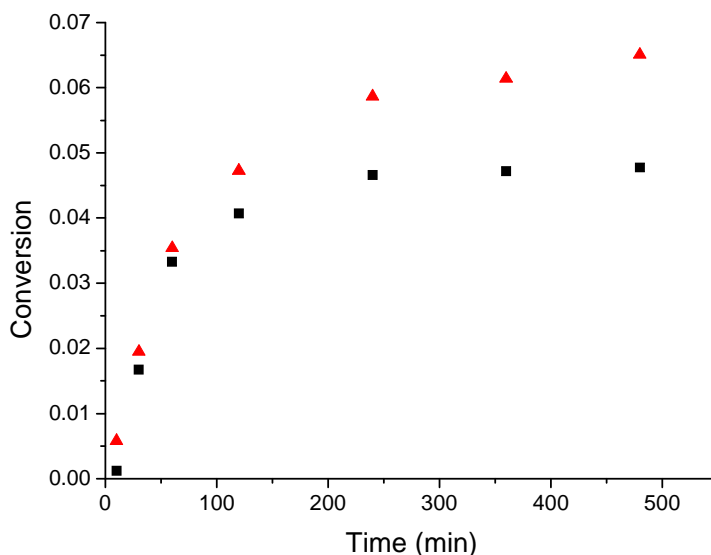


Figure 22. Impact of triphenyl phosphine on the radical polymerization of MMA initiated by NiNO. 50 mg of NiNO at 70°C in 40 mL of toluene and 10 mL of MMA without ■ or with ▲ 3 eq of PPh₃

Surprisingly, the reaction profiles are different. Indeed polymerization is more efficient in presence of triphenyl phosphine. The initial rate of polymerization is equivalent however the half-life time increases of about 20 min to reach 220 min in the presence of PPh₃. This increase explains most of the raise in yield obtained since the efficiency factor remains almost unchanged (it only slightly increases).

Consequently, the addition of triphenyl phosphine impacts the initiator system itself and reduces the dissociation rate of the nickel carbon bond. Moreover since initial rate of polymerization is identical the efficiency factor of the initiator may also increase.

These results prove that the phosphine is not spectator of the initiation but must interact with the NiNO complex. Since NiNO is already complexed by a triphenyl phosphine another coordination position must be used in order to modify the kinetic of the cleavage.

Moreover, when additional PPh₃ is added no signal of Ni^I and Ni^{III} species is observed in EPR investigations. This could indicate that the coupling of paramagnetic species is more efficient in the presence of PPh₃. Consequently we propose this type of mechanism (see Figure 23).

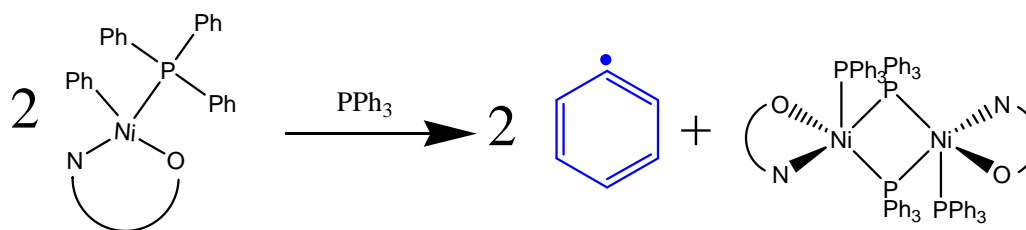


Figure 23. Proposed mechanism for triphenyl phosphine effect

Moreover ³¹P NMR shows that new signals appear which indicates that other phosphine ligand coordinations take place. Indeed the ³¹P NMR spectrum performed after heating the NMR tube during 1 hour at 70°C shows four signals: 23.5 ppm corresponding to the initial coordinate PPh₃, -5.3 ppm of free PPh₃, and two signals at 24.3 and 23.3 ppm which can be attributed to the proposed bimetallic Ni^I species.

b) Effect of other phosphines

Since triphenyl phosphine impacts the reaction profile, other phosphine ligand can also be used in order to modify the kinetics of the MMA polymerization initiated by NiNO. The next figure shows some examples of reaction profiles obtained in the presence of various phosphines.

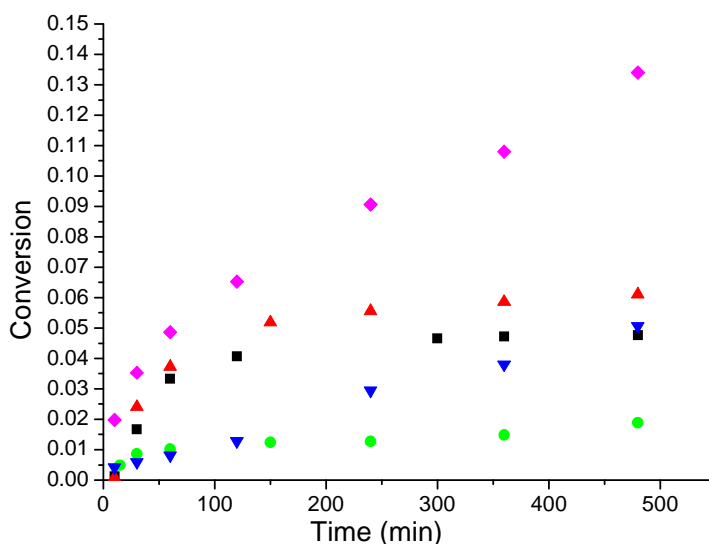


Figure 24. Impact of phosphine ligand on the radical polymerization of MMA using 50 mg of NiNO at 70°C in 40 mL of toluene and 10 mL of MMA without ■ or with 3 eq. of ▲ P(o-Tol)₃, ● PCy₃, ▼ PBu₃, ◆ P^tBu₃

As expected, reaction profiles are strongly impacted by additional phosphine. For example in the presence of PBu_3 (▼) the profile is almost linear indicating a high half-life time of the initiator. In the presence of P^tBu_3 (◆) higher yields are obtained and conversions reaches 14% in 8 hours. Polymerization can also be slowed down for example in the presence of PCy_3 (●).

Consequently, phosphine ligand strongly influences the initiation mechanism. Some phosphines raise the efficiency factor of the initiator while other decrease it, moreover half-life time can also be increased or decreased.

c) Effect of phosphites

Similar identical series of experiments are performed using phosphite ligands (see Figure 25).

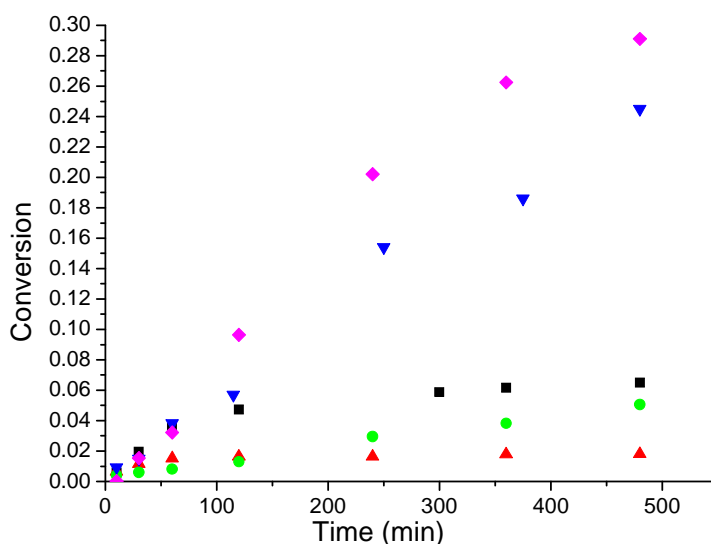


Figure 25. Impact of phosphite ligands on the radical polymerization of MMA using 50 mg of NiNO at 70°C in 40 mL of toluene and 10 mL of MMA with 3 eq of ■ PPh₃, ▲ P(OPh)₃, ● PBu₃, ▼ P(OBu)₃, ◆ P(OEt)₃

Phosphine and phosphite ligands exhibit totally different behaviors. Indeed aryl phosphites (▲) lead to less efficient polymerization than aryl phosphines (■). But alkyl phosphites (▼) are extremely efficient compared to their phosphines counterparts (●). In the presence of alkyl phosphite, conversion around 30% was reached in 8 hours with almost linear reaction profile indicating higher half-life time.

In order to understand all these results we perform QALE (Quantitative Analysis of Ligand Effects) analysis on half-life time and efficiency of our systems.

d) Rationalisation of the phosphorous ligand effect

Indeed mono-phosphorous ligands are usually described using QALE model by four independent parameters [9]:

- χ_d [10, 11] – describes the *s* electron donor capacity. A small χ_d value means a highly *s* electron donor. χ_d is from -0.9 to 43 for phosphorous ligands.
- θ [12] – corresponds to Tolman's cone angle. A large value of θ is associated with a large ligand. θ is from 87° to 184° for phosphorous ligands.
- Ear [13] – describes the secondary electronic effect (origin unknown). Originally called the 'aryl effect' because in association with aryl groups on phosphorous. Nowadays authors have found that this effect is not limited to aryl groups. For example, PCl_3 has one of the largest Ear value determined so far. We now refer to this effect as the 'Ear' effect. Ear range is from 0 to 4.1 for phosphorous ligands.
- π_p [14] – describes the *p* electron acceptor capacity (π acidity). A large value indicates a strong π acid. π_p range is from 0 to 13.2 for phosphorous ligand.

Here is a table of these parameters for the phosphorous ligand used:

Table 2. QALE parameters of phosphorous ligand used [9]

Ligand number	Phosphorous ligand	χ_d	θ	Ear	πp
1	PPh ₃	13.25	145	2.7	0
2	P(o-Tol) ₃	10.65	178	2.7	0
3	PBu ₃	5.25	136	0	0
4	P ^t Bu ₃	0	182	0	0
5	PCy ₃	1.4	170	0	0
6	P(C ₆ F ₅) ₃	34.8	184	4.1	0
7	P(p-MeO-Ph) ₃	10.5	145	2.7	0
8	P(OPh) ₃	23.6	128	1.3	4.1
9	P(OBu) ₃	15.9	110	1.3	2.7
10	P(OEt) ₃	15.8	109	1.1	2.9

In the presence of these phosphorous ligands half-life times cover a wide range from 60 to 360 min and efficiency factor from 4% to 100% during the MMA polymerization initiated by NiNO.

Therefore using these four parameters (χ_d , θ , Ear, πp), a linear relation is found with half life time and efficiency of the initiator. In the following figure, we plot relative half-life time ($t_{1/2}/t_{1/2PPh_3}$) and efficiency factor f/f_{PPh_3} vs. QALE parameters (see Figure 26).

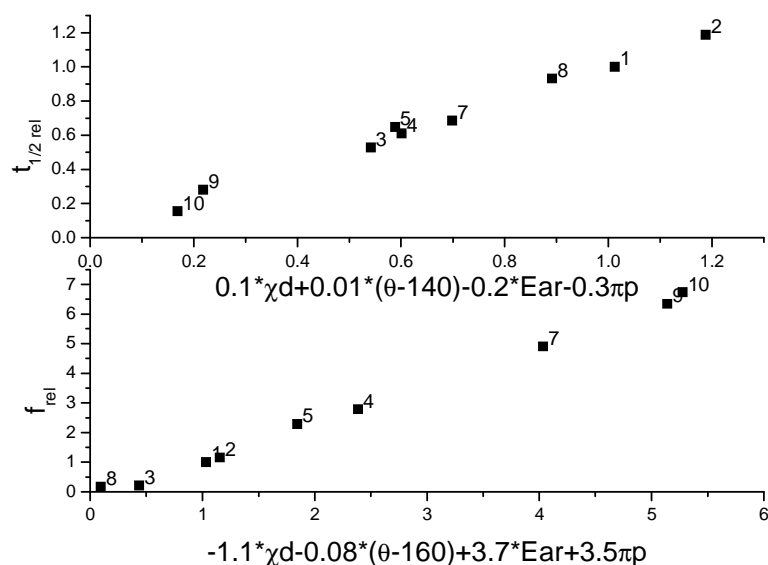


Figure 26. Master curves between QALE parameters and efficiency or half-life time of the initiator (labels correspond to ligand number in Table 2)

It should be noted that the correlation between $t_{1/2}$ and f with QALE parameters are different. Low s donation or high Tolman's angle increases half-life time but decreases efficiency. Different contributions are also obtained for the two other parameters.

In an overall view, strongly interacting phosphine (highly s donated, π retrodonated, low θ and high Ear) leads to low half-life time and high efficiency factor. Therefore a trade-off between QALE parameters must be done in order to obtain the best initiator systems. Indeed high half-life time will usually lead to low efficiency factor and *vice-versa*.

Since every phosphorous ligands which are less interacting than the initial PPh_3 impact the polymerization in this case at least two ligands (PPh_3 and the additional phosphorous ligand) must interact with NiNO during the initiation mechanism. Indeed less interacting ligand cannot replace the initial phosphine and consequently impact the initiation mechanism. For ligands more interacting than PPh_3 , one or more phosphorous ligands can be involved (see Figure 27).

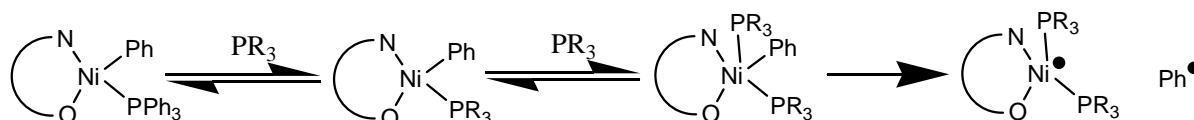


Figure 27. Proposed mechanism for the impact of phosphorous ligand on initiation mechanism (in the case of a lowly interacting ligand, the first equilibrium does not take place)

e) Case of multidentate phosphine ligands

In order to access a better understanding of the system we perform the polymerization using different di-, tri- or tetraphosphines using 3 molar equivalents of phosphorous atoms per Ni.

For tri- and tetraphosphines, no effect is observed. Indeed the three multidentate phosphines investigated (see Figure 28) do not lead to different reaction profiles except for lower efficiency than the one predicted by the master curve (Figure 26), due to a concentration effect.

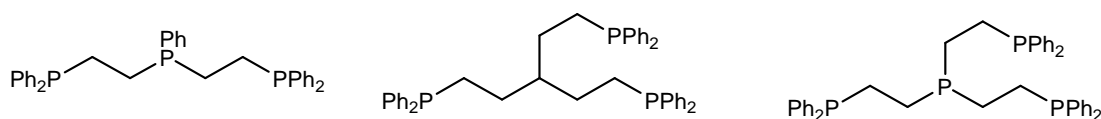


Figure 28. Tri- and tetraphosphines studied

However with diphosphine, a bidentate coordination effect is observed (reaction profile is not in agreement with the master curve obtained for monophosphine ligand) indicating that two phosphines may be involved in the initiation mechanism which is in agreement with our proposed mechanism (see Figure 23).

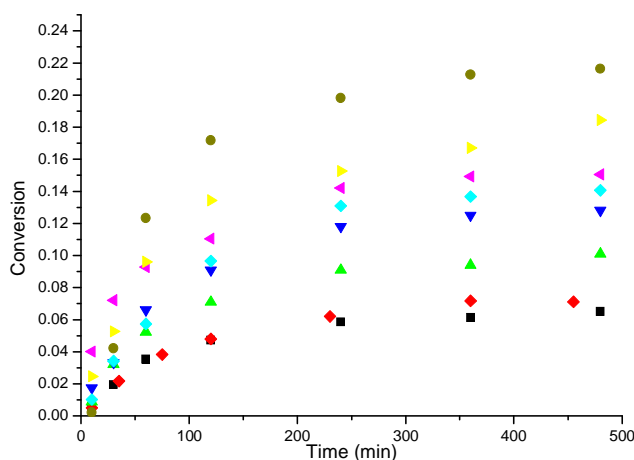


Figure 29. Impact of diphosphine ligands on the radical polymerization of MMA using 50 mg of NiNO at 70°C in 40 mL of toluene and 10 mL of MMA with 3 eq of ■ PPh₃, 1.5 eq. of ♦ DPPH, ▲ DPPM, ▼ DPPE, ◆ DPPP, ▲ DPPB, ► DPPPe, ● DPPH

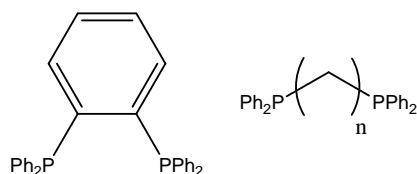


Figure 30. Diphosphine used with phenyl as spacer (DPPH) or alkyl (DPPM n=1 to DPPH n=6)

Triphenyl phosphine (■) and DPPh (◆) exhibit similar behavior therefore DPPh does not provide bidentate coordination effect. For other diphosphine yield increases with the length of the spacer between the two phosphines. In fact compared to the theoretical reaction profile obtained in the presence of 3 eq. $P(Ph)_3$ (the equivalent monophosphine), DPPM (▲) lead to lower yield and DPPE (▼) to DPPB (◀) exhibit similar reactivity profile. For DPPM it must be due to the impact of the second phosphorous atom on the QALE properties compared to the monophosphine.

Consequently only DPPPe (▶) and DPPH (●) exhibit a significant bidentate coordination effect. Half-life time remains almost unchanged but efficiency increases. This induces that the “bite angle” between the two phosphines should be over 100° (see Table 5). This infirms a square planar structure with an axial/equatorial complexation but is more compatible with a tetrahedral structure (see Figure 31).

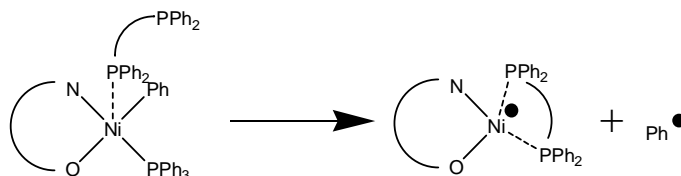


Figure 31. Schematic bidentate effect on the initiation by NiNO

It should be noted that since no tri- nor tetradentate coordination effects have been identified only two phosphorous atoms should be involved in the resulting species created after the homolytic cleavage of the nickel carbon bond.

2. Effect of the phosphorous ligand on the catalytic polymerization

Since phosphorous ligands strongly impact the homolytic cleavage of the nickel carbon bond, there should also exist an effect during the ethylene catalytic polymerization. Therefore the radical ethylene polymerization initiated by NiNO is investigated in the presence of phosphorous ligand.

It should be noted that this study is at the opposite of the usual use of NiNO, in which phosphine scavengers (such as $NiCOD_2$) are added in order to release the vacancy where ethylene will coordinate and therefore activate the ethylene catalytic polymerization. Therefore since ligand is added, a deactivation should be expected.

Since we demonstrated that phosphorous ligands induce effect on the homolytic cleavage of the nickel carbon bond which is a potential deactivation pathway of NiNO

ethylene polymerization catalyst, therefore we perform ethylene polymerization at lower temperature (50°C instead of 70°C) in order to study the effect of ligand on the catalytic polymerization only, with negligible loss of metal carbon bond via homolytic cleavage.

As mentioned before, in these experimental conditions, no radical polymerization of ethylene takes place.

Consequently polymerizations are performed using 20 mg of NiNO and 1 molar equivalent of phosphorous atom per Ni in 250 mL of toluene at 50°C during 1 hour under 20 bar of ethylene pressure.

a) Effect of phosphines

Results are summarized in the following table.

Table 3. Phosphines effects on the ethylene polymerization by NiNO catalyst^a

Additional phosphine	Activity (g mmol ⁻¹ h ⁻¹)	Mn (g/mol) ^b [PDI] ^b	Melting Temperature (°C) ^c
-	94.7	7150 [2.2]	117.9
PPh ₃	209	16150 [2.2]	118.1
P(o-Tol) ₃	146	14200 [1.9]	113.3
PBu ₃	1.1	nd [nd]	nd
P ^t Bu ₃	40.6	nd [nd]	118.1
PCy ₃	201	23700 [2.1]	118.0
P(C ₆ F ₅) ₃	135	10600 [2.1]	110.9
P(p-MeO-Ph) ₃	96.1	16300 [2.3]	115.6

^a: Polymerizations are performed during 1 hour using 20 mg of NiNO at 50°C in 250 mL of toluene under 20 bar of ethylene pressure with 1 molar equivalent of PR₃. ^b: determined by HTSEC. ^c: determined by DSC.

As expected we observe a dependence of activity, PE molecular weight and melting point on phosphine ligands. However, surprisingly some additional ligands activate the catalytic polymerization of ethylene. Indeed triphenyl phosphine and tricyclohexyl phosphine induce an activation of the polymerization. Alkyl phosphines such as tributyl or tritertbutyl phosphine decrease the activity.

$P(o\text{-Tol})_3$ also slightly increases the activity but leads to a decrease of 5°C of the melting point. Similar findings are obtained in the presence of $P(C_6F_5)_3$. Only in the presence of these two phosphines an important decrease of melting point is observed.

MWD remains narrow whatever the phosphine used. Mn increases in the presence of phosphines. Indeed the number of chains per nickel remains almost constant for different phosphines (10-13 chains per Ni) except for $P(p\text{-MeOPh})_3$ (6 chains per Ni). This last phosphine exhibits a specific behavior since the activity remains almost unchanged and the melting point decreases only of 2°C but transfer constant is divided by a factor 2.

In conclusion, additional phosphines do not act as spectator during the ethylene polymerization. They induce change in activity, transfer constant and branches content.

b) Effect of phosphites

Ethylene polymerizations in presence of phosphites are also performed at 50°C (see Table 4).

Table 4. Phosphines and Phosphites effects on the ethylene polymerization by NiNO catalyst^a

Additional phosphorous ligand	Activity (g mmol ⁻¹ h ⁻¹)	Melting Temperature (°C) ^a
-	94.7	117.9
PPh ₃	209	118.1
P(OPh) ₃	14.1	117.5
PBu ₃	1.1	nd
P(OEt) ₃	53.5	119.2

^a: Polymerizations are performed during 1 hour using 20 mg of NiNO at 50°C in 250 mL of toluene under 20 bar of ethylene pressure. ^b: determined by DSC.

The presence of phosphites leads to low activity. However, the alkyl phosphite induces higher activity than the polymerization in the presence of alkyl phosphine counterpart. Moreover contrary to phosphine, the polymerization with aryl phosphite is less active than the one in the presence of alkyl phosphite.

c) Rationalization of the activity in presence of phosphorous ligands

Again using QALE model we can propose some tendency to explain the impact of ligand on activity with the four parameters of phosphorous ligand. For activity no master curve can be found which may indicate a change of mechanism depending on the phosphorous ligand used. Phosphines and phosphites seem to act by two different mechanisms but for each of them σ donation increase leads to a decrease of activity and so do π back donation, while bulkiness of ligand increase leads to an increase of the activity. A simple mechanism can nevertheless explain the activities observed (see Figure 32).

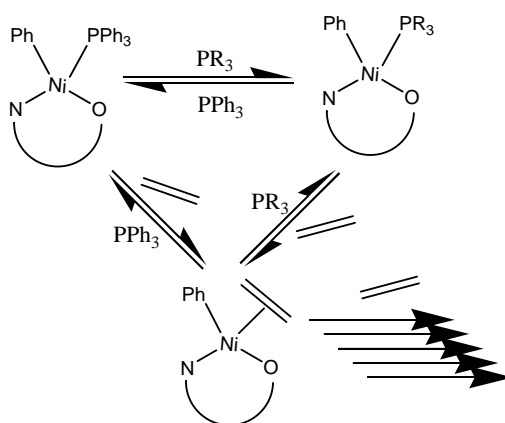


Figure 32. Proposed mechanism of interaction of phosphorous ligand during ethylene polymerization

The more interacting the phosphorous ligand is, the harder it will be for ethylene to coordinate and insert in the nickel carbon bond, consequently activity of the polymerization decreases. It is worthy to mention that this mechanism only explains the decrease of activity compared to the polymerization without additional ligand.

The activation of the polymerization by triphenyl phosphine can be explained using the axial coordination position demonstrated during the study of part C-1 (see Figure 33).

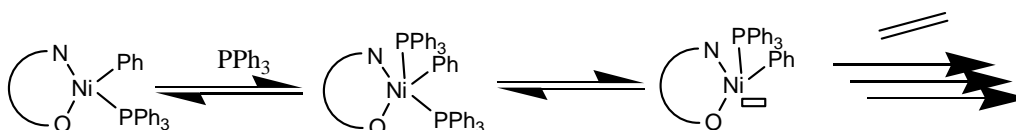


Figure 33. Proposed explanation for ligand activation of the ethylene polymerization

The axial PPh_3 coordination may favor the release of the *cis* vacancy and therefore increase the activity of the ethylene polymerization.

For melting point and number of chains per Ni, further investigations need to be performed in order to obtain more experimental evidences of influence of phosphorous ligand. Then some tendency could be observed.

d) Effect of diphosphines

We also investigate the effect of diphosphines. Results are summarized in the following table.

Table 5. Diphosphine effect on the ethylene polymerization by NiNO catalyst^a

Phosphine	Bite angle (°)	Activity (g mmol ⁻¹ h ⁻¹)	Mn (g/mol) ^b [PDI] ^b	Melting temperature (°C) ^c
-	-	94.7	7150 [2.2]	117.9
PPh_3	-	209	16150 [2.2]	118.1
DPPPh	109	201	18200 [2.1]	115.1
PEtPh_2	-	54.1	15794 [3.2]	119.6
DPPM	<80	117	16100 [2.3]	117.1
DPPE	85	155	12700 [2.5]	116.2
DPPP	91	120	18400 [2.2]	115.4
DPPB	98	21.7	11000 [1.9]	116.2
DPPPe	111	344	9450 [2.6]	111.8
DPPH	120	21.0	10100 [2.0]	114.4

^a: Polymerizations are performed during 1 hour with 20 mg of NiNO at 50°C in 250 mL of toluene under 20 bar of ethylene pressure. ^b: determined by HTSEC. ^c: determined by DSC.

Surprisingly a strong bidentate coordination effect has been observed. PPh_3 and DPPPh induce almost same activity and average molecular weight however PE synthesized in the presence of DPPPh possesses more branches as melting point decreases of 3°C .

For the other diphosphines series, diphosphine with spacer from 1 to 3 carbon length increases the activity of polymerization, and then in presence of DPPB or DPPH the polymerization is almost inefficient. DPPPe leads to the most efficient polymerization with activity of $344 \text{ g mmol}^{-1} \text{ h}^{-1}$. Moreover with this diphosphine, PE melting point decreases of 6°C indicating a higher chain-walking probability.

This very specific efficiency in the presence of DPPe indicates a well defined ethylene polymerization catalyst involving a chelate phosphine which fit only for a pentyl spacer. As N,O ligands can not be removed an octahedral geometry can be proposed (see Figure 34).

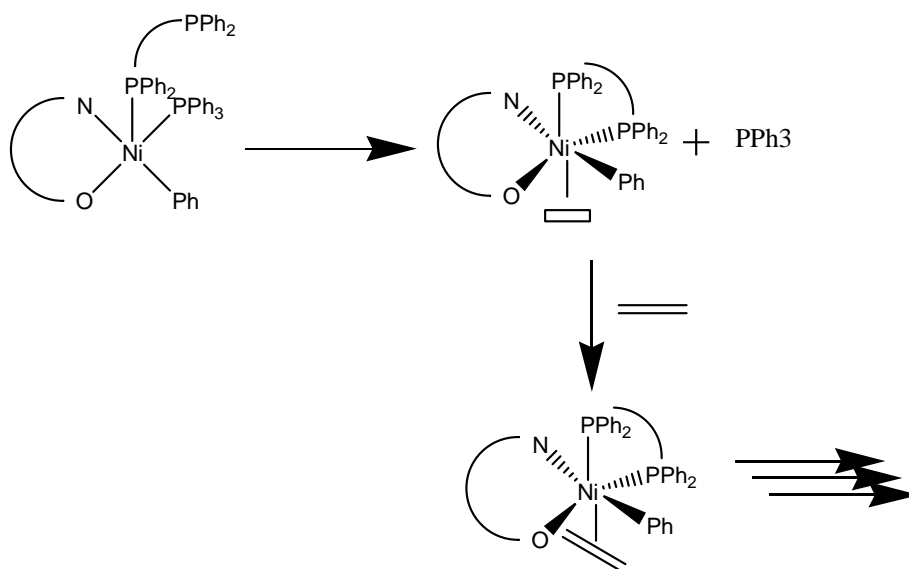


Figure 34. Proposed ethylene catalyst in situ synthesized with DPPPe

This octahedral catalyst is more active during ethylene polymerization than the initial NiNO square planar catalyst and leads to more branched PE. Moreover number of PE chains per Ni increases by a factor three indicating a high chain transfer ability which is in agreement with the high branching content.

Experimental investigations to crystallize the resulting complex from the interactions between NiNO and DPPPe are in progress.

e) Other ligands

Finally other classes of ligands are used from NPh_3 to SbPh_3 in similar experimental conditions. Results are summarized in the next table.

Table 6. Influence on the ethylene polymerization by NiNO catalyst with ligands of other atoms^a

Ligand	Activity (g/mmol/h)	Melting Temperature (°C) ^b
	94.7	117.9
NPh_3	398	111.4
PPh_3	209	118.1
AsPh_3	134	114.7
SbPh_3	76.5	116.4

^a: Polymerizations are performed during 1 hour using 20 mg of NiNO at 50°C in 250 mL of toluene under 20 bar of ethylene pressure. ^b: determined by DSC.

Activity decreases from nitrogen to antimonies. It is linked to the fact that the Tolman's angle remains almost constant in this series while s donation decrease (from N to Sb) and π retrodonation increase. These results are in agreement with the previous findings.

D. Conclusion

In this chapter we demonstrate that a homolytic cleavage of the nickel carbon bond of the NiNO complex takes place under some of our experimental conditions. This cleavage appears to be monomer dependent since half-life time and efficiency factor are different between the polymerization of MMA and styrene. Moreover VAc and BuA can not be polymerized by NiNO.

Moreover, this cleavage can be optimized by adding AIBN to the system. A real synergy between the catalytic and radical polymerization takes place since the radical and catalytic polymerizations are more efficient in the presence of AIBN. These indicate that radicals can interact with Ni complexes. These exchange mechanisms by S_{R1} and S_{R2} have been demonstrated by EPR.

Moreover additional phosphorous ligand effects have been studied for ethylene and MMA polymerization.

In the last case the additions of phosphine change dramatically efficiency factor (from 4 to 100%) and half-life time (from 60 to 360 min) of the initiation system. This behavior has been rationalized using QALE parameters.

Additionally during the catalytic polymerization activity (0 to $400 \text{ g mmol}^{-1} \text{ h}^{-1}$), PE number of chains synthesized per nickel and PE melting point can also be modified by addition of ligand. Again using simple argumentation this behavior has been rationalized.

Consequently phosphorous ligands could be used to tune the system: for example the radical polymerization or the catalytic polymerization can be improved in the same experimental conditions using a specific phosphorous ligand (for example in the presence of $P^t\text{Bu}_3$ radical reactivity is high and catalytic reactivity is low).

We dispose now from two ways to increase the efficiency of the system: addition of phosphorous ligand or addition of radicals/AIBN. However, a single phosphorous ligand can not increase both catalytic and radical reactivities of NiNO. Moreover the phosphine effect remains extremely complex. Consequently in the next chapter we will use the most efficient and simple way of improvement of the system based on NiNO catalyst and an additional source of AIBN in order to perform hybrid copolymerization of ethylene with polar vinyl monomer.

References:

- [1] D. Guironnet, P. Roesle, T. Runzi, I. Gottker-Schnetmann, and S. Mecking *J. Am. Chem. Soc.*, vol. 131, p. 422, 2009.
- [2] A. Nakamura, S. Ito, and K. Nozaki *Chem. Rev.*, vol. 109, p. 5215, 2009.
- [3] A. Leblanc, *Copolymerization d'olefines et de monomères polaires: à la frontière des chimies de coordination et radicalaire*. PhD thesis, Université Claude Bernard-Lyon 1, 2008.
- [4] C. Navarro, A. Leblanc, V. Monteil, R. Spitz, C. Boisson, and J.-P. Broyer *FR 2937643*, 2010.
- [5] C. Navarro, A. Leblanc, V. Monteil, R. Spitz, C. Boisson, and J.-P. Broyer *WO 2010049633*, 2010.
- [6] A. Leblanc, J.-P. Broyer, C. Boisson, R. Spitz, and V. Monteil *Macromolecules*, 2010, submitted.
- [7] G. Odian, *Principles of polymerization*. Wiley-Interscience, 2004.
- [8] T. R. Younkin, E. F. Connor, J. I. Henderson, S. K. Friedrich, and R. H. Grubbs *Science*, vol. 287, p. 2320, 2000.
- [9] <http://www.bu.edu/qale/>.
- [10] T. Bartik, T. Himmler, and H. S. K. J. Seevogel *J. Organomet. Chem.*, vol. 272, p. 29, 1984.
- [11] H. Liu, E. Eriks, A. Prock, and W. P. Giering *Organometallics*, vol. 9, p. 1758, 1990.
- [12] C. A. Tolman *Chem. Rev.*, vol. 77, p. 313, 1977.
- [13] M. R. Wilson, D. C. Woska, A. Prock, and W. P. Giering *Organometallics*, vol. 12, p. 1742, 1993.
- [14] A. L. Fernandez, C. Reyes, and A. P. W. P. Giering *Perkin Trans. 2*, p. 1033, 2000.

Chapter VI : Application of the hybrid radical/catalytic mechanism to the copolymerization of ethylene with polar vinyl monomer

A.	Versatility in copolymerization available using hybrid copolymerization	VI-330
1.	Copolymerization with NiNO alone	VI-330
a)	Methacrylates copolymerization with ethylene.....	VI-332
b)	Acrylates copolymerization with ethylene	VI-333
c)	Styrene and α -methylstyrene copolymerization with ethylene.....	VI-334
d)	Other polar vinyl monomers	VI-334
2.	Copolymerization from a classical radical initiator: AIBN	VI-335
3.	Copolymerization with the hybrid mechanism	VI-338
a)	Methacrylates copolymerization with ethylene.....	VI-340
b)	Acrylates copolymerization with ethylene	VI-341
c)	Styrene and α -methylstyrene copolymerization with ethylene.....	VI-341
d)	Other polar vinyl monomers copolymerization with ethylene	VI-342
(1)	Acrylonitriles copolymerization with ethylene	VI-342
(2)	Acids and amides vinyl monomers copolymerization with ethylene.....	VI-342
(3)	Acetates copolymerization with ethylene	VI-343
(4)	Crotonate copolymerization with ethylene	VI-343
4.	Conclusion	VI-344
B.	Case of the ethylene MMA copolymerization	VI-345
1.	Influence of the ethylene pressure.....	VI-345
2.	Fine and original copolymer characterization by LC-CC at high-temperature	VI-346
3.	Influence of the MMA concentration.....	VI-348
4.	Effect of the catalyst and AIBN concentration	VI-349
5.	Influence of the temperature	VI-352
6.	^{13}C NMR microstructure analysis of these copolymers	VI-353
7.	Conclusion	VI-359

C.	Case of styrene, BuA and VAc copolymerization with ethylene.....	VI-360
1.	Ethylene copolymerization with styrene	VI-360
a)	Effect of ethylene pressure.....	VI-360
b)	Effect of catalyst concentration.....	VI-361
2.	Ethylene copolymerization with BuA	VI-363
3.	Copolymerization of vinyl acetate with ethylene.....	VI-364
4.	Conclusion	VI-364
a)	Proposed mechanism for the hybrid copolymerization	VI-364
b)	Copolymers available by hybrid radical/catalytic copolymerization.....	VI-365
D.	Hybrid copolymerization using an ATRP system.....	VI-366
1.	Why ATRP system is a promising pathway?	VI-366
2.	Introduction of radicals from ATRP equilibrium.....	VI-368
3.	Case of reverse ATRP	VI-370
E.	Conclusion.....	VI-372

Up to now we have studied ethylene radical homopolymerization and copolymerization. Copolymerization under ethylene pressure as high as 250 bar does not give access to the complete range of copolymer composition. For example with comonomer such as MMA or BuA, ethylene insertions over 60% are extremely difficult to reach by a pure radical copolymerization. Moreover, almost no succession of ethylene units is present in the polymer chain.

In order to achieve more efficiently the copolymerization of ethylene with some polar vinyl monomer we develop a hybrid polymerization by combining radical and catalytic polymerization (see Figure 1).

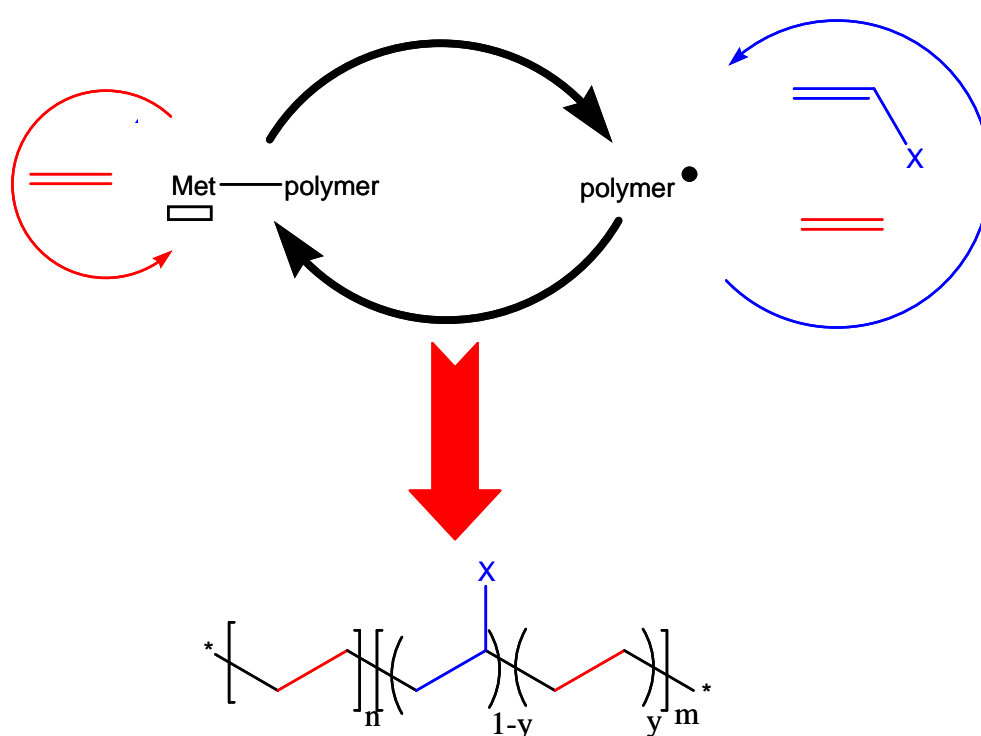


Figure 1. Hybrid radical/catalytic mechanism of polymerization

These type of mechanism can be considered to have some formal similarities with the chain shuttling catalytic polymerization recently developed [1]. In this kind of polymerization, two different polymerization catalysts are present and the growing chain “shuttles” (usually implicating a chain shuttling agent (CSA)) between these two catalysts. Multiblocks of linear PE and branched PE (see Figure 2) have been synthesized using this technology.

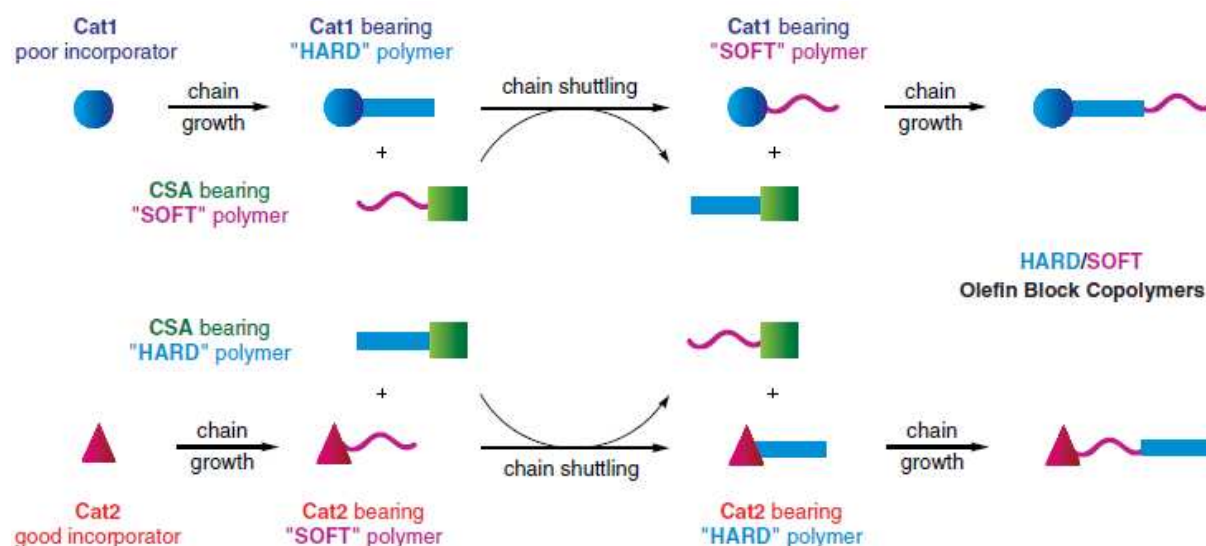


Figure 2. Chain shuttling mechanism from Arriola et al. [1]

In our case (hybrid radical/catalytic copolymerization), we investigate the possibility of chain shuttling not between two different catalysts but between an ethylene polymerization catalyst and a macroradical which will polymerize polar vinyl monomer. The shuttling of a growing polymer chain between a radical and an organometallic species is already well known and used to control the radical polymerization of various monomer via a reversible termination (e.g. CMRP). The success of the new concept of hybrid polymerization requires that the organometallic species is also a catalyst of olefin polymerization.

In the previous chapter, we demonstrated that NiNO ethylene polymerization catalyst suffers a spontaneous homolytic cleavage of the nickel carbon bond in our experimental conditions. Moreover, this cleavage can be optimized by adding AIBN to the system. A real synergy between the catalytic and radical polymerization takes place since the radical and catalytic polymerizations are more efficient in the presence of AIBN. These indicate that exchange between the radical and the organometallic species via S_R1 and S_R2 takes place.

Consequently, this nickel complex is an interesting candidate for the hybrid copolymerization by a radical/catalytic mechanism. Indeed the non polar ethylene block will be synthesized by a coordination-insertion mechanism and the polar block by a radical polymerization. As S_R mechanisms have been demonstrated using a radical initiator such as AIBN, we can expect that multiblocks will be synthesized. Figure 3 highlights the mechanism of chain shuttling between radical and catalytic polymerization.

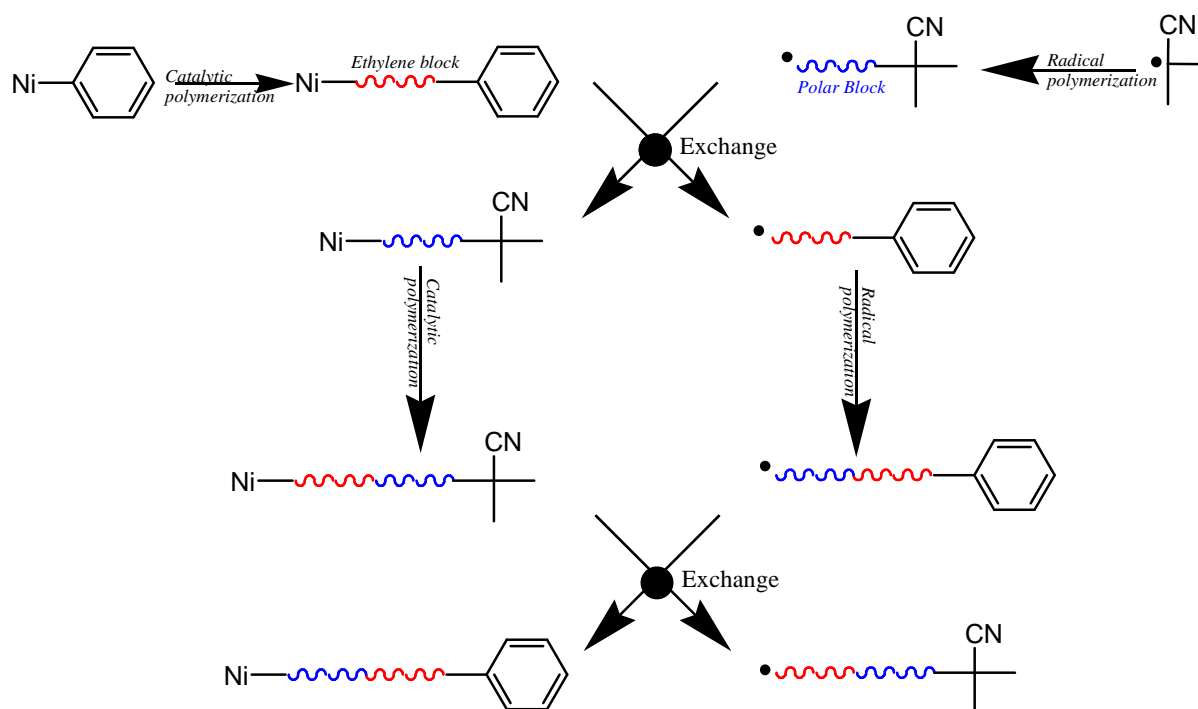


Figure 3. Copolymerization by chain shuttling between catalytic and radical polymerization

This mechanism needs a synergy between the two types of polymerization and a balance between both mechanisms in order that they take place at the same time.

In this chapter we report copolymerization of ethylene with various polar monomers using the same experimental conditions for NiNO or AIBN alone and the combination of both initiators. The superiority of the last method will be then demonstrated. Then the influence of other parameters such as ethylene pressure, monomer initial concentration and AIBN/NiNO ratio will be discussed. The multiblock architecture of ethylene/MMA copolymer will be demonstrated. Finally, the possibility to use CRP method for the radical part of the hybrid mechanism will be reported in order to access a better control of the chain microstructure and comonomer insertion.

A. Versatility in copolymerization available using hybrid copolymerization

In the previous chapter we demonstrated that NiNO ethylene polymerization catalyst can release a radical which can initiate the radical polymerization of polar vinyl monomer. This homolytic cleavage can be optimized using a phosphorous ligand or AIBN. However, only in the presence of AIBN, the efficient addition of radical on the NiNO and therefore the chain exchange takes place.

Copolymerization is first performed using 50 mg of NiNO and/or ½ molar equivalent of AIBN (potentially 1 radical per nickel) in 250 mL of toluene with 25 g of polar vinyl monomer under 20 bar of ethylene pressure at 70°C overnight. Keep in mind that these AIBN concentrations are much lower than these used in the radical polymerization in the second chapter (4mg in this case compared to 50 mg used usually in chapter II).

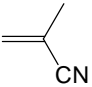
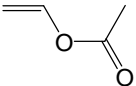
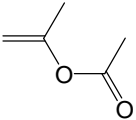
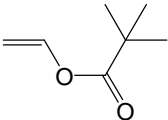
A wide range of comonomer is used in order to link the activity and comonomer insertion to the chemical structure of comonomer. Three successive series of experiments are performed using NiNO alone, AIBN alone and both NiNO and AIBN in order to compare the different systems of polymerization.

1. Copolymerization with NiNO alone

Polymerization using only the ethylene polymerization catalyst NiNO is performed with a wide range of monomer: acrylates, methacrylates, styrenics, etc. Results are summarized in the following table.

Table 1. Copolymerization of ethylene with several comonomers using NiNO alone^a

Comonomer		Yield (g)	Comonomer molar insertion (%) ^b
MMA		2.8	4.3
BuMA		5.5	3.3
tBuMA		6.3	4.5
MA		0.02	nd
BuA		0.05	95
tBuA		0.1	97
Sty		0.1	100
MSty		6.6	0.1
AN		0.2	nd

Comonomer		Yield (g)	Comonomer molar insertion (%) ^b
MAN		0.1	nd
VAc		0.2	1.3
PAc		6.1	0.6
VPiv		0.2	0.9

^a: Polymerizations are performed during 12 hours with 50 mg of NiNO at 70°C in 250 mL of toluene with 25 g of comonomer under 20 bar of ethylene pressure. ^b: determined by ¹H NMR.

Only the copolymerization with methacrylate monomers yields significant amount of polar copolymer. Copolymerizations with MSty, and PAc provide also high yield but the polymer produced is mostly composed of ethylene. With these two comonomers, the ethylene polymerization seems to be nearly unaffected by the presence of comonomer.

a) Methacrylates copolymerization with ethylene

Methacrylates copolymerizations with ethylene are more efficient using bulky comonomer (MMA < BuMA < ^tBuMA, see Table 1). However, comonomer insertions remain almost constant in the range of 4%. Therefore conversion in both ethylene and comonomer increase with the bulkiness of the comonomer.

For the ethylene part, the more bulky the comonomer is, the less the comonomer can be coordinated and consequently ethylene coordination is favored.

For the methacrylate part, since monomer propagation rate slightly decreases with bulkiness, the increase of conversion is due to the better initiation of radical polymerization.

We can assume that the cleavage of the metal carbon bond takes place after the first methacrylate insertion. Therefore the bulkiness of the comonomer should weaken the metal carbon bond and moreover the readdition of the released radical is disfavored (see Figure 4).

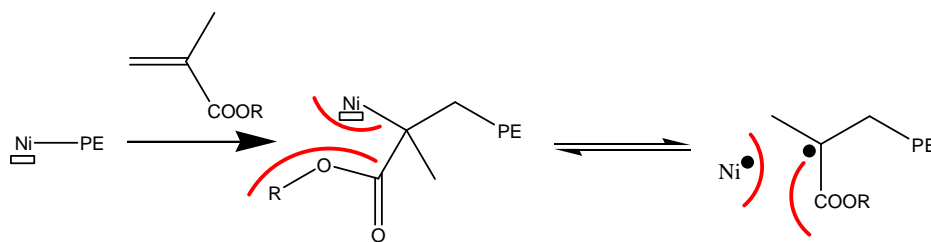


Figure 4. Possible mechanism of cleavage for methacrylate copolymerization with ethylene

It should be noted that the polar monomer insertion cannot be performed only by coordination/insertion since ^{13}C NMR spectrum of ethylene/MMA copolymer shows standard signals for PE and PMMA, no isolated MMA seems to be present in the polymer chain. Therefore, shuttling between a catalytic and radical polymerization should take place.

All these copolymers exhibit a melting point around 100°C . These indicate that long sequences of ethylene able to crystallize are built. Moreover, the molecular weight distributions are monomodal and remain narrow ($\text{PDI} \approx 2$). No copolymer fraction becomes soluble in THF. These indicate that no polymethacrylates or copolymer rich in methacrylates are synthesized.

b) Acrylates copolymerization with ethylene

In presence of acrylates almost no polymer is synthesized (see Table 1). However, as for methacrylates, the yield slightly increases with the bulkiness of the comonomer. This confirms the fact that the inhibition of the ethylene polymerization decreases with increasing bulkiness of the comonomer.

The presence of the methyl group on the vinyl seems to have a critical importance during the copolymerization: with MA, the copolymerization is almost totally inhibited and with MMA, 2.8 g of copolymer are produced. Moreover the copolymer produced in presence of MA is extremely rich in acrylates and almost no ethylenes units are present in the chain contrary to copolymers synthesized in presence of MMA.

These results are in contradiction with what is usually observed during a catalytic copolymerization. Indeed the copolymerizations reported in this case with acrylates are

generally more efficient than with methacrylates, due to the possibility or not of transfer and chain walking after the insertion of the polar vinyl monomer (see chapter I).

Moreover, acrylates are more reactive than methacrylate toward a radical polymerization. Then in order to understand this deactivation, we need to assume the crucial role of the methyl group for the homolytic cleavage which may increase the probability of cleavage.

c) Styrene and α -methylstyrene copolymerization with ethylene

With styrenic comonomers similar behaviors are observed since with styrene only 0.1 g of homopolystyrene are produced and with MeSty 6.6 g of almost homo-polyethylene (see Table 1). Once again the methyl group has a decisive influence on the copolymerization.

Since MeSty exhibits usually an extremely slow radical polymerization the potential radical block cannot be synthesized by radical mechanism which explains why no MeSty units are inserted in the polymer chain.

With styrene the interaction with NiNO is so strong that no ethylene polymerization takes place under our conditions. This could be linked to the efficiency factor determined during the radical polymerization of styrene and MMA by NiNO. Indeed an efficiency factor of 4% only for MMA indicates a limited interaction of MMA with NiNO. Therefore the possibility of coordinating and inserting ethylene is observed. The efficiency factor obtained during styrene homopolymerization is higher (25%), which indicates a stronger interaction of the monomer with NiNO. This could explain the impossibility of polymerizing ethylene in presence of styrene.

d) Other polar vinyl monomers

Other polar vinyl monomers are investigated; acrylonitrile, vinyl acetate and their derivatives (see Table 1). With methacrylonitrile and acrylonitrile, copolymerizations are extremely inefficient as for vinyl acetate and VPiv.

However polymerization in the presence of PAc provides high yield of polyethylene with low insertion of PAc. For the acetates family monomers, insertions of the polar unit remain in all cases extremely low indicating a strong inhibition of the system.

Acrylates and acetates seem to exhibit similar behavior as they provide almost no polymer. However with acrylates, the polymers synthesized are closer to homo-polyacrylates and with acetates to homo-polyethylene. Consequently, the inhibition mechanism of the copolymerization should to be different.

For acetate comonomers, classical β -OAc elimination can be responsible of the deactivation of the system and lead to low acetate insertion in the polymer chain since no homolytic cleavage takes place. For acrylates, behavior is more complex and a strong interaction with the NiNO in order to inhibit the coordination of ethylene seems to take place.

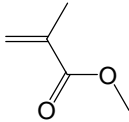
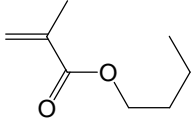
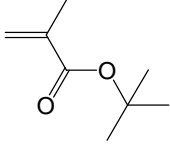
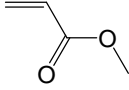
In conclusion, the copolymerization with NiNO alone provides as expected copolymers with various monomers content in low yield. However this polymerization is fully inefficient with several types of comonomers such as acrylates or acetates.

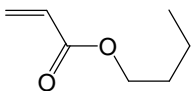
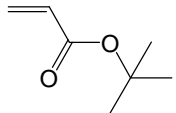
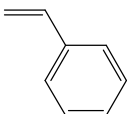
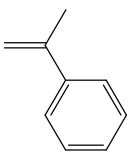
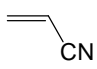
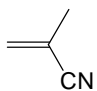
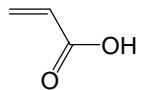
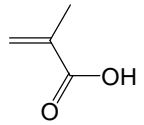
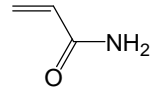
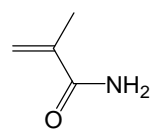
The addition of organic phosphorous ligands or radical initiator would improve this copolymerization. However, we will only study the influence of additional AIBN to NiNO system because the radical exchange has been evidenced in this case only.

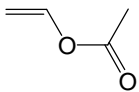
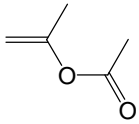
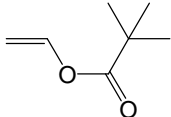
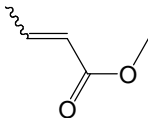
2. Copolymerization from a classical radical initiator: AIBN

We also perform the same polymerization with AIBN alone in order to separate the copolymer which can be formed by a radical polymerization to the copolymer synthesized by a hybrid catalytic/radical copolymerization. Results are summarized in the following table.

Table 2. Copolymerization of ethylene with several comonomers using AIBN alone^a

Comonomer		Yield (g)	Comonomer molar insertion (%) ^b
MMA		13.3	>99
BuMA		14	>99
tBuMA		11.6	>99
MA		16.4	>99

Comonomer		Yield (g)	Comonomer molar insertion (%) ^b
BuA		13.2	>99
tBuA		18	>99
Sty		2.8	>99
MSty		0.1	nd
AN		1.5	>99
MAN		0.1	nd
AA		25	>99
MAA		24.7	>99
AAm		25	>99
MAAm		24.3	>99

Comonomer		Yield (g)	Comonomer molar insertion (%) ^b
VAc		0.3	nd
PAc		0.15	nd
VPiv		0.6	nd
MCr		0.2	nd

^a: Polymerizations are performed during 12 hours with 4 mg of AIBN at 70°C in 250 mL of toluene with 25 g of comonomer under 20 bar of ethylene pressure. ^b: determined by ¹H NMR.

As expected at this low ethylene pressure with such low AIBN concentrations, only homopolymers of polar vinyl monomers are synthesized. The expected reactivity is obtained as acrylates lead to higher conversion than methacrylates, styrenic and acetates.

Methacrylic and acrylic acid as well as the corresponding amides lead to almost 100% of conversion in our experimental conditions.

MeSty, acetates and crotonate (MCr) only lead to conversion below 3%. With these comonomers the radical polymerization can be assumed as negligible.

Finally, whatever the polar vinyl monomer used no important insertion of ethylene has been observed.

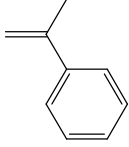
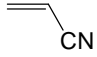
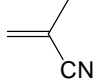
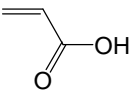
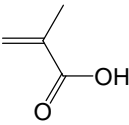
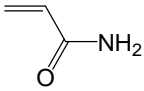
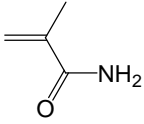
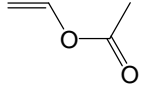
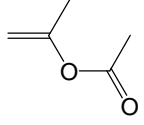
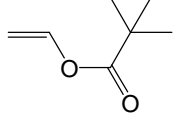
In the previous series of experiments using NiNO catalyst alone, copolymers synthesized with acrylates contained some ethylene in the polymer chain (5% for BuA). Almost no ethylene is inserted in the polymer chain using AIBN alone. Consequently, the ethylene incorporation implies the nickel metal and not a pure radical mechanism.

3. Copolymerization with the hybrid mechanism

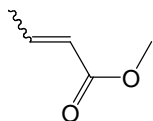
Finally, copolymerizations with NiNO and AIBN are performed in similar experimental conditions. Results are summarized in the following table.

Table 3. Copolymerization of ethylene with several comonomers using NiNO and AIBN^a

Comonomer		Yield (g)	Comonomer molar insertion (%) ^b
MMA		12.0	60
BuMA		12.7	54
tBuMA		17.3	35
MA		12.0	88
BuA		16.0	75
tBuA		15.5	51
Sty		3.3	82

Comonomer		Yield (g)	Comonomer molar insertion (%) ^b
MSty		8.3	0.5
AN		3.1	27
MAN		0.1	33
AA		32	35
MAA		25	60
AAm		25	64
MAAm		24	15
VAc		0.3	28
PAc		3.6	3
VPiv		0.5	14.6

Comonomer	Yield (g)	Comonomer molar insertion (%) ^b
MCr	0.1	31.5



^a: Polymerizations are performed during 12 hours with 50 mg of NiNO and ½ molar equivalent of AIBN at 70°C in 250 mL of toluene with 25 g of comonomer under 20 bar of ethylene pressure. ^b: determined by ¹H NMR.

This system leads to totally different results than the two previous ones. Indeed copolymers are synthesized with high efficiencies with almost all the polar vinyl comonomers investigated using the same experimental conditions.

a) Methacrylates copolymerization with ethylene

Copolymerization with methacrylate monomers is strongly dependent on the bulkiness of the monomer (see Table 3). Yield increases with this bulkiness and insertion of the monomer decreases. Contrary to NiNO alone where only 4% of methacrylates insertion is reached and AIBN in which homo-polymethacrylates are synthesized, with this system the comonomer content is in the range from 35% to 60% depending on the comonomer. These copolymers exhibit a melting point between 105°C (in the presence of ^tBuMA) and 98°C (in the presence of MMA) which indicates that long sequences of ethylene are present in the polymer chain. Moreover, monomodal molecular weight distributions are obtained by HT-SEC with a low PDI (≈2). These indicate that probably only one type of copolymer should be synthesized and therefore no polyethylene or polymethacrylates are produced during the polymerization.

Finally the relative activity is in agreement with an interaction between the comonomer and the catalyst. The more bulky the monomer is, the less it will interact with NiNO therefore the higher the ethylene catalytic activity is.

Conversion of methacrylates is almost constant for all comonomers used. It indicates that the initiation of polar block is not controlled anymore by the bulkiness of the monomer as described with NiNO alone (see Figure 4).

The homolytic cleavage of the nickel carbon bond may be induced by a radical addition on the catalyst by a S_R mechanism. If the predominant mechanism was S_{R1} the bulkiness of the comonomer would control the substitution. It is not the case therefore the predominant mechanism seems to be a S_{R2} mechanism (see Figure 5). Contrary to the copolymerization with NiNO alone the cleavage can take place before or after the insertion of the first methacrylate unit.

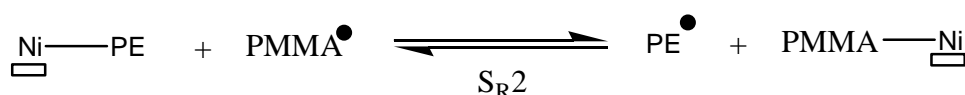


Figure 5. Schematic mechanism of chain exchange between radical and catalytic polymerization

b) Acrylates copolymerization with ethylene

With acrylates, contrary to NiNO alone, copolymers are synthesized efficiently (see Table 3). Once again, yield increases with the bulkiness of the monomer and insertion decreases. Insertion of acrylates between 88% and 51% are measured. Yields are similar than with methacrylates but ethylene conversion is about two times lower. Consequently as expected acrylates appear to be better inhibitor of the ethylene polymerization than methacrylates.

All these copolymers are soluble in THF indicating that no homopolyethylene is produced. And monomodal narrow molecular weight distributions are obtained, consequently no polyacrylate seems to be synthesized as well.

The simultaneous presence of AIBN and NiNO is mandatory. In the presence of NiNO alone, no copolymerization takes place, it could be due to the absence insertion of acrylates and consequently no cleavage of metal carbon bond takes place (or the cleavage does not occur after the insertion of acrylate).

In presence of AIBN and NiNO, the cleavage is induced by the addition of a radical fragment on the nickel. Consequently the insertion of acrylate in the polymer chain can be performed without the requirement of a first coordination-insertion into the metal carbon bond.

c) Styrene and α -methylstyrene copolymerization with ethylene

For styrenic monomers, copolymers are produced with both styrene and MSty (see Table 3). Results obtained are similar than the ones with NiNO alone.

Indeed MSty is not inserted in the polymer chain and does not polymerize by a pure radical mechanism therefore AIBN acts as spectator of an ethylene catalytic polymerization on nickel.

With styrene, 3.3 g of copolymer are produced containing 82% of styrene units and having a melting point at 93°C indicating long sequences of ethylene. Moreover this copolymer is not soluble in THF therefore no homopolystyrene is synthesized.

This result evidences that the copolymer synthesized can not be statistical as with only 18% of ethylene in the polymer chain, the copolymer exhibits a melting point. Indeed statistical copolymers synthesized by AIBN alone at higher ethylene pressure (see chapter IV) do not exhibit melting point.

d) Other polar vinyl monomers copolymerization with ethylene

In this section we report the copolymerization of ethylene with comonomers known to be extremely difficult to incorporate in polyethylene chains via a catalytic mechanism [2, 3].

(1) *Acrylonitriles copolymerization with ethylene*

In the presence of acrylonitrile 3.1 g of copolymer are produced containing 27% of AN units. The copolymerization with MAN is almost inefficient. Since MAN is not polymerized by a radical pathway and totally inhibits the ethylene catalytic polymerization, it must be one of the most difficult copolymers to produce.

MAN remains one of the last polar comonomer which is not inserted efficiently in the polymer chain by a hybrid radical/catalytic mechanism.

(2) *Acids and amides vinyl monomers copolymerization with ethylene*

With acrylic acid and acrylamide extremely high productivities are obtained (see Table 3). Ethylene is inserted in the polymer chain with contents up to 85% with MAAm. The high ethylene insertion and high activity indicate an extremely efficient system of copolymerization. Moreover to our knowledges, these copolymers are the first examples of direct copolymerization of ethylene with this kind of comonomer. The copolymers produced represent a tremendous interest.

Indeed these copolymers containing ethylene sequences are soluble in water (basic aqueous solution for acid monomer AA and MAA and neutral water for AAm and MAAm)

which indicates that no homo-polyethylene is produced. Moreover these copolymers self-organize in water and form nano-objects with e.g. a PE hydrophobic core and a hydrophilic shell. These objects seem to aggregate in solution in order to form more complex architectures as the average particles diameters determined by DLS just after a sonication is 12 nm (with $PI \approx 0.05$) and 50-75 nm (with $PI \approx 0.25$) after 1 hour at ambient temperature, whatever the copolymer used. Then these dispersions are stable for months.

A critical micelle concentration (cmc) was measured for AA and MAA copolymers with ethylene. For ethylene/AA copolymer, the cmc was measured at 0.1 g/L and 0.4 g/L for ethylene/MAA.

Moreover these copolymer exhibit a melting point around 100°C indicating long sequences of ethylene incorporating in the polymer structure.

This block architecture represents an additional advantage since crystallinity can be maintained even at high polar monomer content.

(3) *Acetates copolymerization with ethylene*

With acetates derivatives monomers, the copolymerization remains inefficient but high insertion of acetate is evidenced by NMR (see Table 3 - for example 28% VAc are inserted in the copolymer chain) contrary to the copolymerization in the presence of NiNO alone.

No fraction of polymer is soluble in THF and molecular weight distributions determined by HT-SEC are monomodal and narrow. Moreover these copolymers possess a melting point around 100°C. All these results indicate that block copolymers have been synthesized.

(4) *Crotonate copolymerization with ethylene*

Finally with crotonate the copolymerization is totally inefficient (see Table 3). In comparison, MA and MMA copolymerizations with ethylene exhibit much higher efficiencies while these monomers differ only by the presence or the position of the methyl group on the double bond.

This monomer does not polymerize in our experimental conditions by radical pathway (as does MSty) but the insertion becomes quite important 31%. Consequently this insertion must be performed by a nickel-mediated mechanism.

This comonomer highlights how important the chemical nature of the vinyl polar monomer is for the hybrid radical/catalytic copolymerization.

4. Conclusion

The hybrid copolymerization via a shuttling mechanism between catalytic and radical polymerization is extremely efficient to produce a wide range of copolymers. Copolymerizations are performed using acids and amides vinyl monomers, (meth)acrylates, acrylonitriles, styrenics. Indeed NiNO alone only permits the copolymerization of ethylene with methacrylates.

The simultaneous presence of a radical initiator, AIBN, and an ethylene polymerization catalyst able to suffer a homolytic cleavage of the nickel carbon bond, NiNO, permits the copolymerization. Even some comonomers known to be extremely difficult to copolymerize with ethylene (AN, AA, AAm, etc), are inserted in the polymer chain using this hybrid copolymerization.

Consequently, this hybrid radical/catalytic copolymerization using NiNO and AIBN represents a versatile pathway in order to obtain copolymers with various polar functions and in a wide range of chemical compositions.

The block microstructures of the synthesized copolymers have been demonstrated as almost all copolymers exhibit a melting point and a monomodal narrow MWD. With water-soluble vinyl monomers, more evidences were obtained as water-soluble copolymers were produced which form micelle-like particles with extremely low critical micelle concentration.

Finally concerning the polymerization mechanism the important role of the bulkiness of comonomer is highlighted. Indeed usually ethylene insertions increase with the bulkiness of the comonomer. With NiNO alone, we assumed that the cleavage of the metal carbon bond should take place after the insertion of a polar monomer (see Figure 4). With additional AIBN, the most efficient system, the cleavage is induced by a radical addition on the nickel itself via a S_R2 mechanism (see Figure 5).

In the next section we investigate further the copolymerization of ethylene with MMA, styrene, BuA, and VAc and especially highlight the role of the relative kinetics of respectively radical and catalytic polymerizations. We will confirm the multi-block nature of copolymer using fine ^{13}C NMR studies and a chromatographic method that separates polymer according to their chemical nature.

B. Case of the ethylene MMA copolymerization

Copolymerization of MMA and ethylene has proved to be one of the most efficient system for hybrid copolymerization. The effect of the initial concentration of ethylene and MMA is reported in this section. Moreover, characterization of these copolymers by NMR and liquid chromatography in critical condition of PMMA (LC-CC) are reported in order to confirm the microstructures of copolymers.

1. Influence of the ethylene pressure

Two series of experiments are performed at 70°C in 40 mL of toluene and 10 mL of MMA with 20 mg of NiNO during 4 hours and with or without ½ molar equivalent of AIBN under different ethylene pressures. Results are summarized in the following figure.

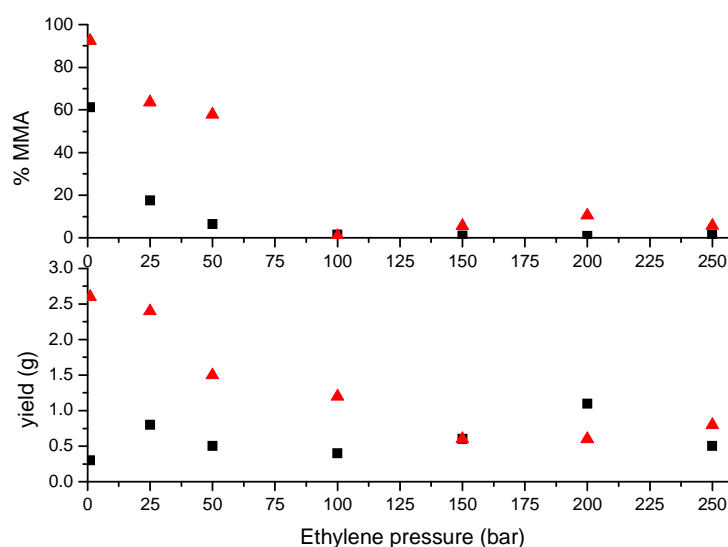


Figure 6. Effect of ethylene pressure on the yield and MMA molar insertion^a during the copolymerization of ethylene with MMA. 20 mg of NiNO in 40 mL of toluene with 10 mL of MMA at 70°C during 4 hours with ▲ or without ■ AIBN. ^a: determined by ¹H NMR

As expected, at low pressure yields are higher in the presence of AIBN and so do MMA incorporations. Over 100 bar of ethylene pressure the system leads to almost constant yield and MMA insertion. Insertions of MMA roughly decrease with the ethylene pressure from 90 % to 1%.

In the presence of AIBN a slight increase of MMA insertion is observed between 100 bar and 200 bar of ethylene pressure. This increase indicates that a change occurs in the mechanism of the copolymerization. Indeed no reactivity ratio can be calculated for this kind

of copolymerization (ethylene insertion does not steadily increase with the increase of ethylene pressure).

Except for the copolymers synthesized at 1 bar of ethylene pressure, all other products exhibit a melting point around 100-105°C. Moreover, in the presence of AIBN, the melting point is always lower even at low and similar MMA insertion. For example, copolymers synthesized under 100 bar of ethylene pressure contain only 1% of MMA for both systems (NiNO alone and NiNO in presence of AIBN), however, without AIBN the melting point is 105.6°C and with AIBN 102.8°C.

This may indicate a better homogeneity of MMA incorporation in the polymer chain which disturbs the crystallization of PE sequences in the case of polymerization in the presence of AIBN.

Molecular weights of the copolymer are also determined using HT-SEC (see Table 7). In all cases, monomodal narrow molecular weight distributions are observed ($PDI \approx 2$) which may indicate that only one type of copolymer is synthesized. M_n is always lower in presence of AIBN than without. Molecular weights first decrease for copolymers obtained at ethylene pressure until 100 bar then slightly increase to 150 bar until reaching a plateau.

2. Fine and original copolymer characterization by LC-CC at high-temperature

Copolymers produced in the presence of NiNO and AIBN at different ethylene pressures are also analyzed using specific chromatographic technique in order to elute the copolymer in function of their chemical compositions. This work needs a long and difficult optimization of the elution design and has been done at the DKI (see chapter IV). The chromatograms obtained clearly confirm that no homopolymer (PE and/or PMMA) is synthesized during the hybrid radical/catalytic copolymerization (see Figure 7).

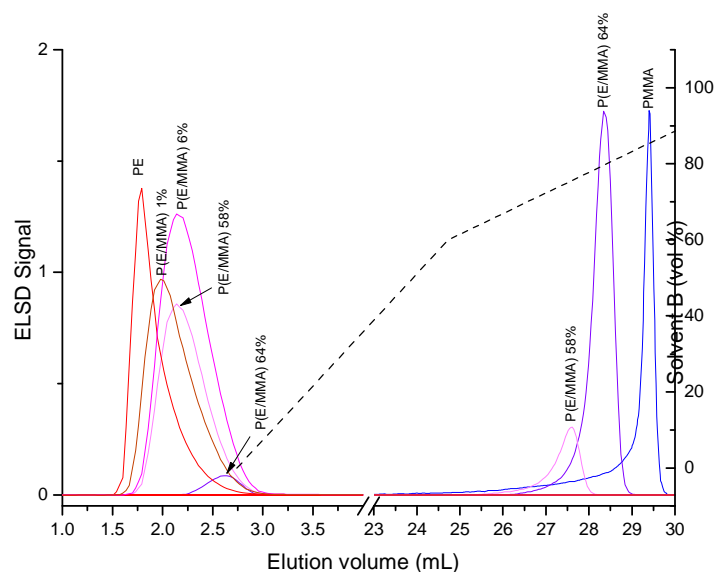


Figure 7. Overlay of chromatograms of P(E/MMA) samples. Stationary phase: Perfectsil 300. Mobile phase: TCB and gradient TCB → TCB/cyclohexanone (20/80 v/v). Temperature: 140°C. Gradient of solvent is indicated by a dotted line

For copolymers synthesized at ethylene pressure below 50 bar two different peaks are observed. These may indicate that two different copolymers are synthesized: a PE-rich and a PMMA-rich. Copolymers obtained between 100 bar and 250 bar exhibit only one peak. These peaks of elution seem to be in agreement with the previous correlation between elution volume and MMA molar content (see Figure 8) previously observed using copolymers of ethylene/MMA synthesized by a pure radical polymerization.

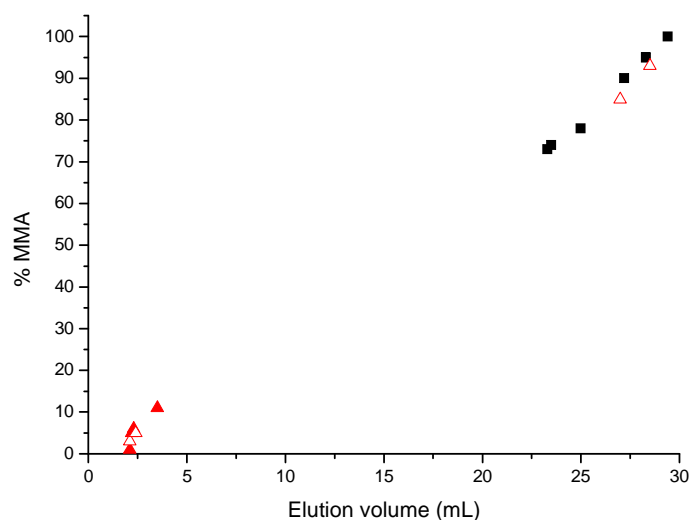


Figure 8. Correlation between elution time and MMA insertion determined by ^1H NMR.
■ Ethylene MMA copolymers synthesized by radical copolymerization, ▲ Ethylene MMA copolymers synthesized by hybrid copolymerization (▲ are estimated MMA insertions using the relation of elution volume with molar % of MMA)

Then, using this relation, the real insertion of the two families of copolymer can be estimated for copolymers synthesized at 25 and 50 bar. At 25 bar, two different copolymers are formed one containing 93% of MMA and the other 5% of MMA (for the copolymer produced at 50 bar 3% and 85%).

It should be noted that the relative concentration of these copolymers cannot be easily determined using the chromatograms because the intensity of the signal depends of the copolymer composition (MMA unit exhibits a higher response than ethylene units). However, for the copolymers synthesized under 50 bar of ethylene pressure chromatogram integral indicate that the average composition of MMA determined by this method cannot be in agreement with the average composition determined by NMR.

This may be because we assumed that the correlation between elution time and MMA insertion determined by NMR is equivalent to the one for radical synthesized copolymer. However the microstructures of the copolymer are different (statistical for pure radical copolymerization and multiblock for hybrid radical/catalytic mechanism), therefore the correlation should be different. In fact, theoretically the dependence of elution time will be for multiblock copolymers mostly dependent of the average block length of MMA units. Consequently only IR or NMR post analyses of separate fractions of copolymers could give an estimation of their compositions.

Moreover, two different copolymers with the same MMA amount but different block lengths should not exhibit the same elution volume. Only the fine ^{13}C NMR study of the separate copolymer can confirm the polymer microstructure.

3. Influence of the MMA concentration

Other series of experiments are performed using similar conditions at several MMA initial concentrations from 10% vol. to 100%. Copolymerizations are done at 70°C during 1 hour with 20 mg of NiNO under 100 bar of ethylene pressure with or without $\frac{1}{2}$ molar equivalent of AIBN (see Figure 9).

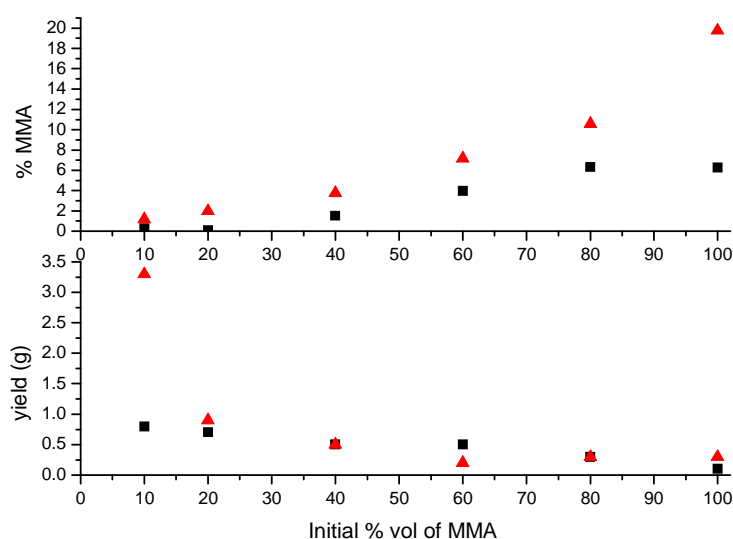


Figure 9. Influence of MMA concentration on the copolymerization yield and MMA molar insertion.^a 20 mg of NiNO in 50 mL of toluene MMA mixture at 70°C under 100 bar of ethylene pressure during 1 hour with ▲ or without ■ AIBN. ^a: determined by ¹H NMR

As expected yield decreases with increasing MMA concentration with or without AIBN which confirms that MMA slows down the copolymerization. Insertions of MMA increase from 1% to 6% without AIBN and up to 20% in the presence of AIBN. Average molecular weights also decrease in both sets of experiment from 40000 to 18000 g/mol with AIBN and 26000 to 9000 g/mol without. As for the previous set of experiments, molecular weights are lower without AIBN than with AIBN. Moreover, polydispersity index remains between 2 and 3 and monomodal molecular weight distributions are obtained.

All these results indicate that only one family of copolymers is synthesized allowing the determination of conventional reactivity ratios. In the presence of NiNO and AIBN, using Kelen-Tüdös method $r_{\text{MMA}}=0.98$ and $r_{\text{E}}=29.8$ is obtained, with NiNO alone $r_{\text{MMA}}=4.17$ and $r_{\text{E}}=228$. Consequently the AIBN addition favors the MMA insertion inside the polymer chain.

4. Effect of the catalyst and AIBN concentration

The concentrations of the catalyst and AIBN have also a crucial effect on the copolymerizations. We perform different experiments with excesses of AIBN or NiNO and at two different concentrations. Experiments are performed at 70°C during 2 hours in 40 mL of toluene and 10 mL of MMA under 25 bar of ethylene pressure (see Table 4).

Table 4. Influence of NiNO and AIBN concentration on the copolymerization at low ethylene pressure.^a

NiNO (mg)	AIBN (molar eq)	Yield (g)	Molar insertion of MMA (%) ^b
20	1/2	1.3	60
50	1/2	3	58
20	2	1.6	81
50	1/8	4	8

^a: Polymerizations are performed during 2 hours at 70°C in 40 mL of toluene with 10 mL of MMA under 25 bar of ethylene pressure. ^b: determined by ¹H NMR.

Results show that the global concentration has only an effect on the activity of the polymerization but insertions of MMA remain equivalent. If an excess of AIBN is used the incorporation of MMA increases. With an excess of NiNO only 8 % of MMA are inserted compared to 58 %.

It should be noted that without AIBN a copolymer containing 17% of MMA is synthesized. This evidenced that AIBN interacts with NiNO even at this low concentration with the consequence to decrease the MMA insertion.

These results evidence how important the ratio between AIBN and catalyst is in order to control the copolymerization yield and comonomer insertion. Moreover with an excess of AIBN a bimodal distribution of molecular weight is observed. As we already mentioned polymerization at 25 bar lead to two different copolymers: a MMA rich and a MMA poor. The ratio between these two copolymers could be monitored by the ratio of AIBN/NiNO. At high AIBN over NiNO ratio, the rich MMA copolymer would be mostly synthesized. At low AIBN over NiNO ratio, the synthesis of the ethylene rich copolymer would be favored.

The same experiments are performed at 100 bar with similar results (see Table 5).

Table 5. Influence of NiNO and AIBN concentration on the copolymerization at high ethylene pressure.^a

NiNO (mg)	AIBN (molar eq)	Yield (g)	Molar insertion of MMA (%) ^b
20	1/2	0.8	1.5
50	1/2	3.7	1.2
20	2	1.0	6
50	1/8	2.1	0.4

^a: Polymerizations are performed during 2 hours at 70°C in 40 mL of toluene with 10 mL of MMA under 100 bar of ethylene pressure. ^b: determined by ¹H NMR.

Once again the global concentration at constant ratio of AIBN/NiNO does not change the insertion of MMA but influences only the yield of polymerization. With an excess of AIBN higher insertion is obtained. However, the HT-SEC show a bimodal distribution and a part of the material obtained can be solubilized in THF. Consequently, PMMA or MMA rich copolymer could have been synthesized. With excess of NiNO only 0.4% of MMA is inserted in the polymer chain.

Similar results have been obtained using a 50% in volume solution of MMA. Indeed at 100 bar MMA insertion increases from 5% to 22% with excess of AIBN and decreases to 2% with excess of NiNO. In this particular case no soluble fraction of polymer is extracted by THF. This indicates that no PMMA-rich copolymer is synthesized under these experimental conditions even with an excess of AIBN contrary to the polymerization performed in 20% v/v of MMA.

In Consequence it appears that the AIBN/NiNO ratio has to be close to 1/2 in order to improve the exchange between the catalytic mechanism and the radical one. Indeed at low ratio, catalytic polymerization is too important and at higher, it is the radical one which predominates by far.

5. Influence of the temperature

Copolymerizations are also performed at different temperatures in order to evidence a potential temperature effect.

Table 6. Influence of the reaction temperature on the copolymerization of ethylene with MMA^a

Temperature (°C)	Pressure	Yield (g)	Molar insertion of MMA (%) ^b
50	25	3.3	77
70	25	1.3	60
90	25	0.4	52
50	100	1.5	7
70	100	3.7	1.2
90	100	1.2	1.5

^a: Polymerizations are performed during 2 hours with 20 mg of NiNO and ½ molar equivalent of AIBN in 40 mL of toluene with 10 mL of MMA. ^b: determined by ¹H NMR.

We observe that the MMA insertions decrease with increasing temperature when polymerizations are performed under 25 bar or 100 bar of ethylene pressure. Under 25 bar of ethylene pressure, yield also decreases with increasing temperature which is not the case for copolymerization performed under 100 bar of ethylene pressure.

Moreover the melting point of the copolymer decreases as expected with increasing temperature: T_m is found at 115°C when polymerization is performed at 50°C, and T_m=85°C if polymerization takes place at 90°C for polymer synthesized at 100 bar of ethylene pressure. Since MMA insertions also decrease with increasing temperature, the melting point decrease is ascribed to a more uniform distribution of MMA in the polymer chain (average PE block length decrease) or an increase of branch content.

6. ^{13}C NMR microstructure analysis of these copolymers

We have demonstrated that several experimental factors exhibit dramatic effect on the composition of the ethylene/MMA copolymer. Indeed MMA insertion decreases with increasing ethylene pressure and temperature. It increases with MMA initial content and AIBN concentration. Therefore all these factors can be adjusted in order to obtain the desired MMA insertion from 99.9% to 0.1%.

Now, we will investigate the ^{13}C NMR spectra of these copolymers in order to confirm the multi-block microstructure.

Radical copolymerization of ethylene with MMA at several ethylene pressures give access to a range of copolymers which are investigated by ^{13}C NMR. The characteristic signals of isolated ethylene units and successive ethylene sequences are determined this way. Indeed as already mentioned in chapter IV, below 100 bar of ethylene pressure only isolated ethylene units are present, while over 100 bar of ethylene pressure some successive ethylene units are present in the polymer chain. CH_2 peaks at 43.8 ppm and 19 ppm are assigned to isolated ethylene units. For two successive ethylene units, the peaks are identified: 41 ppm, 24 ppm, 32.4 ppm (see Figure 10).

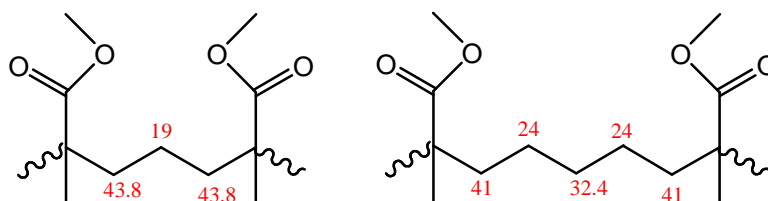


Figure 10. ^{13}C NMR signals of ethylene units in a copolymer with MMA

Further analyses of copolymers obtained by the hybrid radical/catalytic mechanism exhibit numerous new signals compared to the statistical ethylene/MMA copolymers.

The spectrum of copolymer obtained (in green in Figure 11) is compared to the spectrum obtained for a homo-polyethylene synthesized using the same experimental conditions without MMA (spectrum in red) and a homo-PMMA (in blue) synthesized in the same experimental conditions without ethylene. All additional signals should be due to the block-end carbons.

Finally these additional carbon signals are compared to the computed signals of CH_2 in α (42.3 ppm), β (24 ppm), γ (31.5 ppm) and δ (29.5 ppm) of a block MMA using an incremental method from the statistical ethylene/MMA results.

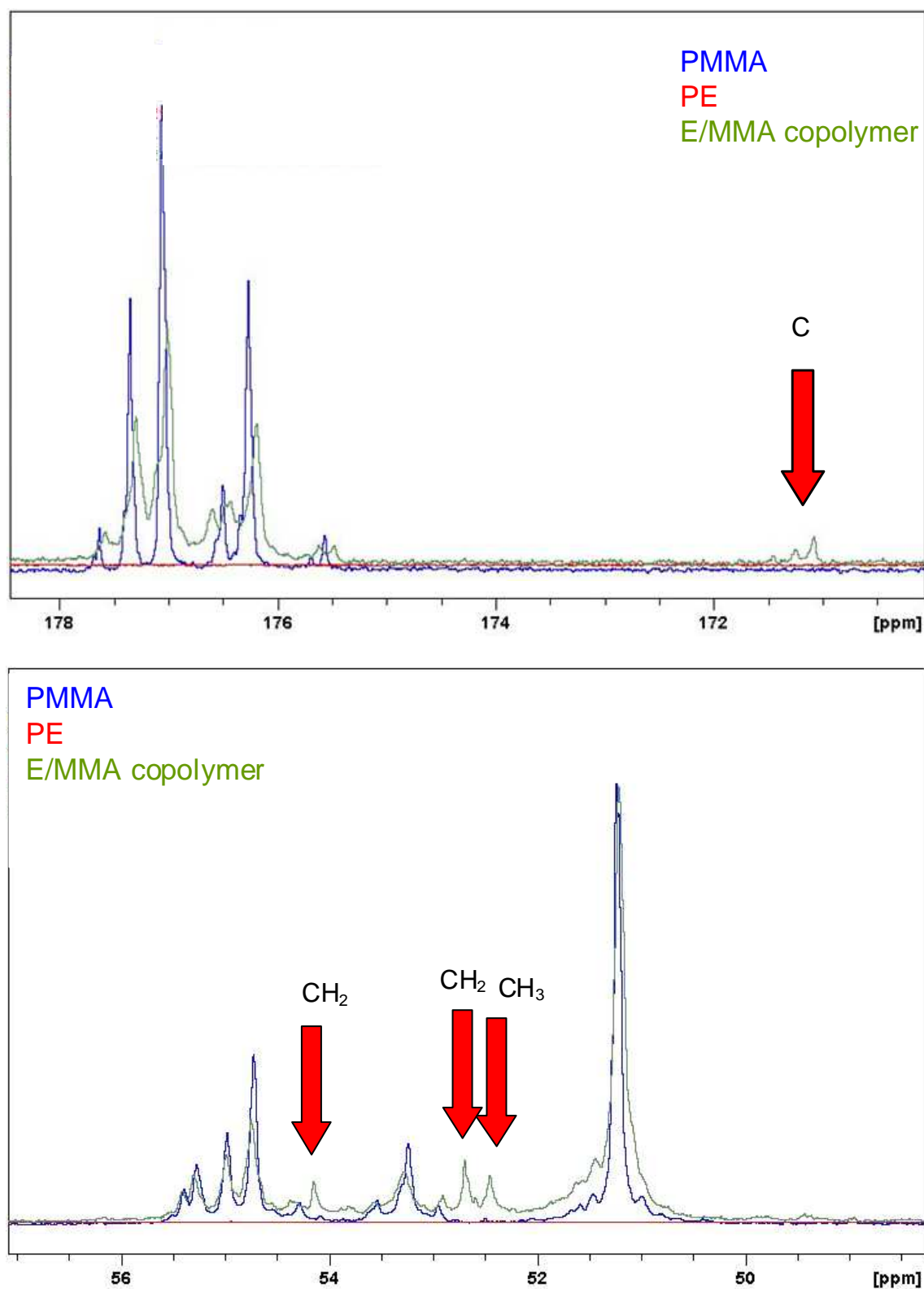


Figure 11. NMR spectrum of a copolymer MMA/Ethylene. In red a homo-polyethylene synthesized using the same experimental conditions without MMA, and in blue a homo-PMMA synthesized using same experimental conditions without ethylene (CH₃ means primary carbon, CH₂ secondary, CH tertiary, C quaternary determined by DEPT spectrum).

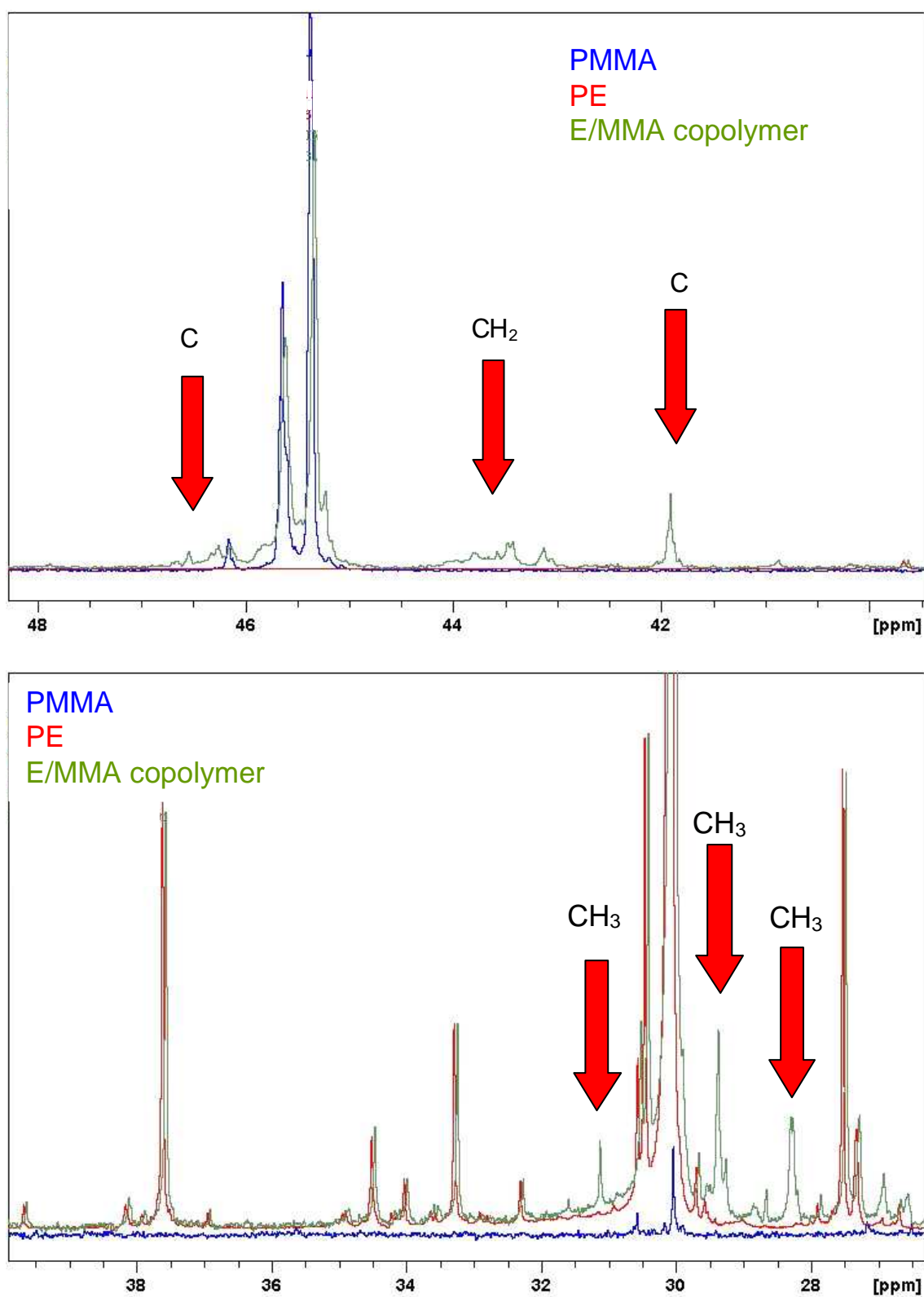
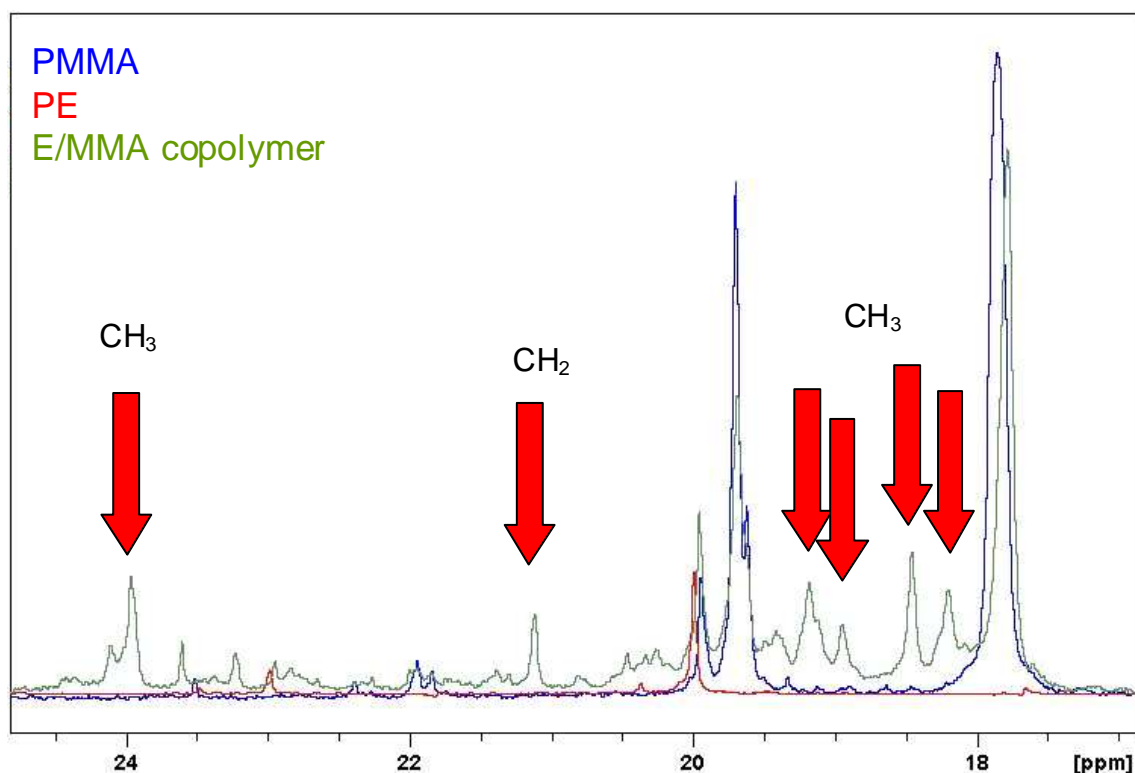


Figure 11 (continued)

**Figure 11 (continued)**

The spectra of the copolymers are extremely complex due to the tacticity of MMA sequences and the branched nature of ethylene sequences.

Among these additional signals, the carbonyl carbon between 171-171.5 ppm is easy to assign. This signal shows a tacticity contribution as standard PMMA carbonyl signal therefore it can be attributed to a carbon of a carbonyl group at the end of a MMA block.

Moreover an additional signal at 52.4 ppm is attributed to the methoxy carbon at the end of MMA block. Finally an additional signal of a quaternary carbon at 41.9 ppm is also attributed to the MMA block-end.

The CH₂ end signal of ethylene blocks are in agreement with the one predicted by the incremental method (α =43-44 ppm, β =21 ppm). However several CH₃ and CH carbon signals are also present. This could indicate that the ethylene block-end seems to contain a methyl branch.

It should be noted that in these copolymers synthesized by hybrid polymerization no isolated ethylene or MMA unit is identified. Moreover the signals of the MMA block-ends indicate that there is no tail-tail or head-head sequence. This is a crucial remarks since it means that the MMA insertion in the nickel carbon bond before the homolytic cleavage (see Figure 4) is a 2,1 insertion.

Another important remark is that the block-end MMA signals show a tacticity equivalent to the tacticity of a pure radical PMMA which may imply that this block is synthesized by a standard radical polymerization. As ethylene block cannot be synthesized using a radical pathway it should exist a “shuttling” between radical and catalytic polymerization.

We summarized these NMR findings in the following figure.

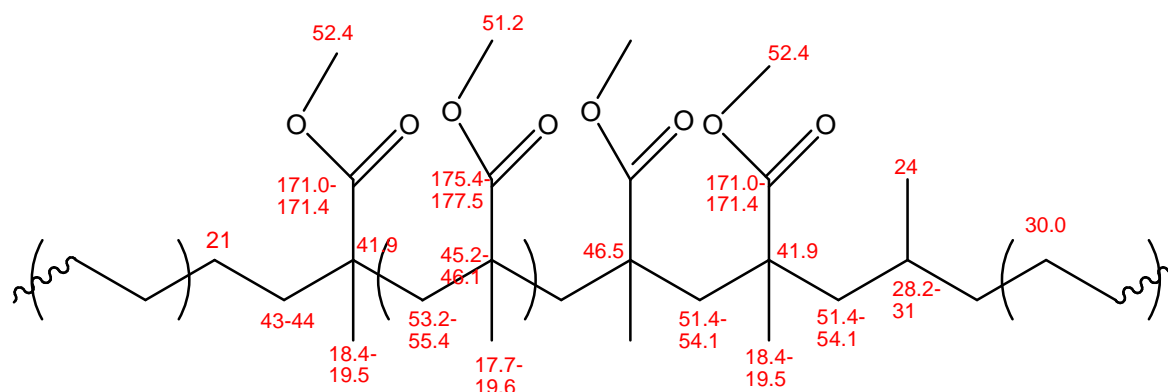


Figure 12. ^{13}C NMR signals of a MMA/Ethylene copolymer

These results are in good agreement with the predicted peaks determined using the incremental technique.

From these results, average block length can be calculated by integrating the respective NMR signals. For MMA, we calculate the block length using methoxy carbon and/or carbonyl and/or quaternary carbon (see equation 1). We obtain typical length between 1 and 40 MMA. For ethylene block we cannot use block-end signal of CH_2 because the microstructure is unknown (some block-ends seem to exhibit methyl branches). Therefore we use the MMA block-end signal to determine the average length of ethylene block (see equation 2). Indeed the composition of two successive blocks (one of MMA and another of ethylene) must be equal to the composition of the entire copolymer.

$$x_{\text{MMA}} = \frac{2I_{52.4}}{I_{52.4}} + 2 = \frac{2I_{175.4-177.5}}{I_{171.0-171.4}} + 2 = \frac{2I_{45.2-46.1}}{I_{41.9}} + 2 \quad (1)$$

$$\frac{x_{\text{MMA}}}{x_{\text{MMA}} + x_{\text{E}}} = X_{\text{MMA}} \quad (2)$$

With x the average block length of respectively MMA (x_{MMA}) and ethylene (x_{E}), I_y the integral value of the signal at y ppm, and X_{MMA} the MMA molar composition of the copolymer determined by ^1H NMR.

The comparison of the average blocks lengths obtained to the molecular weight of the copolymer determines if diblock or multiblock copolymers are synthesized (see Table 7).

Table 7. Blocks average length of the copolymer produced with NiNO and AIBN

Pressure (bar)	Molar insertion of MMA (%) ^a	Average length of MMA block per block end ^b	Average length of ethylene block per block end ^b	Mn (g/mol) [PDI] ^c
25	63.5	35	20	28400 [2.5]
50	57.8	25	18	17900 [2.3]
100	1.0	1	99	9200 [3.1]
150	5.6	2	25	13300 [2.6]
200	10.6	3	21	15000 [2.2]
250	5.8	2	33	14000 [2.1]

^a: determined by ¹H NMR, ^b: determined by ¹³C NMR, ^c: determined by HT-SEC

Below 100 bar of ethylene pressure, diblock copolymers seem to be synthesized since the molecular weight of two blocks corresponds almost to the molecular weight of the copolymer. However, previous results indicate that these copolymers are not homogeneous. Consequently, we can assume that the two diblock copolymers correspond to one which started by a radical mechanism and the other by the catalytic mechanism. Since kinetic rates are different the compositions of these two diblock copolymers should be different if the termination (or transfer) rate is identical.

Over 150 bar of ethylene pressure, we observe that molecular weights of the copolymers are over the molecular weight of block. Consequently, multiblock copolymers seem to be obtained.

These results are the first evidence that the cleavage of the nickel carbon bond can be reversible. For example at 200 bar, sixteen consecutive ethylene and MMA blocks compose the copolymer of 15000 g/mol. Consequently, the fragmentation and addition of the metal

carbon bond takes place 16 times before an irreversible transfer or termination. This high frequency of exchanges averages the difference between a radical initiation and a catalytic initiation of the polymer chain. This has been confirmed by chromatographic method as only one family of chemical composition is identified on these copolymers (see Figure 7).

Without AIBN, NMR results indicate that only diblock copolymers are synthesized. Moreover for copolymers synthesized over 150 bar no additional signal is observed which indicates a possible mixture of homopolymers (LC-CC analyses need to be performed in order to confirm the nature of copolymers).

7. Conclusion

In this section, the hybrid radical/catalytic copolymerization of ethylene with MMA has been performed using NiNO in the presence of AIBN and NiNO alone. These systems allow the formation of copolymers covering the whole range of composition with significant activity.

Moreover, LC-CC analyses performed on these copolymers confirm that no homopolyethylene is present and ^{13}C NMR provides a confirmation of the multiblock microstructures of these ethylene/MMA copolymers. In the presence of NiNO alone, diblock only seems to be synthesized.

These kinds of copolymers are totally new and the multiblock architectures should represent significant interest for their physical properties (via e.g. an original nano-structuration of these blocks).

The ratio AIBN/NiNO has a crucial importance since with an excess of NiNO mostly PE is synthesized and mostly PMMA with an excess of AIBN. The composition of the copolymers can also be monitored by reaction parameters as ethylene pressure and initial amount of MMA used.

In consequence this hybrid polymerization appears to be a promising method to undergo efficient copolymerization of ethylene with polar vinyl monomer.

C. Case of styrene, BuA and VAc copolymerization with ethylene

Other comonomers are also studied more in depth in order to access a better understanding of the mechanism of polymerization.

1. Ethylene copolymerization with styrene

Styrene is one of the most interesting monomer as the polymerization in the presence of NiNO alone or AIBN alone produces homopolystyrene while the copolymerization in the same experimental conditions with NiNO and AIBN produces a copolymer of styrene and ethylene.

It is noteworthy that these copolymers can be synthesized using pure catalytic mechanism (statistical or block ethylene/styrene copolymers) using for example CGC catalysts [4, 5].

a) Effect of ethylene pressure

We investigate the polymerization at different ethylene pressures with styrene instead of MMA with NiNO alone or with AIBN. Reactions are performed at 70°C in 40 mL of toluene with 10 mL of styrene during 4 hours, 20 mg of NiNO and with or without ½ molar equivalent of AIBN. Results are summarized in Figure 13.

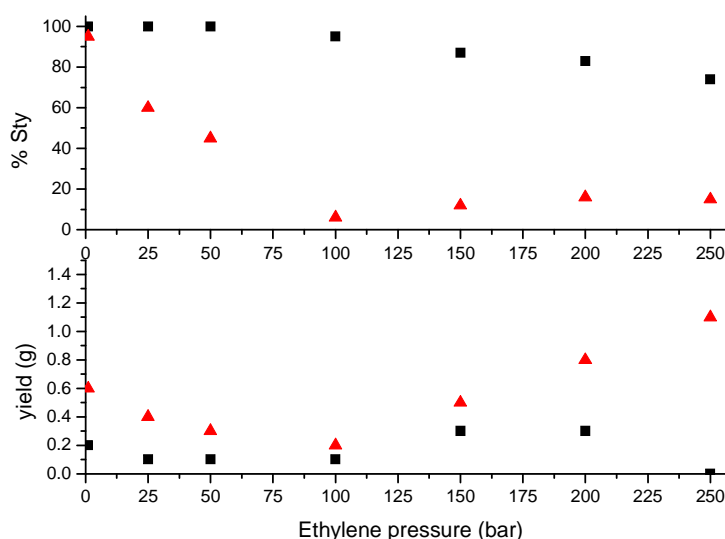


Figure 13. Effect of ethylene pressure on yield and styrene molar insertion^a during the copolymerization of ethylene with styrene. 20 mg of NiNO in 40 mL of toluene with 10 mL of styrene at 70°C during 4 hours with ▲ or without ■ AIBN. ^a: determined by ¹H NMR

As for MMA, copolymerization yields are higher when polymerization is performed with NiNO in the presence of AIBN whatever the ethylene pressure. In the presence of AIBN yield first decreases with increasing ethylene pressure and then increases over 100 bar. Using NiNO alone, yield remains almost constant whatever the ethylene pressure. Moreover insertion of styrene varies from 95% to 5%. In the presence of AIBN and NiNO insertion of ethylene drastically decreases with the ethylene pressure until 100 bar of ethylene pressure then slightly increases. Using NiNO alone the ethylene insertion remains low with a maximum at 20% for copolymer synthesized under 250 bar of ethylene pressure. For copolymer synthesized without AIBN no melting points is observed for copolymers. With AIBN, copolymers exhibit a melting point at 95-110°C which increases with the ethylene pressure.

b) Effect of catalyst concentration

We also investigate the effect of concentration of the catalyst and radical initiator on the copolymerization. Two different initial concentrations of styrene are investigated

Table 8. Influence of NiNO and AIBN concentration on the ethylene/styrene copolymerization at low ethylene pressure.^a

NiNO (mg)	AIBN (molar eq)	Initial vol. % of styrene	Yield (g)	Molar insertion of styrene (%) ^b
20	1/2	20	0.2	66
50	1/2	20	0.5	64
20	2	20	0.4	86
50	1/8	20	0.2	95
20	1/2	50	0.5	97
50	1/2	50	1.2	95
20	2	50	0.6	98
50	1/8	50	0.4	100

^a: Polymerizations are performed during 2 hours at 70°C in 50 mL of toluene styrene mixture under 25 bar of ethylene pressure. ^b: determined by ¹H NMR.

As for MMA copolymerization with ethylene, the global concentration of the catalyst and AIBN (without changing the ratio AIBN/NiNO) does not affect the monomer insertion but only the yield of the polymerization.

The most interesting behavior is observed when an excess of NiNO or AIBN is used. In both cases the copolymer produced is close to homopolystyrene. For example at 20% v/v of styrene the insertion is 66% in the presence of $\frac{1}{2}$ molar equivalent of AIBN, 86% using 2 equivalents and 95% using $\frac{1}{8}$ equivalent. Therefore an ideal ratio AIBN/NiNO exists in order to insert efficiently ethylene in the polymer chain.

Very similar results are obtained if the copolymerization is performed under 100 bar of ethylene pressure (see Table 9).

Table 9. Influence of NiNO and AIBN concentration on the ethylene/styrene copolymerization at high ethylene pressure.^a

NiNO (mg)	AIBN (molar eq)	Yield (g)	Molar insertion of styrene (%) ^b
20	$\frac{1}{2}$	0.2	6
50	$\frac{1}{2}$	0.6	7
20	2	0.3	86
50	$\frac{1}{8}$	0.2	80

^a: Polymerizations are performed during 2 hours at 70°C in 40 mL of toluene with 10 mL of styrene under 100 bar of ethylene pressure. ^b: determined by ¹H NMR.

However at this ethylene pressure, the effect is even more dramatic: from 6% of inserted styrene in the presence of $\frac{1}{2}$ molar equivalent of AIBN to more than 80% if an excess or default of AIBN is used.

These sets of experiments highlight the importance to adapt the ratio AIBN/NiNO in order to induce an efficient copolymerization. To obtain the highest ethylene insertion $\frac{1}{2}$ molar equivalents of AIBN is required. This optimum appears to be a compromise between a polymerization mostly controlled by catalysis at low AIBN/NiNO ratio and another one controlled by AIBN at high AIBN/NiNO ratio.

2. Ethylene copolymerization with BuA

Ethylene/BuA copolymerizations are performed in experimental conditions similar to ethylene MMA and styrene copolymerizations. Copolymerizations with BuA highlight the importance of AIBN. Without AIBN whatever the ethylene pressure, no activity is obtained (see Figure 14).

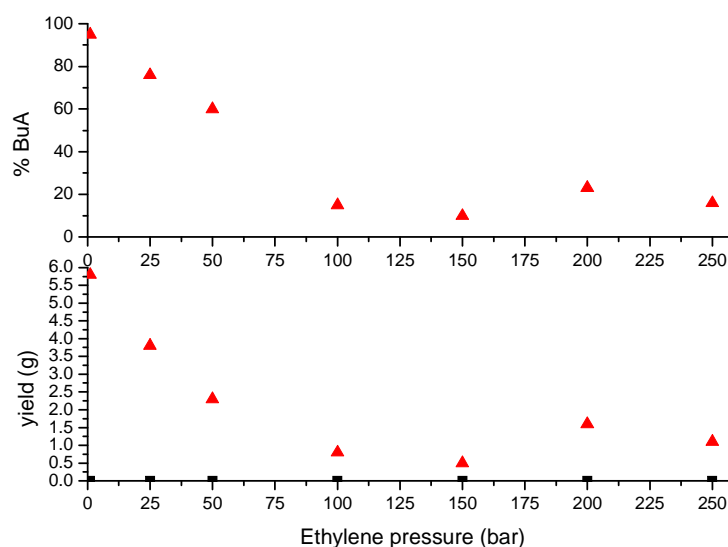


Figure 14. Effect of ethylene pressure on yield and BuA molar insertion^a during the copolymerization of ethylene with BuA. 20 mg of NiNO in 40 mL of toluene with 10 mL of BuA at 70°C during 4 hours with ▲ or without ■ AIBN.
^a: determined by ¹H NMR

In the presence of AIBN and NiNO, the yield first decreases then reaches a plateau over 100 bar of ethylene pressure. Same behavior is obtained for BuA insertion. Consequently copolymers with BuA insertions from 90% to 10% are synthesized by increasing the ethylene pressure only.

Once again over 100 bar of ethylene pressure, insertion of BuA seems to be almost constant around 10%. This value is higher than for MMA (5%) and styrene (7%). This polar monomer insertion seems not to be controlled by a radical mechanism otherwise the insertion at this “equilibrium” should be lower with styrene than MMA which is not the case. Indeed the insertion is controlled by the exchange kinetic between radical and catalytic mechanism. This exchange is more favored with BuA than with styrene and MMA. However, the exact nature of the exchange mechanism remains to be determined.

3. Copolymerization of vinyl acetate with ethylene

Copolymerizations with VAc are also performed under ethylene pressure up to 250 bar of ethylene pressure using similar experimental conditions. However, whatever the ethylene pressure, yield remains extremely low with or without additional AIBN.

This copolymerization remains almost inefficient. As the ethylene catalytic polymerization can be performed in pure ethyl acetate [6], and the copolymerization take place with MMA or BuA, it indicates that in this case the β -OAc elimination could play a crucial role. Indeed, this elimination would totally inhibit the ethylene catalytic polymerization.

4. Conclusion

a) Proposed mechanism for the hybrid copolymerization

From the previous results, we can assume that the NiNO catalyst can also insert a polar vinyl unit in the polymer chain by coordination-insertion. Then in the case of VAc, β -OAc elimination takes place and terminates the polymer chain.

However, with other monomers the catalytic center is dormant after this insertion. Moreover, with MMA no chain-walking could take place because no hydrogen is present in β after a 2,1 MMA insertion (it should be noted that the ^{13}C NMR confirms that MMA block-end do not contain head-head and tail-tail sequences, therefore no 1,2 insertion of MMA seems to take place). This species could be referred as a dormant species until a radical substitution take place. Then another ethylene block can grow (see Figure 15).

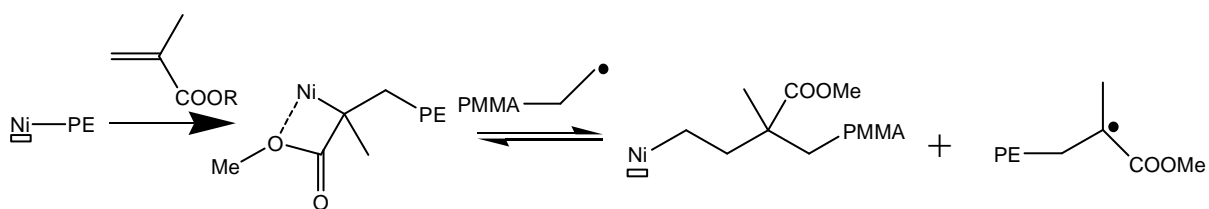


Figure 15. Proposed mechanism of exchange

This mechanism is in agreement with the initial MMA concentration dependence of the multiblock copolymer composition. If the radical which reacts with the catalyst is a MMA radical (for example) the catalyst remain dormant while with an ethyl radical the catalyst is not dormant anymore and the ethylene polymerization can take place (see Figure 15).

Consequently the efficient $Sr2$ takes place after the insertion by coordination-insertion of a polar vinyl unit in the catalytic-made block (Ni-PE) and the insertion of an ethylene unit in the radical made block (see Figure 15).

Since ethylene insertion in a radical chain is easier with BuA than MMA (reactivity ratios determined in chapter IV give under similar experimental condition $r_{BuA}=5.6$ and $r_{MMA}=28.1$) this mechanism is also in agreement with the order in the “equilibrium” composition observed at high ethylene pressure.

b) Copolymers available by hybrid radical/catalytic copolymerization

This hybrid system appears to be extremely efficient to provide various ethylene/polar vinyl monomer copolymer in all the range of chemical composition from the almost pure PE to the homo-polar polymer.

We demonstrated that the copolymer synthesized exhibits a unique chemical composition and possesses a specific multiblock microstructure. These copolymers can exhibit very interesting physical properties due to the potential nano-structuration of ethylene block and polar block.

MMA, BuA have been especially studied. The composition can be controlled by the amount of polar vinyl monomer, the ethylene pressure or the ratio AIBN/NiNO.

One potential improvement for this hybrid radical/catalytic copolymerization is to access to the copolymerization of VAc with ethylene. Indeed VAc remains one of the last comonomer which totally inhibits the copolymerization. However, PAc (isopropenyl acetate) shows some promising result.

D. Hybrid copolymerization using an ATRP system

In order to access a better control of the introduction of additional radicals, we attempt a hybrid copolymerization using a controlled radical polymerization system as a source of radicals.

1. Why ATRP system is a promising pathway?

As we already mentioned, in the second chapter we performed some tryouts in order to control the radical polymerization of ethylene. The most promising systems were the CMRP and RAFT polymerization.

However, here we choose to investigate the hybrid catalytic/controlled radical polymerization using an ATRP system for the following reason. The CuBr and the PMDETA (pentamethyldiethyltriamine) ligand activate the ethylene polymerization by NiNO catalyst contrary to a RAFT agent or nitroxide which inhibit totally the ethylene polymerization (see Table 10).

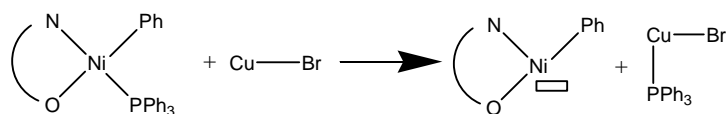
As comparison Ni(COD)₂ a classical phosphine scavenger, known to activate ethylene polymerization, has been also added to the catalyst (see Table 10).

Table 10. Activation of ethylene catalytic polymerization by ATRP controlled agent^a

Additional compounds (molar equivalent vs. NiNO)	Activity (g/mmol/h)	Mn (g/mol) ^b [PDI] ^b	Melting Temperature (°C) ^c
-	94.7	7150 [2.2]	117.9
Ni(COD) ₂ (1.5 eq)	406	12150 [2.2]	118.3
CuBr (1.5 eq)	352	9750 [2.2]	118.2
PMDETA (1.5 eq)	397	13200 [1.9]	112.2
CuBr (1.5 eq) + PMDETA (1.5 eq)	232	11500 [3.2]	115.7
CuBr ₂ (1.5 eq)	302	9900 [2.3]	117.8
CuBr ₂ (1.5 eq) + PMDETA (1.5 eq)	217	10500 [3.0]	114.3

^a: Polymerizations are performed during 1 hour with 20 mg NiNO at 50°C in 250 mL of toluene under 20 bar of ethylene pressure. ^b: determined by HT-SEC. ^c: determined by DSC.

The mechanism of activation should be equivalent between Ni(COD)₂ (nickel biscyclooctadiene), a phosphine scavenger which release the coordination site on which ethylene will coordinate, and CuBr (see Figure 16).

**Figure 16. Phosphine scavenger mechanism of CuBr on NiNO**

For PMDETA, the mechanism of activation should be similar to the one developed in the previous chapter for additional ligand.

When both compounds (CuBr and PMDETA) are added to the catalytic system the polymerization is still activated but less than with only one compound. Moreover the molecular weight distribution is broader. These results may indicate that the mechanism of activation of CuBr and PMDETA are different and can not take place at the same time (this is expected since one is a Lewis acid and the other a Lewis base).

CuBr₂ act also as an activator of the ethylene polymerization therefore reverse ATRP can also be used to control radical polymerization during the hybrid copolymerization.

2. Introduction of radicals from ATRP equilibrium

Polymerizations are performed at 70°C, overnight, in 250 mL of a toluene/MMA mixture at 5% v/v in MMA over different ethylene pressure, with 100 mg of NiNO, 1.5 molar equivalents vs. NiNO of PMDETA and CuBr, and 10 molar equivalent vs. CuBr of ethyl 2-bromo-2-methylpropanate (standard initiator of MMA by ATRP, we will call it in the following MMABr). Results are summarized in the following table.

Table 11. Influence of pressure on the hybrid copolymerization coupled with ATRP^a

Ethylene pressure (bar)	Soluble in THF	Yield (g)	Molar insertion of MMA (%) ^b	Average length of MMA block per block end ^c
4	Yes	2.3	51	30
10	No	1.7	9	nd
	Yes	5.9	48	20
20	No	5	21	9

^a: Polymerizations are performed during 12 hours with 100 mg NiNO at 70°C in 250 mL of toluene/MMA mixture (19/1 v/v) with 1.5 molar equivalents of PMDETA and CuBr and 10 molar equivalent vs. CuBr of MMABr. ^b: determined by ¹H NMR. ^c: determined by ¹³C NMR.

At low ethylene pressure (4 bar) the polymers produced are totally soluble in THF and then as expected high MMA insertions are observed with long MMA sequences. At 10 bar, two types of copolymer, one soluble in THF and the other insoluble, are produced. The soluble one exhibits lower MMA insertion and shorter MMA sequences than the copolymer synthesized under 4 bar of ethylene pressure. Finally, at 20 bar no fraction of the synthesized material is soluble in THF. 21% of MMA are incorporated in the polymer and short sequences of MMA are synthesized.

Finally MALDI-TOF analyses are performed in order to characterize the specific type of copolymer. Only low molecular weights polymers can be detected and analyzed. This analysis could evidence the coupling of a catalytic initiation (phenyl chain-end group) and ATRP termination (Br chain-end group). This family is actually present in MALDI-TOF spectrum (see Figure 17).

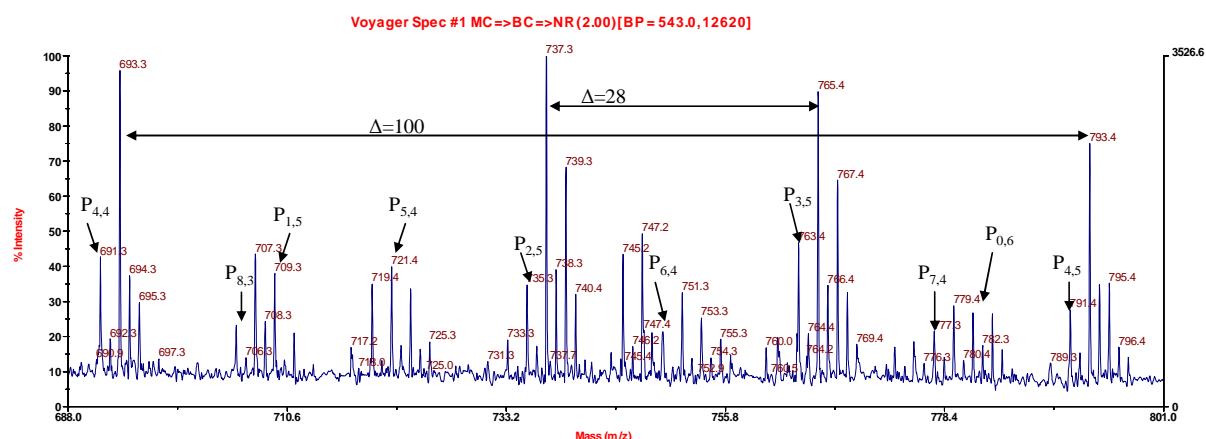


Figure 17. MALDI-TOF spectrum of copolymer produced (zoom between 680 and 800 g/mol).

This spectrum shows separation between the distribution of 28 g/mol corresponding to an additional ethylene unit or 100 g/mol corresponding to an additional MMA unit. The nature of the copolymer ethylene/MMA is then confirmed.

Signals indexed $P_{x,y}$ corresponds to copolymer with the microstructure $\text{Ph}(\text{E})_x(\text{MMA})_y\text{Br}$. The presence of these signals testifies that an exchange exists between the catalytic polymerization of ethylene and the ATRP of MMA. These signals are in good agreement with the theoretical one (see Table 12).

Table 12. Agreement between theoretical and observed signals

Polymer	Formula	Na ionize mass	Isotopic abundance	Observed peak
Ph(E) ₂ (MMA) ₅ Br	C ₃₅ H ₅₃ O ₁₀ Br	735,27	0,3333	735,3
		736,27	0,1337	736,3
		737,27	0,357	737,3
		738,27	0,136	738,3

As for the standard hybrid system (NiNO and AIBN) the ratio between NiNO and ATRP initiator can monitor the MMA insertion in the polymer chain. Indeed in the presence of 20 molar equivalents of ATRP agents (CuBr, PMEDTA with 10 eq. of MMABr), insertion of MMA in the produced copolymer (2g) increases to 45% and average length of MMA per block-end decreases to 7. This copolymer is not soluble in THF. This decrease of MMA block length indicates that the frequency of exchange between radical and catalytic polymerization is increased. This can be due to a higher radical concentration at the equilibrium.

In conclusion this ATRP system seems to be compatible with the NiNO catalyst and the copolymerization can then be performed using an elegant method to introduce radicals to our systems. Moreover, we demonstrate that a shuttling exists between ATRP and catalytic polymerization.

This is a promising method of copolymerization and further investigations need to be done in order to access a living hybrid copolymerization.

3. Case of reverse ATRP

We also investigate the copolymerization using CuBr₂ or NiBr₂ in order to create a reverse ATRP equilibrium. This system is the easiest to perform since the radical created by the homolytic cleavage of the nickel-carbon bond will be involved in the ATRP equilibrium.

This copolymerization is performed at 70°C, overnight, in 250 mL of a toluene/MMA mixture at 5% v/v in MMA over 20 bar of ethylene, with 100 mg of NiNO

using two different ATRP agents, CuBr₂ or NiBr₂, at 1.5 molar equivalents vs. NiNO and 1.5 equivalent of PMDETA. Results are summarized in the following table.

Table 13. Ethylene/MMA copolymerization with NiNO using reverse ATRP^a

ATRP system	Soluble in THF	Yield (g)	Molar insertion of MMA (%) ^b	Mn (g/mol) ^c
-	No	2.8	4.3	8500 [2.3]
CuBr ₂	No	4.5	1	6000 [1.7]
	Yes	0.5	11	12000 [1.8]
NiBr ₂	No	0.4	1	6300 [1.9]
	Yes	1.3	40	14000 [1.8]

^a: Polymerizations are performed during 12 hours using 50 mg NiNO at 70°C in 250 mL of toluene/MMA mixture (19/1 v/v) under 20 bar of ethylene pressure with 1.5 molar equivalents of PMDETA and CuBr₂ or NiBr₂. ^b: determined by ¹H NMR. ^c: determined by HT-SEC.

Contrary to NiNO complex alone, both copolymerizations using reverse ATRP lead to two distinct copolymers one soluble in THF and the other non-soluble.

As expected the two different systems do not lead to the same yield and MMA insertion. Copolymerization with CuBr₂ is more efficient and the synthesis of low MMA content polymer is favored. With NiBr₂, lower yield is achieved however high MMA content is obtained in higher amount.

However, with both reverse ATRP systems higher MMA incorporations are achieved compared to the standard system. This may indicate that without reverse ATRP agent the radical suffers radical termination very rapidly therefore does not incorporate MMA anymore. With reverse ATRP, the probability of irreversible termination or transfer decreases consequently more MMA can be inserted in the polymer chain and higher incorporation are achieved.

E. Conclusion

In this chapter we demonstrated the efficiency of this new approach of copolymerization of ethylene with polar vinyl monomer. Many polar vinyl monomers can be copolymerized by this hybrid radical/catalytic mechanism with NiNO and AIBN. In particular unusual monomers were efficiently copolymerized with ethylene such as acrylonitrile, (meth)acrylic acids or (meth)acrylamides. For the two last families, polymers exhibit very interesting behaviors in water (water-soluble, nano-structuration)

We investigated the importance of ethylene pressure and MMA concentration on the composition of the produced multiblock copolymers. Ethylene insertion increases with the pressure of polymerization and decreases with the MMA initial concentration.

We also shown the importance of the ratio AIBN/NiNO concentration. For MMA copolymerization, large AIBN excess leads to PMMA-like copolymer and large NiNO excess provides PE-like copolymer.

In consequence, by adjusting wisely all these parameters, the whole range of compositions can be reached from a pure polyethylene to a pure PMMA for example.

Finally ethylene/MMA copolymer microstructures have been studied by NMR and multiblock architectures demonstrated. LC-CC and ^{13}C NMR studies have been only performed in depth up to now with ethylene/MMA copolymer, however similar investigations are under process for BuA copolymers.

During styrene copolymerization only the right AIBN/NiNO ratio will lead to high ethylene insertion in the polymer chain. In the case of BuA copolymerization the presence of AIBN is mandatory in order to obtain a copolymer.

Investigation of the ATRP coupled to catalytic polymerization is also reported. The copolymerization is not controlled however the shuttling between a catalytic ethylene polymerization and ATRP of MMA is demonstrated by MALDI-TOF. This kind of copolymerization needs to be studied further in order to reach the controlled hybrid copolymerization of ethylene.

References:

- [1] D. J. Arriola, E. M. Carnahan, P. D. Hustad, R. L. Kuhlman, and T. T. Wenzel *Science*, vol. 312, p. 714, 2006.
- [2] A. Berkefeld and S. Mecking *Angew. Chem. Int. Ed.*, vol. 47, p. 2538, 2008.
- [3] A. Nakamura, S. Ito, and K. Nozaki *Chem. Rev.*, vol. 109, p. 5215, 2009.
- [4] D. J. Arriola, M. Bokota, R. E. Campbell, J. Klosin, R. E. Lapointe, O. D. Redwine, R. B. Shankar, F. J. Timmers, and K. A. Abboud *J. Am. Chem. Soc.*, vol. 129, p. 7065, 2007.
- [5] L. Caporaso, L. Izzo, I. Sisti, and L. Oliva *Macromolecules*, vol. 35, p. 4866, 2002.
- [6] T. R. Younkin, E. F. Connor, J. I. Henderson, S. K. Friedrich, and R. H. Grubbs *Science*, vol. 287, p. 2320, 2000.

Conclusion and perspectives

The aim of this thesis was the copolymerization of ethylene with a polar vinyl monomer via a hybrid radical/catalytic mechanism. For this purpose, we chose to introduce a source of radicals in presence of a traditional catalyst of olefin polymerization in order to favor an exchange of the growing polymer chain between radical and catalytic mechanisms.

During this work the ethylene radical polymerization and copolymerization in organic and water dispersed media has also been investigated.

We achieved quite unexpected results and fulfilled the initial goal of this thesis. The radical polymerization of ethylene is now understood in detail. Indeed now we know the limitation of the free radical polymerization in yield and microstructures. Moreover, the development of ethylene radical polymerization in water dispersed media allowed to synthesize high molecular weight PEs with high yields. Radical copolymerization even at higher pressure than the one usually used in academic studies does not give access to the full range of composition and microstructures of copolymers. Therefore the development of a hybrid radical/catalytic polymerization appeared to be mandatory. The hybrid mechanism of polymerization was also investigated. Only catalysts associated to a radical flux allows to produce copolymers with a wide range of compositions and a broad diversity of polar functions brought by MMA, AA or AN for example.

In the first part of this manuscript, we developed the free ethylene radical homopolymerization under experimental conditions usually assumed to be inefficient. Indeed no real investigation had been done using milder conditions than the industrial process for LDPE synthesis ($P > 2000$ bar and $T > 200^\circ\text{C}$). We demonstrated that ethylene can be polymerized in a solvent at ethylene pressure as low as 5 bar and temperature as low as 10°C without using any specific activating compounds. Ethylene polymerization was performed in various experimental conditions at temperatures ranging from 10°C to 110°C and ethylene pressures from 5 bar to 250 bar. Polyethylene exhibited unexpected low branches content from 5 to 10 branches per 1000 C. Molecular weights of synthesized PE remained low because of chain transfer reaction to solvent but when polymerization took place in DEC higher molecular weights were achieved ($M_n \approx 20000$ g/mol). Finally melting points ranging from 122°C to 85°C were obtained.

Ethylene free radical polymerization can be performed either in a unique supercritical medium or a biphasic medium. In the latter the ethylene polymerization takes place mostly in the liquid phase where some ethylene is dissolved. The transition between these two different systems has been determined experimentally and theoretically. For this purpose the ethylene solubility has been determined in several solvents at different temperatures and under ethylene pressures up to 140 bar.

Ethylene free radical polymerization showed a high solvent activation effect. Indeed ethylene free radical polymerization without solvent produced almost no polymer in the experimental conditions investigated. Polymerization in THF was shown to be almost 6 times more efficient than polymerization in toluene in the same experimental conditions. A broad range of solvents has been investigated in order to determine the critical parameters which control the ethylene polymerization activity. This effect has been rationalized using Keesom interaction parameters. Moreover, solvents also impact the molecular weight of synthesized PE and can lead via transfer reaction to functionalized polyethylene. Indeed THF-ended or chloro-ended polyethylene were obtained. This can be used for producing macromonomer for example.

Some promising results were obtained towards the control of the radical polymerization of ethylene especially using CMRP. Indeed molecular weight increases linearly with conversion and the number of chains remains constant during the polymerization. Some RAFT agents also show promising results as the molecular weight increases with conversion, however the number of polyethylene chains also increases during the polymerization. One last promising way to control ethylene radical polymerization is by alkyl metal agent through a controlled mechanism via a degenerative transfer close to RAFT mechanism. These results represent an important breakthrough in the radical polymerization since ethylene is one of the last “uncontrolled” monomer among all these polymerized by radical pathway.

The polymerizations in organic solvent under milder experimental conditions than the industrial ones were then transposed to emulsion radical polymerization. Stable PE latexes with solid content up to 40% were synthesized using a free radical polymerization in water using AIBA as initiator and with or without CTAB as surfactant. In emulsion PEs of high molecular weights were produced ($M_n > 10^6$ g/mol, $PDI > 4$). Particles diameters from 20 nm to 150 nm were obtained leading from transparent to white latexes (see Figure 1). Two different morphologies of PE particles were obtained: sphere-like PE particles with some facets when

ethylene polymerizations are performed with a low surfactant concentration or cylinder-like particles if polymerizations are performed using a high surfactant concentration. Standard emulsions initiated by APS in or without the presence of SDS were also used however these systems appeared to be less efficient and eventually lead to flocculation in the presence of SDS. Finally, hybrid nanoparticles were obtained using polystyrene or silica cores.



Figure 1. Light transmission through two different native PE latexes obtained at 6% of solid content

In a second part of this work, we investigated the copolymerization of ethylene with a polar vinyl comonomer using free radical polymerization in organic solvent or in water. In this section we particularly highlighted the ambivalent role of the comonomer. Indeed comonomers are solvents which modify the ethylene reactivity (as ethylene radical polymerization presents a high solvent activation effect) on one hand and on the other hand, they are comonomers which can be inserted in the polymer chain. Consequently the reactivity ratios of a copolymerization can be tuned by controlling the comonomer initial content and the organic solvent used. In this section we demonstrated that in these experimental conditions, insertion of ethylene remained limited (having more than 50% of ethylene content was almost never reached except during VAC/ethylene copolymerization) and almost no sequence of successive ethylenes was present in the copolymer chain.

Therefore another mechanism of polymerization needed to be developed in order to produce the complete range of copolymer composition from 0.1% to 99.9% of ethylene content.

In the last part, we developed the hybrid copolymerization concept. First we demonstrated that the chosen nickel catalyst suffers a spontaneous homolytic cleavage and can also undergo radical substitution. Indeed, this homolytic cleavage of the nickel carbon bond can induce polymerization of polar vinyl monomers such as MMA or styrene. Moreover this cleavage kinetics can be adjusted by adding some phosphorous ligand to the system. Then for example the half-life time of the system can be monitored from 60 min to 360 min and

efficiency factor from 4% to 100% just by changing the phosphorous ligand. In the same way the catalytic polymerization parameters (activity, molecular weight and melting point of the synthesized PE) can be modified using the same ligands. Some of the phosphorous ligand almost totally inhibits the polymerization but other activate ethylene catalytic polymerization by a factor of 4. These results were unexpected because usually the addition of Lewis bases to an ethylene catalyst deactivates the ethylene polymerization. Finally a synergy effect has been demonstrated between the radical polymerization and the catalytic polymerization, since AIBN activates the ethylene polymerization catalyzed by NiNO and the radical polymerization initiated by NiNO. A mechanism of initiation of the polar monomer polymerization and interaction with AIBN has been proposed and confirmed using EPR techniques.

Then we used the combination of NiNO and AIBN in order to perform efficient copolymerization of ethylene with various polar vinyl monomers from (meth)acrylates to (meth)acrylic acids or (meth)acrylamides. Mechanism of the hybrid radical/catalytic copolymerization has been investigated (see Figure 2). The superiority of the hybrid polymerization using an additional source of radical has been demonstrated. Multiblock copolymers have been produced with ethylene insertions from 0.1% to 99.9%. Finally, in order to improve this mechanism we investigated the possibility of coupling a catalytic polymerization with an ATRP system. Some promising results were obtained and the “shuttling” between the catalytic polymerization and ATRP demonstrated.

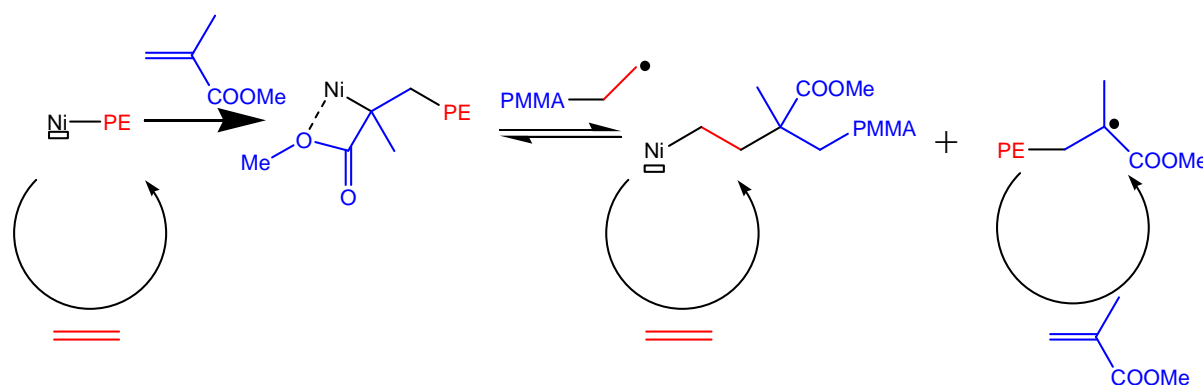


Figure 2. Proposed mechanism of hybrid copolymerization of ethylene with MMA

This thesis discloses new fields which need to be investigated further.

In regards to the homopolymerization of ethylene, the fine study of the solvent activation effect using quantum calculations remains to be done. Indeed, ethylene free radical polymerization presents the unique advantage to be extremely simple to modelize compared to other monomers. This is then a unique opportunity to access a fine understanding of the solvent activation effect during radical polymerization. Some preliminary collaboration has been initiated during this PhD with Dr. Sylvain MARQUE and his team in the laboratory CROPS in Marseille (France).

Moreover, transfer reaction to solvent during the radical polymerization of ethylene can also be used to produce functionalized PE such as macromonomer for example in order to access new architectures. For instance, polylactones with PE branches could be obtained.

The development of ethylene controlled radical polymerization must also be investigated further with for example the synthesis of block copolymers by CMRP.

In emulsion, the properties of PE latexes should be investigated and especially their coating properties. Indeed, these latexes could represent a cheap way to produce hydrophobic films. Moreover the core-shell nanoparticles based on PE should also be developed, especially the synthesis of HDPE core/LDPE shell nanoparticles could present some interesting properties. This kind of particles may have very promising physico-chemical properties.

On the ethylene radical copolymerization, a closer investigation on ethylene vinyl acetate copolymerization needs to be done. Indeed with VAc, ethylene insertion up to 95% can easily be achieved. Since CRP techniques are available for the control of the polymerization of this monomer, a controlled radical copolymerization of ethylene with VAc may be possible.

Concerning the hybrid mechanism, other catalysts need to be investigated. Indeed NiNO catalyst provide branched ethylene block, which increase the complexity of ^{13}C NMR spectrum and therefore the copolymer microstructures is much difficult to investigate. Therefore the development of a hybrid polymerization with a catalyst which does not exhibit chain-walking would lead to linear ethylene block and therefore simplify the structure of the copolymer. Moreover, this kind of copolymer would possess different physico-chemical properties which remain to investigate.

The approach developed in this manuscript is to find an ethylene polymerization catalyst which could exchange its alkyl fragment via a radical substitution. Other pathways can be imagined such as hybrid catalytic/anionic or cationic polymerization, or one could search for a control agent of radical polymerization which allows the coordination and insertion of ethylene. Also the photo-induced cleavage of the metal carbon bond remains to investigate.

Moreover, this hybrid polymerization could be transposed to other non polar monomer such as propylene, butadiene or styrene (especially *s*PS), and to other processes such as emulsion, miniemulsion.

The development of a controlled hybrid polymerization using a living ethylene coordination/insertion polymerization and a controlled radical polymerization system remains an important improvement to perform.

Finally, the physico-chemical properties of new multiblock copolymers need to be deeply investigated by mechanical methods, DMA (dynamic mechanical analysis) for example. Indeed the potential nanostructuration could lead to interesting properties. These new material should exhibit some new properties which can be used in specific applications.

Experimental part

A.	Synthesis of organometallic compounds.....	384
1.	NiNO synthesis	384
a)	Ligand synthesis	384
b)	Nickel precursor synthesis	385
c)	Synthesis of the NiNO catalyst	386
2.	NiPO synthesis.....	387
a)	Ligand synthesis	387
b)	Nickel precursor synthesis: Ni(COD) ₂	388
c)	Catalyst synthesis.....	389
B.	Method of polymerization.....	390
1.	Polymerizations without ethylene.....	390
2.	Ethylene homo- and copolymerization at low-pressure (P<25 bar).....	390
3.	Ethylene homo- and copolymerization at high-pressure	391
a)	High-pressure reactor design.....	392
b)	About the on-line measurement of ethylene consumption during the polymerization	395
C.	Analytical methods.....	397
1.	Polymer analyses	397
a)	SEC.....	397
b)	DSC	397
c)	NMR	397
d)	IR	397
e)	MALDI-TOF	398
2.	Colloidal analyses	398
a)	DLS.....	398
b)	TEM.....	398
c)	AFM.....	398
d)	TGA	399
e)	Surface tension measurements	399
f)	X-Ray scattering	399
3.	Organometallics and organic compounds	400
a)	NMR	400
b)	EPR.....	400

All chemicals are handled using standard Schlenk procedures under argon atmosphere. Syntheses of catalysts are performed under inert atmosphere and products are stored in a glove box.

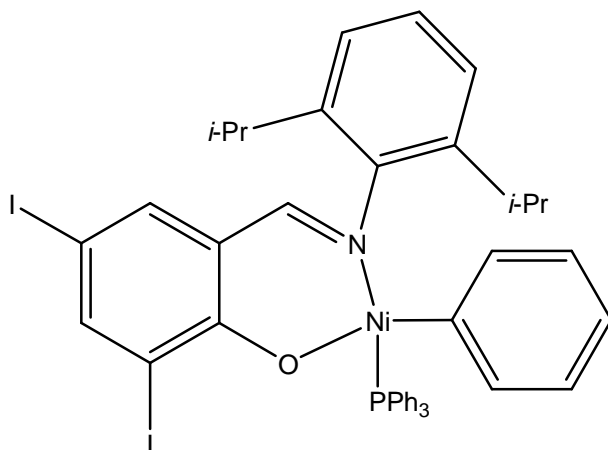
Organic solvents are distilled or dried and degassed under argon. THF, pentane and diethyl ether are dried over sodium/benzophenone then distilled. Alcohols, dichloromethane and pyridine are dried over CaH_2 and distilled. Other solvents are dried on molecular sieves. Water is purified using Milli-Q academic system (Millipore Corporation) and degassed under argon.

Ethylene (purity 99.95%) is purchased from Air Liquide and used without any further purification. All other liquid monomers (1-hexene, MMA, BuA, etc) are purchased from Acros and dried over CaH_2 (except AA, MAA, AAm, MAAm) and cryodistilled. AA and MAA are first dried on molecular sieves and then cryodistilled. AAm and MAAm are used without any further purification.

Radical initiators (AIBN, AIBA, APS, etc) are purchased from Acros and used without any further purification. Other compounds (such as surfactant, phosphorous ligand) are purchased from Acros or Sigma-Aldrich and used without any further purification.

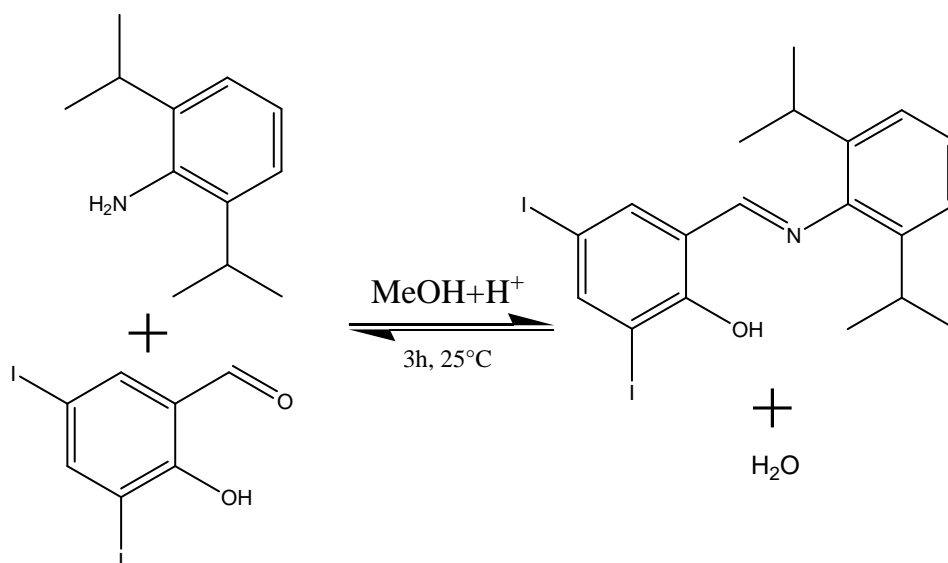
A. Synthesis of organometallic compounds

1. NiNO synthesis



a) Ligand synthesis

The ligand synthesis was performed according to Grubbs procedure [1].



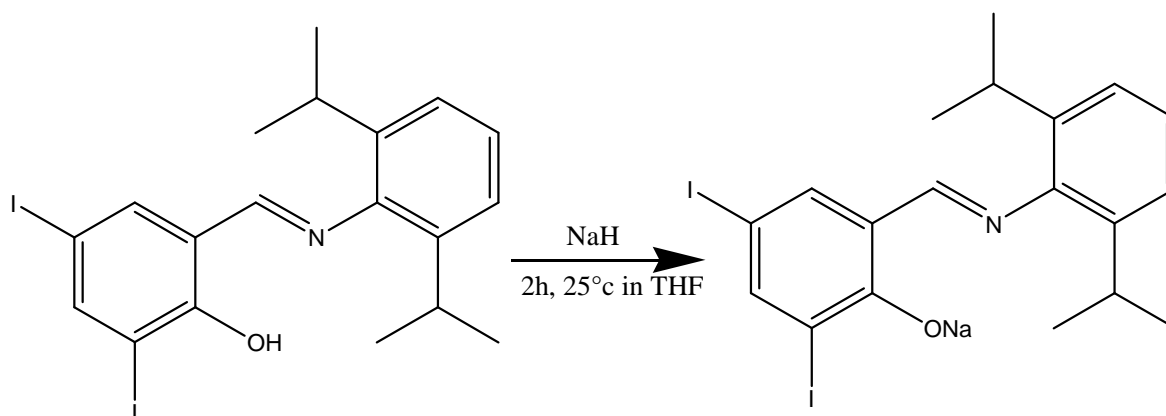
In a Schlenk under argon 100 mL of methanol were added to 5 g of 3,5-diiodosalicylaldehyde (13 mmol). Then 3.5 mL of 2,6-diisopropylaniline (1.3 eq) were added to the suspension at ambient temperature. 0.5 mL of formic acid were finally added dropwise. A yellow suspension was obtained. After three hours, a yellow solid was isolated by filtration. The solid was washed with 3 x 30 mL of methanol. Then the solid was dissolved in diethyl ether and dried by sodium sulphate during 1 hour. The salts were removed by filtration. The solvent was evaporated under vacuum. A yellow solid was obtained and dried under vacuum (yield 85%).

NMR

^1H (C_6D_6 , 300 MHz): 14.2 (*s*, OH , 1H), 7.9 (*d*, H_{ar} , 1H), 7.3 (*s*, $\text{CH}=\text{N}$, 1H), 6.9-7.1 (*m*, H_{ar} , 4H), 2.8 (*m*, CHMe_2 , 2H), 1.0 (*d*, CHMe_2 , 2H) ppm

^{13}C (C_6D_6 , 75 MHz): 165.8 ($\text{C}=\text{O}$), 161.2 ($\text{C}=\text{N}$), 150.0, 146.0, 141.1, 139.1, 126.9, 124.0, 120.7, 88.4 ($\text{C}-\text{I}$), 80.9 ($\text{C}-\text{I}$), 28.9 (CHMe_2), 24.0 (CHMe_2) ppm

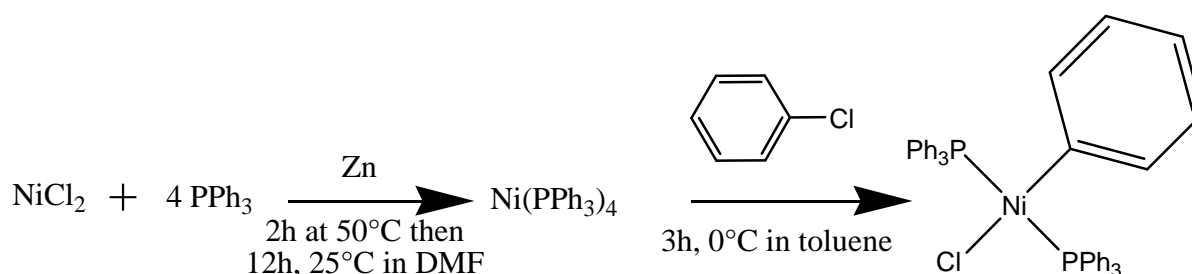
The ligand was then deprotonated.



7 g of ligand (14 mmol) were dissolved in 100 mL of freshly distilled THF. To this yellow solution 1 g of NaH (3.1 eq) was slowly added. The mixture was stirred during 2 hours at ambient temperature. After filtration and removal of the solvent under vacuum, the resulting solid was washed with 2 x 20 mL of cold pentane. A beige solid was obtained and dried under vacuum (yield 89%). Purity of the product was evidenced by the absence of the O-H bond vibration on IR spectrum.

b) Nickel precursor synthesis

The $\text{trans}-(\text{PPh}_3)_2\text{NiPhCl}$ synthesis was performed according to Zeller procedure [2].



In a Schlenk, 1.3 g of nickel (II) chloride (10 mmol), 0.66 g of Zn powder (10 mmol) and 11 g of triphenyl phosphine (42 mmol) were stirred in 100 mL of DMF. A green

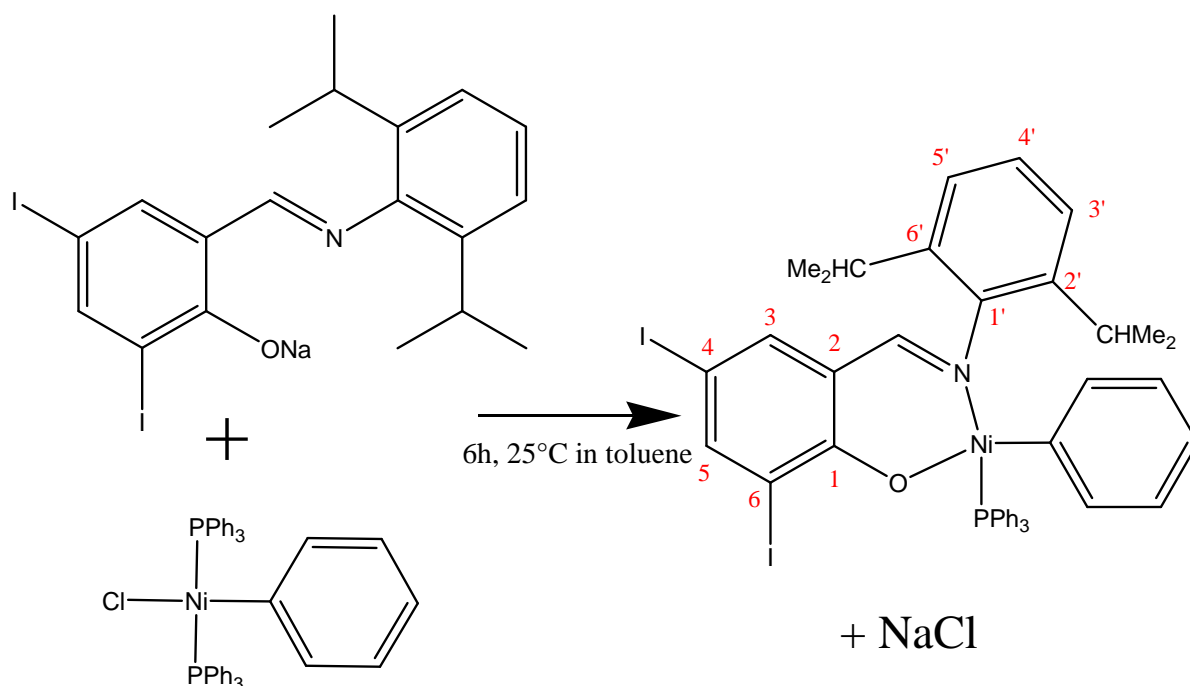
suspension was obtained. The mixture was stirred during 2 hours at 50°C then overnight at ambient temperature. A red suspension was then obtained. Solvent was removed under vacuum at low temperature ($T < 40^\circ\text{C}$) and 200 mL of toluene was added. The red solution was cooled down at 0°C then 3.1 mL of chlorobenzene (25 mmol) were added dropwise. The mixture was stirred during 3 hours at 0°C . A brown suspension was obtained. After filtration and evaporation of the solvent, the solid was washed with 2 x 50 mL of heptane. An orange powder was obtained (yield 60%).

NMR

^{13}C (C_6D_6 , 75 MHz): 148.9 (s, *i*-C of Ni-Ph), 138.5 (t, *o*-C of Ni-Ph), 135.5 (t, *o*-C of PPh_3), 133.0 (t, *i*-C of PPh_3), 130.0 (s, *p*-C of PPh_3), 128.4 (t, *m*-C of PPh_3), 127.3 (s, *p*-C of Ni-Ph), 121.4 (s, *m*-C of Ni-Ph) ppm

c) Synthesis of the NiNO catalyst

The nickel complex synthesis was performed according to Grubbs procedure [1].



In a Schlenk 2.5 g of $\text{trans}-(\text{PPh}_3)_2\text{NiPhCl}$ (3.59 mmol) were stirred in 50 mL of toluene. Then 1.95 g of deprotonated ligand (1.1 eq) were added to the orange suspension. This mixture was stirred at ambient temperature during 6 hours and turns red. After filtration, toluene was removed under vacuum. A red oil was obtained. This oil was washed with 3 x 40 mL of distilled pentane. An orange powder was obtained (yield 45%). The purity of the complex was confirmed by the absence of free phosphine determined by ^{31}P NMR (absence of a peak around -5 ppm).

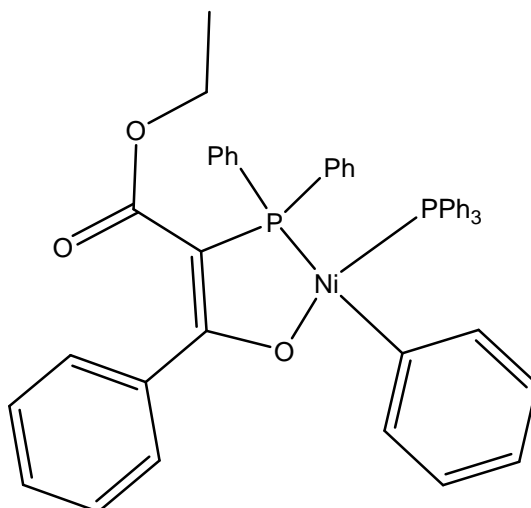
NMR

^1H (C_6D_6 , 300 MHz): 8.2 (*d*, $\text{CH}=\text{N}$, 1H), 6.3-7.2 (*m*, H_{ar} , 25H), 4.0 (*m*, CHMe_2 , 2H), 1.2 (*d*, CHMe_2 , 6H), 1.1 (*d*, CHMe_2 , 6H) ppm

^{13}C (C_6D_6 , 75 MHz): 165.8 (*s*, C1), 163.5 (*s*, $\text{HC}=\text{N}$), 150.5 (*s*, C5), 149.9 (*s*, C1'), 142.6 (*s*, C3), 140.8 (*s*, C2' and C6'), 137.7 (*d*, *o*-C of Ni-Ph), 135.3 (*d*, *o*-C of Ni-PPh₃), 132.9 (*t*, *i*-C of Ni-Ph), 132.1-131.5 (*d*, *i*-C of Ni-PPh₃), 130.5 (*s*, *p*-C of Ni-PPh₃), 127.7 (*t*, *m*-C of Ni-PPh₃), 126.8 (*s*, *p*-C of Ni-Ph), 125.9 (*s*, C4'), 123.4 (*s*, C3' and C6'), 122.1 (*s*, C2), 121.0 (*s*, *m*-C of Ni-Ph), 97.6 (*s*, C6), 73.9 (*s*, C4), 29.4 (*s*, CHMe_2), 26.0 (*s*, CHMe_2), 23.2 (*s*, CHMe_2) ppm

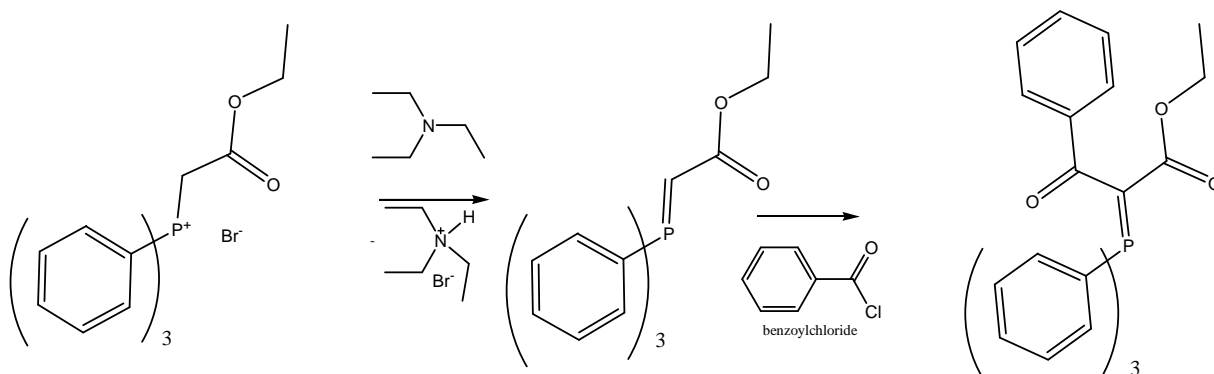
^{31}P (C_6D_6 , 121 MHz): 23.5 (*s*, Ni-PPh₃) ppm (-5 ppm, free PPh₃)

2. NiPO synthesis



a) Ligand synthesis

The ligand synthesis was performed following the procedure derived from literature and developed at the LCPP during Benjamin Saillard thesis [3].



At T=0 °C, 6.1 g of triethylamine (60 mmol) were added dropwise to a suspension of 12.94 g of (ethoxycarbonyl methyl)triphenylphosphonium bromide (30 mmol) in 60 mL of THF. The suspension was stirred for 30 min. Then, 4,2 g of benzoylchloride (30 mmol) were added dropwise.

The suspension was warmed up to room temperature during 1 h. The salts were removed by filtration. The remaining solvent was removed under vacuum. The white solid obtained was dissolved in 50 mL of methanol. To precipitate the white solid, 200 mL of distilled water were added. The solid was filtered, washed with 3 x 10 mL of petrolether and dried under vacuum. A white powder was obtained (yield 60%).

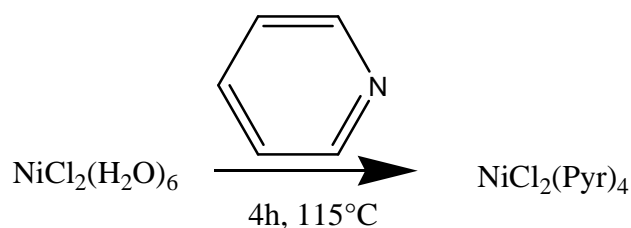
NMR

^1H (acetone-d₆, 300 MHz): 7.58-7.30 (*m*, H_{ar} , 20H), 3.54 (*q*, OCH_2CH_3 , 2H), 0.57 (*t*, OCH_2CH_3 , 3H) ppm

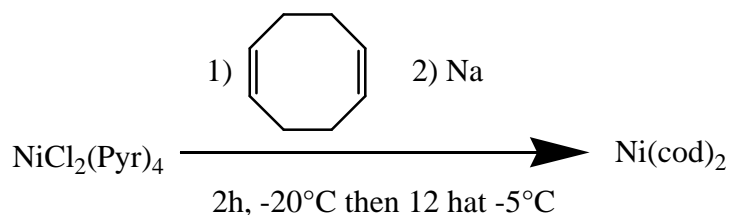
^{13}C (acetone-d₆, 75 MHz): 134.8 (*d*, $\text{O}-\text{C}=\text{O}$), 133.2 (*d*, $\text{O}=\text{C}-\text{Ph}$), 130.4-122.7 (C_{ar}), 59.1 (*s*, OCH_2CH_3), 14.7 (*s*, OCH_2CH_3) ppm

b) Nickel recursor synthesis: $\text{Ni}(\text{COD})_2$

The $\text{Ni}(\text{cod})_2$ synthesis was performed following the procedure derived from literature and developed at the LCPP during Benjamin Saillard thesis [3].



59.1 g of nickel (II) chloride hexahydrate (250 mmol) were dissolved in 600 mL of pyridine. The resulting blue suspension was stirred during 4 hours at 115°C. Then after cooling down the mixture, a solid was obtained by filtration and washed with 3 x 100 mL of heptane. 117g of a blue powder of $\text{NiCl}_2(\text{Pyr})_4$ were obtained (yield 95%).

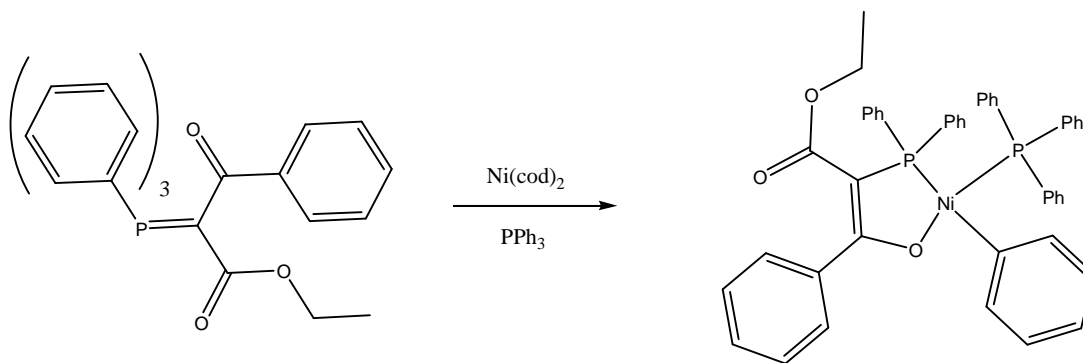


20.8 g of $\text{NiCl}_2(\text{Pyr})_4$ (52.0 mmol) was added in 150 mL of THF. The mixture was cold down to -20°C then 25.4 mL (4 eq) of 1,5-cyclooctadiene freshly distilled were added dropwise. The mixture was stirred during 2 hours at -20°C . Then 2.3 g of sodium wire (101 mmol) were slowly added to the mixture (≈ 30 min). The mixture turns green and was stirred overnight at -5°C . The purple solution was transferred through cannula in 350 mL of cold methanol at -5°C . A yellow solid precipitates. After filtration, the solid was washed with 6 x 50 mL of methanol. 6 g of $\text{Ni}(\text{cod})_2$ were obtained (yield 63 %).

NMR

^1H (C_6D_6 , 300 MHz): 4.3 (s, $\underline{\text{CH}}$, 4H), 2.1 (s, $\underline{\text{CH}_2}$, 8H) ppm

c) Catalyst synthesis



The catalyst synthesis was performed following the procedure derived from literature and developed at the LCPP during Benjamin Saillard thesis [3].

A solution of 2.24 g (8.2 mmol) of $\text{Ni}(\text{cod})_2$ in 40 mL of THF was added to a suspension of 3.76 g (8 mmol) of the ligand and 2.21 g (8.1 mmol) of triphenyl phosphine in 60 mL of THF. The mixture was stirred for 1 h, then the solvent was removed under vacuum. The residue was dissolved in 30 mL of toluene. 200 mL of heptane were added to precipitate a yellow solid. After filtration the product was washed with 3 x 10 mL of heptane and dried under vacuum (yield 60%).

RMN

^1H (CDCl_3 , 300 MHz): 8.20-6.14 (m, $\underline{\text{H}}_{\text{ar}}$, 35H), 3.8 (q, $\text{O}-\underline{\text{CH}_2}\text{CH}_3$, 2H), 0.6 (t, $\text{O}-\underline{\text{CH}_2}-\underline{\text{CH}_3}$, 3H) ppm.

^{13}C (CDCl_3 , 75 MHz): 165.4 ($\underline{\text{C}}=\text{O}$), 134.3, 133.6, 133.5, 131.3, 129.7 – 129.3, 129.0, 127.8, 126.7, 126.0, 121.2, 91.0, 58.3 (s, $\text{O}-\underline{\text{CH}_2}\text{CH}_3$), 13.8 (s, $\text{O}-\underline{\text{CH}_2}-\underline{\text{CH}_2}$) ppm

B. Method of polymerization

1. Polymerizations without ethylene

Polymerizations of liquid monomers were performed in a Schlenk under inert atmosphere with a magnetic stirring.

Standard polymerization procedure (e.g. MMA homopolymerization)

The radical initiator and/or the catalyst were dissolved in the desired volume of solvent and the desired quantity of monomer in a Schlenk tube under argon. The mixture was heated up to the desired temperature under magnetic stirring. During the polymerization, we regularly collected samples in order to determine the kinetic profile by gravimetry. At the end of the polymerization, the mixture was cooled down and acidic ethanol was added in order to quench the reaction.

We also perform polymerization under argon pressure. In this case the procedure was similar to the one developed for high-pressure ethylene polymerization except that we charged the reactor thanks to a commercial argon gas cylinder at 200 bar.

2. Ethylene homo- and copolymerization at low-pressure (P<25 bar)

Beside the high-pressure reactor, two other 500 mL ethylene polymerization reactors were used at lower pressure with a similar *modus operandi*: a glass reactor in which polymerization can be performed up to 4 bar of ethylene pressure and a steel reactor from SFS with ethylene pressure up to 25 bar.

Standard polymerization procedure

Caution, all polymerizations involve high pressure and explosive gaz.

The radical initiator and/or the catalyst were dissolved in the desired volume of solvent and eventually the desired quantity of comonomer was added in a Schlenk tube under argon. The mixture was introduced through cannula into the reactor. Ethylene was introduced from an intermediate tank (charged from commercial ethylene gas cylinder) at the given pressure using a manometer and the mixture was heated at the desired temperature under stirring (250 rpm). The pressure was maintained constant during the entire polymerization by continuous feeding with ethylene intermediate tank. A pressure sensor on the ethylene tank

records the fall of pressure during the reaction and a thermocouple in reactor measures temperature. Using these sensors, we can follow easily the kinetic of the reaction on-line. Indeed in this case the intermediate tank does not suffer important decompression. The temperature remains almost constant near ambient temperature; therefore the consumption of ethylene in the intermediate tank allows the calculation of the reaction profile. At the end of the polymerization, the reactor was slowly cooled down and degassed. The polymer was then dried under vacuum at 70°C and washed.

3. Ethylene homo- and copolymerization at high-pressure

Standard polymerization procedure

Caution, all polymerizations involve high pressure and explosive gaz.

Ethylene polymerizations were done in a 160mL stainless steel autoclave (equipped with safety valves, stirrer, oven) from Parr Instrument Co.. To manage safely polymerization over 50 bar of ethylene we have used a 1.5 L intermediate tank. The tank was cooled down to -20°C to liquefy ethylene at 35 bar. When thermodynamic equilibrium was reached, the intermediate tank was isolated and heated to reach up to 300 bar of ethylene pressure. This tank was used to charge the reactor, and maintain pressure of ethylene constant in the reactor by successive manual ethylene additions.

The radical initiator and/or the catalyst were dissolved in the desired volume of solvent and eventually the desired quantity of comonomer was added in a Schlenk tube under argon. The mixture was introduced through cannula into the reactor. Ethylene was introduced and the mixture was heated at the desired temperature under stirring (250 rpm). At the end of the polymerization, the reactor was slowly cooled down and degassed. The polymer was then dried under vacuum at 70°C.

Similar *modus operandi* was used for ethylene emulsion except that the latexes obtained were split. A part was dried and washed with water in order to perform analyses such as NMR, DSC, HT-SEC, etc. The other part was used to determine the latex colloidal properties (DLS, TEM, X-ray, etc).

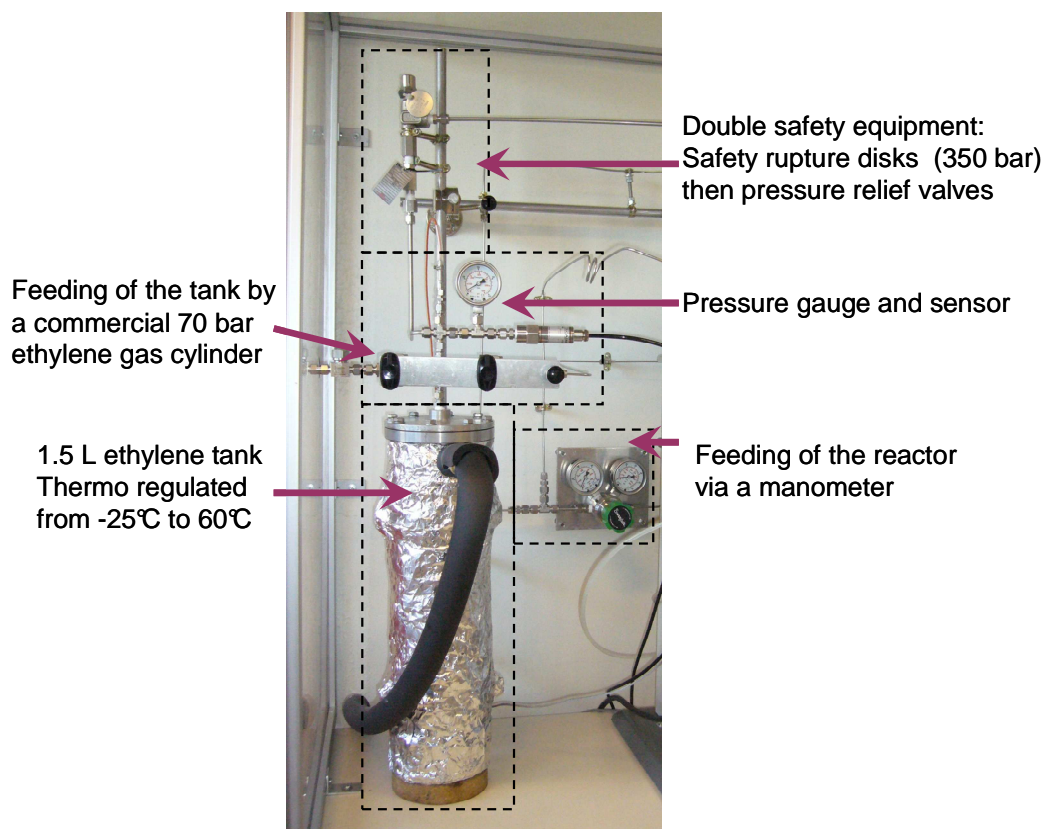
a) High-pressure reactor design

Overall view of the reactor



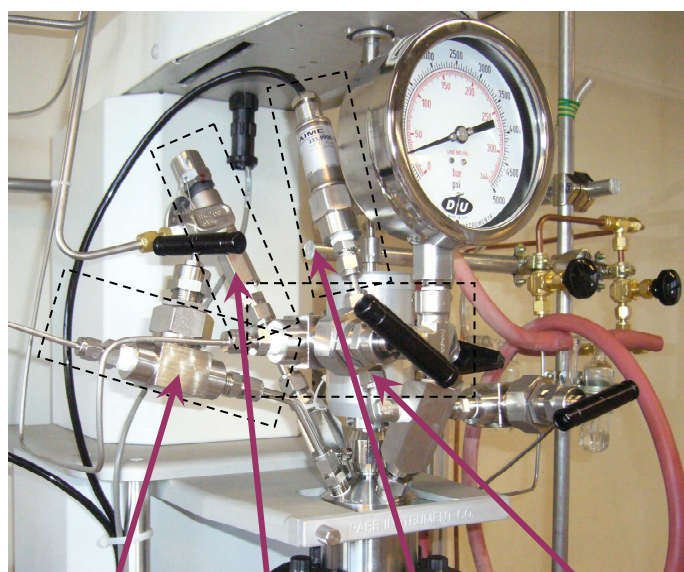
Built by Jean-Pierre Broyer

Intermediate ethylene tank



Design by Roger Spitz

Feeding of the reactor

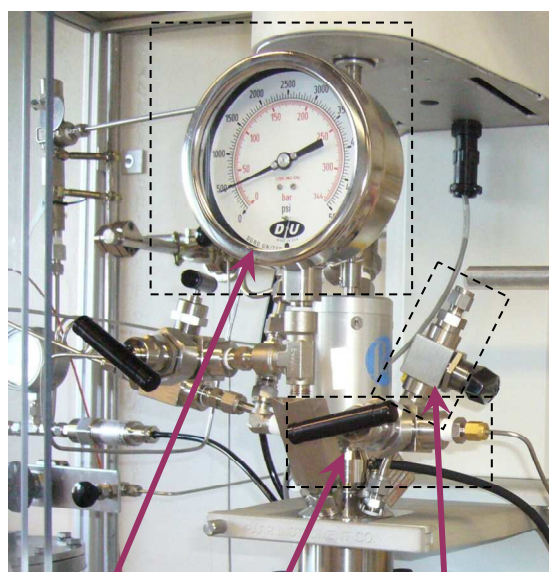


Ethylene release valve

Double safety equipment

Pressure sensor

Ethylene inlet valve

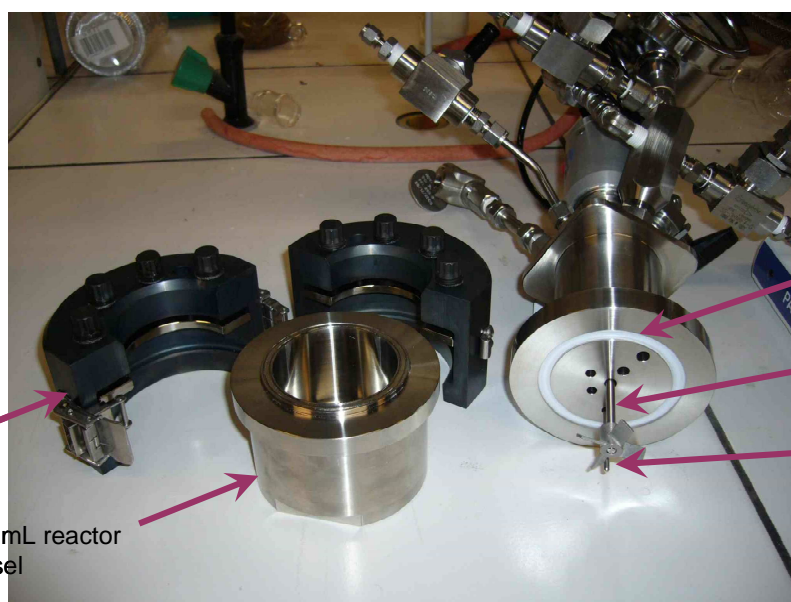


Pressure gauge

Argon inlet valve

Reactant inlet valve

Reactor vessel



Solid-ring with cap screws for fixed head vessel

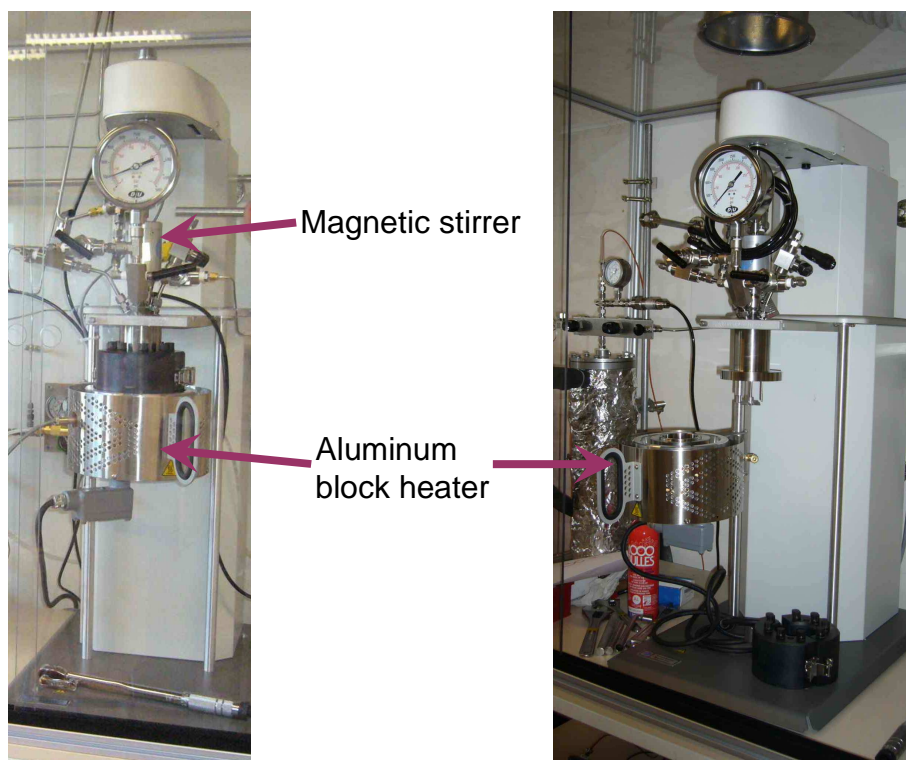
160 mL reactor vessel

Flat PTFE gasket

Internal stirring system

Thermocouple

Reactor stirrer and heater



b) About the on-line measurement of ethylene consumption during the polymerization

Both intermediate tank and reactor itself are equipped with online monitoring of temperature and ethylene pressure. Generally during ethylene polymerization ethylene consumption in the intermediate tank is registered in order to obtain the kinetic of the reaction. However in this case the tank is submitted to a smaller decompression.

Indeed if the reactor is charged at 100 bar of ethylene pressure the thermodynamic equilibrium of the intermediate tank is reached only after several hours (see Figure 1). Usually the intermediate tank pressure decreases of almost 200 bar and temperature of 10°C.

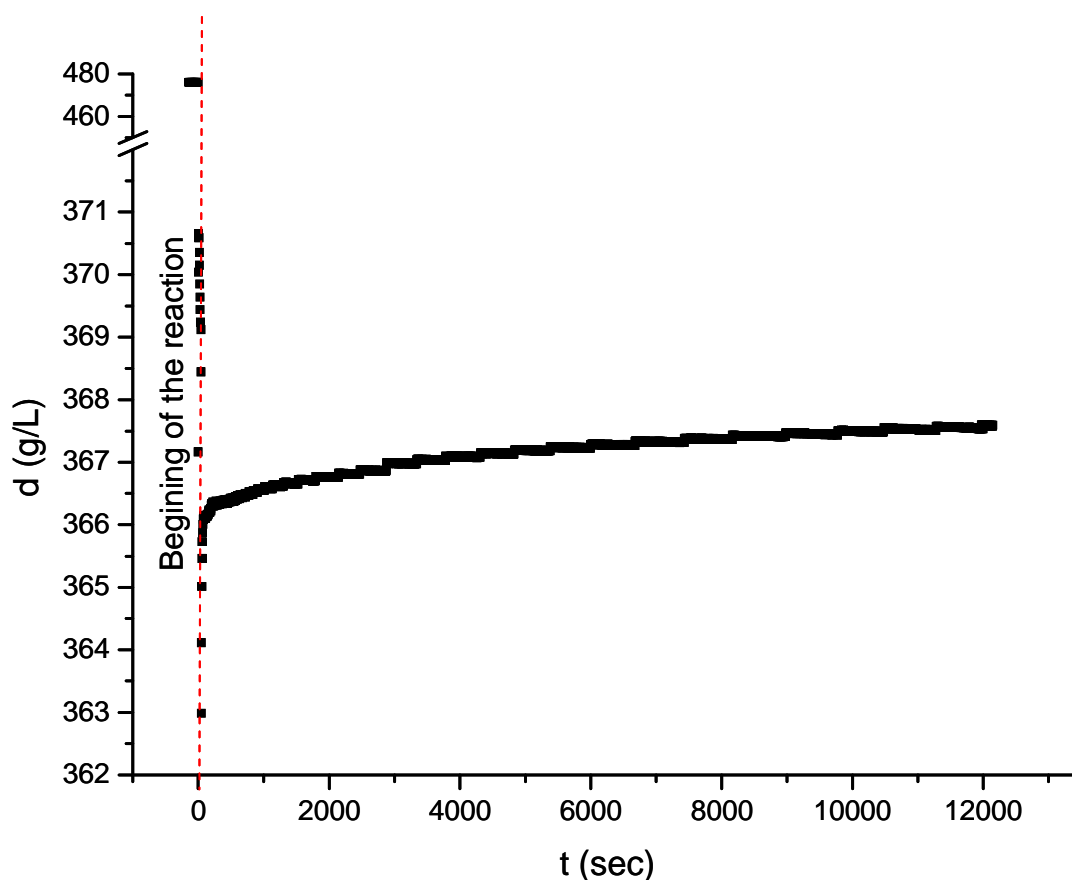


Figure 1. Density calculated inside the ethylene tank using measured temperature and ethylene pressure. A $t=0$ sec the reactor is charged then after $t=30$ sec the inlet valve of the reactor is closed during the reaction

As shows Figure 1, the thermodynamic equilibrium is not reached during the polymerization. Consequently, the ethylene consumption cannot be measured by this method and the reaction profile needs to be determined by another method such as the one developed in our manuscript (several experiments in same experimental conditions during different times).

The reaction profile can also be determined thanks to the ethylene pressure and to the temperature of the reactor but as we have chosen to work at constant ethylene pressure during the polymerization we can not use this method.

Moreover during the filling of ethylene intermediate tank, the thermodynamic equilibrium is reached only after 1h30 of condensation (see Figure 2).

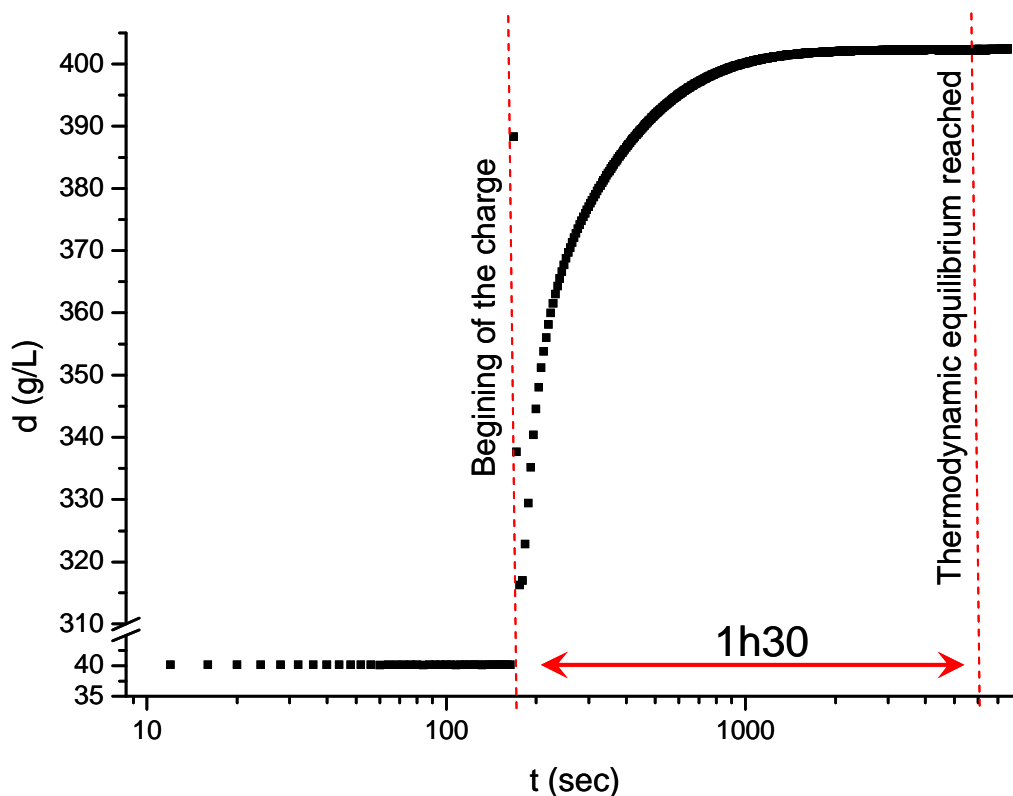


Figure 2. Density of the ethylene tank during the condensation of ethylene.

All these results indicate that temperature and ethylene pressure of the intermediate tank cannot be used to follow the reaction profile. The tank must be equipped of a stirrer in order to decrease the time to reach the thermodynamic equilibrium. Therefore if this time was dramatically decreased (few minutes) the reaction profile could be measured directly.

C. Analytical methods

1. Polymer analyses

a) SEC

Molecular weights of polyethylene are determined by size exclusion chromatography (SEC) using a Waters Alliance GPCV 2000 instrument (columns: PLgel Olexis) with two detectors (viscosimeter and refractometer) in trichlorobenzene (flow rate: 1 mL/min) at 150°C. The system is calibrated with polystyrene standard sample using universal calibration.

For THF-soluble polymer, molecular weights are determined by size exclusion chromatography using a WATERS 717 injector, four columns (one precolumn PLgel Olexis guard and three columns PLgel 5 μ m Mixed C) at 30°C. Two detectors are used (light scattering and refractometer) in order to obtain the absolute molecular weight.

b) DSC

For PE melting points, differential scanning calorimetry (DSC) is performed on a Mettler Toledo DSC1 at a heating rate of 5 K/min from 20°C to 150°C. Two successive heatings and coolings of the samples are performed. We consider data (T_m values, crystallinity) obtained during the second heats.

c) NMR

High-resolution liquid nuclear magnetic resonance (NMR) spectroscopy is carried out with a Bruker DRX 250 spectrometer operating at 250 MHz for ^1H at the Service commun de RMN du Réseau des Polyméristes Lyonnais in Villeurbanne. Spectra are obtained with a 5-mm QNP probe. PE samples are examined as 10–15 % (w/v) solutions using a mixture of tetrachloroethylene (TCE) and perdeuterobenzene (C_6D_6) (2/1 v/v) as solvent at 363 K. Chemical shift values (δ) are given in ppm in reference to internal tetramethylsilane (TMS).

d) IR

Infrared analysis (IR) is performed on a Nicolet Protégé 460 Spectrometer ESP with a resolution of 4 cm^{-1} from 500 cm^{-1} to 3800 cm^{-1} . A background spectrum is collected and subtracted from the spectrum of the sample. Samples are prepared by mixing the powder with KBR and pressing the mixture into pellets. The presences of the inserted comonomer in the polymer chain are confirmed by this method.

e) MALDI-TOF

MALDI-TOF (matrix-assisted laser desorption/ionisation – time-of-flight mass spectrometry) spectrum is obtained using PerSeptive Biosystems Voyager 4130 DE-STR with sodium ionisation performed at the Institut de Biologie et de Chimie des Protéines in Lyon. Samples are prepared by mixing a polymer solution in toluene and a solution of THAP (2,5-dihydroxybenzoic acid) in toluene.

2. Colloidal analyses

a) DLS

Particle size is determined by dynamic light scattering (DLS) using a Malvern Zetasizer 1000 HAS autosizer apparatus with a detection angle of 90° at 25°C. The measurements are performed on highly diluted samples in order to rule out interaction and multiple scattering effects. The intensity average diameter is computed from the intensity autocorrelation data using the cumulant analysis method. The final data is the average of 5 measurements for each sample.

b) TEM

TEM (transmission electron microscopy) analyses is performed after placing a droplet of the particle suspension on a copper grid (3.05mm copper grid with Formvar/Carbon support Film, 200 mesh (Agar Scientific)) and dried before analysis. TEM is performed on a Philips CM120 transmission electron microscope, at an acceleration voltage of 80 kV (Centre Technologique des Microstructures (CTμ) - Plateforme d'Imagerie Integrative (PI²), Claude Bernard University, Lyon, France).

TEM tomography is performed on the same microscope by tilting the samples every 2° from -70° to +70°, then image processing is performed in order to picture the 3D shape of particles.

c) AFM

AFM (atomic force microscopy) analyses are performed after placing a droplet of the particles suspension on a mica surface and dried before analysis. AFM is performed in a AFM nanoscope using tapping mode (287 KHz, 16 mV) in the CLYME (Centre Lyonnais de Microscopie Electronique) in Lyon.

d) TGA

TGA (thermogravimetric analysis) is performed on a Mettler Toledo DSC/ATG 1 at a heating rate of 20 K/min from 30°C to 800°C. Organic content is obtained by measuring the weight loss during the heat.

e) Surface tension measurements

The surface tension of aqueous solution of CTAB and PE latexes at 25°C are measured using the Wilhemy plate method owing to the Krüss Digital Measuring Instrument Tensiometer K12C in the range of 0-80 mN/m with a resolution of 1 mN/m. The cmc value is determined at the sharp break point in the surface tension versus the surfactant concentration

The area per adsorbed surfactant molecule (A_s) is estimated by tensiometry at 25°C using the method developed by Maron [4]. This method consists of determining the cmc of the surfactant in pure water and in the presence of the latex particles. The difference between the two cmc corresponds to the quantity of adsorbed surfactant at the particles surface. Therefore it is easy to calculate A_s .

f) X-Ray scattering

X-Ray analysis is performed in collaboration with Jean-Pierre ALBOUY in the LPS (Laboratoire de Physique du Solide) at the University of Orsay. Crystallinity and average crystallite dimension are measured by a X-ray scattering using Cu K α radiation ($\lambda=1.54 \text{ \AA}$) from a 1.5 kW rotating anode generator. PE latex is placed in a glass capillary for X-Ray experiment.

Crystallinity is measured by adding the crystalline and amorphous spectra in order to obtain the experimental spectrum. X-Ray diffusion of hexadecane is used for the amorphous spectra. Diffusion water, air and the capillary background need also to be determined and subtracted from the spectrum of the samples.

Average crystallite dimension are calculated by the Scherrer formula [5].

$$H_l = \frac{0.89\lambda}{\tau \cos \theta}$$

With τ the crystallite dimension, λ the X-ray radiation, H_l the mid-height thickness of the X-ray peak, θ the angle of scattering.

Therefore crystallite diameters can be estimated even though the thickness of the crystallite cannot be determined by this method.

3. Organometallics and organic compounds

a) NMR

NMR analyses ^1H , ^{13}C , ^{31}P are performed in team “Chimie Organométallique de Surface” of C2P2 laboratory in Villeurbanne on a spectrometer Brücker AC300 300 MHz at 22°C. Analyses of air-sensitive products are performed using Young tubes.

b) EPR

EPR (electron paramagnetic resonance) analyses are performed in Chemistry laboratory at ENS Lyon (thaks to Laurant BONNEVIOT) on a spectrometer Brucker Eleksys E500 X-band (9.4 GHz) spectrometer with a standard cavity. The magnetic field is measured on time by a gaussmeter. Analyses of air-sensitive products are performed using Young tubes.

References:

- [1] C. Wang, S. Friedrich, T. R. Younkin, R. T. Li, R. H. Grubbs, D. A. Bansleben, and M. W. Day *Organometallics*, vol. 17, p. 3149, 1998.
- [2] A. Zeller, E. Herdtweck, and T. Strassner *Eur. J. Inorg. Chem.*, p. 1802, 2003.
- [3] B. Saillard, *Polymerisation de l'éthylène catalysée par des complexes activés de métaux de transition*. PhD thesis, Université Claude Bernard-Lyon 1, 2005.
- [4] S. H. Maron, M. E. Elder, and I. N. Ulevitch *J. Coll. Sci.*, vol. 9, p. 89, 1954.
- [5] A. L. Patterson *Phys. Rev.*, vol. 56, p. 978, 1939.

Annex I : Influence of the PE microstructures on its melting point

The influence of molecular weight and degree of branching on the melting temperature of PE is critical [1]. Some studies have reported a correlation between molecular weight, microstructure and melting point.

These studies have a great importance since they allow estimation of the microstructure of PE without performing a ^{13}C NMR spectrum.

A. Melting point of linear PE

The melting point of linear PE can be extrapolated from the melting point of corresponding alkanes [2] (see Figure 1).

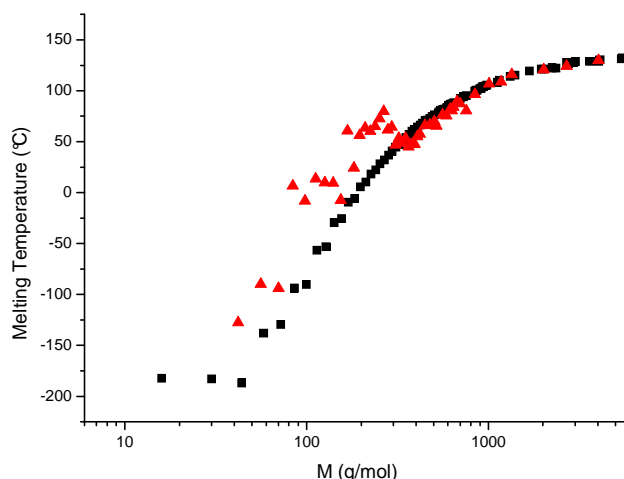


Figure 1. Melting temperature of oligomers; ■= alkanes, ▲= cycloalkanes

As shown on the figure, over 5000 g/mol the melting point attains a value almost equal to the one of linear polyethylene ($T_m=121^\circ\text{C}$ at 2000 g/mol and $T_m=132^\circ\text{C}$ at 5000 g/mol). The extrapolation of this curve at infinite molecular weight gives a melting point of about 140°C . However this value cannot be reached due to entanglement effects. Indeed the ultra high molecular weight polyethylenes (UHMWPE) have lower crystallinities and melting point than classical HDPE (drop of 5°C from 50000 g/mol to 10^7 g/mol) [3]. The maximum in melting point and crystallinity for a linear PE is usually reported of around 100000 g/mol [4].

B. Melting point of branched PE

As early as 1949 Flory [5, 6] developed the crystallization theory of polymers. It modelizes the simplest case of copolymers in which one monomer unit can form crystallite and the other one does not form any by itself and no co-crystallization occurs: the theory can be summarized in a unique equation 1.

$$\frac{1}{T_m} - \frac{1}{T_m^0} = \frac{R}{h_u} \left(-\ln X_A - \mu'(1 - v_A)^2 \right) \quad (1)$$

Where T_m is the melting temperature of the copolymer, T_m^0 the melting point for corresponding homopolymer with the same molecular weight, h_u the heat of fusion per repeating unit, μ' the heat of mixing parameter, and X_A and v_A are respectively the mole fraction and volume fraction of the crystallizing structural unit in the copolymer.

This equation can be applied for ethylene copolymer, and branched PE in first approximation. However, the molecular weight influence is not included in Flory equation.

It is known experimentally that the melting point of the crystallites is related to the lamellar thickness [7-9] and therefore at any given temperature there is a certain thickness required to provide a stable crystallite. Consequently the lamellar thickness of the crystallites formed in a branched PE will be determined in part by the length of the ethylene units sequence providing that the comonomer unit is excluded from the structure (branches are considered as non-crystallisable units). The thickness of lamellas can be accessed by X-ray analysis, but generally only DSC is available to study PE so we will focus only on the relation between melting temperature and heat of fusion with the microstructures of the PE.

The real influence of branches degree on PE melting point is more complicated. Mandelkern [8-11] reported a correlation between melting point, crystallinity and crystallite dimension to the PE microstructures and molecular weights. His results are summarized in the Figure 2.

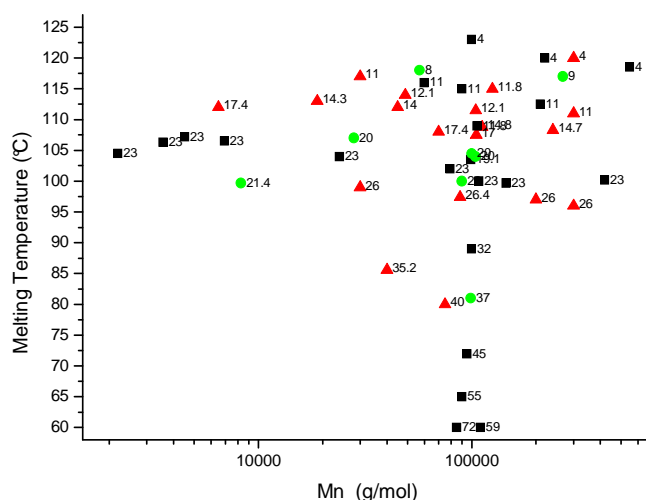


Figure 2. Melting temperature of polyethylene; ■ = ethylene-butene copolymers, ▲ = ethylene-hexene copolymers, ● = ethylene-octene copolymers, label correspond to the number of branches per 1000C [8-11]

In all this part, we only plot the melting temperature after a fast crystallization obtained by Mandelkern (cooling rate over 5°C/min). Indeed the melting temperature is strongly dependant for branches PE to the cooling rate. At very low cooling rate the difference in T_m could be over 5°C and the tendency with degree of branches could be different. Therefore it is mandatory to perform DSC analyses always in similar experimental conditions.

At constant high molecular weight, a correlation is found between the melting point and the degree of branches (see Figure 3). Whatever the kind of branches from ethyl to butyl, the melting point decreases with the degree of branches following the same curve.

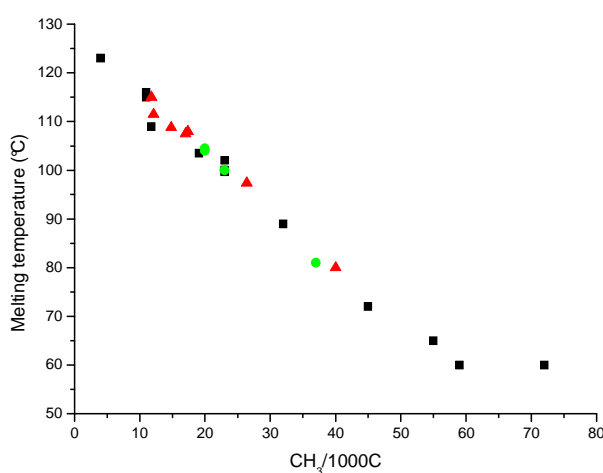


Figure 3. Correlation between melting temperature and branches content at constant $M_w=90000\pm20000$ g/mol; ■ = ethylene-butene copolymers, ▲ = ethylene-hexene copolymers, ● = ethylene-octene copolymers [8-11]

This curve is used in this manuscript in order to estimate the branching level of our synthesized PE.

For methyl branches the behavior is totally different due to the possibility of co-crystallization of ethylene and propylene units into a new crystallite [12-14]. In this case the copolymer can exhibit several melting points for each sort of crystallite.

For higher α -olefins, such as 1-dodecene or 1-octadecene, the relation between melting temperature and degree of branches diverges. The melting point is lower than expected at low branches degree [15] because longer branches induce a higher perturbation of the crystallization due to a higher free volume. Flory equation takes into account this contribution in the term $\mu'(1-v_A)^2$.

Finally at constant degree of branches, melting temperature slightly decreases with the molecular weight. An unexpected behavior is observed at low molecular weight (see Figure 4). The melting point first increases with the molecular weight until a maximum (around $M_n=5000$ g/mol) then decreases as expected. This maximum is still not understood and the evolution of this maximum with the branches type and the degree of branches is not studied to the best of our knowledge. Moreover, this maximum vanishes if the copolymer is submitted to an isothermal crystallization. Consequently this maximum seems to be related to a kinetic effect and not to a thermodynamic one.

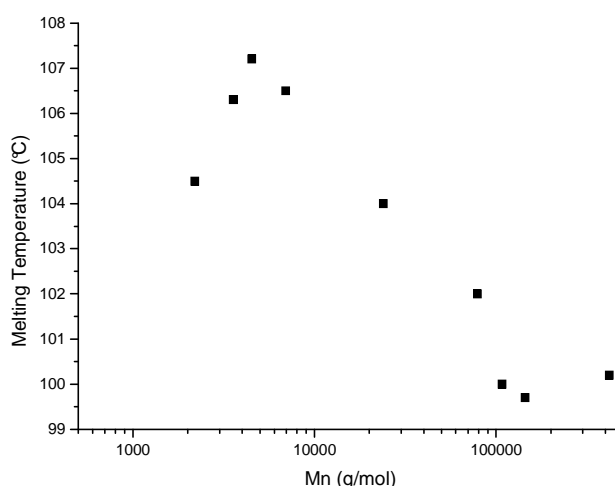


Figure 4. Influence of the molecular weight on the melting point at constant degree of branches 23C/1000C for ethylene-butene copolymer [8-11]

In conclusion these results show that the melting point of a branched PE depends on two major parameters: the molecular weight of the polymer and the degree of branches. Usually melting points decrease with the branches content and molecular weight. However no global relation has been described up to now linking all these parameters.

C. Crystallinity of branched PE

For crystallinity the relationship with branches is well known [16]. The heat of fusion for a random copolymer per weight fraction of ethylene (ethylene is the only comonomer which contributes to crystallization $\Delta H'_m = \Delta H_m / W_E$ with W_E the weight fraction of ethylene in the copolymer) can be related to the ethylene mole fraction (x_E) by the equation 2.

$$\ln \Delta H'_m = \ln k + n' \ln x_E \quad (2)$$

Where k is a constant related to the enthalpy of fusion of the parent homopolymer, n' corresponding to the critical sequence length below which no monomer sequence will crystallize. The constant k is likely to be affected by parameters such as M_w and PDI, heterogeneity of copolymer composition, thermal history of the sample, and presence of nucleating impurities.

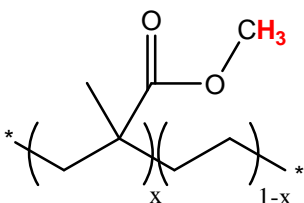
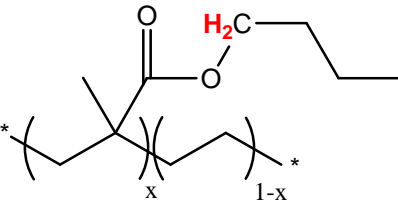
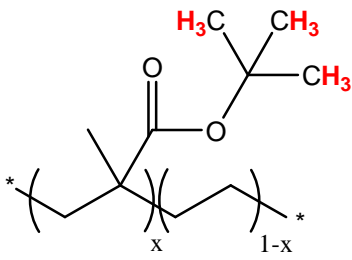
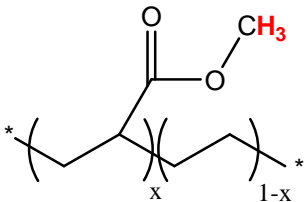
As expected n' increase with the branches length (5 for ethyl branches, 13 for isobutyl).

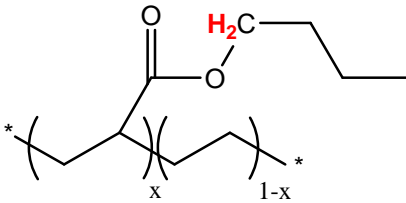
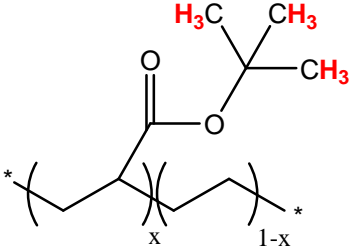
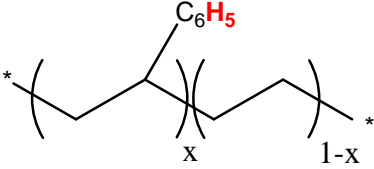
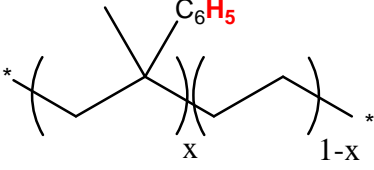
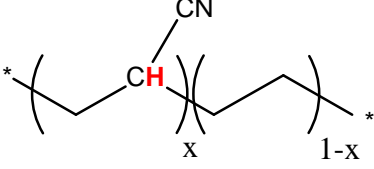
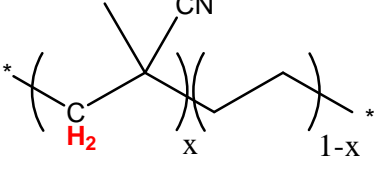
References:

- [1] L. Mandelkern *Biophys. Chem.*, vol. 112, p. 109, 2004.
- [2] J. Brandrup, E. H. Immergut, and E. A. Grulke, *Polymere handbook*. WILEY-INTERSCIENCE, 1999.
- [3] L. Mandelkern *Acc. Chem. Res.*, vol. 23, p. 380, 1990.
- [4] E. Ergoz, J. G. Fatou, and L. Mandelkern *Macromolecules*, vol. 5, p. 147, 1972.
- [5] P. J. Flory *J. Chem. Phys.*, vol. 17, p. 223, 1949.
- [6] P. J. Flory *Trans. Faraday Soc.*, vol. 51, p. 848, 1955.
- [7] D. R. Burfield and P. J. T. Tait *Makromol. chem*, vol. 186, p. 2657, 1985.
- [8] R. Alamo and L. Mandelkern *Macromolecules*, vol. 22, p. 1273, 1989.
- [9] R. G. Alamo, B. D. Viers, and L. Mandelkern *Macromolecules*, vol. 26, p. 5740, 1993.
- [10] R. Alamo, R. Domszy, and L. Mandelkern *J. Phys. Chem.*, vol. 88, p. 6587, 1984.
- [11] R. G. Alamo, E. K. M. Chan, L. Mandelkern, and I. G. Voigt-Martin *Macromolecules*, vol. 25, p. 6381, 1992.
- [12] M. J. Richardson, P. J. Flory, and J. B. Jackson *Polymer*, vol. 4, p. 221, 1963.
- [13] C. H. Baker and L. Mandelkern *Polymer*, vol. 7, p. 7, 1966.
- [14] S. N. Gan, D. R. Burfield, and K. Soga *Macromolecules*, vol. 18, p. 2684, 1985.
- [15] J. Yoon, D. Lee, E. Park, I. Lee, D. Park, and S. O. Jung *Polymer*, vol. 41, p. 4523, 2000.
- [16] D. R. Burfield *Macromolecules*, vol. 20, p. 3020, 1987.

Annex II : Calculation of comonomer molar insertion

Comonomer molar insertions are measured by ^1H NMR in TCE/ C_6D_6 2/1 at 90°C . For each copolymer, the hydrogen atoms in red in the following table are integrated and calibrated. Then the peak between 1-2.5 ppm (except for MAN, AA, MAA, AAm and MAAm) are integrated (A). Finally using the following formula the comonomer insertions are determined.

Comonomer	Calibration [peak (ppm)]	Comonomer molar insertion
MMA 	3 [3.6]	$\frac{1}{1 + \frac{A-5}{4}}$
BuMA 	2 [4]	$\frac{1}{1 + \frac{A-12}{4}}$
tBuMA 	9 [3.5]	$\frac{1}{1 + \frac{A-5}{4}}$
MA 	3 [3.3]	$\frac{1}{1 + \frac{A-3}{4}}$

Comonomer	Calibration [peak (ppm)]	Comonomer molar insertion
BuA	2 [4]	$\frac{1}{1 + \frac{A-10}{4}}$
		
tBuA	9 [3.5]	$\frac{1}{1 + \frac{A-3}{4}}$
		
Sty	5 [5.7-7.4]	$\frac{1}{1 + \frac{A-3}{4}}$
		
MSty	5 [5.7-7.4]	$\frac{1}{1 + \frac{A-5}{4}}$
		
AN	1 [3.5]	$\frac{1}{1 + \frac{A-2}{4}}$
		
MAN	2 [2.2]	$\frac{1}{1 + \frac{A-3}{4}}$
		

Comonomer	Calibration [peak (ppm)]	Comonomer molar insertion
AA	1 [2.5]	$\frac{1}{1 + \frac{A-2}{4}}$
MAA	2 [1.9]	$\frac{1}{1 + \frac{A-3}{4}}$
<hr/>		
AAm	1 [2.5]	$\frac{1}{1 + \frac{A-2}{4}}$
MAAm	2 [2]	$\frac{1}{1 + \frac{A-3}{4}}$
<hr/>		
VAc	1 [4.7]	$\frac{1}{1 + \frac{A-5}{4}}$

Comonomer	Calibration [peak (ppm)]	Comonomer molar insertion
PAc	3 [3.5]	$\frac{1}{1 + \frac{A-5}{4}}$
VPiv	1 [4.7]	$\frac{1}{1 + \frac{A-11}{4}}$
MCr	3 [3.5]	$\frac{1}{1 + \frac{A-5}{4}}$

Annex III : Table of cohesive pressure, dielectric constant and dipole momentum of solvents

Run	Solvent	c : cohesive solvent pressure (MPa) ^a	ϵ : Dielectric constant (at 20°C) ^b	μ : Dipole momentum (10 ⁻³⁰ C.m) ^b
1	None	151	-	0
2	Cyclohexane	285	2.0	0
3	Heptane	219	1.9	0
4	Toluene	337	2.4	1
5	DMSO	708	46.4	13.5
6	Acetonitrile	581	35.9	11.8
7	DEC	324	2.8	3.7
8	DMF	581	36.7	10.8
9	Dibutylether	256	3.1	3.9
10	Ethanol	676	24.5	5.8
11	Acetone	488	20.6	9
12	Dimethylcarbonate	412	3.2	3.7
13	Butanone	383	18.5	9.2
14	Butyrolactone	665	39.0	14.2
15	Butan-2-ol	488	16.6	5.5
16	Cyclohexanone	364	16.0	10.2

Run	Solvent	c : cohesive solvent pressure (MPa) ^a	ε : Dielectric constant (at 20°C) ^b	μ : Dipole momentum (10 ⁻³⁰ C.m) ^b
17	Butan-1-ol	485	17.5	5.8
18	Ethyl acetate	331	6.0	6.1
19	Dichloromethane	414	8.9	5.2
20	1,4-dioxane	388	2.2	1.5
21	THF	365	7.6	5.8

^a: obtained from Reichardt, C., In Solvents and solvent effects in organic chemistry, 2nd ed.; Reichardt, C. Ed.; VCH:Weinheim 1988. ^b; obtained from Loupy, A., In Effets de milieu en synthèse organique: Des effets de solvants aux méthodes d'activation non classiques, 2nd ed.; Loupy, A. Ed.; Dunod 1996.

Free Ethylene Radical Polymerization under Mild Conditions: The Impact of the Solvent

Etienne Grau, Jean-Pierre Broyer, Christophe Boisson, Roger Spitz, and Vincent Monteil*

CNRS UMR 5265 Laboratoire de Chimie Catalyse Polymères et Procédés (C2P2), LCPD team, Université de Lyon, CPE Lyon, Bat 308F, 43 Bd du 11 novembre 1918, F-69616 Villeurbanne, France

Received July 23, 2009

Revised Manuscript Received August 26, 2009

Ethylene is industrially polymerized either by radical polymerization under severe conditions or by catalytic polymerization at lower temperatures and pressures. Free radical polymerization of ethylene is performed under high pressure (1000–4000 bar) and high temperature (200–300 °C) in bulk.^{1,2} Under these conditions radical polymerization provides a branched polyethylene due to uncontrolled transfer reactions to polymer. Polymers possess a degree of crystallinity of 45–55% and melting points of 105–115 °C. They contain 15–25 short-chain branches and 2–5 long-chain branches per 1000 carbon atoms. Catalytic polymerizations^{3,4} generally occur at low pressure (1–50 bar) and low temperature (near or below 100 °C). Under intermediate conditions (100–200 °C, 100–500 bar) an anionic oligomerization^{5,6} of ethylene (“Aufbau” reaction) occurs leading to a linear polyethylene with low molecular weight.

At ethylene pressure below 300 bar and low temperature (<100 °C) radical polymerization has been shown to be inefficient, unless ethylene is activated by strong Lewis acid such as original lithium cations.⁷ Clark’s calculations^{8,9} of the gas-phase activation energy of methyl radical addition to ethylene predicted a decrease from 60 to 25 kJ/mol when ethylene is complexed with Li⁺.

The development of radical polymerization of ethylene under mild conditions ($P < 250$ bar and $50\text{ °C} < T < 90\text{ °C}$) is an important challenge since it may open a new field of radical ethylene polymerization allowing the use of solvents, organic additives and classical radical initiators such as diazo compounds. Solvent effects have been observed in radical polymerization with common vinyl monomers,^{10,11} although this effect remains tiny except for vinyl acetate. To our knowledge, the influence of the solvent has not been discussed for radical polymerization of ethylene. In the present paper, radical ethylene polymerization is reported using two solvents having different polarities: toluene and THF. The solvent influences on productivity and polyethylene molecular weight are discussed and rationalized.

Radical polymerization of ethylene was performed at 70 °C in the range of 10 to 250 bar using AIBN as initiator in toluene (Figure 1). Toluene was chosen in a first approach as a typical solvent of the slurry catalytic polymerization of ethylene performed using similar conditions.

Under 50 bar of ethylene pressure, no polymer was obtained. From 50 to 250 bar, polymerization occurred but conversion of ethylene remained very low (3% conversion considering a solubility of ethylene¹² of 470 g/L under 100 bar at 70 °C). As expected the radical polymerization of ethylene was inefficient under mild conditions using toluene as solvent.

We investigated ethylene polymerization in THF (typical solvent for radical polymerization), with the aim to improve yield. Surprisingly polymerization in THF occurred down to 10 bar of ethylene, an unusual pressure range for pure radical polymerization of ethylene. At 100 bar 3.9 g of polyethylene were isolated, corresponding to 17% of conversion. Radical polymerization of ethylene was about 6 times more efficient than in toluene. As already mentioned, solvent impact is usually a tiny effect in radical polymerization, but in the case of ethylene polymerization solvent seems to play a major role.

The produced polyethylenes were moderately branched in both solvents (7 branches/1000C in toluene and 9 branches/1000C in THF) as determined by ¹³C NMR¹³ (see Supporting Information, Figures S1 and S2) and have a melting point between 115 and 119 °C and a crystallinity of 55–70% (see Supporting Information, Table S1). ¹³C NMR spectra showed only butyl and longer chain branches and no vinyl chain end. Transfer to solvent provided respectively phenyl-ended and THF-ended polyethylenes which were fully identified by ¹³C NMR (see Supporting Information, Figures S1 and S2). In the case of transfer to THF two different structures (1- and 2-polyethylenyl-THF, see Supporting Information, Figure S2) were identified.

Molecular weights were lower in THF than in toluene. As expected molecular weights increased with ethylene concentration: from 950 to 4300 g/mol with toluene and from 440 to 2400 g/mol with THF. At pressure below 100 bar, melting points and molecular weights dropped (runs 3, 8–10, see Supporting Information Table S1) and oligomers were produced.

The number of chains per initiator was about 10 times higher in THF than in toluene. Molecular weights in THF were about 0.6 times lower than in toluene. Assuming AIBN dissociation being similar in both solvents, the rate of polymerization in THF was 6 times higher than in toluene.

To examine the variation of kinetic constants, the kinetic law of the free radical polymerization (eq 1) was checked for both toluene and THF solvents. We plotted $\ln(1/(1-x))$ versus time (Figure 2)

$$\frac{1}{1-x} \frac{\partial x}{\partial t} = k_p \sqrt{\frac{2fk_d[I]}{k_t}} = k_{tot} \quad (1)$$

with x = ethylene conversion, $[I]$ = AIBN concentration, f = efficiency factor of the initiator, and k = kinetic constants of initiator dissociation (k_d), propagation (k_p), and termination (k_t).

A linear relation with a good correlation was observed for polymerization in THF and toluene. The slope k_{tot} for THF was 6 times higher than the toluene one. After 8 h under 100 bar of ethylene, 7.8 g of polyethylene were produced with THF as solvent (33% of conversion) and only 1.3 g with toluene (5.5% of conversion). A factor of 6 was observed as expected.

For each solvent, there was neither significant change in the melting point nor in the molecular weight during the polymerization (see Supporting Information, Table S2).

Various concentrations of initiator were evaluated at 100 bar of ethylene pressure and 70 °C (see Supporting Information, Figure S3, Table S3). We plotted $\ln(1/(1-x))$ versus $[I]^{1/2}$. Equation 1 was once again confirmed. As expected molecular weight decreased according to the concentration of initiator, due to an increase of the termination rate. Melting points remained unchanged between 115 and 117 °C.

*monteil@lcpd.cpe.fr.

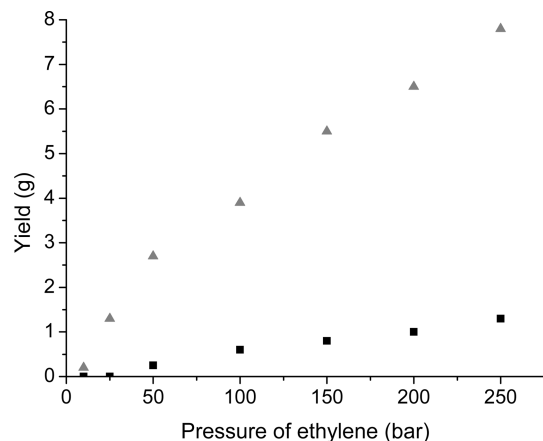


Figure 1. Pressure influence on ethylene radical polymerization: (■) 50 mg of AIBN, 50 mL of toluene, 4 h at 70 °C under ethylene pressure; (▲) 50 mg of AIBN, 50 mL of THF, 4 h at 70 °C under ethylene pressure.

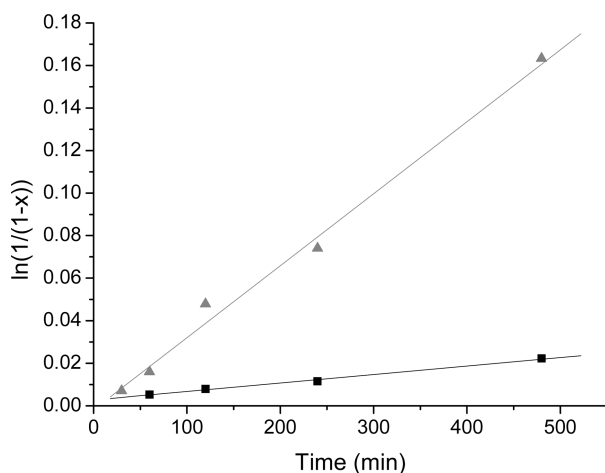


Figure 2. Influence of time on radical polymerization of ethylene: (■) 50 mg of AIBN, 50 mL of toluene at 70 °C under 100 bar of ethylene pressure; (▲) 50 mg of AIBN, 50 mL THF at 70 °C under 100 bar of ethylene pressure.

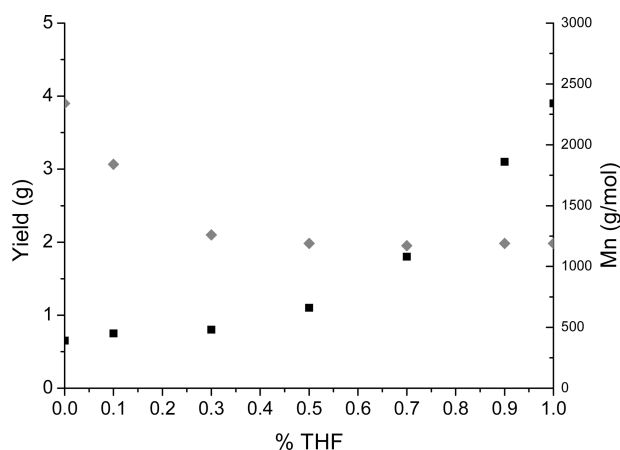


Figure 3. Impact of solvent composition in volume on radical polymerization of ethylene: (■) 50 mg of AIBN, 50 mL of solvent, 4 h at 70 °C under 100 bar of ethylene pressure; (◆) M_n (g/mol) determined using High Temperature SEC.

To further investigate the THF effect, polymerizations of ethylene under 100 bar at 70 °C were performed with different mixtures of THF and toluene as solvent (Figure 3).

Table 1. Arrhenius Parameters of Ethylene Polymerization (Assuming the Validity of the Arrhenius Law)

solvent	E_{tot} , global activation energy (kJ/mol)	$\ln(A_{tot})$, global pre-exponential factor
toluene	27.7	7.6
THF	32.8	10.3

The yield did not increase linearly with the solvent composition. The observed activation was not proportional to the THF amount in the solvent mixture. Below 40% of THF the yield remained even and drastically increased over 40% of THF only. Molecular weights decreased with the addition of THF (see Supporting Information, Table S4) due to transfer to THF.

How To Explain This Unexpected Effect of Solvent? The THF activation can be explained by a change of polymerization rate. To go further we aim to calculate the global activation energy and global pre-exponential factor. For this purpose we performed polymerizations at several temperatures (50, 70 and 90 °C) and ethylene pressures (from 50 bar up to 250 bar) in both solvents. One can remark that ethylene conversion seemed not to be linked to ethylene pressure (see Supporting Information, Table S5). At 90 °C ethylene conversion reached 40% after 4 h of polymerization.

From these experiments we plotted k_{tot} versus $1/T$ to determine the Arrhenius parameters. Corresponding E_{tot} and $\ln(A_{tot})$ are summarized in Table 1.

Ideally, the determination of the Arrhenius parameters for each polymerization step should be performed, but this kind of study is currently incompatible with our conditions of pressure (since stopped flow or pulsed laser polymerizations techniques cannot be used).

$$k_{tot} = k_p \sqrt{\frac{2fk_d[I]}{k_t}}$$

$$= A_{tot} \exp\left(\frac{-E_{tot}}{RT}\right) \left\{ \begin{array}{l} E_{tot} = E_p - \frac{1}{2}E_t + \frac{1}{2}E_d \\ A_{tot} = A_p \sqrt{\frac{2fA_d[I]}{A_t}} \end{array} \right. \quad (2)$$

The global activation energy and the pre-exponential factor (eq 2) are lower in toluene than in THF. Lower global activation energy is usually linked to a more favorable reaction. In both solvents the polymerization mechanism was considered to be the same, so the change in the global activation energy was only due to the relative stabilization of intermediate and activated states, which differ from one solvent to the other.¹⁴ Solubilization by toluene provides a lower energy barrier than in THF.

Despite lower global activation energy, toluene was less efficient than THF. The global pre-exponential factor is higher for THF, which explains, in the range of temperature used, the better efficiency of radical ethylene polymerization in THF. The global pre-exponential factor is proportional to the frequency of efficient shocks. With a higher pre-exponential factor the probability of the mechanism involved is supposed to increase. Differences in geometry of activated states in toluene and in THF could explain the difference of pre-exponential factors. Toluene is less electron donor than THF, more toluene molecules may therefore be necessary to stabilize the radical corresponding to a denser solvation shell. This could explain a higher pre-exponential factor in THF than in toluene.

In summary, this work showed that radical ethylene polymerization can be effective under mild conditions

(50 °C < T < 90 °C and P > 10 bar in THF) contrary to what used to be assumed. The polymerization was 6 times more productive in THF than in toluene: conversions of ethylene up to 40% were obtained. Because of transfer to solvent, 1- or 2-polyethylenyl-THF were synthesized. Calculations of Arrhenius parameters have been done to understand THF activation. THF efficiency is not due to a lower global activation energy but to a higher pre-exponential factor corresponding to a higher efficient shock frequency. Further investigations with other solvents of various polarities are under progress in order to discriminate the solvent effect and to increase polyethylene molecular weights by reducing the transfer capacity of solvent.

Acknowledgment. E.G. thanks the “Ministère de la Recherche et de l’Enseignement Supérieur” for fellowship.

Supporting Information Available: Text giving experimental details, figures showing NMR spectra, influence of initiator concentration on radical polymerization of ethylene, tables showing the influence of ethylene pressure, polymerization time, concentration of initiator, solvent composition, and temperature on the radical polymerization of ethylene. This material is available free of charge via the Internet at <http://pubs.acs.org>.

References and Notes

- (1) Doak, K. W. In *Encyclopedia of Polymer Science and Engineering*, 2nd ed.; Mark, H. F., Bikales, N. M., Overberger, C. G., Menges, G., Eds.; WileyInterscience: New York, 1985; Vol. 6, pp 386–428.
- (2) Aggarwal, S. L.; Sweeting, O. J. *Chem. Rev.* **1957**, 57, 665–742.
- (3) Mulhaupt, R. *Macromol. Chem. Phys.* **2003**, 204, 289–327.
- (4) Beach, D. L.; Kissin, Y. V. In *Encyclopedia of Polymer Science and Engineering*, 2nd ed.; Mark, H. F., Bikales, N. M., Overberger, C. G., Menges, G., Eds.; WileyInterscience: New York, 1985; Vol. 6, pp 454–489.
- (5) Ziegler, K.; Gellert, H.-G.; Holzkamp, E.; Wilke, G. *Angew. Chem.* **1955**, 67, 425.
- (6) Ziegler, K.; Gellert, H.-G. *Angew. Chem.* **1952**, 64, 323.
- (7) Vyakaranam, K.; Babour, J. B.; Michl, J. *J. Am. Chem. Soc.* **2006**, 128, 5610–5611.
- (8) Horn, A. H. C.; Clark, T. *J. Chem. Soc., Chem. Commun.* **1986**, 1774.
- (9) Horn, A. H. C.; Clark, T. *J. Am. Chem. Soc.* **2003**, 125, 2809.
- (10) Kamachi, M. *Adv. Polym. Sci.* **1981**, 38, 55–87.
- (11) Beuermann, S.; Buback, M. *Prog. Polym. Sci.* **2002**, 27, 191–254.
- (12) Solubilization is a low kinetic process in absence of stirring. Thus to calculate the ethylene solubility in a solvent we charged the reactor with ethylene pressure without stirring and we recorded the pressure and temperature until the equilibrium under stirring. The difference in density between the initial step and the equilibrium gave us the solubilization of ethylene. Identical solubilities were estimated for toluene and THF.
- (13) Galland, G. B.; de Souza, R. F.; Mauler, R. S.; Nunes, F. F. *Macromolecules* **1999**, 32, 1620–1625.
- (14) Reichardt, C. In *Solvents and solvent effects in organic chemistry*, 2nd ed.; Reichardt, C., Ed.; VCH: Weinheim, Germany, 1988; pp 121–205.

Supercritical behavior in free radical polymerization of ethylene in the medium pressure range†

Etienne Grau,* Jean-Pierre Broyer, Christophe Boisson, Roger Spitz and Vincent Monteil*

Received 18th March 2010, Accepted 28th June 2010

DOI: 10.1039/c004447d

Free radical polymerization of ethylene in an intermediate pressure and temperature range ($P_{\text{ethylene}} < 250$ bar and $50\text{ °C} < T < 90\text{ °C}$) in the presence of an organic solvent has been studied. Under selected conditions (P , T) and according to the amount of organic solvent added, either a supercritical monophasic or a biphasic medium is obtained. In the case of a biphasic medium, polymerization occurred in the liquid phase in which radical initiator and ethylenes are dissolved. The transition between a monophasic to a biphasic medium has been predicted using thermodynamic calculations and has been related to experimental observations such as the dependence of polymerization activity *versus* solvent volume.

Introduction

Free radical polymerization of ethylene is industrially conducted under high pressures (1000–4000 bar) and temperatures (200–300 °C).^{1,2} Under these conditions, polymerization occurs in a monophasic supercritical medium without any use of solvent. Polymerization of ethylene with an organic solvent as diluent can be considered under milder conditions but free radical polymerization of ethylene is generally assumed to be inefficient except when some strong Lewis acids are used to activate the monomer.^{3–5} We have recently reported that the solvent was not spectator and that a simple change of solvent can increase drastically the efficiency of the free radical polymerization of ethylene⁶ under mild conditions (ethylene pressure up to 250 bar; $T = 70\text{ °C}$).

Low molecular weight polyethylenes ($M_n < 5000\text{ g mol}^{-1}$) have been produced exhibiting a slightly branched microstructure (7 branches/1000 C in toluene and 9 branches/1000 C in THF) and a melting temperature between 110 and 120 °C. Crystallinity ($\sim 70\%$) was below catalytic PEHD but higher than for standard LDPE produced at high temperature and pressure by a free radical process. The development of the free radical polymerization of ethylene under mild conditions is an attractive challenge, because it can be a tool for creating new functionalized polyethylenes (*e.g.* using chain transfer to solvent) with controlled molecular weight distribution and microstructure, as was described in our previous paper.⁶

There is a lack of study on ethylene polymerization in this intermediate range of pressure. As a consequence, all the data allowing to understand in which conditions the chemistry

takes place are not available and cannot be extrapolated from the two better known ranges of reaction conditions.

Actually coordination catalysis^{7,8} is performed in the low pressure range (up to 40 bar), while free radical polymerization is performed much over 1000 bar at high temperature. An important issue for our intermediate conditions concerns the determination of the phase diagram of the polymerization medium: whether the polymerization takes place in a biphasic or in a monophasic medium. Low pressure and temperature coordination catalysis can be compared to a biphasic system. In this case polymerization is located in the liquid phase where some ethylene is dissolved from the surrounding ethylene gas phase. Solubility of ethylene in a broad range of organic solvents has been fully determined under 40 bar of ethylene pressure.^{9–11}

At high pressure and high temperature, the system is constituted by a unique supercritical phase (usually ethylene is used without any additional solvent).

In the intermediate pressure range either one or two phases could be envisaged depending on the ethylene pressure, the amount of solvent (slurry conditions) and the temperature. The biphasic or monophasic medium will not lead to the same polymerization activity and polyethylene microstructure. Therefore the determination of the phase transition is of great interest.

In the present paper, the transition has been highlighted experimentally and confirmed using simple thermodynamic calculations leading to a complete description of our polymerization system with, for instance, the exact composition of the polymerization medium.

Experimental

All chemicals were handled using standard Schlenk procedures under argon atmosphere. Solvents (tetrahydrofuran (THF) and toluene) were distilled from drying agents or degassed under argon. Ethylene (purity 99.95%) was purchased from Air Liquide and AIBN from Acros and used without further purification.

Université de Lyon, Univ. Lyon 1, CPE Lyon, CNRS, UMR 5265 Laboratoire de Chimie Catalyse Polymères et Procédés (C2P2), LCPP Team, Bat 308F, 43 Bd du 11 novembre 1918, F-69616 Villeurbanne, France. E-mail: monteil@lcpp.cpe.fr, grau@lcpp.cpe.fr; Fax: +334 7243 1768; Tel: +334 7243 1781

† Electronic supplementary information (ESI) available: Experimental information on polyethylene characterization, figures and tables showing influence of toluene or THF volume, AIBN concentration on radical polymerization of ethylene, *modus operandi* to calculate ethylene solubility. See DOI: 10.1039/c004447d

Standard polymerization procedure

Caution, all polymerizations involve high pressure and explosive gas. Ethylene polymerizations were done in a 160 mL stainless steel autoclave (equipped with safety valves, stirrer, oven) from Parr Instrument Co. The azobisisobutyronitrile (AIBN) was dissolved in the desired volume of solvent (THF or toluene) in a Schlenk tube under argon. The mixture was introduced through cannula into the reactor. Ethylene was introduced and the mixture was heated at the desired temperature under stirring (300 rpm). To manage safely polymerization over 50 bar of ethylene we use a 1.5 L intermediate tank. The tank was cold down to $-20\text{ }^{\circ}\text{C}$ to liquefy ethylene at 35 bar. When thermodynamic equilibrium was reached, the intermediate tank was isolated and heated to reach up to 300 bar of ethylene pressure. This tank was used to charge the reactor, and maintain the pressure of ethylene constant in the reactor by successive manual ethylene addition. After 4 h of polymerization the reactor was slowly cooled down and degassed. The polymer was then dried under vacuum at $70\text{ }^{\circ}\text{C}$.

Result and discussion

Experimental evidence of the phase transition with polymerization conditions

Polymerization of ethylene was performed in a batch reactor by increasing the amounts of THF as organic solvent at $70\text{ }^{\circ}\text{C}$ under a pressure of 100 bar of ethylene (Fig. 1). Note that at this pressure and temperature free radical polymerization of ethylene is usually assumed to be inefficient and this unusual activity observed has been directly related to the activation of polymerization by THF.⁶ Thus only 0.1 g of low molecular weight PE was synthesized in the absence of THF ($M_n = 3010\text{ g mol}^{-1}$).

The results showed a break of behavior between 40 and 45 mL of tetrahydrofuran (THF). At a low amount of THF, the yield increased according to the volume of the solvent. On the contrary it decreased slightly for a higher volume of THF.

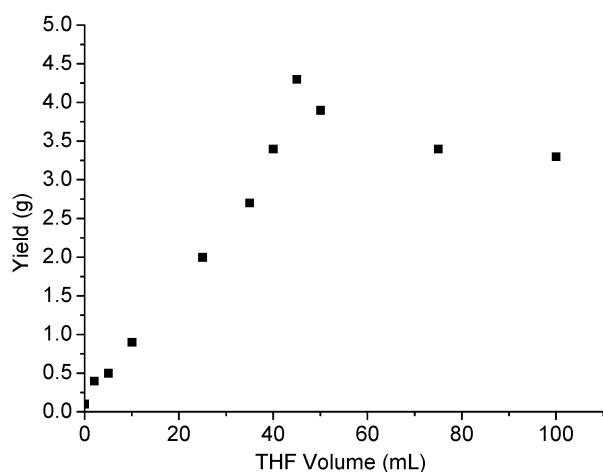


Fig. 1 Influence of THF content on radical polymerization of ethylene ■: 50 mg AIBN, 4 h at $70\text{ }^{\circ}\text{C}$ under 100 bar of ethylene pressure.

This behavior cannot be due to the THF itself because no polyethylene was synthesized without AIBN in THF in the same experimental conditions. The highest conversion was reached around the break between 40–45 mL where the yield was over 4.5 g.

These observations could be compatible with a phase transition between a monophasic medium at low THF volume, where the reaction takes place in a single supercritical phase (ethylene + THF = 1 phase), and a biphasic medium at higher volume, where the polymerization takes place in the liquid phase in which ethylene is dissolved.

In the case of a biphasic medium, no AIBN is in the gaseous phase and thus polymerization occurred only in the liquid phase.^{12,13} Over 45 mL of THF, the polymerization became less efficient due to a dilution of the initiator while the ethylene concentration remains constant with increasing amounts of THF. Below 40 mL of THF, the reaction seems to be accelerated by a solvent activation effect evidenced in our previous work.⁶ In this case the initiator concentration remains constant and the ethylene concentration decreases with increasing amounts of THF (the partial pressure of ethylene P_E decreases while the total pressure P_{tot} remains constant: $P_{\text{tot}} = P_E + P_{\text{THF}}$). Without solvent the reaction is almost inefficient and activation with THF is almost proportional to THF amount. Radical polymerization occurred efficiently only in the presence of THF for solvating the propagating radical.⁶ Note that at this stage the conversion of our system can not be estimated as the real fraction of THF and ethylene are unknown, due to the complexity of the polymerization medium.

A similar set of experiments was also performed in toluene (see ESI Fig. S1).[†] The same behavior was observed with toluene, but the activation was less impacted. Polymerization yield slightly increased with increasing amounts of toluene until a maximum around 40–45 mL of solvent and then finally decreased. The ratio between activation with THF and toluene did not remain constant with the solvent amount. Below 40 mL of solvent the relative activation (yield in THF vs. yield in toluene) increased up to a factor 6, and remained constant above this volume.

The produced polyethylenes had a melting point between 110 and $117\text{ }^{\circ}\text{C}$ and crystallinity of 50–60% (see ESI Tables S1 and S2).[†] As expected, polyethylene molecular weight decreased with increasing solvent volumes due to transfer of propagating radical to the solvent. In addition, the molecular weight dropped over 45 mL due to the sudden increase of solvent concentration in the liquid phase after the assumed phase transition. Over 45 mL the molecular weight decreased with the solvent volume.¹⁴ Moreover, low polydispersity index (PDI) values were measured and the molecular weight distributions of polyethylenes were always monomodal, which strongly suggests that polymerization occurred in one phase, respectively, in the supercritical phase (solvent + ethylene) for a monophasic medium and in the liquid phase for a biphasic system.

In order to confirm this phase transition, polymerizations were performed at $70\text{ }^{\circ}\text{C}$ under 100 bar of ethylene with 50 mL of THF using various amounts of AIBN (see ESI Table S3).[†] If no phase transition occurs this set of experiment could be

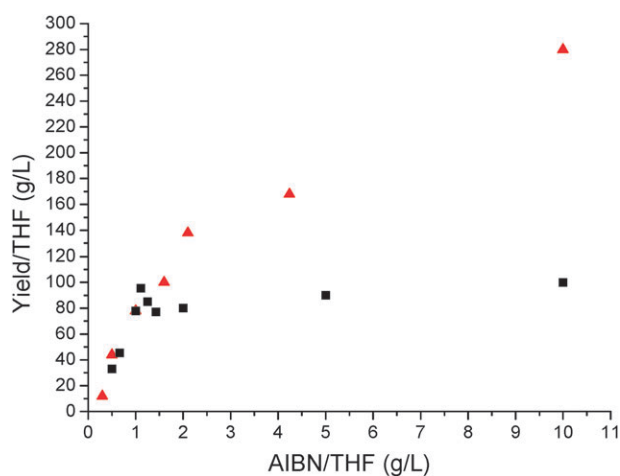


Fig. 2 Influence of AIBN/THF ratio on the radical polymerization of ethylene ■: 50 mg AIBN, 4 h at 70 °C under 100 bar of ethylene pressure, various volume of THF ▲: 50 mL of THF, 4 h at 70 °C under 100 bar of ethylene pressure, various amount of AIBN.

related to the previous one (same amount of AIBN but various volume of THF). For this purpose we plotted yield/THF vs. the initial ratio AIBN/THF (Fig. 2).

The two sets of experiments diverge from the ratio AIBN/THF of 1.11 g L^{-1} corresponding to 45 mL of THF (50 mg AIBN). This could be related to the aforementioned phase transition. Below this amount both set of experiments follow the same curve (biphasic medium).

How to determine this phase transition theoretically?

The previous findings highlighted the importance of the nature of the reaction medium (supercritical vs. liquid). To determine theoretically the phase diagram in order to validate our hypothesis we need as prerequisite to calculate experimentally the solubility of ethylene in the solvent phase. As far as we know, ethylene solubility was well determined up to 40 bar in organic solvent.^{9–11}

Ethylene solubility determination (40–130 bar)

To determine ethylene solubility at higher pressure we assume that solubilization is a slow kinetic process without stirring. The reactor was then charged with ethylene at a desired pressure and then stirring was started until thermodynamic equilibrium. Pressure and temperature evolution were recorded throughout the whole experiment (see ESI Fig. S2).†

A Peng-Robinson equation of state,¹⁵ was chosen after examination of numerous available equations of state as an excellent compromise between simplicity and efficiency. According to this equation, the density of ethylene (d) is known in the supercritical phase for each P , T (eqn (1) and (2)). The difference in density between the initial step (i) (before stirring) and the equilibrium (f) is due to the solubilization of ethylene in the solvent (s_E). To perform the calculation the total inner volume of the reactor has been determined ($V_R = 230 \text{ mL}$).¹⁶ The volume of the solvent being known (V_S), solubility was calculated by mass balance through the eqn (3). The dilatation of solvent (V_E) due to the solubilization

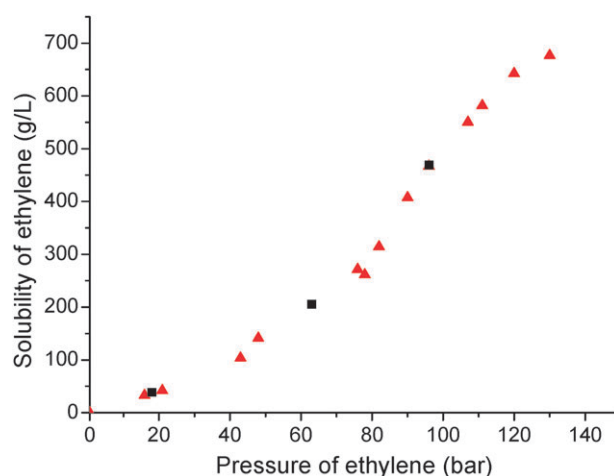


Fig. 3 Solubility of ethylene at 70 °C (in grams of ethylene per initial volume of solvent) ■: in THF, ▲: in toluene.

of ethylene was determined by varying the volume of solvent at a constant P_f .

$$d_i = EOS(P_i, T_i) \quad (1)$$

$$d_f = EOS(P_f, T_f) \quad (2)$$

$$d_f(V_R - V_S) - d_f(V_R - V_S - V_E) = s_E V_S \quad (3)$$

According to this *modus operandi*, ethylene solubility in toluene and THF was determined up to 130 bar of ethylene pressure at 70 °C (Fig. 3). The solubility at 50 °C and 90 °C in toluene was also measured.

As an illustration, at 100 bar about 24 g of ethylene is dissolved at 70 °C in 50 mL of solvent initially introduced (usual conditions of our polymerization experiments). At low pressure the slope was about $2 \text{ g L}^{-1} \text{ bar}^{-1}$ in agreement with the literature. Over 50 bar an increase of the slope to $9 \text{ g L}^{-1} \text{ bar}^{-1}$ was observed. Solubility seems to be mostly independent of the nature of the solvent. Solubility varies linearly with ethylene density with a slope of 3.04 (see Fig. 4). This linear relationship is valid whatever the temperature and the nature of the solvent.

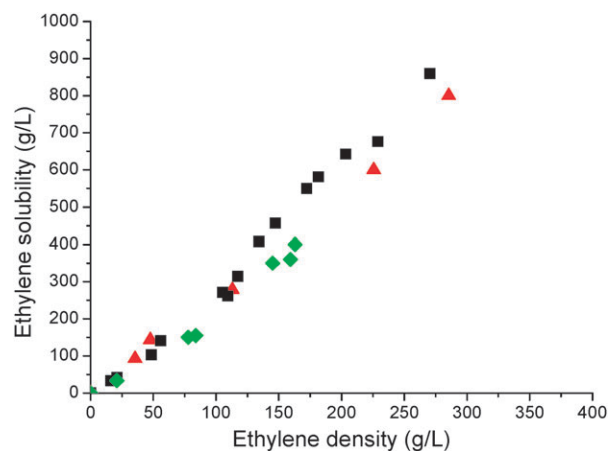


Fig. 4 Correlation between ethylene density and solubility in toluene ▲: at 50 °C; ■: at 70 °C; ◆: at 90 °C.

A linear relationship also occurred between ethylene density and the effective ethylene solubility, *i.e.* the solubility in the ethylene expanded solvent. The liquid phase is about 1.8 times more concentrated in ethylene than the supercritical ethylene phase, which explains in part (in addition to solvent activation effect) why the free radical polymerization of ethylene is more efficient in a solvent than without any solvent in this pressure range.

Phase transition determination

Ethylene solubility has been determined up to 130 bar, but the phase transition between a biphasic medium at low pressure and a monophasic medium at higher pressure still has to be determined. This was done using the Peng-Robinson equation of state¹⁷ (eqn (4)–(8)) and the standard mixing rules for coefficients *a* and *b* (eqn (9)–(10))¹⁷ for a bicomponent system (ethylene and solvent).

The Peng-Robinson equation of state:

$$P = \frac{RT}{v-b} - \frac{a}{v^2 + 2bv - b^2} \quad (4)$$

$$a = \frac{0.45724R^2T_c^2}{P_c} [1 + f\omega(1 - T_r^{1/2})]^2 \quad (5)$$

where

$$f\omega = 0.37464 + 1.54226\omega - 0.26992\omega^2 \quad (6)$$

and

$$T_r = \frac{T}{T_c} \quad (7)$$

$$b = \frac{0.07780RT_c}{P_c} \quad (8)$$

Mixing rules:

$$a = \sum_{i=1}^N \sum_{j=1}^N x_i x_j a_{ij} \text{ where } a_{ij} = \sqrt{a_i a_j} \quad (9)$$

$$b = \sum_{i=1}^N \sum_{j=1}^N x_i x_j b_{ij} \text{ where } b_{ij} = \frac{b_i + b_j}{2} \quad (10)$$

where *P* is the pressure, *T* the absolute temperature, *v* the molar volume, *R* the ideal gas constant, *P_c* the pressure at the critical point, *T_c* the absolute temperature at the critical point, *ω* the acentric factor,¹⁸ *x_i* the molar fraction of compound *i* (solvent or ethylene).

To calculate the transition we have to determine at each temperature (because *a* depends of *T*), critical pressure and temperature of the ethylene–solvent mixture using eqn (5)–(10) for all compositions.

The mixture composition depends on three parameters only: temperature, pressure of ethylene (which determines the amount of ethylene),¹⁹ and volume of solvent (which determines the amount of solvent). For each composition and temperature *a* and *b* were thus calculated using eqn (9) and (10). Then the critical parameters of the mixture have been determined (eqn (5) and (8)). These critical parameters also depend on ethylene pressure, temperature and solvent volume.

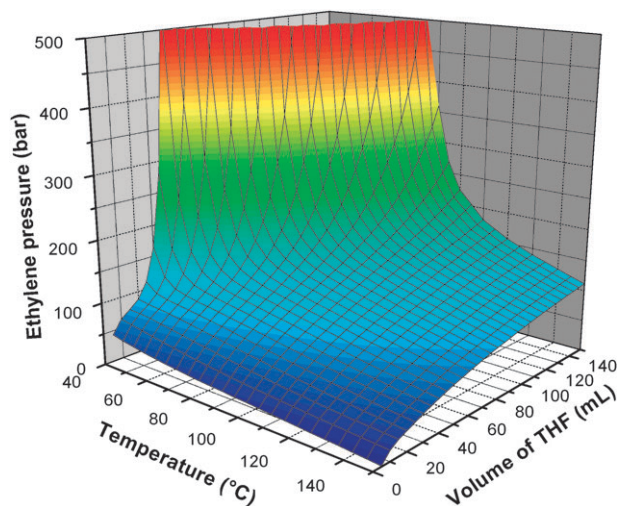


Fig. 5 Phase diagram for ethylene/THF mixture.

At a given temperature, if $T_{c,mixture} < T$ and $P_{c,mixture} < P$, the medium is supercritical and monophasic. If $T_{c,mixture} > T$ a biphasic system is expected with a liquid phase of solvent containing dissolved ethylene. $P_{c,mixture} > P$ and $T_{c,mixture} < T$ never occur due to the intrinsic properties of the mixture.

From these calculations a phase transition surface can be obtained depending on temperature, ethylene pressure, and amount of solvent as shown in Fig. 5, and the medium composition can be estimated for each coordinate.

Above the phase transition surface the system will be a supercritical monophasic medium (THF and ethylene in a unique supercritical phase) and below the surface it will be biphasic (2 phases with ethylene in both). Note that the transition surface possesses a certain thickness (second order transition) which cannot be precisely determined using our calculation method.

Our method was also used for various solvents such as toluene and the phase transition was determined for each solvent (see Fig. 6 for comparison of transition between THF and toluene at a constant volume of solvent: 50 mL).

At iso-volume, THF and toluene present almost the same phase transition. For example, at 70 °C, 50 mL of solvent, the

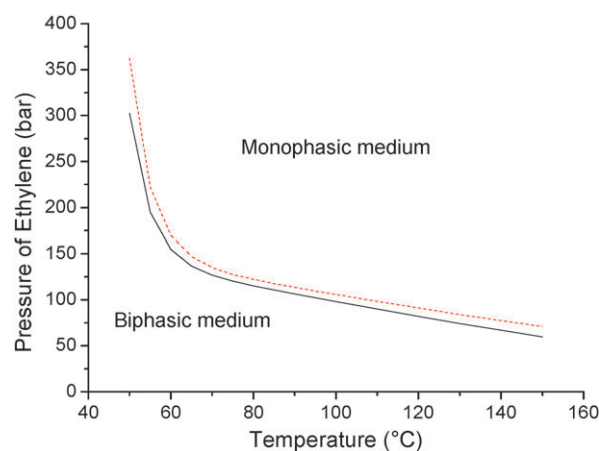


Fig. 6 Phase diagram of ethylene/solvent system —: with 50 mL THF, ---: with 50 mL Toluene.

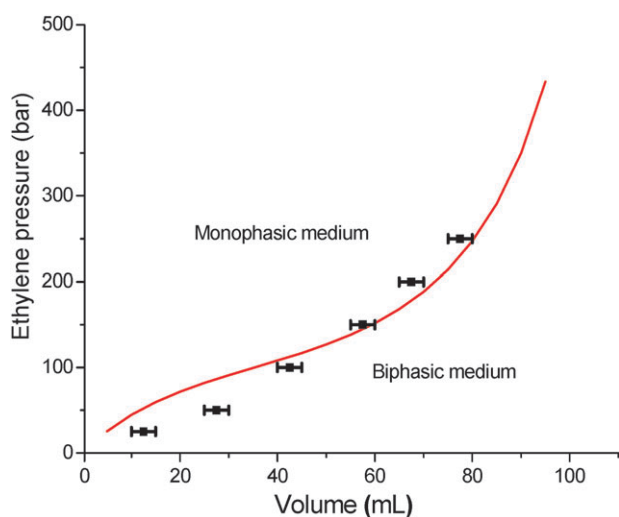


Fig. 7 Phase diagram for ethylene/THF mixture at 70 °C —: theoretical measure, ■: experimental measure.

transition is at 128 bar in THF and at 135 bar in toluene. This transition could explain the impossibility of measuring ethylene solubility over 130 bar.

Are these calculations accurate?

Calculations show a phase transition under 100 bar at 70 °C for THF between 36 and 37 mL (39–40 mL for toluene) which can be related to the experimental behavior in ethylene free radical polymerization (Fig. 1). As proposed, the break in activity corresponds to the phase transition which experimentally occurs between 40 and 45 mL solvent using these polymerization conditions (100 bar, 70 °C). To validate our calculations we performed polymerization at different pressures (25–250 bar) at 70 °C to experimentally determine the transition between monophasic and biphasic medium (Fig. 7) by varying the volume of THF. The break in activity was determined for each pressure (see ESI Fig. S3, Table S4).†

Our methodology seems to predict the transition of the system with a good correlation. The difference between theoretical and experimental transition could originate from the non-ideality of the THF/ethylene mixture. Our cubic Peng-Robinson model may be considered tentative at the present stage, and presumably describes the mixture of ethylene and THF best for the mid-range temperatures and pressures.

Conclusions

In summary, the activity profile for free radical polymerization of ethylene shows a break that can be related to a phase transition between a biphasic medium (two phases with ethylene in both) and a supercritical monophasic medium (solvent + ethylene). This phase transition depending on ethylene pressure, temperature and amount of organic solvent was fully determined by thermodynamic calculations using Peng-Robinson EOS and mixing rules for a bicomponent system (ethylene and solvent). For this purpose the solubility of ethylene was determined up to 130 bar in various solvents: solubility was mostly found to be independent of solvent

properties. The full description of the polymerization medium proposed from these calculations allows to understand better the free radical polymerization of ethylene in the intermediate pressure range ($20 < P_{\text{ethylene}} < 300$ bar) and opens the door to accurate copolymerization studies, the co-monomers playing the role of a solvent. Note that our calculation method is not restricted to ethylene but could be applied to other supercritical fluids.

Acknowledgements

E.G. thanks the “Ministère de la Recherche et de l’Enseignement Supérieur” for fellowship. The authors thank Mettler-Toledo for the thermal analysis.

References

- 1 K. W. Doak, in *Encyclopedia of Polymer Science and Engineering*, ed. H. F. Mark, N. M. Bikales, C. G. Overberger and G. Menges, Wiley Interscience, New York, 1985, vol. 6, pp. 386–428.
- 2 S. L. Aggarwal and O. J. Sweeting, *Chem. Rev.*, 1957, **57**, 665.
- 3 K. Vyakaranam, J. B. Babour and J. Michl, *J. Am. Chem. Soc.*, 2006, **128**, 5610.
- 4 T. Clark, *J. Chem. Soc., Chem. Commun.*, 1986, 1774.
- 5 A. H. C. Horn and T. Clark, *J. Am. Chem. Soc.*, 2003, **125**, 2809.
- 6 E. Grau, J. P. Broyer, C. Boisson, R. Spitz and V. Monteil, *Macromolecules*, 2009, **42**, 7279.
- 7 R. Mülhaupt, *Macromol. Chem. Phys.*, 2003, **204**, 289.
- 8 D. L. Beach and Y. V. Kissin, in *Encyclopedia of Polymer Science and Engineering*, ed. H. F. Mark, N. M. Bikales, C. G. Overberger and G. Menges, Wiley Interscience, New York, 1985, vol. 6, pp. 454–489.
- 9 L. S. Lee, H. J. Ou and H. L. Hsu, *Fluid Phase Equilib.*, 2005, **231**, 221.
- 10 L. S. Lee, R. F. Shih, H. L. Ou and T. S. Lee, *Ind. Eng. Chem. Res.*, 2003, **42**, 6977.
- 11 M. Atiqullah, H. Hammawa and H. Hamid, *Eur. Polym. J.*, 1998, **34**, 15511.
- 12 P. Ehrlich and G. A. Mortimer, *Adv. Polym. Sci.*, 1970, **7–3**, 386.
- 13 When the condensable fractions of the gaseous phase corresponding to a mixture of 500 mg of AIBN in 50 mL of THF at 70 °C and under 100 bar of ethylene were recovered in a glass vial, no significant amount of AIBN was detected.
- 14 The decrease of molecular weight over 50 mL is unexpected because the average length of PE is controlled by transfer to THF. This decrease is associated to an increase of PE branching level (T_m decrease from 115 °C to 100 °C). Both of these effects can be explained by considering the swelling of the amorphous part of PE which increases with the solvent volume. Growing PE radicals (located in the amorphous phase) exhibit higher mobility thus higher back-biting and transfer to solvent probability.
- 15 R. C. Reid, J. M. Prausnitz and B. E. Poling, in *The properties of gases and liquids*, ed. R. C. Reid, J. M. Prausnitz and B. E. Poling, McGraw-Hill Book Company, Singapore, 1988, pp. 29–35.
- 16 The total reactor volume was calculated by studying the pressure fall of the intermediate tank when we charge the empty reactor. A mass balance gives us: $d(V_T) = d(V_T + V_R)$ with V_T the tank volume.
- 17 R. C. Reid, J. M. Prausnitz and B. E. Poling, in *The Properties of Gases and Liquids*, ed. R. C. Reid, J. M. Prausnitz and B. E. Poling, McGraw-Hill Book Company, Singapore, 1988, pp. 74–84.
- 18 Critical parameters for ethylene ($T_c = 282.4$ K, $P_c = 50.4$ bar, $\omega = 0.089$), THF ($T_c = 540.1$ K, $P_c = 51.9$ bar, $\omega = 0.217$), and toluene ($T_c = 591.8$ K, $P_c = 41$ bar, $\omega = 0.263$) from R. C. Reid, J. M. Prausnitz and B. E. Poling, in *The Properties of Gases and Liquids*, ed. R. C. Reid, J. M. Prausnitz and B. E. Poling, McGraw-Hill Book Company, Singapore, 4th edn, 1988, pp. 656–732.
- 19 The amount of ethylene was calculated thanks to the Peng-Robinson EOS for the gas phase and the solubility in the hypothetical liquid phase, because $m_{E \text{ total}} = m_{E \text{ gaseous}} + m_{E \text{ liquid}}$.

Aqueous Dispersions of Nonspherical Polyethylene Nanoparticles from Free-Radical Polymerization under Mild Conditions**

Etienne Grau, Pierre-Yves Dugas, Jean-Pierre Broyer, Christophe Boisson, Roger Spitz, and Vincent Monteil*

Polyethylene, the top manufactured polymer by volume, is usually synthesized from low-pressure and -temperature catalytic processes^[1,2] or from a high-temperature (above 200 °C) and -pressure (greater than 1000 bar), highly energy-consuming free-radical polymerization process.^[3–5] In the latter case a branched, low-density, polyethylene is produced (LDPE), in contrast to Ziegler–Natta catalysis, which enables the synthesis of high-density polyethylene (HDPE) that exhibits higher crystallinities and melting temperatures. These well-established polymerization processes require improvement: reduction of energy consumption and of the use of volatile organic compounds (VOCs) are important targets. The VOC issue has been largely solved for low-pressure catalytic Ziegler–Natta polymerizations by using solvent-free gas-phase processes. For slurry polymerization, new catalysts compatible with “green” diluents such as supercritical CO₂^[6,7] or water^[8–11] have been developed.

Recently we successfully produced polyethylene (PE) by a radical pathway under less energy-consuming conditions: medium pressure below 250 bar and a low temperature of 70 °C using organic solvents (toluene or THF).^[12] PE was synthesized in high yields and exhibited intermediate melting points and crystallinities in comparison to HDPE and LDPE ($115 < T_m < 119$ °C; crystallinity of 55–70 %). However, polymer molecular weights remained low (number-average molecular weight $M_n < 5000$ g mol^{−1}, polydispersity index PDI ≈ 2) because of frequent transfer reactions to the solvent.

Transposition to an emulsion polymerization in aqueous dispersed medium (benefiting from the compartmentalization of radicals and from the low transfer ability of water) should be useful to increase both molecular weight and yield and at the same time to solve the VOC issue.

Only a few studies of free-radical polymerization (FRP) of ethylene in aqueous dispersed media have been

reported,^[13–17] and these use relatively high pressures ($P > 300$ bar) and a wide range of temperatures. The interpretation of the results in these early works (1945–1975) is difficult because of the lack of analytical tools available at the time to study colloidal properties of the obtained polymer dispersions.

Note that the emulsion process for ethylene polymerization cannot be a classical one. Ethylene is introduced as a supercritical gas, and consequently no ethylene droplets exist during the polymerization and no unreacted liquid monomer can remain in the latex. Furthermore, PE is a crystalline material, in contrast to most conventional polymers produced by FRP.

Herein, FRP of ethylene in emulsion under mild conditions has been investigated, representing an innovative, low-energy, “green”, efficient way to produce PE by a free-radical mechanism. The transposition of the ethylene polymerization process to aqueous medium has been achieved by using a cationic water-soluble initiator, 2,2-azobis(2-amidinopropane) dihydrochloride (AIBA). FRP of ethylene was performed in water at 70 °C with and without a standard cationic surfactant (CTAB, cetyltrimethylammonium bromide) to assist nucleation and particle stabilization. In all cases, ethylene was polymerized with significant yields, and stable dispersions of PE particles were obtained for ethylene pressure up to 250 bar (Figure 1). Interestingly, PE can be synthesized by this FRP process down to a pressure of 50 bar.

In the surfactant-free system, yield is lower than that obtained using the same amount of initiator in THF but is

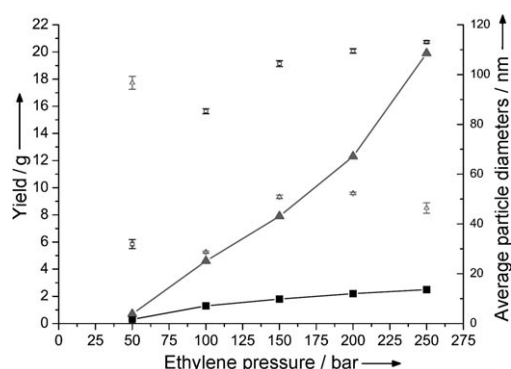


Figure 1. Free-radical polymerization of ethylene in aqueous dispersed medium: ■ yield and □ average particle diameter versus ethylene pressure (80 mg AIBA, 50 mL water, 4 h at 70 °C under ethylene pressure); ▲ yield and △ average particle diameter versus ethylene pressure (80 mg AIBA, 50 mL water with 1 g L^{−1} CTAB, 4 h at 70 °C under ethylene pressure). Average particle diameter determined by DLS.

[*] E. Grau, P.-Y. Dugas, J.-P. Broyer, Dr. C. Boisson, Dr. R. Spitz, Dr. V. Monteil
UMR 5265 Laboratoire de Chimie Catalyse Polymères et Procédés (C2P2), LCP team
Université de Lyon, Univ. Lyon 1, CPE Lyon, CNRS
Bat 308F, 43 Bd du 11 novembre 1918, 69616 Villeurbanne (France)
Fax: (+33) 4-7243-1768
E-mail: monteil@lcpp.cpe.fr

[**] E.G. thanks the “Ministère de la Recherche et de l’Enseignement Supérieur” for his fellowship. We thank Mettler-Toledo for the thermal analysis. We are indebted to C. Graillat and Prof. B. Charleux for their valuable contributions to this research.

Supporting information for this article, including experimental details, is available on the WWW under <http://dx.doi.org/10.1002/anie.201001800>.

higher than in toluene.^[12] The stabilization of PE particles is assumed to result from the cationic fragments of the initiator attached at the chain end, which induce electrostatic repulsion. Average particle diameters (D_p) measured by DLS (dynamic light scattering) increase with the ethylene pressure (and consequently with the yield) from 30 to 110 nm. Polydispersity indexes of the particle size distribution remain very low ($PI \approx 0.05$), thus indicating the monodisperse character of particle size distribution. Furthermore, the yield/ D_p^3 ratio, standing for the number of particles, remains constant whatever the ethylene pressure.

When polymerizations were performed in the presence of a standard cationic surfactant (CTAB) at 1 g L^{-1} (above the critical micelle concentration of 0.2 g L^{-1} at 25°C), much higher activities were found (Figure 1). This emulsion system is even more efficient than the polymerization in THF.^[12] In these non-optimized conditions, up to 40% solid content is obtained (after degassing the 250 bar ethylene). Average particle diameters seem to reach a plateau at 50 nm with increasing ethylene pressure. This result indicates that the number of particles increases with the yield. Surprisingly, polydispersity indexes measured by DLS remain higher ($PI \approx 0.5$) than for the surfactant-free process.

The produced PE exhibits a low melting point ($T_m \approx 100^\circ\text{C}$) and low crystallinity (30–40%). Highest values were obtained in the case of the surfactant-free polymerization process (see the Supporting Information, Table S1). As expected, high molecular weights PE ($M_n = 10^4$ – 10^5 g mol^{-1}) were produced. The number of PE chains synthesized is greater with CTAB, thus indicating a possible transfer to surfactant (see the Supporting Information, Figure S1). The PE obtained is moderately branched under both conditions (Figure S1: 30 branches per 1000 carbons without surfactant and 37 branches per 1000 carbons with CTAB) as determined by ^{13}C NMR spectroscopy,^[18] which is in agreement with the crystallinities and melting temperatures measured. This higher branching level in water than in an organic solvent (THF: 9 branches per 1000 carbons or toluene: 7 branches per 1000 carbons)^[12] can be explained by the compartmentalization of the growing PE chains, which increases transfer reactions to the polymer. The proportion of short chain branches is lower in emulsion (25 vs. 35% in organic solvent) owing to favored intermolecular over intramolecular transfer reactions in a confined environment.

To link solvent and emulsion processes, the influence of the addition of organic solvents to water (water-miscible THF or immiscible toluene) was investigated. PE molecular weights dropped in the presence of solvents (see the Supporting Information, Table S2). The M_n value dropped from $50\,500 \text{ g mol}^{-1}$ in water to 8300 and 2350 g mol^{-1} for toluene/ H_2O (1:4) and THF/ H_2O mixtures, respectively, in the presence of CTAB. This decrease can be attributed to an increased frequency of transfer reactions to solvent (contrary to water, THF and toluene exhibit high transfer abilities),^[12] which has been confirmed by NMR spectroscopy (see the Supporting Information, Figure S2). With THF, the transfer reaction should take place in the continuous aqueous phase or at the particle surface and not in the particles, because THF is not an efficient swelling agent for amorphous PE (the same

D_p is observed before and after removal of THF by partial reduced-pressure evaporation). For toluene, the D_p drops by about 10 nm after removal of the organic solvent (toluene is a swelling solvent for PE), so transfer could additionally take place inside the particles.

Surfactant-free and classical emulsion polymerization processes were compared by investigating the reaction profile at 70°C under 100 bar ethylene (Figure 2). For the surfactant-free system, particle diameters increase with yield and the yield/ D_p^3 ratio remains constant, thus no renucleation or aggregation takes place during the polymerization.

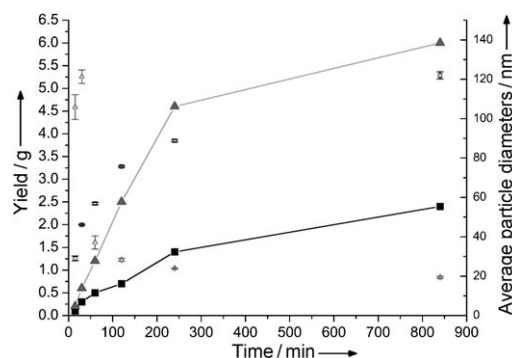


Figure 2. Reaction profile for free-radical polymerization of ethylene in aqueous dispersed medium: ■ yield and □ average particle diameter versus time (80 mg AIBA, 50 mL water at 70°C under 100 bar); ▲ yield and △ average particle diameter versus time (80 mg AIBA, 50 mL water with 1 g L^{-1} CTAB at 70°C under 100 bar). Average particle diameter determined by DLS.

In the presence of CTAB the behavior is quite different. Initially, particles with large diameters are formed, which seem to disappear with time to generate only small particles ($D_p \approx 30 \text{ nm}$) after 2 h. The mechanism for the extinction of large particles to generate very small particles still remains unknown, but preliminary experimental results suggest a crucial role of the surfactant itself. For example, if 1 g L^{-1} CTAB is added to surfactant-free PE latex, after stirring at 70°C small particles are recovered (see the Supporting Information, Figure S3).

The PE latexes were also characterized using TEM analysis (Figure 3). In the surfactant-free process, quasi-spherical particles were observed. The rigid lamellas of semicrystalline PE prevent the formation of spheres (as already observed for latex prepared by catalytic emulsion polymerization).^[19] Nevertheless, particles show relatively homogeneous diameters, in agreement with DLS measurements (low PI).

In the presence of CTAB, TEM pictures show a low contrast for the surface of particles, which could be an indication of flat particles. This morphology has been confirmed by tilting the sample: disks were observed at 0° and ellipses at 60° . Note that no significant changes were observed when the PE latex obtained from surfactant-free polymerization was tilted. From the hypothesis of cylinder-like particles, the dimensions of these objects were estimated

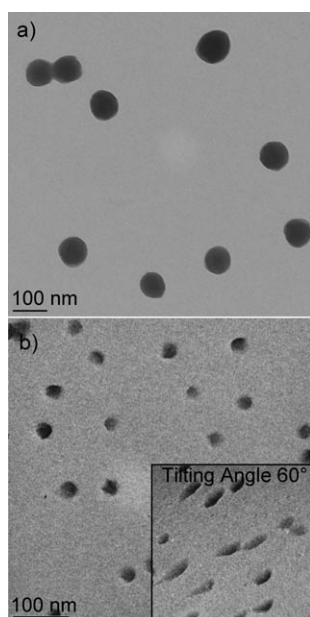


Figure 3. TEM pictures of PE latex: a) Standard particles without CTAB, 100 bar, 4 h at 70 °C. b) Standard particles with 1 g L⁻¹ CTAB (inset: tilting angle of 60°), 100 bar, 4 h at 70 °C.

(average disks diameters about 35 nm and thickness about 3–4 nm). From these findings we can better explain the high values of PI (ca. 0.5) obtained by DLS (the autocorrelation function of DLS is calculated for a size distribution of spherical particles), which were not in agreement with the apparent homogeneity in the diameters of particle sizes observed by TEM.^[20]

In summary, compartmentalization in water from emulsion processes (with or without surfactant) is a very promising way to produce high-molecular-weight polyethylenes in the low to very low density range by FRP under mild conditions from a water-soluble cationic initiator. PE yields are higher than for the solvent processes previously developed. From a colloidal point of view, FRP in emulsion exhibits unexpected original behavior. In the presence of surfactant, very small cylindrical PE particles are generated, while larger quasi-spherical particles were formed in the surfactant-free process.

The coating properties of these attractive PE nanoparticles are currently being investigated.

Received: March 26, 2010

Revised: June 7, 2010

Published online: August 16, 2010

Keywords: emulsions · nanoparticles · polyethylene · polymerization · radicals

- [1] R. Mülhaupt, *Macromol. Chem. Phys.* **2003**, *204*, 289–327.
- [2] D. L. Beach, Y. V. Kissin in *Encyclopedia of Polymer Science and Engineering*, Vol. 6, 2nd ed. (Eds.: H. F. Mark, N. M. Bikales, C. G. Overberger, G. Menges), Wiley Interscience, New York, **1985**, pp. 454–489.
- [3] K. W. Doak in *Encyclopedia of Polymer Science and Engineering*, Vol. 6, 2nd ed. (Eds.: H. F. Mark, N. M. Bikales, C. G. Overberger, G. Menges), Wiley Interscience, New York, **1985**, pp. 386–428.
- [4] S. L. Aggarwal, O. J. Sweeting, *Chem. Rev.* **1957**, *57*, 665–742.
- [5] S. P. Ehrlich, G. A. Mortimer, *Adv. Polym. Sci.* **1970**, *7*, 386–448.
- [6] M. Kemmere, T. de Vries, M. Vorstman, J. Keurentjes, *Chem. Eng. Sci.* **2001**, *56*, 4197–4204.
- [7] A. Bastero, G. Francio, W. Leitner, S. Mecking, *Chem. Eur. J.* **2006**, *12*, 6110–6116.
- [8] L. Kolb, V. Monteil, R. Thomann, S. Mecking, *Angew. Chem.* **2005**, *117*, 433–436; *Angew. Chem. Int. Ed.* **2005**, *44*, 429–432.
- [9] A. Held, F. M. Bauers, S. Mecking, *Chem. Commun.* **2000**, 301–302.
- [10] R. Soula, C. Novat, A. Tomov, R. Spitz, J. Claverie, X. Drujon, J. Malinge, T. Saudemont, *Macromolecules* **2001**, *34*, 2022–2026.
- [11] S. Mecking, *Colloid Polym. Sci.* **2007**, *285*, 605–619.
- [12] E. Grau, J. P. Broyer, C. Boisson, R. Spitz, V. Monteil, *Macromolecules* **2009**, *42*, 7279–7281.
- [13] H. Hopff, R. Kern, *Modern Plastics* **1946**, 153–220.
- [14] A. F. Helin, H. K. Stryker, G. J. Mantell, *J. Appl. Polym. Sci.* **1965**, *9*, 1797–1805.
- [15] A. F. Helin, H. K. Stryker, G. J. Mantell, *J. Appl. Polym. Sci.* **1965**, *9*, 1807–1822.
- [16] T. Suwa, H. Nakajima, M. Takehisa, S. Machi, *Polym. Lett. Ed.* **1975**, *13*, 369–375.
- [17] H. K. Stryker, G. J. Mantell, *J. Polym. Sci. Part C* **1969**, *27*, 35–48.
- [18] G. B. Galland, R. F. de Souza, R. S. Mauler, F. F. Nunes, *Macromolecules* **1999**, *32*, 1620–1625.
- [19] F. M. Bauers, R. Thomann, S. Mecking, *J. Am. Chem. Soc.* **2003**, *125*, 8838–8840.
- [20] High PI can also be partially due to a wide distribution in cylinder thickness.

Ni dieu, ni maître

Sauf Roger !

Abstract:

This work aims to study ethylene polymerization from the free radical polymerization process to the copolymerization by a hybrid radical/catalytic mechanism. PE is synthesized by free radical polymerization under milder experimental conditions than industrial ones ($P > 1000$ bar and $T > 100^\circ\text{C}$). Indeed free radical polymerization of ethylene is efficient even down to pressure of 5 bar and temperature of 10°C . Several unexpected behaviors are observed such as a high solvent activation effect. Beside the slurry process in organic solvent, polymerization in aqueous dispersed media is also performed. Stable PE latexes are obtained with solid contents up to 40%. Two different PE particles morphologies are observed cylinder-like and sphere-like. Then free radical copolymerization is studied using a broad range of polar vinyl monomers in organic solvent and emulsion. Insertions up to 50% of ethylene are obtained under mild conditions. The ambivalent role of comonomer as monomer and activator of the polymerization is highlighted. In order to obtain a wide range of composition of polar/non-polar copolymers a new technique of polymerization has been developed. A nickel complex is used to initiate the free radical polymerization and to catalyse the coordination/insertion ethylene polymerization. This nickel complex is capable of a reversible homolytic cleavage of its nickel-carbon bond. Finally, this hybrid process is used to copolymerize efficiently ethylene with various polar vinyl monomers. Multiblock copolymers with ethylene content from 1% to 99% are obtained by simply varying the monomer feeds.

Key-Words:

Ethylene/Polar monomer/Copolymerization/Free radical polymerization/Catalysis/High pressure/Emulsion

Titre :

Polymérisation de l'éthylène : de l'homopolymérisation radicalaire à la copolymérisation hybride radicalaire/catalytique

Résumé :

Ce travail concerne l'étude de la polymérisation de l'éthylène allant de l'homopolymérisation purement radicalaire jusqu'à la copolymérisation utilisant un mécanisme hybride radicalaire/catalytique. Ce travail montre que le polyéthylène peut être synthétisé par voie radicalaire dans des conditions expérimentales beaucoup plus douces que celles utilisées industriellement ($P > 1000$ bar et $T > 100^\circ\text{C}$). L'éthylène a été polymérisé à partir de 10°C et 5 bar de pression d'éthylène. Un important effet activateur du solvant a été mis en évidence. De plus la polymérisation en milieu dispersé aqueux de l'éthylène a aussi été étudiée. Des latex stables de PE avec des taux de solide de 40% ont pu être obtenus. Deux morphologies de nanoparticules, cylindre ou sphère, ont été observées. La copolymérisation radicalaire avec des monomères vinyliques polaires a été également étudiée en solution ou en émulsion. Des insertions d'éthylène jusqu'à 50% ont été obtenues. De plus l'influence du comonomère et du solvant organique utilisé sur la polymérisation radicalaire de l'éthylène a été quantifiée. Une nouvelle technique de polymérisation hybride radicalaire/catalytique a été développée pour pouvoir obtenir toute la gamme de compositions possibles de copolymères éthylène/monomère polaire à partir d'un complexe de nickel qui amorce la polymérisation radicalaire et catalyse également la polymérisation de l'éthylène. Ce complexe subit une rupture homolytique réversible de la liaison nickel carbone et permet la synthèse de copolymères multiblocs. Des insertions d'éthylène de 1% à 99% ont été obtenues en faisant varier la pression d'éthylène et la concentration en comonomères polaires.

Mots-clés:

Ethylène/Monomère polaire/Copolymérisation/Polymérisation radicalaire/Catalyse/Haute pression/Emulsion

Laboratoire C2P2 – Equipe LCPP
CPE Lyon – Bât. F308, B.P. 2077
43 Bd. du 11 Nov. 19118
69616 Villeurbanne

